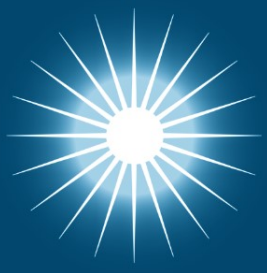
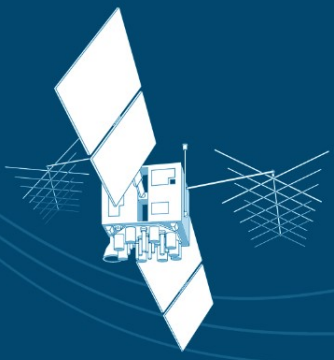
Space Weather & Telecommunications

JOHN M. GOODMAN







SPACE WEATHER & TELECOMMUNICATIONS

THE KLUWER INTERNATIONAL SERIES
IN ENGINEERING AND COMPUTER SCIENCE

SPACE WEATHER & TELECOMMUNICATIONS

JOHN M. GOODMAN
Radio Propagation Services, Inc., USA
JMG Associates, Ltd., USA
Alexandria, Virginia, USA

Springer

John M. Goodman
Radio Propagation Services, Inc. (RPSI)
Alexandria VA 22308-1943

Email: jm_good@cox.net

Library of Congress Cataloging-in-Publication Data

A C.I.P. Catalogue record for this book is available
from the Library of Congress.

Goodman, John M.
Space Weather & Telecommunications / John M. Goodman
p.cm.—(The Kluwer International Series in Engineering and Computer Science)
Includes bibliographical references and index.

ISBN 0-387-23670-8 (HC) ISBN 0-387-23671-6 (eBook) Printed on acid-free paper.

© 2005 Springer Science+Business Media, Inc.
All rights reserved. This work may not be translated or copied in whole or in part without the written permission of the publisher (Springer Science+Business Media, Inc., 233 Spring Street, New York, NY 10013, USA), except for brief excerpts in connection with reviews or scholarly analysis. Use in connection with any form of information storage and retrieval, electronic adaptation, computer software, or by similar or dissimilar methodology now know or hereafter developed is forbidden.
The use in this publication of trade names, trademarks, service marks and similar terms, even if the are not identified as such, is not to be taken as an expression of opinion as to whether or not they are subject to proprietary rights.

Printed in the United States of America.

9 8 7 6 5 4 3 2 1 SPIN 11049883 (Hard cover) / 11341390 (eBook)

springeronline.com

DEDICATION

To my wife Jane, our three children and their families:

Mary Jane Goodman & Eugene Giddens and their children: Hannah, Caroline, Elliot, Benjamin, Isaac and Noah;

John Michael Goodman, Jr. & Victoria Risbrough;

Jenny Rebecca Goodman & Hans Hansen and their children: Steven, John, Luke and Gage

CONTENTS

PREFACE xiii
1. INTRODUCTION 1
1.1 Summary 1
1.2 Definition of Space Weather 2
1.3 An Historical Perspective 3
1.4 The Advent of Space Weather Programs 20
1.5 Categories of Radio Systems 21
1.6 Other Influences on Systems 22
1.7 Space Weather Data Utilization 23
1.7.1 Availability of Space Weather Data 23
1.7.2 Operational Terminals & Workstations 24
1.8 Conclusions 24
1.9 References 25
1.10 Bibliography 27
2. THE ORIGINS OF SPACE WEATHER 29
2.1 Introduction 29
2.2 The Sun and its Influence 31
2.2.1 Solar Structure and Irradiance Properties 31
2.2.2 On the Nature of Solar Activity and Sunspots 36
2.2.3 Active Regions, Coronal Holes, and Solar Wind 39
2.2.4 The Canonical Sunspot Cycle 42
2.2.5 Prediction of the Sunspot Cycle 43
2.2.6 Solar Variability 45
2.2.7 Solar Flares 50
2.2.8 Storms and Declining Solar Activity 51
2.3 Magnetosphere and Geomagnetic Storms 54
2.3.1 The Geomagnetic Field 55
2.3.2 Magnetospheric Topology 60
2.3.3 Geomagnetic Activity Indices 62
2.3.5 Real-Time Geomagnetic Data 64
2.3.6 Magnetic Storms and the Ionosphere 65
2.3.7 The Halloween Storm Period of 2003 73
2.4 Motivation for Space Weather Observations 76
2.5 References 78
3. THE IONOSPHERE 81
3.1 Introduction 81
3.2 General Properties of the Ionosphere 82
3.2.1 Basic Structure 82
3.2.2 Formation of the Ionosphere 84

3.2.3 Ionospheric Layering 87
3.2.4 Chapman Layer Theory 90
3.3 Equilibrium Processes 92
3.4 Description of the Ionospheric Layers 95
3.4.1 Sounder Measurement Method 95
3.4.2 The D-Region 97
3.4.3 The E-Region 98
3.4.4 The F1-Region 101
3.4.5 The F2-Region 103
3.4.6 Anomalous Features of the F-Region 104
3.4.6.1 Diurnal Anomaly 105
3.4.6.2 Appleton Anomaly 105
3.4.6.3 December Anomaly 106
3.4.6.4 Winter (Seasonal) Anomaly 106
3.4.6.5 F-Region High-Latitude Trough 106
3.4.7 Irregularities in the Ionosphere 106
3.5 Diurnal Behavior of the Ionospheric Layers 108
3.5.1 Mean Variations 108
3.5.2 Short-Term Variations 108
3.6 Long-Term Solar Activity Dependence 112
3.7 Sporadic-E 114
3.7.1 General Characteristics 114
3.7.2 Formation of Midlatitude Sporadic E 114
3.7.3 Sporadic E at Non-temperate Latitudes 116
3.8 The High Latitude Ionosphere 116
3.8.1 Description of Plasma Blobs and Patches 120
3.8.2 Arctic Radio Propagation 122
3.8.3 Early Diagnostic Studies 122
3.8.4 Recent Diagnostic Studies 124
3.9 Ionospheric Response to Solar Flares 127
3.10 The Ionospheric Storm 129
3.10.1 Early Attempts at Storm Modeling 130
3.10.2 The NOAA-SEC STORM Model 132
3.10.3 Storm Studies Using NTS-2 Navigation Signals 134
3.10.4 The Halloween 2003 Storm 137
3.11 Ionospheric Current Systems 141
3.12 Ionospheric Models 141
3.12.1 Data Assimilation and Kalman Filters 146
3.12.2 GAIM 148
3.12.3 European Union COST Action Models 149
3.12.3.1 COST Action 238 150
3.12.3.2 COST Action 251 150

3.12.3.3 ESA Space Weather Working Team 152
3.12.4 Ionospheric Modeling Panel at IES2002 153
3.12.4.1 User Needs 154
3.12.4.2 Storm Modeling 154
3.12.4.3 Observations & Data Issues 155
3.12.4.4 Empirical Models 155
3.12.4.5 Data Sources for Modeling 156
3.12.4.6 Future of Ionospheric Modeling 156
3.12.4.7 Data Assimilation Modeling 157
3.12.4.8 Solar EUV Modeling 157
3.12.4.9 WBMOD Overview 157
3.12.4.10 Weather Model for Scintillation 157
3.12.4.11 Panel Discussion Synopsis 158
3.12.4.12 Panel Conclusions 161
3.13 Ionospheric Predictions 161
3.14 Science Issues and Challenges 163
3.15 References 164
4. TELECOMMUNICATION SYSTEMS 175
4.1 Introduction 175
4.2 Outline of Ionospheric Effects 178
4.3 Terrestrial Telecommunications 181
4.3.1 Longwave Propagation 181
4.3.2 Extremely Low Frequency 183
4.3.3 Very Low Frequency and Low Frequency 184
4.3.4 Medium Frequency 185
4.3.5 High Frequency (shortwave) 187
4.3.5.1 Operational HF Systems 193
4.3.5.2 System Performance Modeling 196
4.4 Earth-Space Telecommunications 198
4.4.1 Integrated Propagation Effects 198
4.4.1.1 Refraction 199
4.4.1.2 Phase and Group Path Variation 202
4.4.1.3 Ionospheric Doppler Shift 206
4.4.1.4 Faraday Rotation 206
4.4.1.5 Time Dispersion 209
4.4.1.6 Absorption 209
4.4.1.7 Comments on Total Electron Content 210
4.4.2 Differential Effects and the *Ne* Distribution 213
4.4.2.1 Diurnal Variation of Scintillation 214
4.4.2.2 Global Morphology of Scintillation 216
4.4.2.3 Modeling of the Scintillation Channel 219
4.4.2.4 Mitigation Schemes 220

4.5 Space Weather Support for Systems 221
4.5.1 Military C3I Requirements 221
4.5.2 Systems Combating Space Weather 223
4.5.2.1 GLOBALink/HF 225
4.5.2.2 FAA WAAS System 237
4.5.3 Practical Approaches 240
4.5.4 Benefits of Space Weather Information 243
4.6 References 246
5. PREDICTION SERVICES & SYSTEMS 255
5.1 Introduction 255
5.2 Requirements 257
5.3 Elements of the Prediction Process 258
5.4 Organizational Approaches 260
5.4.1 Forecasting Services 260
5.4.2 International Space Environment Service 263
5.4.3 NOAA 265
5.4.3.1 Space Environment Center 265
5.4.3.2 National Geophysical Data Center 283
5.4.4 RWC Canada (NRCan) 285
5.4.5 RWC Australia 287
5.4.6 Jet Propulsion Laboratory 289
5.4.7 Rutherford Appleton Laboratory 293
5.4.8 Institute of Communications and Navigation 293
5.4.9 RWC Warsaw and IDCE 295
5.4.10 RWC Brussels and SIDC 296
5.4.11 Military Systems 296
5.4.11.1 Air Force Weather Agency 296
5.4.12 Special Product: Email Alerts 298
5.5 Commercial Forecasting Services 298
5.5.1 Vendor Industry 299
5.5.1.1 Northwest Research Associates 299
5.5.1.2 Radio Propagation Services 301
5.5.1.3 Solar Terrestrial Dispatch 302
5.6 Systems for Forecasting 302
5.6.1 OPSEND 303
5.6.2 SCINDA 304
5.7 Concluding Remark 305
5.8 References 306
6. RESEARCH ACTIVITIES & PROGRAMS 309
6.1 Introduction 309
6.2 National Space Weather Program 311
6.3 Living with a Star 315

6.4 Data Assimilation and Transfer 317
6.5 Military Space Weather Involvement 317
6.5.1 Early DoD Activity 317
6.5.2 Space Weather Architecture 318
6.5.3 Existing Capabilities 319
6.5.4 Areas for Improvement 320
6.5.5 Space Weather Architecture "Vector" 323
6.6 International Initiatives 324
6.6.1 European Union COST Actions 325
6.6.1.1 COST Action 238 325
6.6.1.2 COST Action 251 325
6.6.1.3 COST Action 271 326
6.6.1.4 COST Action 724 326
6.6.2 European Space Agency 327
6.6.3 Sweden 327
6.6.4 France 328
6.6.5 Japan 328
6.6.6 Canada 329
6.6.7 Australia 329
6.7 Scientific & Professional Organizations 329
6.7.1 URSI 329
6.7.2 COSPAR 330
6.7.3 SCOSTEP 331
6.7.4 ITU-R 331
6.7.5 NCEP 332
6.7.6 CSWIG 332
6.7.7 Space Weather Week 333
6.8 Research Programs & Activities 334
6.8.1 CEDAR 334
6.8.2 GEM 335
6.8.3 SHINE 336
6.8.4 CISM 336
6.8.5 CAWSES 337
6.8.6 Additional Missions & Activities 337
6.9 Agencies, Institutions & Companies 341
6.10 Comment on Internet Resources 344
6.11 References 345
7. EPILOGUE 347
- Featuring an interview with the Director of SEC
ACRONYMS & TERMS 355
INDEX 367
About the Author 381

PREFACE

Space weather has an enormous influence on modern telecommunication systems even though we may not always appreciate it. We shall endeavor throughout this monograph to expose the relationships between space weather factors and the performance (or lack thereof) of telecommunication, navigation, and surveillance systems. Space weather is a rather new term, having found an official expression as the result of several government initiatives that use the term in the title of programs. But it is the logical consequence of the realization that space also has weather, just as the lower atmosphere has weather. While the weather in space will influence space systems that operate in that special environment, it is also true that space weather will influence systems that we understand and use here on terra firma. This brings space weather home as it were. It is not some abstract topic of interest to scientists alone; it is a topic of concern to all of us. I hope to make this clear as the book unfolds.

Why have I written this book? First of all, I love the topic. While at the Naval Research Laboratory (NRL), I had the opportunity to do research on many topics including: Thomson scatter radar and satellite beacon studies of the ionosphere, utilization of the NASA Gemini platform for ionospheric investigations, microwave radar propagation studies, HF signal intercept and direction-finding experiments, and multi-disciplinary studies of certain physical phenomena relevant to weapon systems development. Some of the latter studies were undertaken by NRL under its role as an independent arm for the DoD to engage in "responsible myth chasing" and resolution of dubious system performance claims by contractors or other government agencies. However, one of the more interesting facets of my NRL career did not involve a great deal of science, but did involve the development of tools and applications of solar data in support of military systems thought to be vulnerable to solar flares and related phenomena. My role, as manager of the SOLRAD Environmental Data Analysis Center (SEDAC), brought me in touch with many renowned solar physicists at NRL and elsewhere. I had the opportunity to leverage my ionospheric and communication system background with a legitimate understanding of solar-terrestrial-physics; and this brought to mind some novel schemes that might have the potential for improvement in system design and performance. Along the way I have served as the convener for the triennial *Ionospheric Effects Symposia*, and this activity was stimulated in part by my SOLRAD experiences. So, I have written this book to bridge an untidy gap in the relationship that exists between the following two disciplines: space weather and telecommunication system performance. There are a number of books that address one of the two

disciplines in some detail, but generally mention the other as an afterthought. I have tried to marry the two disciplines so that the readership can see the connections more clearly. Hopefully I have achieved this goal.

There are many Internet Web sites dedicated to the provision of space weather data sets that can be directed to an estimation of the onset, magnitude and duration of various forms of system impairment. Counted among the government organizations with such sites are: the Space Environment Center (SEC) and the National Geophysical Data Center (NGDC) of NOAA in the USA; CRC in Canada; the Ionospheric Prediction Service (IPS) of the Space Weather Agency in Australia, and others. There are also commercial activities that are generally a little closer to the ultimate customers, and, as a result, can provide tailored products. The Commercial Space Weather Interest Group (CSWIG) is an association of firms that provide space weather products and services, and it includes a number of companies specifically focusing on telecommunication performance predictions. Without access to the fundamental space weather data provided by SEC and other government sources, commercial activities such as those undertaken by CSWIG members could possibly fail and would surely be more expensive. The value of SEC and its international partners in the provision of fundamental space weather data to customers, both military and civilian, is hard to gauge accurately. But this data source is clearly very important for the operation of a variety of systems that are impacted by space weather, and for many of these systems, it may be essential.

As would be expected, the various services of SEC and its R&D backbone are under periodic scrutiny by the parent agency, currently NOAA, and by Congress itself. National priorities and other exigencies can sometimes lead to budgetary constraints, and SEC is not immune from this phenomenon. In my view it is imperative that SEC, or an organization with equivalent functionality, remain viable as a national resource, and it is hoped that funding sufficiency and continuity can be achieved. Space weather services are that important. It is noteworthy that SEC has found a new home with the National Weather Service, and this would appear to validate the importance of space weather to the nation, with SEC as the focus for implementation of national space weather objectives.

It should be noted that the national and international defense establishments do recognize the importance of space weather to operational systems that are reliant upon earth-space and terrestrial radio propagation. Indeed there are some very important activities for which the requirements of both military and civilian users have common themes. Accordingly, some activities are necessarily similar, and distinctions of approach to final application can appear blurred. This book will not strive to carve distinctions

where none exist, but we will attempt to point out those activities that have distinctly military or civilian applications.

The first chapter provides a general overview of important space weather issues and the relevance to telecommunication systems. It could be regarded as a summary since glimpses of the entirety of topics covered within the book are provided, although in abbreviated form. The definition of space weather is examined in light of the significant usage of the expression in programmatic terms, published paper titles, and the popular press. We look briefly at the categories of radio systems, distinguishing between those that derive their full utility based upon the presence of the ionosphere from those that regard the ionosphere as a nuisance. Next we look at modern electronic systems that are influenced by space weather, and the ionospheric weather as a subset. Brief summaries of modeling and climatological approaches, model updating methods for forecasting, and technological solutions to the system impairments associated with space weather effects are discussed. We look at deficiencies in space weather data (i.e., the knowledge base) as well as deficiencies in the proper application of space weather data that are already available. There is a logical bifurcation in the set of space weather data, and we refer to these varieties as "upstream" and "downstream". The upstream variety includes parameters related to the following regimes: (i) solar surface, (ii) the corona, (iii) the solar wind, and (iv) the interplanetary magnetic field. The "downstream" variety is directly related to telecommunication system performance and consists of the plasmasphere and the ionosphere.

In Chapter 2, "The Origins of Space Weather", we turn our attention to the solar-terrestrial environment. We examine the rudiments of solar structure and processes, the genesis and consequences of solar activity, the solar wind and the interplanetary magnetic field (IMF), elements of relevant magnetospheric processes, and solar-terrestrial relationships. We cover solar activity cycles and indices and their importance in specified prediction systems. In recent years, the importance of the corona, including coronal holes and coronal mass ejections (i.e., CMEs), has emerged, and a treatment of these phenomena is provided. We shall conclude with a discussion of recent progress in the development of space weather prediction systems and will identify those services that are available for forecasting purposes. New observational satellites that may provide better imaging or improved vantage points for solar montoring are identified. An important feature of the chapter is the phenomenon of the geomagnetic storm. This topic is central to the matter of any intermediate ionospheric forecasting system since the magnetospheric substorm is strongly coupled to the ionosphere. The ionospheric storm is the response of the ionosphere to the geomagnetic storm. As an example of the magnetic storm signature, we identify the so-called *Halloween Storm* of 2003. This period was decidedly dramatic in the

hierarchy of space weather terms, including the ionosphere and the system interactions. Accordingly we revisit the ionospheric response of the Halloween Storm period in Chapter 3, and the telecommunication effects in Chapter 4. We conclude Chapter 2 with a discussion of the motivation for space weather research.

In Chapter 3 we examine the influence of space weather on the ionosphere, beginning with general properties under benign conditions and concluding with disturbed properties under pathological conditions. We discuss ionospheric layers and their individual characteristics as functions of solar cycle, season, and time of day. Differences in the ionospheric personality are the most definitive when data are organized in terms of geomagnetic coordinates, and we discuss the regional differences for polar, auroral, trough, mid-latitude, and equatorial regions. The earliest quasi-theoretical descriptions of the ionosphere were based upon the Chapman hypothesis, and we examine the various departures from this model, including the Appleton, December, winter, and diurnal anomalies, and the high latitude trough. Other features of interest are described, such as sporadic E, spread F, and traveling ionospheric disturbances. The sun has a marked impact on the ionospheric layers, in the form of Sudden Ionospheric Disturbance (SIDs), solar proton events, and enhanced solar wind transients. There are a number of modeling approaches depending upon the application and these are outlined. The GAIM technology and region-specific models such as UAF Eulerian Parallel Polar Ionosphere Model are mentioned. We conclude with a discussion of ionospheric predictions with a view toward their utilization in radio propagation forecasting. Fundamental science issues and challenges are brought up at the end of the chapter.

In Chapter 4 we start with a survey of legacy 20th Century telecommunication systems to establish a baseline for the technology. This is followed by an examination of certain improved and emergent systems of the 21st Century. There are a variety of operational communication systems that are strongly dependent upon the ionosphere, and there are others that are merely influenced by the ionosphere. In the dependent category, we have short-wave (i.e., MF and HF systems) and long-wave systems (i.e., VLF and LF systems). In the influenced category we have meteor-burst communications (at VHF), systems, and satellite-based navigation systems. This book will examine the hierarchy of communication systems, including legacy terrestrial systems and important earth-space systems. It will address various resource management issues for specified operational systems, and the relationship with aspects of space weather will be discussed. Some examples where space-weather information is used in existing systems are presented. We also identify how space weather information could be used in those situations where it is currently unused. Of considerable importance in

the context of telecommunication system performance forecasting is an understanding of the methodologies and tools that are available. Methods involving climatological updating, recurrence, persistence, neural networks, and various combinations are examined throughout the book, including Chapter 4. Of course, aspects relevant to ionospheric modeling are covered in Chapter 3, while aspects specific to products and services are discussed in Chapter 5.

Radio Communication and broadcasting systems may be either controlled by the ionosphere, as in HF skywave systems, or simply influenced by it, as in transionospheric radio communication and navigation systems. In the former case, the ionosphere is actually an inexorable part of the system; while in the latter case, the ionosphere is fundamentally a nuisance. In both instances an account of the ionosphere is at least beneficial to system design and operation. In the case of HF skywave systems, the accounting may be a critical factor in system performance. What is not well understood is that radio communication systems that are affected by the ionospheric personality are not necessarily inferior to systems that are little influenced by the ionosphere. Intelligent use of space-weather information may lead to significant improvements in performance of adaptive HF systems. In fact, under some conditions, HF digital communication can be just as reliable as satellite communication. This may be surprising to some communication specialists, and it indicates the power of adaptive system design as powered by space-weather data. It is noteworthy that our emphasis is on *intelligent* exploitation of space-weather data as part of an adaptive HF system incorporating sufficient levels of time, path and frequency diversity. We must be clear on that point. We describe several systems that cope successfully with many classes of ionospheric disturbances using space weather data in an intelligent way. Two systems are the ARINC GLOBALink/HF system and the FAA WAAS system. We conclude Chapter 4 with the benefits of space weather data ingestion.

In Chapter 5 we outline the space weather vulnerabilities and the mitigation schemes that are employed. A major part of the chapter identifies those organizations that provide space weather data and services. These include government sources and private vendors. Modeling and forecasting techniques are identified as appropriate. We conclude Chapter 5 with a discussion of certain operational systems used in the provision of forecasting products.

In Chapter 6 we identify the wide-ranging set of national and international programs dealing with space weather or activities that are congruent with space weather concerns. For many years, there were a number of activities that were actually space weather in nature but not identified as such. In the last decade, the "community" has become more coordinated

under the space weather banner. In rare instances some programs exploit the banner as a matter of expedience, but for the most part, the programmatic association is genuine. The chapter includes a discussion of the *National Space Weather* program, NASA's *Living with a Star* program, as well as related programs. International initiatives are outlined, and we identify scientific and professional organizations, research programs and campaigns, and corporate entities that participate in space weather activities.

Chapter 7, the Epilogue to the book, provides a synopsis of the main points we have attempted to cover plus some final remarks. As should be clear before reading the Epilogue, most forecasting systems that support the disciplines of communication, navigation, and surveillance depend upon fundamental data sets made available through various publicly funded organizations. In the United States, the Space Environment Center of NOAA is one of those organizations. As a special feature, we are happy to include some remarks from Dr. Ernest Hildner, the Director of SEC. Since these remarks are largely prompted by queries from the author, I take full responsibility for any inadequacy in scope or any misinterpretations arising from Ernie's insightful commentary.

A book of this type is not written in a vacuum. Many individuals have directly or indirectly contributed to the material that is presented herein. It would be tedious to provide a complete listing of all contributors, but hopefully my numerous references to key individuals and relevant works will suffice. Even so, I especially appreciate the information on special topics that was graciously provided by Tim Fuller-Rowell and Joe Kunches of NOAA-SEC, John Patterson and Brian Gaffney of ARINC, Anthea Coster of MIT-Haystack, Patricia Doherty of Boston College, Greg Bishop of AFRL, David Boteler of NRCan, and Jim Secan of NWRA. I would also like to acknowledge the numerous organizations, which allowed me to use certain graphics from their web sites.

I would be remiss if I did not mention some recent books that cover various aspects of space weather. The works include: *Space Storms and Space Weather Hazards* [Daglis, 2000]; *Storms in Space* [Freeman, 2001]; *Space Weather* [Song et al., 2001]; *Storms from the Sun* [Carlowicz and Lopez, 2002]; and *The Sun and Space Weather* [Hanslmeier, 2002]. From the vantage point of telecommunications I have borrowed heavily from my earlier book *HF Communications: Science & Technology* [Goodman, 1991], and have also found *Radio Techniques for Probing the Ionosphere* [Hunsucker, 1991] and *Ionospheric Radio* [Davies, 1990] to be valuable resources. Full citations for these works are included in the Bibliography at the end of chapter 1. There are many more books, conference proceedings, reports and papers that I have drawn upon, and hopefully I have referenced all material properly. Like all current authors of non-fiction, I am an enthusiastic user of the Internet, not

only to obtain real-time solar and space weather data, but also to derive fodder for this manuscript. The Internet can be remarkably helpful at times, but the apparent utility can be deceptive if not exploited with care and discretion. Complete citations for published works appear at the end of each chapter.

I want to acknowledge the support of my friend and colleague John W. Ballard, President of Radio Propagation Services, for enduring the many months required to complete this manuscript. I would also like to thank the Springer Science & Business Media, Inc. (previously, Kluwer Academic Publishers) and its editorial staff for having patience with me during all of the delays associated with reformatting and revisions, especially during the latter stages of the project. Ms. Suzanne Guilmineau of NRL was responsible for much of the figure preparation and artwork appearing in this book, and I appreciate her efforts as well.

The most important acknowledgement is reserved for Jane Brooks, my wife for some 45 years. While her field is not physics, she proved to be a good sounding board on matters of clarity and grammar. More importantly, she has been understanding of my mood swings during the course of this project, and she has brightened my days with her continuing support and encouragement without which this book would have been impossible to complete.

Finally, it can be accurately stated that there are always improvements to be made in a book of this type. While doing my final review of the draft manuscript, I noted several areas that would be worthy of expansion, and some other material that could be suppressed or even eliminated. Also, while spell-check software is helpful, there may be some residual errors in author names, especially in the references. I apologize for this. Eventually one runs out of time and energy. Nevertheless, I would certainly appreciate any feedback you may have, and would welcome any suggestions for changes that could be applied in latter editions.

John M. Goodman

Chapter 1
INTRODUCTION

> Space weather, in part, represents those *"conditions on the sun and in the solar wind, magnetosphere, ionosphere, and thermosphere that can influence the performance...of technological systems..."*
> [National Space Weather Program Strategic Plan, 1995]

1. 1 SUMMARY

This chapter provides a general overview of important space weather issues and their relevance to telecommunication systems. It could be regarded as a synopsis since glimpses of topics covered within the book are provided, although in abbreviated form. As a logical point of departure, the definition of space weather is examined in light of the significant usage of the expression in programmatic presentations, published paper titles, and the popular press. Next we provide an historical perspective, with an emphasis on space weather phenomena that are important to telecommunication systems and related technologies.

The advent of space weather programs – domestic and international – has led to a greater awareness and focus on the underlying issues of solar-terrestrial physics (i.e., STP) and its impact on telecommunication systems. It is clear that the term *space weather* connects with a wide audience and offers the technical cache long sought by STP research teams. But the space weather moniker is certainly more than a marketing construction, and there should be no doubt about its fundamental importance in the development of modern technological systems.

In this book we look at two primary categories of radio systems: (i) those that depend on the ionosphere, and (ii) those for which the ionosphere may be regarded as a nuisance. An example of the former category is HF communication, and an example of the latter category is satellite communication. Aside from space weather, there are other influences on telecommunication systems, and these are mentioned in the book. Broadband radio noise originating from weather systems (i.e., lightning strokes) and man-made interference can be major factors in the performance of radio systems.

We address selected aspects of space weather data utilization in Section 1.7. In the conclusion to this chapter, we offer some thoughts about upstream and downstream data sets, and preferred methods for forecasting and prediction.

1.2 DEFINITION OF SPACE WEATHER

What is space weather? The US Department of Defense, in its implementation plan [OSD, 2000], indicates, "space weather refers to adverse conditions on the sun, the solar wind, and in the earth's magnetosphere, the ionosphere, and the thermosphere." Indeed this definition portrays those aspects of space weather that are generally of most concern, namely the more pathological elements. But space weather, and ionospheric weather, in particular, can be turbulent or benign. All aspects of space weather should be included in the definition. Indeed, from a telecommunications perspective, it can be safely stated that quiet conditions are not always good and disturbed conditions are not always bad. From the NRL Plasma Physics Division web site comes a rather crisp definition: "space weather refers to the state of the magnetosphere and ionosphere which is determined by the solar wind." The National Space Weather Program [NSWP, 1995] has defined space weather as representing "conditions on the sun and in the solar wind, magnetosphere, ionosphere, and thermosphere that can influence the performance and reliability of space-borne and ground-based technological systems." This definition is more appropriate for our purposes in this book. On the NOAA/SEC web site, it is indicated "space weather describes the conditions in space that effect Earth and its technological systems." It goes on to say, "space weather is a consequence of the behavior of the sun, the nature of Earth's magnetic field and atmosphere, and our location in the solar system". This is also a useful definition.

In this monograph, the vantage point of the telecommunications specialist drives our view of space weather. Specifically we treat ionospheric and plasmaspheric weather as the most important from a nowcasting perspective. On the other hand, we treat the space weather generated within the magnetosphere and the extra-magnetosphere as primary in the context of forecasting and prediction services. I want to emphasize this point, not only because the effects on various communication systems derive from near-space regions just above the troposphere, but because it identifies the hierarchy of very important terrestrial sensors that have played (and continue to play) a significant role in our knowledge of the ionosphere. These sensors are a major part of the space weather remote sensing "network" and are basically ionospheric diagnostic instruments.

Space weather phenomena have been affecting legacy communication systems involving longwave and shortwave signaling since the dawn of the radio communication era. The impact of the ionosphere on radio transmission is well known through the consideration of the Appleton-Hartree expressions that detail the relationship between plasma and signals that propagate within

that medium. Over the 20th Century, a wide range of telecommunication systems have been developed, and many have been fielded for operational use. While many of the systems received their impetus through military necessity, the utility of telecommunications is evident in virtually all aspects of human activity. Space weather, a relatively new terminology, loosely defines the hierarchy of all phenomena within the earth-sun environment that may impact biology and systems that reside within that environment.

Earthbound telecommunication practitioners would be tempted to use a more restrictive term such as the geoplasma environment, to include the magnetosphere and ionosphere, as an appropriate definition of the primary region of interest since that is the focus of effects that can be observed or calculated. Indeed, only the closest geoplasma region, the ionosphere, is the primary focus for nowcasting and assessment of effects on many telecommunication systems. We will focus principally upon the ionosphere and its interactions with communication systems, especially in Chapters 3-5. However it is obvious that space weather is the real driver of pertinent properties of the ionosphere. Hence a treatment of the hierarchy of effects on telecommunication systems is really a more general space weather problem.

1.3 AN HISTORICAL PERSPECTIVE

The author is not an historian, but he recognizes the benefit of retrospective examination of the great scientists, their achievements, and the role they play in the advance of space weather and communication technologies. A good deal of the information in this historical perspective is derived from the author's earlier book on *HF Communication: Science & Technology* (i.e., Goodman [1991]). Another excellent source is a series of articles in *EOS* by E.W. Cliver [1994a, 1994b, 1995] dealing with solar activity. A bibliography of additional reading is provided at the end of Chapter 1.

As we go through this brief history of the space weather discipline, it will become apparent that adaptive communication system developments and observations of space weather phenomena and the ionosphere are closely related. (See Figure 1-1.) This was especially true in the early years. Our knowledge of the ionosphere and the development of radio communications both derive from 20th Century science and technology. However some vestiges of space weather have been known for many centuries. In fact, auroras, long known for their visual beauty and complexity, have been chronicled since the dawn of recorded history. In the modern history context, auroras are also related to a variety of communication disturbances at high latitudes.

One of the most significant solar-terrestrial observables is the sunspot, a phenomenon related to solar activity. (See Chapter 2 for details.) Sunspots have been associated with certain terrestrial phenomena, including aurora, for more than a century, and the sunspot number has also been a convenient index for many 20th century climatological models of the ionosphere. The number of sunspots has exhibited an eleven-year periodicity for the last 250 years, as shown in Figure 1-2. The first telescopic observations of sunspots were made in 1611 by a number of observers, the most famous being Galileo. Sunspots have been monitored continuously since that time, although a pronounced minimum occurred between 1645 and 1715 (the Maunder minimum), during which time hardly any auroras were observed.

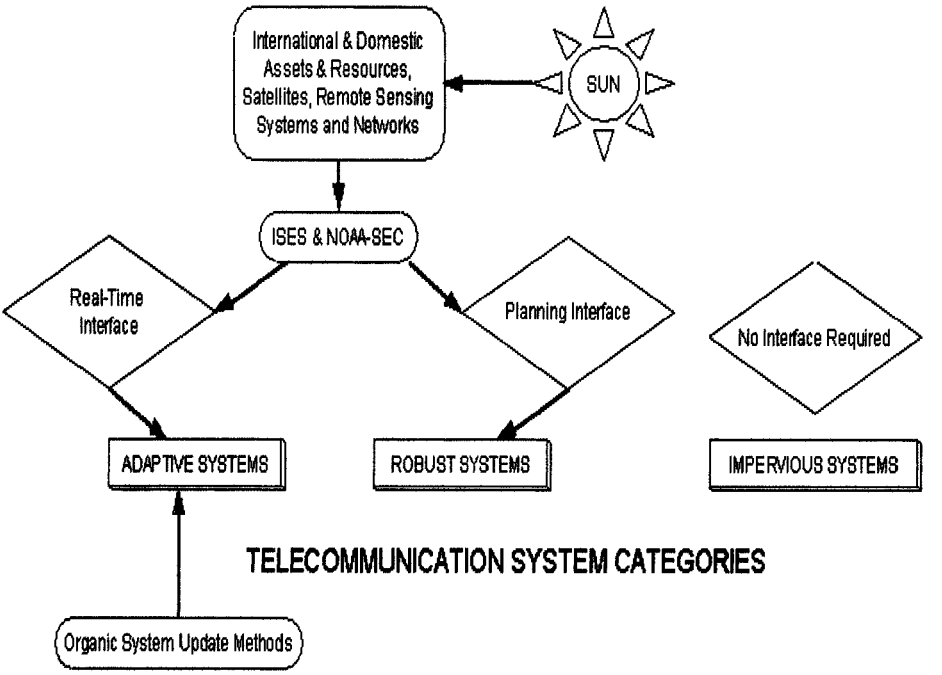


Figure 1-1: Relationship between space weather, the ionosphere, and communications system development. Adaptive telecommunication systems require either (i) organic methods for updating system parameters (viz., the frequency family to be exploited, or power-aperture product to be used) or (ii) non-organic methods from real-time interfaces. These real-time interfaces may involve access to data from NOAA-SEC or the ISES group of Warning Centers. It might also involve data procured from 3rd party vendors.

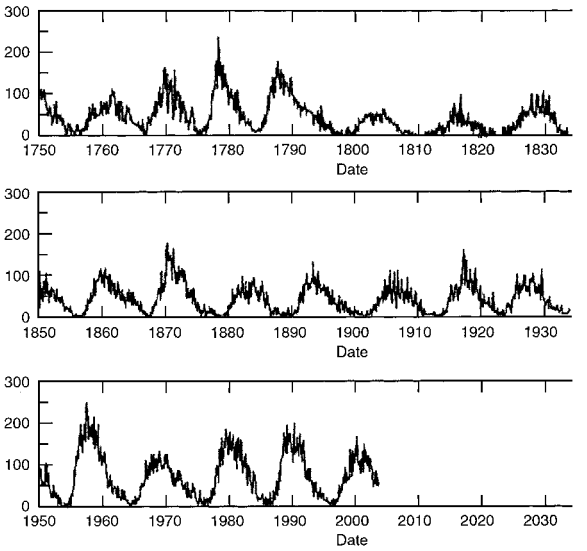


Fig. 1-2: Depiction of the sunspot number for the last 250 years.

While sunspots are indicative of many space weather phenomena, the role of geomagnetism in understanding the nature of the ionospheric personality is important, if not central, in many radio propagation applications. This is especially true of terrestrial systems that exploit the skywave mode of propagation at high latitudes (viz., MF/HF systems). The impact of the geomagnetic field on earth-space systems can also be significant, since geoplasma distributions are controlled by the magnetic field, and geophysical phenomena such as scintillation and Faraday fading are also influenced by it.

According to Sidney Chapman [1968], in his book *Solar Plasma, Geomagnetism, and the Aurora*, the first picture of the so-called auroral oval centered about the geomagnetic pole was drawn by Elias Loomis of Yale University in 1860. In 1878 Balfour Stewart suggested that ionization in the upper atmosphere would account for some of the magnetic field fluctuations that had been observed. By 1892 Stewart had identified the existence of an electrified layer in the upper atmosphere. Subsequently Arthur Schuster recognized this layer to be the origin of electric currents responsible for compass variations. Schuster, who coined the term "ring current", also developed a dynamo theory to explain the diurnal component of ionospheric currents, and he associated the currents with tidal motions of the neutral atmosphere. An aurora, as observed from a fixed terrestrial site, is displayed in Figure 1-3; and a depiction of the instantaneous auroral oval, as observed

from space, is provided in Figure 1-4. Chapter 2 will provide more details about auroras and their consequences.



Fig. 1-3: Depiction of the aurora from Alaska. Adapted from image on website of the Alaska Vacation Store in Anchorage, Alaska. Courtesy of Alaska Department of Community and Economic Development

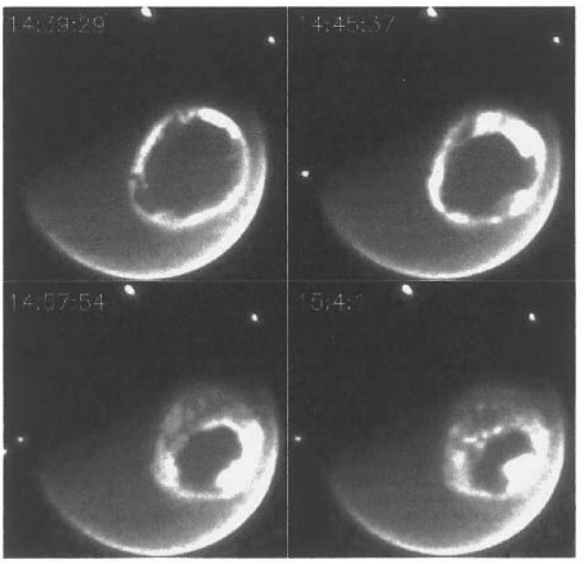


Fig. 1-4: Auroral Oval. IMAGE satellite images of the auroral oval during the Bastille Day storm of 15 July 2000. Note the dynamic behaviors, as each image is only minutes apart. From Lu et al. [2001], by permission.

The geomagnetic field, as represented by the position of a compass needle, was observed to undergo transient fluctuations as early as the 1700s. Swedish scientist Anders Celsius discovered that magnetic storms exhibited a global characteristic and were not isolated events like tropospheric weather cells. He also discovered the correlation of optical auroras with magnetic activity, and in 1741 he determined that auroral forms were aligned with the geomagnetic field vector. These observations predated the first theory of magnetism developed by Simeon-Denis Poisson in 1824, and Johann Carl Friedrich Gauss made the first systematic measurements of the earth's magnetic field. In 1839 Gauss postulated the existence of ionized regions in the upper atmosphere in his work *General Theory of Terrestrial Magnetism.* Who actually should get credit for the first suggestion of ionospheric existence is rather controversial. This is because there are some reports that Michael Faraday (in 1832) and Lord William Thomson Kelvin (in 1860) made similar suggestions. Despite these early suggestions, Balfour Stewart generally gets the credit on the basis of his theory on diurnal variations of the geomagnetic field, which was published in 1878.

The most remarkable feature of the upper atmosphere is the visible aurora, a luminous display that appears in the nocturnal sky in high latitudes. Its generic designation is *Aurora Polaris*, but is termed *Aurora Borealis* in the Northern Hemisphere and *Aurora Australis* in the Southern Hemisphere. The *Aurora Borealis* is sometimes called the *Northern Lights*. It is now known that auroras occur at any time of day, but cannot be observed in the presence of competing sunlight. Carl Stormer developed one of the earliest explanations of auroral formations by 1911, and one of his most significant contributions was the theory of charged particle motion in the geomagnetic field.

In the years following the work of Stewart and Schuster, work on convenient indices of magnetic activity indices was undertaken. Although magnetic indices were being published by 1885, the first real step toward defining a geomagnetic index at an international level was not achieved until the early 1900s [Mayaud 1980]. J. Bartels used magnetic activity indices in 1932 in connection with his discovery that the mysterious M-regions on the sun were associated with 27-day recurrence cycles of magnetic activity. These 27-day cycles were also shown to be related to the mean period of solar rotation. Many years later, magnetic indices have been used to explain the terrestrial effects caused by high-speed solar wind streams associated with the appearance of geoeffective coronal holes and coronal mass ejections (i.e., CMEs).

Let us now depart from classical space weather development and examine some important telecommunication milestones that are relevant to the issues of telecommunications and ionospheric effects. Half a century before Stewart made his suggestion about the existence of the ionosphere

(although that specific term was not used at the time), the English physicist Michael Faraday developed a theory of the electromagnetic field; and 17 years before Stewart's announcement, Maxwell had predicted the existence electromagnetic waves. Maxwell's work specifically dealt with the speed at which magnetic disturbances travel, but his equations are now the cornerstone of electromagnetic theory. Unfortunately his predictions about radiowaves could not be verified at that time, and experimental confirmation of the theory was left to the German physicist Heinrich Hertz. In 1887, Hertz developed the first radio transmitter and loop receiver. With this simple equipment he was able to determine the basic transmission properties of radiowaves.

In 1901 Italian inventor Guglielmo Marconi, transmitted the first long distance (trans-Atlantic) signals from a site at Poldu, England to Newfoundland. It is thought that he used a radio frequency of 313 kHz (in the MF band), a frequency appropriate for ionospheric bounce, and a phenomenon that was unknown at the time. Because of the startling nature of Marconi's result additional theoretical work in EM wave propagation was triggered. The trans-Atlantic experiment by Marconi created a puzzle since the earlier work of Hertz had conclusively demonstrated that radiowaves travel in straight lines unless some object deflects them. This brings us back to the 19th century suggestion by Stewart of a conducting stratum in the upper atmosphere, based upon magnetic disturbances. Perhaps this conducting medium could serve as such an obstacle for electromagnetic waves as well, a suggestion made independently by Arthur Kennelly and Oliver Heaviside in 1902. For many years, that which we now call the E region of the ionosphere was termed the Kennelly-Heaviside layer. It should be noted that the "reflection" mechanism for signal propagation for such long distances, and espoused by Kennelly and Heaviside was itself controversial. Noted physicists including Lord Rayleigh, Henri Poincaré and Arthur Sommerfeld had concluded that diffraction around the surface of the earth was the mechanism, a theory that was ultimately disproved by precise field strength experiments. Marconi shared the Nobel Prize in physics with Karl Ferdinand Braun in 1909 in recognition of their contributions to the development of wireless telegraphy.

Following World War I more improvements were made in radio apparatus, and both theoretical and experimental studies continued. In the United Kingdom, Edward Appleton, who is currently associated with the equatorial fountain effect (i.e., Appleton Anomaly), made substantial contributions to magneto-ionic theory. In the United States, Gregory Breit and Merle Antony Tuve, of the Carnegie Institute in Washington DC, conducted landmark radio pulse experiments and later developed the well-known theorem that bears their names. The Breit and Tuve collaboration was the first known experimental verification of the ionosphere using the radio pulse method, and they discovered ionospheric layer height changes from day to

night. In 1924, Appleton and Barnett unequivocally proved the existence of the ionosphere using a wave interference method, and this led to the development of new techniques for probing the region. Workers at the newly established Naval Research Laboratory (NRL) in the USA also contributed, using the HF pulse technique in 1925 that provided unique proof of multiple layers in the ionosphere. This technique was later applied by NRL in the development of radar. In the period between 1925-28 NRL investigators conducted additional experiments proving the existence of multiple hops and "skip zones" for oblique propagation of radio waves. Figure 1-5 is an example of "round-the-world" radio propagation, as well as the novel concept of "splashback" or signal backscatter. The backscatter phenomenon later led to the development of Over-the-Horizon-Radar (OTH-R). It should be noted that most of the experiments conducted during the 1920s were motivated by the need to communicate via the new wireless medium. But there was a growing synergy between emergent ionospheric scientists and radio communication engineers.

One of the more prominent scientists involved in early investigations of the ionosphere was Sidney Chapman, who in 1931 published a paper dealing with the Kennelly-Heaviside layer, and who, like E.O. Hulburt before him, provided a foundation for our current understanding of the ionosphere. To this day the Chapman hypothesis for ionized layer formation, while relatively simplistic, is a useful model, especially for the lower layers of the ionosphere.

The theory of radio wave propagation in ionized media has been fascinating from the beginning. In 1912, W.H. Eccles discovered that the refractive index of ionized gas was less than unity, leading to the interesting fact that radiowaves are bent away from the medium normal in a plasma environment and thus toward the horizontal. Joseph Larmor, in 1924, concluded that obliquely launched radiowaves at a specified frequency would be refracted downward, but could escape from the earth if the waves are launched above a certain critical angle. This leads to the notion of an ionospheric iris above a given transmitter through which waves may penetrate, and the existence of skip distances. From the theoretical vantage point, Joseph Larmor, Hendrik Lorentz, E.V. Appleton, and D.R. Hartree provided a clear understanding of radiowave propagation in magneto-ionic media, and the Appleton-Hartree formula for the radio refractive index is of fundamental importance in the analysis and prediction of media effects. In 1932, Appleton published a complete theory of radio propagation in magnetoionic media, such as the Kennelly-Heaviside layer, and he coined the term ionosphere to describe the ionized strata upon which MF and HF skywave propagation depend. Appleton also proposed the nomenclature we now employ for the multiplicity of ionospheric layers (i.e., D, E, F). Now, of course, we recognize the importance of the work of Appleton in a number of

areas other than skywave propagation (e.g.; earth-space propagation). Sir Edward Victor Appleton was awarded the Nobel Prize in Physics in 1947 for "his investigations of the physics of the upper atmosphere especially for the discovery of the so-called Appleton Layer". The Appleton layer is now called the F layer, or more properly the F region.

A period of considerable activity in the realms of ionospheric physics and radio engineering characterized the years leading up to World War II and afterward. There were some extraordinary international campaigns that have provided vital information about the ionosphere and associated regions. For background purposes, it is noted that the 1st International Polar Year (IPY-1) was held in 1882-1883. Only a handful of countries were involved and the relevant topics included: solar radiation, the aurora, and geomagnetism. It was the first truly international collaborative scientific activity.

The 2nd International Polar Year (IPY-2) was held in 1932-1933 and was an activity of great significance. It was a multidisciplinary effort, but the science categories of main interest to us within the space weather constituency included: geomagnetism, auroral physics, aeronomy, and ionospheric physics. Appleton chaired the ionospheric science component and the sub-topics were comprised of (i) regular ionosonde measurements of electron density and layer heights, (ii) characteristics of radio propagation, and (iii) the effects of magnetic storms. The data sets obtained were not fully analyzed and some of the data were lost as the result of the ravages of World War II. It is understood that the final publication of the results came as late as 1950. While the negative impact on IPY-2 was significant, the experience gained and discipline associated with international cooperation on a large scale was not lost on the world scientific establishment. More campaigns would follow.

The 2nd World War, because of the importance of radio communication, target tracking and surveillance to the warring parties, invigorated the development of a number of new technologies. We previously alluded to radar, simultaneously invented in the UK and the USA. Communication systems and radio navigation aids were also developed, as well as rudimentary countermeasures. It was not long before OTH radar, based upon ionospheric bounce, was developed for long distance surveillance and targeting. Radio electronics blossomed following WWII and during the Cold War that followed. The field of radio astronomy, while directed at the cosmos, provided some interesting glimpses of refractive turbulence in the ionosphere (i.e., scintillation).

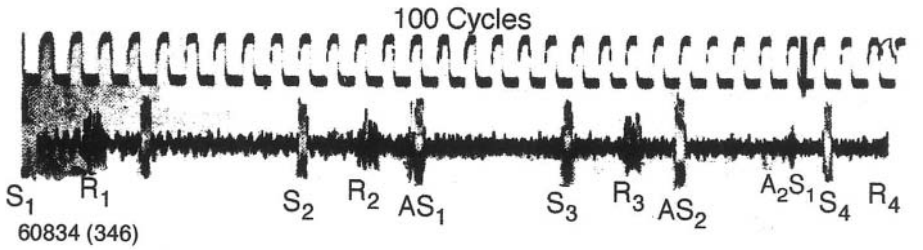


Figure 1-5: A typical chart display of various propagation phenomena in 1928. S_1, S_2, and S_3 are pulses initiated by NRL's transmitter. R_1, R_2, and R_3 are "splashback" echoes from the first reflection zone via the ionosphere. AS_1 and AS_2 are received pulses that have traveled around the world. A_2S_1 is the received pulse that has circled the earth twice. Figure adapted from Gebhard [1979].

While rockets, developed by the Germans, were designed to have weaponized payloads, the technology of rocket science also found a use in ionospheric and space research following the war. NRL scientists used captured V2 rockets to probe the ionosphere and to explore solar emissions from the vantage point of the tenuous upper atmosphere. Early workers at NRL led by Herbert Friedman, made significant contributions in solar physics, aeronomy and ionospheric physics.

It is only logical that the value of space would be recognized in the Defense Department. By the early 1950's it was clear that artificial satellite systems were going to be developed, and these might be quite useful for surveillance purposes. Two specific activities were initiated during the Eisenhower administration (i.e., moon-bounce radar and earth satellites). Both the US Navy and the US Air Force were involved in lunar studies, with NRL leading the charge in the evaluation of passive reception of communication signals of potential adversaries. A large 600-foot dish antenna was partially constructed at Sugar Grove, West Virginia, an extremely quiet site, but the enormous project was abandoned, when it was determined that satellite techniques would be superior and less expensive. However, there was still a problem with artificial earth satellites as surveillance-gathering tools. The passage of a satellite over another country could be deemed to be violation of its airspace. Fortunately, President Eisenhower had his problem solved by the propositions of the International Geophysical year (IGY), including the stipulation that artificial earth satellites be launched for studies of the earth's surface.

The IGY was held in 1957-58, a period of maximum solar activity. The goals of the IGY were patterned from the IPY campaigns, but IGY emphasized worldwide studies. Additionally, rocket probe availability made it possible to conduct *in situ* measurements as well as vertical sounding measurements. As mentioned above, the IGY called for the launching of artificial earth satellites to be used as a tool for mapping the earth's surface. As an ingredient of the US component of the IGY scientific program, NRL was designated to place an artificial satellite in orbit, and the project was called Vanguard. As part of this project the first global network for satellite tracking was established.

As is well known, the satellite age began in the late 1950s with launch of the Russian Sputnik satellites, followed by the American Vanguard satellite, a matter we shall revisit below. Maximum solar activity having been investigated during the IGY, the international scientific community embarked upon another coordinated campaign during 1964-65, a period of minimum solar activity. Satellites were available during this period, and the campaign was dubbed *The International Years of the Quiet Sun,* (IQSY).

During the IGY (solar max: 1957-58) and the IQSY (solar min: 1964-65) a considerable amount of ionospheric sounding was accomplished at an increasing number of stations worldwide. There was also some solar minimum data obtained prior to the IGY, and the period 1954-1958 exhibited a strong rise from solar minimum activity to the largest epoch of sunspot activity in recorded history. During this 5-year period, a data archive of ionospheric sounding records was obtained from roughly 150 stations around the world. Because of a paucity of soundings from the Southern Hemisphere during the 1954 period of minimum activity, the data set was augmented by soundings obtained during the IQSY. From this augmented data sample it was possible to characterize the basic ionospheric parameters, including the layer maximum densities and heights. This led to the so-called *CCIR Model of Ionospheric Characteristics*, and the mapping methods employed were based upon the work of Jones and Gallet [1962, 1965]. We shall mention the CCIR (now ITU-R) modeling methods in later chapters. It is noted that mapping issues arise from the use of a sparse network of sounding stations, especially if they are irregularly spaced. Topside sounding data can assist in the resolution of these difficulties.

In October of 1957, the Soviet Union was the first to successfully place a satellite in orbit. In fact, the USSR had two successful launches before the United States finally succeeded with Vanguard-I, which was placed into orbit on 17 March of 1958. One of the scientific achievements of the Vanguard program was the discovery that the earth is pear-shaped. The success of Sputnik, as an engineering feat, was a seminal event in space research history and had significant geopolitical implications as well. It created alarm in the United States, and the DoD responded by charging the

Redstone Arsenal team led by Werner von Braun to begin work on the Explorer Project, in parallel with the Vanguard program. Explorer-I, successfully launched in January of 1958, carried a scientific payload developed by James Van Allen, which led to the discovery of the earth's radiation belts (i.e., the Van Allen belts). The Explorer program was associated with a succession of small scientific satellites. The American response to the Sputnik launch was the creation of a civilian space agency in the United States, the National Aeronautics and Space Administration (NASA).

The United States and the Soviet Union engaged in vigorous space programs since the Sputnik-Vanguard days, driven by national pride and strategic concerns. Both countries have managed successful astronaut and cosmonaut programs, although each has experienced major human disasters along the way. There have also been striking successes of the manned and unmanned programs. It is beyond the scope of this short historical survey to itemize all the various space launches and scientific advances tied to them. It is worth mentioning a few key activities of special relevance to space weather and its impact on telecommunication systems.

The race to the moon was an exciting event during the 1960's. While the endeavor was largely driven by geopolitics, there was already keen interest in our nearest celestial neighbor, the moon. Before the age of satellites, the field of radar astronomy was emerging (see excellent book by Evans and Hagfors, [1968]). In the late 1940s, both the US Army (i.e. Project Diana) and NRL scientists succeeded in reflecting signals off the moon, but little information was ever published because of security concerns. In the late 1950s, John V. Evans, using the Jodrell Bank Radar Observatory in the UK, studied radar signals reflected from the moon and concluded that slow regular fading of the echoes was caused by the Faraday effect, probably the first observation of the phenomenon outside the field of magneto-optics. This enabled Evans and his team to derive the line integral of the electron population between the earth and the moon, the so-called cislunar electron content. Other attempts at measurement of the electron content using the moon bounce method followed, but the most important measurements of the ionospheric electron content were made using artificial earth satellites rather than lunar echoes.

In 1960, NASA launched Echo 1, a large metalized balloon that was designed to perform as a passive reflector of radiowave signals. It was used as a reflector of radio, television, and telephone signals, enabling intercontinental communication. Radar echoes from the large Echo 1 and 2 were also employed for calibration of earth-space and search radars and some rudimentary ionospheric studies. While the Echo program was significant in the development of various ground station and space tracking techniques, it

was abandoned in favor of active satellites from a communications perspective.

A large number of low earth orbiting satellites (i.e., LEOs) were launched in the 1960s and beyond, and they were equipped with telemetry beacons, typically at VHF (i.e., 136 MHz). These beacons were used for propagation studies although that was not their original intent. Faraday rotation, dispersive Doppler, and hybrid methods were used to obtain information about horizontal structure of the ionosphere. Much was learned by these methods, but the most significant advance in ionospheric measurement by the middle 1960s was the so-called topside sounder.

The Alouette satellite was launched into a 1000 km circular orbit in September 1962. It was a polar orbiting satellite with an inclination of 80 degrees. The instrumentation consisted of a swept-frequency sounder from 0.5 to 11.5 MHz, as well as some auxiliary instruments. With Alouette data, the variation of the $N(h)$ as a function of latitude can be determined. Figure 1-6 depicts the topside electron density distribution between 64°N and 45°S along the 75°W meridian. As suggested earlier, there were some horizontal inconsistencies in the global maps derived from ground-based ionosonde. Topside sounder data assists in the resolution of these problems, especially in regions such as the high latitude trough and the equatorial anomaly.

Geosynchronous satellites were an important advance in the art of ionospheric study. Since the satellites were positioned in the equatorial plane with a rotational period of 24 hours, they were almost geostationary. While LEOs that moved rapidly over a given field of view represented a "frozen" picture or virtual snapshot of the ionosphere, the so-called GEOs enabled ionospheric investigators to examine the time variation of the ionosphere.

The Mercury and Gemini programs preceded the Apollo program, which was associated with successful lunar landings in the late 1960s and early 1970s. The Gemini series of satellites provided several opportunities for propagation experiments to be conducted, including measurements of the subsatellite electron content using Faraday rotation [Goodman, 1967].

The first successful monitoring of solar x-ray and Lyman-alpha radiation by a satellite was performed using SOLRAD-1 in 1960. The Naval Research Laboratory launched a series of solar radiation satellites, culminating in SOLRAD 11A and 11B (i.e., a pair of satellites dubbed SOLRAD HI, at an altitude of 65,000 nautical miles) in the late 1970s. The only mission of the SOLRAD satellites was to monitor all aspects of the solar activity. The telemetry data from the satellite was received at the Blossum Point, Maryland and then conveyed to the NRL campus (Washington, D.C.) for processing and dissemination to users such as NOAA Space Environment Services Center (SESC; and currently NOAA-SEC) and the US Air Force Global Weather Central (or its equivalent). SOLRAD HI data was utilized in various near-real time prediction systems such as PROPHET (see below).

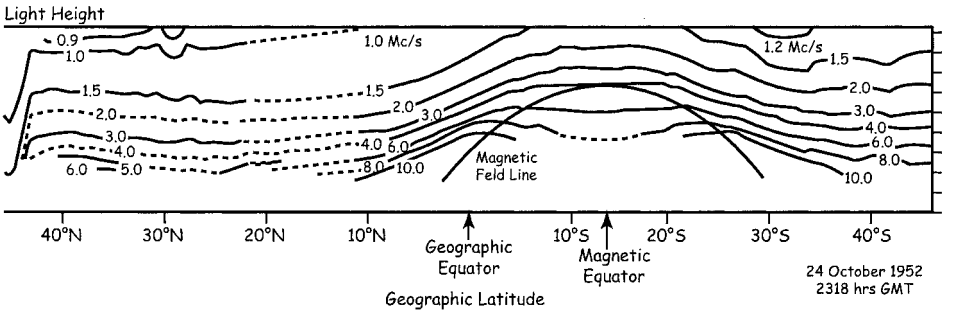


Figure 1-6: Alouette ionograms were analyzed along a pass along the 75°W meridian on 24 October 1962. The equatorial anomaly is evident in this early record. From Brown [1965], after Lockwood and Nelms [1964].

Probably the first use of space weather data to identify and solve real-time communications problems was carried out by U.S. Navy investigators [Argo and Rothmuller, 1979; Richter et al, 1976]. The U.S. Navy was vitally interested in the performance of communication and navigation systems, and in the late 1970s, these systems included: the emergent Global Positioning Satellite System operating at SHF, the Fleet Satellite Communications System, HF and VLF Fleet Broadcast, and VLF and ELF strategic communications. These systems still exist is various forms. Engineers at Naval Ocean Systems Center (NOSC) in San Diego, CA developed a minicomputer platform, called PROPHET, which was used to develop real-time estimates of system effects derived from ionospheric and solar data sets. PROPHET used phenomenological, statistical, and semi-empirical models of the various phenomena; and these models and their outputs supported the OMEGA navigation system, satellite communication systems, and a number of HF communication and surveillance systems. Table 1-1 is a description of the forecasting models employed by PROPHET. The imbedded models were not all developed in-house, and a noteworthy example of this was a simplified scintillation model derived from the work of Fremouw and Rino [1973], Pope [1974] and LaBahn [1974].

Table 1-1: PROPHET was the first system to use Space Weather data to derive near-real-time performance predictions and operational guidance. Adapted from Argo and Rothmuller, [1976].

MODEL (SOURCE)	FUNCTION	CAUSATIVE SOURCE	SECTION	ACTION
Flare detection	Disturbance warning	1 to 8Å x-rays	All HF VLF navigation	Warning
Flare detection estimate (NOSC)	Disturbance warning	1 to 8Å x-rays	All HF VLF navigation	Warning
SID GRID (NOSC)	Disturbance warning-SWF	1 to 8Å x-rays	All HF	HF comm — Freq Shift — Reroute traffic HFDF — Net impact assessment
PCA/VLF (NOSC)	Disturbance warning-PCA	10 MeV Particles	VLF navigation (Omega)	Correction factor for transpolar circuits
SPA/VLF (NOSC)	Disturbance warning-SPA	1 to 8Å x-rays	VLF navigation (Omega)	Correction factor for sunlit circuits
LOF Split (NOSC)	Tactical (reduced intercept vulnerability)	Solar diurnal transition 1 to 8Å x-rays	Covert HF systems	Optimum frequency selection against known receivers
Scintillation grid (SRI)	Disturbance warning/tactical	Unknown (Statistical model)	VHF/UHF satellite communications	Advisory -dB fade probability based on location
PCA/HF (NOSC)	Disturbance warning-PCA	10 MeV Particles	All HF	Advisory -dB — Freq Shift — Reroute traffic HFDF — Net impact assessment
Quiet MUF (ITS/GMC)	MUF during normal times		All HF	HF comm normal operations
QLUF	LUF during normal times		All HF	HF comm normal operations
Raytrace	Receiver accessibility		All HF	HF comm normal operations

The PROPHET environmental prediction terminal is depicted in Figure 1-7. Data from a number of satellites such as SOLRAD-11 (e.g., SOLRAD HI), and from service centers such as the NOAA Space Environment Services Center (SESC) and the Air Force Global Weather Central (AFGWC), was conveyed to the NOSC data fusion center in San Diego for data sorting and quality control, and then disseminated to the individual (deployed) minicomputer platforms that hosted the PROPHET software. Engineers at NOSC also conducted field tests of the various products using selected communication stations (e.g., Stockton Naval Communication Station). The operating personnel found the system to be very useful and concluded that communication outages for the HF circuits were reduced by 15-20% using the near-real-time system.

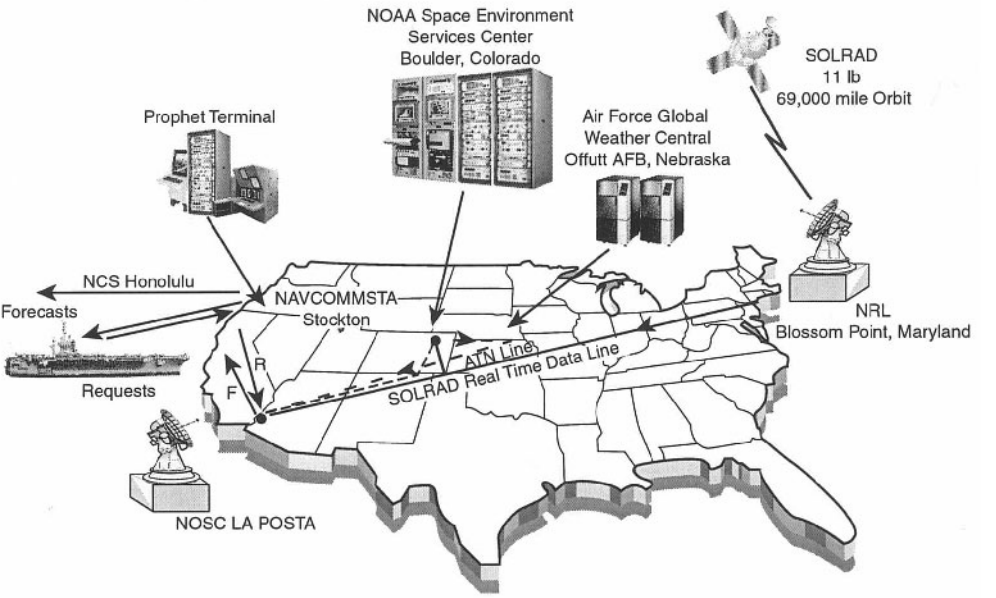


Figure 1-7: The PROPHET concept developed by US Navy Engineers at NOSC was the first attempt to use real-time space weather data operationally with success. The information flow for the system is shown. Adapted from Argo and Rothmuller [1976].

One of the monumental achievements of the 20th Century was the development of satellite navigation, culminating in the operational Global Positioning System (GPS). The Naval Center for Space technology at NRL developed the concept of passive ranging from space in 1964 and successfiully demonstrated the feasibility of satellite navigation systems in

1967-68 with the launch of the Timation-1 and Timation-2. In 1973, management of the Timation program was assumed by the US Air Force to form the NAVSTAR/GPS program. The first NAVSTAR/GPS satellite was launched in 1978. The GPS space segment currently consists of a constellation of 24 operational satellites, with 4 satellites in each of 6 orbital planes, at an altitude of 11,000 nautical miles, and having an orbital period of 12 hours. Users can "see" between five and eight satellites from anywhere on the earth. The GPS system has been designed to eliminate the excess ionospheric group path delay since two frequencies are employed for compensation. Still there are ionospheric and space weather effects to be concerned with. Strong radiowave scintillation can cause GPS receivers to malfunction, and single-frequency users can suffer large errors during magnetic storms.

There are now two other systems in use or under development: GLONASS (Russia) and Galileo (European Space Agency). There are numerous military and civilian uses for satellite navigation systems, and we shall investigate the various applications in more detail in later chapters.

It should be noted that the GPS system is being exploited for ionospheric studies. Jules Aarons, currently with Boston University, has stimulated interest in global scintillation studies using GPS. Scintillation is discussed in the paragraph below. It should also come as no surprise that the GPS is also being used to investigate the Total Electron Content (TEC) on a global basis. The various mapping schemes using various GPS receiver networks will be covered in a later chapter. The GPS system is constantly finding additional uses, and upgrades are being developed for specific purposes such as precise landing. The U.S. FAA WAAS system is but one example.

It is well known that stars twinkle because of atmospheric turbulence resulting in refractive index fluctuations in the optical portion of the electromagnetic spectrum. Stars that emit radio waves are called radio stars, and have been used to examine the twinkling of radio signals. Such twinkling of signals received from radio stars is generally referred to as scintillation, and it was deduced that radio star scintillation was largely due to temporal and spatial variations in ionospheric refractivity. A number of investigators used radio star scintillation measurements to investigate ionospheric inhomogeneous structures such as spread-F in the equatorial region. J.P. Wild [1956] used signals from a source in the constellation Cygnus to derive dynamic spectra, and apparently observed focusing irregularities. Other early investigators included B.H. Briggs [1958] and M. Dagg [1957]. One of the major disadvantages associated with the use of radio stars in propagation studies is the paucity of discrete sources. There are only two sources that have proven to be very useful, and they are both located in the northern sky: Cygnus A and Cassiopeia A.

Radio and radar astronomy preceded satellite studies for ionospheric investigation. Jules Aarons [1963] provides a good summary of competing methodologies, circa 1962, in an Introduction to the volume *Radio Astronomical and Satellite Studies of the Atmosphere.* While analysis of radio stars and analysis of lunar reflections provided some interesting information about the intervening ionosphere, it is clear that satellite studies have provided more detailed and synoptic information. However, we should not lose sight of the contributions made by rocket probes, especially in the early days. Other techniques have also been brought to bear, including: incoherent backscatter radar (i.e., Thomson scatter), and terrestrial radars used for ionospheric monitoring. Robert Hunsucker, in his book *Radio Techniques for Probing the Terrestrial Ionosphere*, has discussed various experimental methods.

It wasn't long before investigators began to exploit satellite transmissions as a replacement for radio stars. Workers at the Air Force Cambridge Research Laboratory (AFCRL), now called the Air Force Geophysics Laboratory (AFGL), and led by Jules Aarons, have made significant contributions to this field, and much of our understanding of the climatology of ionospheric scintillation derives from investigations conducted by U.S. Air Force scientists and affiliated organizations. It should be noted that Jules Aarons was a pioneer in beacon satellite studies of the ionosphere, and is credited for promoting an international investigation of scintillation morphology on a global scale.

NASA obtained a considerable amount of telemetry data over the years using the Minitrack system, and the VHF signals exhibited disruptions due to scintillation, especially at certain equatorial and high latitude stations. Tom Golden, a NASA communication network engineer, recognized that a model of the worldwide scintillation activity would have operational merit. Other agencies subsequently developed an interest. A significant amount of satellite data, including data from a multi-beacon satellite DNA-002 (i.e., Wideband), was used to develop a semi-empirical model (Fremouw and Rino [1973]; Pope, [1974]). The firm Northwest Research Associates (NWRA) maintains the current operational model, WBMOD, for the U.S. Air Force with certain improvements in the equatorial and high latitude regions (Secan [1995, 1997]). This climatological model provides a baseline estimate of ionospheric scintillation in the absence of real-time methods.

An anecdote is in order. TACSAT-1 was the largest communications satellite ever put in orbit at the time of launch in 1969, and it served the mobile user needs of the US military. UHF was a critical band for tactical communications, especially during the Viet Nam War period. It should be noted that a period of maximum solar activity occurred in the period 1968-1972, leading to enhanced scintillation probability, especially over the equatorial regions (i.e., $\pm$ 20° from the magnetic equator). Conventional wisdom at the time suggested that the roll-off of scintillation with increasing

frequency above VHF was relatively steep, being based upon an incomplete theory and limited data sets. But, alas, this was not the case. Significant outages were observed, and this led to increased emphasis on the development of scintillation countermeasures (i.e., diversity schemes) at UHF and the consideration of even higher frequencies. The significant level of scintillation activity at UHF also led to further investigations of the underlying theory of scintillation. These issues are covered more fully in Chapter 4.

It is clear that the various DoD mission areas are the primary drivers for many of the space weather applications relating to telecommunications (i.e., communications, navigation, and surveillance). While scientists at NRL can be credited with many firsts in the area of ionospheric phenomenology, it can be safely said that the geophysicists and engineers at the AFCRL/AFGL have contributed significant amounts of operationally useful information in the context of telecommunications and space weather. This is not to say that there have not been significant civilian and university contributions as well.

Since the 1980s, there are three things that have provided the greatest boost in our capabilities for assessment and prediction of space weather parameters, especially those of importance in real-time support of telecommunication systems. There are: (i) faster and more capable computers, (ii) the Internet and improved data accessibility, and (iii) more observational capability. There have been significant developments in data-driven modeling and data assimilation approaches, similar to those methods used in the tropospheric weather prediction business. Mapping technologies have been improved and novel methods for prediction have been advanced.

1.4 THE ADVENT OF SPACE WEATHER PROGRAMS

Space weather observation and prediction began in earnest in the middle of the 20th century in order to support radar and communication systems that were found to be vulnerable to solar disturbances, various ionospheric phenomena and magnetic storms. Vigorous forecasting services were developed in a number of countries, including the USA, and these became internationalized over time. Much of this data sharing was fostered by the realization that the solar-terrestrial environment is of global concern. In Chapter 5, prediction systems are described, and Table 5-4 is a list of some historical milestones.

In the middle 1990s, the United States embarked on a multi-agency initiative entitled the National Space Weather Program, NSWP, based upon the need to improve the Nation's ability to specify and forecast space weather. A strategic plan has been published along with an implementation plan [NSWP, 1995, 2000]. This effort has provided considerable focus to the space weather issue, and the implementation plan serves as a useful guide. Being

broadly directed across many technological disciplines, the NSWP may put a different slant in its portrayal of what constitutes mission success. In the rather narrow field of radio communications, this author has looked at things that will provide the greatest level of improvement in actual system performance. Clearly the emphasis in this manuscript is on improvements achievable in the realm of ionospheric specification while recognizing there is a distinct need for improvement in more general forecasting technologies for geospace applications.

The NSWP is but one of many efforts that are focused on the phenomena of space weather and its consequences. A summary of civilian agency and DoD initiatives are described in Chapter 6, including regional programs (i.e., Australia, Asia, Canada and Europe) and international programs such as those organized under the aegis of COSPAR.

1.5 CATEGORIES OF RADIO SYSTEMS

Radio Communication and broadcasting systems may be either controlled by the ionosphere, as in HF skywave systems, or simply influenced by it, as in transionospheric radio communication and navigation systems (see Section 1.1). In the former case, the ionosphere is actually an inexorable part of the system; while in the latter case, the ionosphere is fundamentally a nuisance. In both instances an account of the ionosphere is at least beneficial to system design and operation. In the case of HF skywave systems, the accounting may be a critical factor in system performance. What is not well understood is that radio communication systems that are affected by the ionospheric personality are not necessarily inferior to systems that are little influenced by the ionosphere. Intelligent use of space weather information may lead to significant improvements in performance of adaptive HF systems. In fact, under some conditions, HF digital communication can be just as reliable as satellite communication. This may be surprising to some communication specialists, and it indicates the power of adaptive system design as powered by space weather data. It is noteworthy that our emphasis is on *intelligent* exploitation of space weather data as part of an adaptive HF system incorporating sufficient levels of time, path and frequency diversity. We must be clear on that point.

The influence of the ionosphere on radio systems falls into two general categories. Category 1 involves those systems that depend upon the ionosphere (i.e., involve the ionosphere as part of the system); and Category 2 involves those systems for which the ionosphere is simply a nuisance. In addition to these categories, we may organize the various systems into three disciplines: communication navigation, and surveillance. This issue is covered

more fully in Chapter 4. From Table 1-2, we see that all three disciplines may be found in listings of category 1 and 2 systems.

Table 1-2. Categories of Radio Systems in Terms of Ionospheric Dependence

Category 1	Category 2
VLF-LF Communication and Navigation	Satellite Communication
MF Communication	Satellite Navigation (e.g., GPS & GLONASS)
HF Communication	Space-based Radar & Imaging
HF Broadcasting ("shortwave" listening)	Terrestrial Radar Surveillance & Tracking
OTH Radar Surveillance	Meteor Burst Communications
HFDF and HF SIGINT	Any other system for which the ionosphere is not necessary for conveyance

In this chapter, we have not offered any new technical data regarding particular space weather observables and communication system impairments, as the literature is already replete with such associations. Rather, the author's goal is to offer some observations based upon many years of R&D experience within government and industry. The basis for these observations derives from early work at the Naval Research Laboratory supporting civilian and DoD communication and surveillance activities. Within the same time frame, we incorporated various methodologies for assessment and prediction of communication performance, including the ionospheric measurements using sounder systems and solar measurements using satellite platforms. Indeed, Navy specialists were the first to develop an approach for application of space weather data in a near-real-time computer platform, PROPHET, which was a quasi-operational system [Rothmuller, 1978].

1.6 OTHER INFLUENCES ON SYSTEMS

While space weather is a term in vogue, it should recognized that there are a number of external (environmental) factors that influence the performance of radio communication systems. While the energy that fuels variability of the ionosphere may ultimately derive from the sun, it is clear that secondary energy sources from below the ionosphere may also instrumental in the development of ionospheric irregularities. In some cases, the interaction between space weather and the neutral atmosphere may be just as important as its interaction with the ionosphere and plasmasphere. Atmospheric gravity waves that produce traveling ionospheric disturbances (TID) come to mind. The process whereby space weather influences the character of upper atmospheric winds is becoming understood, but the process

of forecasting the direction, magnitude, and wavelength of TIDs has not been fully developed.

Radio communication systems operate at maximum efficiency in a high signal-to-noise environment. The community spends a great deal of time discussing the ionospheric (and space weather) impact on the strength of radio signals, but very little time examining its impact on the atmospheric and cosmic noise components. The general radio noise environment has a climate of its own, and it is modulated by space weather parameters. Existing models of radio noise are climatological in nature and are not generally amenable to update. It can be safely stated that a fundamental weakness in radio system performance predictions is the lack of precision in the specification of the noise and interference background.

1.7 SPACE WEATHER DATA UTILIZATION

The use of ionospheric measurements for development of accurate ionospheric maps has yet to be embraced by the civilian user community in any significant way. This is true whether or not emergent space weather data is actually applied for improved specifications (i.e., nowcasts and forecasts). There are a number of reasons for this, not the least of which is education. Education goes both ways. For example, the constituency of ionospheric specialists and space weather advocates is not fully conversant with the problems of system architects and engineers. They don't know what is needed, and often offer solutions to the wrong problem. On the other hand, the community of system specialists has limited awareness of the growth of space weather science and technology, and has limited capacity to exploit the results. This has spawned a 3rd-party vendor community designed to fill the gap (see Section 1.7.1).

1.7.1 Availability of Space Weather Data

Public availability of primary space weather data is made more convenient by the Internet. The space weather constituency is growing and one finds a vast array of web sites that provide data and information to serve this constituency. Many of these sites are cross-linked and have repackaged data from government sites such as NOAA-SEC. Other organizations make use of available data, add value, and provide unique services and products. There are a growing number of companies having systems that exploit current models and data to provide direct space weather support to customers. Recently, a number of private firms in the USA have formed a Commercial Space Weather Interest Group (CSWIG). This organization was facilitated

through with the support of NOAA-SEC, and meetings are typically held at annual Space Weather Week workshops.

As an example of the balance between public and private resources, we make note of the Dynacast® service provided by RPSI that makes considerable use of government data but uses its own array of sounders for added value. Many companies belonging to CSWIG use similar strategies.

In Section 6.10, we revisit this data availability issue, and identify some entities that make space weather data available. It is remarked that it is rather easy to locate information on the Internet, provided one is reasonably conversant with search engines. With some regret, we have steered away from listing the URLs for relevant sites in this manuscript, principally because of our experience with broken links and outdated information. We were also influenced by a strong recommendation from our editor to avoid publishing web sites that may change or disappear altogether over the lifetime of the book.

1.7.2 Operational Terminals and Workstation Applications

We have mentioned earlier that the Naval Ocean Systems Center (now defunct) and the Naval Research Laboratory teamed in the development of a terminal concept for evaluation of system impairments introduced by ionospheric effects [Rothmuller, 1978]. The SOLRAD satellite provided space weather data, and the terminal contained an imbedded set of simplified models that could be updated by the satellite data in real time. This was probably the first attempt to exploit space weather data in an operational environment. Tests were successful but the program was eventually cancelled to fund other priorities.

A regional nowcasting and forecasting system for UHF and L-Band scintillation has been developed by the USAF and is currently being tested. This system, called SCINDA, utilizes data from terrestrial receivers to generate tailored products, and might be regarded as an intelligent scintillation detection and tracking system [Caton et al., 2002]. The USAF has also developed an Operational Space Environment Network Display (OpSEND) that provides easy-to-visualize displays of space weather effects on designated systems. Nowcast and forecast options are available [Bishop et al, 2002]. (The reader should refer to Section 4.5.3 and 5.6.)

1.8 CONCLUSIONS

From a communication vulnerability perspective, space weather influence derives from two classes of data: (a) ionospheric (or *downstream*)

data, and (b) exoionospheric (or *upstream*) data. The *upstream* space weather information can have a significant operational impact on terrestrial HF and SATCOM systems only if accurate forecasting algorithms relating the *upstream* data to pertinent ionospheric disturbances (i.e., the *downstream* data) can be developed. Such information will aid in top-level resource management decisions.

In the context of short-term forecasting and nowcasting, near real-time assimilation of ionospheric data (e.g., GAIM technology) is preferred over methods based upon purely *upstream* data assimilation. However neither approach should proceed in a vacuum. Without meticulous assimilation of the upstream and downstream data, a real solution to the forecasting problem will not be obtained. This solution is in fact a primary goal of the National Space Weather Program. It is encouraging to see that in the priority list showing the key physical parameters for the ionosphere and the thermosphere, the Space Weather Program Implementation Plan has the following listed as among the 1st priorities: *Ne* and its intrinsic variability and $\delta Ne/Ne$ (NSWP, 2000).

For certain communication systems, an accurate specification or forecast of the geoplasma distribution is a key ingredient to the improvement of performance. Robust systems have been developed, based upon the gloomy prospect that this "key ingredient" will never be available in a timely or with sufficient accuracy. But these robust approaches are more limited than should be necessary.

Some basic needs include the development of new and/or improved physical relationships between space weather parameters (e.g., IMF characteristics) and the global distribution of *Ne* in the ionosphere and plasmasphere. In addition we need further development of sensors and/or techniques for the timely delivery of space weather parameters.

1.9 REFERENCES

Argo, P.E., and I.J. Rothmuller, 1979, "PROPHET: An Application of Propagation Forecasting Principles", in *Solar-Terrestrial Predictions Proceedings, Vol. 1:Prediction Group Reports*, R. F. Donnelly (editor), ERL, NOAA, U.S. Department of Commerce, Boulder CO.

Bishop, G., T. Bullett, K. Groves, S. Quigley, P.Doherty, E. Sexton, K. Scro, and P. Citrone, 2002, "Operational Space Environment Network Display (OPSEND)", *2002 Ionospheric Effects Symposium*, J.M. Goodman (Editor-in-Chief), NTIS, Springfield VA, September 15, 2002.

Briggs, B.H., 1958, "A Study of Ionospheric Irregularities Which Cause Spread-F Echoes and Scintillations of Radio Stars", *J. Atmospheric Terrest. Phys.*, 12, pp.34-45.

Caton, R.G., W.J. McNeil, K.M. Groves, and Sa. Basu, 2002, "GPS Proxy Model for Real-Time UHF Satcom Scintillation Maps from the Scintillation Network Decision Aid (SCINDA)", *2002 Ionospheric Effects Symposium*, J.M. Goodman (Editor-in-Chief), NTIS, Springfield VA, September 15, 2002.

Chapman, S., 1931, "The Absorption and Dissociative or Ionizing Effect of Monochromatic Radiation in an Atmosphere on a Rotating Earth", Parts 1 and 2, Proc. Phys. Soc., 43, 26 and 484.

Cliver, E.W., 1994a, "Solar Activity and Geomagnetic Storms: The First Forty Years", *EOS*, Transactions of the American Geophysical Union, Vol. 75, No.49, pp.569, 574-575, 1994.

Cliver, E.W., 1994b, "Solar Activity and Geomagnetic Storms: The Corpuscular Hypothesis", *EOS*, Transactions of the American Geophysical Union, Vol.75, No.52, pp. 609, 612-613, December 27, 1994.

Cliver, E.W., 1995, "Solar Activity and Geomagnetic Storms: From M Regions and Flares to Coronal Holes and CMEs", *EOS*, Transactions of the American Geophysical Union, Vol.76, No.8, pages 75 and 78, February 21, 1995.

Dagg, M., 1957, "Diurnal Variations of Radio-Star Scintillations, Spread-F and geomagnetic Activity", *J. Atmospheric Terrest. Phys.*, 10, pp. 204-214.

Evans, J.V., and T. Hagfors, 1968, *Radar Astronomy*, McGraw-Hill, New York.

Jones, W.B. and R.M. Gallett, 1962, "Methods for Applying Numerical Maps of Ionospheric Characteristics", J. Res. NBS, Vol. 66D, 6 (Radio Propagation), 649-662.

Fremouw, E.J., and C.L. Rino, 1973, "Modeling of Transionospheric Radio Propagation", *Radio Science*, 8, 213.

Goodman, J.M., 1967, "Electron Content Inhomogeneities in the Lower Ionosphere", J. Geophys. Res. Vol. 72, pp. 5542-5546.

LaBahn, R.W., 1974, "Development of a Scintillation Prediction Grid", NELC Technical Note 2814, NELC, San Diego, CA.

Lu, G., A. Richmond, T. Immel, H. Frey, F. Rich, M. Hairston, and D. Evans, 2001, "Global Ionospheric/Magnetospheric Response to the Bastille Day Storm", presentation at AGU meeting.

Lockwood, G.E.K., and G.L. Nelms, 1964, *J. Atmospheric Terrest. Phys.*, 26, 569.

Mayaud, P.N., 1980, *Derivation, Meaning, and Use of Geomagnetic Indices*, Geophysical Monograph 22, American Geophysical Union, 2000 Florida Avenue N.W., Washington, DC 20009.

OSD, 2000, "Space Weather Architecture Transition Plan", Office of the Assistant Secretary of Defense for Command, Control, Communications, and Intelligence", 22 May 2000.

NSWP, 1995, "Space Weather Strategic Plan", National Space Weather Program Office, 1995

Pope, J.H., 1974, "High Latitude Ionospheric Irregularity Model", *Radio Science*, 9, 675.

Richter, J.H., I.J. Rothmuller, and R.B. Rose, 1976, "PROPHET: Real Time Propagation Forecasting Terminal", *7th Technical Exchange Conference*, El Paso, Texas, Nov. 30th – Dec. 3rd, 1976.

Rothmuller, I.J., 1978, "Real Time Propagation Assessment", AGARD-CPP-238, Ottawa, Canada, 24-28 April, 1978.

Secan, J.A., R.M. Bussey, E.J. Fremouw, and Sa. Basu, 1995, "An Improved Model of Equatorial Scintillation", *Radio Science*, 30, pp 607-617.

Secan, J.A., R.M. Bussey, E.J. Fremouw, and Sa. Basu, 1997, "High-Latitiude Upgrade to the Wideband Ionospheric Scintillation Model,", *Radio Science*, 32, pp 1567-1574..

Wild, J.P., 1956, "The Spectrum of Radio-Scintillations and the Nature of Irregularities in the Ionosphere", *J. Atmospheric Terrest. Phys.*, 8, pp 55-75.

1.10 BIBLIOGRAPHY

Aarons, J. (Editor), *Radio Astronomical and Satellite Studies of the Atmosphere*, Proceedings of the Corfu Summer School, 17-29 June 1962, North-Holland Publishing Company-Amsterdam, Interscience Publishers, a Division of John Wiley and Sons, Inc., New York, 1963.

Brown, G.M. (Editor), *Progress in Radio Science 1960-63, Volume III, The Ionosphere*, Elsevier Publishing Co., Amsterdam, London, New York, 1965

Carlowicz, M.J., and R.E. Lopez, *Storms from the Sun*, The Joseph Henry Press, an imprint of the National Academy Press, 2101 Constitution Avenue, Washington DC 20418, 2002.

Daglis, I.A. (editor), Space Storms and Space Weather Hazards, NATO Science Series, Physics and Chemistry, Volume 38, Kluwer Academic Publishers, Dordrecht, Boston, and London, 2000.

Davies, K., Ionospheric Radio, IEE Electromagnetic Waves Series 31, Peter Peregrinus Ltd., London, UK, 1990.

Freeman, John W., *Storms in Space*, Cambridge University Press, London, New York, Oakleigh (Australia), and Capetown (South Africa), 2001.

Gebhard, L.A., *Evolution of Naval Radio-Electronics and the Contributions of the Naval research Laboratory*, NRL Report 8300, U.S. Government Printing Office, Washington DC, 1979 (NTIS, Springfield VA)

Goodman, J.M., *HF Communications: Science & Technology*, Van Nostrand Reinhold, New York, 1991. (JMG Associates, Ltd., 8310 Lilac Lane, Alexandria VA 22308).

Hanslmeier, A., *The Sun and Space Weather*, Astrophysics and Space Science Library, Vol. 277, Kluwer Academic Publishers, Dordrecht, Boston, and London, 2002.

Hunsucker, R.D., *Radio Techniques for Probing the Terrestrial Ionosphere*, Series: Physics and Chemistry in Space, Volume 22, Springer-Verlag, Berlin, Heidelberg, New York, London, Paris, Tokyo, Hong Kong, Barcelona, and Budapest, 1991.

Song, P., H.J. Singer, and G. Siscoe (editors), *Space Weather*, American Geophysical Union, 2000 Florida Avenue N.W., Washington DC 20009, 2001.

Tsurutani, B.T., W.D. Gonzalez, Y. Kamide, and J. Arballo (editors), 1997, *Magnetic Storms*, AGU Geophysical Monograph 98, American Geophysical Union, 2000 Florida Avenue, Washington DC 20009.

Chapter 2
THE ORIGINS OF SPACE WEATHER

2.1 INTRODUCTION

In this chapter, we turn our attention to the solar-terrestrial environment. We examine the rudiments of solar structure and processes, the genesis and consequences of solar activity, the solar wind and the interplanetary magnetic field (IMF), elements of relevant magnetospheric processes, and solar-terrestrial relationships. We cover solar activity cycles and indices and their importance in specified prediction systems. Relevant prediction systems and services are covered in Chapter 5.

The first title of this chapter was "The Anatomy of Space Weather", but it was changed for several reasons. First of all, the term anatomy suggests a precise dissection of the various processes on the sun and its environment that lead to space weather phenomena. Our real intent is to provide a relatively short overview of such phenomena to the extent they are relevant to our real objective, that of understanding the impact upon telecommunication systems. Moreover there are numerous books that detail solar physics, and these details need not be repeated here. Secondly, it has been noted that up to 70% of space weather occurs in the ionosphere [Meier, 2000]. It certainly appears logical to place the sun and its importance *up front* in this particular book, but it is also sufficient to present the topic in summary fashion, since we dare not diminish the role of the ionosphere that should be at the heart of any dissertation on space weather. Having dispensed with this rationalization for an abbreviated treatment of the sun and space weather origins, let us proceed.

In recent years, the importance of the corona, including coronal holes and coronal mass ejections (i.e., CMEs), has emerged. Certainly a treatment of these phenomena is needed to grasp the impact of transient phenomena that tend to dominate methods of short-term forecasting. An associated phenomenon of major importance is the geomagnetic storm. This topic is central to the matter of any intermediate ionospheric forecasting system since (i) the geomagnetic activity is strongly coupled to the ionosphere, (ii) the ionospheric response is delayed with respect to flare effects, and (iii) the impact is global and relatively long-lasting. The latter property makes the treatment of geomagnetic storms and their causal mechanisms an invaluable component of performance assessment for telecommunications systems that operate in the ionospheric environment. It is duly noted that an ionospheric storm is the response of the ionosphere to a geomagnetic storm. As suggested

above, we shall intentionally limit our treatment of ionospheric storms and related disturbances in the present chapter, leaving these important topics until Chapter 3. In the present chapter we largely restrict our discussion to the origins of space weather. A discussion of new satellite observation systems and other space weather resources will be deferred until Chapter 6. The reader will find many excellent texts that deal almost exclusively with solar and magnetospheric physics, and the author will not attempt to duplicate them either in terms of scope or rigor. For detailed discussions of the sun and the magnetosphere, the bibliography at the end of the chapter should be consulted.

The importance of solar activity as it relates to telecommunication systems is well established. It is recognized that the sun exhibits sudden outbursts of energy that are called solar flares, and that these events may play havoc with the performance of certain radiowave systems including commercial television. However these events are relatively short-lived, typically lasting the order of an hour or less. Other well-known influences of the sun include those changes associated with an intensification in the extent and magnitude of the visible and radio auroras. These events affect high latitude terrestrial and earth-space communication to be sure, but the disturbances are actually global in nature. This is evidenced by the fact that ionospheric storms introduce significant alterations in HF coverage at middle latitudes, as well as enhanced scintillation of signals traversing earth-space paths. These scintillation enhancements are due to a descent of the scintillation boundary, corresponding to an equatorward expansion of the auroral zone. We shall find that solar influences on the ionosphere, may generally be characterized as immediate or delayed, with the long-term occurrence of these categories following an 11-year cycle. A well-known index of solar activity that exhibits the cyclic pattern is the sunspot number. This index roughly characterizes the number of spots on the visible solar disk, and is proportional to that component of solar activity that most severely influences telecommunication systems. The 11-year solar cycle is not subject to precise characterization in terms of onset, duration, or magnitude; and its direct influence on the ionosphere is not always clear. Nevertheless, we use indices of solar activity, or proxies of same, in all current long-term prediction programs. The role of ionospheric models is covered in Chapter 3 and prediction systems are covered in Chapter 5.

The ionosphere owes its existence to the sun, but it would clearly exist even in the absence of the 11-year cycle of sunspots. Indeed, the ionosphere possesses some rather interesting features even during periods of few sunspots. Without the 11-year modulation of activity, the ionosphere would possess a reasonably deterministic variability, which is associated with the local solar zenith angle, including diurnal and seasonal effects that are

appreciably controlled by geometry. Moreover, even the benign ionosphere is characterized by relatively unpredictable variations that arise because of the constitution and dynamics of the underlying neutral gas. In fact there are a host of temporal fluctuations, which originate from sources other than the sun including neutral atmospheric weather patterns and turbulence. This, of course, does not suggest a lack of ultimate linkage to the sun. In any case, this residual class of fluctuations poses interesting challenges for ionospheric forecasting specialists who have long concentrated on the more obvious and direct association between the sun and the ionosphere.

2.2 THE SUN AND ITS INFLUENCE

Following the tradition of many monographs dealing with radiowave propagation and texts on magnetospheric and ionospheric physics, we shall include a review of the nature of solar activity. However, since we are ultimately interested in telecommunication disciplines and not solar physics, our treatment will exclude the more esoteric topics and consider mainly those issues that will provide an insight for the telecommunication specialist.

2.2.1 Solar Structure and Irradiance Properties

A qualitative picture of the modes of outward energy flow from the sun is given in Figure 2-1. The source of solar activity lies within the central core region. The process by which the energy is generated within the core is similar to the mechanism exploited in the detonation of fusion weapons, but in the case of the sun these reactions are hidden from us because they are constrained by the enormous gravitation pressure of the overlying solar layers.

Figure 2-2 depicts the complex structure of the sun and shows a number of the features that have been studied by solar scientists as well as by engineers involved in the prediction of ionospheric impact on terrestrial systems. Solar physicists now have a good understanding of many of the basic characteristics of the sun, including its average temperature, mass, size, constituents, etc. The sun is about 93 million miles from the earth, it has a mass of about 330 thousand earths, it is a gaseous body, and it rotates (from left to right as viewed from the earth) with a period of about 27 days.

The sun is composed of 90% hydrogen and 9% helium, the latter being formed by the fusion of hydrogen, and 1% heavier trace elements. The energy-producing fusion reactions occur in the central core region, generating a temperature of approximately 10 million degrees Kelvin (°K). The energy from the fusion reactions takes 1 million to 50 million years to reach the solar surface.

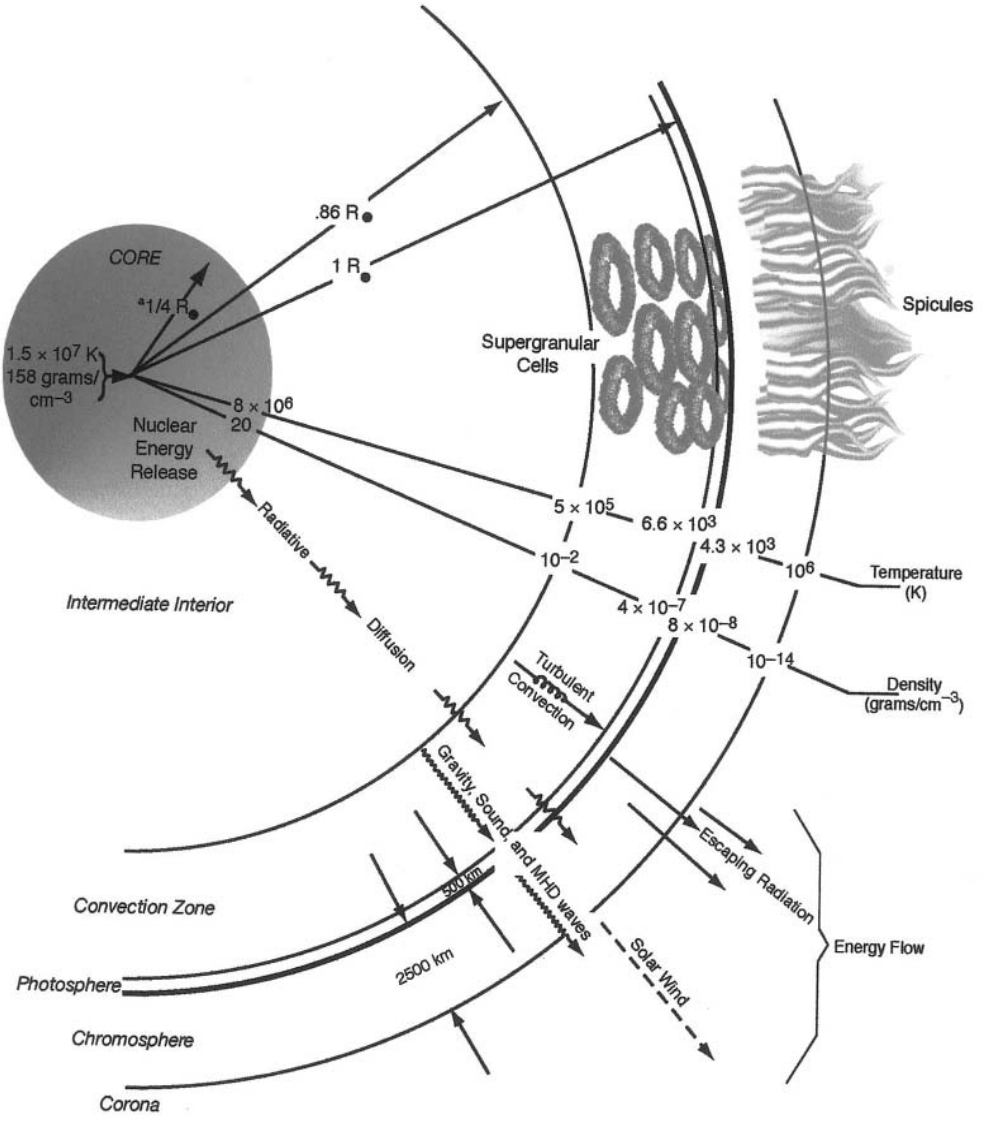


Figure 2-1: A model of energy flow from the sun. Shown are the temperature, density, and phenomenological profiles. The central core region is the seat of energy production. The major zones in the outer region (i.e., > 0.86 R_S) include the convection zone, the photosphere, the chromosphere, and the corona. The corona is observed with a coronograph or during a solar eclipse. The personality of the corona is of major significance in space weather predictions. Adapted from Jursa [1985]

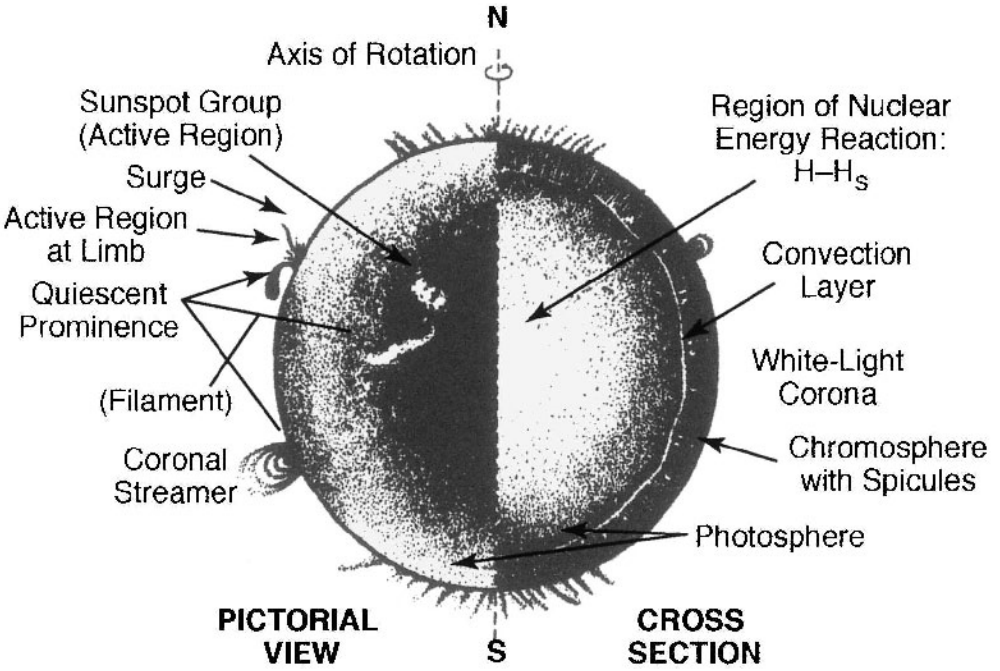


Figure 2-2: Cartoon showing principle features on the sun. Regions are not to scale. Refer also to Figure 2-1. Adapted from Goodman [1991], after Valley [1965].

As observed in Figure 2-1, the temperature of the solar regions diminishes from millions of degrees in the core to its minimum value of several thousand degrees in the lower chromosphere. It rises again to roughly a million degrees in the tenuous solar corona. The equivalent blackbody temperature of the photosphere of the sun is about 6000 °K for electromagnetic wave emissions having wavelengths less than 1 cm. Solar images taken with different wavelengths can be associated with different altitudes. From the photosphere, both UV and visible radiation is emitted. The energy associated with a gas having a temperature T is given by:

$$E \cong kT \tag{2.1}$$

where k represents Boltzmann's constant = 1.38×10^{-23} J/^{0}K, T is the absolute temperature (^{0}K), and E is in Joules (J).

Typically workers use electron volts (eV) as a measure of the energy. One electron volt is the energy of an electron that has been accelerated through a potential difference of one volt. In terms of electron volts we use the following transformation:

$$V = E/q \tag{2.2}$$

where V is the equivalent energy in electron volts (eV), E is the energy (J), and q is the charge of an electron = 1.6×10^{-19} Coulombs.

Wien's Displacement Law allows one to determine the wavelength corresponding to the maximum radiation in the spectral distribution. We have:

$$\lambda = 2.9 \times 10^{-3} T^{-1} \tag{2.3}$$

where λ is in meters, and T is the absolute temperature. As the temperature goes to higher levels, the wavelength decreases, and, of course, the frequency increases. Table 2-1 is a listing of wavelengths, and energy levels corresponding selected values of gas temperature. One can convert to frequency using the relation $\lambda f = 300$, where f is in MHz and λ is in meters.

Table 2-1: Temperature, Energy, and Wavelength and Spectral Designation

Temperature (^{0}K)	Energy (eV)	Wavelength (10^{-9} m)	Spectral Designation
1000	0.1	2900	Infrared
7000	0.6	414	Visible
10,000	0.9	290	Ultraviolet
70,000	6.0	41	Extreme Ultraviolet
700,000	60	4	soft x-rays

Solar radiation can be categorized either as thermal (and broadband) or as line spectral radiation. The line spectra arise as extra-nuclear electrons adjust their positions (and energy levels) following collisional ionization from an electron-atom interaction.

At one time it was thought that the integrated electromagnetic flux from the sun as reckoned at a fixed distance from the solar surface was a constant. However, even correcting for earth-sun distance variation, the solar constant, which is a measure of the total solar irradiance at a distance of one astronomical unit (1 a.u.), has been found to fluctuate slightly. Its value is approximately 1370 watts/m^2. Figure 2-3 illustrates the relative importance of selected bands in the electromagnetic spectrum.

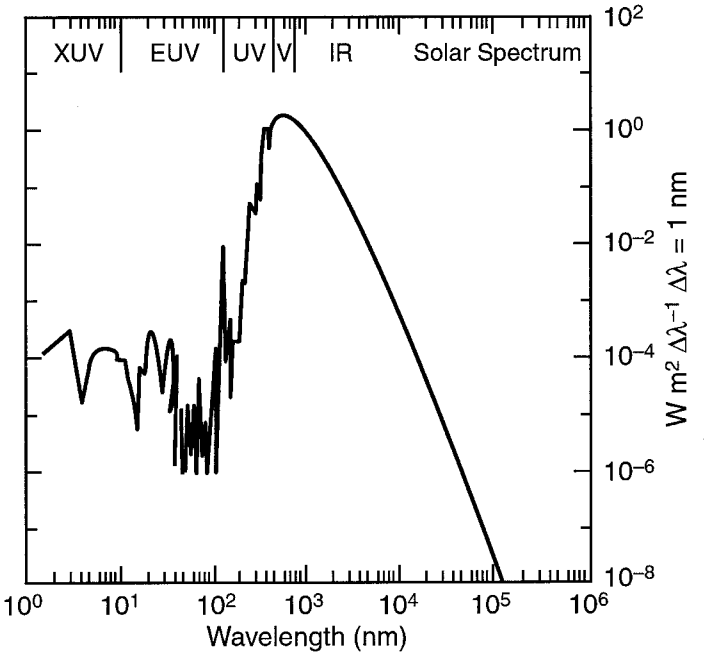


Figure 2-3: The solar spectral distribution from the x-ray band through the radio band. The plot represents irradiance (watts/m^2) versus wavelength (nm) where the irradiance is normalized to a wavelength increment of 1.0 nm. Increasing wavelength is to the right, and increasing energy/photon is to the left. The numbers represent approximate percentages of the solar constant, H ~ 1366 watts/m^2. The visible spectrum is between 400 and 700 nanometers (nm), where 1 nm = 10^{-3}microns. The irradiance curve is adapted from data due to Space Environment Technologies.

The largest contribution to solar irradiance variability (in percentage rather than absolute terms) may be found on the extremes of the spectrum exhibited in Figure 2-3. These regions of greatest variability (i.e., the radio region and the x-ray region) have the most profound effect on the constitution of the upper atmosphere and the ionosphere. Unfortunately, for the purpose of observational science, but fortunately, for purposes of biological safety, a large proportion of the high-energy component corresponding to the ultraviolet (UV), extreme ultraviolet (EUV) and x-ray bands (XUV) is strongly absorbed in the atmosphere. The radio components are virtually unaffected.

EUV and x-ray components are quite influential in photoionization processes, and the UV component is related with ozone layer production. The low energy component of spectral irradiance corresponding to the radiowave

region provides information about energetic particle events and about the general level of solar activity. In fact radio data at 10.7 cm (2800 MHz) may be used as a measure of solar activity since such data is more reliable (and perhaps more meaningful) than the well-known sunspot number. Space Environment Technologies, a commercial firm specializing in irradiance measurements and forecasts, finds that the solar constant, S, changes slightly over time and the currently accepted value is ~ 1366 W/m^2.

Solar physics is a complex subject and many of the fundamental solar phenomena are still incompletely understood. Therefore, at the present time, the important components of electromagnetic and corpuscular flux exiting the sun would appear to exhibit a degree of chaotic behavior. This chaotic behavior is exclusive of more familiar tendencies toward regularity in the temporal pattern of radiation; especially those phenomena associated with the solar rotation period (27 days), and the 11-year solar cycle of sunspot population. As would be expected, the regular patterns are more amenable to prediction. Nevertheless, the chaotic behavior generally controls the short-term environment making near-term forecasts of solar behavior difficult. Moreover, a clear relationship between a particular solar event and its properties (the cause) and the terrestrial disturbance (the effect) is generally lacking. This has a profound effect upon our ability to predict ionospheric behavior and, of course, telecommunication performance.

Because of the circumstantial relationship existing between sunspot number and ionosphere state, considerable effort has been directed toward the development of sunspot number prediction methods. Various prediction methods have been reviewed by Withbroe [1989]. Neural networks have been used to provide estimates of the maximum number of sunspots and when the maximum level will occur [Koons and Gorney, 1990].

2.2.2 On the Nature of Solar Activity and Sunspots

Solar physics provides a basis for our comprehension of solar phenomena, and we use this knowledge to explain previous solar events or to forecast future activity. The relationship between sun and earth is of profound importance for a variety of reasons. An unequivocal linkage between certain solar phenomena and the ionospheric state was established decades ago, largely the result of ionospheric measurements using HF sounders, incoherent scatter radars and rocket probes. More recently, advanced satellite observation platforms has made the case even stronger. Herbert Friedman's *Sun and Earth* [1985] is recommended for additional reading.

To study the origin of sunspots, it is necessary to examine the magnetic field structure on the sun, because, in the absence of the solar magnetic field, current theory does not explain the generation of sunspots or

their cyclic behavior. To first order, the sun's field is oriented N-S in its quiescent configuration (sunspot minimum), and its intensity is little more than that of the earth's magnetic field, being approximately I gauss. However, the sun differs from the earth, where the primary source of the field is within the metallic core, because the solar field is confined near the surface. The field is *frozen-in* to the surface plasma that can move, transporting the field lines with it. In short, the magnetic field is generally too weak to extricate itself from the control of the highly ionized solar plasma. Since the sun and its surface plasma rotate about its NS axis, co-rotation of the surface magnetic field also occurs. However, since the sun is a fluid, this rotation is not uniform as a function of solar (or heliographic) latitude. Indeed, the solar surface rotates differentially, with the equatorial region moving more rapidly than higher heliographic latitudes. This causes the solar magnetic field to become wrapped around the sun over a period of time. It also increases the equatorward magnetic field. Eventually the neighboring stretched field lines become intertwined because of turbulent motion originating in the underlying convection zone. Figure 2-4 shows how this happens. The twisted field lines are hidden below the visible surface and the most intense regions are associated with local magnetic fields of about 4000 gauss. Such fields exert enormous magnetic pressure on the surrounding plasma. As the magnetic pressure begins to exceed the plasma pressure, the fields penetrate the surface and appear as bipolar loops. This phenomenon arises first at a solar latitude of ~ 40 degrees where the field line stretching and convergence is most intense. At the points where the field lines protrude from the surface, the magnetic field intensity is so large that energy is prevented from reaching the surface. These points of opposite polarity are several thousand degrees cooler than their surroundings and appear as dark spots on the photosphere.

Sunspot pairs usually occur in large groups and are contained within rather long-lived (calcium plage) regions. The *preceding* sunspots of the sunspot pairs have the same polarity as the pole of their hemisphere, whereas the *following* sunspots have the opposite polarity. Because of differential rotation, the *following* sunspots lag the overall group motion and form distended unipolar regions that gravitate toward the pole. As a result the latitude of maximum stress moves equatorward and the polar fields become eroded. At sunspot maximum, the polar fields have become completely neutralized. Beyond this point in time, the pole reversal process begins, and the amount of sunspots, now being formed near the low latitude region of limited differential rotation, begins to wane.

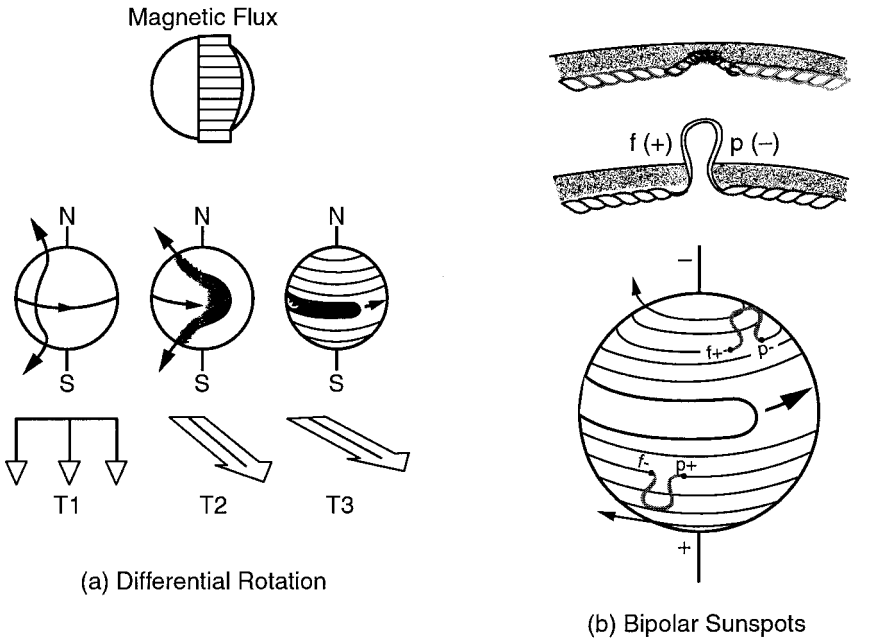


Figure 2-4: Effects of differential rotation on the sun: (A) Development of east-west component of the surface field as the field lines become stretched out between the times T_1, T_2, and T_3. This brings the lines of magnetic flux closer together. (B) Formation of kinks in the plasma field configuration, leading to the development of bipolar sunspots. An eventual reversal of the field at the poles results from the effective poleward migration of the following spots, which have an algebraic sign opposite to that of the pole in their hemisphere. Adapted from Gibson [1973].

By the time the polarity of the magnetic field has completely reversed, no sunspots are evident. Near solar minimum, the field lines that had been intertwined return to a mostly longitudinal (i.e., N-S) configuration. It takes about 11 years for this process to be completed, and it takes about 22 years for the original magnetic configuration to recur. The process is shown in Figure 2-5. From the figure, we see that the spots first start to appear below 40 degrees latitude, both north and south. The maximum solar activity, as represented by the sunspot area index, occurs several years after sunspots first emerge and several years before the last sunspots appear near the equator.

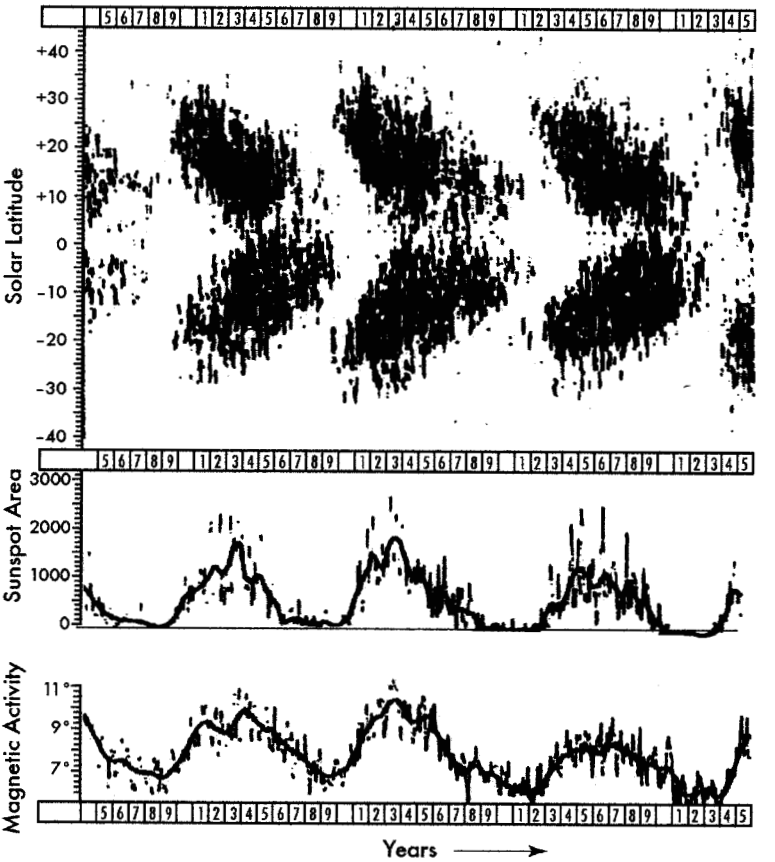


Figure 2-5: The top curve is a so-called *Butterfly diagram*, which shows the migration of sunspots from high latitudes to low as the solar cycle progresses. Also shown is the area of sunspots (middle plot) and a measure of magnetic activity (bottom). Adapted from Chapman [1968].

2.2.3 Active Regions, Coronal Holes, and the Solar Wind

Active areas on the sun are the regions where there arise many phenomena whose form depends upon the region of the spectrum being monitored. Sunspots are best observed in the visible wavelengths, whereas disturbances in the coronal area overlying the disk are best examined in the soft x-ray band with satellite or rocket-borne instruments that are not affected by atmospheric absorption. X-ray emissions are not observable at ground level, and white light observations of the tenuous corona are made problematic by the overwhelming brightness of the solar disk.

The earliest measurements of the solar corona were made during solar eclipses or by using a special instrument called a coronagraph. By superposing successive limb scans, it has been possible to reconstruct an image of coronal disturbances in the visible part of the spectrum. While this method does not generate a frozen picture in time (i.e., a snapshot), it allows coronal observations to be mapped over the entire disk area. The first direct x-ray and UV maps of coronal disturbances were made using rocket probes, but it remained for instruments aboard the Skylab satellite to produce the first comprehensive observations of these disturbances and call attention to coronal holes.

What is a coronal hole? Employing a coronagraph, the visible manifestation of a coronal hole is a lack of coronal brightness in certain regions surrounding the disk; this diminution usually arises and persists near the solar poles. These regions, termed coronal holes, are not devoid of plasma but the density is much less than that found in the surrounding gas. These holes are coupled to underlying unipolar active regions where the field lines are nearly radial. Such a configuration allows plasma to escape the sun and propel itself into space. The observation of coronal holes near the north and south poles of the sun is not surprising, since field lines are naturally vertical in those regions. The existence of coronal holes at low latitudes is a direct result of the generation of bipolar sunspots, progressively in the equatorward direction, and the growth of large unipolar regions. Figure 2-6 shows a coronal hole, which was observed from the Skylab x-ray telescope. This hole extended from the North Polar Region into the southern hemisphere, and was persistent in this general form for over six 27-day rotations of the sun. Through a hole of this type, solar plasma has an escape route similar to that which it has from the polar region.

It is thought that the original notion of a continuous stream of plasma emanating from the sun was born in the early 1950s, based upon comet tail deflections. Subsequently, E.N. Parker [1959] first coined the term *solar wind* to refer to the logical expansion of the solar corona. Solar wind plasma that escapes from the sun carries a signature with it, the embedded magnetic field that may be either sunward or anti-sunward. This coronal magnetic field is transported by the expanding corona into interplanetary space along distended spiral arms, which are called Archimedes spirals. These spirals resemble a rotating gardenhose. They appear as spirals for the following reason. Initially, the solar magnetic field is dominant within the corona causing an initial corotation of the exiting plasma. However, with increasing distance from the sun, the kinetic energy of the plasma will gradually dominate the magnetic field energy resulting in a lag in rotational component of plasma motion. Hence, the expanding coronal plasma appears to fall behind with respect to the rotation solar disk. Parker's solar wind transports the solar magnetic field,

known as the Interplanetary Magnetic Field (IMF), throughout the heleosphere.

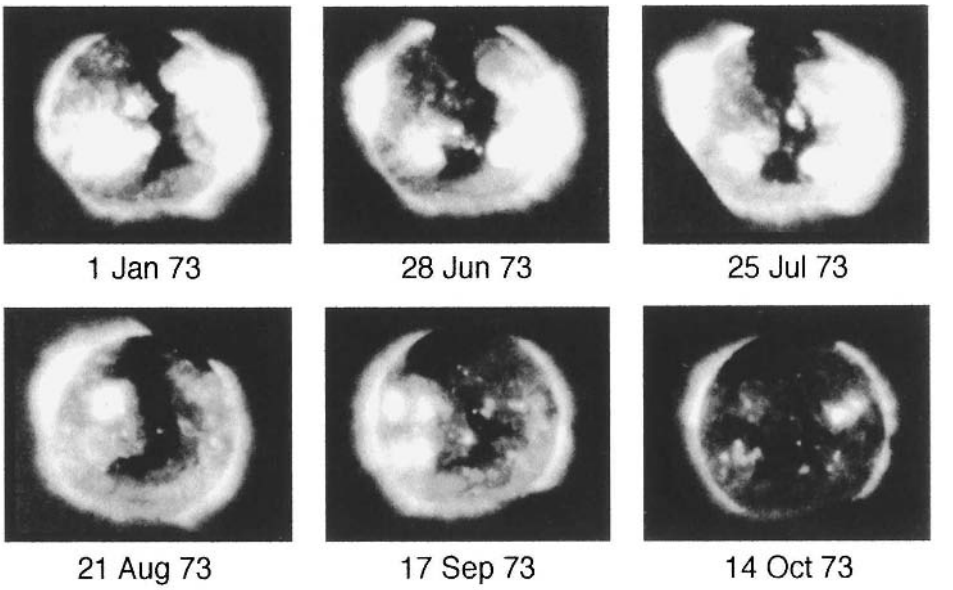


Figure 2-6: Example of a coronal hole observed with Skylab. This event occurred during the decreasing portion of solar cycle 20. Each photograph is separated from its neighbor by 28 days, the average period of a solar rotation. Selected photographs are taken from Figure 1-29 in the Air Force Handbook [Jursa, 1985].

Returning to the sun, we usually find that the predominant magnetic field polarities within the large unipolar regions in the southern and northern solar hemispheres have opposite signs. Opposing fields from the large unipolar regions tend to reconnect at a great distance from the sun producing a neutral sheet in the neighborhood of the ecliptic plane. Looking down on the pole, a sector structure of the IMF is observed, with the magnetic field polarity in adjacent sectors being reversed. This interesting feature is the result of a latitudinal undulation in the neutral current sheet that, under quiescent conditions, would reside in the neighborhood of the ecliptic. The solar wind speed is greatest away from sector boundary crossings. Wind speeds may vary from 700 km/sec during disturbed times and within the center of a sector, to 300 km/sec in the neighborhood of a sector boundary crossing. Greater wind speeds cause more significant ionospheric effects.

Measurements of the IMF and the solar wind speed are useful for the derivation of indices for estimating ionospheric effects. Missions such as Ulysses, IMP-8, ISEE and WIND have shed considerable light on the subject and the ACE satellite is now providing operational data. Some research has suggested that scintillation of selected interstellar radio sources (using measurements made by ground-based radio telescopes) may be associated with the plasma density inhomogeneities within the solar wind. More information regarding ACE may be found in Chapters 5 and 6.

Solar wind speed and IMF characterization are both important in the ultimate impact on the magnetosphere and underlying ionosphere. Solar wind speeds vary, as do magnetic field orientations. It has been demonstrated that the solar wind speed associated with coronal holes is generally much faster that the average solar wind speed. Table 2-2 provides some data on solar wind properties:

Table 2-2: Representative Solar Wind Properties

Solar Wind Parameter	Minimum	Average	Maximum
Flux (particles $cm^{-2}sec^{-1}$)	1	3	100
Speed (km sec^{-1})	200	400	900
Density (particles cm^{-3})	0.4	6.5	100
Magnetic Field, B (nT)	0.2	6	80

2.2.4 The Canonical Sunspot Cycle

Sunspots are indicators of other phenomena that can be important to space weather, and ultimately to ionospheric effects on telecommunication systems. Actually, sunspots are probably overrated as indicators of space weather phenomena. Nevertheless, sunspots have been monitored for centuries and have proved to be a useful if imprecise index. Indeed, because of its historical record and availability, most predictive models are at least partly based upon some measure of the sunspot number.

The most common index of solar activity is based upon a count of the number of sunspots on the solar disk. The fundamental index is the relative sunspot (or Wolf) number that is reckoned daily. It is given by the following relationship developed by Rudolf Wolf who was the first director of the Swiss Federal Observatory in Zurich:

$$R = k(10g + s) \tag{2.4}$$

In Equation 2.4, k is a correction factor dependent upon the observatory, g represents the number of sunspot groups, and s is the number of individual spots. For many years the Wolf number was compiled from measurements

compiled at Zurich. Until 1981, when it was discontinued, it formed the basis for many solar and ionospheric studies. After 1981, the Zurich number (termed R_Z) was replaced by the International sunspot number, R_I. About 25 stations are involved in the construction of R_I. Throughout the chapter we will use the term SSN as a generic for various forms of sunspot number, including R_Z and R_I.

Records of daily and averaged sunspot numbers are archived by the World Data Center A for Solar-Terrestrial Physics through the National Geophysical Data Center located in Boulder, Colorado. The Solar Influences Data Center (SIDC) in Brussels, also a Regional Warning Center, compiles the International Sunspot number and various other products (See Chapter 5).

Another index of solar activity used by many because of its ease of determination and its power as a representative index of solar activity is the noontime value of the 10.7 cm (i.e., 2800 MHz) solar flux, ϕ, from either the Penticton Radio Observatory or from Ottawa. This index is expressed as a monthly mean value in units of 10^{-22} Watts m^{-2} Hz^{-1}. Stewart and Leftin [1972] have compared the Ottawa flux index with the sunspot number and have derived the following relationship:

$$\phi_{12} = 63.7 + 0.728\, R_{12} + 8.9\,(10^{-4})\, R_{12}^2 \qquad (2.5)$$

where ϕ_{12} and R_{12} are the 12-month running mean values of ϕ and R respectively. Note that at solar minimum, the flux level is not zero. For a sunspot number of 100, the solar flux would be ~ 145 according to the Equation 2.5 approximation.

Figure 2-7 gives the range of daily variability in the sunspot number for a period of 170 years, and Figure 2-8 exhibits the 10.7 cm (2800 MHz) solar flux from 1947-2003. Both day-to-day and month-to-month variability in both ϕ and R may be significant; but is it important from a practical standpoint? We will explore this matter in Section 2.2.6. But first we will mention a few things about prediction of the sunspot cycle.

2.2.5 Prediction of the Sunspot Cycle

All techniques used for long-term prediction of sunspots have significant error bars, and, because of this, the value of long-term predictions is questionable for any detailed propagation analysis or a meaningful evaluation of telecommunication impairments. While system performance assessment and system design factors both depend upon solar activity, long-term predictions are of more value in the latter instance. Other matters such as station-keeping, orbital decay probability, and spacecraft charging, which depend upon sunspot number at some level, can influence design parameters.

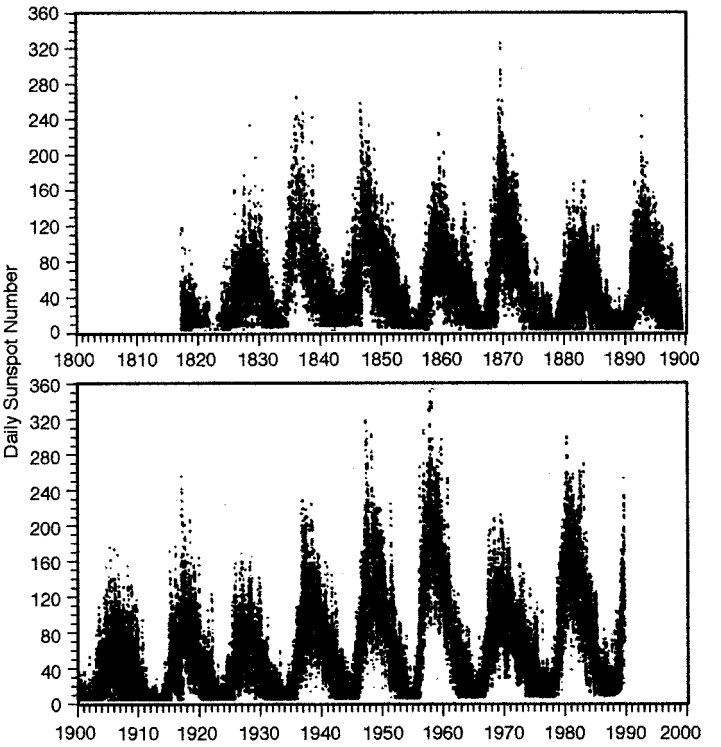


Figure 2-7: The variation of the daily sunspot number from January 1881 to January 1989. Curve is adapted from *EOS Trans, AGU*, vol.70, No. 32, 1989.

These parameters might include the fade margins and link parameters that must be imbedded in the engineering of specified telecommunication systems. Predictions might also be useful for estimating the anticipated level of impairments years in advance by associating outages incurred in the past under the same conditions as predicted. Long-term planning for military exercises could exploit good information regarding the 11-year cycle. But how good are we at doing this?

A number of methods have been used to evaluate future sunspot cycles and no method is very precise. There are several metrics to consider, including the accuracy in prediction of the maximum amplitude, the time of the maximum, and the general shape of the cycle. For the solar cycle 23, workers at NASA have examined this problem and have predicted a maximum value of 154 $\pm$ 21, whereas the maximum of the running average was observed to be $\sim$ 125, slightly below the margin of error. A panel of experts organized by NOAA-SEC, and sponsored by NASA, produced a

report entitled *Solar Cycle 23 Project: Summary of Panel Findings* [Joselyn et al., 1996]. Without going into a description of the methods, Table 2-3 gives the range of values for the various techniques, and the consensus prediction, according to the panel.

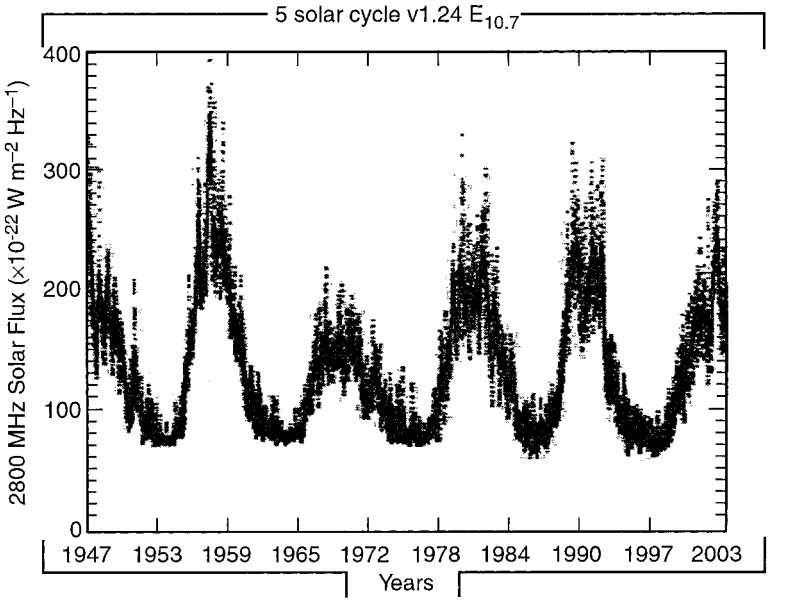


Figure 2-8: Five solar cycle pattern of the 10.7 cm solar flux from 1947-2003. This data set is derived from the SOLAR2000 model, which was developed by Space Environment Technologies (SET). Figure is provided courtesy of Kent Tobiska of SET.

It is evident from Table 2-3 that the timing of the sunspot cycle maximum is predicted with acceptable accuracy, whereas the observed value of the amplitude (i.e., 12-month running average of spots) is outside (i.e., below) the predicted range. Of all the methods cited, the "full" climatology technique appears to be best, followed by the neural network approach. This brief discussion serves to illustrate the point that even a panel of experts can have difficulty in assembling a prediction for a future sunspot cycle before its onset.

2.2.6 Solar Variability

The solar electromagnetic and particulate flux reaching the earth exhibits considerable short-term variability, and the (long-term) time-averaged behavior tracks the general tendency, but not the detailed

morphology, of solar active regions and sunspots. This narrow bandwidth behavior is well known. As one increases the bandwidth of the observational filter, we begin to see more irregular behavior. Indeed, in the time domain, the temporal variability ranges from minutes to years.

- - -

Table 2-3: Forecast of Sunspot number for Solar Cycle 23

Technique	Low End	Maximum	High End
Even/Odd behavior	165	200	235
Precursor	140	160	180
Spectral	135	155	185
Recent climatology	125	155	185
Neural Network	110	140	170
Full climatology	75	115	155
Panel's Consensus of SSN amplitude	130	160	190
Panel's Consensus of SSN peak month	January 1999	March 2000	June 2001
Observed SSN peak	-	~ 120	-
Observed peak date	-	~ April 2000	-

Note-1: By inspection of Figure 2-9, the peak monthly value of the SSN was observed to be ~ 175 at ~ July 2000. However, the smoothed (12-month "mean") value is seen to be ~ 120.
Note-2: Sunspot cycle 23 exhibited two "peaks" in solar activity, where the secondary peak was ~ 115 at ~ December 2001.

- - -

Figure 2-9 is the ISES solar cycle 23 sunspot number progression as of 29 February 2004. It is seen that solar cycle 24 will begin on or about January 2007.

Table 2-4 stipulates the general amplitude of sunspot variability as a function of the filter time constant, using the Wolf number as the gauge of sunspot activity. It is clear that daily values of sunspot number are far more variable than monthly values. While we should always consider the highest bandwidth information when considering real-time forecasting issues, this does not always lead to the desired result. Normally one would like to compare cause and effect using the same filter, thereby enabling an improvement in the correlation expected to exist. This strategy works well at the low-frequency (high bandwidth) end, but this yields little data of interest. We really don't care about a yearly-averaged relationship between *SSN* and *foF2*, for example. However, we would like to take advantage of the daily sunspot number and some daily index of ionospheric parameters, such as the midday value *foF2*. Unfortunately, as we infer from Table 2-4, the day-to-day variability in sunspot number is sizable, and this is not reflected in the degree

of ionospheric variability. But, for a number of reasons, we would not expect sunspot number to be highly correlated with ionospheric personality on a day-to-day basis, and certainly not on an intra-day basis. For one reason, the construction of R is based upon a spatial average over the entire solar disk, and this averaging process has a tendency to eliminate very short-term variations of R. Secondly, there is no physical basis for asserting a direct relationship between sunspot number and ionospheric response. If the same question is asked about solar flares, coronal holes, coronal mass ejections, etc, the answer would be different, with the proviso that time lags be considered in some cases.

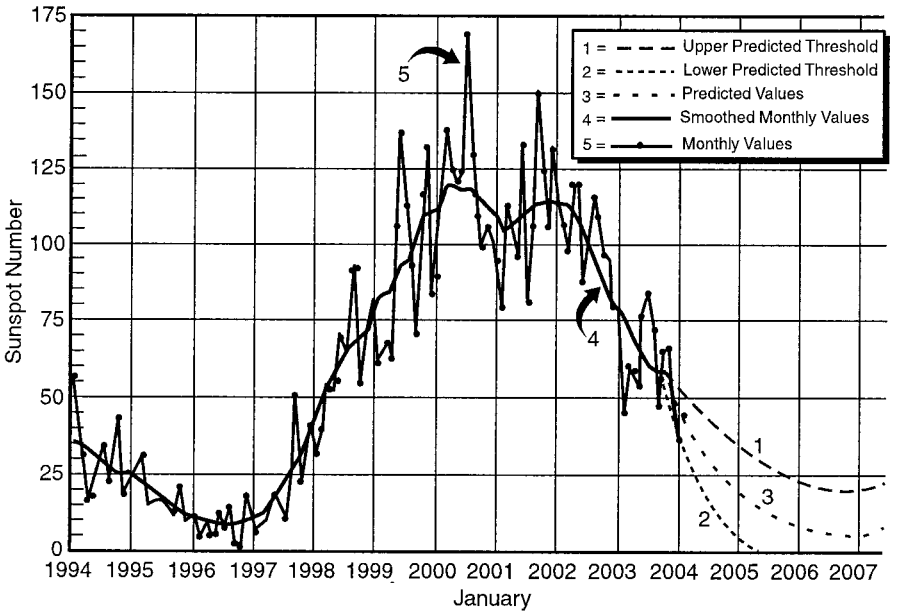


Figure 2-9: Sunspot number variation for solar cycle 23. Monthly averages and smoothed monthly values are given. The dotted lines near the end of the cycle are the upper, median, and lower limits. Data were provided by NOAA-SEC and ISES.

Table 2-4: Sunspot Number Variability

Filter Time Constant	Approximate Sunspot Number Range
11-years	50-100
1-Year	5-150
1-Month	2-175
1-Day	0-350

HF propagation prediction programs in use today all rely on some baseline value of sunspot number (or its proxy), and it is presumed that a running 12-month average of R_z or R_I is to be used as a driver to yield monthly median values of ionospheric parameters (such as *foF2*) as an intermediate product. This is consistent with the fact that the ionospheric data used to formulate almost all climatological models in use today are based upon an evaluation of monthly medians as parameterized by values of SSN, suitably averaged over a 12-month interval. This construction is quite useful for hindcasting, but not as useful for accurate forecasting. Workers have attempted to use monthly or even daily values of the sunspot number. One should be cautious with such approaches, given the inferences of Table 2-4, and the fact that the database indicates that the sunspot number should be entered is the prescribed way for optimization (i.e., 12-month average centered at the time in question). But many HF practitioners have thrown caution to the winds, and have used monthly values without noticeably poor results. On the other hand, use of daily values is a virtual disaster. In fact, it has been shown that an effective sunspot number formed by taking the average over the last five days can strike a good balance between the chaotic behavior of daily values and the damping effect associated with long-term smoothing. Other workers use trend lines or persistence to estimate the sunspot number.

HF prediction models are not the only examples where sunspot number drivers are used in some fashion. TEC and scintillation models also require some sunspot number representation as a driver. We will discuss prediction models in Chapter 5.

An intermediate-term component of sunspot variability can be found by observing the sun through a hypothetical filter having a time constant of several days. The predominant periodicity to be disclosed in this manner is correlated with the solar rotation period, but is significant only if a distinct (longitudinally-isolated) solar active region with a lifetime $\geq$ 27 days exists. If the lifetime is much smaller than the solar rotation period, then recurrence is impossible. Also, if multiple active regions are distributed over the solar disk, then recurrence phenomena can be smeared out or distended, even if the individual active regions are long-lived. Recurrence, when observed, can be used to predict future effects on the ionosphere and telecommunications performance. We have already seen from Figure 2-5 that the long-term trends in solar and magnetic activity are correlated. The coronal hole example in Figure 2-6 illustrates multiple 27-day recurrences, with an obvious forecasting potential.

There is a greater likelihood that active regions will be isolated at solar minimum than at solar maximum. Nevertheless, if an especially active longitude is persistent, it may still introduce a resolvable 27-day modulation

in solar activity even when the average levels are high. This situation was quite evident during a period in 1990, where solar activity is characterized by the observed 10.7 cm solar flux. From Figure 2-10, we note a steady background level of 150 solar flux units, and a 27-day oscillatory component of ± 40 flux units.

We have already mentioned that the 27-day recurrence of active regions on the sun might provide a basis for updates of the predictions of geophysical disturbances, which are otherwise based upon long-term trends, or climatology. Persistence of features on the sun coupled with solar rotation creates the potential for determination of the geoeffectiveness of coronal holes and resultant solar wind speed changes. Sheeley and his colleagues at NRL [Sheeley et al., 1976, 1978; Bohlin, 1977] have suggested that coronal holes can be long-lived phenomena and should allow predictions of increased solar wind speed to be made for ~ six months in advance. The prediction of solar wind speed, along with an understanding of the interplanetary magnetic field, is quite important in the growth of geomagnetic substorms, and ultimately ionospheric storms. Figure 2-11 shows a very good correlation between the appearance of coronal holes, solar wind velocity, and magnetic disturbance.

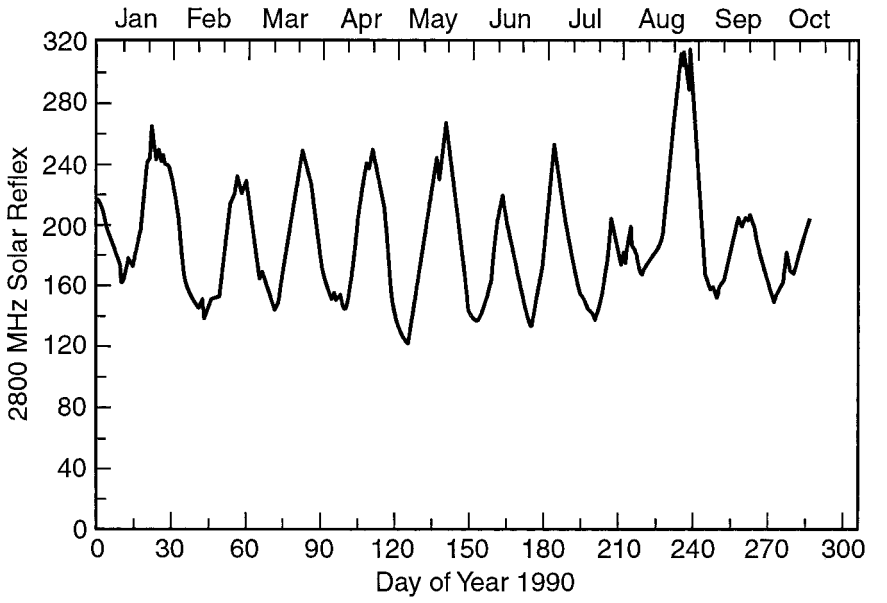


Figure 2-10: Variation of the 2800 MHz solar flux during 1990 showing evidence of a 27-day recurrence in solar activity. Raw data were obtained from NOAA-SEC, Boulder Colorado.

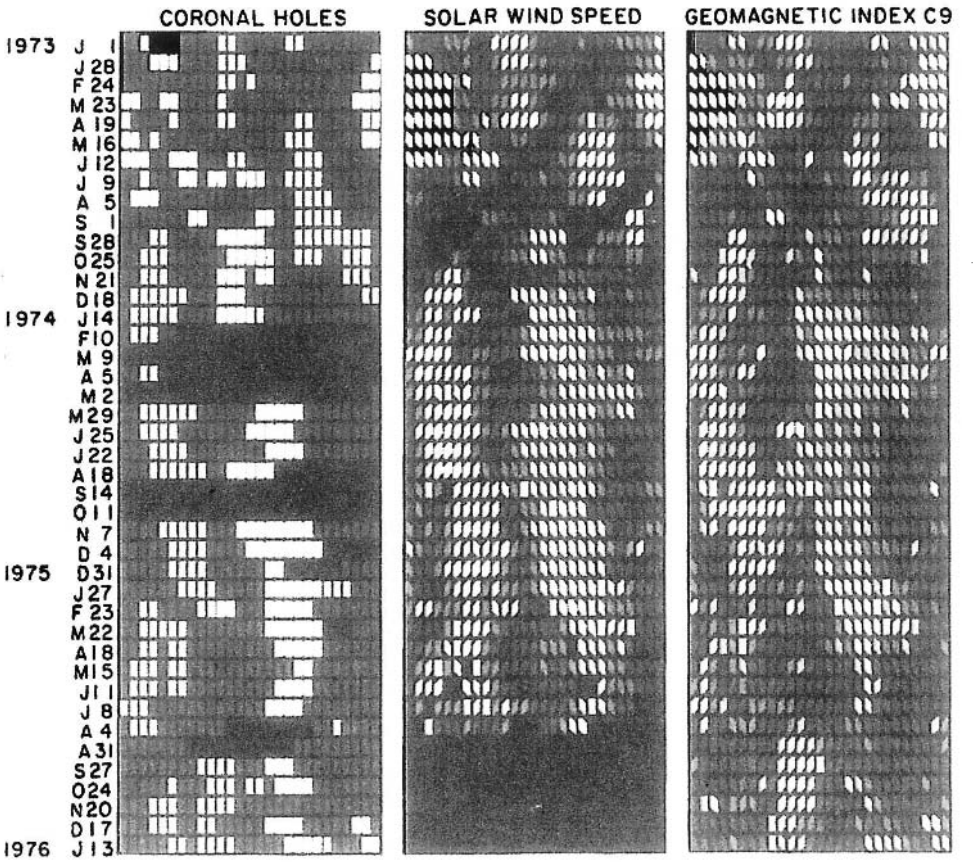


Figure 2-11: A comparison of coronal holes with solar wind speed and magnetic activity. This comparison was made by Sheeley et al. [1976], where the data is arranged in 27-day sequences to correspond to earth rotations.

2.2.7 Solar Flares

One of the more well-known solar events responsible telecommunication disturbances is the solar flare. This is certainly true for HF communications. These events trigger many of the short duration ionospheric events called Sudden Ionospheric Disturbances (SID), and are closely related to other solar phenomena. Sunspot occurrence is closely associated with the observation of solar flares. In general the number of flares observed per solar rotation NF is proportional to the sunspot number.

$$NF = a\,(R - 10) \tag{2.6}$$

where R is the smoothed sunspot number over a 27-day rotation period, and a is a constant which ranges between 1.5 and 2. Thus for $R = 110$ (near solar maximum), the value for NF is about 200. This implies that 7 flares/day will be observed on a global basis.

Flares have been classified in terms of the solar surface area that is enclosed as observed in the hydrogen-α line of the solar spectrum. Subflares cover $\sim \leq 2$ square degrees but the largest class of flares may cover about ~ 25 square degrees of the solar surface.

Another optical designation provides a qualitative indication of the brightness of the flare: F=faint; N=normal; B=bright. The most important flare classification for association with ionospheric effects is the flare strength as measured in the x-ray band. Table 2-5 shows the x-ray classifications in the 1-8 Angstrom band. This is a useful scale; in general only those flares with M and X classifications have any practical significance (i.e., enhanced electron production in the D-layer) leading to radiowave absorption. The process of D-layer absorption is covered in Chapter 4.

Table 2-5: Classification of x ray flares

Class of Flare	X-Ray Energy Output E at Earth (Watt/m^2)
X	$E > 10^{-4}$
M	$10^{-5} < E < 10^{-4}$
C	$10^{-6} < E < 10^{-5}$
B	$E < 10^{-6}$

An important illustration of the relationship between the sunspot number, ionospheric storms, and sudden ionospheric disturbances (SIDs) is given in Figure 2-12. The SIDs are directly related to x-ray flares, and the ionospheric storm variation is directly proportional to the incidence of magnetic storm activity. It is evident from Figure 2-12 that SIDs tend to favor the ascending phase of sunspot activity, whereas ionospheric storms favor the descending phase (see Section 2.2.8).

2.2.8 Storms and Declining Solar Activity

Figure 2-12, corresponding to solar cycle 19, suggests that ionospheric storms have a peak following the maximum in sunspot number. This is evidently a general statement. Still, to this day, the popular view within the public at-large, as well as some otherwise well-informed

telecommunication specialists, is that the sunspot maximum period is all important. The myth that the peak of the smoothed sunspot cycle is the only thing that matters was surely broken in the latter half of 2003, a period of decline in sunspot levels. From Figure 2-9 it is seen that there are two minor peaks in the number of sunspots in July and October-November of 2003 but the 12-month running mean is ~ 60 during the period. The period between mid-October and mid-November of 2003 produced some of the most intense flares and stormy periods seen during the entire solar cycle. Figure 2-13 shows the flare production from active region 486 between 10-24-04 and 11-04-04.

Figure 2-14 is a redrawn version of a white light image of the sun on 28 October 2003. The sunspot regions shown 484, 486, 487, 488, and 492 with region 486 being the most important. It was the largest sunspot region observed since 1990, and it retained its size and complex magnetic structure for the full transit across the visible solar surface. There were 17 major flares from October 19th to November 5th, 2003; and 12 originated from region 486.

The magnetic storm phenomenon is probably the most important ramification of sunspot activity. We will now take an abbreviated look at the magnetosphere and geomagnetic storm activity.

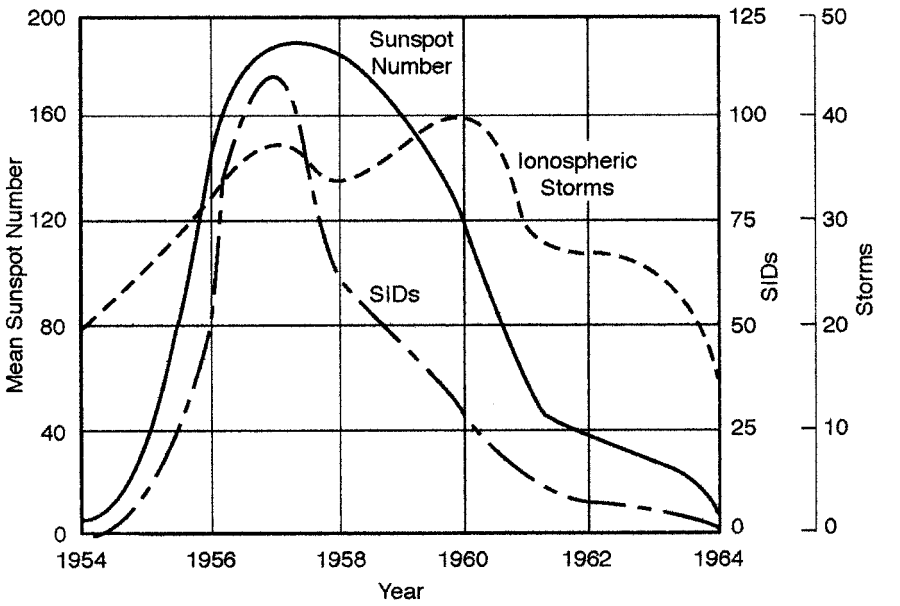


Figure 2-12: Comparison of sunspot number, the number of ionosphere, and the number of SIDs during solar cycle 19 (1954-1964]. After Jacobs and Cohen [1979].

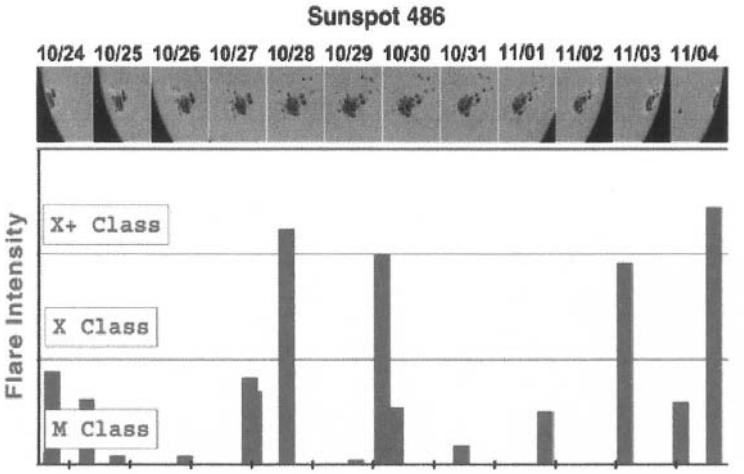


Figure 2-13: Progression of Active Region 486 during the period from 10-24-04 and 11-04-04. The figure is from Simpson [2003]. The image is due to the NASA-SOHO program, the flare data is derived from NOAA, and the compilation is by Metatech Corporation.

- - -

Below we have provided a combined excerpt of NOAA-SEC *Advisory Outlook #03-44* and *Space Weather Advisory Bulletin #03-5.*

Summary for October 27-November 4, 2003:

Space weather during the past week reached extreme levels. The dynamic solar region, NOAA Active region 486, continues to produce high levels of solar activity. Region 486 produced a category R4 (severe) radio blackout on October 28 at 11:10 UTC. Associated with this flare was a category S4 (severe) solar radiation storm beginning at 0025 UTC on 29 October. A coronal mass ejection (CME) was also associated, and it produced a G5 (extreme) geomagnetic storm starting at 0613 UTC on 29 October. This persisted at the G3-G5 levels for 24 hours. Region 486 continued to produce solar activity with yet another major flare at 2049 UTC on 29 October, resulting in an R4 (severe) radio blackout. A CME was also associated with this flare. Moving at 5 million miles per hour, the CME impacted the earth's magnetic field at 1620 UTC on October 30th, and produced a category G5 (extreme) magnetic storm. Stormy conditions persisted for 24 hours. Region 486 grew to become the largest sunspot region of cycle 23.

- - -

Giant sunspot region 486 unleashed another intense solar flare on November 4th at 1950 UTC. The blast saturated sensors onboard GOES satellites. The last time that happened, in April 2001 (i.e., near the peak of the cycle), the flare that saturated the sensors was classified as an X20, the

biggest ever recorded at that time. The November 4th flare appears to have been stronger. Because sunspot region 486 was near the sun's western limb, the blast was not directed toward earth.

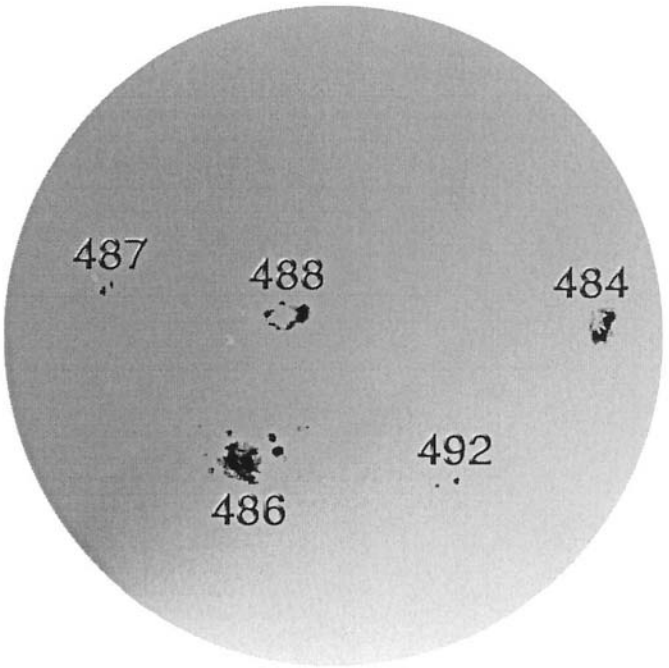


Figure 2-14: Redrawn version of a white light image of the sun on 28 October 2003. This image shows 5 sunspot regions, with Region 486 being the most distinctive. (From EOS, Transactions AGU, Vol.85, No.11, March 16, 2004; the original photograph is courtesy the Solar and Heliospheric Observatory website.)

2.3 MAGNETOSPHERE AND GEOMAGNETIC STORMS

We next turn our attention to the magnetosphere and, in particular, to the coupling of the solar wind, the magnetosphere, and the ionosphere. Much is unknown about these coupling processes, but ongoing studies and campaigns will improve our understanding. We will identify the factors that appear most important, and especially those thought to have a significant bearing on telecommunication systems.

2.3.1 The Geomagnetic Field

To obtain an understanding of the magnetosphere, we must first examine the geomagnetic Field. The earth's magnetic field is an important feature since it generally prevents a direct encounter between the ionosphere and energetic particles of solar origin, and especially solar wind. Mars, for example, does not have a magnetosphere, and it is widely held that solar wind "erosion" has eliminated a good portion of the Martian atmosphere. A geographically localized region that does not afford this protection is found in the neighborhood of the magnetic pole. Since the geomagnetic field is an efficient deflector of the solar wind, why are parameters of the solar wind significant in the morphology of the magnetosphere and the ionosphere beneath it?

The magnetic field of the earth resembles a bar magnetic in many respects. The longitudinal field lines are aligned with the axis of a hypothetical magnet at the ends (poles), and the transverse field lines define an equatorial plane that bisects the magnet. If the field around this bar magnetic were to represent the first-order field of the earth, then we see that the polar field line orientation is nearly vertical while the equatorial field lines are horizontal. This is a good model but there are some differences. First, the geomagnetic field is not purely dipolar, and secondly, the axis of the best-fit dipole does not correspond precisely to the rotational axis of the earth. The geomagnetic field is generated by several sources and current systems located within the earth, the ionosphere, and the magnetosphere. The internal sources include a field produced by currents flowing near the earth's core at a depth of about 3000 km. This component dominates all other sources below about five earth radii. The geomagnetic field may be adequately represented by a magnetic dipole tilted with respect to the earth's rotational axis. Some local anomalies result from direct magnetization of crustal material, but these are generally averaged-out at ionospheric heights. The effects of ionospheric/magnetospheric current system sources depend upon the heights being analyzed, but these components are usually small below a few earth radii.

The simplest approximation to the geomagnetic field is an earth-centered dipole directed southward and inclined at about 11.5 degrees to the earth's rotational axis. Thus the North Pole is 78.5°N, 291°E, and the South pole is 78.5°S, 111°E. This model can be improved by displacing the dipole a distance equal to 0.0685 R_e toward 15.6° N and 150.9°E, where R_e is the earth radius. This modification places the North Pole at 81°N, 84.7°W, and the South Pole at 75°S, 120.4°E. However, there is considerable wander in the precise coordinate placement if the model is slightly changed because of

longitude sensitivity at high latitudes. There are also secular variations of the field associated with gradual reduction in the dipole field strength, a migration of regional anomalies, a northward movement of the dipole, and other variations. Some approximation methods have been based upon the fact that the geomagnetic field decreases in intensity with the inverse cube of geocentric distance, and these methods extrapolate surface values to ionospheric heights. Such approximations tend to emphasize local effects, but the availability of surface magnetic field properties makes the use of such approaches very tempting. Maps of surface values of the total magnetic field, the azimuthal variation of the compass (declination), and the inclination of the magnetic field from the horizontal (dip) may be found in a number of sources. Figure 2-15 shows the conventions associated with measurements of the geomagnetic field. Units vary depending upon application. The primary transformations are given in Table 2-6.

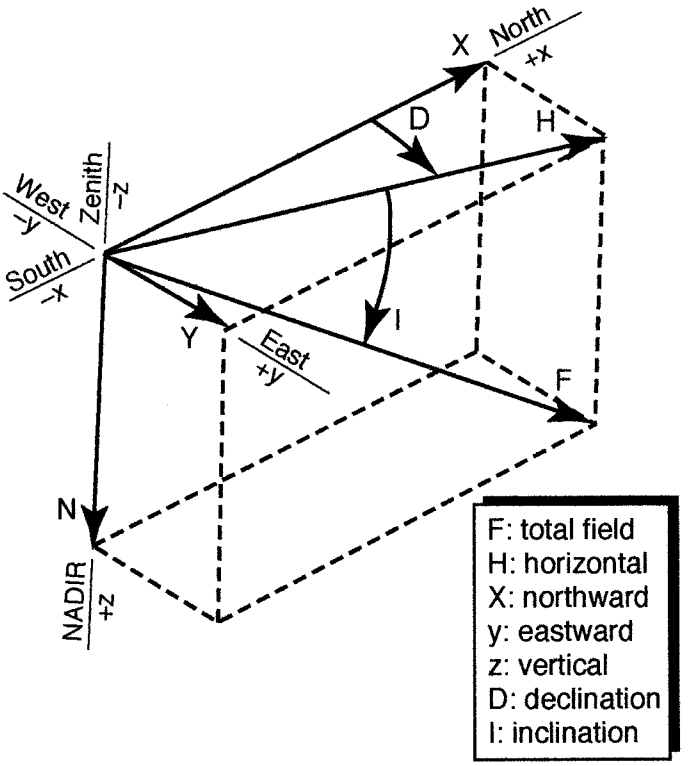


Figure 2-15: Conventions used in Geomagnetic Field Measurements

Table 2-6: Magnetic Field Units and Conversions

Magnetic Induction (B)	1 gamma = 10^{-5} Gauss = 10^{-9} Tesla = 1 nanoTesla
Magnetic Intensity (H)	1 gamma = 10^{-5} Oersted [cgs units] 1 gamma = 10^{-2} $(4\pi)^{-1}$ ampere turns/meter [mks units]

The gamma unit (i.e., γ) is employed in some of the older literature, but it is equivalent to the nanoTesla unit (i.e., nT or 10^{-9} Telsa). Table 2-7 is a listing of various field amplitudes of interest.

Table 2-7: Amplitudes of Selected Magnetic Fields

Earth Surface	~ ½ Gauss	5 x 10^4 nT
Benign Solar Field	~1.0 Gauss	10^5 nT
Disturbed Solar Field	~10^4 Gauss	10^9 nT
Solar Wind		~ 6 nT
Secular Field Decay at the Equator		~ 16 nT/yr
Sq Field Variations from Equatorial Currents		0-50 nT
Lunar-Solar Tidal Variations		~ 3 nT
Geomagnetic Storms at Mid-Latitudes (Kp=9)		~ 10^3 nT

There are a number of representations of the geomagnetic field. A description of the methods is given by Knecht and Shuman [1985]. One of the methods that is most physically attractive for demonstrating ionospheric-magnetospheric interactions is one for which the field is modeled in a so-called *B-L* coordinate frame (see Fig. 2-16). In this system, the field may be exhibited in curves of constant magnetic field intensity *B* and curves of constant *L*. In the *B-L* system, a particular magnetic shell is characterized by a unique *L* value corresponding to the normalized geocentric distance of the field Vector over the equator. Thus, $L = 2$ corresponds to a field line that reaches its maximum height over the geomagnetic equator at 2 *Re*, where *Re* is the earth radius and a convenient normalization factor. This system is quite useful in the study of particles trapped in the magnetosphere such as those found in the Van Allen radiation belts. The terrestrial footprint of a specified field line will occur at two points. These are called conjugate points.

Ionospheric plasma disturbances and resultant telecommunication phenomena are best characterized in terms of geomagnetic rather than geographic coordinates. Accordingly, emphasis should be given to the specification of geomagnetic coordinates for telecommunication terminals, for purposes of space weather assessment.

The dipole method leads to a coordinate system of Geomagnetic Latitudes and Longitudes (i.e., the Geomagnetic Coordinate System). Figure 2-16 depicts a family of Geomagnetic Latitude lines on a Geographic coordinate grid. It is based upon the 1965 IGRF (i.e., International Geomagnetic Reference Field). Other methods include those that replace Geomagnetic Latitude with either Dip Latitude or Invariant Latitude [Jensen et al., 1960]. The Corrected Geomagnetic Coordinate System (CGCS) is a refinement of the Geomagnetic Coordinate system, and like the B-L system, is useful in studies of conjugate effects and other high latitude phenomena.

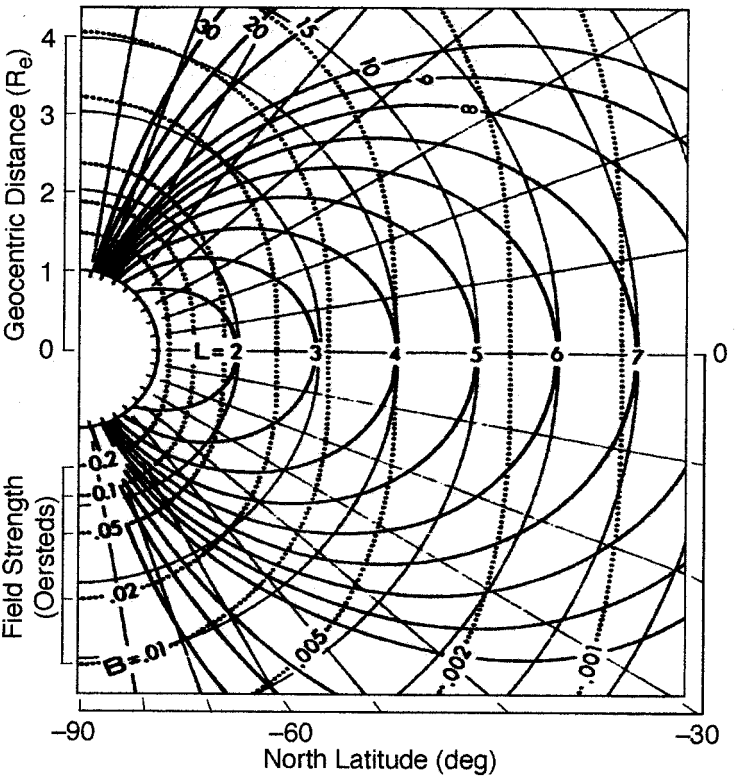


Figure 2-16: The *B-L* Coordinate System. The curves depicted are in the magnetic meridian plane. The *L* parameter is related to the height of the field line over the magnetic equator. *B* is the magnetic field intensity in Oersteds. From Jursa [1985].

Current Methodology uses a representation of the field in terms of a multipole expansion of the magnetic scalar potential function in which the coefficients are based upon a least squares approach to provide a best fit to the field data. This method is now well established and the model, and coefficients, for computing the field are widely available. The internationally

accepted model of the geomagnetic field is the IGRF (mentioned above) with the 1985 version being the most accurate. Previous models have been developed at 5-year intervals beginning in 1965. Coefficients for these models are available from the World Data Center A for Rockets and Satellites at Beltsville, Maryland.

From Figure 2-17, we see that the geomagnetic latitude lines are shifted equatorward in the American sector, relative to Europe and Asia. Knecht and Shuman [1985] have portrayed this situation in a way that gets your attention. They have plotted identifiable land masses in a mercator format, but use Geomagnetic Coordinates for registration (see Figure 2-18).

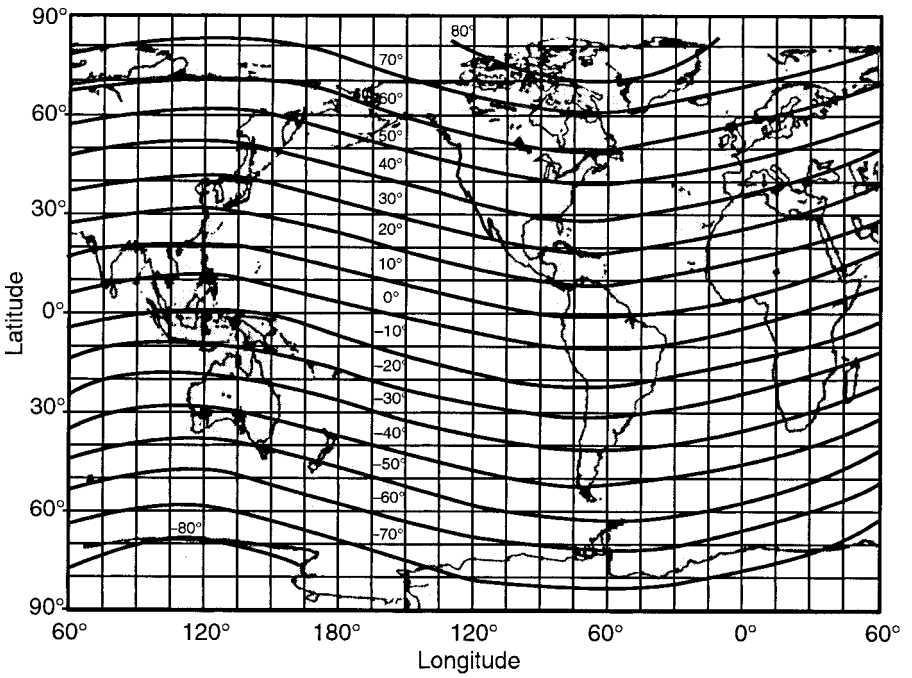
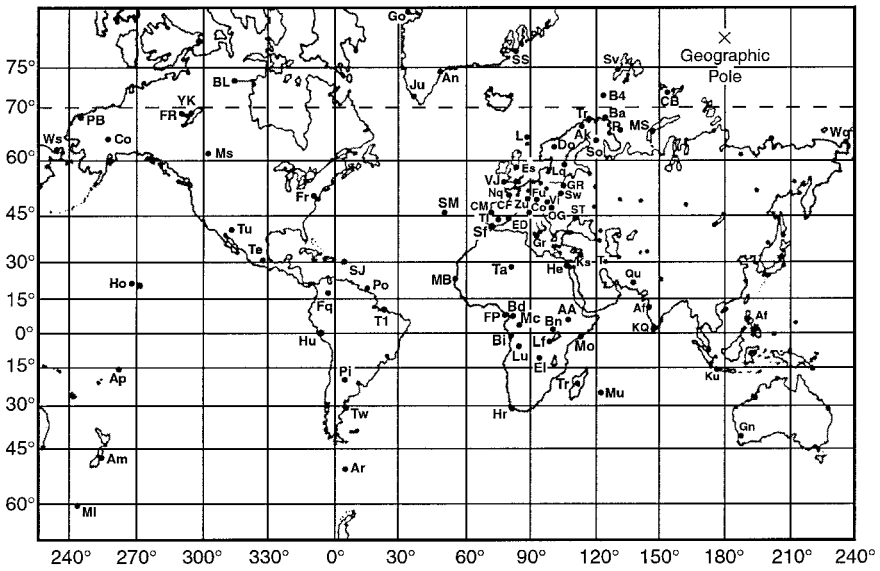


Figure 2-17: Geomagnetic Latitudes (From CCIR [1980]).

Another useful coordinate is the Magnetic Latitude, as opposed to Geomagnetic Latitude. This might be more properly called the Dip Latitude since it is based upon a transformation of observed dip angles by the following formula:

$$Tan\ \Theta = 0.5\ Tan\ I \tag{2.7}$$

where Θ is the Magnetic Latitude and I is the Dip angle.



Figured 2-18: Mecator representation of the world using Geomagnetic Latitudes as the registration format. (From Knecht and Shuman [1985])

Figure 2-19 is a plot of Magnetic (Dip) Latitude. Notice that the magnetic latitude lines passing through the United Kingdom and northern Europe cut through the middle of the continental United States.

2.3.2 Magnetospheric Topology

The geomagnetic field resembles a quasi-blunt object in a supersonic flow field in terms of its interaction with the solar wind stream. The earth's field is compressed on the sunward side and distended on the anti-sunward side, giving rise to a characteristic shape resembling a comet. Within the magnetosphere, solar wind particles are generally excluded, being deflected by the severely distorted geomagnetic field. A collisionless bow shock is formed upstream of the magnetospheric boundary (or magnetopause), and the region between the shock boundary and the magnetosphere is termed the magnetosheath. The magnetosheath is the region of closest approach for the deflected solar wind particles. Within the magnetosphere the motion of plasma is governed by the earth's magnetic field. Since ion-neutral collisions

are not insignificant within the ionosphere, and since this may restrict geomagnetic control of plasma motion, we do not regard the ionosphere as part of the magnetosphere. Moreover, since the geomagnetic field vanishes beyond the magnetopause, to be replaced by the Interplanetary Magnetic Field or IMF, the magnetosheath is actually not part of the magnetosphere either.

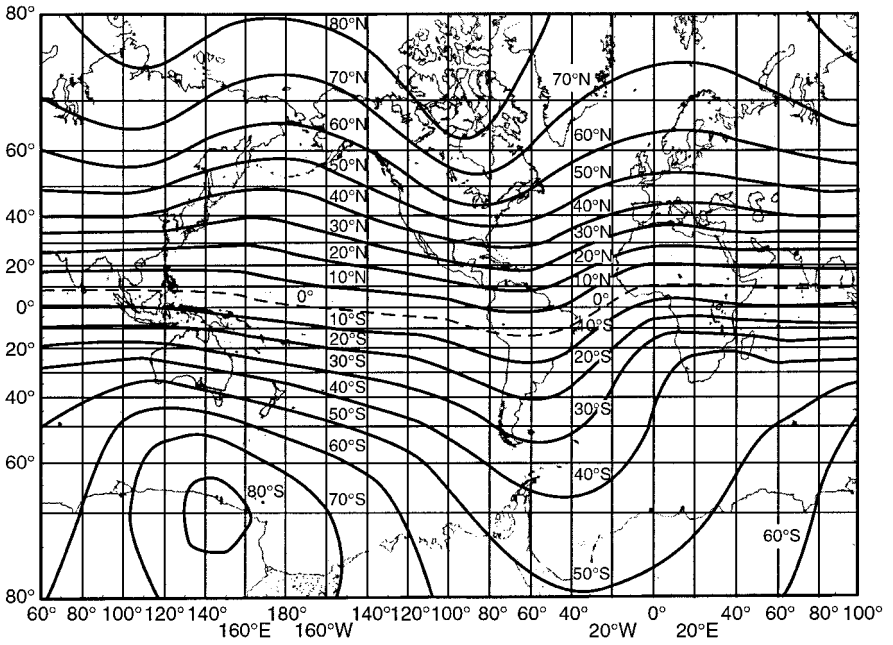


Figure 2-19: Magnetic Latitudes. The dashed line is the Dip equator. This is where the magnetic field is horizontal to the earth's surface. From Valley [1965]

Solar wind particles are typically denied entry to the ionosphere because of the geomagnetic field interaction just mentioned. However, there are some exceptions. Particles may gain entrance through the polar cusp regions. During energetic particle events, this process is enhanced and polar cap absorption (PCA) is the result. Also, because of magnetic merging of the IMF with the geomagnetic field, magnetosheath plasma may be temporarily captured by the plasma sheet (see Figure 2-20).

Another region of interest is the plasmasphere, which serves as a reservoir for ionospheric replenishment during the night and acts as a sink for electrons during the daytime. A very important property of the plasmasphere is its closed field lines. The plasmasphere contains the Van Allen radiation belts. The poleward boundary of the plasmasphere (called the plasmapause)

maps into an ionospheric region called the high latitude trough. Electron concentrations are relaxed in this region. Poleward of the plasmapause, the geomagnetic field lines are no longer closed, but are stretched out well into the magnetotail. This region of open field lines is called the plasma sheet and it has important implications for telecommunication systems at high latitudes. Disturbances within the plasma sheet produce enhanced auroral activity.

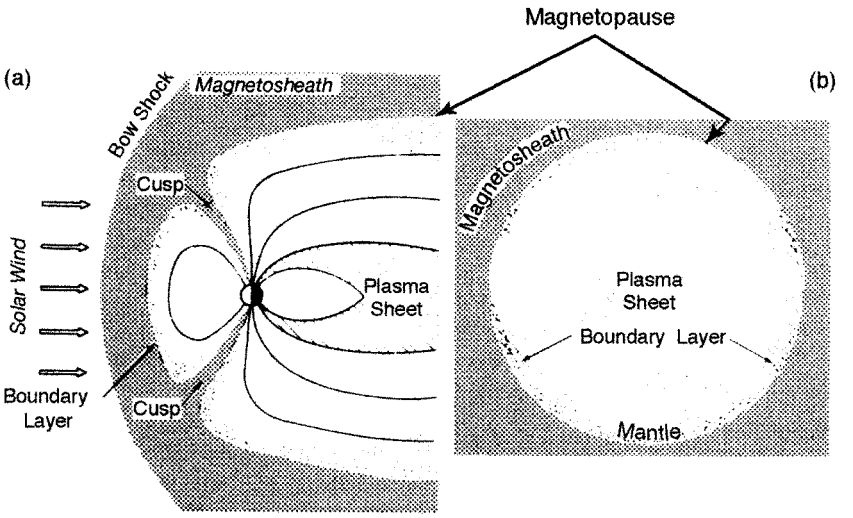


Figure 2-20: A depiction of the magnetospheric regions. From Hill and Wolf [1977].

2.3.3 Geomagnetic Activity Indices

Indices are useful for empirical modeling as well as for forecasting because they provide a convenient parameter set that may be used for driving the model. We have seen that sunspot number R_{12} or the flux index ϕ_{12} are convenient, if not totally representative, of solar activity. The magnetic activity also lends itself to the development of a wide range of index representations. Moreover, the magnetic activity indices are organized and smoothed in a variety of ways that may have the potential for confusing the user who is not an ionospheric specialist. Mayaud [1980] has discussed the array of indices in his book, *Derivation, Meaning, and Use of Geomagnetic Indices*. He traces the history of magnetic index development from the earliest forms to those of the present. Table 2-8 is a list of the current indices

sanctioned by the International Association of Geomagnetism and Aeronomy (IAGA).

Table 2-8: Indices of Magnetic Activity

K-index	Three-hourly quasi-logarithmic index. It is a measure of the irregular variations of the horizontal field component at a specified station or group of stations. For example K_{FR} corresponds to the Fredericksburg site, and K_P is associated with the planetary "average" value. The values of K run from 0-9 with "9" representing the most disturbed condition. K_P is derived from 12 stations between geomagnetic latitudes 48-63 degrees.
Dst-index	Hourly Index associated with low latitude magnetic activity. It is designed to be a measure of the ring current in the magnetosphere (i.e., that region above the geomagnetic equator at ~ 5.6 earth radii). *Dst* stands for "disturbance amplitude storm time", and its units are nT. Four midlatitude sites are used in the construction of *Dst*.
AE-index	Auroral electrojet activity index. This is an hourly index derived from a number of auroral stations.
Q-index	High latitude index with a 15-minute time resolution. It is related to the auroral oval position, and is employed in several propagation prediction algorithms (viz., ICEPAC; see Chapter 3). Q ~ 2Kp –3.5 (The relationship used by AFWA Space Weather Operations Center [ref: NWRA website])
A-index	Daily index of magnetic activity at an individual station or a global array of stations. The A-index ranges between 0-400. It is the linear equivalent to *K*. (See Table 2-9). The three-hourly *K-indices* may be converted to a set of eight three-hourly *A-indices* that are averaged to yield a single daily *A-index*. The U.S. Air Force has developed an operational (planetary) A_p index corresponding to shorter time frames. Such indices can be employed in *foF2* correction models such as STORM (see Chapters 3 and 4).
aa-index	Three-hourly indices computed from *K-indices* of two nearly antipodal magnetic observatories with an invariant latitude of ~ 50 degrees. This index is designed to provide an index of global activity.

The most widely used index is K_P. It is used for ionospheric predictions. However, if we want a simple daily average for the magnetic activity, the fact that K_P is quasi-logarithmic makes it a mathematically poor choice. Even so, a number of studies have used the sum of the eight 3-hourly values of K_P to represent the smoothed daily behavior. The *A-index* is a better choice for use in averaging. Table 2-9 gives a transformation between *A-index* and *K-index*.

Magnetic field data may be obtained from publications and bulletins issued by the International Service of Geomagnetic Indices (ISGI) or the International Association of Geomagnetism and Aeronomy (IAGA) by writing the publications office of the International Union of Geophysics and

Geodesy (IUGG) located in Paris, France. The World Data Centers (WDC) also maintain archives of geomagnetic data. Subcenters of WDC-A (USA) are located in Boulder, Colorado (NGDC) and Greenbelt, Maryland (NSSDC). Bulletins issued by NOAA/NGDC are also mailed to interested users, and NOAA-SEC and Regional Warning Centers of ISES publish reports of the various indices. Generally speaking the *K-index* (or its *A* equivalent) is available from the same sources that issue sunspot number reports and advisories.

Table 2-9: Transformation from *K-index* to *A-index*

K-index	*A-index*
0	0
1	3
2	7
3	15
4	27
5	48
6	80
7	140
8	240
9	400

2.3.5 Real-Time Geomagnetic Data

Magnetometer stations have been established at many locations, and have been quite useful in long-term aeronomic studies as well as in short-term experimental campaigns. A list of stations providing data to the various World Data Centers is given in the compilation by Shea et al. [1984]. Recently attention has been given to a more current assessment of geomagnetic conditions, and the INTERMAGNET program provides near real-time geomagnetic data to Geomagnetic Information Nodes (GINS) for analysis and timely dissemination of data to users [Green, 1990]. The following GIN stations are in operation: Edinburgh, Scotland (British Geological Survey); Golden, Colorado (U.S. Geological Survey); Kyoto, Japan (Kyoto University); Hiraiso, Japan (Communications Research Centre); Ottawa, Canada (Geological Survey of Canada); and Paris, France (Institut de Physique du Globe de Paris). The establishment of this network is consistent with the creation of other real-time ionospheric data networks and solar monitoring systems.

2.3.6 Magnetic Storms and the Ionosphere

It is now widely believed that auroral activity is embodied in the auroral substorm concept described by Akasofu [1964], and that the auroral substorm is only one manifestation of a general process called a magnetospheric substorm [Akasofu, 1968, 1977]. The most dramatic consequence of the magnetospheric substorm is the aurora. The nature of magnetic storms has been refined since the late 1970s. Excellent accounts are found in the one of the NATO science series books, *Space Storms and Space Weather Hazards* [Daglis, 2001], and in AGU Geophysical Monogram 98 entitled *Magnetic Storms* [Tsurutani, 1997].

While the solar wind blows smoothly through the magnetosheath, the topology of the magnetosphere is not disturbed. The plasma sheet is calm and auroral displays are subdued as long as this quiet condition exists. When sunspot activity is at high levels the probability for disturbed aurora and geomagnetic storms is increased. Evidently the enhanced solar wind, which arises when sunspot activity, active regions and solar flares are most prevalent, disturbs the magnetospheric boundary as well as the plasma sheet within the magnetotail. More definitively, coronal expansion phenomena, including Coronal Mass Ejections (CMEs) and coronal holes are major sources of high-speed wind streams. Coronal holes can emerge in a transient fashion, but are usually long-lived and can result in recurrent effects (see Figure 2-6). The coronal hole is a solar feature that can occur even during solar minimum conditions. This can explain why ionospheric disturbances are sometimes observed to occur in the absence of any apparent solar activity (as measured in terms of sunspots).

A crude picture of the magnetic substorm process is given in Figure 2-21. An important factor in the generation of substorm energy is the direction of the Interplanetary Magnetic Field (IMF) along the dipole axis of the earth. When it is directed southward, as shown in Figure 2-20, the plasma sheet becomes pinched driving ionization toward the polar regions. Sheeley et al. [1976] associated high speed solar wind and geomagnetic activity (See Figure 2-11). The current view is that solar wind speed and the IMF direction are fundamental discriminants.

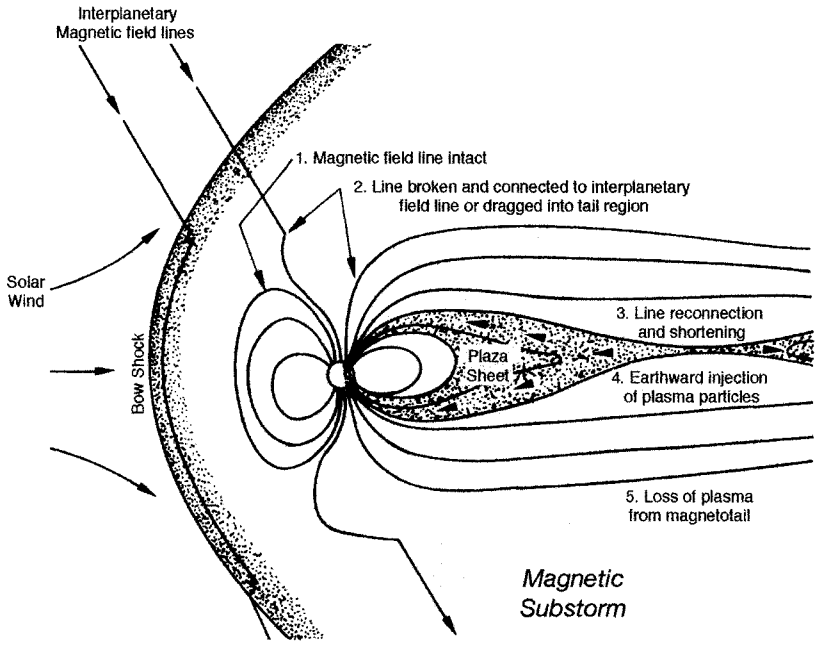


Figure 2-21: Anatomy of a magnetospheric substorm.

The solar wind exhibits fluctuations when high-speed wind streams mix with the ambient solar wind. These fluctuations may be transferred to the N-S component of the IMF. A southward fluctuation may introduce a series of substorms until the excess energy associated with differential merging is exhausted. Differential merging is a process in which the dayside merging rate is in excess of the nightside merging rate. It is a phenomenon that is thought to build up stresses along field lines within the plasma sheet in the tail region. Substorms occur in groups and this process serves to produce a pulsation of the auroral structures. A major geomagnetic storm may be regarded as the integration of a series of substorms. The sequence of events is shown in Figure 2-21.

As the field lines associated with the IMF turn southward, they merge with geomagnetic field lines inside the bow shock region (in the vicinity of the cusp) and flux is transferred from the dayside to the nightside of the magnetosphere. This buildup in potential energy lasts for less than an hour. Subsequently the energy is released as open field lines in the magnetotail become pinched and some of them become reconnected. As the field lines snap into a dipolar configuration, energetic particles are injected toward the earth, forming arcs. These aurorae arcs form beautiful nocturnal displays in regions in the Northern and Southern hemispheres located just poleward of

the midiatitude trough but generally equatorward of the polar cap. These regions were shown by Feldstein to be represented best by ovals anchored at their center by the geomagnetic pole.

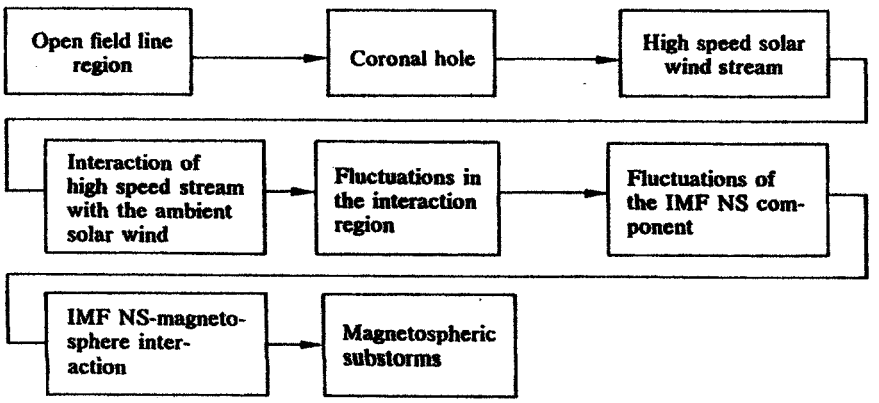


Figure 2-22: Flow Chart of processes leading to the magnetospheric substorm. Working backwards, we see that the conditions for substorm development include (i) a high speed solar wind stream, and (ii) fluctuations of the NS component of the IMF. It has been shown that southward directed B_Z is generally a necessary condition. This high-speed stream generally has its origin in the solar corona. Coronal holes (having long-term effects and potential for recurrence) and transient CMEs are possible sources.

Since the auroral oval is a geomagnetic feature, an interesting diurnal pattern emerges because of the departure of geomagnetic from geographic coordinates. Figure 2-23 shows how the steady state auroral oval appears to move as a function of local time. Notice how Iceland becomes alternately an auroral and nonauroral station even though the magnetic activity is assumed to be fixed. This has important consequences for some telecommunication systems. Our understanding of the dynamics of the aurora and its location has been greatly enhanced by the use of optical imagers from the Defense Meteorological Satellite Program (DMSP). But additional resources have been applied over the years. Striking images of the auroral zone have been obtained over the northern and southern hemispheres using several satellites, including: (i) DMSP (from the 1970s), (ii) the Dynamics Explorer Satellite (from the 1980s; see Figure 2-24), and (iii) IMAGE (currently). From Figure 2-24, we see that Greenland and Iceland are both well circumscribed by the outer ring of the auroral oval. Although the oval may expand and contract over time, it is remarkable how consistent this pattern can appear from space. Refer to Figure 1-4 in Chapter 1 for pictures of the oval during the year 2000 Bastille Day storm using the IMAGE satellite. It is noteworthy that the Solar-

Terrestrial Dispatch organization (STD) publishes on its website selected images of the north polar region from NASA's IMAGE satellite and from the University of Iowa Visible Imaging System (VIS) associated with the POLAR satellite. The company also offers a special product called the STD Auroral Monitor. The STD website is but one example of how the commercial world can use the output from space sensors to offer its customers tailored output. Other companies with web products include Northwest Research Associates, Metatech Corporation, Space Environment Technologies, and Radio Propagation Services. See Chapter 5 for more examples.

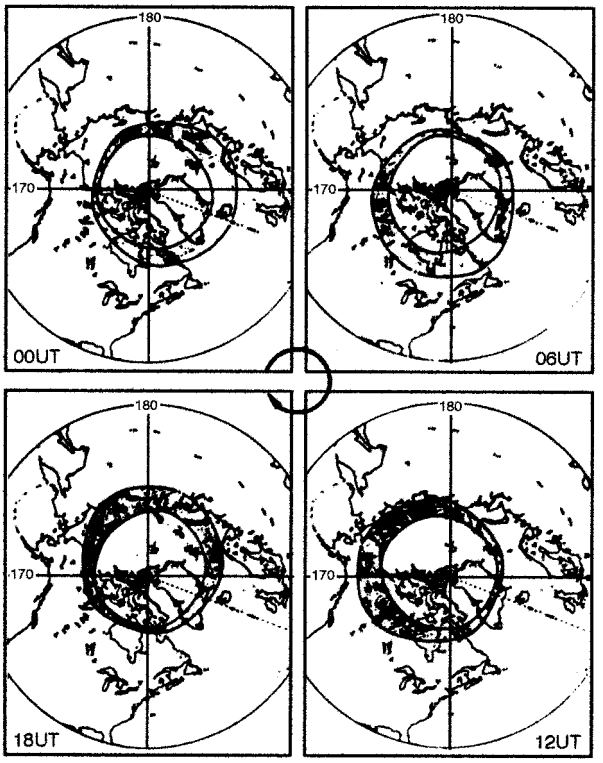


Figure 2-23: The diurnal motion of the auroral oval in geographic coordinates. From Goodman [1991], after Jursa [1985].

Returning to phenomenology, it has been found that the auroral oval thickness increases as the magnetic activity increases and the diameter of the oval expands equatorward. This process is depicted in Figure 2-25. As has been indicated, one of the features of a geomagnetic storm is the equatorward expansion of the auroral oval. Figure 2-26, based upon TIROS observations, shows this characteristic equatorward motion following a period of strong storm activity on November 20-21, 2003. Magnetic activity is highly correlated with the source that drives this motion, and its time history for the period. in terms of the estimated *Kp*, is depicted in Figure 2-27.

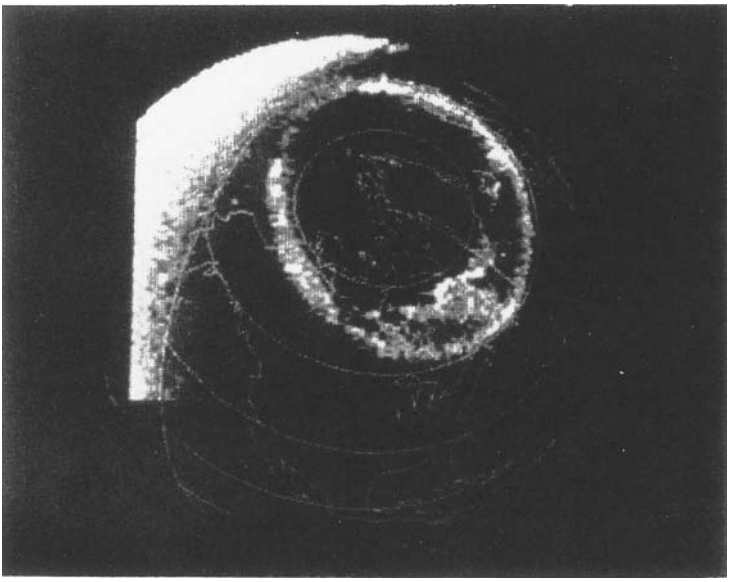


Figure 2-24: Auroral Oval image of North America obtained with the University of Iowa instrumentation aboard the Dynamics Explorer (DE1) on November 8, 1981, a period of intense solar and magnetic activity. From Jursa [1985], after Whalen et al. [1989].

There is a clear lag between the *Kp* time series and the resulting equatorward movement of the oval. There is also a diminution in the total electron content, *TEC* (and the parameter *foF2*) at high latitudes as a result of the storm activity. It turns out that the effective sunspot number, *SSNe*, developed by Northwest Research Associates, is crudely proportional to the globally-averaged *foF2* value. One would expect a global response to be a smoothed-out and somewhat delayed version of the high latitude response. This expectation is consistent with the data in Figure 2-28 that shows the so-called effective sunspot number, *SSNe*, following the same trend in oval

movement, and is delayed in time. The drop in *SSNe* is indicative of a general worldwide diminution in electron concentration. This matter will be discussed further in Chapters 3, 4 and 5.

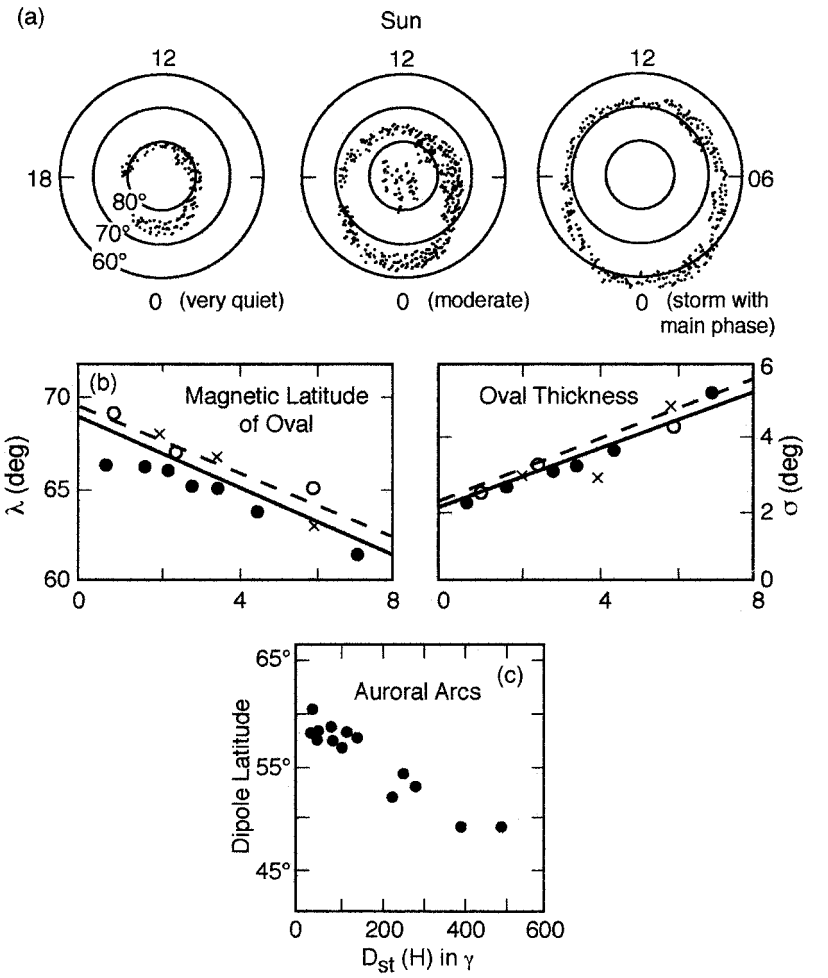


Figure 2-25: (a) Cartoon illustrating the descent of the auroral oval, (b) Median latitude and longitude and oval thickness as a function of *K-index*, (c) Dipole latitude of the oval as a function of the *Dst-index*. Looking at graphs (a), under very quiet conditions, characterized by $Kp < 3$, the auroral oval contracts approaching 70 degrees in the limit. Under disturbed conditions, for which $Kp > 5$, the oval expands approaching 60 degrees in the limit. Equatorward expansion may be larger under strong magnetic storm conditions associated with a main phase. From the depictions (a), we see that the oval is not quite symmetric about the magnetic pole. The nocturnal oval (i.e., anti-sunward side) is more distended equatorward regardless of storm conditions. This is exacerbated in the American sector since the magnetic pole is positioned in northern Canada.

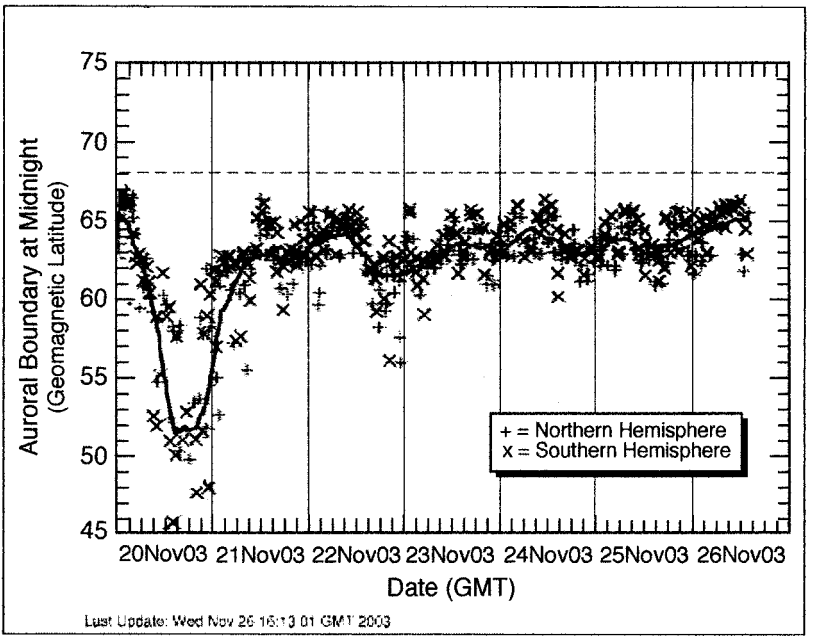


Figure 2-26: The auroral oval boundary position. Graphic courtesy Northwest Research Associates using NOAA-SEC data as input. Refer to Figure 2-27 and Figure 2-28. From NWRA web site, 2004.

A geomagnetic storm develops as the result of the energy transferred from the solar wind to the magnetosphere in a series of substorm events. In macroscopic terms, one may regard the geomagnetic storm as composed of two parts: (i) an initial (short-lived) positive phase associated with an increase in the horizontal component of the magnetic field, which is followed shortly by enhanced auroral displays, and (ii) a main negative phase (or bay) in the horizontal field intensity which may last for several days. The initial phase is associated with short-lived enhancements in electron concentration at ionospheric heights, while the main phase is associated with large-scale diminutions in electron concentration. These effects are often called ionospheric storms to emphasize the ionospheric disturbances involved. It should be noted, however, that the ionospheric response to magnetic storm activity is not always the same. There are differences in latitude, and the effects also depend upon season. More discussion may be found in Chapter 3 where the ionosphere is more fully examined.

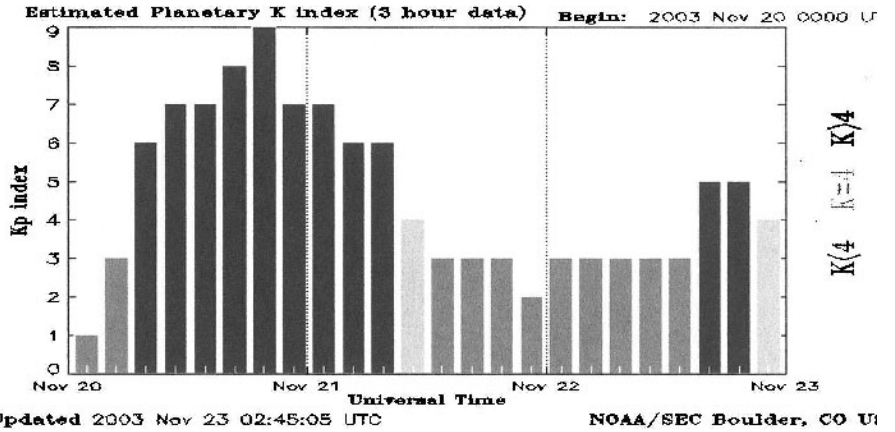


Figure 2-27: Estimated *Kp* index during the November 20-21 storm. Refer to Figure 2-26 and Figure 2-28. Data provided by NOAA-SEC, Boulder CO.

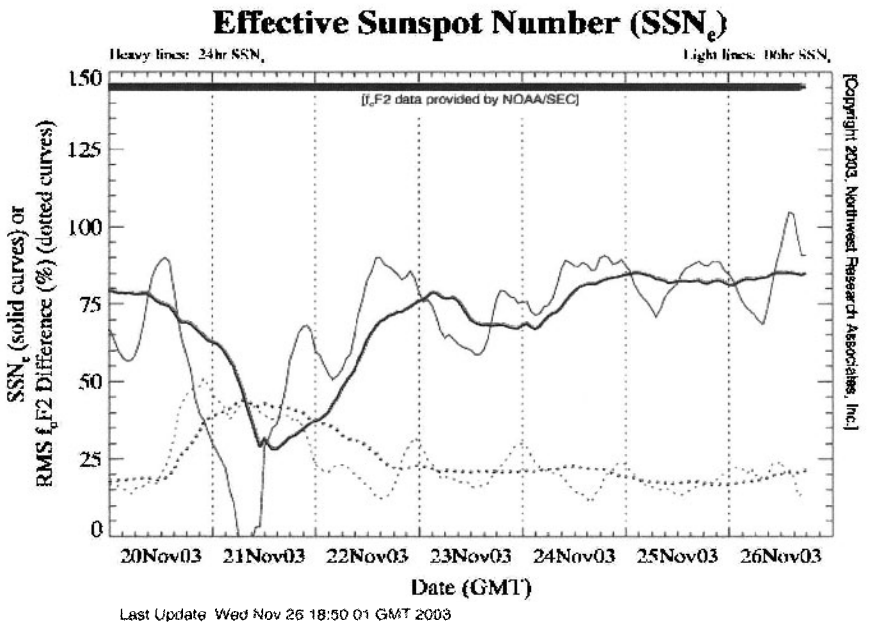


Figure 2-28: Effective Sunspot Number. The effective sunspot number is obtained by matching the tendencies associated with sounder data at selected locations with predictions from a model parameterized by the sunspot number. Graph due to Northwest Research Associates using data from NOAA-SEC sounder database. Refer to Figure 2-26 and Figure 2-27. From NWRA web site, 2004.

2.3.7 The Halloween Storm Period of 2003

As noted in Section 2.2.8, The October 2003 period was an extraordinary period of significant solar activity. Region 486 produced two enormous x-ray flares, with accompanying CMEs, on 28 and 29 October, 2003. The amplitudes of the flares were ~ X17 and ~ X10 respectively as depicted in Figure 2-13. Extreme (i.e., G5) magnetic storms were introduced following impact of both of the CMEs. The second storm has since been termed the Halloween storm in view of its coincidence with the well-known holiday, but its impact on the ionosphere made it noteworthy as well. Figure 2-29 shows the flare activity for the period of interest, and Figure 2-30 shows the magnetic activity response. During these stormy periods, high frequency communications were virtually impossible over uncompensated high latitude paths. The variation in electron concentration was significant for midlatitude sites as well as high latitude sites. We discuss these ionospheric effects in Chapter 3, and some factors related to specific systems in Chapter 4. Indeed, telecommunication performance was degraded for a variety of system types. Ionospheric effects upon the FAA WAAS system are indicated in Chapter 4. The U.S. Department of Commerce (i.e., NOAA, National Weather Service) has published a *Service Assessment* [NOAA-NWS, 2004] detailing the space weather storms of October 19th through November 7th, 2003. Table 2-10 is a chronology of events

Table 2-10: A Summary of Events for the period October 19-November 7, 2003

- October 28, 2003: 1110 UTC: X17 flare from Region 486
- X17 flare produces R4 (severe) radio blackout & solar radio bursts
- X17 flare followed by radiation storm, reaching S3 (strong) levels and S4 (severe) levels after 13 hours
- X17 flare was followed by fast CME. The CME was observed by LASCO on SOHO spacecraft, and had a speed of 2,125 km/sec. The CME reached the earth in 19 hours..
- The X17-related CME impacted the ionosphere and produced a G5 (extreme) geomagnetic storm. This storming lasted 27 hours. This was the 6th most intense storm since 1932.
- October 29: 2049 UTC: X10 flare from Region 486
- X10 flare produces R4 (severe) radio blackout
- X10 flare produces S3 radiation storm
- X10 flare followed by Fast CME with a speed of 1,948 km/sec, reaching the earth in 19 hours. (1600 UTC on October 30, 2003)
- The X10-related CME impacted the earth and introduced a G5 (extreme) geomagnetic storm lasting 24 hours.
- November 4, 2003: 1950 UTC: X28 flare emitted from region 486. This flare occurred near the west limb of the sun, so the impact was minimal. The CME was directed away from the earth. The X28 flare is thought to be the largest since these events have been recorded.

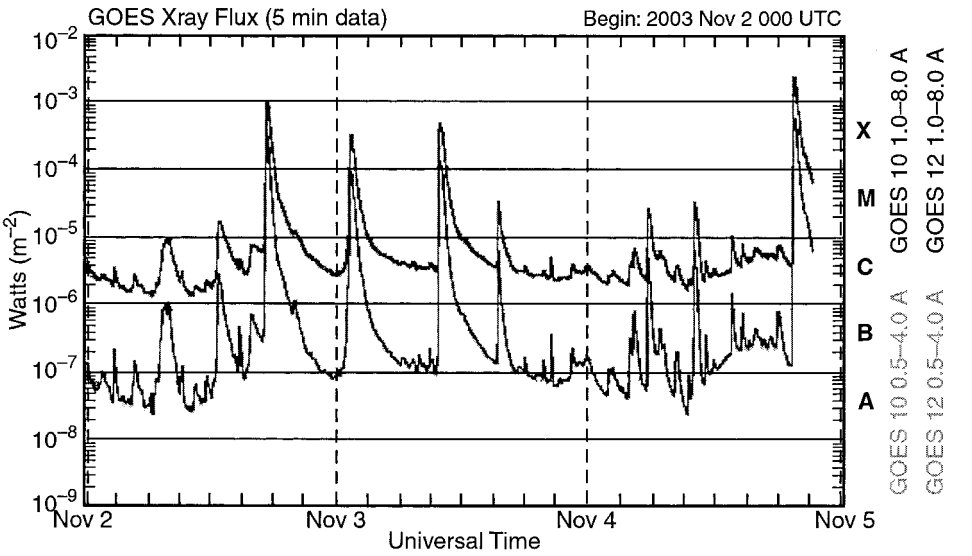


Figure 2-29: GOES X-ray flare activity for the Halloween storm period. Data provided by NOAA-SEC, Dept. of Commerce

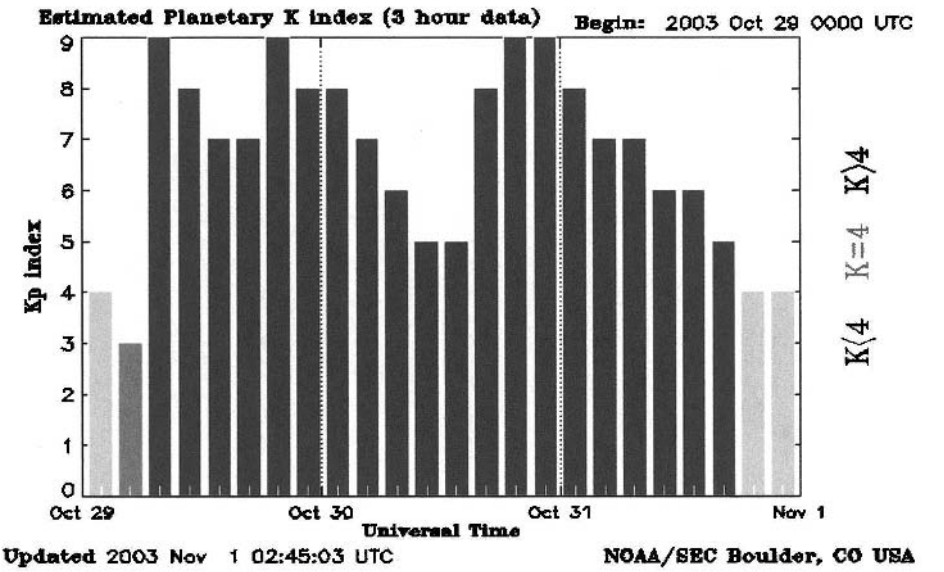


Figure 2-30: Magnetic activity for Halloween storm period. (Data provided by NOAA-SEC, Dept. of Commerce, Boulder CO.)

Given the enormity of the Halloween storm events discussed above, one might say that such isolated situations are sufficient to justify a significant investment in space weather observations and around-the-clock vigilence. But this probably not the case. One has to recognize that such events are not normal occurrences. While they may play havoc, they are rare. From the NOAA assessment report [NOAA-NWS, 2004] a listing of the top 20 radiation storms and the top solar flares have been tabulated. These are given in Tables 2-11 and 2-12. Data for solar cycles 21, 22, and 23 are listed. We see that the Top-20 listing includes 3, 9, and 8 radiation events for cycles 21, 22, and 22 respectively. These events may cause PCA events (of importance to HF communication over the poles) and can lead to radiation exposure for passengers and crew for transpolar flights. One radiation storm from the October-November 2003 period appears in Table 2-11. This occurred on October 28, 2003 (rank 4).

The X-ray flare listing in Table 2-12 indicates that the largest flares numbered 4, 10, and 6 for solar cycles 21, 22, and 23 respectively. Flares cause short wave fades (SWFs) for HF systems, but their importance may be greater as an indicator of delayed effects such as radiation storms, PCA events, and geomagnetic storms. There are 3 flares from the October-November 2003 period in Table 2-12: 11-04-2003 (rank 1), 10-28-2003 (rank 4), and 10-29-2003 (rank 20).

Probably the more important listing is that of magnetic storms. In this instance the NOAA Service Assessment [NOAA-NWS, 2004] has provided the Top-30 Geomagnetic storms since 1932 based upon the Potsdam "running" Ap index. It is well known that geomagnetic storms introduce significant ionospheric perturbations of global significance. Table 2-13 indicates that the largest geomagnetic storm was on December 18, 1941 and that two storms during the "Halloween" period of 2003 (i.e., October 29 and October 30) were respectively ranked 6 and 16 on the 1932-2003 list.

Table 2-11: The Greatest Twenty Radiation Storms (GOES proton flux > 10 MeV since 1976)

Rank	Intensity (pfu) x 10^3	Date (mm-dd-yyyy)	Rank	Intensity (pfu) x 10^3	Date (mm-dd-yyyy)
1	43	03-23-1991	11	7.3	11-30-1989
2	40	10-19-1989	12	4.6	05-09-1982
3	31.7	11-04-2001	13	4.5	09-29-1989
4	29.5	10-28-2003	14	3.5	03-08-1989
5	24	07-14-2000	15	3	06-04-1991
6	18.9	11-22-2001	16	2.9	06-11-1982
7	14.8	11-08-2000	17	2.7	10-30-1992
8	12.9	09-24-2001	18	2.52	04-21-2002
9	10	02-20-1994	19	2.5	04-25-1984
10	9.2	08-12-1989	20	2.36	10-01-2001

Table 2-12: Top Twenty Solar Flares**

Rank	X-ray Intensity	Date (mm-dd-yyyy)	Rank	X-ray Intensity	Date (mm-dd-yyyy)
1	X28e	11-04-2003	11	X12	12-15-1982
2	X20e	08-16-1989	12	X12e	06-04-1991
3	X20e	04-02-2001	13	X12e	06-06-1991
4	X17	10-28-2003	14	X12e	06-11-1991
5	X15e	07-11-1978	15	X12e	06-15-1991
6	X15e	03-06-1989	16	X10	12-17-1982
7	X13e	04-24-1984	17	X10	05-20-1984
8	X13e	10-19-1989	18	X10	01-25-1991
9	X12e	06-06-1982	19	X10	06-09-1991
10	X12e	06-01-1991	20	X10	10-29-2003

** NOAA GOES X-Ray instrument, as observed since 1976. The "e" affixed to the X-ray intensity indicates that the value is estimated since the saturation level for the instrument was reached. By 1993, the saturation level was elevated to the X17.4 level.

Table 2-13: The Top-30 Geomagnetic Storms

Rank	Ap Value	Date	Rank	Ap Value	Date
1	312	09-18-1941	16	220	10-30-2003
2	293	11-12-1960	17	216	07-08-1958
3	285	03-13-1989	18	215	03-28-1946
4	277	03-23-1940	19	214	09-22-1946
5	258	10-04-1960	20	212	03-01-1941
6	252	10-29-2003	21	212	07-26-1946
7	252	07-15-1959	22	203	08-19-1950
8	251	03-31-1960	23	201	09-04-1982
9	241	05-25-1967	24	199	02-07-1946
10	229	07-11-1982	25	199	02-11-1958
11	228	02-07-1986	26	196	05-12-1949
12	226	03-29-1940	26	196	06-04-1991
13	223	08-04-1972	28	195	03-24-1946
14	222	07-05-1941	29	193	05-09-1992
15	221	09-02-1957	30	192	07-14-2000

2.4 MOTIVATION FOR SPACE WEATHER OBSERVATIONS

In this chapter we have examined the nature of solar activity, and have stipulated that a host of events on the sun can give rise to perturbations in the earth's magnetosphere and ionosphere. Electromagnetic radiation does not interact with the geomagnetic field, but X-ray flares can introduce photoionization of atmospheric species. This leads to radiowave absorption in

the lower ionosphere on the sunlit side of the earth. The explosive expulsion of solar cosmic rays (i.e., protons), being deflected toward the polar region, can introduce long-lived radiowave absorption events (i.e., PCA) within the polar cap, and may also introduce radiation hazards for aviation executing transpolar flight plans. While solar flares are a known source of performance impairment for telecommunication systems, the effect of high-energy protons (i.e., solar cosmic rays) and earth-directed coronal plasma (viz., enhanced solar wind and CMEs) are even more important.

For X-ray flares, the impact is virtually immediate; hence the telecommunication system could be designed to compensate by "brute force" rather than through application of diversity techniques. For example, to counter strong power-robbing absorption without trying to play "catch-up", the system should have adequate "margin" incorporated within the design. Often this is too costly. In practice, some systems simply "ride" out the flare effect, which may last less than an hour in most instances, even at HF.

The good news for the non-electromagnetic sources, like CMEs, is that some lead-time is possible for more efficient exploitation by adaptive systems. Moreover the effects usually last awhile. Thus any changes made in system parameters or operational procedures will not have to be undone shortly after making the original change. What a system manager does not want is a situation in which an adaptive subsystem is constantly required to change its operational state. In such a situation, the system spends too much of its time adjusting to the environment, and too little time fulfilling its mission. The overhead required to "chase-down" the telecommunication environment can be too large. This suggests that multiple events that are superimposed can play havoc.

The lesson to be taken from this summary statement is that a timely analysis of solar phenomena can be critical to the successful operation of some telecommunication systems. At the very least, solar observational data sets are critical in forecasting the level of magnetic activity for some time in the future. Having this data might enable an estimation of ionospheric parameter variations from several hours to days in advance.

Table 2-14 is a listing of the solar sources of space weather that have the potential to impair certain classes of telecommunications systems. The ionospheric effects are discussed in Chapter 3 and the system effects are covered in Chapter 4. Forecasting can be used as a countermeasure for systems that are operationally agile or quasi-adaptive in nature. Forecasting systems and real-time data sources are discussed in Chapter 5.

Table 2-14: Solar Sources of Telecommunication System Impairment

Source
Coronal hole
Coronal Mass Ejection (CME)
Energetic Particle (i.e., proton) event
Solar flare
Solar radio burst

- - -

2.5 REFERENCES

Akasofu, S.I., 1964, "The Development of the Auroral Substorm", *Planetary Space Science*, 12:273.

Akasofu, S.I., 1968, *Polar and Magnetospheric Substorms*, D. Reidel Publishing. Co., Dordrecht, Holland.

Akasofu, S.I., 1977, *Physics of Magnetospheric Substorms*, D. Reidel Publishing Co., Boston.

Bohlin, J.D., 1977, "Extreme Ultraviolet Observations of Coronal Holes. 1. Locations, Sizes, and Evolution of Coronal Holes, June 73-Jan 84", *Solar Physics* 51:377-398.

CCIR, 1980, "CCIR Atlas of Ionospheric Characteristics", Supplement No.3 to Report 340, (based upon CCIR Meeting Kyoto, 1978), ITU, Geneva; p.29.

Chapman, S., 1968, *Solar Plasma, Geomagnetism and Aurora*, Gordon and Breach, New York, London and Paris, p.28-32 (references have been made specifically to Figs.1.11 and 1.12 in Chapman's text).

Daglis, I.A. (editor), 2000, Space Storms and Space Weather Hazards, NATO Science Series, Physics and Chemistry, Volume 38, Kluwer Academic Publishers, Dordrecht, Boston, and London, 2000.

Friedman, H, 1985, *Sun and Earth*, Scientific American Books, New York.

Gibson, E.G., 1973, "The Quiet Sun", NASA SP-303, National Aeronautics and Space Administration, USGPO, Washington, DC.

Goodman, John M., 1991, *HF Communication: Science and Technology*, Van Nostrand Reinhold, New York (out-of-print; now available through JMG Associates, 8310 Lilac Lane, Alexandria VA 22308).

Green, A.W, 1990, "Intermagnet, A Prospectus", proposal for global real-time digital geomagnetic observatory network, distributed at First SESC Users Conference, Boulder, CO, 15-17 May 1990.

Hill, T.W. and R.A. Wolf, 1977, "Solar Wind Interactions", in *The Upper Atmosphere and Magnetosphere*, Studies in Geophysics, National Research Council, NAS, Washington, D.C

Jacobs, G. and T.J. Cohen (Editors), 1979, *The Shortwave Propagation Handbook*, Cowan Publishing Corp., Port Washington, NY.

Jensen, D.C., R.W. Murray, and J.A. Welch Jr., 1960, "Tables of Adiabatic Invariants for the Geomagnetic Field, 1955.0", Air Force Special Weapons Center, Kirtland Air Force Base, New Mexico.

Joselyn, J. et al., 1996, "Solar Cycle 23 Project: Summary of Panel Findings", NOAA-SEC panel of experts, sponsored by NASA.

Jursa, A.S. (Scientific Editor), 1985, *Handbook of Geophysics and the SpaceEnvironment*, Air Force Geophysics Laboratory, Air Force Systems Command, U.S. Air Force, NTIS, Springfield, VA.

Knecht, DJ. and B. M. Shuman, 1985, "The Magnetic Field", in *Handbook of Physics and the Space Environment*, edited by A.S. Jursa, AFGL, available through NTIS, Springfield, VA.

Koons, H.C., and D.J. Gorney, 1990, "A Sunspot Maximum Prediction Method Using a Neural Network", *EOS*, AGU Trans., 71(18)677.

Mayaud, P.N., 1980, *Derivation, Meaning, and Use of Geomagnetic Indices*, American Geophysical Union, Washington, DC.

Meier, R.R., 2000, "Aeronomy and Space Weather: "Space Weather Effects and Metrics", article in *The CEDAR Post.*

NOAA-NWS, 2004, "Intense Space Weather Storms October 19 – November 07, 2003", Service Assessment, U.S. Department of Commerce, NOAA, National Weather Service, Silver Spring, Maryland.

Shea, M.A., SA Militello, H.E. Coffey, and J.H. Allen, 1984, *Directory of Solar-Terrestrial Physics Monitoring Stations*, Edition 2, MONSEE Special Publication No.2, published jointly by AFGL (Hanscom AFB, Bedford, MA.) and WDC-A for Solar-Terrestrial Physics (NGDC, NESDIS, NOAA, Boulder, CO.) under aegis of SCOSTEP, AFGL-TR-84-0237, Special Report No.239.

Sheeley, N.R. Jr., J.W. Harvey, and W.C. Feldman, 1976, "Coronal Holes, Solar Wind Streams, and Recurrent Geomagnetic Disturbances, 1973-1976", *Solar Physics*, 49:271.

Sheeley, N.R. Jr., and J.W. Harvey, 1978, "Coronal Holes, Solar Wind Streams, and Geomagnetic Activity During the New Sunspot Cycle", *Solar Physics*, 59:159-178.

Simpson, S., 2003, Massive Solar Storms Inflict Little Damage on Earth", Space Weather Journal, 2003SW000042, 28 November 2003.

Tsurutani, B.T., W.D. Gonzalez, Y. Kamide, and J. Arballo (editors), 1997, *Magnetic Storms*, AGU Geophysical Monograph 98, American Geophysical Union, 2000 Florida Avenue, Washington DC 20009.

Stewart, F.G. and M. Leftin, 1972, "Relationship Between the Ottawa 10.7 cm. Solar Flux and Zurich Sunspot Number", *Telecommunications J*, 39:159-169.

Valley, S.L., (editor), 1965, *Handbook of Geophysics and Space Environments, Air Force Cambridge Research Laboratories*, Office of Aerospace Research, USAF, Hanscom AFB, Bedford, MA.

Whalen, J.A., R.R. O'Neil, and R.H. Picard, 1985, "The Aurora", in *Handbook of the Geophysics and the Space Environment*, edited by A.S. Jursa, AFGL, USAF, NTIS, Springfield VA.

Withbroe, G.L, 1989, "Solar Activity Cycle: History and Predictions!', *J.Spacecraft and Rockets*, 26:394.

Chapter 3
THE IONOSPHERE

3.1 INTRODUCTION

The ionosphere poses an interesting challenge for many radio systems that make use of signal transmission through all or some portion of the medium. Being a magnetoionic medium imbedded in a background neutral atmosphere, it exhibits very interesting refractive properties, including anisotropy, dispersion and dissipation. The laminar ionosphere introduces an array of effects, which are related to the ionospheric component of radio refractivity. These include: ray path bending, phase path increase, group path delay, absorption, Doppler shift, pulse dispersion, Faraday rotation, and magneto-ionic path splitting. Inhomogeneities in the ionosphere give rise to temporal and spatial variations in the effects just cited. An understanding of the ionospheric personality provides information about a wide range of solar-terrestrial interactions, and it has significant space-weather implications. Space weather is a relatively new discipline that includes a wide range of exoatmospheric phenomena of major importance to space systems and their operational effectiveness.

Main features of the ionosphere are well-known although details are still subjects of continuing research. There are many excellent sources of information about the ionosphere, from both a theoretical and experimental perspective. Books by Davies [1965,1987,1990], Ratcliffe [1972], and Giraud and Petit [1978] should be consulted. Theoretical and plasma physics aspects of the ionosphere have been discussed in a book by Kelley [1989]. A readable account of the basic physics of the ionosphere has been developed by Rishbeth [1991]. Other useful references that place the ionosphere within a larger context of the geospace weather system include the Air Force Handbook of Geophysics and the Space Environment [1985], and an Introduction to the Space Environment by Tascione [1988]. Various techniques for probing the ionosphere have been described in a monograph by Hunsucker [1991]. From a practical perspective, Goodman [1991], Johnson et al. [1997], and McNamara [1991] have published expositions on the ionosphere in connection with radio system applications. There are also proceedings of topical conferences and workshops. The Ionospheric Effects Symposia [Goodman, 1975, 1978, 1981, 1984, 1987, 1990, 1993, 1996, 1999, and 2002] have chronicled ionospheric research activities and applications since the early 1970s; and the Commission of the European Communities has published reports dealing with ionospheric prediction and modeling [Bradley, 1999] [Hanbaba, 1999].

The purpose of this chapter is to provide a general understanding of the ionosphere. The emphasis is on those ionospheric processes and phenomena that are encountered by users of radio propagation systems. More complete descriptions of the underlying physical processes may be found in various references cited in the text. At IES2002, a session of ionospheric modeling was convened, and a summary is found in Section 3.12.4. We conclude the chapter with science issues and challenges.

3.2 GENERAL PROPERTIES OF THE IONOSPHERE

3.2.1 Basic Structure

The ionosphere is an ionized region in the upper atmosphere that, by generally accepted convention, lies between an altitude range of 60-1000 kilometers. Nevertheless the region above 1000 kilometers but below 2000 kilometers, called the protonosphere, is also ionized and may be an important region when considering the totality of ionization effects on radio systems. As a matter of convenience, some specialists have combined the ionosphere and protonosphere into a single region of ionization. For example, the integrated electron density from a ground station to a geosynchronous satellite (referenced to the vertical) is referred to as the total electron content of the ionosphere (i.e., TEC), even though both ionospheric and protonospheric electrons contribute to the integral. For the purpose of this article, we shall use the more restricted definition for the ionosphere, generally placing the upper limit at approximately 1000 kilometers. While there are equal numbers of free electrons and positive ions within the ionosphere, it is the electron number density that characterizes the array of interesting phenomena associated with the region. The ionosphere is imbedded in the earth's magnetic field and this situation influences the distribution of the ionized constituents. A clear indication of this may be seen in the worldwide distribution of electron density in the upper ionosphere that tends to be best organized by geomagnetic rather than geographic coordinates. Moreover, being a magnetoionic medium, the ionosphere has a profound impact upon radiowaves that interact with the medium.

The ionospheric electron density distribution is logically evaluated first in terms of its height profile, followed by its geographical and temporal variabilities. Even though there is abundant evidence suggesting a rather complex electron density profile comprised of several peaks and valleys, the basis for understanding fundamental properties of the ionosphere comes from a simple picture of an ionized medium dominated by a single region, or layer, having a distinct maximum in electron density. This is not without some justification since the highest and thickest component region, the so-called F

layer, typically exhibits the greatest electron density. Moreover, in many radiowave applications, it is the F layer that exhibits the dominant interaction. Figure 3-1 depicts the various regions or layers of the ionosphere in terms of the electron number density. It has been observed that the height profile varies diurnally, seasonally, and as a function of solar activity.

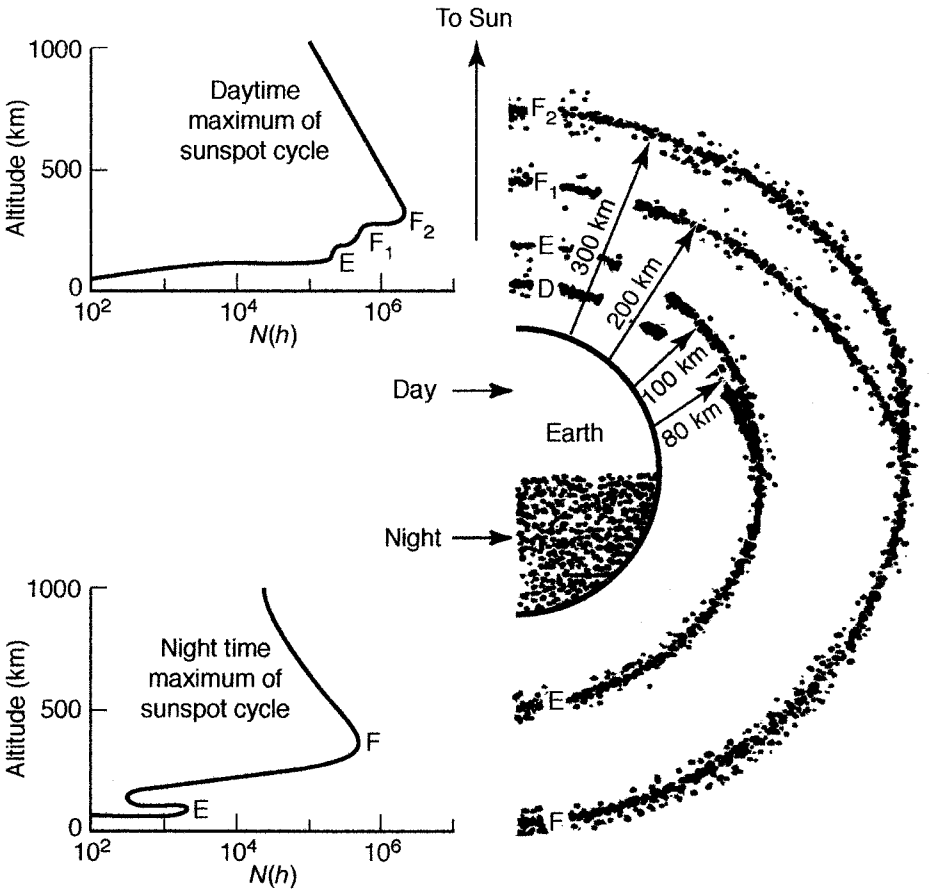


Figure 3-1: Depiction of the Ionospheric Layers for middle latitudes, including the day to night variation. Solar cycle variations are suggested in the cartoon, but seasonal effects are suppressed. The daytime ionosphere is defined by three "refractive" layers: the E-region, the F1-region (or ledge), and the F2-region. The ionosphere also has an "absorption" layer principally for shortwave propagation, termed the D-region. The D-region extends from ~ 50 km to the base of the E-region. The nominal altitude of the ionization peaks for the various layers are: D-region (60 km), E-region (100 km), F1-region (200 km), and F2-region (300 km). However, large variations may occur, especially in the F2-region. During the nighttime, the E- and F1-regions vanish due to recombination. The F2-region diminishes slowly following ionospheric sunset, since electronic loss is governed by an attachment process that has a low cross section. The F2 layer exhibits significant variability that is not under solar control. Overall, the ionosphere exhibits higher ionization densities in the daytime. Cartoon derived from Goodman [1991] and a variety of public domain sources.

3.2.2 Formation of the Ionosphere

The sun exerts a number of influences ever the upper atmosphere, but the interactions of most importance for our discussion are photodissociation and photoionization. Figure 3-2 depicts the neutral atmosphere, its various regions and the depth of penetration of the various components of solar flux.

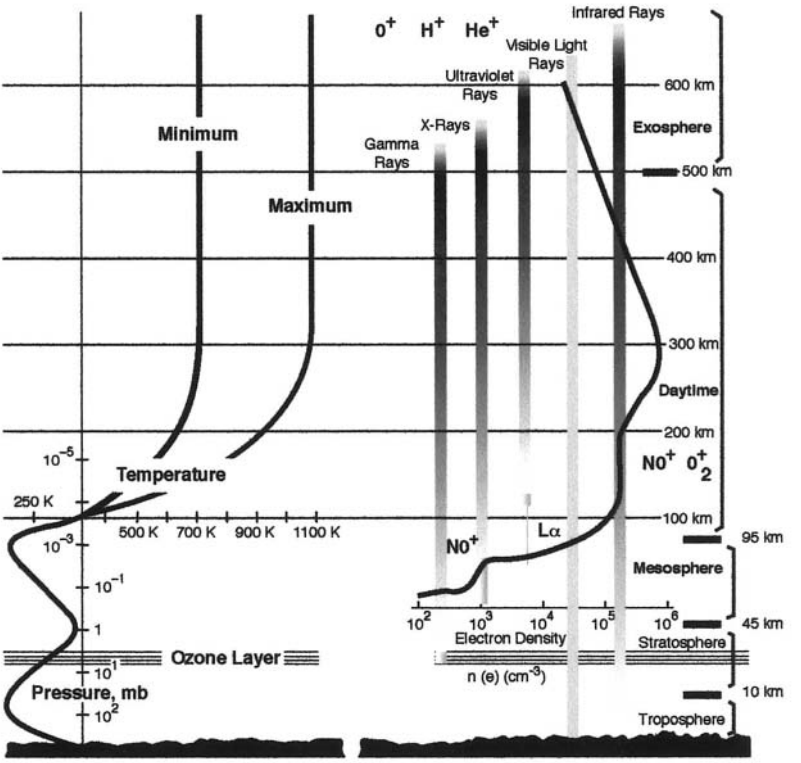


Figure 3-2: Atmospheric and Ionospheric Layers. The primary atmospheric regions are nominally: troposphere (0-10 km), stratosphere (10-45 km), the mesosphere (45-95 km), the thermosphere (95-500 km), and the exosphere (> 500 km). The bulk of the D-region is within the mesosphere. The majority of the ionospheric electron content resides within the thermosphere. The protective ozone layer lies within the stratosphere. The depth of penetration of the solar radiation is also depicted. Large variations in penetration depth exist for specific bands. Below 200 km, the ionosphere is dominated by polyatomic species, a fact that favors recombination processes. Between 200 and 600 km, the F-region is predominantly monatomic oxygen. Eventually an altitude is reached where atomic hydrogen dominates and helium is in evidence, and this region is called the protonosphere. From National Research Council report [NRC, 1981].

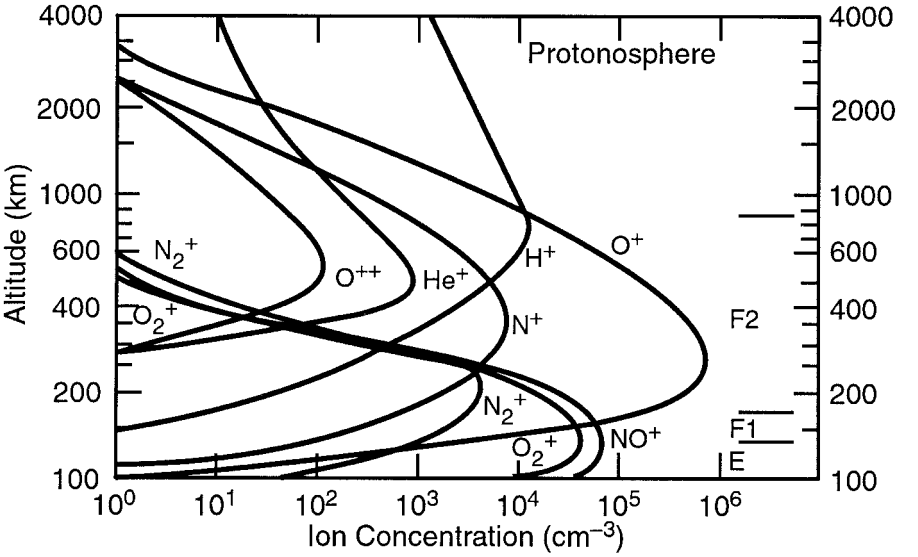


Figure 3-3: Profiles of ion concentration, as a function of height, for midlatitude daytime conditions. Note that even where the ionization density is greatest (i.e., the F2 peak), the neutral density is still larger by several orders of magnitude. There is a distinct E-F valley of ionization during nocturnal hours, which is deeper at solar minimum. This region can be a ducting vehicle for trapping of shortwave signals. Figure from Jursa [1985].

In the lower atmosphere, species such as N_2 and O_2 dominate the constituent population even though other species such as water vapor, carbon dioxide, nitric oxide, and trace element gases are influential in specific contexts. In the upper atmosphere, however, molecular forms are dissociated by incoming solar flux into separate atomic components. Formally the lowest portion of the ionosphere is the so-called D-layer at an altitude of ~ 60 Km ± 20 Km, but the free electron and ion population rises dramatically at an altitude of ~ 100 Km, which is the median altitude of the E-layer. Two things occur at this altitude. First, oxygen becomes dissociated as a result of solar UV radiation. Secondly, the mixing process of the atmosphere, so efficient below 100 Km, ceases rather dramatically, and the region where this occurs is called the turbopause.. This process of dissociation is so efficient that we refer to the distribution of neutral species in a vast segment of the upper atmosphere (i.e., above 200 Km) as a monatomic gas. In the lower atmosphere (i.e., below roughly 200 Km), the gas is largely polyatomic,

although the transition between the two regimes is rather gradual between 100 and 200 Km. This has implications for the lifetime of ion-electron pairs created through photoionization. Also, in the altitude regime above about 200 Km and well above the turbopause, collisions become a rarity with mixing of the various species becoming unimportant in comparison with diffusive forces. As a consequence, diffusive separation occurs, with constituents of the neutral gas seeking their own unique height distributions dictated by their atomic masses, the gas temperature, and the acceleration of gravity. Figure 3-3 shows height profiles of ionic species in the upper atmosphere, and Figure 3-4 contains typical distributions of midlatitude electron density for daytime and nighttime under solar maximum and minimum conditions.

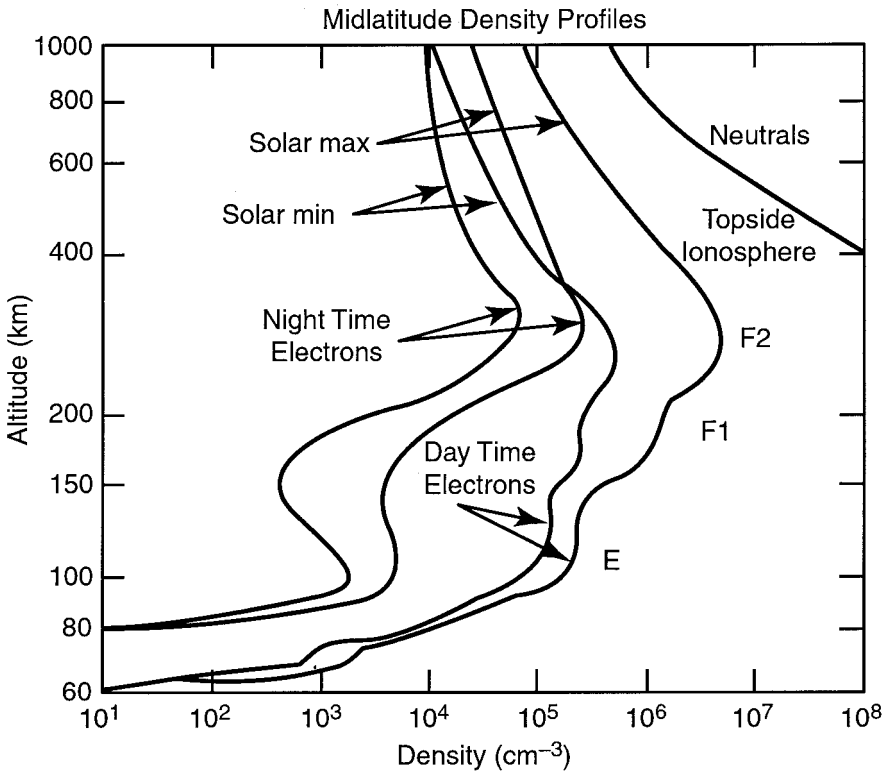


Figure 3-4: Electron Density Distributions for day/night and solar maximum/minimum conditions. Note the dominance of atomic oxygen within the F2-region, where the molecular species have suffered considerable dissociation. Nitric oxide (singly-ionized) is dominant between 100 and 200 km. From Jursa [1985].

It may be seen that ionized monatomic oxygen is the majority ion between roughly 180 and 800 kilometers, and is wholly dominant between about 200 and 500 Km. Atomic hydrogen ions become important above 500 Km, and the region from about 800 to 2000 kilometers is called the protonosphere. It should also be noted that above 500 Km (i.e., the base of the exosphere), the neutral atmosphere is virtually collisionless and particles tend to move about freely. On the other hand, electrons and ions in the exosphere are still influenced by the earth's magnetic field and electrodynamic forces. The electron density distributions in the ionosphere and protonosphere are variable. Because of this, the boundary between the ionosphere and the protonosphere is not sharply defined, being dependent upon a number of factors including time-of-day, season, and solar activity. The protonosphere is often referred to as the plasmasphere, especially by magnetospheric scientists and propagation specialists engaged in measurements of the total electron content (TEC) of the ionosphere using GEOs.

3.2.3 Ionospheric Layering

Table 3-1 provides information about the various ionospheric layers, the altitude ranges of each, the principal ionic constituents, and the means of formation. A comment is appropriate here on the nature of ionospheric layering with some emphasis on the historical distinctions made between the words layer and region as they pertain to the ionosphere. Often the terms are used interchangeably, and while neither is generally preferred, region is the more accurate description. This is because it does not convey the incorrect impression that sharp discontinuities in electron density exist at well-defined upper and lower boundaries. This is especially the case for the F region, and to a lesser extent in the D and E regions. From an historical perspective, the concept of layering derives from the appearance of the ionospheric regions on vertical incidence ionospheric soundings, called ionograms (see Section 3.4.1). Furthermore, the alphabetic designation of the ionospheric regions was also based upon the early sounding studies. On the other hand, there are certain situations for which the restrictive term layer is acceptable. For example, the normal E region may occasionally be characterized by an electron density profile displaying a degree of boundary sharpness. Aside from this, the most significant localized concentration of free electrons in the ionosphere is called sporadic E (or Es) that exists as an isolated layer within the boundaries of the normal E region (see Section 3.7). Since the Es layer exhibits a generally unpredictable temporal and geographical distribution, it is termed sporadic, and because of its limited geographical extent, it is sometimes referred to as a sporadic E patch.

As indicated above, the ionosphere is often described in terms of its component regions or layers. These were the so-called D, E and F regions. These designations are largely based upon data obtained from crude sounder (i.e., ionogram) measurements undertaken in the 1920s and 1930s. These early measurements often exhibited evidence for an additional layer between regions E and F in the daytime ionosphere. This led to the notion that the F region is actually comprised of two distinct regions (i.e., F1 and F2) having different properties. The lowest region of the ionosphere, the D region, is important in the characterization of absorption losses for short-wave systems, but is important as a reflecting layer for longwave communication and navigation systems. There is also evidence for a bifurcation in the D region, with the upper portion (i.e., above 60 Km) being produced by solar flux, and with the lower portion (i.e., below 60 Km) being produced by galactic cosmic rays.

Table 3-1: Properties of the Ionospheric Layers

Region	Height Range (km)	N_{max} Range (m^{-3})	f_p (MHz)	Major Ingredients(s)	Basis of Formation
D	70 to 90	10^8 to 10^9		NO^+, O_2^+	Lα x-rays
E	90 to 130 h_{max} ~110	~10^{11} (day) ~10^{10} (night) (smooth diurnal variation)	~0.3 (night) ~3.0 (day)	O_2^+, NO^+	Lβ x-rays; Chapman Layer
Es	90 to 130	~10^{12} (highly variable)		Metallic Ions	Wind shear and meteoric derbis; equatorial electrojet; Auroral electrojet and precipitation
F_1	130 to 210 h_{max} ~180	~2×10^{11} (day) ~0 (night) (smooth diurnal variation)	~3 to 6 (day) (merges with F_2 layer at night)	O^+, NO^+	Helium II Line; UV Radiation; Chapman Layer
F_2	200 to 1000 h_{max} ~300	~10^{12} (day) ~2×10^{11} (night) (asymmetric diurnal variation)	~5 to 15 (day) ~3 to 6 (night) (presunrise minimum)	O^+	Upward diffusion from the F_1 Layer; photoionization

Ground-based vertical incidence sounder measurements have provided the bulk of our current information about ionospheric structure (see Section 3.4.1). Through application of ionogram inversion technology to account for the radiowave interaction effects, individual sounder stations provide information about the vertical distribution of ionization to the altitude of the F2 maximum (i.e., 300-400 Km). In addition, the worldwide distribution of these systems has allowed a good geographical picture to be developed using sophisticated mapping algorithms. These measurements are somewhat limited in the characterization of certain features such as the so-called E-F valley, and they cannot evaluate ionization above the F2 maximum. There is also a paucity of data over oceanic regions. Satellite measurements (viz., topside sounders and in-situ probes) have been invaluable in the characterization of F-region ionization density over oceanic regions. Rocket probes and incoherent backscatter radar measurements, which provide a clearer representation of the true electron density profile, typically reveal a relatively featureless profile exhibiting a single F region maximum with several underlying ledges or profile derivative discontinuities. Nevertheless, a valley of ionization may often be observed between the E and F regions. Ionization above the F2 maximum may be deduced from satellite probes and Thomson scatter radars, but a large amount of information has been derived from total electron content measurements using Faraday rotation or group path measurements of signals from geostationary satellites or Global Positioning System (GPS) satellites. Hunsucker [1991] describes various ionospheric measurement techniques.

Simple layering occurs as the result of two factors. First, the atmospheric neutral density decreases exponentially with altitude, while the solar ionizing flux density increases with height above sea level. This leads to the formation of single region for which the ionization rate is maximized, and ultimately results in a layer having the so-called Chapman shape. This shape is based upon a simple theory advanced by Sidney Chapman [1931] (see Figure 3-5). We observe nonetheless a degree of structure in the ionosphere, which suggests more than one layer. One cause for multilayer formation is the existence of a multicomponent atmosphere, each component of which possesses a separate height distribution at ionospheric altitudes. But there are other factors. Solar radiation is not monochromatic, as suggested in simple Chapman theory, and it has an energy density that is not evenly distributed in the wavelength domain. Furthermore, its penetration depth and ionization capability depends upon wavelength and atmospheric constitution. All of this results in a photoionization rate, and an associated electron density profile, that are structured functions of altitude. It has been shown that the Chapman model is valid for the D, E, and F1 regions but is not generally valid for the F2 region.

3.2.4 Chapman Layer Theory

One of the basic tenets of Chapman theory is that solar radiation will penetrate to an altitude for which the total number of atoms or molecules P (populating a column of unit cross sectional area directed toward the sun) is equal to the inverse of the absorption (or interaction) cross section a. In other words $P = I/a$. The peak in ionization will be produced in the neighborhood of that altitude, and the concept is valid for oblique solar illumination as well as for the case in which the sun is directly overhead. It is convenient to look at the production rate in terms of its deviation from the peak (overhead) value at height h_0. For this it is useful to define a reduced height z, corresponding to the normalized departure of an arbitrary value of ionospheric height h from h_0.

$$z = (h - h_0)/H \tag{3.1}$$

where h_0 is the peak height for vertically-incident radiation from the sun, and H is the neutral scale height given by the following expression:

$$H = kT/mg \tag{3.2}$$

where k is Boltzmann's constant, T is the absolute gas temperature, m is the atomic or molecular mass, and g is the acceleration of gravity.

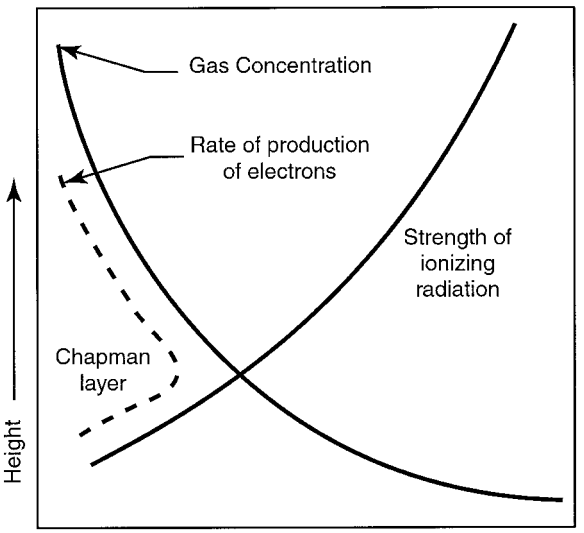


Figure 3-5: An idealized representation of the ionization production in the atmosphere as the solar radiation encounters a neutral gas with exponentially increasing density (with decreasing altitude).

Within the thermosphere (with h above ~ 100 Km), the gas temperature is monotonically increasing, reaching an asymptotic level near the base of the exosphere. The temperature rises from ~ 180°K at the mesopause (and incidentally near the turbopause) to levels approaching a diurnal range of 600 - 1100°K at solar minimum and 800 - 1400°K at solar maximum. The heat sources include solar radiation, the dissipation of atmospheric gravity waves, and particle precipitation. The asymptotic levels of T are due to limits on the thermal conductivity of the gas. The scale height H is a convenient parameter since it may be used as a measure of layer thickness for an equivalent fixed density slab. More importantly, it has a physical meaning. If the atmosphere is in diffusive equilibrium governed by the force of gravity and the gas pressure gradient and N is the atomic or molecular gas density (as appropriate), we have:

$$N = N_0 \exp(-h/H) \tag{3.3}$$

$$H = [(1/N)|dN/dh|]^{-1} \tag{3.4}$$

where N_0 is the atomic or molecular density at some reference height.

In a diffusively separated atmospheric environment, each constituent has its own unique scale height governed by its own molecular (atomic) mass. In an ionized gas in which the electrons and ions are coupled by electrostatic forces, the effective value of the mean molecular mass is ~ ½ the mass of the positive ion. This is because the mass of the electron is essentially zero in comparison with the ion mass.

Figure 3-6 depicts the production rate curves associated with an ideal Chapman-like production profile and a range of solar zenith angles, χ. It is seen that there are a number of curves, parameterized in terms of χ, for which the production rate maxima, q_{max}, may be observed. The largest q_{max} occurs for $\chi = 0$ (overhead case corresponding to $q = q_0$), and we see that other values for q_{max}, corresponding to oblique geometries wherein $\chi \neq 0$, will decrease in magnitude and occur at increasing heights as χ becomes larger (i.e., sun moves toward the horizon). Chapman theory yields the following rate of production formula:

$$q = q_0 \exp\{1 - z - \sec\chi \exp(-z)\} \tag{3.5}$$

At altitudes well above the peak in q, the rate of electron production drops off in an exponential fashion imitating the exponential decrease in gas pressure with height. In order to relate Chapman production curves to actual

electron density distributions, we must examine loss processes and certain dynamical factors.

3.3 EQUILIBRIUM PROCESSES

The equation that expresses the time rate of change of electron concentration, N_e , is the continuity equation:

$$d N_e /dt = q - L(N_e) - div (N_e V) \tag{3.6}$$

where N_e is the electron density, $L(N_e)$ is the loss rate, which is dependent upon the electron density, *div* stands for the vector divergence operator, and V is the electron drift velocity.

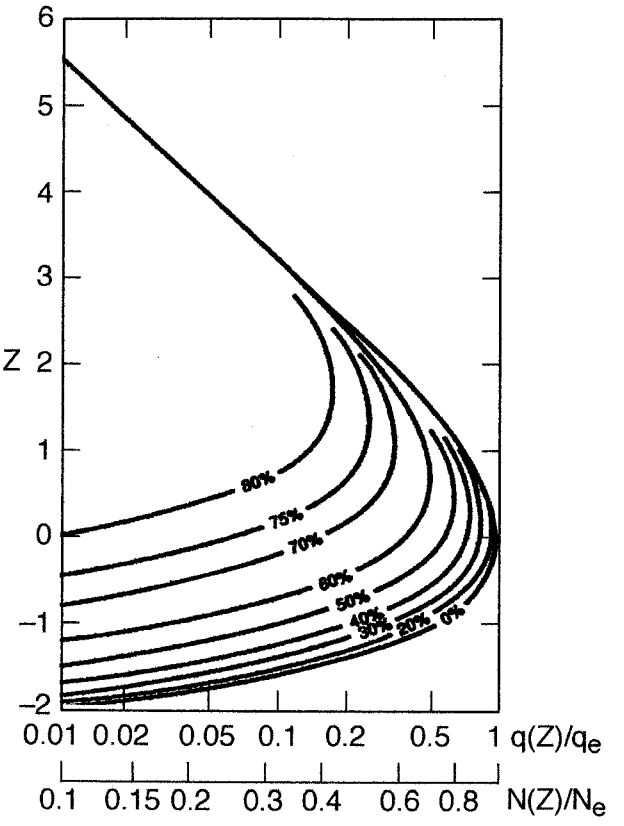


Figure 3-6: Rate of electron production as a function of reduced height (h-h_0) and for selected values of the solar zenith angle. From Davies [1965].

The divergence of the vector in Equation 3.6 is the transport term, sometimes conveniently called the "movement" term. The continuity equation says that the time derivative of electron density within a unit volume is equal to the number of electrons that are generated within the volume (through photoionization processes), minus those that are lost (through chemical recombination or attachment processes), and finally adjusted for those electrons that exit or enter the volume (as expressed by the transport term). To first order, the only derivatives of importance in the divergence term are in the vertical direction, since horizontal N_e gradients are generally smaller than vertical ones. In addition, there is a tendency for horizontal velocities to be relatively small in comparison with vertical drift velocities. Consequently, we may replace $div\ (N_e\ V)$ by $d/dh\ (N_e\ V_h\ )$ where V_h is the scalar velocity in the vertical direction. We rewrite Equation 3.6 as follows:

$$d\,N_e/dt = q - L(N_e) - d/dh\ (N_e\ V_h) \tag{3.7}$$

Now let us look at some special cases. If $V_h = 0$ (no movement), then the time variation in electron concentration is controlled by a competition between production q and loss L. At nighttime, we may take $q = 0$, and this results in

$$d\,N_e/dt = - L(N_e) \tag{3.8}$$

In principle, there are two mechanisms to explain electron loss: one defined by attachment of electrons to neutral atoms (in the upper ionosphere), and the second defined by recombination of electrons with positive ions (in the lower ionosphere). The attachment process is proportional to N_e alone, while recombination depends upon the product of N_e with N_i, where N_i is the number of ions. The process of attachment involves radiative processes and results in an extremely low cross section (probability of occurrence). We may ignore it in many practical situations and take recombination as the only major source for electron loss. Since $N_e = N_i$, the recombination process obeys the equation $L = \alpha\ N_e^2$, where α is the recombination coefficient. Recombination is very rapid in the D and E regions, the process being accomplished in the order of seconds to minutes. Attachment, the electron loss process for the upper ionosphere, has a time constant of the order of hours. This is the primary reason that the ionosphere does not entirely disappear overnight. Another reason is that there exists a second source of electrons associated with the plasmasphere, This reservoir of ionization is built up during the daytime through vertical drift, but "bleeds" into the ionosphere during nocturnal hours.

In the vicinity of local noon, $dN_e / dt = 0$ and we may analyze the quasiequilibrium conditions suggested by Equation 3.7 when the left hand side of the equation = 0. The two main types of equilibrium processes are given in Table 3-2. The equilibrium processes identified in Table 3-2 are the dominant possibilities during daytime when photoionization is significant. During nocturnal hours, equilibrium is seldom achieved at F region heights, although it is approached in the period before sunrise.

Table 3-2: Types of Equilibrium Processes

Type	Property	Equation
Photochemical	Production balanced by loss	$L(N_e) >> d/dh\ (NeV_h)$
Drift	Production balanced by drift	$L(N_e) << d/dh\ (NeV_h)$

While the continuity equation appears quite simple, the generic terms (i.e., production, loss, and transport) represent a host of complex photochemical and electrodynamic processes, which exhibit global variations and are influenced by nonstationary boundary conditions within the atmosphere and the overlying magnetosphere. Notwithstanding these complications, the equation provides a remarkably clear view of the basic processes that account for ionospheric behavior. In fact, the relative contributions of terms in the continuity equation will account for the majority of the anomalous ionospheric properties; that is, those ionospheric variations which depart from a Chapman-like characteristic. This is especially true for the F2 layer within which the movement term attains paramount status. In the E and F1 regions where the movement term is small compared with production and loss (through recombination), photochemical equilibrium exists in the neighborhood of midday. All of this has had a significant bearing on the development of ionospheric models and prediction methods. Indeed, as it relates to the F region of the ionosphere, it may be said that the existence of a nonvarishing divergence term in the continuity equation has been the primary impetus for the development of statistical modeling approaches. Nevertheless, efforts to account for all terms in the continuity equation through physical modeling are ongoing.

The underlying assumptions used by Chapman in his theory of layer production are in substantial disagreement with observation. The Chapman layer was based upon an isothermal atmosphere, and it is well known that the atmosphere has a scale height, kT/mg, which varies with height. Moreover, the basic theory assumes a monochromatic source for photoionization and a single constituent gas. Corrections and extensions to the early Chapman theory have led to better agreement with observation and, to this day, the

Chapman layer provides a fundamental baseline for ionospheric profile modeling.

3.4 DESCRIPTION OF THE IONOSPHERIC LAYERS

3.4.1 Sounder Measurement Method

In any discussion of the ionospheric electron density distribution, it is important to recognize that many experimental methods have been used to arrive at our current understanding. The major ones include: ground-based vertical incidence sounding (VIS), topside sounding using satellite platforms, incoherent backscatter radar, the Faraday rotation and signal delay of satellite signals, as well as in-situ measurements using rocket probes and satellites. The VIS method, which employs the High Frequency (HF) band, was the earliest method and has provided the most comprehensive picture of the lower ionosphere and its worldwide distribution. The ionospheric D layer is an exception, and special methods are needed to determine the electron densities in that region. Much of the current nomenclature involving ionospheric structure and phenomena is a carryover from early VIS investigations. As a consequence we shall briefly examine the VIS method. For a discussion of other methods, the reader is referred to Hunsucker (1991).

The plasma frequency associated with an electron gas, f_p (a natural resonant frequency), is proportional to the square root of the electron density of the gas.

$$f_p = 8.98\ N_e^{1/2} \tag{3.9}$$

where f_p is in Hz and N_e is expressed in electrons per cubic meter.

It may be shown that a radiowave, propagating vertically upward into the ionosphere, will penetrate the region until it reaches a point at which the sounding frequency matches the plasma frequency. All frequencies less than this value will be reflected back to ground. An ionospheric sounder is essentially a radar, which maps out the height-dependent ionospheric electron concentration versus transmission frequency, where the probing frequency is typically a stepwise increasing function of time. A plot of signal echo time delay versus transmission frequency is called an ionogram. A typical ionogram and the corresponding ionospheric profile are given in Figure 3-7.

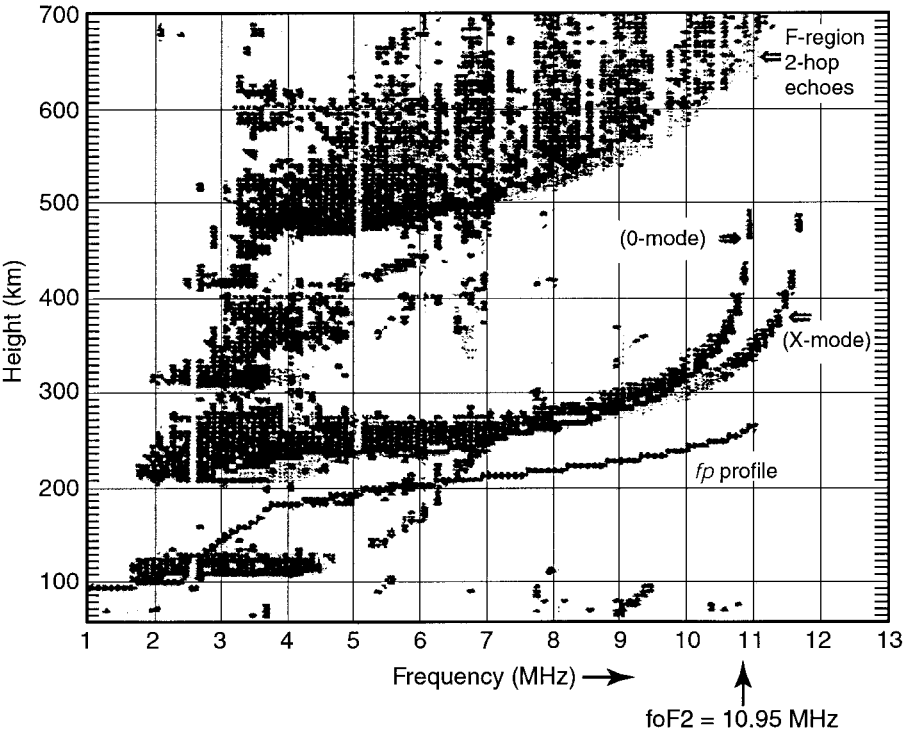


Figure 3-7: A typical vertical-incidence ionosonde recording (i.e., ionogram) and the plasma frequency profile *fp(h)*. The electron density profile is related to the plasma frequency profile by equation 3-9 in the text. This ionogram was obtained from the NOAA-NGDC web site and the sounder instrument was developed by the University of Massachusetts at Lowell for the U.S. Air Force. Information derived from the National Geophysical Data Center, Boulder, CO, NOAA, Department of Commerce.

If N_{max} is the maximum electron density of a layer, then we define a so-called critical frequency of reflection, f_c, which is the maximum plasma frequency within the layer. If the sounder transmission frequency exceeds f_c, then the signal is not reflected and penetrates the layer. There are as many critical frequencies in the ionosphere as there are layers or regions. A more complete treatment of the theory of radio propagation in the ionosphere shows that a magnetoionic medium supports 2 modes of propagation, the so-called ordinary (i.e., O-mode) and the extraordinary (X-mode). These modes encounter slightly different indices of refraction and thus travel with slightly different velocities and directions. As a consequence, each ionogram consists of two traces corresponding to O- and X-mode echoes. These traces may be closely aligned over a large portion of their respective propagation bands but can depart significantly at their respective critical frequencies, with the X-

mode supporting somewhat higher frequency signal reflections. By convention, the O-mode trace is used for conversion of ionogram critical frequencies into maximum electron densities. The following convenient expression is used:

$$N_{max} = 1.24 \times 10^{10} f_o^2 \tag{3.10}$$

where f_o is the ordinary ray critical frequency (MHz) and N_{max} is the maximum electron density of the given layer (electrons/cubic meter). Equation 3.10 is equivalent to Equation 3.9.

From an historical perspective, it is interesting to note that the concept of radar detection of aircraft derived from the early work of ionospheric specialists who were already using ionospheric sounders as a means to "detect" ionospheric layers (see Chapter 1).

3.4.2 The D Region

The D region is responsible for most of the absorption encountered by HF signals, which exploit the skywave mode. In most instances, D region absorption is a primary factor in the determination of the lowest frequency that is useful for communication over a fixed skywave circuit. In addition, the D region supports longwave propagation at VLF and LF, and the medium is exploited in certain legacy navigation systems and strategic low-rate communication systems. The sounder method as described in the previous section is not useful for measurement of the D region since the electron densities are relatively low. Details of D region electron concentration are sketchy in comparison with information available about the E and F regions, principally because of the difficulty in making diagnostic measurements. Moreover, analysis is hampered because many photochemical processes with poorly defined reaction rates take place in the D region. Over 100 reactions have been compiled.

Table 3-1 shows that the D region lies between 70 and 90 Km. In fact, the upper and lower levels are not precisely defined. It is evident that more than one source of ionization gives rise to the D region electron density distribution. Sources include solar radiation at the upper levels and galactic cosmic rays at lower levels. In addition, relatively rare polar-cap absorption events (i.e., PCA) are characterized by highly energetic solar protons that provide an additional source for ionization of the lower D region within the polar cap. Some investigators place the lower boundary of the D region at 50 Km to account for the contribution of galactic cosmic rays in the neighborhood of 50-70 Km. This altitude regime, termed the C region, is not produced by solar radiation. It exhibits different characteristics from the

region between 70 and 90 Km. Specifically, a minimum in electron concentration is observed during solar maximum for the lower portion (viz., region C) while the reverse is true in the upper portion (viz., region D). This can be explained if we assume that the galactic cosmic ray source is partially diverted from the earth by an increase in the interplanetary magnetic field (IMF), which generally occurs during solar maximum conditions.

3.4.3 The E Region

In an (alpha) Chapman layer for which photochemical equilibrium has been established, the following equation represents the electron density distribution as a function of reduced height z:

$$N_e(z) = (q_o/\alpha)^{0.5} \exp [(1 - z - e^{-z} \sec \chi)] \quad (3.11)$$

where α is the recombination coefficient, χ is the solar zenith angle, and q_0 is the maximum production rate in the layer.

Recall that α is the recombination coefficient (see Section 3.3). The quantity (q_o/α) is dependent upon sunspot number and is specific to the region involved, in this case the E-region. The maximum rate of electron production q_0 occurs only for the overhead sun. However, it may be shown that actual maxima for other zenith angles are simply related by this expression:

$$q_{max} = q_0 \cos \chi \quad (3.12)$$

It may be shown that the ordinary ray critical frequency for the E-region, which is directly related to the E-region maximum electron density through Equation 3.10, may be found from Equation 3.11, and is given by:

$$foE = \kappa (\cos \chi)^n \approx \kappa (\cos \chi)^{0.25} \quad (3.13)$$

where κ is a constant of proportionality, which is dependent upon the sunspot number. The exponent n tends to a value 0.25 in terms of the long-term seasonal behavior, and in compliance with Chapman theory, but some workers have found that a value for $n \cong 0.3$ better represents the diurnal dependence. The constant of proportionality κ ranges between about 3 and 4 MHz, bearing in mind that equation 3 represents a climatological median value.

The solar activity dependence of the ratio of peak production to the effective loss (recombination) coefficient has been studied by a number of workers, and the results enable values of *foE* to be deduced. There have also been direct measurements of *foE* using vertical incidence sounders. While

there is some variability to be considered, it is possible to develop a relationship between the median value of *foE*, and the solar zenith angle, and the 12-month running-mean sunspot number. A generally accepted candidate for the daytime E-region critical frequency is:

$$foE(MHz) = 3.3\ [\ (1 + 0.008\ R_{12})\ \cos\chi\ ]^{0.25} \qquad (3.14)$$

where *foE* is given in MHz and R_{12} is the running 12-month sunspot number that may range between roughly 10 and 150.

Equation 3.14 provides an excellent agreement with observation during the daytime, but alternative expressions are found to be more appropriate during the nighttime hours [Davies, 1990]. Moreover, it has been found that Equation 3.14 is inaccurate in the very high latitudes where other means of electron production become important, invalidating the Chapman hypothesis. Internationally adopted relations for monthly median *foE* are due to Muggleton [1975]; and an alternative relation, specific to the European region, has been published [Bradley, 1999].

Figure 3-8a contains an E region critical frequency map for summer solstice conditions in 1958, a period of high solar activity (i.e., R_{12} large). The contours are representative of median conditions as a function of geographic latitude and local time. It is seen that the E-region critical frequencies (and consequently the electron densities) are vanishingly small in those regions devoid of solar illumination. This summer solstice behavior is consistent with Equation 14, and other seasons have also been shown to behave in conformance with $(\cos\chi)^{0.25}$ as well.

Figure 3-8b shows the monthly variation of *foE* for a specified station (i.e., Ft. Belvoir, Virginia) for the year 1958. The solar control is obvious in the median data being plotted.

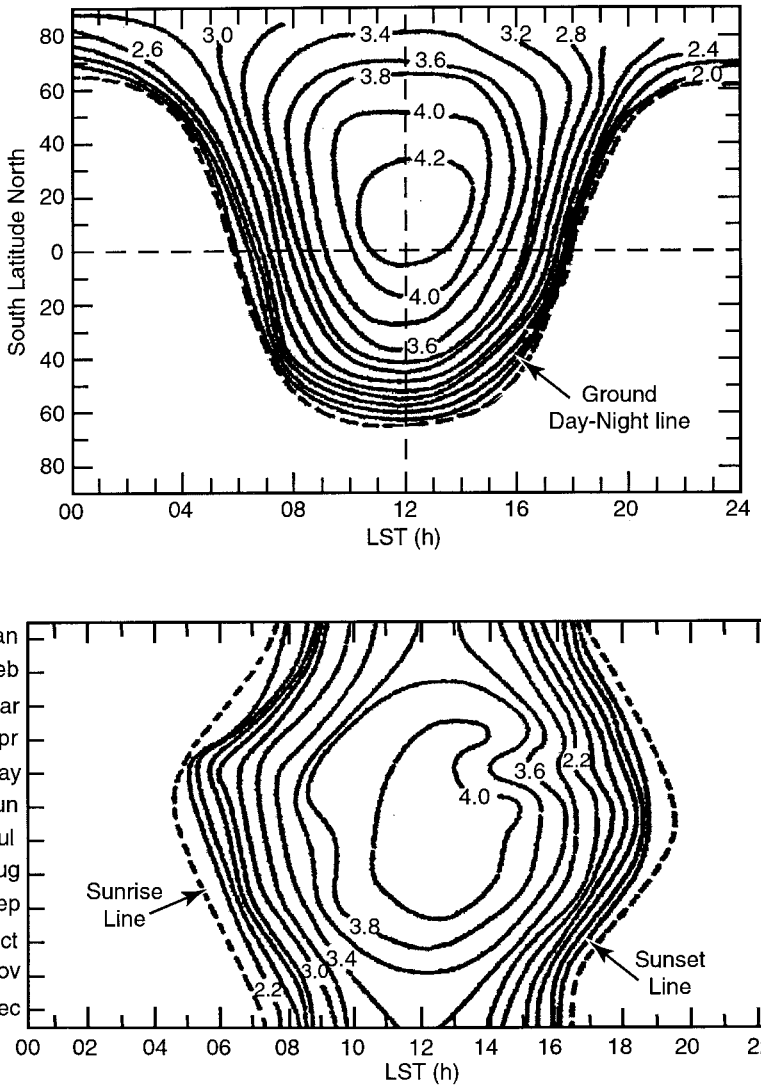


Figure 3-8: (a) Depiction of the local time (LST) and the latitude dependence of *foE* for solar maximum conditions in summer. (b) Contours of *foE* at Fort Belvoir, Virginia in 1958 (solar maximum), showing seasonal variations. The contours are in MHz. From Davies [1965].

3.4.4 The F1 Region

The F1 region is not unlike the E region in the sense that it obeys many of the features of Chapman theory. We look for a relation, which is formally similar to Equation 3.13. A recipe for *foF1* patterned after Chapman principles may be expressed as:

$$foF1 = f_s (\cos \chi)^n \tag{3.15}$$

Like the E region, the F1 region exhibits more complicated behavior than that expressed by such a simple recipe. Specifically, it has been found that the geomagnetic latitude tends to exhibit some control over the F1 region electron densities. The term f_s in Equation 3.15 depends upon sunspot number and magnetic latitude. It is also observed that the F1 region disappears (i.e., merges with the F2 region) at values of the solar zenith angle exceeding a certain value. This value itself depends upon both the sunspot number and the geomagnetic latitude. The Radio Sector of the International telecommunications Union (ITU-R, previously the CCIR) has developed a method for computing foF1 taking all these factors into account [Muggleton, 1975]. The internationally adopted monthly median *foF1* formulation is based on the work of Ducharme et al. [1973]. The relation due to Davies [1990] gives a convenient but approximate expression for the F1-layer critical frequency:

$$foF1 = (4.3 + 0.01 R_{12}) \cos^{0.2} \chi \tag{3.16}$$

Figure 3-9 shows the solar zenith angle control of *foF1* under sunspot maximum and minimum conditions.

The height of the F1 ledge, *hF1*, is taken to be range between 180 and 210 Km. From Chapman theory we anticipate that *hF1* will be lower in summer than in winter, and will be higher at midlatitudes than at low latitudes. Unfortunately the reverse is true. Explanations for this behavior may be found in a detailed study of scale height gradients, a nonvanishing movement term (as expressed in the continuity equation), or gradients in upper atmospheric chemistry.

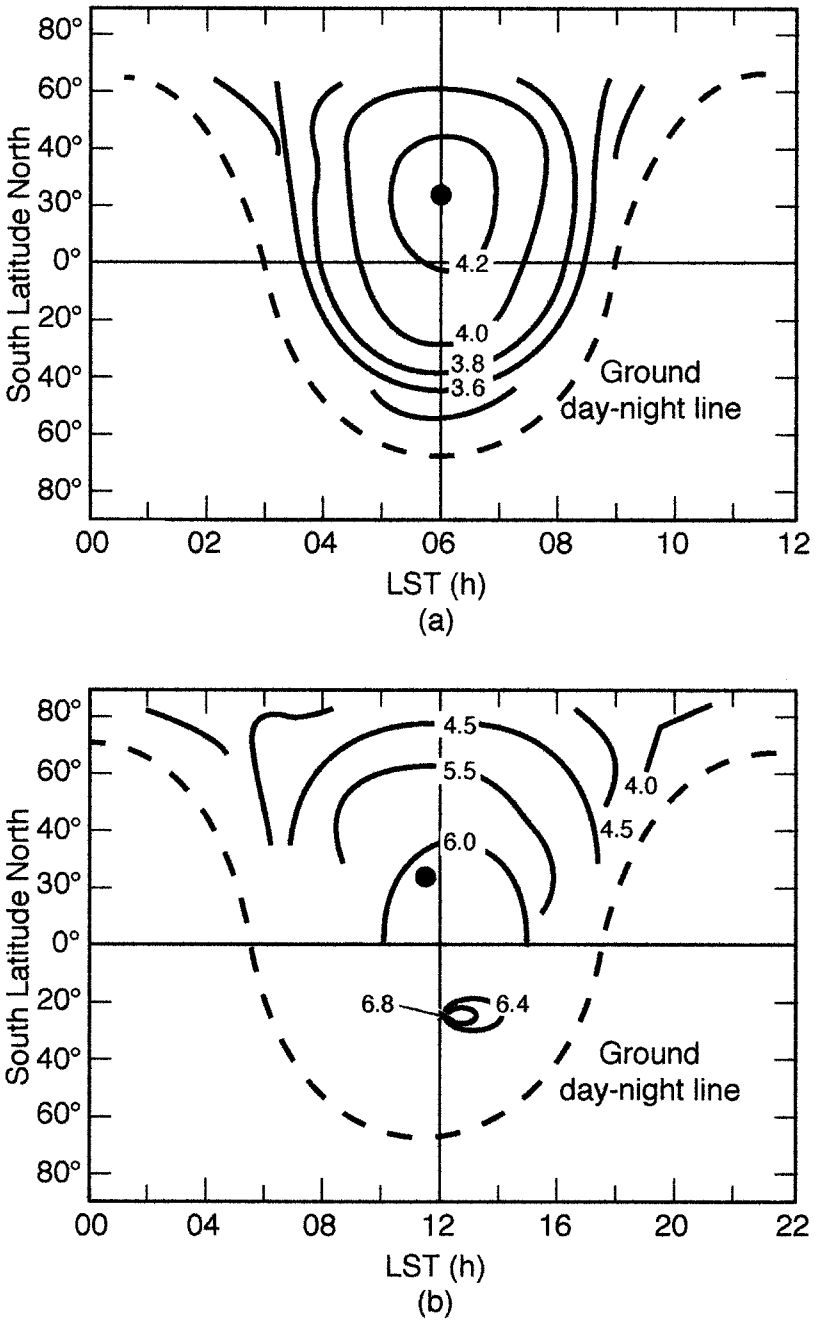


Figure 3-9: (a) Depiction of the local time and latitudinal variation of *foF1* for solar minimum (June 1954). The contours are in MHz. (b) Depiction of the local time and latitudinal variation of *foF1* for solar maximum (June 1958). The contours are in MHz. From Jursa [1985].

3.4.5 The F2 Region

The F2 region is the most prominent layer in the ionosphere, and this significance arises as a result of its median height (the highest of all the component layers) and of course its dominant electron density. It is also characterized by large ensembles of irregularity scales {ΔL} and temporal variations {ΔT}. The F2 region is a vast zone which eludes prediction on the microscale (Δ L < 1 Km) and mesoscale (1 < ΔL < 1000 Km) levels, and even provides challenges to forecasters for global and macroscale (ΔL > 1000 Km) variations. This is largely because of the elusive transport term in the continuity equation. There are also a host of so-called anomalous variations to consider, and these are the subjects of a succeeding section.

As in the E and F1 regions, we may conveniently specify the behavior of the F2 region in terms of equivalent plasma frequency rather than the electron density. For the peak of ionization we have:

$$N_{max}F2 = 1.24 \times 10^{10} (foF2)^2 \qquad (3.17)$$

where *foF2* is the ordinary ray critical frequency.

While *foF2* exhibits solar zenith angle, sunspot number, and geomagnetic latitude dependencies, simple algebraic algorithms do not characterize these relationships. As a consequence, mapping methods are used to describe the F2 region electron density patterns.

The CCIR published its CCIR *Global Atlas of Ionospheric Characteristics*, which includes global maps of F2 layer properties for sunspot numbers of 0 and 100, for every month, and for every even hour of Universal Time [CCIR, 1966]. Figure 3-10 is an illustration of the global distribution of *foF2* for a sunspot number of 100. Such maps are derived from coefficients based upon data obtained from a number of ionosonde stations for the years 1954-1958 as well as for the year 1964. This set of coefficients is sometimes identified by an ITS prefix but is known more generally as the CCIR coefficients. Because of the paucity of data over oceanic areas, a method for improving the basic set of coefficients by adding theoretically derived data points was developed. As a result, a new set of coefficients has been sanctioned by URSI and this is termed the URSI coefficient set. Many communication prediction codes, which require ionospheric sub-models, allow selection of either set of ionospheric coefficients.

3.4.6 Anomalous Features of the Ionospheric F Region

The F2 layer of the ionosphere is probably the most important region for many radiowave systems. Unfortunately the F2 layer exhibits the greatest degree of unpredictable variability because of the transport term in the continuity equation. As indicated previously, this term represents the influences of ionospheric winds, diffusion, and dynamical forces. The Chapman description for ionospheric behavior depends critically upon unimportance of the transport function. Consequently many of the attractive, and intuitive, features of the Chapman model are not observed in the F2 region. The differences between actual observations and predictions derived on the basis of a hypothetical Chapman description have been termed anomalies. In many instances, this non-Chapmanlike behavior is not anomalous at all, but rather typical.

The following subsections indicate the major forms of anomalous behavior in the F2 layer: diurnal, Appleton, December, winter, and the F region trough. A few comments are provided for each major form.

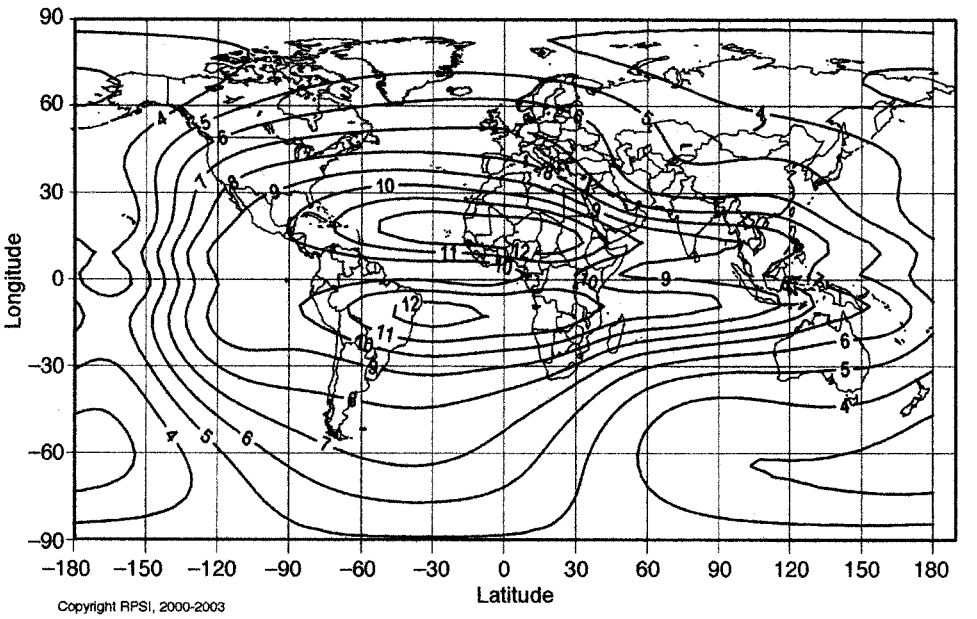


Figure 3-10: Map of foF2 showing the worldwide distribution under the following conditions: 15 November, Sunspot Number = 135, Time = 0000 UTC. The contours of *foF2* are developed using the URSI set of ionospheric coefficients. Curves similar to this are found in the Atlas of Ionospheric Coefficients [CCIR, 1966]. Used by permission, Radio Propagation Services.

3.4.6.1 Diurnal Anomaly.

The diurnal anomaly refers to the situation in which the maximum value of ionization in the F2 layer will occur at a time other than at local noon as predicted by Chapman theory. On a statistical basis, the actual maximum occurs typically in the temporal neighborhood of 1300 to 1500 LMT. Furthermore there is a semidiurnal component which produces secondary maxima at approximately 1000-1100 LMT and 2200-2300 LMT. Two daytime maxima are sometimes observed (one near 1000 and the other near 1400), and these may give the appearance of a minimum at local noon. This feature, when observed, is called the midday "biteout".

3.4.6.2 Appleton Anomaly.

This feature is symmetric about the geomagnetic equator and goes by a number of names including: the geographic anomaly, the geomagnetic anomaly and the Appleton anomaly, as well as the equatorial anomaly. The Appleton anomaly is associated with the significant departure in the latitudinal distribution of the maximum electron concentration within 20 to 30 degrees on either side of the geomagnetic equator. Early in the morning a single ionization peak is observed over the magnetic equator. However, after a few hours the equatorial F-region is characterized by two distinct crests of ionization that increase in electron density as they migrate poleward The phenomenon is described as an equatorial fountain initiated by an $E \times B$ plasma drift (termed a Hall drift), where E is the equatorial electrojet electric field and B is the geomagnetic field vector. This drift is upwards during the day since the equatorial electric field E is eastward at that time. As the electrojet decays, the displaced plasma is now subject to downward diffusion when the atmosphere begins to cool. This diffusion is constrained along paths parallel to B, which maps to either side of the geomagnetic equator. The poleward extent of the anomaly crests is increased if initial Hall drift amplitude is large. This anomalous behavior accounts for the valley in the *EJF(zero)F2* parameter (with peaks on either side) seen at the geomagnetic equator in Figure 3-10. There are significant day-to-day, seasonal and solar controlled variations in the onset, magnitude and position of the anomaly. There are also asymmetries in the anomaly crest position and electron density. Asymmetries in the electron density in the anomaly crests appear to be the result of thermospheric winds that blow across the equator from the subsolar point. The effect of magnetic activity on the anomaly is to constrain the electron density and latitudinal separation of the crests. Magnetic activity is monitored worldwide, and the quasi-logarithmic index *Kp* is used to represent the level of worldwide activity [Mayaud, 1980]. There have been suggestions

that when *Kp* is ≥ 5, the anomaly disappears. But other observations have shown an increased separation of the anomaly crests, a fact that may lead some stations to observe a reduced *foF2* value.

3.4.6.3 December Anomaly.

This phenomenon refers to the fact that the electron density at the F2 peak over the entire earth is 20% higher in December than in June, even though the solar flux change due to earth eccentricity is only 5% (with the maximum in January).

3.4.6.4 Winter (Seasonal) Anomaly.

In this case, the noontime peak electron densities are higher in the wintertime than in the summertime despite the fact that solar zenith angle is smaller in the summer than it is in the winter. This effect is modulated by the 11-year solar cycle and virtually disappears at solar minimum.

3.4.6.5 The F-Region (High Latitude) Trough.

This is representative of a number of anomalous features that are associated with various circumpolar phenomena including particle precipitation, the auroral arc formations, etc. The high latitude trough is a depression in ionization, occurring mainly in the nighttime sector, and it is most evident in the upper F-region [Muldrew, 1965]. It extends from 2 to 10 degrees equatorward of the auroral oval, an annular region of enhanced ionization associated with optical aurora (see Section 3-8). The trough region is associated with a mapping of the plasmapause onto the ionosphere along geomagnetic field lines (see Figure 3-18). The low electron density within the trough results from a lack of replenishment through candidate processes such as antisunward drift, particle precipitation, or the storage effect of closed field lines. The latitudinal boundaries of the trough may be sharp, especially the poleward boundary with the auroral oval. A model of the trough is due to Halcrow and Nisbet [1977].

3.4.7 Irregularities in the Ionosphere

In addition to the various anomalous features of the ionosphere, irregularities in the electron density distribution may be observed throughout the ionosphere. The size, intensity, and location of these irregular formations are dependent upon a number of factors including: geographical area, season, time-of-day, and the levels of solar and magnetic activity. The Traveling

Ionospheric Disturbance (TID, see Section 3.5.2 and Section 3.13) belongs to a special class of irregular formations that are generally associated with significant changes in the electron density (e.g., > a few per cent) over large distances (e.g., > 10 Km). The remaining irregularities, loosely termed ionospheric inhomogeneities, typically develop as the result of ionospheric instability processes and are not directly associated with TIDs. On the other hand, TIDs have been shown to be a possible catalyst in the formation of ionospheric inhomogeneities, especially in the vicinity of the Appleton anomaly. Relatively small-scale ionospheric inhomogeneities are important since they are responsible for the rapid fading (i.e., scintillation) of radio signals from satellite communication and navigation systems. Such effects may introduce performance degradations or outages on systems operating at frequencies between 100 MHz and several GHz. Models of radiowave scintillation have been developed, and these are based upon a basic understanding of the global morphology of ionospheric inhomogeneities.

There are inhomogeneities in all regions of the ionosphere, but the equatorial and high latitude regions are the most significant sources. Hunsucker and Greenwald [1983] have reviewed irregularities in the high latitude ionosphere while Aarons [1977] has examined the equatorial environment. Refer to Section 3-8 for more on high latitude phenomena. Specifically we shall describe the phenomenon of polar patches and blobs.

Equatorial inhomogeneities tend to develop following sunset and may persist throughout the evening but with decreased intensity after local midnight. The irregularities are thought to be the result of an instability process brought about by a dramatic change in F-region height at the magnetic equator following sunset. The scale lengths of the irregularities may range between roughly a meter and several kilometers, and the spectrum of the irregularities has been observed to exhibit a power law distribution. There is a tendency for the irregularities to be field-aligned with an axial ratio of roughly 20 to 1. In addition, the irregularities are organized in distended patches. While the situation is variable, the patch sizes range between ~100 Km and several thousand kilometers in the upper F-region, and have a mean dimension of ~ 100 Km in the lower F region. The equatorial irregularities tend to be more intense and widespread at the equinoxes and at solar maximum, but magnetic activity tends to suppress the growth of the irregularities.

High latitude irregularities exist within the polar cap and the auroral zone, with the latter being primarily associated with the bottomside F-region. The high latitude F-region is quite variable, and unlike midlatitudes, it may have an electron density that is less than the E-region during nocturnal hours. In the wintertime, structured auroral arcs may migrate within the polar cap and the electron density enhancements within these formations may be several

orders of magnitude greater than the normal background, especially during elevated solar activity conditions. During disturbed geomagnetic conditions, structured electron density patches have been observed to travel across the polar cap in the anti-sunward direction. These irregularities may have a significant effect on communication systems. For both the auroral zone and the polar cap, increased geomagnetic activity has a dramatic influence on the growth of irregular ionospheric formations. Moreover, for large and sustained values of *Kp*, it has been observed that the high latitude irregularity patterns tend to migrate equatorward replacing the background midlatitude properties.

3.5 DIURNAL BEHAVIOR OF IONOSPHERIC LAYERS

3.5.1 Mean Variations

As indicated by the Chapman representation for *Nmax*, the respective critical frequencies for the layers D, E, F1, and F2 will generally peak during the daytime. All layers, with the occasional exception of the F2 region, exhibit a peak in the mean electron concentration in the temporal neighborhood of local noon. Figure 3-11 shows the mean diurnal variation of the E, F1 and F2 critical frequencies at solar maximum for a midlatitude site.

3.5.2 Short-Term Variations

Variations in layer critical frequencies will arise on an hour-to-hour and day-to-day basis, especially for the F2 region. Day-to-Day F region variability is exhibited in Figure 3-12 for a period of maximum solar activity and for midlatitudes. It appears that much of this variability owes its existence to the impact of geomagnetic storms, traveling ionospheric disturbances (TIDs), and miscellaneous F region dynamic effects. TIDs are one of the more fascinating features of the ionosphere. They are the ionospheric tracers of neutral atmospheric gravity waves, which derive from a number of sources in the upper atmosphere. These sources include localized heating effects, atmospheric explosions, enhanced auroral activity, and other atmospheric phenomena that are associated with relatively rapid and nonuniform changes in atmospheric pressure. Figure 3-13 shows the variation of *foF2* as a function of time showing the impact of TIDs. Figure 3-14 shows the effect of a large geomagnetic storm.

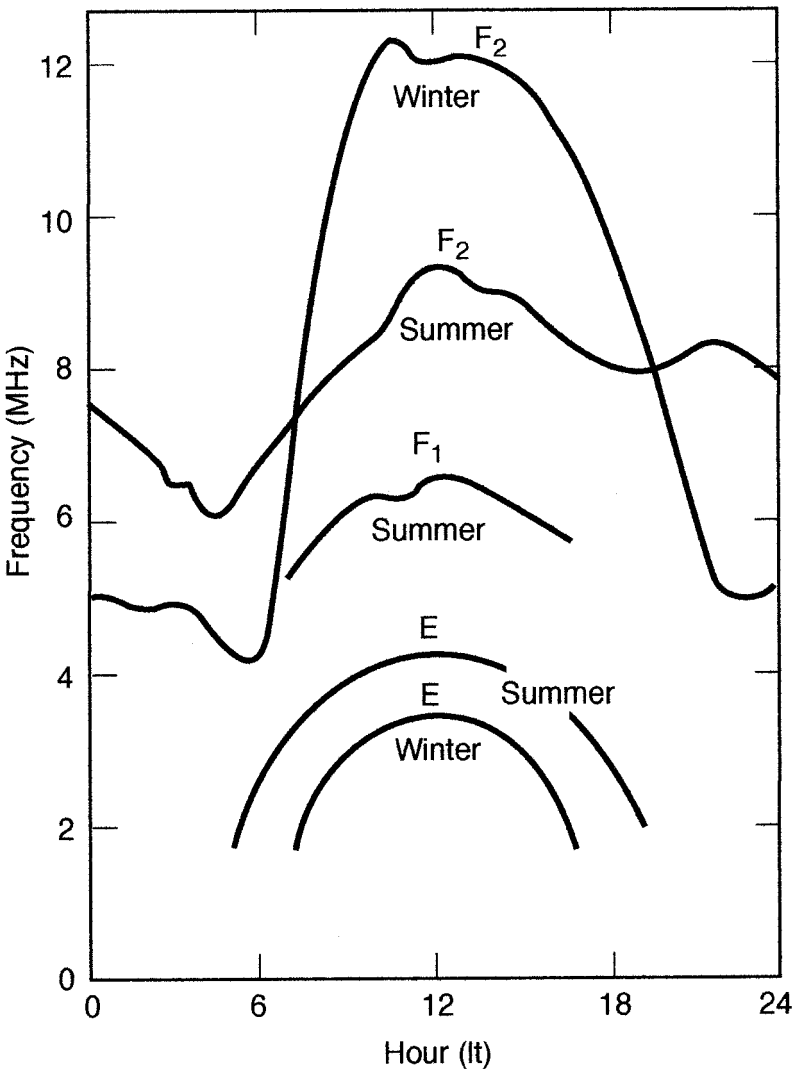


Figure 3-11: Mean diurnal variation of *foE, foF1,* and *foF2* for summer and winter under Northern Hemispheric solar maximum conditions. The seasonal anomaly is clearly evident with the wintertime values of the F2-layer peak electron density being larger than the summertime values. At the same time we note that the E-layer peak density is larger in summer than in wintertime, as suggested by Chapman theory. A late afternoon (pre-midnight) bulge in *foF2* occurs for summertime solar maximum conditions. From Jursa [1985].

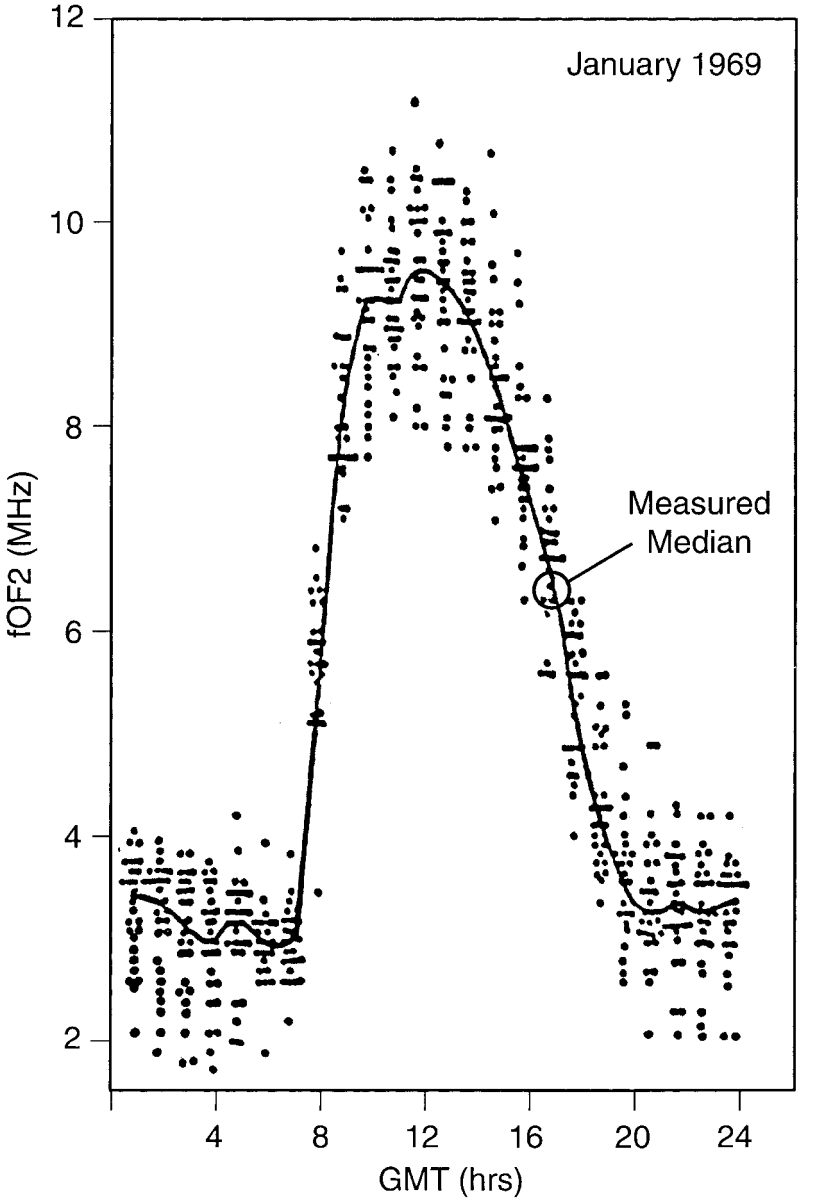


Figure 3-12: Variations in the hourly values of *foF2* as a function of the time of day, for January solar maximum conditions, and Northern Hemispheric sounder site. The range of day-to-day variability in *foF2* is ~ ± 10%, suggesting a variation in *NmaxF2* of ~ ± 5%. From Davies [1965].

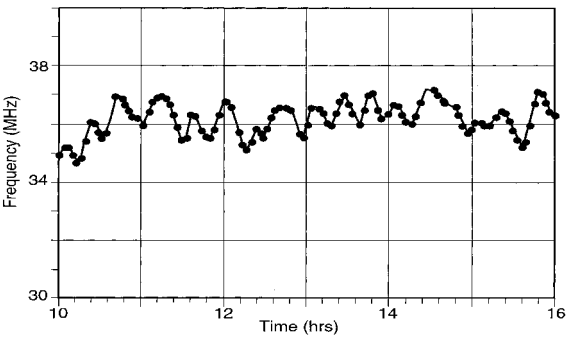


Figure 3-13: Variations in the ionosphere thought to be associated with traveling ionospheric disturbances. The *foF2* variations shown here are of the order of ± 2% and have periods of ~ 20 minutes. The *NF2max* variations are ~ ± 1%. From Paul [1989].

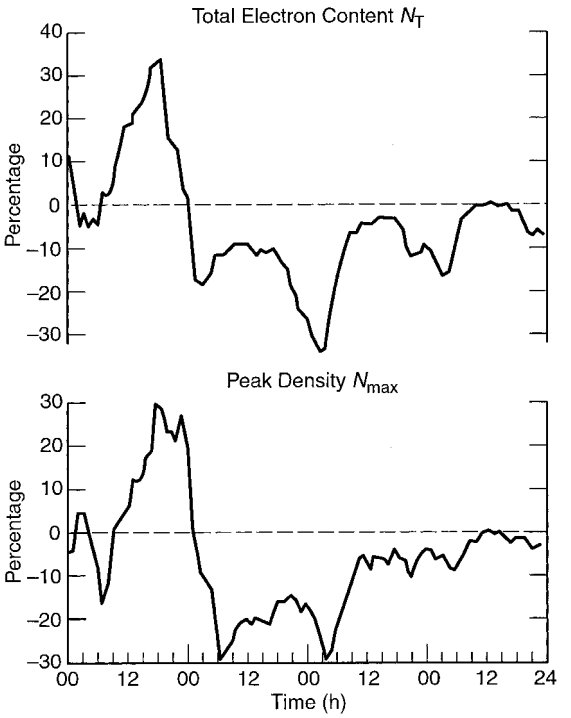


Figure 3-14: Effect of a large geomagnetic storm on *Nmax* and the total electron content N_T. The curves represent average perturbations (%) at hourly intervals, as reckoned from the mean of the 7 days prior to the storm onset. There were some selectivity requirements. The main one was that the storm must begin (i.e., day-1) from a few hours before sunrise to a few hours before sunset. Nocturnal storm onsets generate complications that make a general summary problematic. Illustration derived from Mendillo and Klobuchar [1974b]. (See Section 3.10.)

3.6 LONG-TERM SOLAR ACTIVITY DEPENDENCE

There is a clear tendency for the ionospheric critical frequencies to increase with sunspot number. Figure 3-15 shows the long-term variation of R_{12}, *foF2*, and *foE*, and the D layer absorption level (at 4 MHz) for noontime conditions. The D region is best characterized by the amount of absorption it introduces (see Section 3.4.2). A device for monitoring the D region absorption is the Riometer, where the magnitude of the absorption is proportional to the product of D region electron concentration and the electron collision frequency. From Figure 3-15, a slow 11-year modulation in the ionospheric parameters is evident.

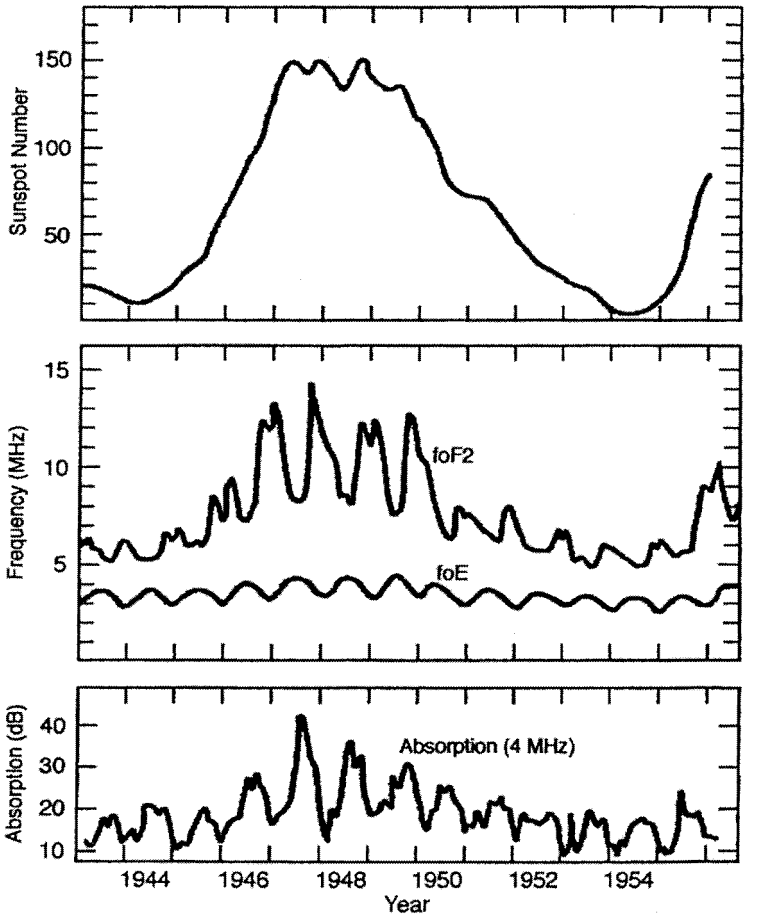


Figure 3-15: Variation in R_{12}, *foF2*, *foE*, and 4 MHz absorption at noontime. The seasonal effects are clearly evident, the foE and D layer variations being out of phase with the *foF2* variations (i.e., the seasonal anomaly). From Goodman [1991].

After smoothing, the results correlate well with sunspot number. Superimposed on this solar epochal variation is an annual variation, with D region absorption and *foE* exhibiting summertime maxima while *foF2* exhibits a wintertime maximum (i.e., seasonal anomaly).

The slow but definite dependence upon mean sunspot number is illustrated in Figure 3-16. This plot is rather unusual since it represents the running 12-month averages of the specified ionospheric parameters as well as the sunspot number. This disguises the seasonal effects observed in Figure 3-15.

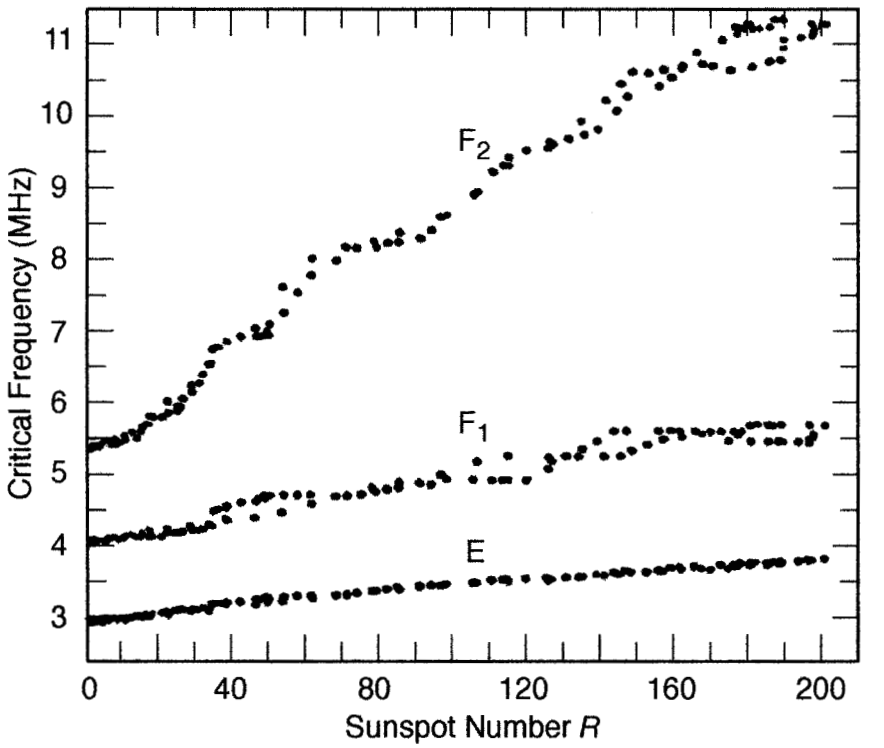


Figure 3-16: Long-term variation in R_{12}, of *foF2, foF1 and foE* at noontime. The x-axis is labeled "critical frequency" (in MHz). The critical frequency is the highest frequency for which skywave propagation can be supported at vertical incidence. The ordinary ray critical frequency can be shown to be equivalent to the electron plasma frequency. The plasma frequency, in turn, is proportional to the square root of the electron density. Because 12-month running averages are used in the plot, the seasonal effects seen in Figure 3-15 are smoothed out. While the critical frequencies for the three layers all increase with solar activity, the F2 layer shows the largest dependence on sunspot number. From Goodman [1991].

3.7 SPORADIC E

3.7.1 General Characteristics

Even though the normal E region is Chapman-like in nature, isolated forms of ionization are often observed in the E region having a variety of shapes and sizes. These ionization forms have been termed sporadic E because they appear quasi-randomly on a day-to-day basis, and they generally defy deterministic prediction methods. Sporadic E (or *Es* ionization) has been observed during rocket flights and with incoherent backscatter radar, and a layer thickness of the order of 2 kilometers has been observed. They are generally large-scale structures, having horizontal dimensions of 100s of kilometers at middle latitudes. Polar and equatorial forms have different structures and causal mechanisms. Although sporadic E consists of an excess of ionization (against the normal E region background) it does not appear to be strongly tied to solar photoionization processes. Still, midlatitude *Es* occurs predominantly during summer days. Sporadic E does exhibit seasonal and diurnal tendencies, which have been examined statistically, and at least three different types of sporadic E ionization have been discovered with distinct geographical regimes. These are low latitude (or equatorial), midlatitude (or temperate), and high latitude ionization. Figure 3-17 depicts the probability of *Es* occurrence.

3.7.2 Formation of Midlatitude Sporadic E

It has been suggested that wind shears in the upper atmosphere are responsible for the formation of sporadic E at midlatitudes. We shall review this process briefly. It should be recalled from examination of photochemistry in the ionosphere that molecular ions such as those, which exist in the E region, introduce relatively rapid electron loss by recombination. At the same time it is recognized that an enormous number of meteors burn up in the E region. This meteoric debris is largely comprised of metallic ions, which are monatomic. Their presence has been confirmed by mass spectroscopy measurements using rockets, and these atomic species include iron, sodium, magnesium, etc. Since monatomic ions exhibit a small cross section for electron capture, the process by which atomic ions become concentrated in well-defined layers will lead to reduced loss rates for ambient free electrons in the interaction region.

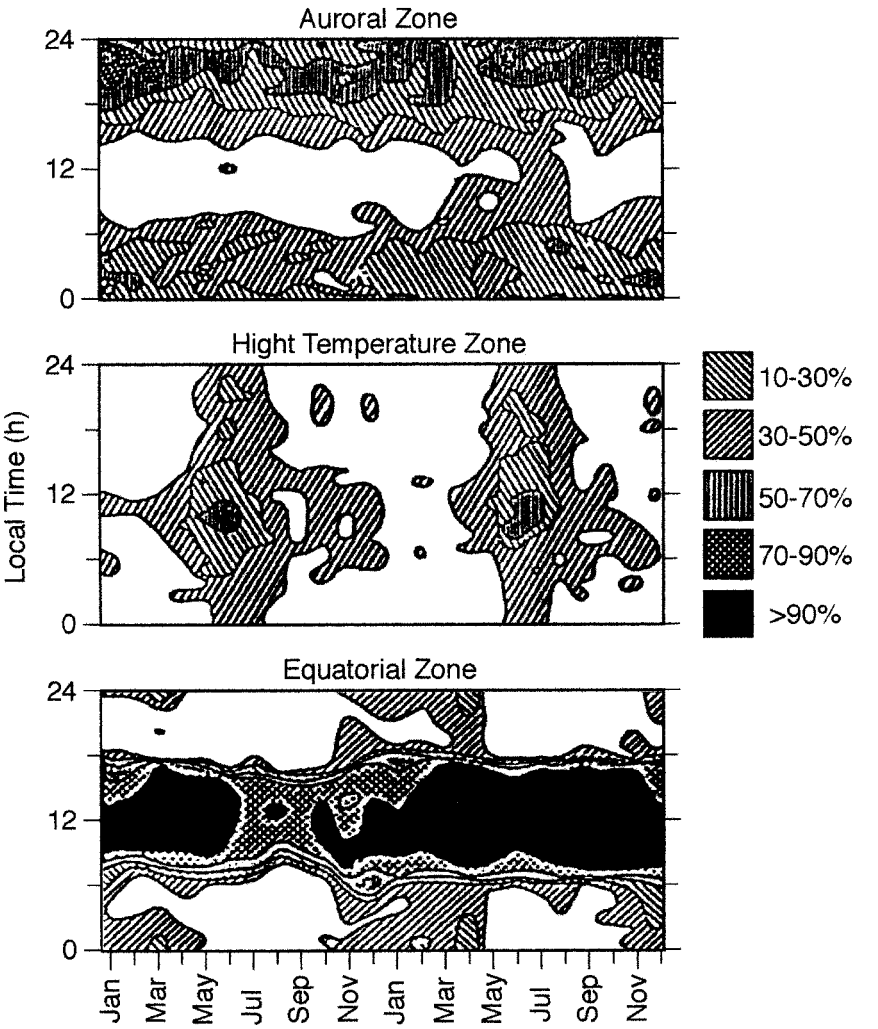


Figure 3-17: Probability of Es occurrence as observed in the period 1951-52. It is representative of the global, seasonal, and diurnal variation of sporadic-E ionization. A form of sporadic E is virtually omnipresent near the auroral zone during nocturnal hours. Another form of Es ionization is evidenced during the midday period at (geomagnetic) equatorial latitides. At middle latitudes, sporadic E is most pronounced during the summer daytime hours. However, no portion of the diurnal cycle is completely immune from the effects of sporadic E. From Goodman [1991], after Davies [1965].

The influx of this foreign mass of metallic ions when distributed over the whole of the E region is still insufficient to overwhelm the omnipresent molecular species (such as NO^+), which are in a state of photochemical equilibrium were it not for a mechanism which preferentially concentrates the meteoric debris ions. Apparently wind shear is this mechanism. The basic wind shear theory was proposed by Whitehead [1970], but it remained for Gossard and Hooke [1975] to outline a process for meteoric ion concentration based upon the interaction of the meteoric debris with atmospheric gravity waves, the latter wave structures being responsible for the development of traveling ionospheric disturbances (TIDs) as well. The ultimate process involves a corkscrew propagation of atmospheric gravity waves and atmospheric tides that results in a rotation of wind velocity as a function of altitude. The velocity rotation effect can cause the wind to change direction over an altitude of only a kilometer or so, sufficient to trap meteoric ions at an intermediate point having zero velocity. This buildup in a narrow region is sufficient to generate an intense sporadic E patch.

3.7.3 Sporadic E at Non-Temperate Latitudes

The high latitude sources are evidently of two types depending upon whether the observation is made in the neighborhood of the auroral oval or poleward of it (i.e.., in the polar cap region). It has been found that auroral Es is basically a nocturnal phenomenon, it is associated with the optical aurora, and is due to auroral electron precipitation. Because of its proximity to the seat of auroral substorm activity, it is not surprising to find some correlation between auroral Es and some appropriate magnetic index. Indeed, it has been found that auroral Es is positively correlated with magnetic activity. On the other hand, polar cap Es may be relatively weak, and is negatively correlated with substorm activity.

Turning equatorward, it has been found that equatorial Es is most pronounced during daylight hours, and evidence points to formation of ionization irregularities within the equatorial electrojet as the responsible agent at low latitudes.

3.8 THE HIGH LATITUDE IONOSPHERE

From a morphological point of view, the high latitude region is the most interesting part of the ionosphere. It has been said that the auroral zone and associated circumpolar features are our windows to the distant magnetosphere, and the presence of visible auroras has fascinated observers for centuries. The interplanetary magnetic field, which may be traced to its solar

origins, has a significant impact on the geomorphology of the high latitude ionosphere and its dynamics, including magnetic substorm development.

The high latitude region is a portion of the ionosphere that is characterized by the hierarchy of phenomena. These are largely orchestrated by magnetospheric and interplanetary events (of a corpuscular nature) rather than solar (electromagnetic) flux variations. Hunsucker [1983] has examined the salient features and they are depicted in Figure 3-18, with particular emphasis on the high latitude trough. The cartoon portrayed in Figure 3-19, from Bishop et al. [1989], exhibits many of the same features are depicted and compared with worldwide features.

The magnetic activity index K_p is generally available and is typically used as the parameter of choice to determine the statistical position of the auroral zone. The concept of the auroral oval was developed by Feldstein and Starkov [1967] on the basis of a set of all-sky camera photographs that were obtained during the International Geophysical Year. Other models exist but the Feldstein picture is found in most models that attempt to include auroral effects in some way. The position of the oval is important, not only as an ionospheric feature itself, but because it also represents a boundary between decidedly different geophysical regimes that are either poleward (i.e., polar cap) or equatorward of it (i.e., midlatitude). Because the position of the auroral zone varies diurnally as well as a function of the index K_p, there are some sites that may be characterized by all four regimes at any given time: polar, auroral, trough, or midlatitude. Iceland is such a location.

One of the most fascinating properties of the various circumpolar features is their latitudinal motion as a function of magnetic activity. The ionospheric plasma is best organized in terms of some form of geomagnetic coordinates, but the high latitude plasma patterns are not fixed in that frame of reference either. The equatorward boundary of the region of precipitating electrons has been deduced from DMSP satellite instruments and it takes the form due to Gussenhoven et al. [1983].

$$L(t) = L_0(t) + a(t)\, K_p \tag{3.18}$$

In Equation 3.18, the Corrected Geomagnetic Coordinates are used, $L(t)$ and $L_0(t)$ are specified in degrees, and $L_0(t)$ is the equatorward boundary of the oval when $K_p = 0$. It is emphasized that $L_0(t)$ and $a(t)$ are functions of time in the Local Magnetic Time (MLT) system.. Both functions are smoothly varying over the diurnal cycle; L_0 ranges between 65 degrees at ~0100 MLT and ~72 degrees at ~1700 MLT, and $a(t)$ varies between ~ -2 at 2400 MLT and -0.8 at ~1500 MLT.

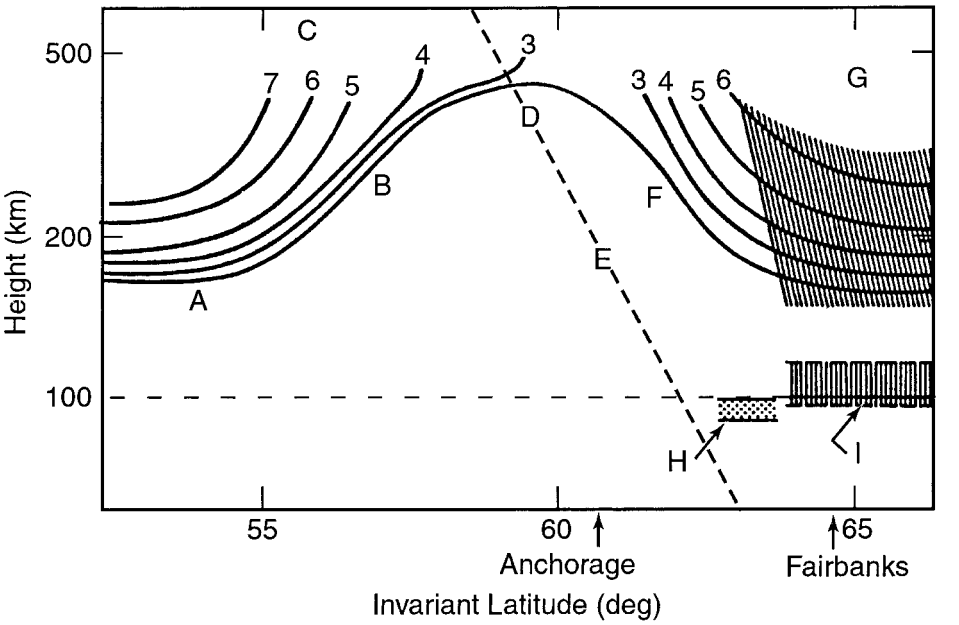


Figure 3-18: Idealized picture of ionospheric plasma frequencies in a north-south plane through Fairbanks and Anchorage, Alaska. (A) the region equatorward of trough; (B) equatorward edge of the trough; (C) plasma frequencies specified in MHz; (D) trough minimum; (E) plasmapause field line; (F) poleward edge of trough; (G) F-region blobs; (H) enhanced D-region absorption; (I) E-region irregularities. Illustration from Goodman [1991] based upon Hunsucker [1983].

We note that the statistical representation of the oval has its greatest equatorward descent during nocturnal hours, and, as already indicated, this equatorward boundary is greatly influenced by magnetic activity. Chubb and Hicks [1970] have found that the daytime aurora descends approximately 1.7 degrees/unit K_p, and the nighttime aurora descends at a rate of 1.3 degrees/unit K_p. The auroral oval and thickness was previously depicted in Figure 2-25. Ultimately the auroral arcs, which reside within the auroral oval, are tied to interplanetary phenomena. Workers have shown that the magnitude of the southward component of the Interplanetary Magnetic field is a key factor is the development of so-called geomagnetic substorms, wherein K_p exhibits large enhancements.

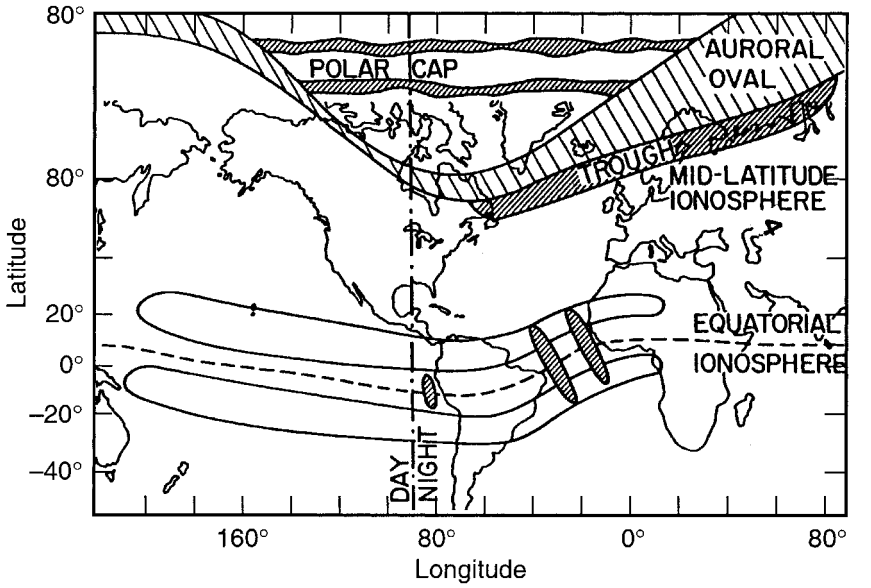


Figure 3-19: Depiction of various ionospheric features at a given time such that the day-night terminator is passing through the middle of the United States (Time is ~ 2300 UTC). Illustration from Goodman [1991], based upon Bishop et al. [1989].

The U.S. Air Force prepares daily summaries of the index Q in order to provide a basis for various analyses of the high latitude ionosphere. The index Q ranges between 0 and 8 with larger values associated with a widening of the oval region and a general increase in intensity of activity within the oval. Consistent with other magnetic activity indices, the equatorward boundary of the auroral oval moves to lower latitudes as Q increases. Since Q, viewed as a parameter, defines the shape and location of the auroral zone, and it is a convenient index for transmission to communication and forecasting facilities. Its utility is dependent upon timeliness and accuracy. As originally designed by Feldstein, the Q index defines only a statistical relationship between the oval position and magnetic activity, the latter being parameterized by the planetary index K_p. Nevertheless, the Feldstein oval concept has been shown to have some utility under real-time circumstances. Satellite imagery is used to deduce an effective index, Q.

Auroral physics is an exceedingly rich and complex subject. Not all phenomena in the high latitude region are understood, and insufficient data are available to fully characterize those factors for which a general understanding exists. One area of renewed interest is the appearance of polar patches and blobs (see Figure 3-18).

Figure 3-20 [Gassman, 1972] shows an instantaneous cross section of the ionosphere along the noon-midnight meridian. It shows the relative position of the auroral region during daytime and nighttime conditions, indicating a distended aurora during nocturnal hours, and very low *Ne* concentration within the polar cap. Representations such as this are all-important when there is a need to evaluate paths through the ionosphere at a variety of elevation (launch) angles. Ray tracing is an application of interest in this connection.

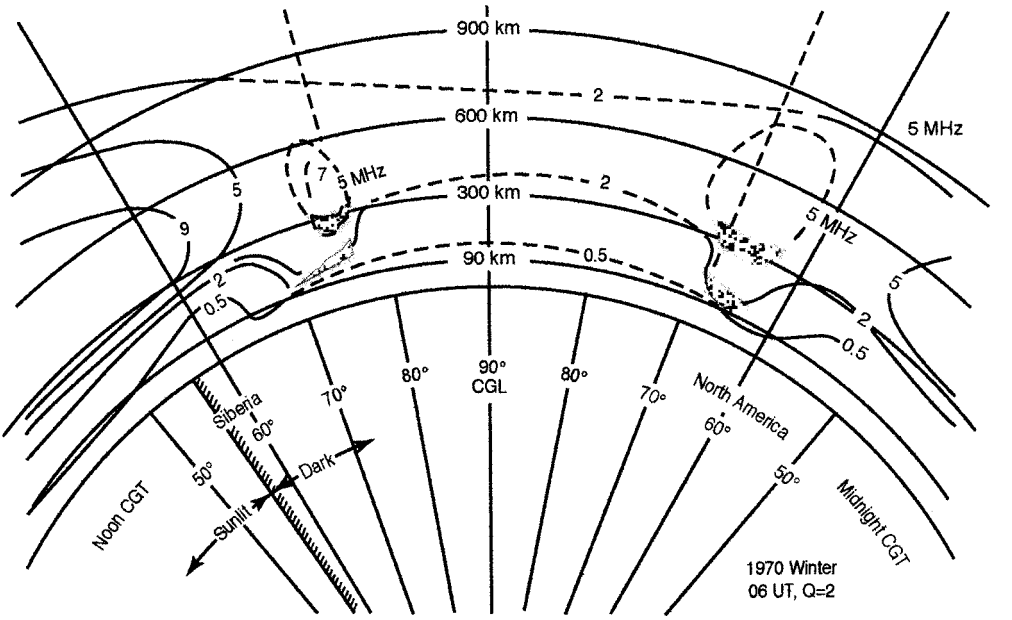


Figure 3-20: Vertical profile of the ionosphere from magnetic noon to midnight. The conditions are winter, 0600 UTC, and quiet magnetic conditions. The contours are in MHz. The vertical scale is 3-times the horizontal scale. From NATO-AGARD-CP-97. [1972].

3.8.1 Description of Plasma Blobs and Patches

Buchau et al. [1983] have examined the wintertime polar cap F-region with an emphasis on its structure and dynamics. Crowley [1996] has reviewed ionospheric patches and blobs, and discusses the distinctions between them. Discrete electron density enhancements occurring in the F region of the ionosphere at high latitudes, with horizontal scales of 100-1000 km are called

patches if inside the polar cap (or entering), and they are called blobs if they have passed through the cap and are outside of it. These plasma enhancements are a factor of 2 or more above ambient, and steep gradients associated with patches and blobs are correlated with small-scale structure (i.e., irregularities).

The status of research about patches provided by Crowley [1996] has been augmented by Rodger [1998, 1999], who describes polar patches as regions of high F-region plasma concentration observed in the polar cap. One of the critical issues remaining is the differentiation in the observations between the distorted tongue of ionization that may convect across the polar cap from "genuine" polar patches which Rodger describes as isolated "islands" of high concentration.

Terminology for the phenomena has been offered in various papers [Crowley, 1996; Rodger, 1999; and Benson and Grebowski, 1999]. The latter authors describe the polar cap as the region poleward of the auroral oval in each hemisphere. In the winter it is subject to prolonged periods of darkness and has a lower electron density (*Ne*) than in the oval but contains both *Ne* enhancements (i.e., tongues, patches, and blobs) and *Ne* depletions (viz., troughs, cavities, and holes). In its simplest conception, ignoring more complicated structures, the average large-scale polar cap *Ne* cavity deepens during the winter night as plasma convects and chemically decays in the absence of a well-defined source of photoionization.

An intriguing result, from stations in Vostok, Mirny, and Dixon, shows a high correlation between noontime *foF2* values (for wintertime solar maximum conditions) and dynamic pressure of the solar wind. Rodger [1999] speculates that the ionospheric convection pattern is quite expanded when the solar wind velocity is high. He reckons that lower latitude plasma is drawn (i.e., entrained) into the cross-polar tongue of ionization and hence over the observatories used in the study.

There are a number of source materials that may be drawn upon. Michael Kelley [1998] has written an impressive book on ionospheric physics. It covers essential theory about high latitude electrodynamics, current systems, convection patterns, and irregularities. Benson and Grebowski [1999] have found that low ionization heights are sometimes observed in topside sounder data. They feel that these lowered heights may have been misinterpreted (by others) as F-region holes since the peak layer heights drop monotonically during disturbed times. The implication of topside sounder results on highly oblique paths is not totally evident. But it is clear that if *Ne* is fixed and the layer height were to drop dramatically, then the maximum observable frequency (MOF) exploiting that disturbed "layer" would increase in proportion to the increase in ray zenith angle, until such time as the height lowering leads to mode switching (i.e., 1-hop to 2-hop conditions).

3.8.2 Arctic Radio Propagation

There have been numerous studies of HF propagation effects and communication capability within the arctic environment. A review of these effects is provided in various books and manuscripts [Lied, 1967; Goodman, 1991; Davies, 1990]. Much of our knowledge of the region has been provided by data obtained in the 1950s through the 1970s. An early account of propagation in the arctic was published under the auspices of NATO-AGARD [Millman, 1972]. Within that volume, papers by Hartz [1972] and Gassman [1972] are instructive of views from an earlier time.

From a morphological point of view, the high latitude region is the most interesting part of the ionosphere. It has been said that the auroral zone and associated circumpolar features are our windows to the distant magnetosphere, and the presence of visible aurora has fascinated observers for centuries. The interplanetary magnetic field, which may be traced to its solar origins, has a significant impact on the geomorphology of the high latitude ionosphere and its dynamics, including magnetic substorm development.

A wide range of phenomena characterizes the high latitude region, and the subject is far too complex to be given proper coverage in this manuscript. These phenomena are largely orchestrated by magnetospheric and interplanetary events (of a corpuscular nature) rather than solar (electromagnetic) flux variations. Hunsucker [1983] has examined the salient features with particular emphasis on the high latitude trough. Bishop et al. [1989] have placed these features in a worldwide context. It is well known that the magnetic pole is tilted toward the American sector. This makes high latitude phenomena more pronounced than would be expected on the basis of geographic coordinates. This fact is important as we consider HF communication for trans-polar flights between the Orient and the United States.

3.8.3 Early Diagnostic Studies

Studies of the polar ionosphere have largely emphasized the ionospheric physics and were less directed toward an understanding of HF communications. While ionospheric data were obtained during the International Geophysical Year (i.e., 1957) and other years leading to the development of useful performance prediction models, many operational issues associated with actual communications were not adequately addressed. One of the more useful forums for examination of practical communications was the 8th meeting of the NATO-AGARD Ionospheric Research Committee at Athens in 1963 [Landmark, 1964]. While this was long ago, a number of arctic communications phenomena were clearly identified, and more fulsome

reports have not been forthcoming since that time. An especially noteworthy paper was presented by Jull [1964].

Jull [1964] examined the results from several studies of oblique-incidence sounding and 30 MHz Riometer absorption with the express objective of using the results to increase the reliability of HF communications over auroral zone circuits. Studies of propagation paths were carried out during high and low intensity Polar Cap Absorption (PCA) events, and moderate and severe magnetic storms, to determine the effect of these disturbances of HF communications. These paths included: (i) a number of fixed point-to-point circuits, and (ii) a mobile circuit from a ground station to an aircraft flown into, and through, the auroral zone and into the polar cap. A key finding made by Jull was that frequency sounding systems can be used to provide direct assistance to communication systems in the selection of optimum communication routes and operating frequencies during PCA events and geomagnetic storms. Also, in order to match the highly variable characteristics of auroral Es and F-layer propagation during geomagnetic storms, it was necessary to provide a well-spaced set of frequency assignments. Finally, because of the rapidity of propagation variability, it was necessary to sample propagation conditions at time intervals no greater than 15 minutes. Jull reports rather marked differences between model predictions and the optimum working frequencies during trans-auroral operations, with sporadic E often providing significant connectivity at frequencies both above and below the classical predicted MUF for the designated circuit. Abnormal propagation at elevated HF bands caused by Es patches was shown to be useful during PCA events when the lowest frequencies are not usable. Jull presented some alternate routing strategies that are not wholly pertinent to the current problem, but it did indicate the necessity for station diversity, a matter that was examined in a comprehensive multiple-path sounding experiment conducted in the 1990s [Goodman et al., 1997]. While Jull found discrepancies between model predictions and experimental data during disturbances, he did note that models are most useful during undisturbed periods. Even under these conditions we must find ways to properly extrapolate ionospheric data. This is because we are generally dealing with an undersampled environment.

Additional studies of the auroral and polar environment using oblique sounders have been reported by Lundborg et al. [1995] and Broms and Lundborg [1994]. In these studies, the paths were trans-auroral, and not exclusively polar. Multipath propagation was found to be a regular feature in the data, as well as splitting of the O- and X-modes of propagation. These factors are problematic for digital communication systems, although fixes are possible. Auroral Es was observed predominantly during nocturnal hours at wintertime, and it was correlated with magnetic activity. The authors contend that auroral Es can be used for a low data rate propagation channel at

frequencies that are higher than normal, reducing the impact of absorption. Spread-F was a major problem and made the effort of communication largely impossible, especially on winter nights and during elevated auroral activity.

3.8.4 Recent Diagnostic Studies

Radio Propagation Services (RPSI) installed a Chirpsounder® system to evaluate the communication path between Svalbard (Spitsbergen) and Barrow, Alaska (see Figure 3-21). This system of measurements was used to update operational ionospheric propagation models used to nowcast the effectiveness of High Frequency (HF) communications over polar paths [Goodman and Ballard, 2004]. Operations were continuous from December 2000 until the Spring of 2002 during which time measurements of the propagation effects were observed. Oblique sounder patterns were observed to be diverse, ranging from standard (i.e., classical) ionograms with a sharp "nose" near the anticipated MUF to rather diffuse patterns. However, the most interesting patterns consisted of non-climatological signals associated with Elevated Maximum Observable Frequencies (i.e., EMOFs). These were first observed to occur during the winter, but they were in evidence throughout the year. The strong signal strengths associated with these EMOF patterns are transient, and consistent with independent ionospheric layers or modulations of existing layers. Figure 3-22 shows the effect of these EMOF signals on the ionogram.

A major consequence of the polar EMOF structures include the potential for use of much higher bands than are currently in use in the polar region. The use of higher bands, if available, will reduce the atmospheric noise competing with signal, and will reduce the amount of ionospheric absorption inflicted on the signal. To accomplish this, regulators must work with radio engineers to allow more spectrum use in the Polar Regions. In some cases, HF bands in the range between 18 and 30 MHz are authorized for use for a given service (e.g., maritime-mobile or aeronautical-mobile) but are not licensed since the requirements are derived on the basis of climatology. And, of course, polar blobs (and polar EMOF signals) are not a part of the archived climatology. Hence the studies described by Goodman et al. [2004] are important as a means to educate system engineers who must field systems in the polar environment.

It is well established that the midlatitude trough, sometimes referred to as the high latitude trough, can also affect long distance propagation of HF signals. Deviations of up to 100 degrees in bearing can sometimes be observed [Stocker et al., 2003]. Moreover, studies of polar patches and arcs have suggested a measurable impact upon the direction of arrival (DOA) of HF signals [Zaalov et al. 2003].

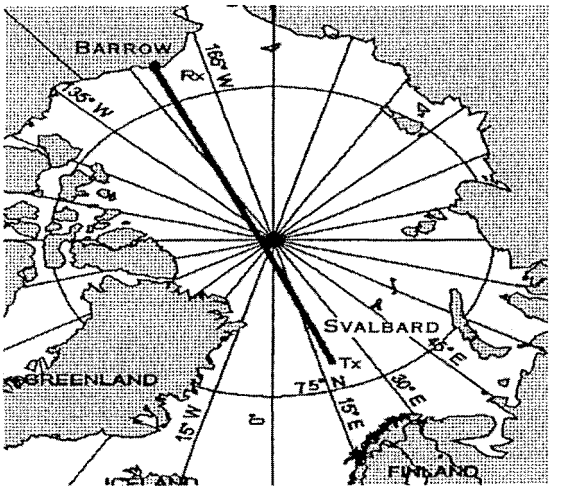


Figure 3-21: Geometry of the RPSI Polar experiment. The Chirpsounder® transmitter was located at Svalbard (courtesy of NDRE), and the receiver was located at Barrow (courtesy of ARINC). From Goodman and Ballard [2004].

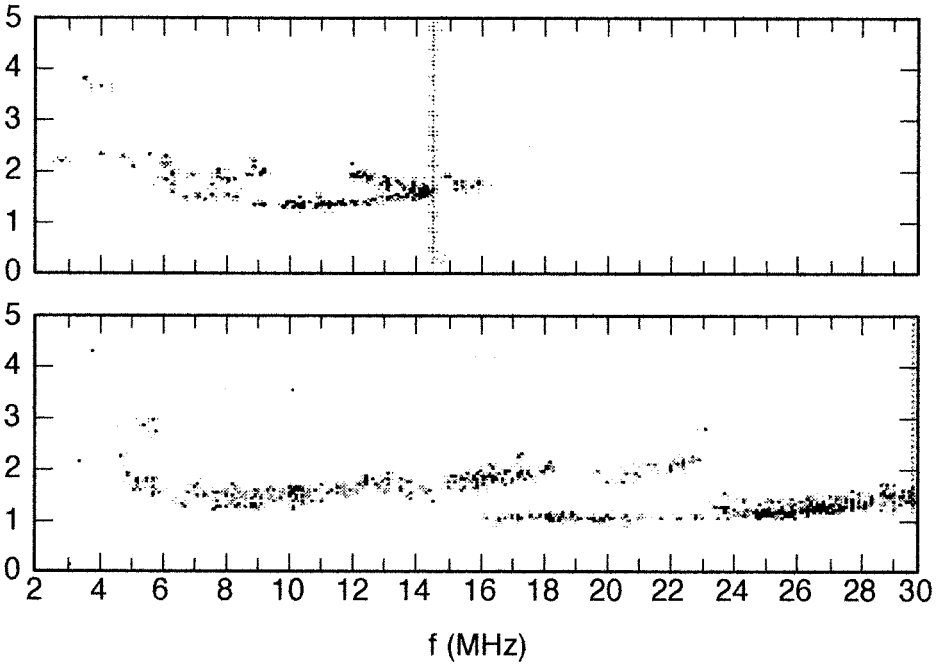


Figure 3-22: Examples of benign (top) and disturbed (bottom) ionograms for the Svalbard to Barrow path. The ordinate scale is the relative propagation time delay (ms). The maximum frequency on the disturbed ionogram far exceeds the predicted MUF for the path. From Goodman and Ballard [2004].

As recognized in Section 3.8.1.1, there are many structured features of the polar ionosphere, Large scale features (i.e., 500-1000 km in dimension) typically originate in the auroral (or sub-auroral) regions and are convected (at speeds of ~1 km/sec) through the auroral zone and into the polar cap. These are referred to as patches or blobs, as the case may be. These are probably the features observed by Goodman et al. [2004] using oblique sounder transmissions. However there are other large-scale features to consider as candidates. Discrete plasma arcs (i.e., theta aurora), with electron densities up to an order of magnitude above the background, have been observed to stretch across the entire polar cap and move transverse to the earth-sun line at roughly $1/10^{th}$ the speed of the polar patches [Nickisch, 2004]. Both categories of large-scale features (viz., patches and arcs) can cause variations in the TEC along the radar lines-of-sight to specified targets, introducing variable excess time delay (i.e., range errors).

There are also important small-scale features to be considered. It has been suggested that the large-scale features (i.e., patches or blobs) are unstable to the $\boldsymbol{E} \times \boldsymbol{B}$ gradient drift instability, and that they decompose into smaller-scale structures as transport progresses [Tsunoda, 1988]. The resulting TEC variations (i.e., inhomogeneities in N_e) can cause radiowave scintillation that will degrade UHF radar operations.

The impact of the arctic environment is significant for individual communication circuits. In Chapter 4 we shall see that station diversity and frequency diversity can both play a role in improvement of communication performance. This is especially true for HF systems. Using oblique-incidence sounder data that sampled the entire HF spectrum every 5 minutes, Goodman et al. [1997] examined the impact upon a communication circuit between Iqaluit and Reykjavik, Iceland for a two-week period in 1995. Referring to Figure 4-28 that exhibits the RPSI Northern Experiment geometry, we see that this path constitutes polar conditions at worst and trans-auroral conditions at best. Figure 3-23 is a plot of HF channel availability computed from the sounder data for a hypothetical data link circuit over the specified path. Daytime averages are shown, and these are compared with a plot of negative *Ap* index. Two availability graphs are given, the first corresponding to use of a single "best" frequency, and the second corresponding to use of any out of eight "best" frequencies. The so-called "best" frequencies were pre-computed using the VOACAP HF prediction program [Teters et al., 1083]. Several things about this experiment are noteworthy. There are: (i) overall channel availabilities for the given circuit are not especially good; (ii) when the availability deteriorates, it makes little difference what the frequency plan is; and (iii) the variation in channel availability has a weak but noticeable correlation with magnetic activity index. The effects on the circuit appear to be broadband in nature, and they appear to persist for a day or more in some instances.

In general, we find that for high latitude circuits, frequency diversity is not as powerful a countermeasure to adverse propagation effects as station diversity. The reader is reminded that station diversity is not the same as path diversity. Path diversity corresponds to reception of signals from a common source by two receivers separated by 10s to 100s of meters. Station diversity refers to the reception of signals from two widely-spaced radio stations by a suitably equipped receiver. Path diversity is designed to counter short-duration diffraction fading due to small-scale irregularities, and station diversity is designed to cope with macroscopic propagation anomalies of medium scale and higher.

The reader should refer to Chapter 4 for more information on the effect of the ionosphere and miscellaneous space weather phenomena on telecommunication systems. Also, we refer the reader to an interesting real-time polar model that has been developed by the University of Alaska-Fairbanks [Maurits and Watkins, 1996]. This is discussed in Section 3.12 dealing with models.

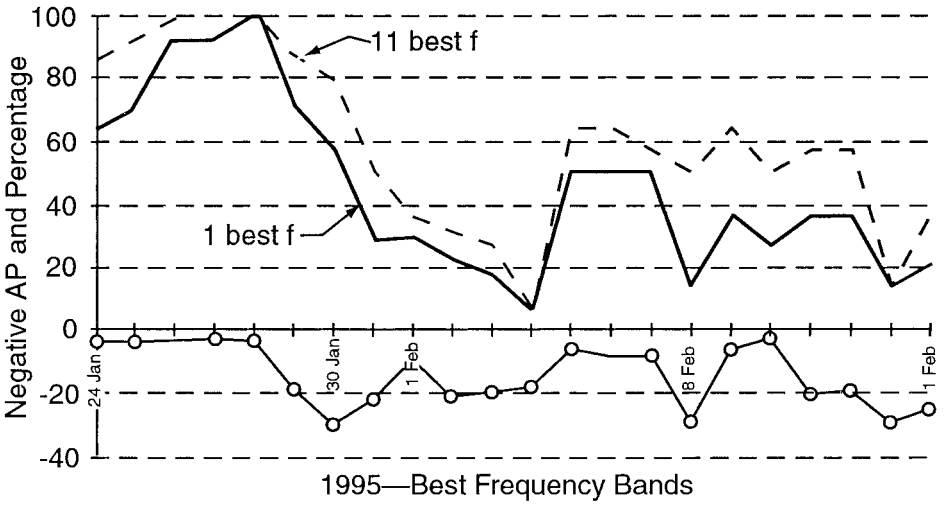


Figure 3-23: Channel availability (@300 bps) during daytime hours between 24 January 1995 and 14 February 1995. The path is from Iqaluit to Reykjavik. Refer to Figure 4-28 for the geometry. Also shown on the chart is the *Ap* index plotted as a negative number.

3.9 IONOSPHERIC RESPONSE TO SOLAR FLARES

Now we shall take note of a special class of effects called Sudden Ionospheric Disturbances (SID). These constitute those events that arise as a result of the atmospheric interaction with electromagnetic flux from solar flares. A book by Mitra [1974] is an excellent treatise on the ionospheric effects of solar flares.

We recognize that the sun is the ultimate source for a large variety of ionospheric and magnetospheric effects. Figure 3-24 exhibits the hierarchy of solar-induced ionospheric effects. There are many types of SID observed, and one of the most important is the Short-Wave-Fade (SWF) which affects HF communication circuits on the sunlit side of the earth. The source of the enhanced D-region ionization responsible for the SWF is typically an impulse burst of x-ray energy from within an active region on the sun (generally a sunspot). An x-ray flare generates a significant increase in D layer ionization with a temporal pattern that mimics the flare itself. This results in an increase in the product of the electron density and the collision frequency. It is the growth of this product that accounts for the absorption of HF signals passing through the D-region. Flares tend to be more prevalent during the peak in sunspot activity, and the individual flare duration distribution ranges between a few seconds to roughly an hour.

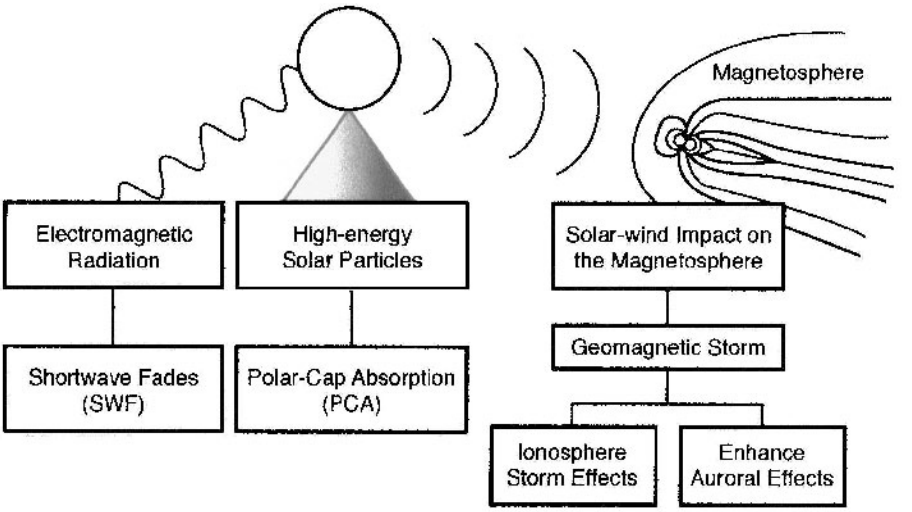


Figure 3-24: Hierarchy of solar-terrestrial effects. From Goodman [1991].

Figure 3-25 below is an example of a short wave fade. As indicated previously, the fade pattern mimics the pattern exhibited by the 1-8 Angstrom x-ray flux. Refer to Chapter 5 for more information about nowcasting these effects. (Figure 5-7 derived from the NOAA-SEC web site depicts a nowcast for global D-region absorption based upon the observation of an x-ray event. An x-ray flare, also extracted from the SEC web site is given in Figure 5-9, albeit for a separate event.) Any forecasting of short wave fade events is

problematic, since only the tendencies can be predicted from other observables (i.e., active regions, etc.).

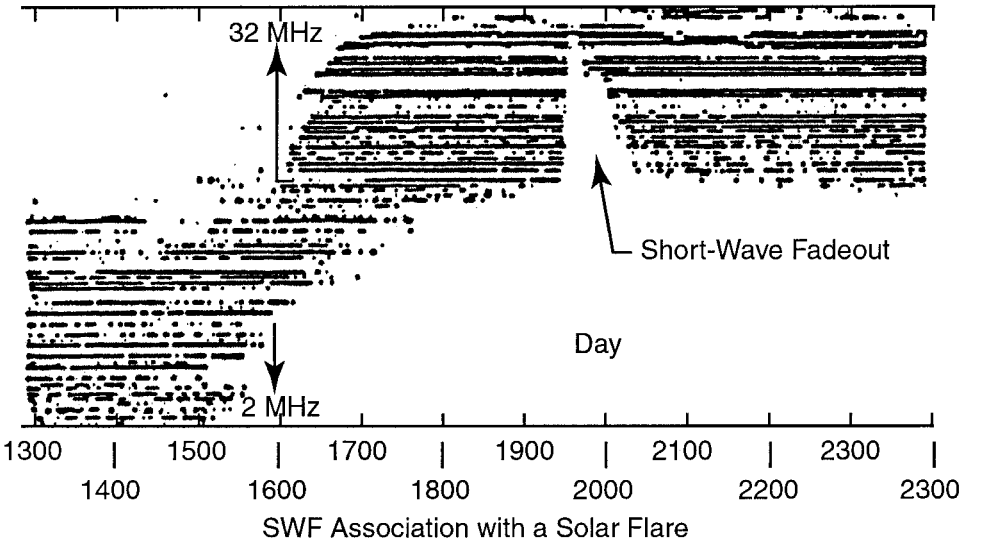


Figure 3-25: Sample short wave fade (SWF). From US Navy sources.

3.10 THE IONOSPHERIC STORM

The magnetic storm is a fascinating geophysical phenomenon, which goes far beyond the visible evidence corresponding to auroral displays at high latitudes. It is central to the issues surrounding what is now referred to as space weather. A discourse on this subject is beyond the scope of this chapter, but the reader is referred to an excellent geophysical monograph edited by Tsurutani et al. [1997]. Current understandings about the ionospheric storm processes appear in a paper by Buosanto [2000].

The ionospheric storm is the ionosphere's response to a geomagnetic storm. While the ionospheric responses to magnetic storms are varied, it has been shown that they may be conveniently classified as either positive or negative in nature. The main attribute of so-called negative storms is that they are generally associated with decreases in *foF2*. Positive storms exhibit the opposite behavior. At midlatitudes the ionospheric storm signature is typically commensurate with the main features of a negative storm, although variations may occur. Often the temporal (or stormtime) pattern is complex. For example, the midlatitude ionospheric response to a large magnetic storm is generally characterized by a short-lived increase in the F-region electron

concentration in the dusk sector following storm commencement (SC), after which it decreases dramatically (see Figure 3-14). But there is also a seasonal dependence and the positive/negative phase pattern may be different for the Northern and Southern Hemispheres. The NOAA STORM model captures this difference. Referring to the Northern Hemispheric response, an initial short-lived enhancement can be observed in *foF2* records and is correlated with the initial positive phase of the storm. The main phase of the geomagnetic storm is correlated with a concomitant *foF2* diminution, and this reduction in *foF2* may last for a day or longer. It is thought that the initial enhancement in *foF2* is a result of electrodynamic forces while the long-term reduction is associated with changes in upper atmospheric chemistry and modification of thermospheric wind patterns. A key factor is atmospheric heating through dissipation of storm-induced gravity waves. This heating effect will cause the thermosphere to expand, and ionospheric loss rates will increase.

3.10.1 Early Attempts at Storm Modeling

Some of the earliest attempts to examine the impact of magnetic activity on the midlatitude ionosphere were carried out by NRL workers in the early 1970s [Goodman et al., 1971; Goodman and Lehman, 1971]. Since the work was only documented in government reports and at a meeting of the American Geophysical Union (i.e., circa 1971-72), its distribution was not broad. Nevertheless we shall dedicate a small amount of space to the main points of the NRL study in the paragraphs that follow.

The Naval Research Laboratory had an incoherent backscatter radar located at its Chesapeake Bay Division some 40 miles from Washington DC. The NRL team was able to determine a number of ionospheric parameters, including the TEC, *NF2max, hF2*, and the equivalent slab thickness using a hybrid Faraday rotation and Thomson scatter radar technique [Goodman, 1970]. Faraday rotation of the radar returns was used to derive an unequivocal estimate of *NF2max*, without resort to a non-organic sounder. Studies of correlation between previous values of the magnetic index from Fredericksburg, Virginia (i.e., K_{FR}) were undertaken using midday conditions of the baseline ionosphere. The object was to derive the impulse response of the ionosphere to excursions in *K*-index at different lag intervals. It is important to note that the NRL data set did not include any major storm days; the data consistent of reasonable quiet conditions. The objective was to determine whether or not there was any particular threshold effect for *K*-index vis-à-vis the ionospheric impact. Having derived the correlation functions, the NRL team then exaggerated the amplitude of the *K*-indices to see if they could mimic a storm. Quite surprisingly, the answer was yes. Figure 3-26

shows a typical result. The general behavior is one in which the F2 maximum height increases initially, in proportion to the amount of magnetic activity, subsequently decreases, and eventually returns to its equilibrium value. It was found that *NF2max* and TEC decrease with increasing lag time, with the greatest diminution occurring at ~ 24 hours on the average. On the other hand, the F2 layer scale height and the slab thickness exhibited no consistent behavior. It should be noted that these are impulse responses. A true magnetic storm response at any given time would require an integration of all of these responses, each weighted by the appropriate value of *K*-index amplitude. This computed pattern of ionospheric perturbation clearly mirrors the pattern of a moderate magnetic storm, which is typically characterized by an initial positive phase followed by a longer-lasting negative main phase.

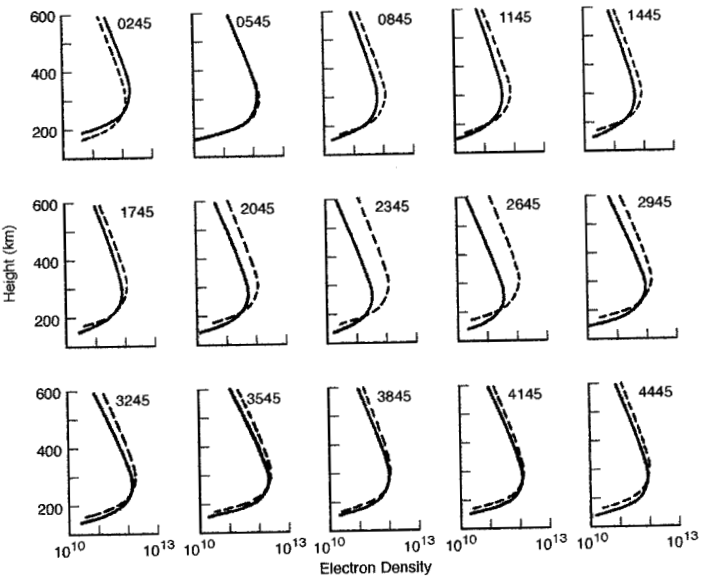


Figure 3-26: Response of the ionosphere to an impulse of magnetic activity. The normal unperturbed ionosphere is shown by the dashed curves, and the perturbed distributions are given by the solid curves. The scale of the perturbed distributions has been exaggerated for illustrative purposes. From Goodman [1971].

It is well known that magnetic activity is correlated with thermospheric heating. One only needs to refer to the premature loss of Skylab as a result of increased satellite drag forces to acknowledge this. Moreover, the dissipation of atmospheric gravity waves is thought to be a major source of heat in the upper atmosphere; and it is well-established that free atmospheric gravity waves and surface waves are coincident with elevated levels of magnetic activity. Since the NRL work was undertaken

during quasi-quiet times, the results suggest that small, and possibly undetectable, gravity wave modes were being generated and becoming available as heat sources, even during periods of modest magnetic activity. This appears to be an important result. The reader is reminded that the NRL correlation studies correspond to data over three consecutive months in 1971 (i.e., springtime and fixed sunspot number) and the results only apply to midlatitude stations.

Workers at AFCRL (now AFRL) conducted a long-term investigation of the ionosphere, based upon TEC measurements using geosynchronous satellites, and assembled the most comprehensive data base from which magnetic storm effects could be derived [Mendillo, 1971; Mendillo, 1973; Mendillo and Klobuchar, 1974a; and Mendillo and Lynch, 1978]. They developed a 62-month atlas of F-region responses to magnetic storms from which storm-time research was undertaken [Mendillo and Klobuchar, 1974b]. See Figure 3-14 for the average pattern in the variation of ionospheric parameters *NF2max* and TEC over 72 storms.

While most studies of the storm-time effects on the ionosphere have been directed at middle latitudes, Yeboah-Amankwah [1976] has examined eight storms and their impact at an equatorial station (i.e., Ghana). The measurements were of the TEC using the VHF Faraday rotation method, and the signal source was the geosynchronous satellite ATS-III. Yeboah-Amankwah finds a general rise in the TEC, with the largest effect at nighttime. Other equatorial investigators have also found that the correlation between the *Kp*-index and TEC is positive for all hours of the day. This equatorial response is different from that of the midlatitude observations.

3.10.2 The NOAA-SEC STORM Model

It is known that the ionosphere behaves quite differently from storm-to-storm, certainly with respect to the details, and there are latitudinal, seasonal, diurnal and solar epochal effects to consider. Moreover, it makes a difference whether the onset of the storm is during the day and during the night. Empirical models are data-driven but most efforts rely upon physical insight to extrapolate results into those domains for which data are sparse or unavailable altogether. Empirical models of magnetic storm effects are elusive, a fact that is not surprising given the fact that not all theoretical questions have been fully answered.

When we speak about modeling of magnetic storm effects, it is important to understand what we use as an input and what we desire as an output. Detman and Vassiliadis [1997] have reviewed techniques for magnetic storm forecasting, and Lundstedt [1997] has described AI (and specifically neural network) approaches. These efforts use downstream data (i.e., solar

and solar wind data) as an input to arrive at an output such as a magnetic activity index (i.e., *Kp* or *Dst*). From the perspective of telecommunications we are not uninterested in these results. But we are a bit more interested in how a given time history of *K*-index translates into ionospheric perturbations. A discussion of the magnetic storm forecasting (as opposed to ionospheric storm forecasting that is based upon magnetic storm attributes) is more properly a topic to be covered in Chapter 2 ("The Origins of Space Weather").

Needless to say, one can envision the marriage of AI technology, as the basis of a model to yield *K*-index time history, to an ionospheric response model (such as STORM, see below), yielding a prediction of *foF2* departures. To go a step further, we would like to promote the notion that the resultant *foF2* departure data set could be exploited in a number of propagation codes that require *foF2* as one of the input parameters. Then we will have successfully linked "upstream" solar data sets to system performance. But that is a little ahead of the game. Let's take a brief look at the STORM model.

Fuller-Rowell et al. [1997] have addressed the question "How does the thermosphere and ionosphere react to a geomagnetic storm?" Fuller-Rowell and his team have developed a model called STORM [Araujo-Pradere et al., 2002]. The model has also been imbedded in the International Reference Ionosphere (IRI2000) [Araujo-Pradere et al., 2002], and the imbedded model shows a 28% improvement in performance during storm days when compared with the model IRI95, which does not contain a stormtime correction. (See Section 5.4.3.1.2 for a brief discussion of the real-time STORM output on the SEC website.)

Fuller-Rowell and his team have developed an empirical model of the ionospheric storm, but it is important to recognize that the model is consistent with theoretical understandings [Prolss, 1993; Fuller-Rowell, 1996]. Table 3.3 is a list of the major points underpinning the model, as indicated by Fuller-Rowell and his team at SEC.

There are many factors that can compromise the assertions implicit in the listing above. Since there are a number of processes at work, the net result depends on the blend of the physical processes. This situation is difficult to specify in a complex physical model, and virtually impossible to represent in an empirical model. While one should not expect perfection in the SEC STORM model predictions, it is currently the only model that appears to capture most of the features of interest, and is simple enough to be operationally useful.

The STORM model is now on-line, and operates in a nowcast mode. However, telecommunication specialists would benefit if certain improvements were to be implemented. First, it would be useful if the model could be modified to work in a forecast mode. It is understood that NOAA-SEC is contemplating a 12-hour forecast. Secondly, it would be useful if the model could be run with different versions of the ionospheric response filter

function, especially for execution at different geomagnetic latitudes. Finally, it would be more convenient to the user if the output were organized in terms of geographic latitude and longitude, with more resolution provided.

Table 3.3: Assumptions forming the Basis for the STORM Model

- Long-lived negative storm effects are associated with neutral composition changes
- The so-called "compositional bulge" is from auroral heating as a result of magnetospheric input
- The neutral air (bulge) is transported to midlatitudes by nocturnal winds that are equatorward
- The neutral air (bulge) is brought to the dayside by earth rotation effects
- Summer-to-Winter circulation is prevailing, sending (molecular rich) gas to middle and low latitudes in the summer hemisphere over a matter of days.
- Poleward winds in the winter hemisphere restrict the equatorward movement of the bulge.
- Result_1: The winter hemisphere has a net decrease in molecular species (resulting from downwelling) and this causes a positive storm.
- Result_2: The summer hemispheric bulge introduces a net decrease in the electron concentration, and a negative storm.

3.10.3 Storm Studies Using NTS-2 Navigation Signals

Using data obtained from the Side-Tone-Ranging Subsystem (STR) of the Orbit Determination and Tracking System (ODATS) of the Navy NTS-2 satellite, NRL scientists were able to derive some interesting information about ionospheric storm effects [Goodman and Martin, 1983]. The NTS-2 satellite, like its predecessor NTS-1, was developed by the Naval Research Laboratory as an experimental prototype of satellites in the NAVSTAR/GPS constellation. The satellite was launched in 1977 into an orbit characteristic of modern day GPS satellites. It had coherent transmissions of 335 and 1580 MHz that could be used to study ionospheric parameters. These included TEC variations and ionospheric inhomogeneities responsible for amplitude and phase scintillation. Data were obtained at four locations: NRL Chesapeake Bay Division, near Washington, DC; Panama; Australia; and Great Britain. It is noteworthy that NTS-2 had two separate navigation subsystems, one the STR-ODATS (previously mentioned), and the second a pseudo random noise (PRN) pulse-ranging system that provided the main navigation signal. It was comprised of transmissions at nominally 1575 MHz and 1227 MHz with a waveform defined by bit rates of 1 or 10 Megabits/sec. For simplicity at the time, the NRL ionospheric studies exploited the STR-ODATS ranging tones at 335 and 1580 MHz instead of the dual frequency (L-Band) PRN waveforms. The ODATS system transmitted ranging tones of 335 and 1580

MHz, as mentioned above, with the UHF and L-Band transmissions consisting of a carrier, a single side-band reference tone and ten ranging tones equi-spaced up to 6.4 MHz, from the reference tone.

Based upon the NTS-2 data, high latitude scintillation observations have been presented by Goodman et al. [1978] and Goodman [1979]. Figure 3-27 shows a period of scintillation to the north of Washington DC as NTS-2 transited the oval and trough regions moving equatorward. Notice the loss of phase lock for part of the pass. This event was unusual since it exhibits a distinct trough region during daylight hours within which the slant TEC is significantly depressed, and this is correlated with scintillation occurrence near the poleward boundary. A fading range in excess of 40 dB was observed at 335 MHz near the poleward segment of the trough. It is noteworthy that on December 2nd, the A-index rose to 46 at Fredericksburg and 191 at Anchorage, while the planetary *Ap* index was ~ 70. The K-indices ranged from 4-6 at Fredericksburg and 3-9 at Anchorage. Clearly storm activity has moved the high latitude trough significantly equatorward.

From the Panama site, it was possible to examine the impact of storm effects on the anomaly crest. Figure 3-28 shows the ODATS output during the October 31-November 01, 1977 period. Two curves are shown, with the upper and lower curves corresponding to the L-Band and UHF signals respectively. Ignoring the data trends, for present purposes, the only significance of the data lies in the (vertical) difference between the two curves. This represents the ionospheric contribution to group path delay. It is seen that the difference is smallest near the closest point of approach of the satellite to the ground station (i.e., the CPA), and this would generally be expected. Of significance is the fact that the greatest difference appears on the N-S transit, somewhat ahead of the meridian transit that is due south. This corresponds to the northern hemispheric crest of the equatorial anomaly. The erosion of the crest is also observed as the satellite moves further southward and goes over the horizon near the meridian transit point. On its northward journey, the NTS-2 maps the same anomaly crest, albeit seven hours later.

Figure 3-29 is the superposition of UHF and L-Band phase data for a number of days. The presentation is a bit peculiar, but we have chosen to preserve the original format. The shaded area approximates the slant TEC at any given time, since it shows the time-delay difference between the UHF and L-Band signals. From the Panama site, and the given orbit, one may only observe the Northern Hemispheric crest of the Appleton Anomaly, as the southern crest is over the horizon. In any case, the northern crest is clearly observed as NTS-2 moves southward, and once again (but less distinctly) when it moves northward. From Figure 3-29, there is some evidence that *Kp* variations are correlated with poleward motion of the anomaly crest. This phenomenon will be revisited below.

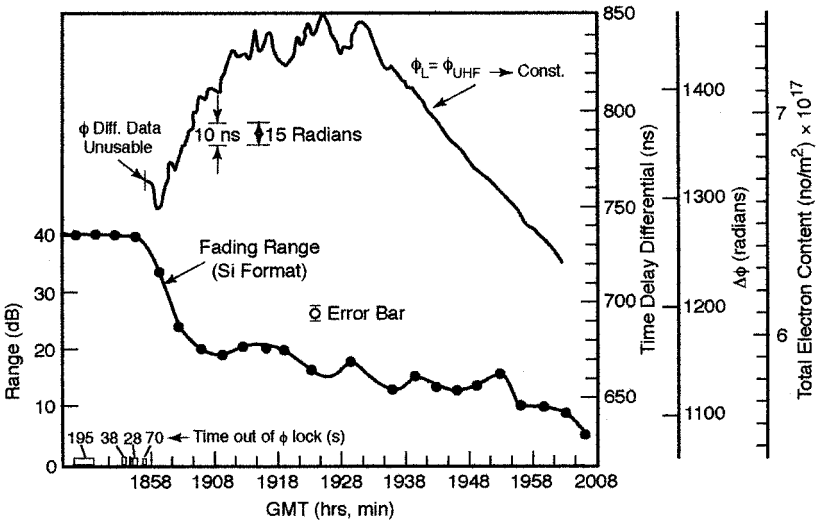


Figure 3-27: (Top): RF phase variation (radians), time delay (ns), and the slant TEC (electrons/m^2 x 10^{17}) for a NTS-2 pass on December 2, 1977. The vantage point is Washington, DC, and the mean ionospheric point (MIP) referenced to 400 km was transiting the Great Lakes region at midday (i.e., 1334-1508 LMT, and 1845-2008 GMT). (Bottom): Fading range at UHF is given in the approximate SI units. Here SI ~ the S4 index. The fading range exceeded 40 dB for more than 10 minutes and there were four periods of phase-lock being lost. From Goodman and Martin, [1983].

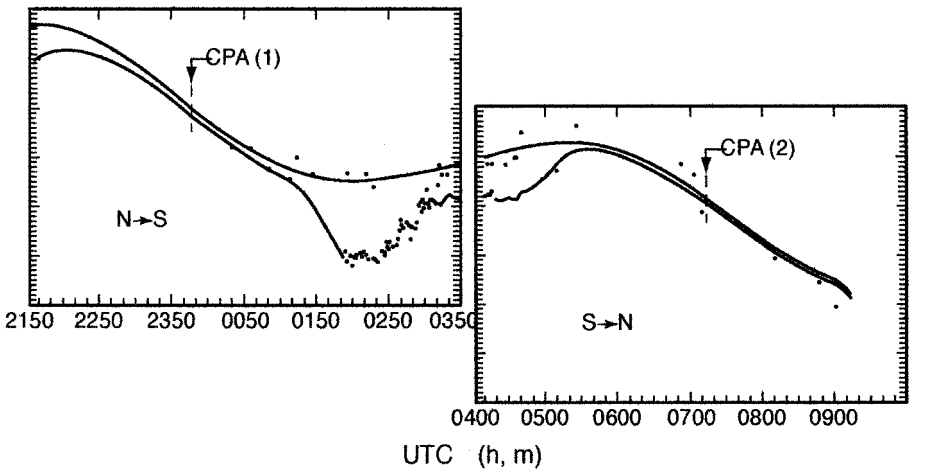


Figure 3-28: STR-ODATS data from NTS-2 signals on October 31- November 1, 1977. The receiver site was at Panama. The difference between the L-band (top curve) and the UHF (lower curve) signals can be translated into the slant TEC. Quasi-periodic fluctuations in TEC are observed equatorward of the anomaly crest. Only the northern hemisphere crest is observed on the N-S and the S-N transits. From Goodman and Martin [1983].

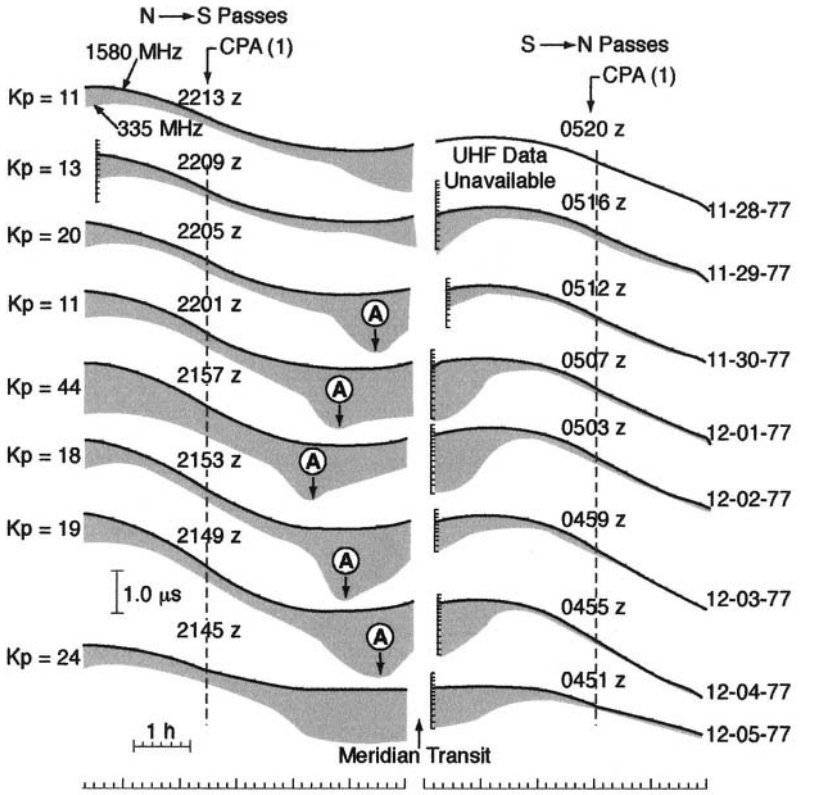


Figure 3-29: NTS-2 data at UHF and L-Band between 11-28-1977 and 12-06-1977. The vertical separation between the 335 and 1580 MHz signals is proportional to the group path delay difference between the two signals (i.e., slant TEC). From Goodman and Martin, [1983].

3.10.4 The Halloween 2003 Storm

The space weather aspects of the Halloween storm period were covered in Section 2.3.8, where the "upstream" aspects were emphasized (i.e., solar emissions, the IMF influences, and the magnetic activity response.) In this short section we will discuss the ionospheric disturbances that occurred during the period (i.e., "downstream aspects) and will compare that with some predictions from the STORM model. Some of the telecommunication system effects are described in Section 4.5.2. Figure 3-30 gives the STORM model prediction for the Northern Hemisphere for the 2-day period from October 31 to November 01, 2003. During the stormy period, a lot of the interesting sites that collected *foF2* data under normal circumstances exhibited vulgarized

data, but. Figure 3-31 and Figure 3-32 show some results for Sondrestrom (77°ML) and Eglin AFB (~40°ML) respectively. A climatological prediction of *foF2* for the sites is also given. We see from the STORM prediction (i.e., Figure 3-30) that there is a marked difference between the high latitude and low latitude dependence of the predicted *foF2* "multiplier". An enhancement is predicted for sites in the lower CONUS and a marked diminution is predicted for the upper CONUS. A comparison of the observations with the (transient) STORM predictions as well as the climatological predictions points out the difficulty associated with any prediction methods. We know that climatological "predictions" cannot account for storms. The STORM model develops its predictions based upon an historical record of storms, and its output is basically an "average" prediction of stormtime effects. But there is no average storm; each storm has its own eccentricities. The Halloween storm was no exception. More work is need in this area.

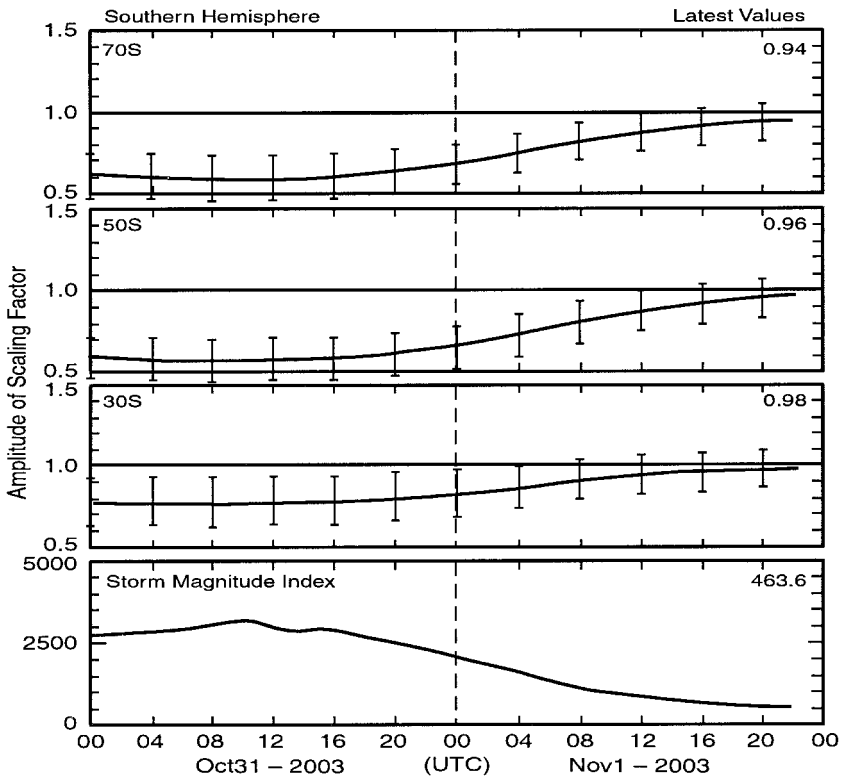


Figure 3-30: STORM model predictions during the Halloween storm period. The plots represent the "multiplier" for the median value of *foF2* based upon URSI-88 coefficients. See Section 3.10.2. The numbers on the RHS of each graph are the last recorded values. and not the maximum values. By permission of NOAA-SEC, Department of Commerce, Boulder, CO.

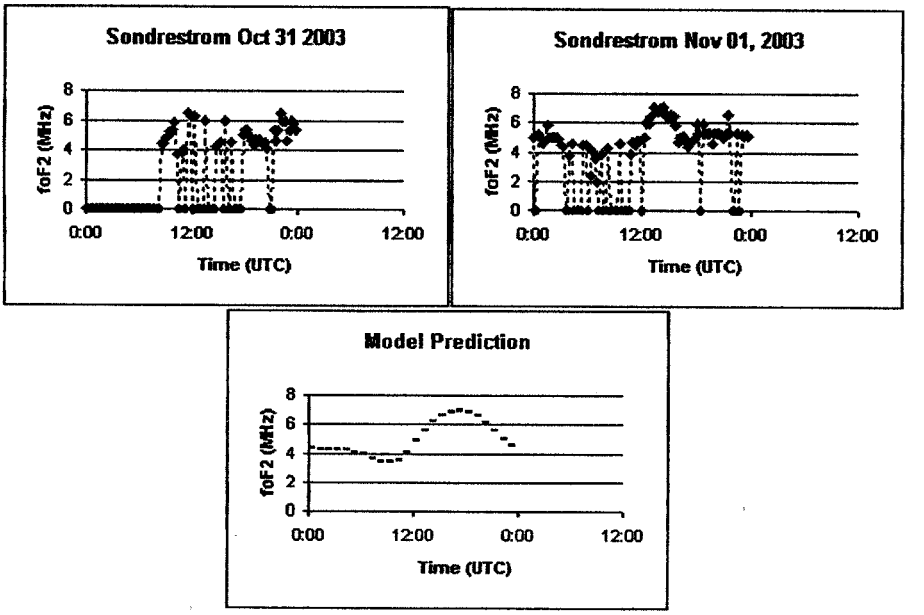


Figure 3-31: *foF2* data from Sondrestrom on Oct. 31-Nov. 01. 2003. A climatological prediction is shown using CCIR coefficients. Raw data was provided by NOAA-SEC.

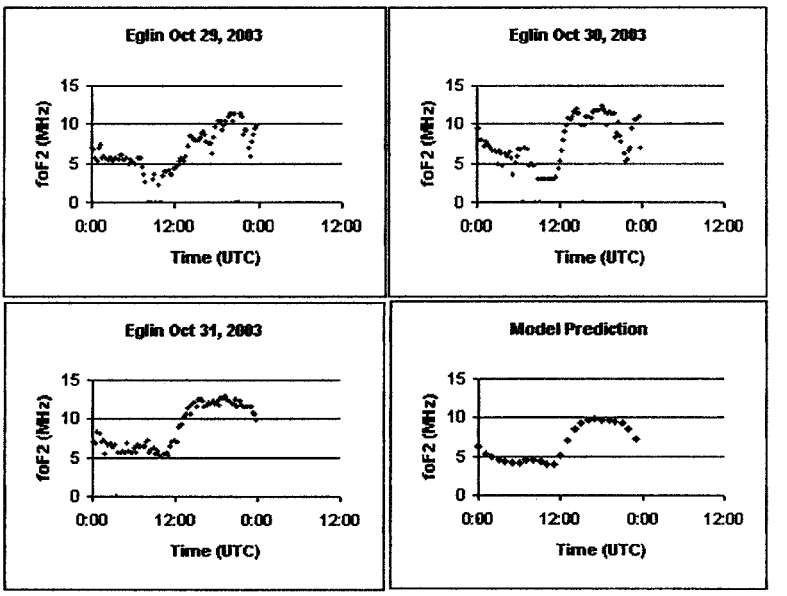


Figure 3-32: *foF2* data from Eglin AFB for Oct. 29-31. A climatological model prediction of the *foF2* is also shown using CCIR coefficients. Raw data was provided by NOAA-SEC.

In some instances, it has been shown [Coster, 2004] that the Equatorial Anomaly (EA) peaks move poleward during geomagnetic storms, and GPS-TEC data seems to support that. This is a very important result, and is consistent with some earlier work of Goodman and Martin [1983] described in Section 3.10.3. It suggests that poleward movement of the anomaly crest can sometimes be coincident with the well-known equatorward expansion of the auroral oval. This implies that during some geomagnetic storms the region we normally call "midlatitudes" may be contracted significantly. From a propagation perspective this introduces some important system considerations.

Figure 3-33 is the depiction of an SED event during the Halloween 2003 storm. We will continue the impact of storms and SEDs in Chapter 4.

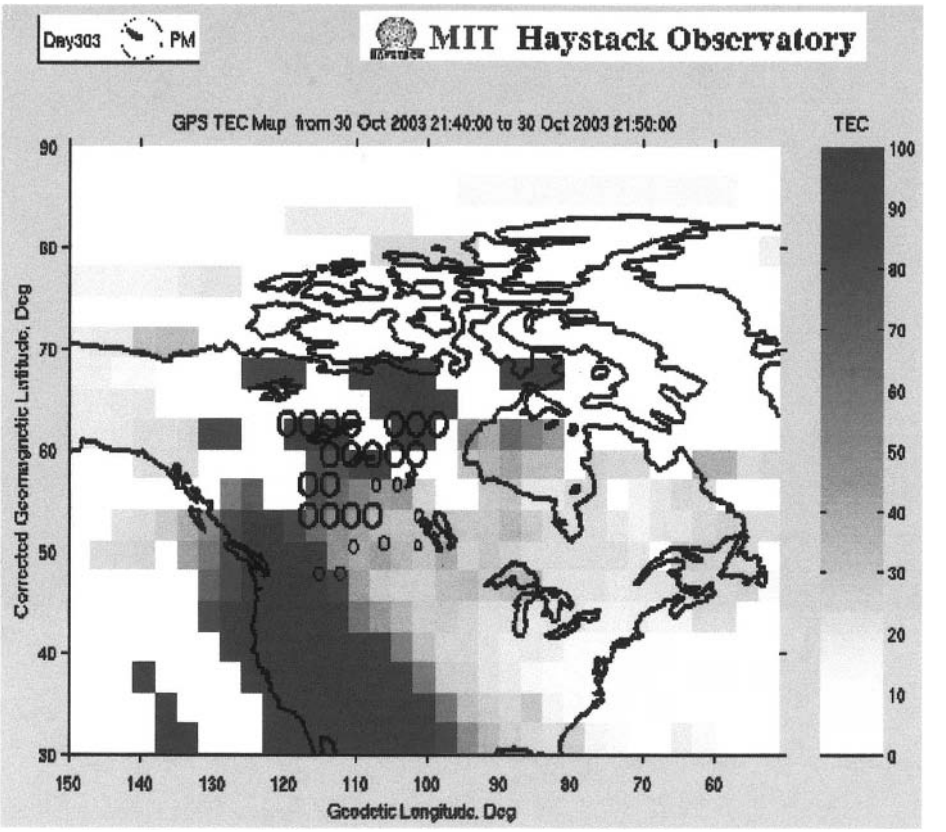


Figure 3-33: Example of SED plume of ionization during the Halloween storm. The circles represent data from scintillation monitors, courtesy Suzan Skone. The dark area over western CONUS and extending sporadically into Canada is the SED plume. Original illustration provided courtesy Anthea Coster and Wm. Rideout, MIT Haystack Observatory.

3.11 IONOSPHERIC CURRENT SYSTEMS

Current systems are important in an understanding of ionospheric perturbations associated with the onset of geomagnetic storms and the progression of these events. There are four principal current systems in the ionosphere that give rise to relatively rapid fluctuations in the geomagnetic field. These systems include: the ring current, the magnetopause current system, the atmospheric dynamo, and various high latitude current systems. The first two are associated with magnetic storms and occur at magnetospheric distances. The atmospheric dynamo is important in an understanding of tidal-driven forces, which interact with the ionospheric plasma causing a vertical drift of the F-region ionization. Descriptions of ionospheric current systems and dynamo theory may be found in a monograph co-authored by Rishbeth and Garriott [1969] and in a book by Ratcliffe [1972]. High latitude currents (i.e., polar and auroral) and atmospheric dynamo currents are observed at lower ionospheric heights in the vicinity of the E-layer.

Brekke [1980] provides a good treatment of relevant high latitude current systems. There is also a current system within the neighborhood of the magnetic equator, the equatorial electrojet, which flows along the geomagnetic equator, eastward by day and westward by night. It is associated with a class of discrete ionospheric formations that are termed equatorial sporadic E.

3.12 IONOSPHERIC MODELS

As in many areas of geophysical study, ionospheric modeling may assume a number of forms ranging from the purely theoretical to the totally empirical. Approaches may also include a combination of these forms, although empirical models dominate the field. Recent developments include allowance for adaptivity within the models to accommodate exploitation in the near-real-time environment for special applications. While physical or theoretical principles are the inspiration for a number of models, in fact most models in use today are largely specified on the basis of semi-empirical relationships derived from observational data.

Ionospheric models fulfill a variety of needs beyond basic research, with the most prominent application being radio system performance assessment and prediction. For example, ionospheric models are the engines that drive HF system performance models such as IONCAP [Teters et al., 1983]. Related models are supported by the U.S. Department of Commerce, including VOACAP, ICEPAC, and REC533. (The latter models may

downloaded from an ITS website [Hand, 2004].) Other applications include evaluation of transionospheric signal parameters and errors in ranging or geolocation introduced by the electron content of the ionosphere. A general discussion of the status of ionospheric modeling in the context of HF communication systems has been covered by Goodman [1991], and recent information regarding telecommunication system planning has been published by the Commission of European Communities [Hanbaba, 1999]. We shall discuss activities of the European Union in the context of COST Actions in Section 3.12.3, Section 5.4.7, Section 5.4.9, and Section 6.6.1

Ionospheric profile models are based upon the superposition of various submodels of the ionospheric layers or regions (i.e., D, E, Es, F1, and F2). The basic purpose of modeling is to represent the electron density profile under a variety of conditions (See Figure 3-4). These profile models may represent the respective layers as thin horizontal sheets (e.g. sporadic E), or quasi-parabolic regions in the vicinity of maximum ionization. The models are specified by the maximum electron density of the layer, the layer height, layer thickness and a functional representation of the layer shape. There are a number of models for the height profile, with the main differences being the manner in which the component layers are combined. Figure 3-34 depicts the general profile shape for the International Reference Ionosphere [Bilitza, 1990], and Figure 3-35 shows the ionospheric model contained in the computer program IONCAP.

There are also geographical, seasonal, and solar epochal variations in the specified ionospheric profiles, and the parameters upon which they are built. An example of the geographical variations in foF2 was shown in Figure 3-10, and the *Global Atlas of Ionospheric Coefficients* was discussed in Section 3.4. Ionospheric coefficients used to produce maps similar to Figure 3-10 are common to virtually every global empirical model of the ionosphere. Currently there are two sets of ionospheric coefficients, which may be specified; and these are the original CCIR (or ITU-R) set, which is sanctioned by the ITU-R, and the newer URSI set [Rush et al., 1989].

Sometimes it is good to keep models relatively simple in order to make subsequent applications more convenient. A sample application would be ray tracing. Simplicity may also be sufficient if the application is not demanding of precision in the profile. A simplistic model of the ionosphere consists of a parabolic E-layer, a linear increase in electron density in the F1 layer followed by a parabolic F2 layer [Bradley and Dudeney, 1973]. At nighttime, the E and F1 layers effectively disappear. A newer ITU-R recipe consisting of multi-quasi-parabolic layers to provide continuity of the overall profile and its height derivatives [Dick and Bradley, 1992] has replaced the so-called Bradley-Dudeney profile model.

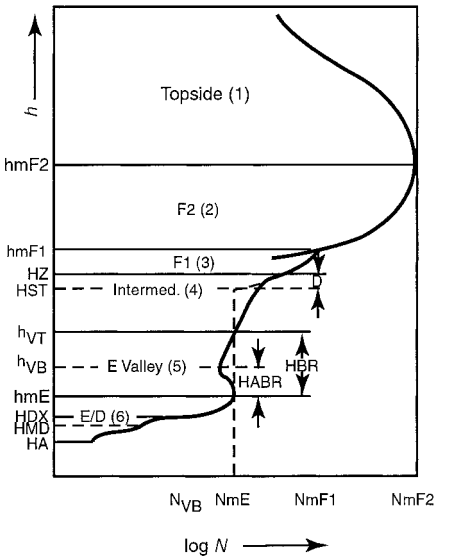


Figure 3-34: Depiction of the general profile shape for the International Reference Ionosphere.

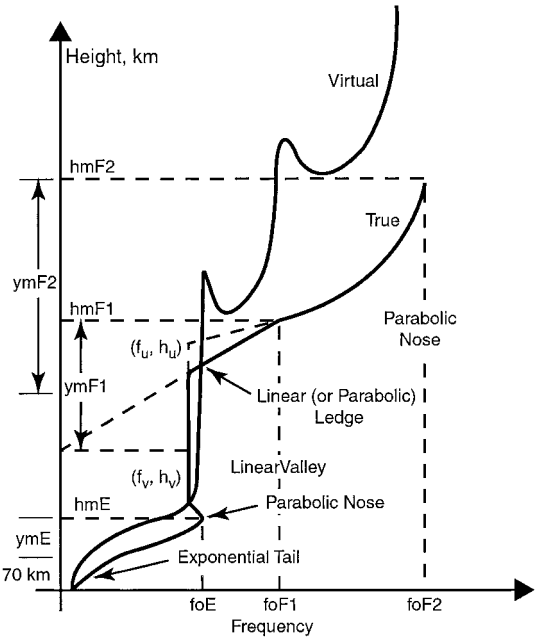


Figure 3-35: Ionospheric model contained in the computer program IONCAP.

Significant improvements in empirical ionospheric modeling have been promoted by military agencies around the world, including the U.S. Department of Defense, the U.K Ministry of Defence, and others. This is not surprising in view of the large number of applications of ionospheric specification in radiowave systems used by the military. The original ICED model was intended to be a northern hemispheric ionospheric specification model to serve the requirements of the US Air Force. It was only a regional model, descriptive of midlatitude behavior but extending into the auroral zone. It was designed to allow for recovery of some of the dynamic features embodied in auroral climatology which are smeared out in most mapping procedures. The model as described by Tascione et al.[1987a, 1987b] is driven by an effective sunspot number and an index derived from auroral oval imagery. The effective sunspot number is not based on solar data at all, but is derived from ionospheric data extracted from the US Air Force real-time ionosonde network. This effective sunspot number is similar to an ionospheric T-index developed by Australian workers, and the pseudoflux concept used by the U.S. Navy for HF predictions [Goodman, 1991]. The ICED model has been generalized to incorporate global considerations, while emphasizing near real-time applications.

Anderson has developed a low-latitude ionospheric profile model, SLIM [Anderson et al., 1987], and a Fully Analytic Ionospheric Model, FAIM [Anderson et al., 1989], in order to eliminate the use of limiting simplifications in the driving parameters associated with prediction models. A discussion of SLIM and FAIM may be found in a paper by Bilitza [1992]. Other developments supporting Air Force requirements include PIM [Daniell et al., 1995] and PRISM. The model PIM, or Parameterized Ionospheric Model, is a global model of theoretical and empirical climatology, which specifies the ionospheric electron and ion densities from 90 to 25,000 Km. The model PRISM, for Parameterized Real-Time Ionospheric Specification Model, uses ground-based and space-based data available in real time to modify PIM thereby providing a near real-time ionospheric specification. Another model (viz., RIBG) discussed by Reilly and Singh [1993] combines ICED and several other models with a general ray tracing utility. Current versions of these models and validation of PRISM is discussed by Doherty et al. [1999]. An earlier survey of computer-based empirical models of the ionosphere has been published by Secan [1989].

The International Reference Ionosphere (IRI), mentioned previously, is a global empirical model that specifies monthly averages of electron, ion, and neutral temperatures, in addition to electron and ion densities from about 50 Km to ~ 2000 Km [Bilitza, 1990; 2001]. The IRI development is a joint project of URSI and COSPAR, and has proven to be a useful model for scientific research. In recent years the IRI has been used in a number of applications and has gained greater acceptability within the operational

community. The IRI is continually updated, and the responsible group holds periodic Task Force Activity meetings. The year 2002 meeting of the URSI-COSPAR IRI Working Group was the 9th meeting; and the major actions were considerations of ionospheric variability and the better understanding of the topside ionosphere [Radicella, 2003]. As was pointed out in Section 3.10.2, IRI2000 has incorporated the STORM model to better represent the ionospheric personality during ionospheric storms. Figure 3-36 gives two global maps of the parameter *foF2* using the IRI model. The conditions are summertime solar maximum and minimum at 00 UTC. Its form is similar to maps found in the original CCIR Global Atlas [CCIR, 1966] and in current ITU-R publications. The IRI has become a defacto standard for a number of applications including HF communication predictions and GPS studies. There is also a proposal to the International Standardization Organization (ISO) to recognize IRI as a standard model for the ionosphere. More information about the IRI model may be found on the NASA-GSFC website. There is also a newsletter that can be useful to researchers, and it is distributed through the ISAS organization. The source code of the IRI is available from the National Space Science Data Center (NSSDC); the documentation is given in Bilitza [1990]; and online computations may be organized from the NASA-GSFC website and the University of Leicester website.

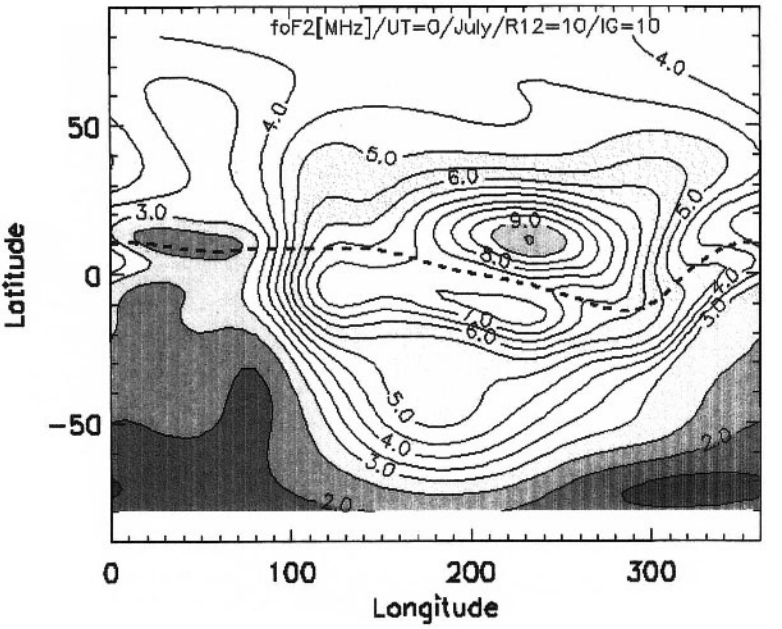


Figure 3-36: The International Reference Ionosphere. Global map of the parameter *foF2* (MHz) for solar minimum (R=10), summertime (July) at 00 UTC. Map provided by courtesy of Dieter Bilitza [2004].

A model of primary interest to workers studying transionospheric propagation effects is the so-called Bent Model, a profile model based upon topside and bottomside sounder data [Bent et al., 1976]. Simplicity is not always important in the age of sophisticated computers, but the Ching-Chiu model [1973] has found a number of scientific applications in cases for which detailed ionospheric specification is not paramount.

Aside from global modeling of the ionosphere, there have been attempts to model selected regions of the world more accurately. During the decade of the 1990s, European scientists affiliated with the COST program have taken a lead in regional modeling and mapping of the ionosphere [Bradley, 1999; Hanbaba, 1999]. More information on COST-related activities is provided in Section 3.12.3.

Another region-specific model is University of Alaska-Fairbanks Eulerian Parallel Polar Ionospheric Model (EPPIM). The EPPIM is a physical model of the polar ionosphere, which uses as inputs current solar and geomagnetic activity supplied by NOAA-SEC using the FTP protocol. The primary real-time geomagnetic activity driver is the U.S. Air Force estimate of *Kp*-index that is supplied hourly. Interplanetary Magnetic Field (IMF) data is obtained from the WIND or ACE satellites; and this is used in conjunction with the Weimer [1995, 1996] electric field model to determine ionospheric drift patterns. The model can be run in a forecast mode (i.e., ~ 1 hour in advance) using the fact that an average solar wind takes between 0.5 hr and 1.5 hr to traverse the ACE-to-earth distance, depending on the solar wind speed involved. Real-time data can be obtained by accessing the special UAF EPPIM web site. Real-time comparisons of the model output and observed values of the F2 layer critical frequency (i.e., *foF2*) are found on the web site. Real-time data from twelve stations belonging to the global ionosonde network are used in the comparisons. The sounder data are found at the NOAA-SEC web site (i.e., daily files). The EPPIM model has been of value when estimating the impact on HF communication circuits in the polar regions. Radio Propagation Services, a provider of HF communication forecasting services has used (i) UAF-EPPIM output, (ii) polar GPS-based TEC maps and (iii) raw ionosonde data from NOAA-SEC to evaluate the influence of the polar ionosphere on air-to-ground HF circuits within the auroral oval.

3.12.1 Data Assimilation and Kalman Filters

As a practical matter, there is a natural tendency to trust data over theory if there is some assurance that the data truly represents the quantity being observed. In practice, data is obtained from measurements by imperfect instruments against a background of noise and other factors that may

camouflage the true values be sought. Even if we are convinced that the data is of high quality, the application of multi-station data in development of an ionospheric "map" can be problematic for a variety of reasons. Some include: a paucity of observations over oceanic areas, and an irregular spacing of data derived from observing platforms in both space and time.

Many attempts have been made to assimilate various data types (i.e., *foF2* from ionosondes) to produce instantaneous maps over regions where observing platforms are sufficiently dense. The European COST 238 and COST 251 Actions come to mind, and these will be discussed in Section 3.12.3. American sector, European region and polar maps of GPS-derived TEC have also been produced with some success. Worldwide maps can be produced by piecing together local "maps". But how can we make the individual maps consistent with each other in the intervening regions where there is little data upon which to develop a data-driven model? One approach is to develop a transitional region that gracefully merges with climatology after a certain distance. This appears to be a method used in the COST Actions pertaining to the ionosphere and radio communications.

The Kalman filter was developed decades ago [Kalman, 1960], and has found many engineering and military applications [Anderson and Moore, 1979]. The IEEE has reprinted a number of classic papers [Sorenson, 1985]. Of special interest is the so-called extended Kalman filter [Costa and Moore, 1991]. The main purpose of the Kalman filter in the present context is to determine the state of a system (e.g., the ionosphere) from measurements that contain random errors. There are a number of error sources in ionospheric measurement systems, and the error variances will depend upon the type of measurement. In simple terms, the question addressed by a Kalman filter is as follows: Given our knowledge of the general physical behavior of the ionosphere, and given all of our diverse measurements at our disposal, what is the best estimate of specified ionospheric variables. We know how the ionosphere should behave on the basis of a physical model, and we have a number of measurements of specified parameters, so how can one evaluate the complete state of the system? It seems obvious that we should be able to do better than simply take the measurements as the only basis for system state estimation, most especially if there is an abundance of measurement noise. The Kalman filter is an algorithm that minimizes the estimation error. The Kalman filter equations may be formulated in a number of ways, and it is beyond the scope of this manuscript to present them. The Kalman filter algorithm involves a considerable amount of matrix algebra in its application, but the reader can review this field of mathematics in books by Golub and Van Loan [1989] and Horn and Johnson [1985]. In the GAIM programs, described in Section 3.12.2, a Kalman filter approach is used.

3.12.2 GAIM

McCoy [2001] has provided background for the Global Assimilating Ionospheric Model (i.e., GAIM), which was sponsored by the U.S. DoD. Specifically it was a Multidisciplinary University Research Initiative (MURI) managed jointly by the Office of Naval Research (ONR) and the Air Force Office of Aerospace Research (AFOSR). The 5-year program began in 1999. Two awards were given: the Utah State University team headed by Robert Schunk, and the University of Southern California team headed by Chunming Wang. Elements of both programs were discussed at IES2002 in Alexandria, VA and were included in the conference Proceedings [Goodman, 2002]. While the MURI component of GAIM is virtually over, the initiative has developed a life of its own, and a number of separate research activities based on GAIM technology are underway.

The purpose of GAIM-MURI was the development of a new generation of ionospheric model based upon near-real-time data assimilation. The idea was the joint vision of Robert McCoy at ONR and Paul Bellaire of AFOSR, derived from the recognition of considerable progress in the last 50 years or so by meteorological investigators in the use of various filtering, data assimilation and variational methods. McCoy points out that more data is always a good thing, but that skill in forecasting requires a precise knowledge of the source of errors. He also notes that raw data assimilation is preferable to the assimilation of secondary products that are derived from data sets. An example of a secondary product would be (vertical) TEC derived by conversion of oblique GPS-TEC measurements. In any case, it is felt that GAIM and its follow-on technologies are certainly a step in the right direction. The telecommunications community eagerly awaits the outcome of this research. It is hoped that versions of the code, or Internet access to specified output data files, can be made available to the public. Schunk et al. [2002] and Wang et al. [2002] outline the two independent DoD-sponsored MURI efforts to develop a GAIM model. Additional work by the groups is described by Scherliess et al. [2002] and Hajj et al. [2002].

It has been recognized for some time that empirical models, with an initial value for a driving parameter, can be updated by forcing the output to match data, thereby deducing an altogether new value of the driving parameter. Using the new value of the driving parameter, we find that the model should do a better job at matching the real world, provided correlation distances are sufficiently long and the raw data is not error prone. This general procedure has been used for HF communication networks for many years [Goodman, 1991]. But GAIM is far more elegant and less simplistic, although the starting point in the GAIM methodology exhibits certain similarities to some of the HF updating methods.

GAIM, as a MURI program, was completed in 2004; however aspects of the program have transitioned to a quasi-operational phase. Work is continuing at NOAA-SEC and the Air Force Weather Agency (AFWA). Fuller-Rowell et al. [2002] and Mintner et al., 2004] of the SEC group have examined the data assimilation of neutral thermospheric species during geomagnetic storms. This research is important since it is well known that the ratio of certain thermospheric species can be the most important driver in *foF2* variations during magnetic storms. The research of the SEC group includes a comparison of Kalman filtering with nudging, and it was concluded that the former method is superior. Nudging is the simplest approximation to the Kalman filter in that it simply ingests raw data into the model without attempting to correct for observational errors. Mintner et al., [2004] maintain that this is equivalent to setting the Kalman gain equal to unity, with full acceptance of recent data, and neglecting the propagation state.

It should be noted that specialized data assimilation efforts have been undertaken, as derivatives of GAIM. Sojka et al. [2002] have examined data assimilation for ARGOS LORAAS tomographically reconstructed electron density profiles near the equator. Keskinen and Dymond [2002] have described data assimilation techniques for mesoscale space weather forecasting. They consider Kalman filters, direct data insertion, the so-called nudging processes, and variational methods. Of special interest is an application associated with spread-F bubbles or plumes.

3.12.3 European Union COST Action Models

The European Union has organized a number of activities under a program termed COST, which stands for *Cooperation in Scientific and Technical Research*, and specific *Actions* under COST have been sanctioned. The Actions are necessarily Eurocentric, although there are clearly certain developments that apply globally. Three of these COST Actions of relevance to ionospheric modeling, forecasting and telecommunication system effects have been designated as Actions 238, 251 and 271. An Action on Space Weather has also been initiated (i.e., Action 724). In this section we shall identify some aspects of the ionospheric models and related products to the extent they have been developed and are applicable. It is the opinion of this author that the various COST actions are a significant advance in the development of ionospheric modeling, especially models of the empirical variety. It is also clear that the COST programs have succeeded in organizing a viable and productive European space weather program.

We shall make a few remarks about specific COST Actions 238 and 251 products below (i.e., Sections 3.12.3.1 and 3.12.3.2). Additional

programmatic information about all Actions, including 271 and 724, are provided in Chapter 6 (i.e., Section 6.6.1).

3.12.3.1 COST Action 238

Details of COST Action 238 may be found in a published final report [Bradley, 1999]. Action 238 is otherwise known as PRIME, standing for *Prediction and Retrospective Modeling over Europe*. The Action was inaugurated in 1991 and completed in 1995. The objective was to develop improved models of the European ionosphere for telecommunication purposes. There were a number of achievements that are relevant not only for the European region, but they can also be useful for consideration elsewhere. A tangible product from the Action was the development of a computer program based upon adopted procedures that provides for electron density profiles of the ionosphere, total electron content, and other ionospheric characteristics under specified conditions. There are 16 separate output options and a range of presentation methods accommodated. The output options and sub-models are discussed in the final report.

3.12.3.2 COST Action 251

This Action is entitled: *Improved Quality of Service in Ionospheric Telecommunication Systems over Europe*. Details of COST Action 251 may be found in a published final report [Hanbaba, 1999]. Like Action 238, Action 251 resulted in a computer program that provides ionospheric information. Specifically it enables the calculation of monthly median and instantaneous values of the parameters *foF2*, *M(3000)F2*, *N(h)*, and the TEC. If necessary, the parameter can be translated to the height of the maximum of F2 layer ionization using a well-known empirical expression. While the emphasis is on the European theater, there are procedures for interfacing seamlessly with global maps. In Table 3.4 we have a listing of key algorithms used in the Action 251 computer program.

The most interesting of the algorithms in the Action 251 computer program from the perspective of near-real-time prediction services (i.e., nowcasting and short-term forecasting) are PLES2, PLES5, COSTPROF, COSTTEC, and CORLPRED. The models MQMF2R, UNDIV, PLES2, and PLES5 use the ITU-R ionospheric model outside of the so-called COST 251 area of interest; COSTPROF uses the IRI model outside of the COST 251 area. CORLPRED predicts *foF2* up to 24 hours in advance at a specified station using an autocorrelation method [Muhtarov and Kutiev, 1998]. At least 20 days of historical data is needed for the CORLPRED program to work properly. There are additional models developed under the Action, not incorporated in the published program.

The CORLPRED software is made available through the Space Research Center in Warsaw, Poland. The basic input data are 23 vertical-incidence sounder stations between 10 degrees West and 90 degrees East Longitude. The latitude range is between ~ 30 degrees North and ~ 70 degrees North. Raw data are converted to maps over this Eurasian region. The forecasting procedure allows prediction of both *foF2* and *MUF(3000)F2* up to 4 days in advance when 60 days of prior data are used as an input for derivation of an auto-regressive filter. The prior data are, of course, *foF2* and *M(3000)F2*, where it is assumed that $MUF(3000)F2 = M(3000)F2 \cdot foF2$. To produce maps of *foF2*, for example, a commercial package is applied. This package is not unlike the SURFER program offered by Golden Software in Boulder, Colorado. It has an option for mapping called Kriging, a method that operates efficiently for sparse data sets. Sample maps of *foF2* for the forecast and measurement mode are shown in Figure 3-37. While this corresponds to a quiet ionosphere, it seems apparent that the results are quite acceptable.

Table 3.4: List of Models contained in Action 251 Computer Program

Program Name	Ionospheric Parameter	Presentation of Output
MQMF2R	*foF2*	long-term map
UNDIV	*M(3000)F2*	long-term map
PLES2	*foF2*	instantaneous map
PLES5	*M(3000)F2*	instantaneous map
COSTPROF	*N(h)*	long-term and instantaneous map
COSTTEC	TEC	long-term map
CORLPRED	*foF2*	short-term forecasting

Other forecasting methods developed under COST 251 included separate neural network approaches advanced by the UK DERA organization and by Tulunay et al. [1999]. The DERA method reportedly can predict from 1 hour to 24 hours in advance. The Tulunay approach was designed to predict *foF2* one hour in advance. Multi-regression approaches for short-term prediction of *foF2* have also been developed under the Action.

Of special interest are forecast models for the TEC. As indicated above, CORLPRED is the Action-approved method for instantaneous values of *foF2* and *M(3000)F2*. Using forecast values of *foF2* and *M(3000)F2* data, and using an appropriate profile model, CORLPRED can be extended to do TEC forecasting and mapping. COSTPROF is the sounder-based model used to forecast the TEC, based upon work by Cander et al. [1999]. Figure 3-38 illustrates some of the difficulties in the approach.

Under the Action 251, GPS-TEC data sources were also investigated, but most of the original emphasis was on extrapolation of sounder results

using COSTPROF. This emphasis has changed in the time since COST Action 251 was finalized. Other "novel" data sources for investigating the effects on earth-space systems include ionospheric tomography and GPS occultation measurements.

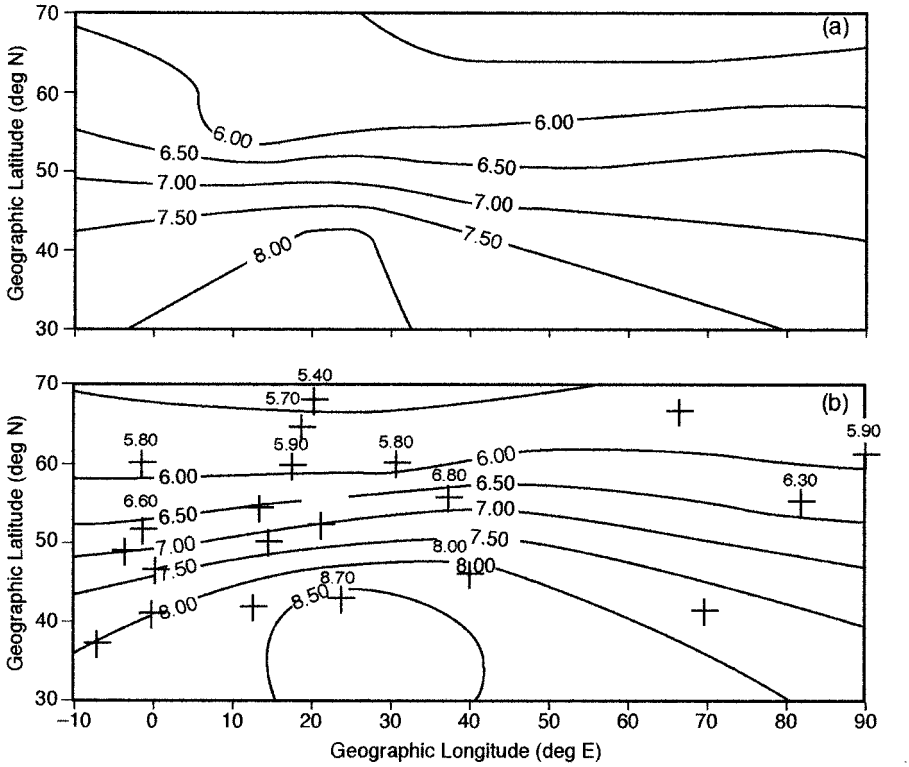


Figure 3-37: Pair of maps showing the actual measured *foF2* for the COST 251 area (top) and the predicted map (bottom). The prediction was 24 hours in advance. The conditions were not disturbed. The period of the forecast was 1200 UT on 12 May 1998. Original illustrations by courtesy of Space Research Center, Warsaw, Poland.

3.12.3.3 The ESA Space Weather Working Team

While not part of the COST program (viz., Action 724), the SWWT was set up to advise the European Space Weather Advisory Committee, and it provides advice to ESA on various space weather strategies. See Section 6.6.1 for additional programmatic information.

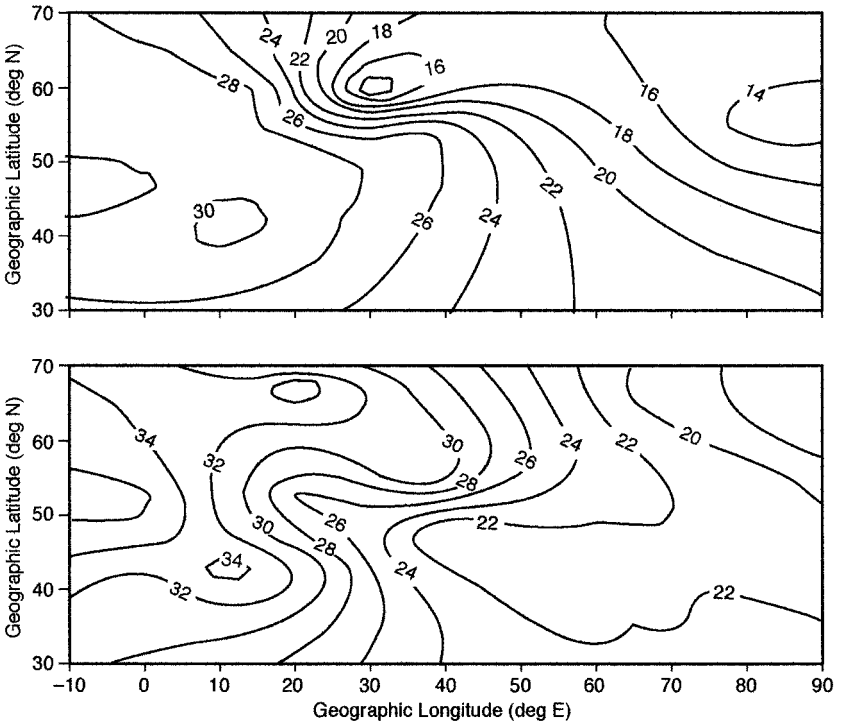


Figure 3-38: Pair of maps showing the actual TEC for the COST 251 area (top) and the predicted map (bottom). The period of the measurement and forecast was 20 January 1999.The prediction was 24 hours in advance. The COSTPROF model was used. The conditions were not disturbed. Illustrations provided by courtesy of the Space Research Center, Warsaw, Poland.

3.12.4 Ionospheric Modeling Panel at IES2002

Author's Note: I have had the good fortune to organize the triennial Ionospheric Effects Symposia since 1975, and the event in 2002 included a special forum on "Ionospheric Models-Current and Future". The Forum was ably chaired by Dr. Ken Davies of NOAA (retired) and Dr. Anthea Coster (MIT-Lincoln Lab, now MIT-Haystack Observatory). The panel co-chairs developed a full summary that is contained in the Proceedings of IES2002. It turned out to be a rather interesting forum, and I felt it would be useful to provide a short synopsis of the summary report written by Davies and Coster. The recorders were Greg Bishop and Patricia Doherty. The panelists included: John Seago (user needs), Tim Fuller-Rowell (storm models and metrics), Jan Sojka (new data and data quality), Dieter Bilitza (empirical models), Terence Bullett (data sources), and Brian Wilson (TEC models). The

discussions were freewheeling and I would like to express my appreciation to Jack Klobuchar for keeping the forum lively.

I have occasionally entered some comments within the text, identified as "Editorial Note", to distinguish my personal views or additions from those of Davies, Coster, and the various contributors at the forum. Finally, it was regrettable that the user community was not as well represented at the forum as would have been preferred. This is always a problem, and needs to be rectified.

Summary Report on Ionospheric Models – Current and Future

By: Ken Davies and Anthea Coster
(as edited by John Goodman)

3.12.4.1 User Needs

John Seago (Honeywell Technology Solutions, Inc.) represented himself as a "novice user", or an individual who is aware of the need to account for ionospheric effects, but lacks the formal training or experience in modeling approaches and techniques to apply them. Mr. Seago recommended that models and documentation be accessible on-line, and be completely self-contained, with software installation instructions, necessary data files, version numbers, and points of contact provided. He also suggested on-line information should include test cases and estimates of model uncertainties.

3.12.4.2 Storm Modeling

Tim Fuller-Rowell (NOAA-SEC) discussed the difficulties in modeling the ionosphere under storm conditions, which he regarded as being comprised of both climatological features and weather features. The climatological features were repeatable from storm-to-storm, but the differences between storms should be properly described as weather. He lamented that the physics of storm phenomena was not yet completely understood. Fuller-Rowell reported that the IRI2000 model, which captures solar cycle, seasonal, geographical, and local time variations, has now included magnetic activity variations (through the STORM model). He remarked that the magnetic activity incorporation, while an improvement, still has problems at low and high latitudes, and the middle latitudes in wintertime. Metrics are still needed, according to Fuller-Rowell, to quantify the amount of variability that has been captured by any specified model, and to determine its utility in any space weather application.

3.12.4.3 Observations and Data Issues

Jan Sojka (Space Environment Corporation) discussed data quality and specified the following sources of error:

- Statistical (Gaussian noise)
- Instrumental effects
- Representation of data vis-à-vis the model targeted
- Absolute or offset values

Sojka expressed the concern that data assimilation models, which require real-time data streaming, are subject to the problem that required data sets might not be properly reviewed. He suggested improved handling of data in order to produce results that assimilation models can effectively use. He also notes that there are some constraints on error distributions. For example the Kalman filters in data assimilation require a Gaussian distribution for errors. In the area of new observations, Sojka reflected on two experiments flying on the ARGOS satellite: (i) Low Resolution Airglow and Aurora Spectrograph (LORAAS) and (ii) The High Resolution Airglow and Aurora Spectroscopy (HIRASS). The LORAAS should provide data useful in validation of *Ne* in models; the HIRASS should provide data useful for thermospheric models that need to be validated. This is important since some ionospheric models have an imbedded thermospheric model.

3.12.4.4 Empirical Models

Dieter Bilitza discussed the fact that empirical models are based upon long records of measured data. He noted the obvious bias of the empirical models to those areas where more data had been accumulated (i.e., Northern Hemispheric middle latitudes). The ocean areas are especially under-represented, as are the equatorial and high latitude regions. Still these empirical models have many applications, and now have the capability to be updated in real-time. Bilitza discussed the attributes of the current version of the International Reference Ionosphere, IRI2001. This version incorporates information on the D-region, the bottomside of the F1 region, the F region peak, electron temperature, and equatorial vertical ion drift. Improvements are considered continually. Specifically, the following improvements are planned: the F2 peak height, spread F, sporadic E, and a quantitative examination of variability in terms of a monthly standard deviation. Bilitza points out that there are a number of organizations that support empirical modeling, including: COSPAR, URSI, and ITU. Moreover, the International Standardization Organization (ISO) is in the process of registering standard

models for the Earth's environment, including the ionosphere. Bilitza refers to the IRI home page.

3.12.4.5 Data Sources for Modeling

Terence Bullett (AFRL) identified a number of on-line sources of data. The categories he considered were: (a) radio remote sensing (e.g., incoherent scatter), (b) ionosondes, (c) topside sounder, (d) coherent scatter radar (i.e., SuperDARN), (e) GPS Network, (f) tomography, (g) occultation, (h) satellite UV, and (i) in-situ probes. Bullett stressed ionosonde data in his presentation. He noted that recent investment in the international network of sounders have largely focused on data availability and timeliness and not on quality. While there is an enormous amount of sounder data available, the issues of data accuracy and latency need to be recognized. Bullet addressed the need for model validation, and suggested that data providers make raw data available.

3.12.4.6 Future of Ionospheric Modeling

Brian Wilson (Jet Propulsion Laboratory) discussed new data types including:

- Additional GPS stations (within IGS and CORS)
- New occultation data sets (current satellites plus COSMIC constellation)
- UV data sets (SSUSI and SSULI on the DMSP)
- Data from the C/NOFS

Wilson illustrated strides made in the area of TEC mapping. Daily maps of TEC are available and a number of groups are moving to the production of hourly maps. JPL's global mapping scheme, GIM, has been validated using TOPEX data as ground truth. Some limitations in the low latitude region have been documented. Differences (in TEC units) between GIM and TOPEX were ~ 3-5 at middle latitudes and 5-10 at low latitudes. The JPL GENESIS web site is a location to obtain occultation data, including data from CHAMP, and SAC-C, and also from IOX, GRACE, and COSMIC (when available). The GIM TEC maps can be found on the Web. Wilson took the opportunity to comment on the GAIM work being carried out by JPL and the University of Southern California. The following data types can be assimilated: (i) GPS-TEC data, (ii) relative TEC from occultation, (iii) ionospheric data from ionosondes, (iv) in-situ data from DMSP, and (v) nighttime UV limb scans. Other data types are planned.

3.12.4.7 Data Assimilation Modeling

Ludger Scherliess (Utah State University) discussed the purpose of data assimilation modeling. He mentioned that the goal is to combine models and data optimally. Models illustrate our knowledge of the physics and data provide information about the true state of the ionosphere. The problem is that both models and data are imperfect, since models require parameterization and data contain observation errors. Scherliess itemized the data subject to assimilation, and expressed the view that millions of data measurements will be available in the next decade, and that physics-based data assimilation models will provide real-time snapshots of the ionospheric behavior.

3.12.4.8 Solar EUV Modeling

Kent Tobiska (Space Environment Technologies) discussed current and future data and measurements, and various models. He identified the most recent EUV model, SOLAR2000, which is now operational. Tobiska noted that nowcast irradiances are produced for use in solar monitoring; and forecasts are being made for operational systems.

3.12.4.9 WBMOD Overview

Jim Secan (NorthWest Research Associates) discussed the wideband model WBMOD. This model is a semi-empirical model of the effects of F-layer plasma density irregularities on trans-ionospheric radio propagation. Included in the model is a propagation component that predicts the S4 index (i.e., the normalized RMS variation in signal power), the phase scintillation parameter, and the probability distribution function. Secan mentioned some of the shortcomings of the model, mostly the result of data source limitations, and he explained that additional data sets would be useful. He indicated that attempts would be made to make the model available to the wider user community, and suggested that more information could be found on the NWRA web site.

3.12.4.10 Weather Model for Scintillation

Santimay Basu (AFRL) described plans for a weather model for scintillation based upon data from the C/NOFS system. This is the Communication/Navigation Outage Forecasting System having the ability to convert observations of ionospheric turbulence to scintillation parameters. Additional information on C/NOFS can be obtained at several web sites.

3.12.4.11 Panel Discussion Synopsis

The discussion began with some views from Jack Klobuchar (Innovative Solutions International), who served as a devil's advocate at the forum. The more relevant comments were as follows:

1) Certain applications, such as the NAVSPASUR system require electron density profiles and not TEC.
2) There are limitations to some of the data sets used in data assimilative modeling.
3) There are limitations in data from the CORS network in that they are not well-calibrated or uniform, multiple receiver types are included in the data sets, and it is difficult for the user to determine the biases for the receivers.
4) The WAAS system is currently available for the CONUS region, and does not suffer from many of the issues that plague the CORS network. Why does the community of data assimilation modelers not use this resource?
5) It was recommended that the STORM model development should be suppressed at low latitudes in favor of ascertaining the effect of vertical drifts on the ionosphere in quiet times, and specifically longitudinal differences. At the least, this information should be evaluated prior to modeling the magnetic storm effects.
6) Daily EUV daily has little correlation with daily TEC, and it is of questionable value in modeling the TEC.
7) The WBMOD scintillation model suffers from limited source data from a few stations. (*Editorial Note: Jim Secan of NWRA generally agrees with the view that WBMOD can be improved with additional data sets, See comments from Secan above*)

There were responses to these views. With respect to #3, Anthea Coster (MIT Lincoln Laboratory, currently MIT Haystack) defended the usefulness and quality of the CORS data set since she had exploited the data successfully in several applications. She also noted its availability on the Internet. Brian Wilson (JPL) also defended the CORS data, and also noted that TOPEX data is used to validate the GIM data, and to determine structures in the equatorial region.

With respect to comment #4, Bob Schunk (Utah State University) indicated the WAAS data is actually equivalent vertical TEC, and thus not useful for data assimilation. His concern was the error introduced when converting the slant TEC to the vertical. Concerned about data smearing, he would prefer to use the original slant measurements. The CORS data has real slant measurements preserved.

Also with respect to #4, Wilson noted that while the WAAS supertruth data contains high quality slant TEC information, it is the result of a lot of post-processing ... and not real-time. Hence it is not a good candidate for data assimilation. Wilson indicates that there is a GPS TEC data uncertainty due to receiver bias; and there is an additional 2-3 TEC unit uncertainty (where 1 TEC unit = 10^{16} electrons/m^2) in the TOPEX TEC.

With respect to #5, Tim Fuller-Rowell (NOAA-SEC) argued the usefulness of ionospheric storm modeling since it was apparent that magnetic storm effects can drastically change the diurnal variation. (*Editorial Note: Klobuchar was essentially saying that priority should be given to the determination the low-latitude quiet-time mean density, so that storm departures would have a meaningful reference.)*

With respect to #6, Kent Tobiska (Space Environment Technologies) commented that the solar irradiance is useful for long-term modeling, and it now becoming better quantified.

A general discussion ensued. Sandro Radicella (Abdus Salam ICTP) indicated that TOPEX data has been shown to be quite useful in validations of the GIM and IRI models. He expressed the concern that supertruth slant TEC data could not be obtained in real-time. In response, Coster indicated that it should be possible to obtain high quality GPS data (~ 2-3 TEC unit accuracy) in real-time if calibration is handled carefully. Wilson agreed that JPL could compute streaming TEC (instead of batch-processed) every few seconds and could provide the data in real time.

On the issue of data availability for assimilative models, Brian Wilson (JPL) cited the use of GPS occultation data. These data sets are useful since they can lead to profiles of the ionosphere to the height of the low orbit satellite. Schunk (Utah State University) commented that topside data was very useful for modeling purposes, including topside data on electron and ion temperatures. Jack Klobuchar noted that there was limited reception in the American zone, vis-à-vis the Alouette satellite.

Coster asked Bilitza (NASA-Goddard) about the validity of the IRI model in the low latitude sector. She had noticed that the IRI underestimates the TEC by ~ 50% near the equator at solar maximum. Bilitza responded that there was a task force structure within IRI to address various problems such as this. He continued by saying topside ISIS data, obtained at high solar activity, will no doubt lead to improvements. The IRI task-force work in 2002 stresses TEC on the topside.

Bodo Reinisch (University of Massachusetts-Lowell) cited the usefulness of the worldwide ionosonde database. He mentioned its availability at a number on Internet web sites, including NOAA-NGDC. Sojka (Space Environment Corporation) commented that real data was extremely important, and that ionosondes are still a leading source of good data. Klobuchar

commented that the integrity of ionosonde data is an issue. Much data is missing because it did not pass the quality control algorithm.

Speaking with reference to the HF community that constitutes ~50% of the customers for the ionosonde network, Terence Bullett (AFRL) wonders if GAIM will benefit them. Bullett also inquired about the treatment of TIDs with the GAIM approach. Would TIDs be visible? Schunk responded by saying that TIDs are not available at present, but future advances may lead to the possibility of detecting TIDs. For example, the addition of 200 spaced receivers could detect TIDs. Bullet said that the addition of D and E-region models would be helpful, and customers would find a 1-hour forecast of TIDs useful.

Both Jim Secan (NWRA) and Jan Sojka, referring to assimilative models, indicated that data providers need to be mindful of the fact that assimilative models have a grid size element (i.e., a volume element) within which ionospheric parameter estimates are made. Data needs to be characterized in terms of variance within a given volume element.

Earlier in the presentations, John Seago (Honeywell) indicated that new model developments might benefit from increased product exposure and "marketing". He was asked to elaborate. Seago pointed out that he was simply noting that users need to be aware of the existence of the models, their capabilities, and how to access them. Tim Fuller-Rowell indicated that the 3rd party vendors would take the responsibility for the transfer of tailored products to the ultimate customer.

On the issue of modelers, data providers, and users, a number of comments were made. Mannucci (JPL) indicated that modelers and data providers should work together. Specifically, data providers should be sensitive to the need by modelers to address error bounds on the data sets they use in model development. Also the data should be well documented and easy to use. Jack Klobuchar responded that in addition to data providers and modelers working together, there was also a need for a more institutionalized way to bring users and scientists together. He pointed out the IES symposia as a good example, given the fact that full papers are provided to the attendees, and that published proceedings are made available. Paul Bellaire (AFOSR) replied that this was also the intent of the annual Space Weather Week, and that presentations and discussions are posted on a designated web site for Space Weather Week. *(Editorial Note: In this connection, the organizers of Space Weather Week have published the SWW Proceedings following the 2004 event, and have provided CDs of all presentations upon request.)* Paul Kintner (Cornell University) followed with the thought that there was a need for a system to bridge the gap between science and application. There has never been adequate funding to do transition to application (i.e., step out of the science realm). Anthea Coster suggested that we should document user needs to help transition science to application.

Mannucci (JPL) inquired about sources of funding. Specifically, what agencies fund data system research? Klobuchar indicated that funding is based upon need, and the researcher should seek funding from sources that specify needs. Klobuchar agrees with Paul Kintner about forcing the transition from science to applications, but reminds the audience that the ionosphere, (and space weather) will never be as relevant as tropospheric weather.

3.12.4.12 Panel Conclusions

(Editorial Note: The following is a fitting conclusion to the forum, and is "lifted" almost verbatim from the summary by Davies and Coster. My apologies go to the authors for some re-ordering of text and occasional additions.)

It is evident that near-real-time data assimilative models, which utilize many aspects of empirical and physics-based models, seem to offer the most promise for capturing the true state of the ionosphere. The future of these models depends on intelligently incorporating the wealth of information from new satellite systems, from the addition of multiple ground-based systems, and, perhaps more importantly, the communication links that will allow this data to flow in near-real-time to the various data processing centers, and from there to the users.

Modelers are concerned with the testing of models with valid data, and since data assimilative models require real-time data, it is essential that data be inspected for quality. This was a recurrent theme. Users suggested that information about state-of-the-art models be made readily available.

A concern, which continues to surround the development of the newer models, is that of funding. Which agencies need and fund data system research? There are real-world applications for this research, but funding is not always available to make the transition from science to applications.

3.13 IONOSPHERIC PREDICTIONS

Ionospheric predictions influence several disciplines including the prediction of radio system performance, a matter of some interest in planning as well as ultimate operations. Long-term predictions are generally based upon predictions of driving parameters such as sunspot number, the 10.7 cm solar flux, magnetic activity indices, etc. Unfortunately these parameters are not easy to predict. We are now unfortunately faced with the job of predicting outcomes from models driven by parameters that also need to be predicted. This is truly double jeopardy. Moreover, the functions relating these parameters to the ionosphere are imprecise. Consequently, long-term

predictions needed for system design are subject to a considerable amount of uncertainty. To first order the uncertainty in the median value of *foF2* for a particular time and location is proportional to the uncertainty in the mean sunspot number.

In addition to the uncertainty in the mean parameters, we must account for the fact that ionospheric parameters have real distributions, and with few exceptions the spread of these distributions is such that errors about the mean may be a dominant contribution. Short-term ionospheric predictions (or forecasts) generally refer to departures from the median behavior, the latter being well characterized by running averages of solar flux and related parameters (viz., sunspot number). The short-term fluctuations may be specified in terms of hour-to-hour, day-to-day, and week-to-week variabilities. There are also second-to-second and minute-to-minute variations but this class of variations generally falls within the realm of unpredictable behavior. Compensation for such fluctuations is quite difficult, but may be accommodated through use of system protocols which enable real-time channel evaluation (or RTCE) measures to be initiated, such as channel sounding or probing. These very short-term forecasts are generally referred to as Nowcasts.

There are four ITU-R documents that are pertinent to the investigation of the ionospheric forecasting problem. The first deals with the exchange of data forecasts [ITU-R, 1995]; the second outlines various measures for forecasting of ionospheric parameters [ITU-R, 1994a]; the third deals specifically with solar-induced ionospheric effects [ITU-R, 1994b]; and the fourth outlines various real-time channel evaluation schemes [CCIR, 1990]. These reports should be consulted.

Distributions of parameters such as *foF2, foEs*, and *hF2* are important since these parameters depart significantly from fundamental intuition and from rules set forth by Sidney Chapman and his classic theory. Distributions of *foF2* and *foEs* are available [Lucas and Haydon, 1966; Leftin et al., 1968] but F2 layer height distributions are not directly available. Ionospheric predictions in the short and intermediate terms provide the most exciting challenge for the ionospheric researchers.

Observational data have shown that Traveling Ionospheric Disturbances (or TIDs) are the ionospheric tracers to a class of atmospheric gravity waves; and these disturbances are a major contribution to ionospheric variability, especially at F region heights. TIDs have a major impact on layer height as well as peak electron density, and possess a variety of scales, from kilometers to thousands of kilometers. The small to intermediate scale TIDs, having wavelengths of less than a few hundred kilometers and periods of the order of 10-20 minutes, arise from local sources and have relatively small amplitudes away from the source region. The large-scale TIDs have sources that are located at great distances, and there is a strong correlation between

this class of disturbances and geomagnetic storms. Evidence suggests that large scale TIDs have an impact over global distances and originate within the auroral zone as a result of atmospheric modifications associated with precipitation and auroral arc formation. A survey of the effects of TIDs on radiowave systems may be found in a review paper by Hunsucker [1990].

The field of ionospheric predictions is undergoing continuous evolution with the introduction of new scientific methods and instruments, which are providing fresh insight. The requirements for quasi-real-time products based upon current ionospheric specification has led to an increased importance of so-called real-time ionospheric models. This class of models, in turn, is driven by a hierarchy of solar-terrestrial observations, which enables the analyst to examine the space-weather environment as an integrated complex of phenomena. This general approach is leading to an improvement in our understanding of ionospheric structure and it variations, if not better short-term forecasts. In the immediate future, it is anticipated that the primary ionospheric specification tools will be comprised of terrestrial sounding systems, including real-time networks of ionospheric sounders [Galkin et al., 1999]. Real-time data services based on these approaches are becoming available [Goodman and Ballard, 1999].

Perhaps the most exciting new development in recent years has been science and technology for ingesting large amounts of real-time data and the assimilation of these data within various models. COST programs in Europe have led the way in the incorporation of data within empirical models, while the American GAIM technology shows great promise in the assimilation of data within physical models with the aid of Kalman filtering and related schemes.

Meanwhile, other more direct methods are being used in a number of practical situations where computational assets are limited. For example, direct ingestion of real-time data can be used for updating climatological models when data sets are sparely distributed and when less precision is required. When data sets are dense, particularly over areas where GPS-TEC and sounding data are available, careful mapping techniques have been applied to capture the most likely continuous distribution of data over selected regions.

3.14 SCIENCE ISSUES AND CHALLENGES

There are a number of challenges facing ionospheric specialists and aeronomists. While theories explaining most facets of ionospheric behavior exist and are generally accepted, the theories do not always provide a good basis for prediction of future behavior. This is because the driving forces and boundary conditions needed in a physical model are not always known, and

estimates must be used. This has led to the development of semi-empirical models for the purpose of system design and these are used for operations as well. By and large these models exploit large ionospheric data bases and yield only median representations of ionospheric parameters. To fix this problem, various "update" schemes have been developed to make the specification of the ionospheric state as current as possible. The physics is then used to let the system evolve. The new GAIM methodologies offer some considerable promise in this regard. Still, all of this can be very unsatisfactory unless an understanding of the nature of ionospheric variability (viz., in both space and time) is established. There are many sources within the earth-sun system that contribute to the growth of ionospheric structure. While these have been characterized to some extent, the characterizations are not sufficient to provide predictions acceptable for many users of the ionospheric channel. Currently this is a major challenge facing the ionospheric research community. Even GAIM technology will be taxed in its quest to map medium-to-small scale ionospheric structure and disturbances, including TIDs.

The following topics require more attention from ionospheric specialists: (a) the driving forces of upper atmospheric winds and the impact on ionospheric structure and dynamics; (b) the hierarchy of energy sources within the earth-sun system that influence ionospheric behavior; (c) the development of geomagnetic storms and the impact that storms have on ionospheric behavior; (d) the development and evolution of ionospheric inhomogeneities; and (e) various methods for ionospheric predictions.

Finally, in the new millennium, the researcher is confronted with an enormous amount of data, both near real-time and archived, that may be accessed via the Internet. Harnessing this information stream, and using the state-of-the-art computational assets, it should be possible to leverage ongoing science efforts, organize more efficient experimental campaigns, and enhance collaborative efforts, all resulting in a more fulsome understanding of ionospheric physics.

3. 15 REFERENCES

Aarons, J., 1977, "Equatorial Scintillations: A Review", *IEEE Trans. Ant. Prop.*, 25, 729-736.

Araujo-Pradere, E.T., T.J. Fuller-Rowell, and D. Bilitza, 2004, "The STORM Response in IRI2000, and Challenges for Empirical Models of the Future", Radio Sci., 39, RS1S24, doi: 10,1029/2002RS002805.

Anderson B., and J. Moore, 1979, *Optimal Filtering*, Prentice-Hall.

Anderson, D.N., M. Mendillo, and B. Herniter, 1987, A Semi-Empirical Low-Latitude Ionospheric Model, *Radio Science*, 22:292.

Anderson, D.N., J.M. Forbes, and M. Codrescu, 1989, "A Fully Analytic, Low Latitude Ionospheric Model", *J. Geophys. Res,*. 94:1520.

Bent, R.B., S.K.Llewllyn, G. Nesterczuk, and P.E. Schmid, 1976, The Development of a Highly-Successful Worldwide Empirical Ionospheric Model and its Use in Certain Aspects of Space Communications and Worldwide Total Electron Content Investigations", in *Effect of the Ionosphere on Space Systems and Communications, IES'75,* edited by J.M. Goodman, USGPO, available through NTIS, Springfield VA, pp.13-28.

Benson, R., and Grebowski, 1999, "Extremely Low Ionospheric Peak Altitudes – Possible Relationship to Polar Holes", in the *1999 Ionospheric Effects Symposium*, edited by J.M. Goodman, NTIS, Springfield VA.

Bilitza, D., 1990, International Reference Ionosphere, NASA, NSSDC 90-22, World Data Center A (Rockets and Satellites), Greenbelt, MD.

Bilitza, D., 1992, "Solar Terrestrial Models and Application Software", *Planet. Space. Sci.*, 40(4) 541-579.

Bilitza, D., 1993, International Reference Ionosphere-Past, Present and Future, I, Electron Density, *Adv Space Res.*, 13(3), 3-13.

Bilitza, D., 2001, "International Reference Ionosphere 2000", *Radio Science*, Volume 36, No. 2, pp.261-275.

Bilitza, D., 2004, private communication.

Bishop, G.J., J.A. Klobuchar, A. E. Ronn, and M.G. Bedard, 1989, "A Modern Trans-Ionospheric Propagation Sensing System", in *Operational Decision Aids for Exploiting or Mitigating Electromagnetic Propagation Effects*, NATO-AGARD-CP-453, Specialised Printing Services Ltd., UK.

Bradley, P.A., 1999, "PRIME: Prediction and Retrospective Ionospheric Modeling over Europe", Final Report, Commission of European Communities, Printed by Rutherford-Appleton Laboratory, UK.

Bradley P.A., and J.R. Dudeney, 1973, "A Simple Model of the Vertical Distribution of Electron Concentration in the Ionosphere", *J.Atmos. Terrest. Phys.*, 35, 2131-2146.

Brekke A., 1980, "Currents in the Auroral zone Ionosphere", in *The Physical Basis of the Ionosphere in the Solar-Terrestrial System*, AGARD-CP-295, Tech. Edit. & Reprod. Ltd., London, pp. 13.1-13.9.

Broms, Mats and Bengt Lundborg, 1994, "Results from Swedish Oblique Soundings Campaigns", Annali Geofisica, Vol. XXXVII, No.2, pp.145-152, May 1994.

Buchau, J., B.W. Reinisch, E.J. Weber, and J.G. Moore, 1983, "Structures and Dynamics of the Winter Polar Cap F-Region", *Radio Science*, 18, 995-1010.

Buosanto, M.J., 2000, "Ionospheric Storms – A Review", *Space Sci. Reviews*, 88, pp.563-601.

CCIR, 1966, Atlas of Ionospheric Characteristics, Report 340, General Assembly held in Oslo, ITU, Geneva.

CCIR, 1990, "Real-Time Channel Evaluation of HF Ionospheric Radio Circuits", Report 889-2, International Telecommunications Union, Geneva

Chapman, S., 1931, "The Absorption and Dissociative or Ionizing Effect of Monochromatic Radiation in an Atmosphere on a Rotating Earth", *Proc. Physical Soc.*, 43:26.

Ching, B.K. and Y.T. Chiu, 1973, "A Phenomenological Model of Global Ionospheric Electron Density in the E, Fl, and F2-Regions", *Atmospheric Terrest. Phys*, 35:1615-1630.

Costa P.J., and W.H. Moore, 1991, "Extended Kalman-Bucy Filters for Radar Tracking and Identification", *Proc. IEEE National Radar Conference*, Aerospace and Electronic Systems Society, Sudbury, MA.

Coster A., 2004, Space Weather Week, NOAA-SEC, Boulder CO

Crowley, 1996, "Critical Review of Ionospheric Patches and Blobs", in *Review of Radio Science*, 1992-1996, edited by Ross Stone.

Davies, K., 1965, *Ionospheric Radio Propagation*, NBS Monograph 80, USGPO, Washington, DC

Davies, K., 1969, *Ionospheric Radio Waves*, Blaisdel Publishing Company, Waltham, Massachusetts

Davies, K. 1990, Ionospheric Radio, IEE Electromagnetic Wave Series 31, Peter Peregrinus Ltd., IEE, London, UK

Daniell, R.E. Jr., L.D. Brown, D.N. Anderson, M.W. Fox, P.H. Doherty, D.T. Decker, J.J. Sojka, and R.W. Schunk, 1995, Parameterized Ionospheric model: A Global Ionospheric Parameterization based on First-Principles Models, *Radio Sci.*, 30, 1499-1510.

Detman, T.R., and D. Vassiliadis, 1997, "Review of techniques for Magnetic Storm Forecasting", *Magnetic Storms*, Geophysical Monograph 98, AGU, 253-266.

Dick M.I., and P.L. Bradley, 1992, "The RAL Quasi-Parabolic Model Ionosphere" in *Proceedings of the COST-PRIME Workshop on Data Validation of Ionospheric Models and Maps*, COST 238TD (93) 001, 67-83.

Doherty, P.H, D.T. Decker, P.J. Sultan, F.J. Rich, W.S. Borer, and R.E. Daniell Jr., 1999, Validation of PRISM: The Climatology", in *Proceedings of IES99* , edited by J. M. Goodman, NTIS, Springfield, VA.

Ducharme, E.D., L.E. Petrie, and R. Eyfrig, 1973, "A Method for Predicting the F1 Layer Critical Frequency Based Upon Zurich Smoothed Sunspot Number", *Radio Science*, 8, 837-839.

Feldstein, Y.I. and GN. Starkov, 1967, "Dynamics of Auroral Belts and Polar Geomagnetic Disturbances", *Planet. Space Sci*, No.15, p.209.

Fuller-Rowell, T., M.V. Codrescu, R.G. Roble, and A.D. Richmond, 1997, "How Does the Thermosphere and Ionosphere React to a Geomagnetic Storm?, *Magnetic Storms*, Geophysical Monograph 98, AGU, Washington DC, pp. 203-225.

Fuller-Rowell, T., M.V. Codrescu, R.J. Moffett, and S. Quegan, 1996, "On the Seasonal response of the Thermosphere and Ionosphere to Geomagnetic storms", J. Geophys. Res., 101, pp. 2343-2353.

Fuller-Rowell T., C. Mintner, and M. Codrescu, 2002, "Data Assimilation for Neutral Thermospheric Species during Magnetic Storms", pp. 239-247, in *Proceedings IES2002*, edited by J.M. Goodman, NTIS, Springfield VA and JMG Associates, Alexandria VA.

Galkin, I.A., B.W. Reinisch, and D. Kitrosser, 1999, Advances in Digisonde Networking, in *Proceedings of IES99*, edited by J.M. Goodman , NTIS, Springfield VA.

Gassmann, 1972, "On Modelling the Arctic Ionosphere", in Radar Propagation in the Arctic, (G.H. Millman, editor), NATO Advisory Group on Aerospace Research and Development (AGARD), Conference Proceedings CP 97, NTIS, Springfield, VA. AD 73891.

Giraud, A. and M. Petit, 1978, *Ionospheric Techniques and Phenomena*, D. Reidel Publishing Co., Dordrecht (Holland), Boston, and London.

Golub G., and C. Van Loan, 1989, *Matrix Computations*, Johns Hopkins University Press.

Goodman, John M., 1970, "On the Morphology of the Midlatitude Ionosphere - a VHF Radar Study using the Faraday Effect in conjunction with Thomson Scatter", Doctoral Dissertation (physics), Catholic University of America, Washington, D.C.

Goodman, John M. (Editor-in Chief), 1975, 1978, 1981, 1984, 1987, 1990, 1993, 1996, 1999, and 2002 *Ionospheric Effects Symposia*, National Technical Information Service, Springfield VA

Goodman, John M., Melvin W. Lehman, 1971, "Midday Electron Density Profiles ove Randle Cliff for March 1971", NRL Memorandum Report 2344, September.

Goodman, J.M., M.W. Lehman, E.L. Gott, K.W. Morin, and E. Piernik, 1972, "Electron Density Profiles of the Ionosphere Observed near Washington D.C. during the Spring of 1971", NRL Report 7395, June 7, 1972 (also presented at AGU meeting, San Francisco, 1972).

Goodman, J.M., R. Zirm, and R. Beard, 1978, "Storm-Time Scintillation Effects Deduced from NTS-2 Observations at Washington, D.C.", XIX General Assembly, URSI, Helsinki.

Goodman, J.M., 1979, "Storm-Time Scintillation and Electron Content Variations Deduced from NTS-2 Satellite Observations", Spring AGU Meeting, Washington, D.C.

Goodman, J.M., and A.J. Martin, 1983, "A Synopsis of Total Electron Content Data Obtained Using the NTS-2 Satellite Transmissions", NRL Memorandum Report, 15 February, 1983.

Goodman, J.M., 1991, *HF Communications: Science & Technology*, Van Nostrand Reinhold, New York.

Goodman, J.M., J.W. Ballard, and E. Sharp, 1997, *Radio Science*, Vol.32, No.4, pp.1705-1715.

Goodman, J.M. and J.W. Ballard, 1999, Dynacast-Assisted Frequency Management for HF Communication and Broadcasting Systems, in *Proceedings of IES99*, edited by J.M. Goodman , NTIS, Springfield VA.

Goodman, J.M., 2001, Ionospheric Characteristics, *Wiley Encyclopedia of Electrical and Electronics Engineering Online*, John Wiley & Sons (http://www.interscience.wiley.com).

Goodman, J.M. and J.W. Ballard, 2004, "An Examination of Elevated Frequency Propagation over a Transpolar path", *Radio Sci.*, 39, RS1S29, doi:1029/2002RS002850.

Gossard, E.E. and W.H. Hooke, 1975, *Waves in the Atmosphere*, Elsevier Scientific Pub.Co., Amsterdam, Oxford, and New York.

Gussenhoven, M.S., DA. Hardy, and N. Heinemann, 1983, "Systematics of the Equatorward Diffuse Auroral Boundary", *J.Geophys.Res*, 88:5692.

Hajj G. A., B.D. Wilson, C. Wang, and X. Pi, 2004, "Ionospheric Data Assimilation by Use of the Kalman Filter", pp. 231-238, in *Proceedings IES2002*, edited by J.M. Goodman, NTIS, Springfield VA and JMG Associates, Alexandria VA.

Halcrow, B.W., and Nisbet, J.S., 1977, "A Model of F2 Peak Electron Densities in the Main trough Region of the Ionosphere", *Radio Science*, 12, 815-820.

Hanbaba, R., 1999, "Improved Quality of Service in Ionospheric Telecommunication Systems Planning and Operations", Final Report, COST-251, published by the Space Research Centre, Warsaw, Poland.

Hand, Greg, 2004, Space Weather Week, NOAA-SEC, Boulder Colorado.

Hartz, T.R., 1972, "Morphology of Radio-Radar Polar Propagation Effects", *Radar Propagation in the Arctic*, G.H. Millman (editor), NATO-AGARD EWP Panel Meeting in Lindau-Harz, FRG, September 1971, NTIS, Springfield, VA. AD738791.

Horn R., and C.Johnson, *Matrix Analysis*, 1985, Cambridge University Press

Hunsucker, R.D., and Greenwald, R.A., (Guest Editors), 1983, "Special Issue, Radio Probing of the High Latitude Ionosphere and atmosphere – New techniques and New results", *Radio Science*, Vol.18, AGU, Washington DC.

Hunsucker, R.D., 1983, "Anomalous Propagation Behavior of Radio Signals at High Latitudes", in *Propagation Aspects of Frequency Sharing,*

Interference and System Diversity, H. Soicher (editor), AGARD-CF-332, available from NTIS, Springfield, VA.

Hunsucker, R., 1990, "Atmospheric Gravity Waves and Traveling Ionospheric Disturbances: Thirty Years of Research", in *Effect of the Ionosphere on Radiowave Signals and System Performance, IES90,* edited by J.M.Goodman, USGPO, NTIS, Springfield, VA.

Hunsucker, Robert D., 1991, *Radio Techniques for Probing the Terrestrial Ionosphere*, Springer-Verlag, New York, Berlin, Heidelberg

ITU-R, 1994a, "Short-Term Forecasting of Critical frequencies, Operational Maximum Useable frequencies and Total Electron Content", ITU-R P.888, International Telecommunications Union, Geneva..

ITU-R, 1994b, "Short-Term Prediction of Solar Induced Variations of Operational Parameters for Ionospheric Propagation", ITU-R P.727, International Telecommunications Union, Geneva.

ITU-R, 1995, "Exchange of Information for Short-Term Forecasts and Transmission of Ionospheric Disturbance Warnings", Rec P.313, International Telecommunications Union, Geneva.

Jull, 1964, *Arctic Communications*, edited by B. Landmark, AGARD Proceedings, Pergamon Press, New York

Jursa, A.S. (Scientific Editor), 1985, *Handbook of Geophysics and the Space Environnment*, Air Force Geophysics Laboratory, Air Force Systems Command, U.S. Air Force, National Technical Information Service (NTIS), Springfield VA.

Kalman R.E., 1960, "A New Approach to Linear Filtering and Prediction Problems", *J. Basic Engineering*, 82, pp. 34-45.

Kelley, Michael C., 1989, *The Earth's Ionosphere*, Plasma Physics and Electrodynamics, Academic Press Inc., San Diego CA.

Landmark, B. 1964, *Arctic Communications*, AGARD Proceedings, Pergamon Press, New York

Leftin, M., S.M. Ostrow, and C. Preston, 1968, "Numerical maps of foEs for Solar Cycle Minimum and Maximum", U.S. Dept. of Commerce, ERL 73-ITS 63, Boulder CO.

Lied, F. (editor), 1967, *High Frequency Radio Communications with Emphasis on Polar Problems*, AGARDograph 104, NATO, published by Technivision, Maidenhead, England.

Lucas, D. and G.W. Haydon, "Predicting Statistical Performance Indices for High Frequency Telecommunication Systems", ITSA-1, U.S. Dept. of Commerce, Boulder CO, 1966.

Lundborg, B., M. Broms, and H. Derblom, 1995, "Oblique Sounding of an Auroral Ionospheric HF Channel", *J. Atmospheric Terrest. Phys.*, Vol.57, No.1, pp.51-63,

Lundstedt, Henrik, 1997, "AI Techniques in Geomagnetic Storm Forecasting", *Magnetic Storms*, Geophysical Monograph 98, AGU, pp. 243-252.

Maurits, S., and B. Watkins, 1996, "UAF Eulerian Model of the Polar Ionosphere", *STEP Handbook of Ionospheric Models*, pp. 95-123.

Mayaud, P.N., 1980, *Derivation, Meaning, and the Use of Geomagnetic Indices*, American Geophysical Union, Washington, DC.

McCoy, R., 2001, "Space Weather – Lessons from Meteorologists", *Space Weather*, Geophysical Monograph 125, pp. 31-37.

Mendillo, M., 1971, "Ionospheric Total Electron Content Behavior during Geomagnetic Storms", *Nature*, 234, 23.

Mendillo, M., 1973, "A Study of the Relationship between Geomagnetic Storms and Ionospheric Disturbances at Midlatitudes", *Planet. Space Sci.*, 21, 349.

Mendillo, M., and J.A. Klobuchar, 1974a, "An Atlas of the Midlatitide F-Region Response to Geomagnetic Storms", AFCRL Technical Rpt. 0065, L.G.Hanscom Field, Bedford, MA, 01730.

Mendillo, M., and J.A. Klobuchar, 1974b, "Seasonal Effect in Ionospheric Storms", COSPAR/URSI Symposium on Satellite Beacon Studies of the Ionospheric Structure and ATS-6 Data, Moscow, USSR, 25-29 Nov., 1974.

Mendillo, M., 1978, "Behavior of the Ionospheric F-Region during Geomagnetic Storms", Dept. Astronomy, Boston University, 725 Commonwealth University, Boston MA 02215, AFGL-TR-78-0092 (II), March 1978.

Mendillo, Michael, and F.X. Lynch, 1979, "The Influence of Geomagnetic Activity on the Day-to-Day Variability of the Ionospheric F-Region", Air Force Geophysics Laboratory, AFGL-TP-79-0074, January.

Millman, G., (editor), 1972, *Radar Propagation in the Arctic*, NATO-AGARD EWP Panel Meeting in Lindau-Harz, FRG, September 1971, NTIS, Springfield, VA. AD738791.

Mintner C.F., T. Fuller-Rowell, and M.V. Codrescu, 2004, "Estimating the State of the Thermospheric Composition using Kalman Filtering", *J. Space Weather*, Vol. 2, S04002, doi.1029/2003SW000006, 2004.

Mitra, A.P., 1974, *Ionospheric Effects of Solar Flares*, D.Reidel Pub.Co., Dordrecht (Holland) and Boston.

Muggleton, L.M., 1975, "A Method for Predicting *foE* at any Place and Time", *Telecomm. J.*, 42 (7), 413-418

Muldrew, D.F., 1965, "F-Layer Ionization Trough Deduced from Alouette Data", *J.Geophys. Res.* 70, 2635-2650.

Nickisch, L.J., 2004, "A Power-Law Power Spectral Density Model of the Total Electron Content Structure in the Polar Region", *Radio Science*, 39, RD1S12, doi:10.1029/2002RS002818.

NRC, 1981, *Solar-Terrestrial Research for the 1980s*, National Research Council, National Academy Press, Washington, DC.

Prolss, G.W., 1993, "On Explaining the Local Time Variation of Ionospheric Storm Effects, *Ann. Geophys.*, 11, pp.1-9.

Prolss, G.W., 1997, "Magnetic Storm Associated Perturbations of the Upper Atmosphere", *Magnetic Storms*, Geophysical Monograph 98, AGU, Washington, D.C. pp.227-241.

Paul, A., 1989, "Ionospheric Variability", Technical Report 1277, Naval Ocean Systems Center, San Diego, CA.

Ratcliffe, J.A., 1972, *An Introduction to the Ionosphere and the Magnetosphere*, Cambridge University Press, London and New York.

Reilly, M.H., and M. Singh, "A Transionospheric Radio propagation Model", in *IES93 Proceedings*, edited by J.M. Goodman, NTIS, Springfield, VA, 1993.

Rishbeth, H. and O.K. Garriott, 1969, *Introduction to Ionospheric Physics*, Academic Press, New York and London.

Rishbeth, H., 1991, "Basic Physics of the Ionosphere", in *Radiowave Propagation* (M.P.M. Hall and L. Barclay, editors), IEE Electromagnetic Series 30, Peter Peregrinus Ltd., UK.

Rodger, A.S., 1998, "Polar Patches – Outstanding Issues", in *Polar Cap Boundary Phenomena*, edited by Moen, Egeland, and Lockwood, NATO ASO Series 509, Dordrecht-Holland, Kluwer Academic Publishers, PP.281-288.

Rodger, A.S., 1999, "Recent Advances in Geospace Research", in *Review of Radio Science 1996-1999*, edited by Ross Stone, URSI, Oxford University Press.

Rush, C.M., M. Fox, D. Bilitza, K Davies, L. McNamara, F.G. Stewart, and M. PoKempner, 1989, "Ionospheric Mapping - an Update of foF2 Coefficients", *Telecomm. J.*, 56, 179-182.

Scherliess L., R.W. Schunk, J.J. Sojka, and D.C. Thompson, 2002, "Development of a Physics-Based Reduced State Kalman Filter for the Ionosphere", pp. 210-221, in *Proceedings IES2002,* edited by J.M. Goodman, NTIS, Springfield VA and JMG Associates, Alexandria VA.

Schunk, R.W., L. Scherliess, J.J. Sojka, D.C. Thompson, D. Anderson, M. Codrescu, C. Minter, T. Fuller-Rowell, R.A. Heelis, M. Hairston, and B. Howe, 2002, "Global Assimilation of Ionospheric Characteristics (GAIM)", in *Proceedings IES2002*, edited by J.M. Goodman, NTIS, Springfield VA and JMG Associates, Alexandria VA.

Secan, J.A., 1989, "A Survey of Computer-Based Empirical Models of Ionospheric Electron Density", Northwest Research Associates Report NWRA CR-89-11038, Bellevue, WA.

Sojka J.J., J.V. Eccles, R.W Schunk, S. Thonnard, and S. McDonald, 2002, "Ionospheric Assimilation Techniques for ARGOS LORAAS

Tomographically Reconstructed Equatorial Electron Density Profiles", pp. 40-49, in *Proceedings IES2002*, edited by J.M. Goodman, NTIS, Springfield VA and JMG Associates, Alexandria VA.

Sorenson H., 1985, *Kalman Filtering: Theory and Practice*, IEEE Press.

Stocker, A.J., E.M. Warrington, and T.B. Jones, 2003, "A Comparison of Observed and Modeled Deviations from the Great Circle Direction for a 4490 km HF Propagation Path along the Midlatitude Ionospheric Trough", *Radio Science*, June 13, 2003.

Tascione, T.F., H.W. Kroehl, R. Creiger, J.W. Freeman, R.A. Wolf, R.W. Spiro, R.V. Hilmer, JW. Shade, and B.A. Hausman, 1988, "New Ionospheric and Magnetospheric Specification Models", *Radio Science*, 23:211-222. (also in proceedings of IES'87).

Tascione, T.F., H.W. Kroehl, B.A. Hausman, and R.C. Cregier, 1987, "A Technical Description of the Ionospheric Conductivity and Electron Density Profile Model, (ICED, Version 196-11)", Hqrtrs Air Weather Service, U.S. Air Force, Scott AFB, Ill.

Tascione, T., 1988, *Introduction to the Space Environment*, Orbit Book Company, Malabar, FL.

Tascione, T.F., H.W. Kroehl, R. Creiger, J.W. Freeman, R.A. Wolf, R.W. Spiro, R.V. Hilmer, JW. Shade, and B.A. Hausman, 1988, "New Ionospheric and Magnetospheric Specification Models", *Radio Science*, 23:211-222.

Teters., L.R., J.L. Lloyd, G.W. Haydon, and D.L. Lucas, "Estimating the Performance of Telecommunication Systems Using the Ionospheric Transmission Channel, IONCAP User's Manual", U.S. Dept. of Commerce, NTIA Report 83-127, PB84-111210, NTIS, Springfield, VA, 1983.

Tsunoda, R.T., 1988, "High Latitude F-Region Irregularities – A Review and Synthesis", Rev. Geophys., No.4, pp.719-760, November 1888.

Tsurutani, B.T., W.D. Gonzalez, Y. Kamide, and J. K. Arballo (editors), 1997, *Magnetic Storms*, Geophysical Monograph 98, published by the American Geophysical Union, Washington, DC.

Wang, C., G. Hajj, X. Pi, I.G. Rosen, and B. Wilson, 2002, "A Review of the Development of a Global Assimilative Ionospheric Model", in *Proceedings IES2002*, edited by J.M. Goodman, NTIS, Springfield VA and JMG Associates, Alexandria VA.

Whitehead, J.D., 1970, "Production and Prediction of Sporadic E", *Reviews Geophys. Space Phys.*, 8:65-144.

Weimer, D.R., 1996, "A Flexible, IMF-dependent Model of High Latitude Electric Potentials having Space Weather Applications", *Geophys. Res. Lett.*, 23, 2549.

Weimer, D.R., 1995, "Models of High-latitude Electric Potential Derived with a Least-error Fit of Spherical Harmonic Coefficients", *J.Geophys. Res.*, 100, 19, 595.

Yeboah-Amankwah, D., 1976, "Increases in the Equatorial Total Electron Content (TEC) during Magnetic Storms", J. Atmospheric. Terrest, Phys., 38, pp.45-50.

Zaalov, N.Y., E.M. Washington, and A.J. Stocker, 2003, "Simulation of Off-Great Circle HF Propagation Effects due to the Presence of Patches and Arcs of Enhanced Electron Density within the Polar Cap", *Radio Science*, June 07, 2003.

Chapter 4
TELECOMMUNICATION SYSTEMS

4.1 INTRODUCTION

Much of this chapter is based upon earlier work [Goodman and Aarons, 1990] published just prior to the peak of solar cycle 22. Since that time, many issues remain the same, but the growth in technology has led to different approaches. The expanded use of GPS within the civilian sector is but one example. Another change is the growth in capability to monitor and assess the real-time environment so that improved predictions can be entertained. But the Internet has arguably provided the most significant leap change in technology, successfully addressing the issue of data transfer, analysis, dissemination, and the potential for real-time forecasting of space weather phenomena. As we migrate through this chapter, the influence of the Internet and the World Wide Web will be evident.

Electronic systems have evolved to address a myriad of problems associated with disciplines such as earth surveillance and mapping, surveying, the maintenance and transfer of time, navigation, search and rescue, emitter location, signal intercept, target tracking, global communication, the command and control of military forces, and electronic warfare, to name a few. Figure 4-1 is a cartoon depicting the various generic systems.

The general topic of ionospheric effects on radiowave systems has been covered in various topical conferences and workshops, the proceedings of which are generally available. Special topics are reported in scientific and technical journals, selected government publications, and certain monographs. The *Handbook of Geophysics and the Space Environment* [Jursa, 1985] published by the Air Force Geophysics Laboratory (AFGL) remains an excellent resource. A comprehensive treatment of radiowave propagation in the ionosphere is beyond the scope of this book, but the interested reader is referred to a monograph by Davies [1990]. Other books include those by Goodman [1991], Tascione [1994], and Hunsucker [1991]. A readable account of radio propagation in the ionosphere has been written by Bradley [1991]. For those seeking a more succinct discussion of various ionospheric effects, a classic survey of earth-space propagation effects was published by Lawrence et al. [1964]. This was updated by Millman [1967] and later by Flock [1987]. Ionospheric effects have also been included in the numerous *Solar-Terrestrial-Predictions Workshops,* the *Ionospheric Effects Symposia,* various conferences organized by the IEEE and the IEE (UK), and meetings sponsored by the NATO Advisory Group for Aerospace Research and development (AGARD). Another major source of information is contained in

documents published by the Radiocommunication Bureau of the International Telecommunication Union (ITU-R), previously known as the International Radio Consultative Committee (CCIR) prior to reorganization in the 1990s. Indeed, the established international positions with respect to ionospheric phenomena and its impact on radiowave systems are found in published ITU-R Recommendations, Reports, and Handbooks. Of relevance are the following ITU-R handbooks: (i) *The Ionosphere and its Effects on Radiowave propagation* [ITU-R, 1998], and (ii) *Radiowave Propagation Information for Predictions for Earth-to-Space Path Communications* [ITU-R, 1996]. The ITU-R *Recommendations on Radiowave Propagation* [ITU-R, 1997] is also an important source of information. For those involved in more fundamental issues of radio science, a bridge is provided by organizations such as the International Union of Radio Science (URSI). The progress of radio science has been reviewed periodically by URSI revealing the state-of-the-art in propagation assessment, modeling, design factors, and mitigation schemes. Some of the more recent editions of the *Review of Radio Science* should be consulted; i.e., Stone [1999].

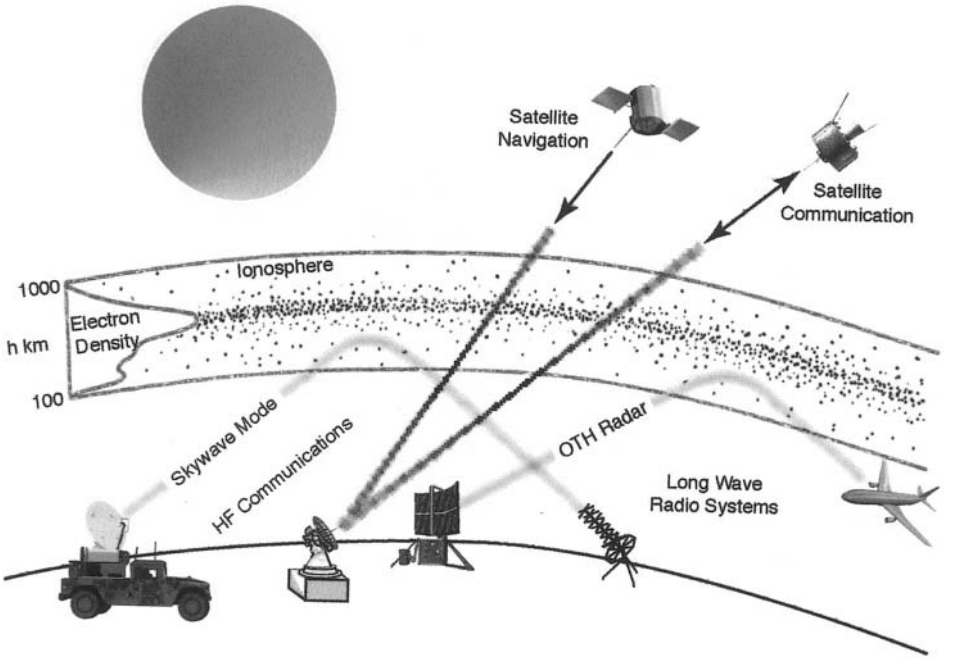


Figure 4-1: The ionosphere has a substantial impact on communication, command, control, and surveillance systems. The cartoon illustrates earth-space paths, skywave (ionospheric bounce) paths, and paths that exploit the earth-ionosphere waveguide. From Goodman and Aarons, [1990].

This chapter examines many of the systems of modern significance vis-à-vis space weather effects, but we will suppress a detailed discussion of the bands from ELF to LF, the so-called longwave bands, given the reduced emphasis on technological systems using that part of the spectrum. Even so, we will identify major effects on longwave systems and provide suitable references to the interested reader. Much of our attention will be directed to the HF communication and surveillance systems, and satellite systems having a variety of missions (i.e., communication, surveillance, navigation, earth observation, and science applications). Other system types will be covered on a case-by-case basis. Satellite systems typically use radio frequencies at VHF-UHF and even higher, and the use of GHz frequencies is substantial. We would expect satellite systems to be less vulnerable to space weather than terrestrial skywave systems since most effects diminish with increasing frequency. Nevertheless we will discover that practical HF systems with space weather compensation are not all that bad, and operational satellite systems are not all that good.

It is well established that the ionosphere is greatly influenced by ionizing radiation emanating from the sun, including both electromagnetic flux and energetic particles. The major sources of this radiation are associated with active regions on the sun that may host a preponderance of sunspots. Over the years, aeronomists and radio engineers have developed algorithms that describe the circumstantial relationship between the number of sunspots and the ionospheric effects that are observed. In recent times, it has become clear that other solar phenomena, such as coronal mass ejections (CMEs) and configurations of the interplanetary magnetic field (IMF), play a prominent role in the ionospheric state, especially in relation to disturbed periods. Even so, sunspots play more than a legendary role in the long-term trends of ionospheric behavior. The daily sunspot numbers were displayed in Figure 2-7, and many system users are tempted to use these values. Generally this is a serious mistake, since the ionosphere does not respond in accordance with daily values. However the median ionospheric properties can be successfully parameterized in terms of smoothed values of sunspot number. Figure 4-2 depicts the smoothed sunspot number from 1800 to the present time. Climatological models are based upon smoothed values of the sunspot number or solar flux, and even quasi-real time models require a degree of sunspot number smoothing (e.g., 5-7 days) to provide optimal results. Solar activity is closely associated with ionospheric structure and dynamics, and higher values typically imply enhancements in the maximum electron concentration within the various layers. The reader is referred to Chapter 2 (on space weather) and Chapter 3 (on the ionosphere).

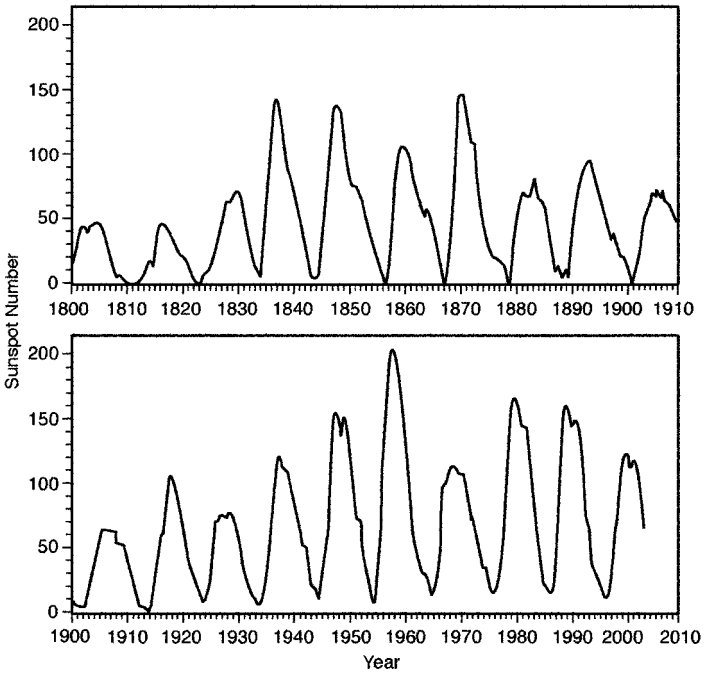


Figure 4-2: Pattern of the smoothed sunspot activity from 1800 to the present. See Figure 2-7 for a representation of the range of daily values.

4.2 OUTLINE OF IONOSPHERIC EFFECTS

The ionosphere is a partially ionized region of the upper atmosphere loosely partitioned into three major regions termed D, E, and F. It extends from roughly 50 km to 2000 km in altitude as defined by its sensible effect upon radiowave propagation systems. The reader is referred to Figure 3-1 in the last chapter. Although only a cartoon, the figure is still instructive. It depicts the "layering" properties of the midlatitude ionosphere for both daytime and nighttime conditions, and these differences are important for system operations. A brief but rather thorough description of the ionosphere and its effects on radiowave propagation is contained within an ITU-R handbook [ITU-R, 1998]. The interaction of radiowaves with the ionosphere depends upon the radio frequency employed as well as the details of the ion and electron density distributions that may be encountered. The interactions are complex, especially at the lowest frequencies, and the governing relationships involving refractive index are embodied in the Appleton-Hartree formalism described in many texts, including Davies [1991]. The ionosphere is immersed in a magnetic field and exhibits the following properties in connection with radiowave propagation:

- *Dispersion:* The index of refraction is a function of frequency, and the group velocity is not necessarily equal to the phase velocity.
- *Absorption:* The ionospheric refractive index is complex, having real and imaginary parts. The absorption is always dissipative and represents a conversion of wave energy into heat through the collision process.
- *Birefringence:* The index of refraction has two distinct values, owing to the presence of the uniform geomagnetic field and free electron mobility. This property suggests the possibility of two ray paths, each characterized by different phase and group velocities.
- *Anisotropy:* Each of the two indices of refraction is a separate function of the orientation of the normal to the surface of constant wave phase with respect to the background (uniform) geomagnetic field.

Dispersion and absorption will exist even in the absence of the earth's magnetic field, but its presence leads to the last two properties, birefringence and anisotropy. The Faraday effect is the most prominent phenomenon that results from birefringence, and it has been long exploited as a scheme to deduce the total electron content (TEC) of the ionosphere. One obvious distinction between the ionosphere and the underlying troposphere is the manner in which radiowaves interact with the respective regions. The ionosphere exhibits a frequency-dependent index of refraction that is less than unity, whereas the troposphere possesses an index that is frequency-independent but greater than unity. Furthermore, we note that the absolute value of the atmospheric index is generally greatest at the surface where the gas density is greatest, and it exhibits a roughly exponential decay with altitude (see Bean et al. [1971]). The absolute value of the ionospheric component, on the other hand, is virtually zero below an altitude of 60-70 kilometers, and rises to a maximum at the peak of electron concentration in the ionosphere, which typically occurs in the range of 250-400 km. The departure of the atmospheric index from unity is quite limited in comparison with the ionospheric index, especially for frequencies at VHF and below. As a consequence, we may generally concentrate on ionospheric interactions in connection with radiowave propagation below, say, 300 MHz. Between 300 MHz and 1 GHz, the effects are competing, and the dominant radiowave interactions depend critically upon the system application and geometrical situation involved. This does not mean that ionospheric effects may be ignored in comparison with tropospheric effects if frequencies in the GHz regime or higher are employed. This is because a proper accounting must be taken of the path lengths involved. Indeed, ionospheric ray trajectories are

typically much larger than their tropospheric counterparts. Furthermore, we must also consider the presence of refractive index inhomogeneities, which will give rise to a different class of effects broadly classified as scintillation. In the ionosphere these refractive index inhomogeneities are directly related to irregularities in the free electron number density.

The ionospheric effects on radiowave systems may be characterized in a number of ways, depending upon the focus of the treatment. Popular breakouts may organize the effects in terms of system type, medium properties, or frequency band. Our plan is to organize the discussion into two broad groups of ionospheric effects: terrestrial systems and earth-space systems. Frequency issues are considered within each group. Table 4-1 is a listing of the radio bands, the frequency range, the wavelength range, and the primary modes of propagation. This is followed by Table 4-2, which shows the primary uses of the specified bands.

Table 4-1: Radio Bands and Primary Propagation Modes

Band	Frequency	Wavelength	Primary Modes
ELF	< 3 kHz	>100 km	Waveguide Groundwave
VLF	3-30 kHz	100-10 km	Waveguide Groundwave
LF	30-300 kHz	10 – 1 km	Waveguide Groundwave
MF	300-3000 kHz	1000-100 m	Groundwave Skywave (E)
HF	3-30 MHz	100-10 m	Groundwave Skywave (E,Es,F1,F2)
VHF	30-300 MHz	10-1 m	LOS Meteor Scatter Es Scatter
UHF	300-3000 MHz	1000-100 mm	LOS
SHF	3-30 GHz	100-10 mm	LOS Troposcatter
EHF	30-300 GHz	10-1 mm	LOS

The full array of ionospheric effects may be organized in terms of specified radio frequency regimes, and these regimes, in turn, may be largely identified with certain propagation "modes." For example, at the low end of the spectrum (viz., ELF and VLF), we may associate the effects with propagation within an effective waveguide bounded by the earth below and the ionosphere above. There is some penetration of the ionosphere at ELF because of the enormous wavelengths involved, but details of ionospheric layering are effectively disguised. Just above the ELF band, at VLF, the penetration of the wave is reduced but lower ionospheric structures become more important. The ionospheric impact gradually increases as we proceed

upward within the longwave part of the spectrum. On the other hand, at the high end of the considered radio spectrum (viz., SHF), the effects are associated with the so-called earth-space mode in which penetration of the sensible ionosphere is complete. For both ELF and SHF, the ionosphere has a definable but limited role. Between these two extremes, centered at HF, one encounters the most intense ionosphere effects; these effects are associated with *skywave* modes otherwise termed ionospheric-reflected or refracted modes. We now will sketch out the main effects in more detail beginning with longwaves.

Table 4-2: *Utilization of the Radio Bands*

Frequency Band	Uses
VLF	Navigation Standard Frequency Standard Time
LF	Broadcasting Navigation
MF	AM Broadcasting
HF	Communication WWV, WWVH OTH Radar Direction Finding Systems Amateur Service Citizens
VHF	Television FM Broadcasting Aviation Communication
UHF	Satellite Communication Radar Surveillance Satellite Navigation and Timing Television
SHF	Satellite Communication Radar Navigation Television

4.3 TERRESTRIAL TELECOMMUNICATIONS

4.3.1 Longwave Propagation: General Remarks

It is worth noting that the investigation of longwave propagation (from ELF through LF) was greatly influenced by ground-based observation of whistlers, a mode of propagation that is strongly influenced by the earth's magnetic field. This mode allows ionospheric penetration but no major system application of this mode has been developed. However, a number of

proposals have recently been made for which longwave transmitters would be orbited, providing longwave terrestrial coverage from space. These concepts would utilize the whistler mode for penetration but significant, and possibly unrealistic, transmitter powers would be required for a system to be useful. A rather thorough discussion on longwave propagation in the ionosphere is found in the aforementioned *Handbook on The Ionosphere and its Effects on Radiowave Propagation* (i.e., Chapter 4 of [ITU-R, 1998]). Additional background on the theory of longwave propagation is found in earlier works, including a document published by AGARD [1982], books by Wait [1970] and Galejs [1972], and the U.S. Air Force Handbook [Jursa, 1985].

For longwaves, the antenna system is a significant component of the overall system. Indeed, the sheer size requirement to efficiently launch longwaves may be a formidable restriction. As indicated by Kelly [1986], considerable ingenuity has been employed to develop relatively efficient antennas that are necessarily large in human terms but small in comparison with a wavelength dimension. Contrary to popular opinion, it is thought that the classic Marconi experiment in 1901, which demonstrated the feasibility of communication over global distances, was actually performed using signals in the MF band, and bordering the longwave part of the radio spectrum. Marconi's success subsequently led to the notion that signals were being refracted from upper atmospheric strata rather than being diffracted along the earth surface. It turns out that the greatest efficiency in coverage by this ionospheric "bounce" process is achieved at HF, since ionospheric properties permit the largest refraction height in this frequency band. At lower frequencies (viz., LF and below), the interaction is restricted to heights on the order of 100 km or less restricting the maximum range for a single hop, while at higher frequencies (viz., VHF and above), the ionosphere has a high probability of being transparent and signals are lost into outer space. Nevertheless, since it has been shown that the lower ionosphere is far less variable (and more predictable) than the upper ionosphere, the longwave communication channel is a highly reliable one at least in comparison with the so-called *shortwave* (or HF) channel. Furthermore, we find that the longwave signal traverses far less of the ionosphere than signals in other frequency regimes, with most of its lifetime spent in the "free space" between the earth and the lower ionosphere. This accounts for the relative stability of longwave signals, but there are other factors that tend to reduce some of this attractiveness. First and foremost, huge power-aperture products are essential to overcome the impact of environmental noise. Also, the longwave channel has a very limited bandwidth, which restricts the ultimate information rate possible to achieve. A major advantage provided by the longwave channel is its seawater and earth penetration capability, especially at ELF.

While the use of longwaves in the practical realm is under decline, there is still a vigorous scientific and popular interest. Amateur monitoring and student activities abound, and an educational corporation has been established to encourage the science of natural radio listening (e.g., "Project INSPIRE"). On the professional level, Stanford University has engaged in a vigorous VLF research program since the middle of the 20th century, and they are still involved in studies of the ionosphere and magnetosphere using natural and man-made VLF signals. They use VLF waves as diagnostic tools to investigate the physical processes in the Earth's low and high altitude plasma environment. Umran Inan heads the VLF group, and it has an illustrious senior staff including Bob Helliwell (who introduced the author to the notion of Whistlers in the 1960s) and Don Carpenter (who is associated with the discovery of "Carpenter's knee" or the plasmapause). The VLF group manages multiple ground-based stations in the continental United States, Canada, and Antarctica; and has observational programs on satellites. Research includes modeling of such phenomena as sprites, blue jets, and elves. Refer to Chapter 6 (on Resources) for information on activities affiliated with the Stanford VLF group, such as HAARP, POLAR, CLUSTER, and IMAGE.

Long wave bands have very attractive ground wave characteristics, which are virtually unaffected by the ionosphere and nuclear-induced Electromagnetic Pulse (EMP). The United States built the Ground Wave Emergency Network (GWEN), a high power VLF communication system operating at 150-175 kHz, and designed to provide survivable connectivity to bomber and tanker bases. The system has been placed in a sustainment mode (circa 2000), but is being considered for other non-military purposes, such as inland navigation.

4.3.2 Extremely Low Frequency

The ELF band (<3kHz) has been the subject of theoretical investigation for a number of years, and Bannister [1986] has reviewed the topic. ELF field strength predictions include methods developed by Pappert and Moller [1978] in which the ionosphere and the earth are both assumed to be homogeneous and sharply bounded. Although this model is a simple one, the bulk of the evidence, both experimental and theoretical, has shown its adequacy. The ionosphere acts almost like a perfect conductor at ELF, and as a result, the earth's magnetic field-induced anisotropy is vanishingly small. Thus, the refractive index is independent of propagation direction. Ionospheric effects are not dominating at ELF; nevertheless certain ionospherically-related phenomena have been observed. They include the following:

(a) Anomalous field strength fluctuations, which may arise as the result of magnetic storms [Bannister, 1980], enhanced particle precipitation, or movement of sporadic E patches [Pappert, 1980]. These events are typically nocturnal, have magnitudes in the range of 3-8 dB, and may be the result of interference between waves reflected from the normal E region and an enhanced sporadic E patch.

(b) Solar-induced effects, such as x-ray flare disturbances, and solar particle events (SPE), which may increase the signal attenuation rates by 1-2 dB per megameter of path length. Field [1982] has reported daytime attenuation rate enhancements of up to 4 dB per megameter.

(c) Non-radial propagation disturbances arising from inhomogeneities, such as the day-night terminator, the polar cap boundary, or significant sporadic E formations. The most significant effects are observed for the situation in which the great-circle path is approximately tangent to the boundary of one of these features.

4.3.3 Very Low Frequency and Low Frequency

There are two primary mathematical formulations associated with the VLF (3-30 kHz) and LF (30-300 kHz) bands corresponding to propagation in these bands, one involving a waveguide approach and the second characterized by wave-hop theory. As would be expected, the former approach is usually employed at VLF, while the latter approach is most utilized at LF.

In the waveguide formulation we find that the cavity between the earth and the ionosphere gives rise to the usual features one would expect, including cutoff frequencies and characteristic reflections from segments of the guide for which sharp electrical discontinuities arise. It is noteworthy that either Transverse-Electric (TE) or transverse-Magnetic (TM) modes may be excited, depending upon the model selected for the antenna current element. TE and TM waves both have their own personalities in terms of mode structure, excitation, height-gain factors, and attenuation rates. Nevertheless, they are not totally uncoupled because of the presence of the earth's magnetic field.

It is felt that neither the waveguide nor the wave-hop formulations are unassailable under all conditions, and should be viewed as complementary methods in a thoughtful analysis of VLF/LF coverage. There are a number of models that allow for the prediction field strength in these bands. Components of the U.S. Navy have long been active in this field (e.g., [Morfitt et al., 1982] [Houser et al., 1981] [Kelly et al., 1984]), although current research interest has waned along with the decline in use of communication and navigation systems at VLF/LF. The ITU-R has

sanctioned two methods for theoretical calculation of field strength [ITU-R Rec. P.684, 1997], based upon wave-hop and waveguide methodologies.

From a propagation viewpoint, the ionosphere has a far greater impact on signals at VLF/LF than at ELF. Accordingly, the space weather impact is also greater. In the absence of significant space weather events, even VLF and LF bands are remarkably stable to benign ionospheric variabilities. Still, performance degradation in the VLF/LF bands, aside from radio noise competition, can result from a number of space weather factors, including solar flares and related phenomena. Sudden Phase Anomalies (SPA) occur at the same time as daytime solar x-ray events that produce an increase in the normal D layer ionization level. These anomalies, if uncompensated, may yield navigation errors of the order of 10 nautical miles or more. Other events of interest include magnetic storms and Polar Cap Absorption (PCA), the latter being caused by solar protons that gain access to the lower ionosphere within the polar cap. These events give rise to both phase and amplitude distortion of signals in the band. Although solar flare-related effects are of interest, the major problem areas in VLF/LF predictions may be related to other factors, including ground conductivity uncertainties and noise variability. There is considerable interest in the high-latitude region, owing to the combination of ionospheric effects, which dominate the arctic environment, and the existence of low conductivity zones characteristic of permafrost, sea ice, and the ice cap itself. Practical VLF circuits from America to Europe cross the Greenland ice cap, and these circuits are especially vulnerable to attenuation arising from ice cap traverse. Moreover, these paths, which are already degraded, are very sensitive indicators of solar proton events. Table 4-3 is a summary of ionospheric effects at VLF. Figure 4-3 shows the phase and amplitude variation during a PCA for an 18.6 kHz path between Washington, D.C and Sweden.

4.3.4 Medium Frequency

Some treatments group Medium Frequency (MF) and High Frequency (HF) together since both may utilize the *skywave* mode of propagation, and, with the possible exception of the lower MF band, operational utility is usually achieved through exploitation of this mode. Additionally, both MF and HF exhibit useful groundwave properties. For example, large-scale D-region absorption events, such as PCA or SWF, will reduce the competing noise at the groundwave receiver terminal arriving by skywave. Hence, a groundwave system will encounter reduced atmospheric noise, and this should increase the SNR and the system performance. This is even the case for absorption due to high altitude nuclear explosions (i.e., HANE events).

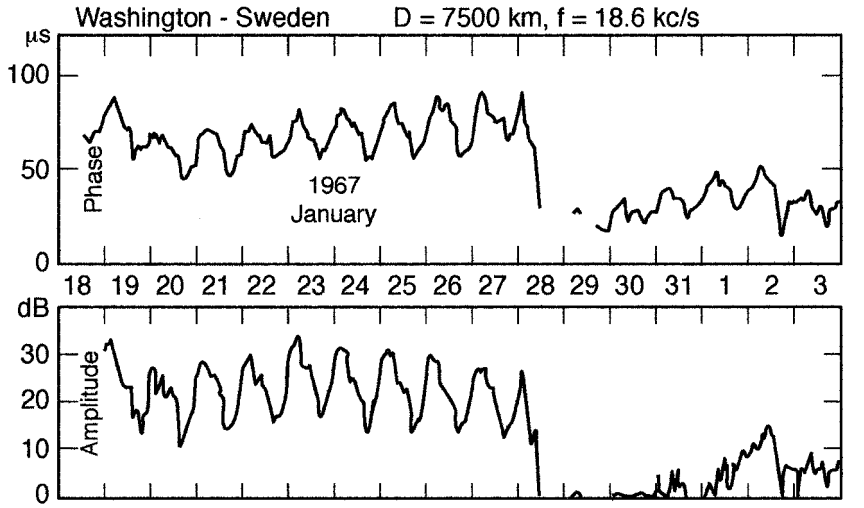


Figure 4-3: Phase and Amplitude Recordings during a PCA Event. From Galejs [1972], after Westerlund et al., [1969].

Table 4-3: Ionospheric Effects at VLF

Event	Ionospheric Change	System Result
Solar Flare	Sudden Ionospheric Disturbances (SIDs): Solar x-rays cause excess ionization below the normal D-layer, on the sunlit side of the earth, changing the effective height of reflection. (wide-area and instantaneous event)	▪ Sudden Phase Anomaly (SPA, or increase in wave phase) ▪ Increase in signal strength above 16 kHz over sunlit paths
Solar Proton Event	Polar cap disturbance due to energetic particle event. This causes excess ionization in the D-layer within the polar cap. (wide-area and instantaneous event)	Phase lag and amplitude decreases: ▪ several hours at midlatitudes ▪ 10-20 days hi-lat/transpolar paths
Magnetic Storm and Auroral Phenomena	Precipitation in the auroral zone causes excess ionization in the D-region, but these events are more localized in space and time.	Irregular variations in phase and amplitude with periodicities of ~10s of minutes, especially at night and over long paths [ITU-R, 1998].

The variabilities in skywave field strength at MF have been outlined by Knight [1982]. While there are sound arguments for consideration of the MF and HF bands as a unified pair of bands, the ITU-R has chosen to group LF and MF together. Indeed, there are two recognized methods for predicting skywave field strength in the LF/MF bands, specifically within the range 150 kHz and 1700 kHz (i.e., [Wang, 1985, 1993] and ITU-R Rec.P.1147 [1997]). There are distinct magnetic and solar activity influences on LF and MF circuits. Figure 4-4 compares long-term MF field strength variations with SSN and *Ap*.

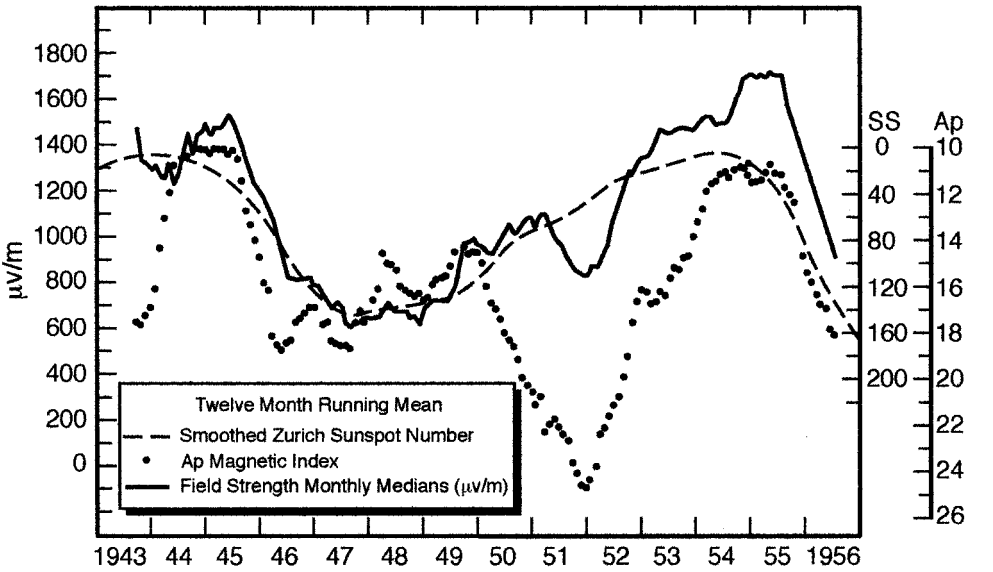


Figure 4-4: Monthly median field strength for a Medium Frequency (MF path) between Cincinnati and Atlanta (600 km) compared with the *Ap* Index and the 12-month running mean sunspot number. (From Davies [1990]).

4.3.5 High Frequency (Shortwave)

The HF band is probably the most difficult regime to characterize, given the fact that it is the most precarious of the bands, vis-à-vis ionospheric propagation. This is because representative electron densities associated with various layers in the ionosphere correspond to critical frequencies (and plasma frequencies) that fall within the HF band. The layer critical frequency is the frequency above which radio waves will penetrate the ionosphere at vertical incidence, and this is the maximum plasma frequency of the layer. For example, a typical midlatitude daytime value of the F2 layer critical frequency is 10 MHz, but it varies considerably depending upon a number of geographical and solar epochal considerations (see Chapter 3). Space weather

effects on HF are significant, and the effects include: solar flare-induced absorption, polar cap absorption, angle-of-arrival fluctuations, auroral scatter, multipath distortion, HF radar ranging errors, broadcast coverage variations, storm-driven MUF variations, and many more. One may refer to Goodman [1991] for additional information. Table 4-4 provides a synopsis of ionospheric disturbances on HF systems.

Table 4-4: Ionospheric disturbances that influence HF radio systems. The magnitude of the HF effects will depend critically upon system parameters.

Ionospheric Disturbances					
			Approximate Occurrence Frequency		
Disturbance	**Propagation Effects**	**Time and Duration**	**Solar Max**	**Solar Min**	**Probable Cause**
a) Sudden Ionospheric Disturbance (SID)	In sunlit hemisphere, strong D layer absorption (shortwave fades), anomalous VLF-reflection, F-region effects.	All effects start approximately simultaneously. Duration ~ 1/2 hour.	2/Week	2/Year	Enhanced solar X-ray and EUV flux from solar flare.
b) Polar Cap Absorption (PCA)	Intense radiowave absorption in magnetic polar regions. Anomalous VLF-reflection.	Starts a few hours after flare. Duration one to several days.	1/Month	0	Solar protrons 1-100 MeV.
c) Magnetic Storm	F-region effects; increase of foF2 during first day, then depressed foF2, with corresponding changes in MUF.	May last for days with strong daily variations.	26/Year	22/Year	Interaction of solar low energy plasma (solar wind) with earth's magnetic field, causing energetic electron precipitation, auroral effects, heating, and TID generation.
d) Auroral Absorption (AA)	Enhanced absorption along auroral oval in areas hundred to thousand kilometers in extent. Sporatic K may give enhanced MUF.	Complicated phenomena lasting from hours to days.	Essentially omni-present		Precipitation of electrons with energies a few tens of keV within an oval region equatorward of the polar cap.
e) Travelling Disturbances (TID)	Changes of foF2 with corresponding changes of MUF sometimes periodic.	Typically the periods are from tens of mnutes to hours.	Essentially omni-present with larger scales enhanced during magnetic storms		Atmospheric waves.

HF signals penetrate the overhead ionosphere if the frequency is greater than the so-called critical frequency (see Equation 3-10). For practical systems, it is necessary to exploit the so-called skywave mode of propagation. Unless we simply want an "umbrella" type of coverage that is limited to 500 km or so, we actually want the transmission frequency to be higher than *foF2*.

This means we lose signals to outer space through an overhead "iris", but we gain the opportunity for greater coverage by oblique propagation. Long-haul skywave propagation is achieved if the transmission frequency is greater than *foF2* but less than the Maximum Observable frequency (i.e., MOF) for the path length required. The MOF can be shown to be proportional to the quantity (k *foF2 sec ø*) where ø is the ray zenith angle, *foF2* is the ordinary ray critical frequency of the F2-layer, and k is a number between 1 and 2 whose value is dependent upon the nature of the process involved. For classical HF skywave propagation, $k \cong 1$, but it approaches 2 for around-the-world propagation involving super-modes, chordal modes and ducted modes. For scatter modes, $k > 1$. Referring to the classical case, we find that as the elevation angle is reduced, a level is eventually reached at which reflection will occur, and it becomes possible to generate skywave modes. This effect is depicted in Figure 4-5.

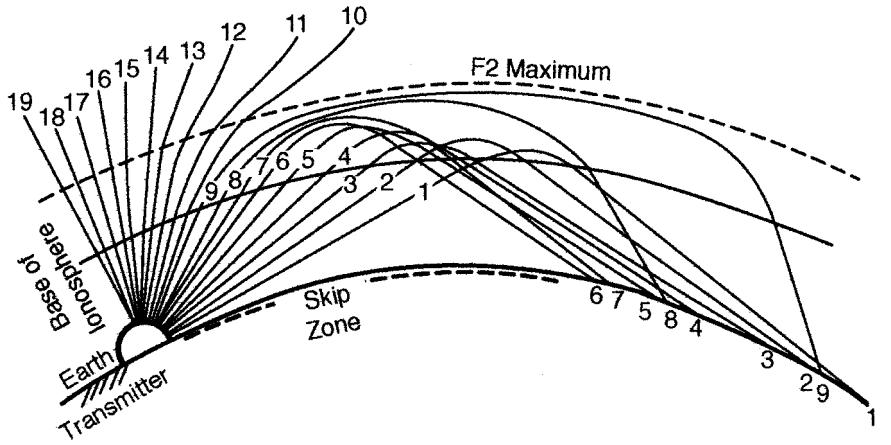


Figure 4-5: Illustration of rays launched into the ionosphere. The numbers are sequenced from the lowest elevation angle labeled "1" at 0 degrees to "19" at 90 degrees. Notice that rays 1-9 participate in skywave propagation, and rays 10-19 escape through the ionospheric iris. A "skip zone" is also introduced. In practice this skip distance is weakly illuminated as the result of non-classical scatter modes. Groundwave and line-of-sight propagation will also provide "local" coverage.

The HF band is most sensitive to ionospheric effects. In fact, HF radiowaves experience some form of virtually every propagation mode or mechanism, as indicated in Table 4-5 and illustrated in Figure 4-6. It has been said that if one can understand radio propagation at HF, a comprehension of all other bands follows naturally.

Table 4-5: List of HF Propagation Mechanisms

Mode or Mechanism	Description
Groundwave	Propagates along surface of the earth or ocean (i.e., surface wave)
Spacewave	Superposition of LOS, earth-reflected signals, and secondary ionospheric modes
Terrestrial Line-of-Sight	Subionospheric rectilinear propagation
Earth-Space Line-of-Sight	Transionospheric quasi-rectilinear propagation
Reflected One-Hop	Earth-to-Earth propagation with intermediate reflection from an ionospheric layer.
Reflected Multi-Hop	Earth-to-Earth propagation with multiple hops using a single ionospheric layer or different layers
Ducted	Wave is trapped between two ionospheric layers (i.e., the E-F "valley" of ionization)
Chordal	Wave, launched from an earth terminal, skips along the base of an ionospheric layer without an intermediate ground reflection (i.e., transequatorial "supermodes")
Scatter	Wave is scattered from ionospheric inhomogeneities or features (i.e., auroral and sporadic-E sidescatter, spread-F scatter)

The major ionospheric layers possess characteristic plasma frequencies that lie within the HF band, and as a result, ionospheric interaction is pronounced. Accordingly, many of the traditional ionospheric diagnostic systems exploit this feature and use HF waveforms to probe the ionosphere and determine its structure. Figure 4-7 depicts the various possibilities. See Hunsucker [1990] for more details.

Propagation factors at HF have been widely explored, and numerous books are available on the subject with most being cited in Section 4.1. Naturally, the author's preference is the HF book by Goodman [1991], having an emphasis on applications, but the book by Davies [1990] is a well-rounded classic.

One of the major problem areas that arise in connection with HF system performance is the variability in coverage and reliability for a fixed transmitter site and a specified frequency. This variability mimics the ionospheric variability itself, and recently schemes have been developed to monitor the ionosphere and adjust certain system parameters in near real time to compensate for the system effects. The value of these Real-Time-Channel Evaluation (RTCE) schemes that may be central in specified adaptive-HF methodologies will be addressed later on in the chapter.

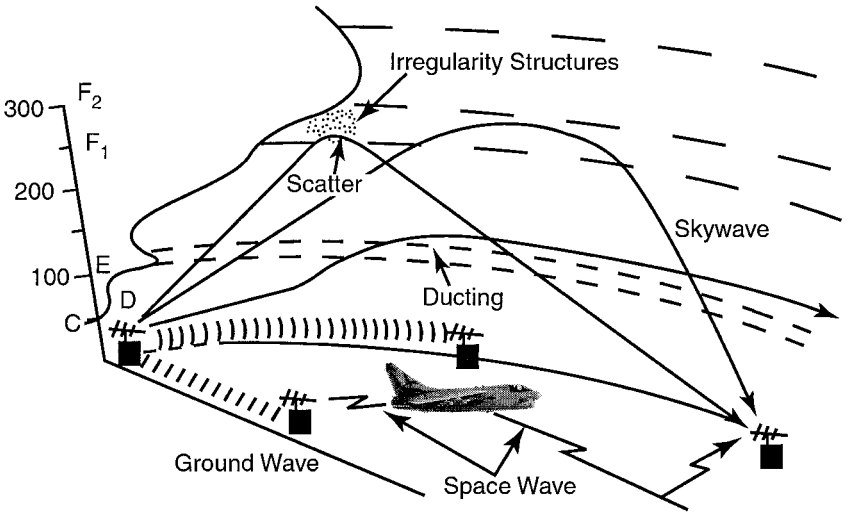


Figure 4-6: Depiction of various propagation mechanisms (i.e., modes) at HF. The most prominent group is the set of *skywave* modes. These fall into three categories: (a) those associated with regular refraction from the ionospheric layers E, F1, and F2; (b) those associated with scatter from sporadic-E, auroral forms, polar patches, blobs, etc.; and (c) those associated with ducted or chordal modes of propagation. There is also scatter from ionospheric inhomogeneities associated with above-the-MUF connectivity. Other non-skywave possibilities include groundwave, spacewave and line-of-sight. (From Goodman [1991]).

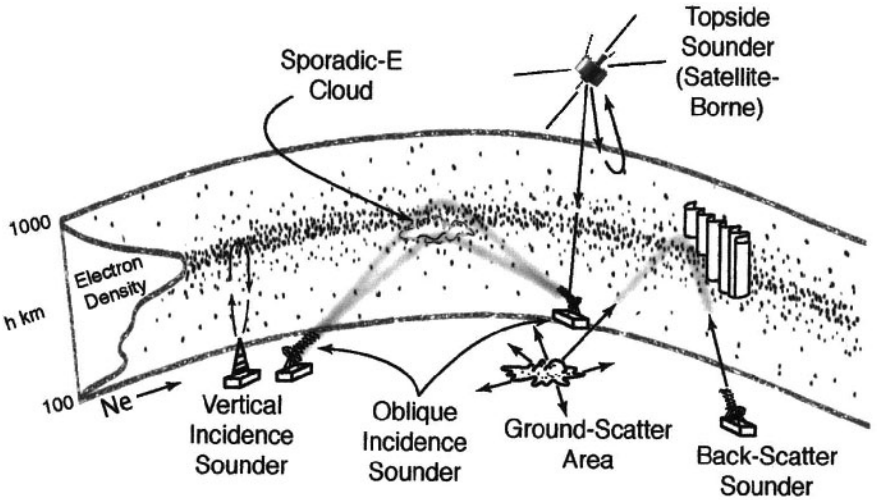


Figure 4-7: Sounding and diagnostic techniques that use the HF band. From Goodman and Aarons, [1990].

Included among the quasi-global disturbance phenomena that may impact long-haul HF systems are: Sudden Frequency Deviations (SFD) and Short Wave Fades (SWF), both of which occur within seconds of the measurement (at earth orbit) of an x-ray flare on the solar surface. These events are important only on the sunlit portion of the ionosphere and the effects are diminished as the ionospheric distance from the subsolar point increases. Less immediate but near-term phenomena associated with energetic solar protons are also encountered. Polar Cap Absorption events (or PCAs) are perhaps the most catastrophic events in connection with HF radio propagation in the high latitude zone, with attenuation over skywave circuits in excess of 100 dB sometimes encountered. These absorption conditions may last from hours to days. Fortunately, they are rare events, which are not typically encountered at solar minimum, and are observed approximately once a month at solar maximum.

Probably the most interesting space weather phenomenon to be encountered at HF is the ionospheric storm, which gives rise to a hierarchy of effects at midlatitudes. Although the time history of ionospheric storms is also of importance in earth-space satellite applications, it may be devastating in the HF band. This is because it may limit ionospheric support in the frequency range $\leq$ the undisturbed MUF, causing a non-absorptive "blackout" of HF trunks in the affected area. An ionospheric storm is an ionospheric manifestation of the geomagnetic storm whose basic phenomenology has been fully described by Akasofu [1977], and has been updated in Geophysical Monograph 98 [Tsurutani et al., 1997], and in a document edited by Daglis [2001]. At HF, we are principally interested in the diminutions in the F2 region electron density, a phenomenon that is highly correlated with the temporal structure of the main phase of the geomagnetic storm. In concert with *foF2* variations, Maximum Observable Frequency (MOF) reductions of up to 50% may be observed for the day of the disturbance with full recovery occurring over several days. (We also note that MOF enhancements are sometimes observed, and these events are designated positive storms.) It was once thought that ionospheric storms would be predominant during solar maximum conditions, but significant disturbances may be observed at any time, especially during the declining phase of the sunspot cycle.

Again, while there are many phenomena of interest, the most important concerns for HF systems vis-à-vis space weather relate to the delayed phenomena associated with particle eruptions or solar wind plasma. These events take a predictable amount of time to impact the earth, and as a consequence allow time to invoke countermeasures. The delayed events include energetic particles (viz., solar protons) that cause long-term fading in the polar region (i.e., PCA). Equatorward of the polar cap, the most important solar phenomena are those associated with expansion of the solar corona (i.e.,

coronal holes) and coronal mass ejections (CMEs). As already described, these events give rise to magnetic storms and, more importantly ionospheric storms. Ionospheric storms are not only defined by large excursions in the electron density of the F layer, but can also introduce large-scale TIDs, enhanced spread-F, and other deleterious effects. Immediate events like solar flares have the potential to cause communication blackout (i.e., SWF) over a large area of the sunlit earth for up to an hour, and they can serve as markers for particle expulsion or solar wind enhancement. But, given this, the x-ray flare is still not as important an event for HF systems as the ionospheric storm.

Most HF systems are only partially adaptive, with the capability to compensate for relatively minor channel variations through equalization and diversity schemes. While HF systems are now designed to take care of traditional HF difficulties, they are ill-equipped to address massive changes in the propagation characteristics, such as total absorption of entire frequency families due to PCA and enhanced auroral absorption, loss of important circuits as the result of exaggerated F-layer depletion, etc. This puts a premium on the forecasting and early detection of magnetic storms. Such information allows the system manager, or possibly a computer controller, to activate new routing strategies and frequency plans, or possibly resort to the use of alternate media.

4.3.5.1 Operational HF Systems

There are several HF systems of interest, and they all depend upon the ionosphere in one way or another. While not the only examples, two types are especially noteworthy: HF communication and HF Over-the-Horizon Radar (OTH-R). Both of these system types are of interest since they have undergone a modest rebirth either as the result the invocation of new technology (as in HF communication) or as the result of a change in mission (as in OTH-R).

4.3.5.1.1 HF Communication

HF communication systems incorporate voice and data missions. In this section we will highlight HF automatic link establishment (ALE) systems since they dominate both the civilian and military marketplaces. HF communication is not married to the non-agile crystal-set mentality of days gone by. The concept of "adaptive HF" is now in vogue. The interested reader should refer to the adaptive HF handbook published by ITS [1998] and a similar handbook recently published by the ITU-R [2002]. Other systems have been designed for special purposes, and may offer superior performance

to ALE under certain conditions. An example is ARINC's HFDL system, GLOBALink/HF (see Section 4.5.2.1).

We discuss ALE in this section of Chapter 4 as an HF system appliqué that could effectively exploit space weather data, but does not do so at present. We also reserve space in Section 4.5.2.1 for the GLOBALink/HF system because it is a system that does use space weather forecasts in the course of its frequency management procedures.

The concept of ALE has been described by the author [Goodman, 1991], but the most comprehensive treatment is provided by Johnson et al. [1997]. Other references include the multi-service document on HF-ALE [ALSA, 2003], and several military standards [viz., MIL-STD-188-141A; MIL-STD-188-141B]. The ALE systems are designed to enable HF radio stations to call and link to the optimum HF channel automatically without operator intervention. In general, ALE radios exploit recently measured radio channel characteristics that are stored in computer memory (i.e., link-quality analysis matrix, LQA) to derive the best frequency for use. This matrix is constantly updated by use of organic sounding within the network, or other methods. When not in use, the radio receiver performs a scan of all of its assigned frequencies, listening for any calls addressed to it. ALE systems are designed to readjust the frequencies used for connectivity based upon the LQA matrix, and it should be noted that the LQA entries depend upon all potential propagation channels in the network, and each has unique ionospheric and noise characteristics. There are a number of generations of ALE in use, and a number of organization employ ALE to improve their HF performance. Systems are employed by all the military services, and civilian agencies also employ the technology.

It has been said by some that ALE works so well that space weather information is not needed to govern its operation or improve its operational efficiency. But this is an overstatement. For example, it has been suggested by Sutherland [1993] that during periods of stress (i.e., propagation disturbances), the system will exhaust a significant portion of its assets in a possibly fruitless search to find the best channel. Goodman et al. [1996] has suggested that non-organic sounding might be used to circumvent the Sutherland "problem". In general one could exploit space weather data (i.e., ionospheric sounding data) to modify the organic LQA matrix or otherwise "steer" the list of assigned frequencies to a more realistic subset, possibly reducing the scan time. From the multi-service document on ALE, it is recommended that a good propagation prediction program be used for planning the network (see Section 4.3.5.2). There are other limitations. For example, ALE will not improve propagation. If poor frequencies are used ALE procedures will not make them work better. ALE was originally designed as a replacement for an HF operator. However a very skilled

operator may still be more efficient than an ALE system. But this is academic since such personnel are quite rare in the present environment. This having been said, ALE is enormously popular with both military and commercial users, and the systems have been promoted vigorously by the U.S. Government and an association of users and ALE radio providers (viz., the HF Industry Association, HFIA). ALE radio networks generally offer predictable performance and support a range of services. An important attribute of the ALE concept is that all ALE radios, built to the standard, perform the same way irrespective of the supplier of the individual radios. This is a huge plus. First and second generation ALE standards have been promulgated with most current systems being compatible with second-generation specifications. Standard methods have now reached the 3rd generation, but most vendors have not produced such advanced radios.

4.3.5.1.2 HF OTH-R

OTH-R was born in the early days of radar system development as described in Chapter 1. The primary mission was radar surveillance of military targets beyond-line-of-sight (BLOS) using large power-aperture products and sophisticated signal processing algorithms. The OTH-R is fundamentally a down-looking radar, so it must always contend with ground or sea clutter. There are also difficulties associated with ionosphere phenomena such as spread-F that can degrade the radar performance. Reviews of OTH-R are given by Headrick and Skolnik [1974] and Headrick [1990]. Sophisticated processing methods are employed to resolve signals in a clutter rich environment, but range determination still requires registration based upon an ionospheric model or a check target at a known range. In the early 1980s, the Relocatable OTH-R (ROTHR) was developed for the U.S. Navy. Two ROTHR systems (Virginia and Puerto Rico) were operational in 1998, and another was being proposed for Puerto Rico. OTH-R plays a major role in the Counter-Drug Program. A summary of the current technology is found in a special issue of *Radio Science* [Berkey, 1998].

Aside from the USA, countries involved in OTH-R research and technology include Australia, China, and Russia. Australia has developed the Jindalee radar system located at Alice Springs with research supported by the Defense Science and Technology Organization (DSTO) [Anderson, 1986]. The Jindalee Operational Radar Network (JORN) is being developed based upon this effort. Work in the Ukraine and Russia has been described by Evstratof et al. [1994].

OTH-R is currently used in non-military roles, including: (i) as a research instrument, (ii) as a system to track tropical storms and hurricanes, (iii) to monitor sea state, and (iv) to detect illegal aircraft engaged in drug smuggling. OTH-R systems are also used in a diagnostic capacity, vis-à-vis

the ionosphere. These diagnostic systems, including SuperDARN, are resources for science rather than operations, and are mentioned in Chapter 6.

4.3.5.2 System Performance Modeling

There are a number of HF system performance models (i.e., IONCAP, VOACAP, ICEPAC, ASAPS, and REC533) that can be used to assist in frequency management and related endeavors. There is an ITS-Boulder web site from which VOACAP, ICEPAC, and REC 533 may be downloaded. (Suggestion: Go to the ITS website using your browser, click on radio propagation software, and then on HF models.) A detailed discussion of these and other models may be found in Chapter 5 of Goodman [1991]. The internationally accepted HF system performance model is REC533 [1997], but a number of system engineers and HF practitioners in the United States prefer VOACAP. A valuable resource outlining many of the VOACAP features is now available [Lane, 2001].

Many workers in the Pacific Rim and Australasia use the ASAPS model [McNamara, 1991], and it has also developed a following in other regions as well. One interesting feature about ASAPS is that it uses a so-called T-index as a proxy for sunspot number. The T-index is based upon ionospheric measurements, and like the sunspot number, is readily available for use as a driver in the calculations.

The models cited above are based upon ionospheric submodels that may be either simple or complex. But it is important to recognize that the ionospheric submodels are largely based upon the same climatology (i.e., the same set of values for *foE, foF1, foF2, M3000F2*, etc.) for the same periods of time and circuit geometries. Hence, to first order, the system performance models yield similar, although certainly not analogous, results. Differences derive from how the parameters like signal-to-noise ratio and system reliability are handled, and the differences can be quite significant. Table 4-6 provides some information about selected full performance prediction models. Bare in mind that there are additional less capable models developed for special limited purposes, such as simply computing the maximum and minimum frequencies for a specified circuit (i.e., MUF and LUF). The U.S. Navy MINIMUF program is well-known model of this category. In general, the MUF and LUF information is not sufficient to run a circuit properly, nor understand its idiosyncrasies.

From a space weather perspective, we are mainly interested in the determination of storm-driven departures from climatological predictions. We can hope that we have conducted our analysis properly, and can run VOACAP or REC533 using the proper set of system parameters. Typically we specify a running average sunspot number, and possibly some

representation of magnetic activity. With this information, we derive median ionospheric properties and system performance parameters such as the signal strength distribution function and the system reliability.

Table 4-6: HF Communication Performance Models (since 1970)

MODEL NAME	ORIGINATOR	REFERENCE
FTZ	Deutsche Bundespost	Ochs [1970]
CCIR-252-2	CCIR/ITU	CCIR Rpt.252-2 [CCIR, 1970]
CCIR-252-2 (Supplement)	CCIR/ITU	CCIR Rpt.252 Supp [CCIR, 1982]
CCIR-894-1	CCIR/ITU	CCIR Rpt.894 [CCIR, 1986]
HFBC84	WARC/ITU	[ITU-WARC, 1984]
REC533	ITU-R	[ITU-R REC533, 1987]
HFMUFES	ITS-Boulder	[Haydon et al., 1976]
IONCAP	ITS-Boulder	[Teters et al., 1983]
VOACAP	ITS-Boulder/NRL/VOA	ITS website (see text)
ICEPAC	ITS-Boulder/U.S. Air Force	ITS website (see text)
RADARC	ITS-Boulder/NRL	[Lucas et al., 1972] [Headrick et al., 1971]
ASAPS	IPS-Australia	[McNamara, 1991]

It is understood that the ionosphere has a recognized level of anticipated variability, even when the ionosphere is undisturbed, and some of this is accounted for in the model. However, the "common" climatological data base (referred to earlier) does not include ionospheric storm data. In short, the manner in which the ionosphere behaves under magnetic storm conditions is not contained in the historical record. Hence, the ability to predict ionospheric response, and HF performance, under storm conditions is typically based upon ad-hoc algorithms or software patches to existing codes. Some methods use imbedded ray tracing, and estimate signal strength through an analysis of ray path density within the coverage area, but these methods can be problematic in a realistic ionosphere. Furthermore there is no guarantee of consistency. A practical solution to the evaluation of large disturbances is to modify certain parameters within the ionospheric submodel, such as the *foF2* value. In a number of models this can be accomplished easily. A more pressing problem is how to make climatological models like VOACAP or ICEPAC useful for future operations. To do so, one must have confidence in space weather forecasting algorithms (e.g., the STORM model discussed in Chapter 3), and a system that is blessed with a degree of resilience (i.e., organic adaptability). For practical reasons, it is more important to have a forecast of ionospheric properties for HF system utilization than a current assessment or nowcast. This is because it takes time for system resources to be reorganized and managed. The good news is that upstream space weather data tends to be correlated with lagged values of pertinent ionospheric factors. Lane [2004] has suggested that VOACAP, with

suitable modification, can be used in connection with ALE radios, even in the absence of space weather data.

4.4 EARTH-SPACE TELECOMMUNICATIONS

Telecommunications have expanded enormously since the advent of the space age. In general, we are no longer limited to the coverage dictated by terrestrial systems, nor the data rate limitations and catastrophic ionospheric effects so long associated with lower frequencies. But this does not mean we are rid of the ionosphere and space weather effects. Table 4-7 contains a representative listing of effects for frequencies between 100 MHz and 1 GHz corresponding to a single traverse through the ionosphere at an elevation angle of 30 degrees. Also given is the frequency dependence. As may be seen, ionospheric effects are not entirely negligible at frequencies normally utilized on space platforms. For example, at 1 GHz, 250 nS corresponds to a group path delay error of ~ 250 feet, and this creates a problem for some single-frequency users of GPS systems requiring highly accurate radionavigation.

Table 4-7: Representative Maximum Effects on Earth-Space Systems
(Note: The EC = 10^{18} electrons/m^2, and the elevation = 30 degrees)

Effect	100 MHz	1 GHz	Frequency Dependence
Faraday Rotation	30 rotations	108 degrees	f^{-2}
Ionospheric Delay	25 μS	250 nS	f^{-2}
Refraction	< 1 degree	<0.6 Minutes	f^{-2}
Absorption	5 dB	0.05 dB	f^{-2}
Time Dispersion	0.4 pS/Hz	0.0004 pS/Hz	f^{-3}

For the time being we ignore Doppler effects and radiowave scintillation. Scintillation, arising from ionospheric inhomogeneities, has had a major influence on the selection of frequencies used for earth-space communication, and even with the upward drift in transmission frequencies, scintillation is still a factor. We shall soon see that for earth-space paths the estimated maxima given in Table 4-7 are directly related to the values of the Total Electron Content (TEC) of the ionosphere. As a result, measurements and predictions of the TEC take on a special significance for many applications.

4.4.1 Integrated Propagation Effects

Ionospheric effects encountered by systems operating in the frequency bands above HF are generally associated with earth-space propagation. A treatment of these effects appears in an excellent, but dated,

pair of documents by Lawrence et al. [1964] and by Flock [1987]. Goodman [1980] treats the subject with an emphasis on applications. The reader should consult ITU-R documents for more current information [ITU-R, 1996]. It must be remembered that all of the significant radiowave parameters such as signal amplitude, wave polarization, and wave phase vary as the radiowave traverses the ionospheric medium, and the exiting wave retains a "memory" of the integrated variations. Many of the system impairments, with the exception of scattering and scintillation effects that depend upon detailed distributions, are directly related to the integrated electron density, often referred to as the electron content (EC) that is encountered by the radiowave. This is the integral of the electron density from an earth terminal to the satellite platform or target. In general, this is a slant value of the electron content, unless the path is along an earth radial. In practice, analysts measure the Slant Electron Content (i.e., EC), and then compute the Total Electron Content (i.e., TEC), which references the measured EC to the vertical. Table 4-8 exhibits the relationship between the EC and the effects of interest, viz., Faraday rotation, group-path-delay, phase advance, ionospheric Doppler, and signal dispersion. Estimated maxima for effects is provided in Table 4-7.

4.4.1.1 Refraction

Ionospheric refraction and group path delay errors are especially important for radar ranging and surveillance problems. The last row in Table 4-8 indicates the amount of wedge refraction that is introduced as a radiowave penetrates the troposphere and then traverses the ionosphere. Figure 4-8 gives the geometry.

Table 4-8: Effects Related to the Electron Content

EFFECT	Comment	UNITS	FORMULAE
Faraday Rotation	See Table 4-5; Section 4.3.1.4	Rad	$2.97\,(10^{-2})\,f^{-2}\,H_L\,(EC)$
Group Path Delay	See Table 4-5; Section 4.3.1.2	Sec	$\sim 1.34\,(10^{-7})\,f^{-2}\,(EC)$
Phase Path length	See Section 4.3.1.2	Meters	$-40.5\,f^{-2}\,(EC)$
Group Path Length	See Section 4.3.1.2	Meters	$\sim 40.5\,f^{-2}\,(EC)$
Phase Change	See Section 4.3.1.2	Rad	$-8.44\,(10^{-7})\,f^{-1}\,(EC)$
Doppler Shift		Hertz	$-1.34\,(10^{-7})\,f^{-1}\,d/dt\,(EC)$
Time Dispersion	See Table 4-5	Sec/Hz	$-2.68\,(10^{-7})\,f^{-3}\,(EC)$
Phase Dispersion		Rad/Hz	$-8.44\,(10^{-7})\,f^{-2}\,(EC)$
Wedge Refraction	See Table 4-5; Section 4.3.1.1	Rad	$40.5\,f^{-2}\,d/dx\,(EC)$

Note: The units of EC are electrons/m^2, and H_L is that component of the geomagnetic field that lies along the ray path. The units are MKS (i.e., ampere-turns/meter). The Total Electron Content (TEC) is related to the EC by a secant factor. We have EC = TEC sec φ where φ is the ray zenith angle based upon a mean ionospheric height of ~ 400 km.

The amount of "wedge" refraction due to the ionosphere is given by:

$$\tau = 40.5 f^{-2} \, d/dx \, (\int N \, ds) \qquad (4.1)$$

where $\int Nds$ is the integrated electron density along the ray path (or the slant electron content, EC), and "d/dx" implies a transverse gradient. The refraction τ is in radians, and MKS units are used throughout.

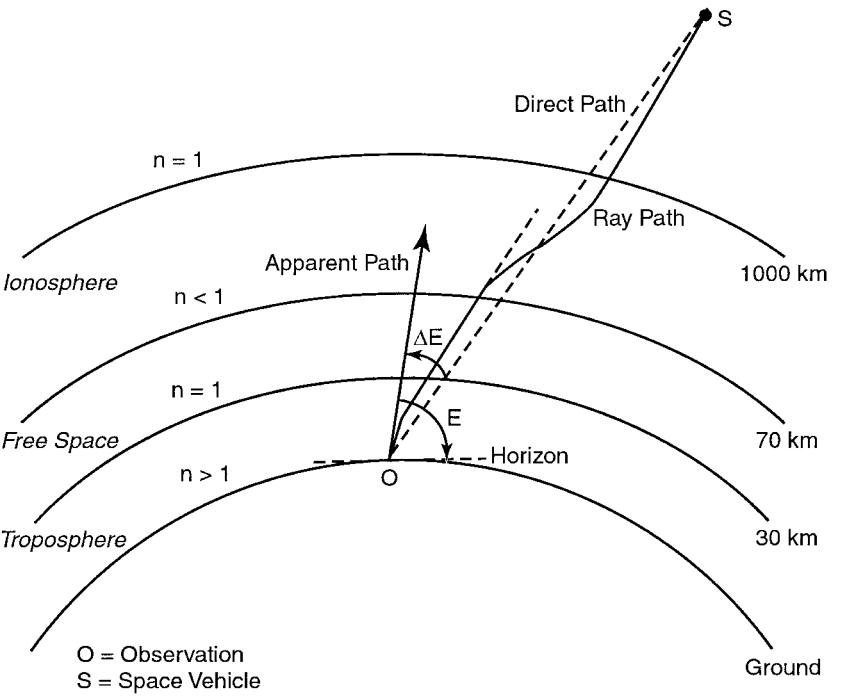


Figure 4-8: Radiowave trajectory through the troposphere and ionosphere. Note that the refractive index n < 1 in the ionosphere, n = 1 in free space, and n > 1 in the troposphere. The apparent elevation angle is higher than the actual (straight line) elevation to the space vehicle After Millman [1967].

Assuming a rather sharp 10% gradient over 10 km and a frequency of 100 MHz, we arrive at a value for τ of 4 x 10^{-3} radian (i.e., 4 milliradians or ~ 1/20 degree). At 1 GHz, the frequency dependence drives the wedge refraction level to a negligible number ~ 40 microradians. Figure 4.9 shows the total refraction error at 100 and 200 MHz as a function of altitude.

Elevation angles of 0, 5 and 20 degrees are exhibited. It is seen that at 100 MHz, the difference between the total daytime refraction (i.e., including the ionosphere and troposphere) and the daytime tropospheric refraction is ~ 6 milliradians for an elevation angle of 0 degrees.

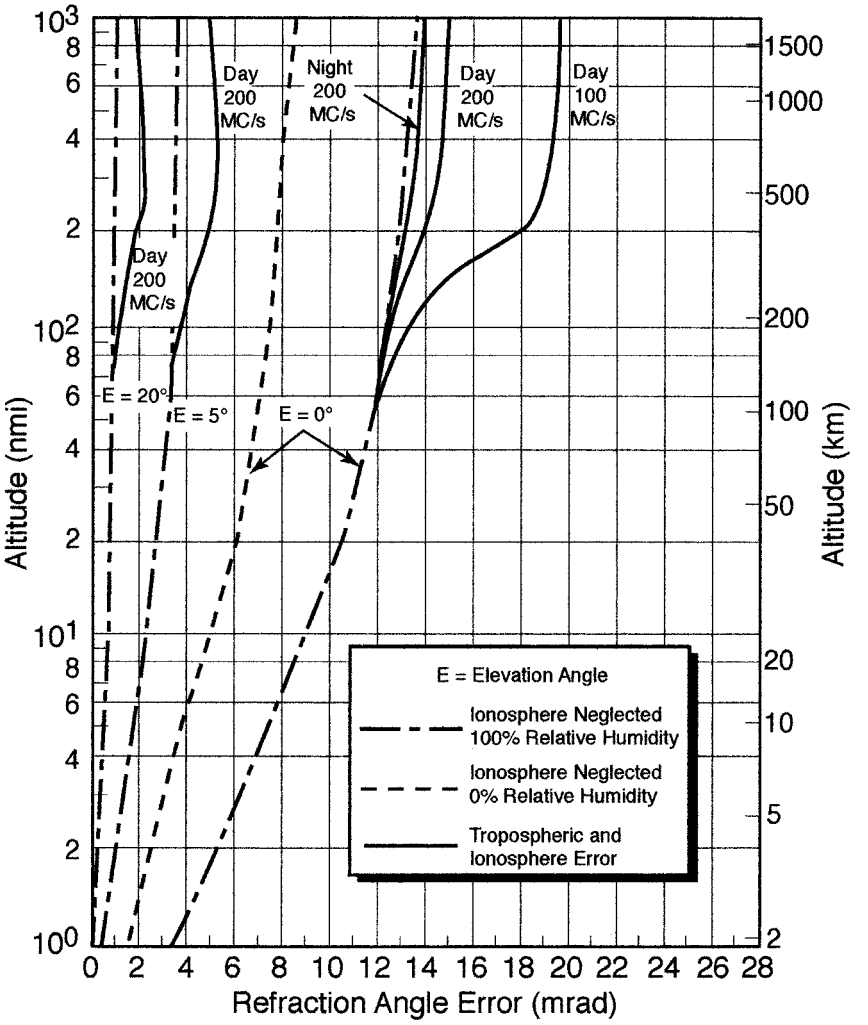


Figure 4-9: Total refraction error at 100 and 200 MHz as a function of altitude with elevation angle as parameter. The refractive error increases dramatically as the elevation angle moves toward the horizon, and as the frequency is reduced. (Note Mc/s = MHz.) Original illustration courtesy of George Millman [1967].

4.4.1.2 Phase Path and Group Path Variation

The change in the phase path, ΔL, at VHF and above, is given by the integrated difference between the refractive index in the ionosphere and unity:

$$\Delta S \text{ (meters)} = \int (n-1)ds = -40.5 f^{-2} EC \qquad (4.2)$$

The negative sign indicates that the impact of the ionosphere is to reduce the phase path length relative to free space.

The group path length $\Delta S_g \sim -\Delta S$ at VHF and above. To obtain the time delay ΔT_g, we simply divide by the speed of radio propagation (i.e., c = 3 x 10^8 m/sec) to obtain:

$$\Delta T_g \text{ (seconds)} = \Delta S_g/c = \sim 1.34 (10^{-7}) f^{-2} (EC) \qquad (4.3)$$

The ionospheric time delay is an important parameter in connection with satellite navigation. Figure 4-10 illustrates how ΔT_g varies with radio frequency, using the electron content as parameter. Note that the TEC may range between ~ 10^{16} and 10^{18} electrons/m^2. The EC may be ~ 3 times larger for highly oblique paths. Taking the EC to be 3 x 10^{18}, and f = 1.6 GHz, we find ΔT_g = 157 nanoseconds.

To obtain the phase change, we recognize that it is simply the phase path length ΔS times $2\pi/\lambda$ where λ is the wavelength. This leads to the result:

$$\Delta\varphi \text{(radians)} = -8.44 (10^{-7}) f^{-1} (EC) \qquad (4.4)$$

The range error associated with the ionospheric path is obtained by integrating $(n_g - 1)$ along the refracted path, where n_g is the group refractive index. This is just the change in group path length, and it is a positive number. At 100 MHz and above, $n_g \approx 1/n$, where n is the real part of the index of refraction. Figure 4-11 gives the representative limiting values for range error (i.e., troposphere + ionosphere) at 100 and 200 MHz. In Figure 4-12 there is a display of the diurnal variation of elevation error and range error is given at 400 MHz for a typical midlatitude profile of electron density. To go from one frequency to another, recall that the scaling factor will be f^{-2}.

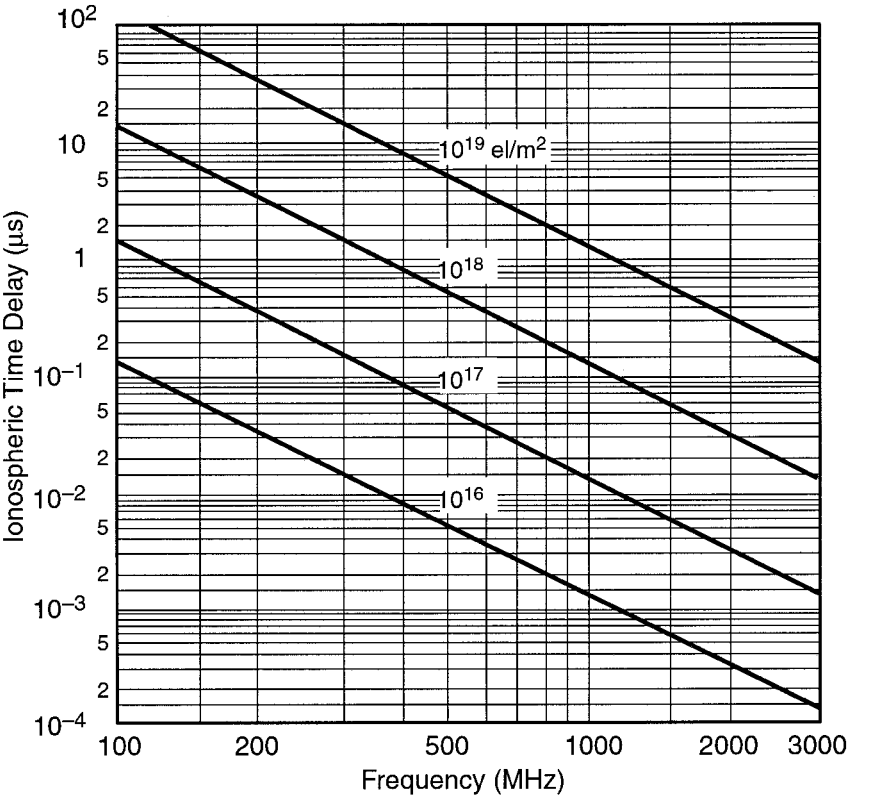


Figure 4-10: Ionospheric time delay as a function of radio frequency with electron content as parameter. From ITU-R [1996].

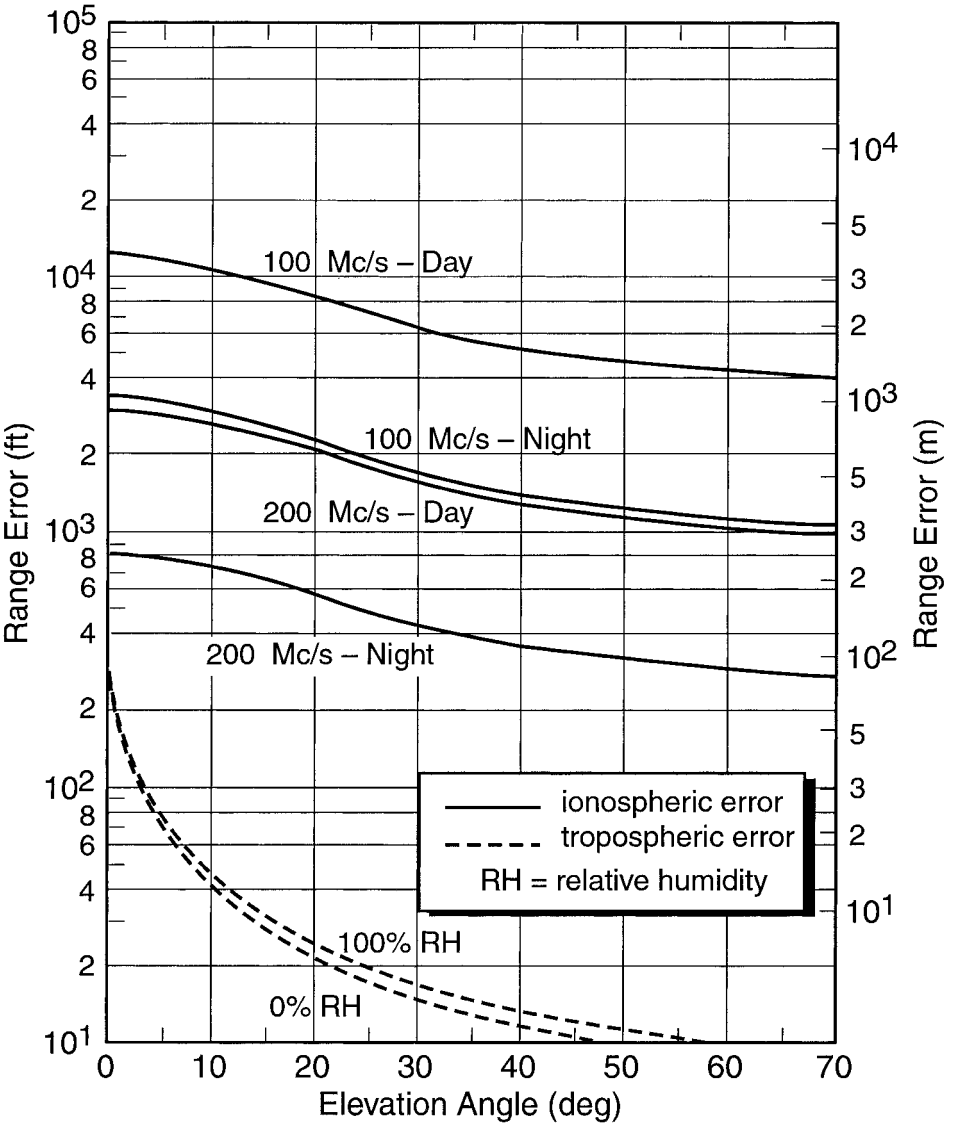


Figure 4-11: Limiting values for ionospheric and tropospheric range errors From Millman [1967].

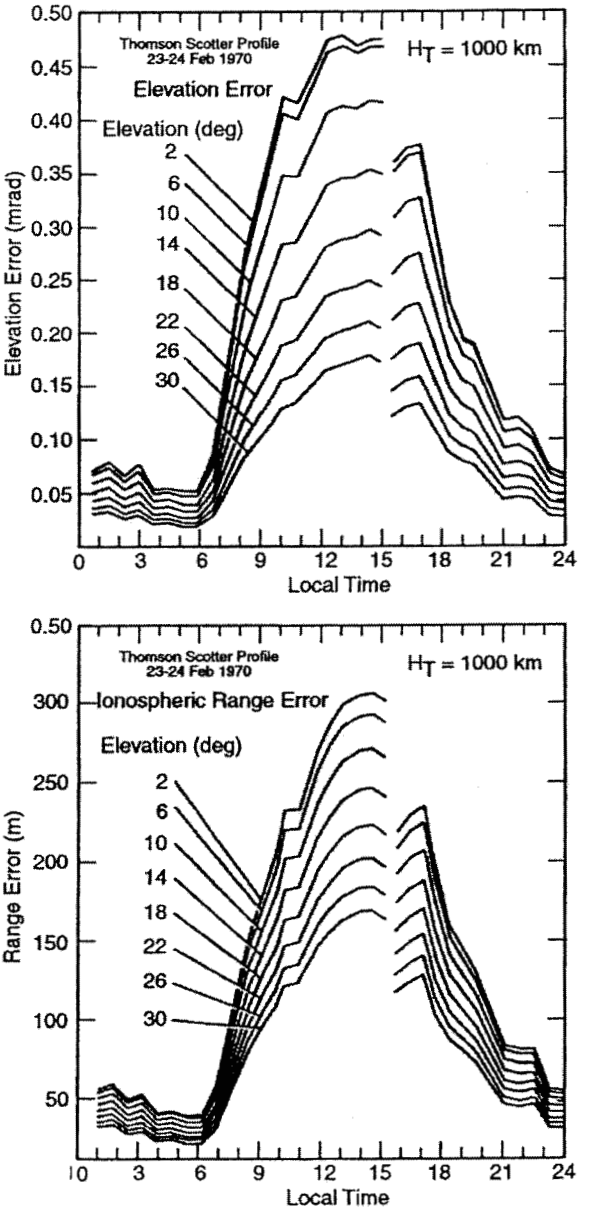


Figure 4-12: Ionospheric refraction and range errors through a real ionosphere. The profile was derived using the Millstone Hill incoherent (Thomson) scatter radar. The 400 MHz elevation error is given in the top curve, and the range error is given in the bottom curve. From Evans and Wand [1975].

4.4.1.3 Ionospheric Doppler Shift

Ionospheric Doppler is given by the time rate of change of the ionospheric phase change times the quantity ($1/2\pi$). In other words, simply divide Equation 4.4 by 2π. We then have the following:

$$\Delta f = -1.34\,(10^{-7})\,f^{-1}\,d/dt\,(EC) \tag{4.6}$$

This effect is not very significant if the transmission frequency is sufficiently high. For example, for a rapidly moving satellite, *d/dt (EC)* would be ~ order of the *EC* divided by ~ several minutes. We assume $d/dt\,(EC) \approx \Delta(EC)/\Delta t$, where $\Delta(EC)$ and Δt are finite values. Taking $\Delta(EC) \sim 10^{17}$ electrons/m^2 and $\Delta t \sim 60$ seconds, the ionospheric Doppler shift at 1.6 GHz is about 0.1 Hz. At 160 MHz, it is ~ 1 Hz, and at 16 MHz, it is ~ 10 Hz under the stated conditions. Figure 4-13 shows the free space and ionospheric Doppler for a satellite transmitting at 20 MHz.

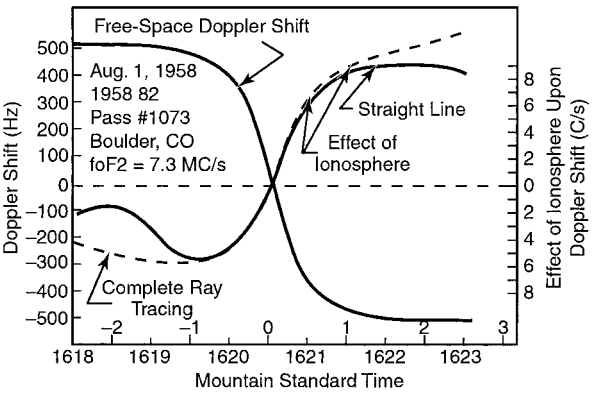


Figure 4-13: Computed Doppler, including the ionospheric component, for a rapidly moving LEO satellite. The transmission frequency is 20 MHz. From Lawrence et al., [1964].

4.4.1.4 Faraday Rotation

Linearly polarized radiowaves may be considered as equivalent to the superposition two equal amplitude circularly polarized waves, but of opposite sense. Faraday rotation occurs in the ionosphere as a result of the fact that two modes (i.e., ordinary and extraordinary waves) propagate in the magneto-ionic medium (i.e., the ionosphere) at different phase velocities. The phase difference between the two modes is proportional to the product of the

magnetic field strength and the *EC*, and inversely proportional to the square of the radio frequency. At any position along the ray trajectory one may compute the resultant orientation of the electric vector of the resultant linearly polarized wave. The amount of (one-way) Faraday rotation throughout the ionosphere is given by the approximate formula:

$$\Omega = 2.97\,(10^{-2})\,f^{-2}\,H_L\,(\int N\,ds) \tag{4.7}$$

where Ω is in radians, H_L is the magnetic field component in ampere-turns per meter, and $\int N\,ds$ is the slant electron content *(EC)* in electrons/m^2. The magnetic field component is given by $H_L = H\cos\theta$, where θ is the angle between the ray path and the magnetic field vector. In its most general form Equation 4-7 retains the parameter H_L under the integral sign since it is not a constant but varies slowly along the path of integration. However we may invoke the mean value theorem to bring out a representative value of H_L; in this way we can conveniently isolate the electron content. The ionospheric "mean" is given by $\langle h\rangle = \int hN\,dh / \int N\,dh$. It is also convenient to replace *ds* by *dh sec* χ where *dh* is a height increment and χ is the ray zenith angle. Using the mean value theorem, we extract the value of the so-called magnetic field parameter $H\cos\theta\sec\chi = \Psi$ evaluated at the mean height $\langle h\rangle$. A typical value for $\Psi = \sim 50$ ampere turns/meter for a mean altitude of $\langle h\rangle$ = 400 km. Taking the *EC* to be 3 x 10^{18}, this implies Ω = 1.75 radians at 1.6 GHz. This can be serious if linearly polarized antennas are employed. At lower frequencies, the amount of Faraday rotation may be enormous, and may translate to periodic fading. The rate of fading will depend upon the motion of the satellite (or target) and/or the diurnal variation of the *EC*. Figure 4-14 illustrates Faraday rotation as a function of frequency with *EC* as parameter.

Manual methods for computing the amount of Faraday rotation for arbitrary path appear in an NRL report [Goodman, 1965]. It should be recognized that for a radar situation, the amount of Faraday rotation is doubled. For the radar situation, the amount of Faraday rotation becomes:

$$\Omega = 5.95\,(10^{-2})\,f^{-2}\,\Psi\,\int N\,ds \tag{4.8}$$

where the rotation angle Ω is given in radians and, as before, MKS units are employed.

The parameter Ψ may be computed for various ground stations and values for the ionospheric height. Figure 4-15 shows the elevation and azimuthal dependence of Ψ for a site near Washington DC.

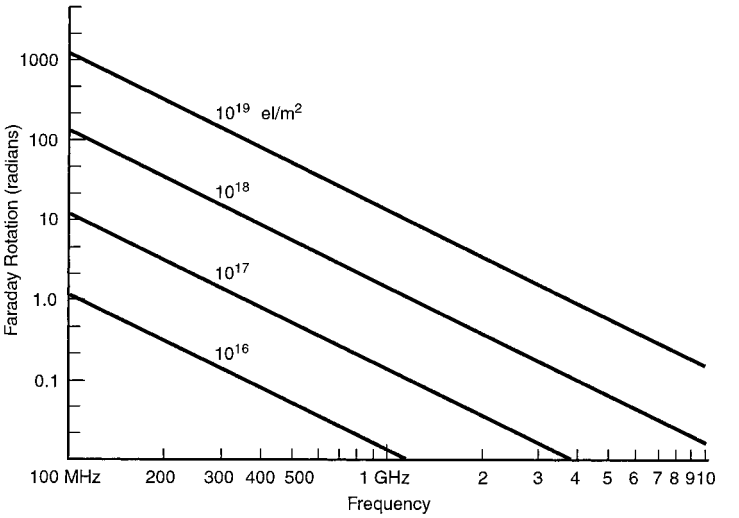


Figure 4-14: Faraday rotation angle as a function of frequency with the electron content as a parameter. Remember this is the "slant" electron content and not the Total Electron Content (TEC), which is defined along the vertical. From ITU-R [1996].

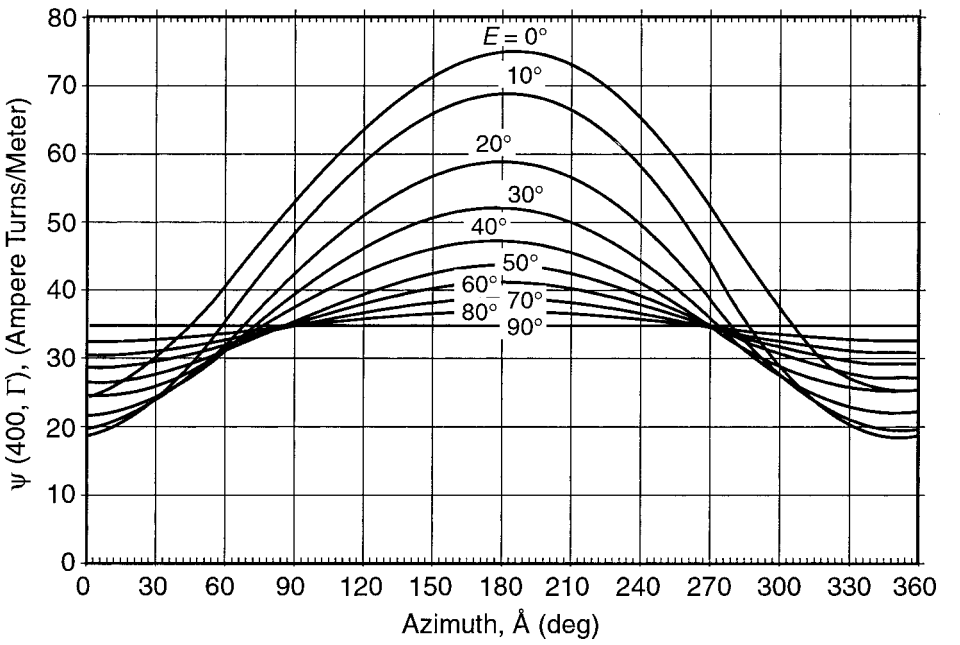


Figure 4-15: The $\Psi = H \cos\theta \sec\chi$ values for an ionospheric height of 400 km and a site near Washington, D.C. For the Northern Hemisphere, it is seen that Faraday rotation peaks toward the south and reaches a minimum toward the north (from Goodman [1965]).

For system design purposes where only order of magnitude values are needed, the following expression suffices for estimation of the amount of Faraday for a superionospheric radar target, an arbitrary radar path, and midlatitude location:

$$\Omega(radians) \sim Order\ of:\ \{10^4\ (foF2/f)^2\ ;\ f >> foF2 \qquad (4.9)$$

This is only a representative number, not a maximum value. In Equation 4.9, we have assumed that the effective slab thickness of the ionosphere is 360 km, and Ψ = 40 ampere turns/meter. (Note that the TEC is given by the product of the F2 maximum electron density and the effective slab thickness.). Thus, if the value of *foF2*, obtained from a sounder, is 10 MHz, and the transmission frequency is 100 MHz, the value of $\Omega \sim 100$ radians. If the value of f = 1000 MHz, then $\Omega \sim 1$ radian. Since this is for a two-way radar path, the one-way radio path would be ½ of these values.

4.4.1.5 Time Dispersion

Since the ionosphere is a dispersive medium, separated frequencies travel with different velocities. When a pulse is represented in the frequency domain, we find that the spectral width is inversely proportional to pulse length. As a result, short pulses suffer a larger relative distortion following ionospheric transit than longer pulses. Millman and Olsen [1980] have examined ionospheric dispersion effects in wideband transmissions. Figure 4-17 shows the pulse distortion impact (i.e., group time delay difference) as a function of frequency with pulse width as parameter. We see for a 100 MHz channel, and a pulse width of 1 μsec, that the time delay difference is ~ 0.1 μsec. This is a 10% distortion effect. Of course the situation will get worse if the pulse length is reduced. On the other hand, at 900 MHz, the time delay difference is only 0.0002 μsec.

4.4.1.6 Absorption

Absorption will arise as a radiowave interacts with electrons in the D and lower E-region of the ionosphere where the collision frequency is relatively large. The electron collisions have the effect of robbing energy from the radiowave and converting it to heat in the interaction region. It may be shown that the absorption in dB can be related to the product of the electron density N and the collision rate ν. The formula for absorption follows:

$$A\ (dB) = 1.16\ (10^{-6})\ f^{-2} \int N\ \nu\ ds \qquad (4.10)$$

Figure 4-17 shows the variation of electron density and electron collision rate as a function of altitude. During solar flares and PCA events, there is an enhancement in the value of N in the D region. As indicated in Section 4.3.5, absorption can be a significant problem at lower frequencies like HF. Indeed, absorption is the primary control for the lowest propagation band supported by the ionosphere, and an x-ray flare can cause complete disruption of communication for the duration of the flare. In the polar cap region, energetic particle events (i.e., solar cosmic rays or protons) can cause absorption of 100 dB or more. On the other hand, since D-region absorption is inversely proportional to the radio frequency squared, most satellite frequencies (i.e., $f >$ 250 MHz) are operationally unaffected even during PCA events.

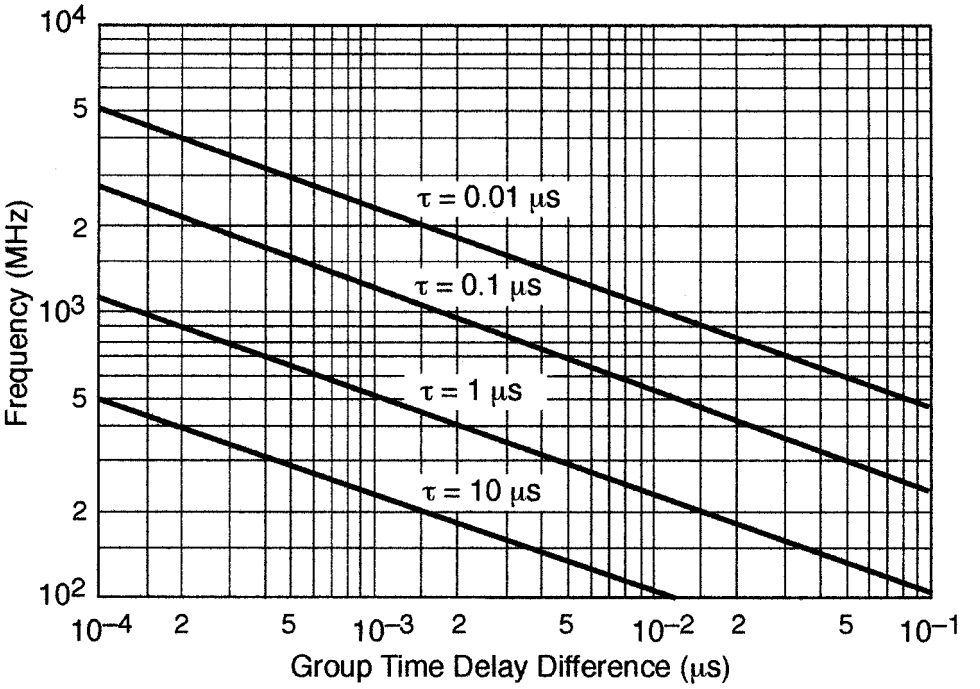


Figure 4-16: Time delay dispersion. The group time delay difference is a measure of the pulse distortion. (From ITU-R, 1996]).

4.4.1.7 Comments on Total Electron Content

Clearly, the TEC is a significant parameter in the assessment of system effects, and considerable effort has been directed toward the modeling

of TEC over the years. In general, the product of two factors controls the TEC: the so-called slab thickness and the peak electron density. Although there are differences, we find that the climatological behavior of TEC is quite consistent with that of the F-region parameter *foF2*, which has been determined from vertical incidence sounders. In systems work, it is important to recognize that the TEC referred to in reported models is the TEC throughout the full ionosphere for an equivalent zenithal path. In Table 4-8 the electron content (i.e., EC) is reckoned along the ray trajectory, which may be oblique and may even terminate within the ionosphere for low orbit satellites. Provided the full ionosphere is involved in both forms of the electron content, we may transform the modeled (overhead) value to the oblique value through multiplication of the former by the secant of the earth curvature-corrected ray zenith angle at the ionospheric mean height.

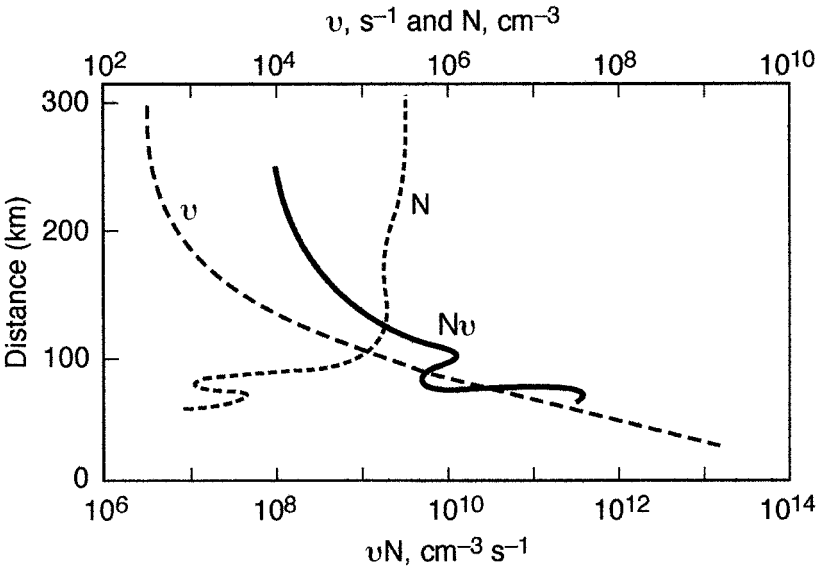


Figure 4-17: Electron density and electron collision frequency versus altitude. From Goodman [1991].

In view of the importance of the TEC in the analysis of earth-space propagation effects from VHF through the lower part of the SHF band, a considerable amount of research has been directed toward the development of models for the TEC. From such models, predictions of system effects such as excess group path delay, Faraday rotation, dispersive Doppler, and ionospheric wedge refraction can be made. Two modeling approaches have been generally used, the first based upon integration of selected worldwide electron density profile models, and the second based upon a direct analysis of the TEC data alone. The most successful model in the former category is due

to Bent et al. [1975], while Klobuchar et al. [1970; 1977] have developed the most useful models in the latter category. Without going into details about the various available global models, one finds that they generally deliver relative accuracies of the order of 75-80% during the daytime and 65-70% at night. Models perform best at midlatitudes, where most of the contributing data have been obtained. The state-of-the-art global representation of TEC is due to Klobuchar [1975], and a simple version tailored for single-frequency GPS users provides for a 50% reduction in the error introduced by the ionosphere. Greater accuracies may be obtained through use of region-specific modeling approaches and real-time update approaches. For example, new data has been obtained at high latitudes [Klobuchar, 1987] and also at the equator [Anderson and Klobuchar, 1983]. Significant increases in the TEC, which are not predicted by the quiet-day TEC models, have been observed for ray trajectories penetrating the polar cap and, although understood theoretically, are not properly accounted for in existing operational algorithms. A low-latitude TEC model has been developed by Anderson et al. [1985], providing a better representation of the so-called equatorial anomaly region.

Models of TEC for use in estimation of effects such as Faraday rotation or group path delay are critically dependent upon the selection of the underlying sub-model of the ionospheric distribution and how well it describes reality. Considerable activity in the general area of global model improvement has occurred in recent years, and we anticipate a significant improvement in the capability to predict propagation factors that depend upon TEC in the future. Simple models such as the Bent model may be replaced by hybrid versions of more complete models such as the IRI [Rawer, 1981] [Bilitza, 2001], or may be improved by use of update-capable empirical models such as ICED [Tascione, 1988]. Rush et al. [1984] has improved the global model from which the electron concentrations and *foF2* may be obtained.

Figure 4-18 gives the diurnal and seasonal variation in TEC for a mid-latitude site. This curve is only representative, but it clearly demonstrates the large day-to-night differences. Although models that attempt to replicate these data trends are more inexact at night (on a percentage basis), the impact of the inaccuracy may not be very profound in practice. This is because system effects depend upon absolute values of TEC and its changes. So far we have been talking mainly about the smoothed ionospheric properties, thereby ignoring structured plasma effects such as those associated with traveling ionospheric disturbances (or TIDs) and other irregularities in TEC which may give rise to focusing and defocusing of radiowaves. On a smaller scale, other effects become important, such as scintillation. Separate methods are appropriate for this class of irregularities, and this will be the logical point of departure for our next section.

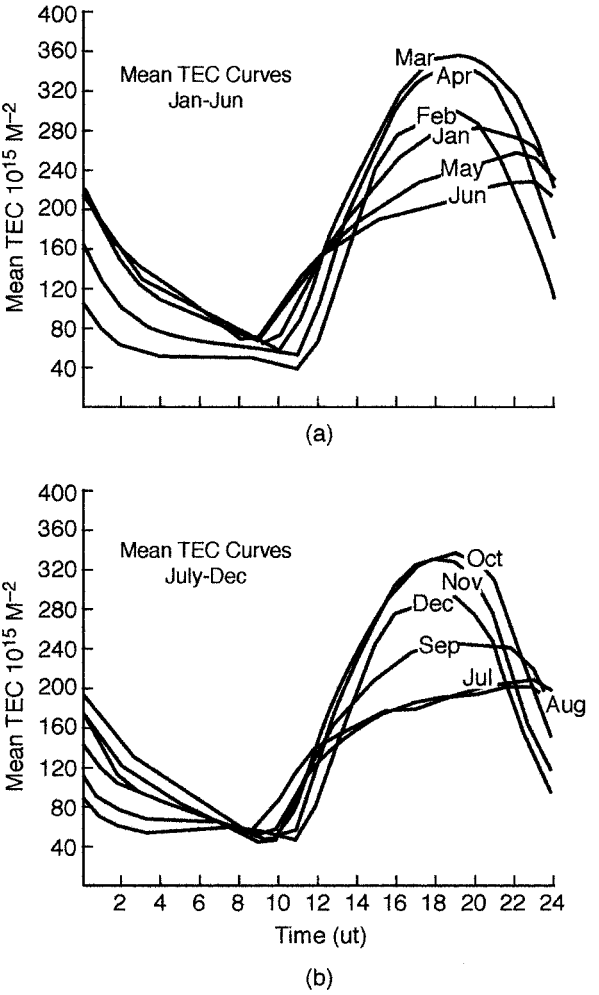


Figure 4-18: Representative midlatitude diurnal and seasonal variation of the Total Electron Content (TEC). (a) Monthly means for January-June; (b) Monthly means for July-December

4.4.2 Differential Effects and N_e Distribution

Fluctuations in signal power and phase often accompany radio wave propagation over earth-space paths as a result of inhomogeneities in the ionospheric electron density. In the case of the ionosphere, the fluctuations are due to irregularities in electron density predominantly at F region heights, from 200-600 km. This phenomenon, analogous to the twinkling of stars in

the visible part of the electromagnetic spectrum, has been the object of research for roughly half a century, and is referred to as scintillation in the context of radio propagation. It is difficult to do justice to this interesting phenomenon in the space available. Fortunately, there is a plethora of papers dealing with scintillation, and some important ones are cited herein. In any case, scintillation is probably the single most important deleterious factor affecting future systems utilizing the earth-space propagation path in the GHz frequency region. Recall our mention in Chapter 1 regarding the failure of TACSAT at UHF to fulfill its mission due to scintillation effects. In fact, even at 4 GHz the worst-case scenarios exhibit peak-to-peak fading greater than 9 dB over periods of ½ hour or longer in the equatorial anomaly region. The virulence of equatorial scintillation has been examined by Basu and Basu [1981]. A general discussion of the scintillation phenomenon may be found in previously cited handbooks [Jursa, 1985; Flock, 1987], and reviews of the subject have been prepared by Aarons [1982] and Liu and Franke [1986]. The overall morphology is now fairly well established, although details remain to be clarified. Basu et al. [1985, 1988] have summarized the equatorial and high-latitude data in statistical form for both solar maximum and minimum conditions. The areas of main importance of this effect are given in Fig. 4-19.

4.4.2.1 Diurnal Variation of Scintillation

Scintillation varies diurnally, and it is principally a nighttime phenomenon. It exhibits a climatology that is unique to four geographical regions: equatorial, midlatitude, auroral, and the polar cap. The most virulent zone corresponds to the post-sunset equatorial region, and the least active zone is at middle latitudes. Scintillation at equatorial latitudes peaks shortly following sunset and may persist throughout the evening but with decreasing virulence after local midnight. At high latitudes, scintillation is also more intense during the night in concert with the natural growth in oval intensity, but midlatitude scintillation may arise during storms as the scintillation boundary descends equatorward. Moreover, the normal diurnal variation of scintillation may become distorted by the superposition of storm-time influences.

Daytime scintillation events may also arise at midlatitudes as a result of sporadic E, and these events are sometimes termed "ringing irregularities" as a result of the quasi-periodic nature of the fading events [Goodman, 1967]. Figure 4-20 illustrates daytime scintillation occurrence at VHF (i.e., the geosynchronous Early Bird satellite downlink) compared to sporadic E (i.e., Es) and spread-F. Figure 4-21 is an example of the quasi-periodic disturbances caused by the interference of direct rays and refracted rays from the sharp edges of sporadic E patches.

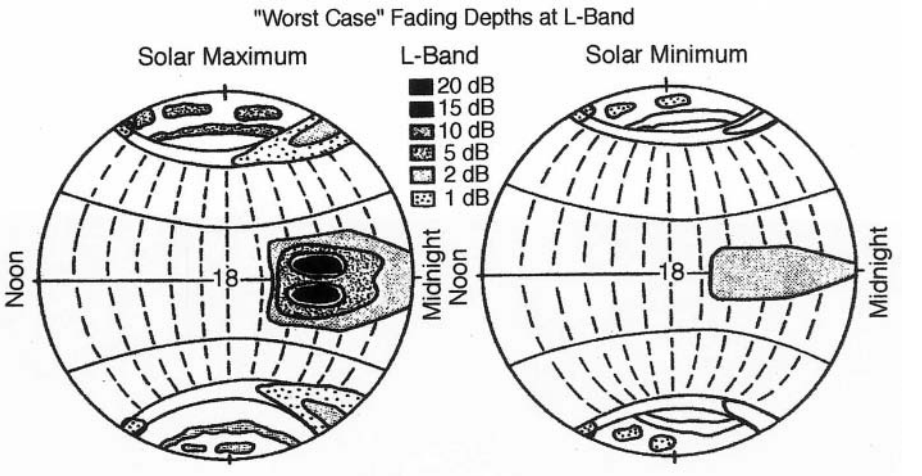


Figure 4-19: Representation of ionospheric scintillation for solar maximum and minimum at L-band. From Goodman and Aarons [1990], courtesy of Santimay Basu.

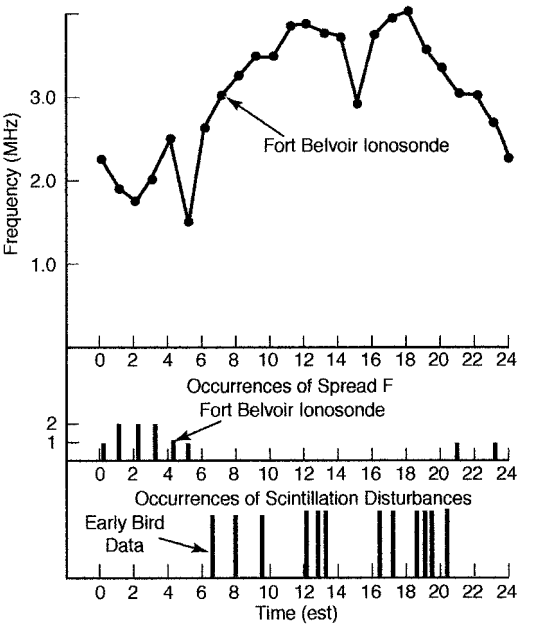
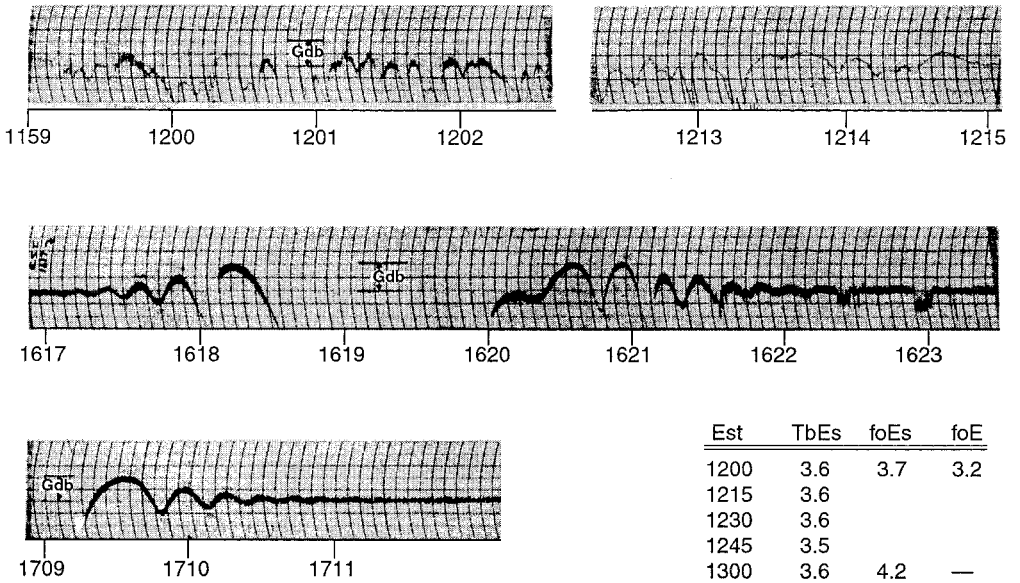


Figure 4-20: VHF scintillation occurrences near Chesapeake Beach Maryland and compared to the 8-day averaged *foEs* and instances of spread-F measured at Fort Belvoir, Virginia. The experiment ran from May 21- May 28, 1965. While this evidence is circumstantial, Figure 4-21 shows the correlation between scintillation and Es more clearly. From Goodman, [1967].



Est	TbEs	foEs	foE
1200	3.6	3.7	3.2
1215	3.6		
1230	3.6		
1245	3.5		
1300	3.6	4.2	—
1600	3.5	3.7	3.0
1615	3.7		
1630	5.4		
1645	7.0		
1700	7.0	7.0	2.6
1715	8.4		
1730	8.7		
1745	8.7		
1800	5.0	6.8	—

Figure 4-21: Depiction of noisy and quasi-periodic scintillation thought to be the result of sporadic E edge refraction. It is noteworthy that the sporadic E "blanketing" frequency *fbEs* reached high levels during the period of time the disturbances were observed. The distance between the Ft. Belvoir ionosonde and the relevant ionospheric piercing point for the radio path was ~ 300 km (with the *Es* height taken to be 100 km). Hence we would not expect perfect correlation. From Goodman [1967].

4.4.2.2 Global Morphology of Scintillation

Region-specific examinations of the scintillation effect have been published for both high-latitude [Basu et al., 1985] [Weber et al., 1985] [Aarons et al., 1988] [Basu et al., 1988b], and equatorial latitude zones [Basu and Basu, 1981] [Mullen et al., 1985]. Figure 4-22 indicates the nature of scintillation at UHF and L-Band for equatorial regions [Basu, 2003].

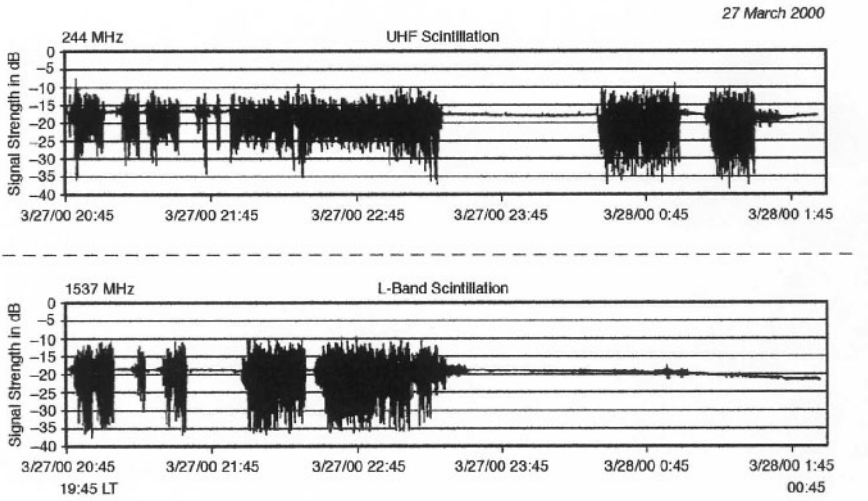


Figure 4-22: Characteristics of scintillation as observed at Ascension Island in March 2000. The scintillation is "saturated" for both bands for the first half of the record. The L-Band scintillation virtually disappears for the last part of the record. We note that the scintillation is patchy in nature. [Sa. Basu, 2003]

The nature of the ionospheric structures, which give rise to radiowave scintillation, has been the subject of numerous theoretical studies and experimental campaigns. Other aspects important are dependencies on solar and magnetic activity. The regionally-averaged scintillation activity increases over the equatorial region as the sunspot number increases. This is particularly true for the equatorial anomaly region, that area approximately 20 degrees from the magnetic equator, where the most intense GHz scintillation is noted. For the high-latitude regions, the same is true. Even when the magnetic conditions are held constant, scintillation activity is observed to be higher during years of enhanced solar flux [Aarons et al., 1980]. Although sunspot number and magnetic activity are not perfectly correlated, we still find that the number and intensity of magnetic storms increases with an increase in solar activity. This general observation may be specialized somewhat for specific instances of scintillation that arise within the auroral zone and polar cap regions. We find that scintillation intensity is directly related to magnetic index within the auroral region [Rino and Matthews, 1980] whereas, within the polar cap, irregularity intensity (which is proportional to scintillation) is more closely related to solar flux. It is interesting to note that within the polar cap the irregularity intensity is vanishingly small during years of low solar flux [Buchau et al., 1985].

The most interesting aspects of the current drive to understand the problem have been attacked from the view point of three differing observational effects of irregularities: (i) radar backscatter of small-scale structures (meters), (ii) scintillation caused by ionospheric inhomogeneities of intermediate scale (hundreds of meters), and (iii) detection of large-scale electron content variations (blobs, bubbles, plumes and patches, of the order of many kilometers). Much of the current scientific activity is focused on the scintillation cause-and-effect relationships, both in the auroral zone and the equatorial region. The auroral physics is more complex but the equatorial region is of continuing interest since the scintillation effects are more intense. Clearly, the instabilities that give rise to plume development are of major concern in understanding the scintillation problem. The scintillation that occurs at both equatorial and high latitudes is thought to arise from one of several related interchange instabilities (i.e., Rayleigh-Taylor, gradient drift, *ExB*, current convective, and flux-tube interchange) plus structured low energy electron precipitation and shear mechanisms. These are described lucidly by Tsunoda [1988].

Plumes are very large-scale depletions in ionization, frequently of the order of several hundred kilometers and extending from 250 km to 800 km in altitude. These are major sources of scintillation near the equatorial anomaly. Are large scale diminutions responsible for similar scintillation events at high latitudes? Probably not. In fact, large-scale increases in electron density (i.e., blobs and patches) are thought to be the cause of auroral zone scintillation. Also, in this region a high correlation exists between intense irregularity levels and the variations of the earth's magnetic field, as represented by the planetary magnetic activity index *Kp*. When magnetic storms occur, the irregularities in the auroral region spread in latitude and become more intense [Rino and Matthews, 1980]. A considerable advance in the total understanding of ionospheric scintillation phenomenology as well as the underlying physical processes involved has been achieved through utilization of data sets obtained via the WIDEBAND DNA-002 program [Fremouw et al., 1978] [Fremouw et al., 1985a] as well as the HiLat Satellite [Fremouw et al., 1985b] [Fremouw, 1985]. Fig. 4-23 is a model of high-latitude scintillation proposed by Aarons [1982].

The modest scintillation observed at midlatitudes is now thought to be a combination of the extension of the auroral effects of magnetic storms and substorms plus the after effect of the decay of ions in the earth's ring current, which produce both Stable Auroral Red Arcs after a magnetic storm and irregularities at sub-auroral latitudes. Nevertheless, it has been shown that sporadic E patches can give rise to some isolated scintillation events, while they are unlikely to be observed at UHF and above.

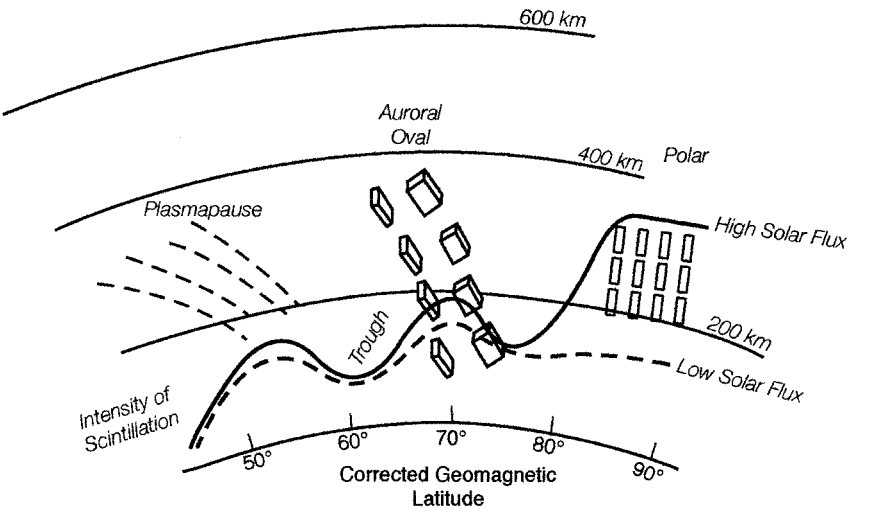


Figure 4-23: Model of high latitude irregularity structures. From Aarons [1982].

4.4.2.3 Modeling of the Scintillation Channel

A considerable amount of effort has been directed toward the development of algorithms to describe the effect, with the ultimate objective of communication channel modeling. The approach has been to deduce the morphology from all available scintillation data and to derive the channel properties from the hypothesis of a two-component signal statistical model [Fremouw and Lansinger, 1982]. It has been demonstrated that signal amplitude, signal phase, and the angle-of-arrival of the wave fluctuates during scintillation episodes. The generally accepted parameter for amplitude scintillation is the so-called S4 index [Whitney et al., 1969] [Fremouw et al., 1980], which is defined as the square root of the variance of received power normalized by the mean power. The probability density function for signal amplitude is well described by a Nakagami distribution, characterized by a single parameter m, which reduces to a Rayleigh distribution when scintillation is saturated (i.e., S4 ~ 1) [Aarons et al., 1988]. The phase is modeled generally as a Gaussian (normal) distribution [Fremouw et al., 1980].

The frequency dependence of moderate amplitude scintillation is consistently observed to vary as $f^{-1.5}$ over a range of frequencies between VHF and L band [Fremouw et al., 1985a] and phase scintillation varies as f^{-1}. As the scintillation intensifies, the amplitude scintillation drops off more gradually with frequency, and the parameter *S4* tends toward unity (i.e., Rayleigh fading conditions).

The power spectra of scintillation typically reflect the nature of the underlying inhomogeneity wave number spectra. For an inhomogeneity one-dimensional form power-law spectrum of the form k^{-p}, the spectra of the fluctuations (in both amplitude and phase) behaves as $F^{(1-p)}$ at the higher frequency part of the spectrum, where p is of the order of 3.5 and F is the fluctuation frequency. At the lower frequency part of the spectrum, the amplitude scintillation exhibits a peak at the so-called Fresnel frequency and is diminished below this frequency [Fremouw et al., 1980]. On the other hand, phase scintillation suffers no such filtering action and the lowest frequency terms dominate the phase effects. These are associated with the largest scale irregularities in TEC. Figure 4-24 shows typical amplitude and phase spectra at 138 MHz at Poker Flat Alaska. [Secan, 1998].

Models have been developed to describe the global scintillation behavior. The currently available model, WBMOD, provides estimates of signal statistical parameters based upon the efforts of many investigators over the years [Secan et al., 1987]. However, as of this writing there are still areas omitted in this model, including the intense polar and equatorial anomaly scintillations.

4.4.2.4 Mitigation Schemes

A considerable effort has been directed toward the elucidation of parameters that are important to the design of earth-space systems in order to counter the scintillation problem. Communications systems may counter the effects of substantial fading by using space diversity. If the paths from a single satellite are sufficiently well separated (depending upon the details of the inhomogeneity wave number spectrum), then fading in the two links is uncorrelated and a net performance gain may be achieved through use of diversity. Separations of the order of a kilometer are involved, but these useful minimum separations are certainly larger than ship dimensions and will only function most efficiently for ground installations. As a result, shipboard and airborne terminals must be designed to provide compensation through pursuit of other countermeasures. One might logically suspect that radio links sufficiently separated in frequency, polarization, or transmission time would be independent and could be effective in combating scintillation. Unfortunately, this generalization is not true, even for orthogonal polarizations. Furthermore, separations of up to 100 MHz may be required to obtain an adequate diversity improvement in the frequency domain. However, time diversity is a demonstrated procedure for overcoming scintillation at UHF for disadvantaged mobile platforms.

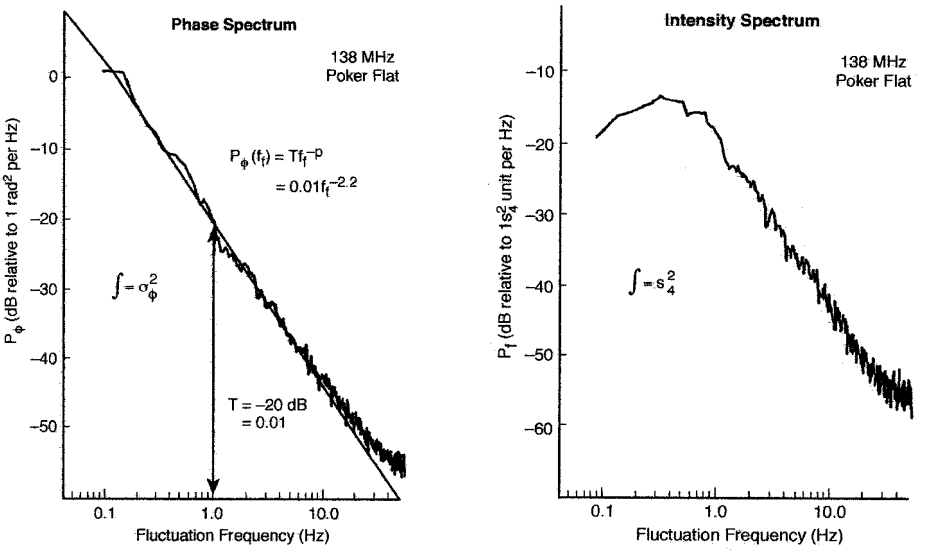


Figure 4-24: Scintillation data at 138 MHz obtained at Poker Flat, Alaska. The abscissa is fluctuation frequency (Hz) for both types of power spectra. (a) Phase spectrum. (b) Intensity spectrum. The so-called S4 index is the integral of the intensity spectrum. Most of the contribution to this integral is at the low frequency Fresnel frequency cutoff. This is a geometrical effect that is not encountered with the phase spectrum, which has no low frequency cutoff. From Secan [1998].

4.5 SPACE WEATHER SUPPORT FOR SYSTEMS

4.5.1 Military C3I Requirements

As has been inferred throughout this monograph, military requirements have dominated the development of operational systems that incorporate space weather information, either actively or passively. In Table 4-9 is a listing of telecommunication disciplines that are influenced or even controlled by the ionosphere and its variations. The ionospheric variability is, of course, a manifestation of space weather. Other military mission areas include missile warning, and the dissemination of weather information and imagery, but these may be generally incorporated within the list in Table 4-9.

Table 4-9: Requirements for Command, Control, Communications, and Intelligence (C3I)

- ❑ Global and long-haul communications (HF and Satcom)
- ❑ Tactical communication (LOS, NVIS, Satcom)
- ❑ Navigation services (legacy, GPS, Glonass)
- ❑ Search, tracking, and fire-control radar
- ❑ Signal intelligence and target geolocation

One of the more important services provided the military is navigation, and the lineage of the two-frequency Global Positioning System is traced to military experiments in the 1960s. The original U.S Navy design used L-band and UHF, with the latter being used for removal of ionospheric group-path delay. Ionospheric compensation is achieved in the current Air Force system by using dual L-band signals, a design that reduces, but does not eliminate, scintillation effects on system performance. The GPS constellation of satellites with its ground segment and the array of user systems, likely represents the most significant technological achievement in the field of telecommunications in the last several decades. Figure 4-25 depicts the GPS space segment. The GPS system is critical for a range of military requirements besides navigation. The effect that is most significant for the dual-frequency GPS system and its users is scintillation, with phase scintillation probably being the most critical since it may lead to receivers losing lock.

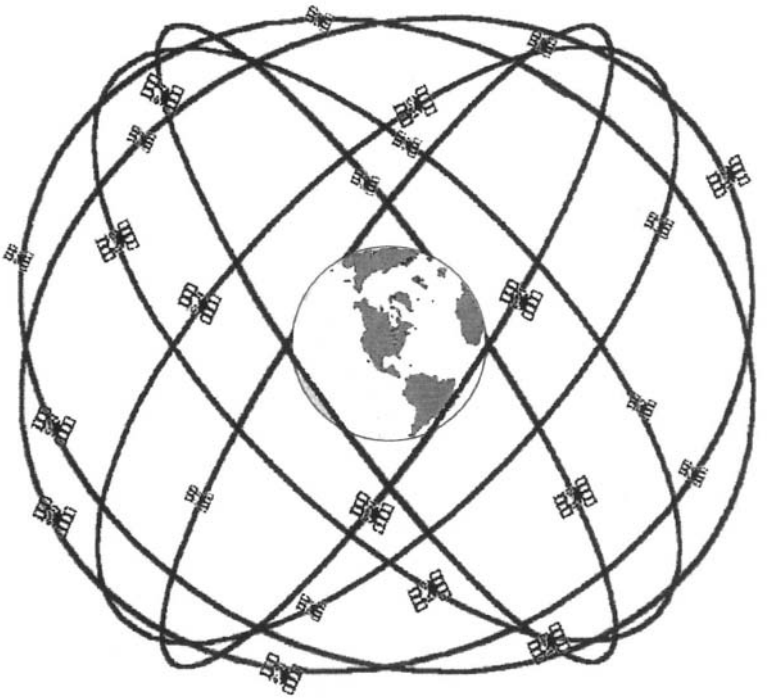


Figure 4-25: Nominal GPS Constellation. There are 24 satellites in 6 orbital planes, with 4 satellites in each plane. The space segment is located at 20,200 km altitude, and each plane is at a 55° inclination.

Space target tracking is a mission of the military, with aspects handled by the U.S. Navy and U.S. Air Force. The radar cross sections of targets may appear to vary as the result of scintillation, and ionospheric inhomogeneities may also introduce angular jitter and group-path delay variations. These effects are not always a major concern, but radar tacking through auroral clutter can be problematic.

Long-haul connectivity, using both HF assets and satellite links, is important to maintain a global communication capability. There are also tactical requirements within theater, and a variety of bands and possible platforms are used to satisfy this mission. Ionospheric effects do not seriously impact all of these possibilities, but many are at least influenced. Near-Vertical-Incidence-Skywave (NVIS) at HF is a peculiar method of connectivity used by tactical commanders to overcome limitations associated with the exploitation of Line-of-Sight (LOS) methods in rugged terrain or jungles. Ionospheric variations can have a serious impact on the utility of this mode, which is restricted to frequencies below the overhead MUF (i.e., $foF2 + \frac{1}{2} fg$, where fg is the electron gyrofrequency).

Any system that uses ionospheric bounce, such as HF radar or HF communication, is strongly influenced by the ionosphere and related space weather effects. While Over-The-Horizon-Radar, OTHR, has a rather limited role in the military at this time, there is a continuing interest in Re-locatable OTH radar by the U.S. Navy (i.e., ROTHR). The OTHR methods are used in civilian agencies of government, such as the "Drug War" and for remote sea state monitoring. Target registration is an important function in the detection and surveillance of targets, and HF ray trajectories can be significantly distorted by ionospheric profile changes. Hence, space weather factors can play havoc with the performance of HF radar systems, where the problems are generated by large MUF excursions, TIDs, PCAs, and SWFs.

To the extent that hostile forces use HF communications, the discipline of HF direction-finding (i.e., HFDF) will remain important. There are obvious ionospheric influences for these systems.

In short, the military has a requirement for surveillance as well as the conveyance of voice and data using a variety of platforms (e.g., fixed-station, space-based, air-mobile, land-mobile). Large telecommunication "pipes" are necessary to support transmission of images, and for use in data fusion and assimilation applications. Good information support is a force multiplier for military operations.

4.5.2 Systems Combating Space Weather

Outside the military arena, it is hard to find many telecommunication systems that take space weather into account as an integral component of the

system. In the commercial world, designers typically use diversity to circumvent or mitigate against various forms of impairment. This process is not always successful even for systems that use frequencies at L-band and above. The GPS constellation is a case and point. As indicated above, scintillation can persist well into the GHz frequency regime. (See Section 4.4.2).

While GPS, like many satellite radiocommunication systems, can suffer scintillation in phase and amplitude, it has been designed to eliminate the impact of group-path delay errors associated with TEC. Two-frequency receivers can eliminate the ionospheric effect since the GPS L1 and L2 channels suffer different amounts of signal delay for a fixed level of TEC (see Equation 4.3). By measuring the time delay (or phase path) difference between the two channels, one can solve for the TEC, and using this information, subtract the excess path delay due to the ionosphere. Unfortunately two-frequency GPS systems are expensive, and equipage is not widespread. However, engineers are not without imagination. For example, DGPS systems, used by the U.S. Coast Guard, among other organizations, exploit judiciously located (and fully equipped) reference stations that develop corrections for users within a certain correlation distance. The accuracy of DGPS systems is directly related to the separation between the reference station and user set. The FAA WAAS system uses a similar principle, but is far more sophisticated.

We have described a number of forecasting schemes and systems in this chapter. For the most part, the outputs (i.e., the forecasts) must be transmitted to system operators who use the data to modify system parameters or operational rules. In short, the forecasting systems are usually non-organic in nature. Non-organic strategies predominate because the alternative methods imply increased cost and complexity, but, sadly, lack of foresight is another reason. Of course, it makes no sense to invest in organic forecasting systems if the forecasts are not associated with a clear-cut mitigation strategy. In the following section, we discuss systems that are designed to counter, or at least cope, with space weather effects.

In Section 4.3.5.1.1 (HF Communication) we discussed HF automatic link establishment (ALE) systems. ALE is an HF system process that automates many labor-intensive operator manipulations. It also has the provision to use organic sounding to exploit the most appropriate propagating band from among those available. While the system is superior to conventional HF radio, it is still vulnerable to ionospheric effects. ALE systems could be designed to exploit space weather information, including real-time ionospheric data, but ALE processes do not include this option at present. To cope with ionospheric effects, ALE systems exploit diversity countermeasures without the benefit of space weather data to "steer" the

system parameters. Under moderate disturbances ALE systems can perform quite well, and operators are generally well satisfied with ALE, certainly in comparison with the performance of plain vanilla HF radios. However, under highly disturbed conditions, an ALE network can spend an inordinate amount of time reorganizing itself for optimal operation. With space weather nowcasting and forecasting information, it might be possible to improve the efficiency of link establishment and link maintenance functions. It should be noted that such a suggestion is unlikely to gain much traction, since the ALE is fairly efficient with its existing frequency management strategy, and non-organic improvements are likely to be an unwelcome expense. In any case, HF-ALE does *not* belong to the class of systems that have provisions for combating influences of space weather directly. But by virtue of its design it can perform adequately in the face of modest space weather effects.

We now discuss two other systems that exploit space weather directly. Like ALE developments mentioned above, which are deeply rooted in the aviation community, these additional systems also support commercial and military aviation. They are: (i) ARINC GLOBALink/HF (viz., an HFDL system), and (ii) the FAA-WAAS system.

4.5.2.1 GLOBALink/HF

Everyone recognizes that HF communication systems have a bad reputation, and most feel this reputation is richly deserved. The HF radio band (i.e., 3-30 MHz) is extremely vulnerable to ionospheric effects under the best of circumstances. During disturbances caused by space weather conditions, individual circuits can be annihilated or rendered virtually useless. At other times predicted coverage patterns may become distorted by magnetic storms, and sporadic E phenomena may introduce deleterious screening effects. In short, the situation can be quite unpleasant for a communicator unless steps are taken to cope with the environment. As odd as it may seem, some circuits may actually be improved with respect to climatology. The secret to making adaptive HF systems perform optimally is to track the channel conditions. Optimal system performance for a given circuit is achieved if one can successfully match the system parameters to channel conditions. This matching process is not always possible, but there are successful methods for approaching the ideal situation. One method is to employ sounding. This is usually achieved with an imbedded sounder to derive channel properties, but it can involve nonorganic sounders as well. Modern ALE systems employ an imbedded channel probe to assist in organization of an optimal transmission frequency scan list. While there is some vulnerability to imbedded sounding, it is currently the default standard. These methods have been described by Goodman [1991] and in the ALE Handbook [ITS, 1998]. In the final analysis,

the best way for HF systems to cope with space weather events is to apply two principles of design and operation: diversity and adaptivity. The GLOBALink/HF system, designed and managed by Aeronautical Radio Inc. (ARINC), employs these principles. In the context of space weather, the GLOBALink/HF system counters pathological changes in the environment by selecting frequencies that are optimal for use under current conditions, albeit temporally- and spatially-averaged. This is achieved by monitoring the environment through a Dynacast® system that delivers Active Frequency Listings (AFTs) to the network operations center in Annapolis, MD.

High Frequency Data Link (HFDL) is certified and has industry approvals based upon findings of the International Civil Aviation Organization (ICAO), the Radio Technical Commission for Aeronautics (RTCA) and the Airline Electronic Engineering Committee (AEEC). ARINC is the sole provider of HFDL service (viz., GLOBALink/HF), which was inaugurated in 1995.

The HFDL data transmission speed is governed adaptively by the prevailing radio propagation conditions. The rates are 300 – 1800 bps. These rates are relatively low but acceptable for the mission involved. There are 14 ground stations as listed in Table 4-10 to satisfy global coverage requirements, including polar coverage.

Table 4-10: Ground Network for HFDL Network

Station	Latitude	Longitude	Geomagnetic Latitude	Global Service	Polar Service
Dixon, CA, USA	38.38 N	121.76 W	+44	Yes	Yes
Molokai, HI, USA	21.18 N	157.18 W	+23	Yes	
Reykjavik, Iceland	64.08 N	21.85 W	+65	Yes	Yes
Riverhead, NY, USA	40.88 N	72.64 W	+52	Yes	Yes
Auckland, New Zealand	37.02 S	174.81 E	-43	Yes	
Hat Yai, Thailand	6.94 N	100.39 E	-7	Yes	
Shannon, Ireland	52.73 N	8.93 W	+51	Yes	Yes
Johannesburg, South Africa	26.13 S	28.21 E	-37	Yes	
Barrow, AK, USA	71.30 N	156.78 W	+70	Yes	Yes
Santa Cruz, Bolivia	17.67 S	63.16 W	-9	Yes	
Krasnoyarsk, Russia	56.17 N	92.51 E	+52	Yes	Yes
Al Muharraq, Bahrain	26.27 N	50.64 E	+21	Yes	
Pulantant, Guam	13.47 N	144.40E	+9	Yes	
Las Palmas, Canary Islands	28.12 N	15.28 W	+18	Yes	

Of the 14 ground stations, three of them are clearly within the equatorial region (viz.., Hat Yai, Santa Cruz, and Pulantant); three are near the crest of the equatorial anomaly (viz., Molokai, Al Muharraq, and Las Palmas); two would be classified as high latitude sites (viz., Reykjavik and Barrow), and the remainder would be considered midlatitude sites. Of the high latitude sites, Barrow is always poleward of the auroral oval and would be expected to

represent polar cap conditions, whereas Reykjavik is typically a site that straddles the oval. Due to the fact that the auroral oval, a primary geophysical marker, can move decidedly equatorward under magnetic storm conditions, a number of stations could be considered transient high latitude sites (viz., Riverhead, Shannon, and Krasnoyarsk) when *Kp* indices are highly elevated.

Figure 4-26 is a map of the HFDL network of ground stations, and Figure 4-27 illustrates commercial air traffic for a given day (top) and month (bottom). It is obvious that the traffic patterns are not distributed uniformly. Moreover the traffic patterns display well-known diurnal patterns and seasonal tendencies. Other factors such as world conditions (i.e., economy, war, calamity, etc.) can also drive the patterns askew. The top curve is a 24-hour representation for May 26th, 2004; the bottom curve is for the entire month of April 2004.

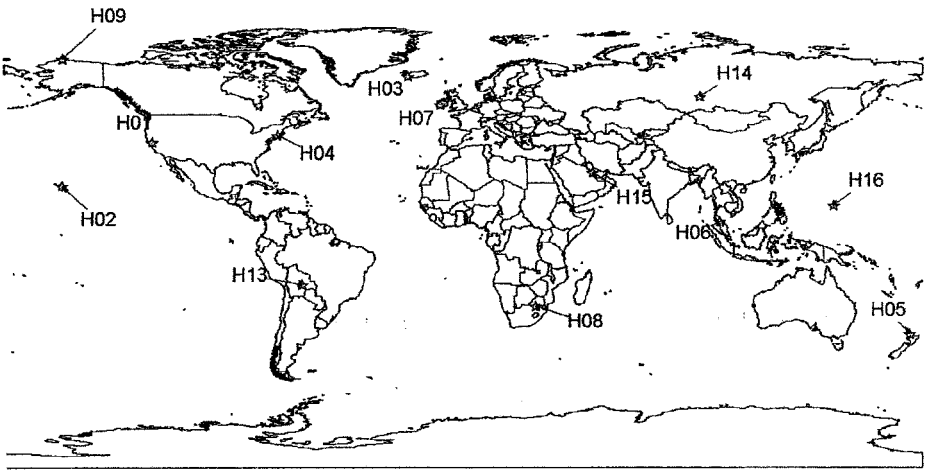


Figure 4-26: Map of the HFDL network (GLOBALink/HF). From ARINC, by permission.

The frequency management subsystem involves an appreciation of HF propagation (i.e., coverage patterns) for all propagating frequencies as well as airline traffic patterns. While knowledge of real-time ionospheric conditions is primary in an adaptive frequency management system, we need to derive a set of canonical coverage patterns over which frequency optimization is to be established. While purely dynamic considerations are possible in the pattern analysis, it was decided to convolve the seasonally-averaged traffic patterns with the standard HF coverage associated with each ground station, taking the system parameters into account (i.e., antenna, transmitter power, etc.). To first order, this is a modification of the plain

vanilla model (i.e., VOACAP and/or ICEPAC). However, in this instance, the gridpoint population defining the desired coverage is weighted by the aircraft traffic patterns.

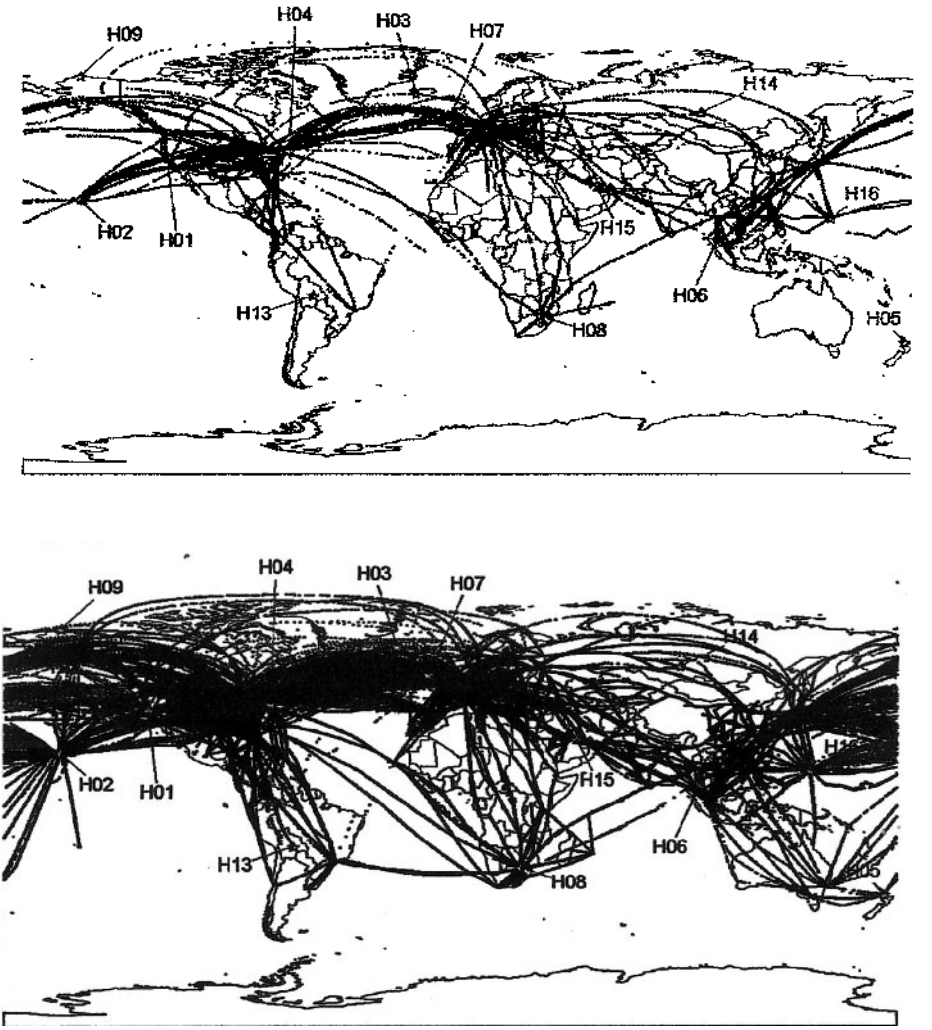


Figure 4-27: Maps exhibiting aggregate commercial air traffic using HFDL. The top curve corresponds to a day (viz., May 26, 2004). The bottom curve corresponds to a month (viz., April 2004). There is no time information retained in these composite plots, but they show the general traffic patterns. There is obviously more traffic in the Northern Hemisphere, and there are certain corridors that dominate the commercial traffic. From space weather analysis perspective, the more dense traffic regions are the ones that demand the most attention. Maps from ARINC, by permission. [Patterson, 2004]

At any given time, an HFDL ground station is designed to activate two distinct frequencies. The challenge is to activate the best two bands for the desired coverage area for each ground station from among a limited group of available frequencies. This generally requires a near real-time adjustment in the ionospheric model used to derive the propagation parameters, although the cadence of the adjustment is typically rather modest (i.e., hourly-to-daily). The data sets used as input to the modified ionosphere come from vertical sounders and oblique-incidence sounders. Other options include the use of global TEC maps suitable analyzed to derive an estimate of the near real time *foF2* values for insertion into the propagation model. The Dynacast program manages this process and provides an optimal pair of frequencies for each station, taking potential interference and other factors into account.

The frequency management product used by HFDL is called an Active Frequency Table (AFT), a computer file that specifies the active frequencies for each ground station over a 24-hour period. Under benign conditions, the Dynacast system submits weekly versions of the AFT; but Emergency AFTs are submitted to net control as required by space weather conditions. Emergency AFTs are needed during certain pathological conditions, with ionospheric storms and PCA events being prime examples. Emergency AFTs are also needed if certain system elements are changed (i.e., new frequencies added, etc.) Network control disseminates the AFT files to all ground stations for coordination and action. The GLOBALink/HF system includes the features given in Table 4-11.

Table 4-11: Characteristics of the GLOBALink/HF system

- HF data radio (ground segment and aircraft)
  - Modem uses adaptive equalization for optimum receiver performance (decision feedback)
  - TDMA protocol for message collision avoidance
  - Unique Squitter message and format for system status for protocol control and timing information
- Constellation of 14 ground stations
  - Two transmitters per station
  - Interconnected network
- Network Control (Annapolis)
- Non-organic Frequency Management System (Dynacast®)
  - Weekly AFTs derived from climatology as updated by short-term forecasts of solar-terrestrial observations (e.g., space weather)
  - Emergency AFTs derived from nowcasts and short-term forecasts of the environment (i.e., current *Kp* time history, sounder data, etc.

The communication traffic for the HFDL system generally exceeds 400,000 messages per month and the average message success rate is greater than 97%. This is comparable to satellite availability and is far better than typical HF voice circuits, even under benign conditions. This clearly shows the benefit of (i) a multi-node network architecture (i.e., for path diversity), (ii) an adaptive HF data radio using (i.e., exploitation of time diversity and code diversity), and (iii) adaptive frequency management (i.e., frequency diversity).

4.5.2.1.1 Diversity Experiments as a Basis for HFDL

It has been shown [Goodman et al., 1997] that HFDL communications can be as reliable as satellite systems given the diversity attributes than can be applied. Frequency diversity is well established as a way to improve communications connectivity for point-to-point circuits. Since aircraft have multiple opportunities for connectivity (i.e., in terms of stations and frequencies), it should not be a surprise that HFDL can be successful. For example, if an aircraft has access to 8 bands per station and four stations within the calling area, there are potentially 32 independent circuits to choose from. In general there are fewer circuits than this, but the diversity is still substantial. By contrast, a satellite circuit, while advantaged in other ways, does not have the same diversity advantage (i.e., station and frequency diversity). It has been pointed out that a combination of satellite and HF data link can provide a very high level of connectivity. Since the failure mechanisms of HF and Satcom are likely to be different, an HF availability of 0.9 and a Satcom availability of 0.99 implies a composite availability of 0.999, for an integrated unavailability of ~ 9 hours/annum or ~ 1.5 minutes/day. Given this high system availability, what can we say about the distribution of residual system outages? As one would expect, there is a tendency for one class of residual outages to cluster in the temporal neighborhood of space weather disturbances. Other outages are systematic and unrelated to space weather.

A comprehensive study of HF propagation conditions was carried out between 1994-1997 using Chirpsounder® assets. Figure 4-28 depicts the geometry of the campaign. The SNRs for all frequency bands in the aeronautical spectrum were continuously monitored and archived for a substantial number of propagation paths in the Northern Hemisphere [Goodman et al., 1997]. From this database, it was possible to deduce the availability of communication for selected subnetworks. This experimental investigation was the basis for certain feasibility studies for HFDL during architecture and standards development. Four subnet clusters were examined, each having a four-pronged star configuration, meaning that each clusterhead,

simulating an aircraft position, was always connected to four other nodes. The clusterheads for the star subnets, arranged in order of highest geomagnetic latitude to the lowest, were located at Churchill (Canada), Reykjavik (Iceland), St. Johns (Newfoundland), and Henrico (North Carolina). Figure 4-29 is an examination of stormy and quiet conditions. It is clear that stormy conditions can introduce significant (but not devastating) unavailability increases for the highest latitude networks (i.e., Churchill and Reykjavik). For the St. Johns clusterhead the effect was small, and for the Henrico clusterhead the effect of storms was virtually non-existent. It is noted that the communication availability is close to 95% even for high latitudes under the worst possible conditions. Naturally, one would not expect this for individual HF circuits. This was strong evidence that HFDL would be successful once implemented.

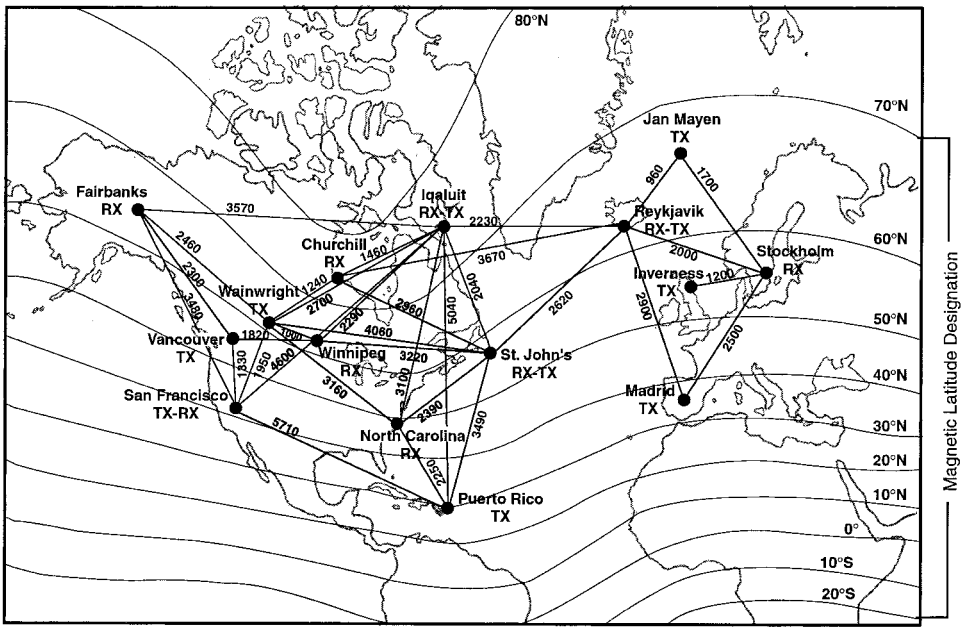


Figure 4-28: Geometry of the Northern Experiment directed by TCI/BR Communications. From Goodman et al. [1997].

Figure 4-30 shows the advantage achieved if one were to exploit Real-Time-Channel-Evaluation (RTCE) as opposed to climatological predictions. All conditions have been combined. The figure indicates that nowcasting can provide a substantial gain in availability if measurements are applied, especially at higher latitudes. For lower latitudes, it is evident that climatological predictions are not so bad, and are competitive with real-time measurements. In such studies, it should be noted that short-duration disturbances are masked by the predominantly quiet periods.

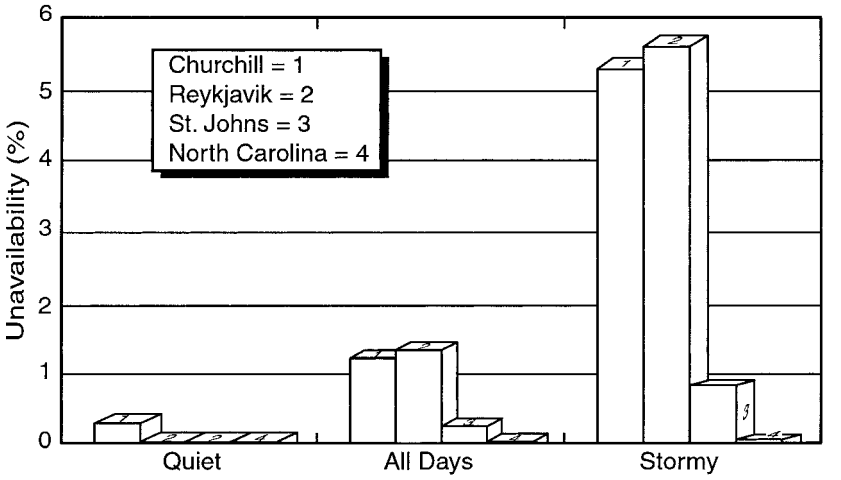


Figure 4-29: Simulation of the impact of storms on diversity networks such as HFDL. Real data from oblique sounders was used in the simulation. The conditions are for four star-net clusters during April of 1995, a period of wide-ranging *Ap* values. The clusterheads are at Churchill, Reykjavik, St. Johns, and northeastern North Carolina, and each cluster consists of four paths terminating at the clusterhead. Each star-net had access to one frequency in each of the eleven aeronautical-mobile bands, and these frequencies are shared between the four links of the cluster. The most stormy period was between 7-12 April when 22>*Ap*>100. From Goodman et al. [1997] and ITU-REC.F.1337.

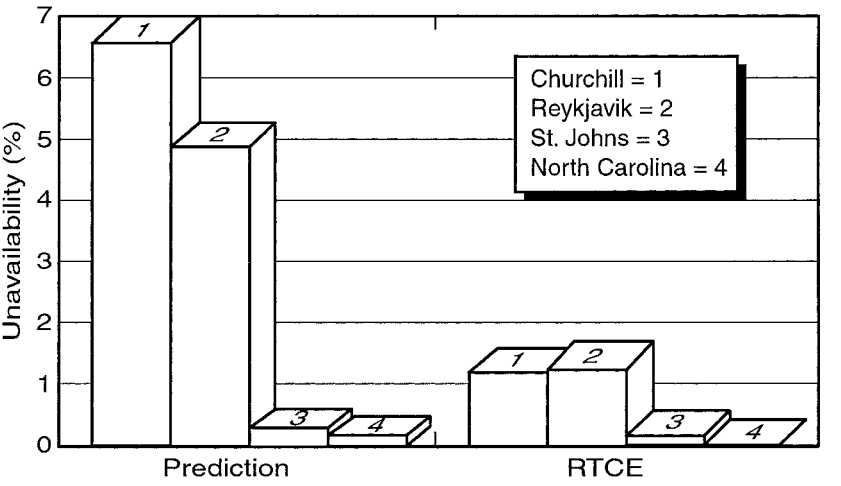


Figure 4-30: Advantage of Real-Time-Channel-Evaluation (RTCE) on diversity networks such as HFDL. The scheme marked "prediction" corresponds to a condition where the VOACAP preselects the three "best" frequencies. The scheme marked "RTCE" (for real-time channel evaluation) corresponds to use of the "best" frequency found from real-time oblique sounding. From Goodman et al. [1997] and ITU-REC.F.1337.

4.5.2.1.2 Halloween Storm Impact on HFDL

The Halloween storm period of October-November 2003 was a period of significant ionospheric effects. Large geomagnetic storms were evidenced (see Section 4.5.4). Patterson [2004] of ARINC has examined the impact on HFDL of the various phenomena observed during this period, and has provided certain data shown in Table 4-12. It is a listing from October 19th – November 7th of a daily metric that is proportional to the performance of the global HFDL system. We have added the magnetic activity index *Ap* for comparison. We see that some impact on HFDL performance on October 29-31 may be arguably present, but it is minimal in amplitude. While HFDL is based upon HF propagation, a medium known for its vulnerability to ionospheric variability, the system performance metric does not reflect this vulnerability to a significant degree.

Table 4-12: HFDL Performance during the Halloween Storm period (10/19/2003 to 11/07/2003). The metric selected is the uplink block success rate in percent. The message success rate is much higher since there are typically several attempts made to send a block of data, and time diversity provides a gain in most instances. The diversity gain can be significant if the tries are independent and if multiple tries are attempted within the allotted time span. For example if the block success rate is 60%, and four tries are afforded, the maximum block delivery rate would be > 99%, using statistical arguments. More than four attempts can be made to attempt transmission of a given block. On the other hand, some messages may be larger than a block in length. Data provided by Patterson [2004], courtesy ARINC.

Date	Uplink Metric	Est. *Ap*	Date	Uplink Metric	Est. *Ap*
Oct.19	59	32	Oct.29	51	04
Oct.20	63	30	Oct.30	55	08
Oct.21	59	39	Oct.31	55	93
Oct.22	58	33	Nov.01	56	21
Oct.23	58	07	Nov.02	59	18
Oct.24	57	34	Nov.03	57	10
Oct.25	58	14	Nov.04	57	31
Oct.26	59	10	Nov.05	57	09
Oct.27	56	15	Nov.06	60	14
Oct.28	60	20	Nov.07	57	08

It is evident from Table 4-12 that the three lowest reliability days, in terms of the uplink block success rate, are October 29-31. While this is interesting, the proper interpretation is elusive. For example, the metric has an average value of 58% for all days for which $Ap \geq 30$, and is 56% for all days for which $Ap \leq 10$. Thus, if there is any significant impact of the environment on HFDL, it must be reflective of other factors than magnetic activity. There

are also system effects than can be important, and these can disguise the ionospheric perturbations. The bottom line is that the Halloween storm period did not impact the operational capacity of HFDL.

Patterson and Grogan [2004] remark that "ARINC engineers monitor the solar data coming from the NOAA satellites and issue frequency changes to the ground stations that will be impacted by the solar event."

They go on to say, "this (i.e., timely recognition of solar and geomagnetic storm activity) is the heart and soul of the adaptive frequency management system of HFDL. During the stormy weeks of October and November, ARINC issued over seven changes to the Automatic Frequency Tables (i.e., AFTs) used by every HFDL station. These changes helped the HFDL network to maintain a delivered message success rate of 97%".

The adaptive frequency management system referred to by Patterson and Grogan is the RPSI Dynacast® system, discussed earlier.

4.5.2.1.3 Polar Flights

One of the important achievements in recent years has been the opening of polar routes. There are a number of benefits. First, the required flight distances from North America and Asia is considerably reduced, and the participating commercial carriers can offer an attractive non-stop service to passengers. Secondly, more direct routes can provide rather significant time and fuel savings. The elimination of an intermediate stop can reduce flight times by an hour or more, and fuel savings can be of the order of a few thousand pounds. Another advantage of trans-polar routes originating in North America is that reduced headwinds are encountered. Unfortunately this is not the case on the return from Asia to America. The return trip is usually accomplished over conventional southerly routes in which favorable tailwinds make non-polar flights more attractive. Typical timesavings in minutes and dollars per flight are estimated in Table 4-13. One flight per day for the New York-Singapore flight would amount to a savings of ~ $16 million dollars per annum.

Table 4-13: Estimated Dollar and Time Savings per Flight (CY04 dollars)

Flight	Time Savings (minutes)	Dollar Savings ($k)
Atlanta-Seoul	124	44
Boston-Hong Kong	138	33
Los Angeles-Bangkok	142	33
New York-Singapore	209	44
Vancouver-Beijing	108	33
Vancouver-Hong Kong	125	33

The polar region does not have satellite coverage above about 80 degrees. For a number of standard path segments over-the-pole, the only means of communication is HF voice and HFDL. At first blush this would appear to be a troublesome situation, given the vulnerability to high latitude propagation effects. Figure 4-31 illustrates the flight geometry for Polar-1 through Polar-4. Figure 4-32 indicates the radio stations that are used for ATC and/or LDOC (voice) communications. Refer to Figure 4-26 for a map of the global HFDL system. The ATC stations include: Cambridge Radio (Arctic), Tiksi Radio (Russia), Norilsk Radio (Russia), Churchill, Montreal Radio (Iqaluit), Iceland Radio, and Bodo. The LDOC stations include: Cedar Rapids Radio, Rainbow Radio, Stockholm Radio, Iceland Radio, Speedbird London, Berne Radio, Houston Radio, ARINC-New York, and ARINC-San Francisco.

ATC communications is far more viable than LDOC when polar flights are being served. Assets for LDOC service (and ATC to a lesser extent) are generally found to be insufficient for adequacy of reliable and rapid voice communication service. To enable an improvement in voice services for transpolar flights, ARINC has installed voice communications capability at Barrow, the location of one of its HFDL stations. This has helped immensely. It is noteworthy that the ARINC's GLOBALink/HF node at Barrow provides the only data link capability specific to the polar cap region, even though augmented arctic service is provided by stations in Reykjavik (Iceland), Shannon (Ireland), New York (USA), Dixon (USA) and Krasnoyarsk (Russia), as indicated in Table 4-10. This is the result, in part, because HF signals can propagate over significant distances by multiple hops, although less reliably. In a similar fashion, the ARINC Barrow site enables acceptable (but not exemplary) voice service to be accommodated for transpolar flights, with the consideration of support from cooperating voice stations.

It bears repeating. The availability of HF communication by voice or data link is only a reality if there are sufficient assets to be applied. This means both stations and frequencies. RPSI is supporting ARINC in examination of approaches for exploiting space weather data to improve the quality of voice and data communications for commercial aviation in the high latitude region. Magnetic storms are an obvious concern at high latitudes, but PCA events can also lead to communication failures on another level. For example, energetic particle events can be sufficient to introduce radiation hazard. During the stormy period in October 2003, and based upon alerts provided by NOAA-SEC, there were a number of diversions of polar flights to avoid radiation hazards associated with radiation storms. Aircraft diversions are expensive, so accurate predictions are essential.

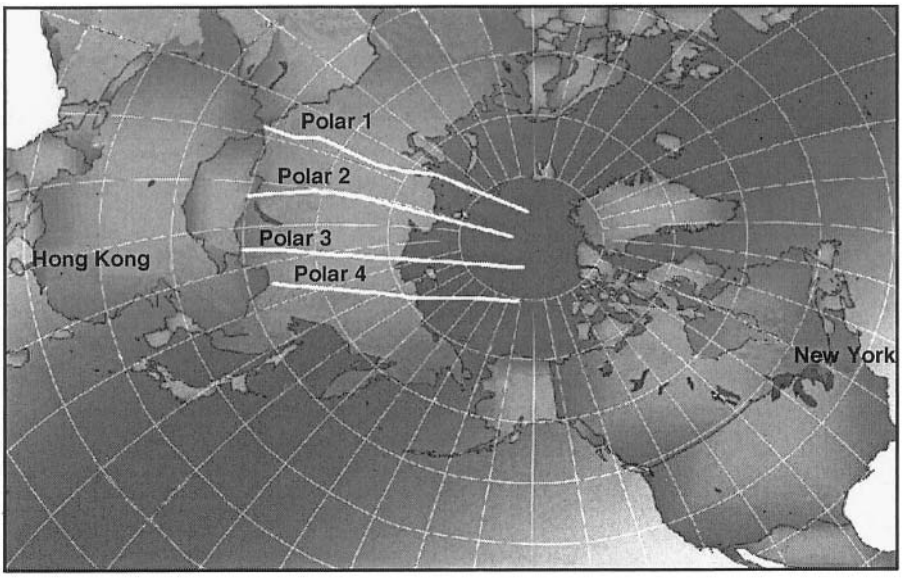


Figure 4-31: Polar Flights Information. Shown are Polar-1, Polar-2, Polar-3, and Polar-4 routes.

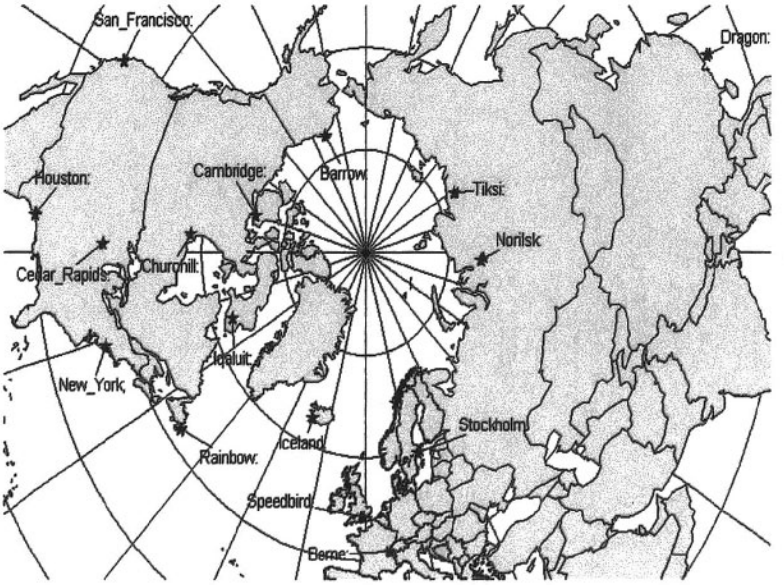


Figure 4-32: Radio Stations serving LDOC and ATC Communications

4.5.2.2 FAA WAAS System

4.5.2.2.1 General Description

The Global Positioning System (GPS) has many applications, and one of the more important ones is the Wide-Area Augmentation System (WAAS). The system supports en route, terminal, nonprecision approach (NPA), NPA with vertical guidance (NPV), and Category 1 (i.e., CAT 1) precision approach (PA) flight operations. The WAAS system broadcasts clock data, satellite ephemeris, and ionospheric corrections to aviation users. These corrections are applied to the GPS measurements by the aviation user equipment, and this equipment also converts error bounds into position. The advantage of WAAS is that GPS can be authorized to provide certain flight operation services if vertical and horizontal position error bounds fall below a designated threshold. Unfortunately the ionosphere can be an important error source. Space weather effects, such as large geomagnetic storms, can introduce substantial horizontal and temporal gradients in the TEC, and this can result in ranging errors (and error bounds) that exceed the threshold. The availability of the WAAS system to support flight operations is reduced in direct proportion to the fraction of time that the error bounds exceed the designated (allowable) thresholds. A good review of the WAAS system has been published by Bakry El-Arini et al. [1999], and pertinent details of the WAAS architecture are derived from this paper. Table 4-14 outlines the Concept of Operations (CONOPS) for WAAS. Figure 4-33 shows the WAAS system architecture, and Figure 4-34 shows the gridpoint constellation for the WAAS system.

4.5.2.2.2 Response of WAAS to Space Weather Events

By now the reader should be quite familiar with the Halloween storm events of 2003. Various aspects of the stormy period have been described in Chapters 2 and 3. As indicated in the CONOPS, ionospheric variations are detected by the WAAS system and corrections supplied to the users. The Halloween storm of October 2003 was a significant challenge for the new system. Remark that WAAS had only been commissioned for operational use for approximately three months by the time the storm period occurred.

The impact of space weather on WAAS has been reported by Doherty et al. [2004]. Geomagnetic storms give rise to ionospheric storms and TEC variations, as described in Chapters 3 (Section 3.10). When WAAS detects a storm, increased error bounds (i.e., GIVEs and UDREs) are computed for effected grid points (IGPs). These numbers determine the efficacy of WAAS services. If they are too large, near-precision approaches can be obviated.

Specifically, during the Halloween storm, the Lateral Navigation (LNAV) and Vertical Navigation (VNAV) capabilities deteriorated. While these near-precision approach services of WAAS were degraded, non-precision approach services were never unavailable during the storms. The WAAS storm detection procedures worked as planned. Specifically, the system increased the error bounds at the affected IGPs during the storm period, and increased the user protection levels.

Table 4-14: WAAS Concept of Operations (from Bakry El-Arini et al. [1999]

Item	Description
1	WAAS Reference Stations (WRSs) are installed at locations throughout CONUS to measure pseudoranges and carrier phases on L1 and L2 channels from all GPS satellites within view.
2	WRSs send Item-1 data to WAAS Master Stations (WMSs). The WMSs calculate clock and ephemeris corrections for each GPS satellite, ephemeris for each geostationary satellite (GEO) being used for broadcast purposes, and ionospheric vertical delays on a grid. The GEO broadcast services for WAAS include: (i) an integrity monitoring function to alert users of out-of-tolerance conditions, (ii) corrections to GPS signal-in-space, and (iii) additional GPS-equivalent signals. Note: The grid is has a 5°x5° resolution within a designated area. Elements in the grid are called Ionospheric Grid Points (IGPs) and reckoned at an altitude of ~ 350 km.
3	The WMSs compute error bounds for ionospheric corrections. These are called Grid Ionospheric Vertical Errors (GIVEs) at each IGP. Also computed are errors bounds for clock and ephemeris corrections for each visible satellite. These are called User Differential Range Errors (UDREs).
4	The WMSs send Item-3 corrections and error bounds to the designated users (e.g., aircraft) via broadcast services of the specified GEOS (i.e., Inmarsat). The GEO data rate is 250 bps.
5	User avionics modify the pseudoranges using the corrections from Item-4 in order to improve the accuracy of position estimates. The user gear also exploits the UDREs and GIVEs to deduce error bounds on position errors in the vertical and horizontal domains (i.e., vertical protection level, VPL and horizontal protection level, HPL).

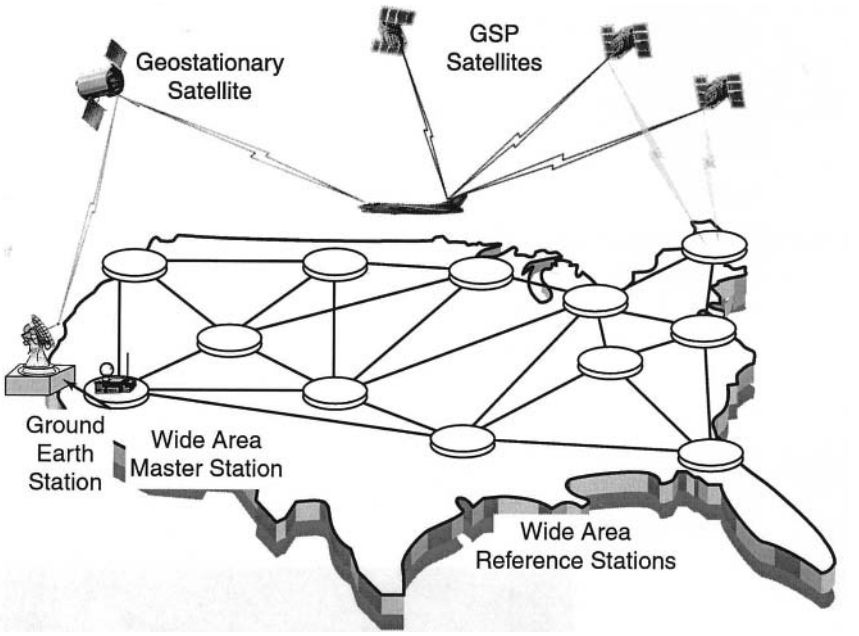


Figure 4-33: WAAS System Architecture. From Doherty et al. [2004].

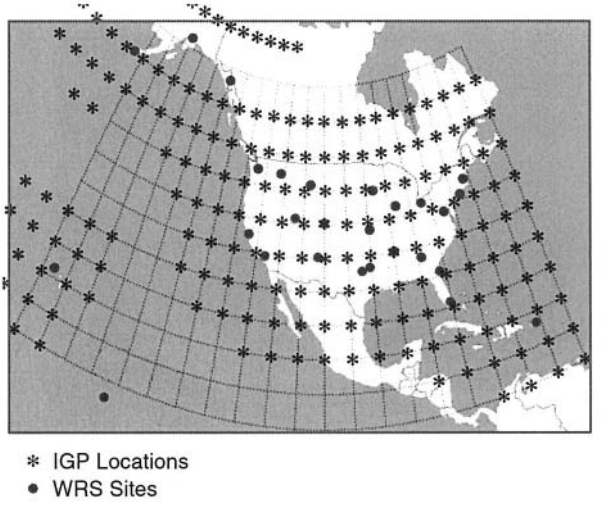


Figure 4-34: WAAS Gridpoint Constellation Outputs from WAAS include the IGPs, IPPs, GIVEs, and UDREs. User calculations include: (i) improved range measurements from the IGP data, (ii) computed VPL and HPL values from GIVEs and UDREs, and (iii) VPL and HPL comparison with horizontal and vertical alarm limits (HAL and VAL) to assess WAAS availability. From Doherty et al.. [2004].

Figures 4-35 and 4-36 shows the IGP data and GIVEs on October 28 (2100-2300 UTC) and October 30 (2100-2300 UTC) respectively. The disturbed period on October 30th shows elevated IGP values and GIVEs. These are associated with a large positive storm effect, described by Coster [2004] as a plume of storm-enhanced density (SED). Figure 4-37 shows the WAAS TEC map and a 200 station GPS grid for October 29th at 2200 UTC.

In sum, it was found that the WAAS performance was degraded due to the Halloween storms, with the most significant effect being the loss of vertical navigation capability. The capability was lost for 15 hours on October 29th and 11.3 hours on October 30th. The non-precision approach services (NPA) were never affected by the storms. The WAAS system operated as required, detecting storm TEC variations, thus yielding elevated GIVEs, UDREs, and user protection levels. This did cause precision approach (PA) services to be interrupted.

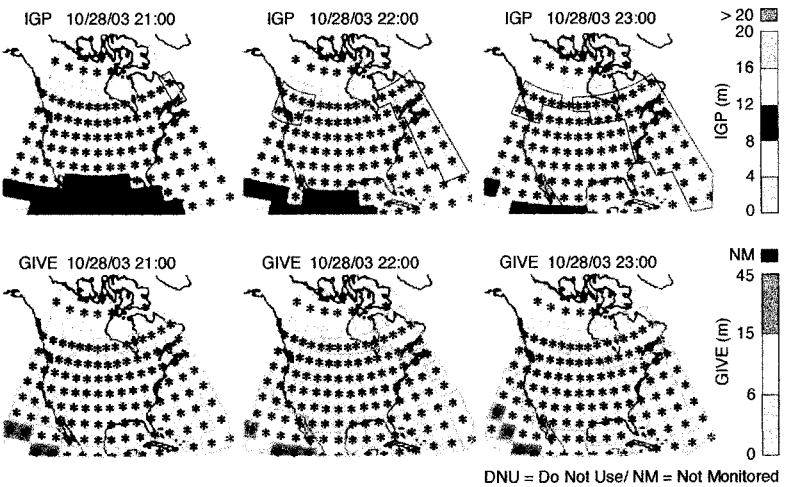


Figure 4-35: IGP data and GIVEs. October 28 (2100-2300 UTC). From Doherty et al. [2004]

4.5.3 Practical Approaches

A general treatment of ionospheric effects on systems has been given in Sections 4.1-4.4. We have also mentioned various system countermeasures. When it comes to specific systems, impairment that may arise from space weather events is a difficult issue to address. For most commercial system managers, there is a real disincentive to announce problems in a competitive environment. The government-run systems are typically more open when it comes the identification of problems and the search for solutions. Disclosure

is assisted when the problems are hard to hide, as in the case of various legacy systems, such as HF communications. It is certainly true that most people understand that systems operating at HF and below are constrained by the ionosphere, and that this constraint may become a hangman's noose when strong space weather events occur. For satellite systems, the matter becomes less clear. The author spent many years trying to identify space weather issues to telecommunication managers, and to encourage the incorporation of available information into their thinking. The activity was not always successful, except at HF. One of the early HF success stories was the development of a system performance prediction platform, called PROPHET, which was developed by U.S. Navy engineers at Naval Ocean Systems Center, now SPAWAR, and the Naval Research Laboratory. It is felt that this forecasting terminal, described in Chapter 1, was of major significance in that it was the first system to exploit space weather data in real time for the benefit of the ultimate user, the naval communicator. This prediction system actually supplied tailored products based upon space weather data to the system operators, and they were delighted. In Chapter 5 we describe other systems that use similar, but more advanced approaches. Getting tailored information to the user is extremely important, especially if he can do something with it. The U.S. Air Force has developed the OpSEND system to provide the military analyst and operator with an array of propagation tools based upon space weather observables and advanced models.

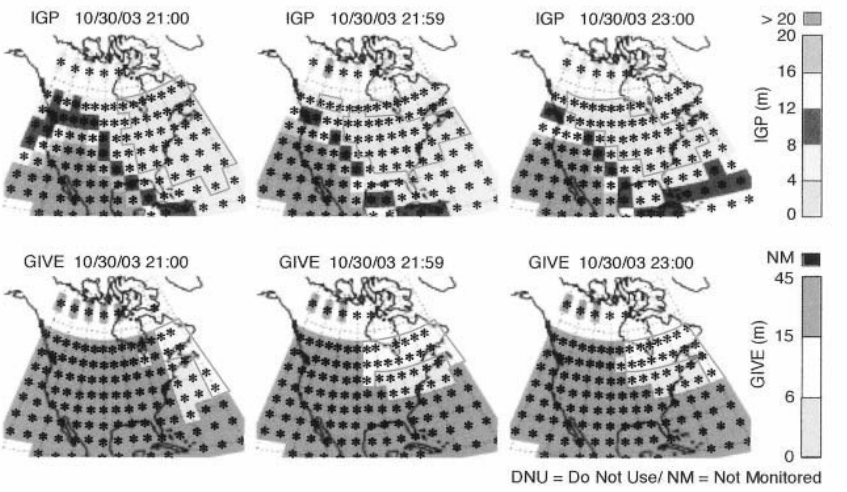


Figure 4-36: IGP data and GIVEs. October 30 (2100-2300 UTC). From Doherty et al. [2004]

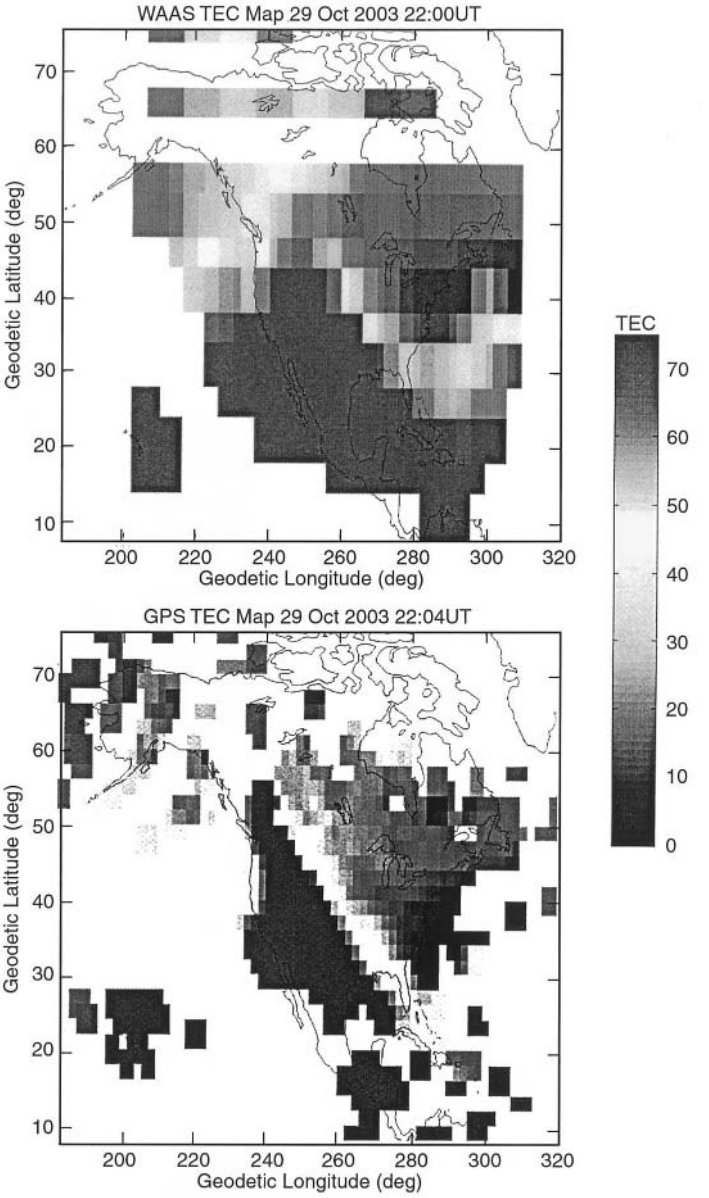


Figure 4-37: WAAS TEC map (top) and a 200-station GPS grid (bottom) for October 29th at 2200 UTC. The original illustration, from Doherty et al. [2004], was in color. This gray-scale representation tends to make the darker red (high TEC values) look similar to the darker blue (low TEC values). The darker "red" band running through the Gulf of Mexico and western CONUS and into southwestern Canada constitutes a region of enhanced TEC (or Storm-Enhanced Density, SED), in the 60-70 TEC range. The narrower band of "white" that is eastward of the SED is in the 40-50 TEC range. Northeastward of the SED the values fall into the darker "blue" category, the 5-20 TEC range.

With satellite communication and navigation systems, the main problem without question is amplitude and phase scintillation. What role does the space weather community play in mitigation of this particular effect? To answer this, we need to understand the phenomenology of scintillation, and the main drivers. We must also be aware that climatological solutions are inadequate but they do provide guidance. There are several flavors to the solution, and they begin with a set of possible countermeasures that may be imposed by the system, given proper space weather data. Satellite communication systems typically operate at a fixed frequency, so that frequency management is not really an option. In any case, scintillation is correlated over a wide range of frequencies limiting any frequency management options that might exist. It goes without saying that satellite communication systems are designed to cope with a range of fading conditions, and they exploit time and space diversity to counter the generic problem. However no system can easily recover from severe scintillation events without some loss in throughput. There is a premium on the circumvention of the problem through use of alternatives and robust countermeasures. The approach to solution depends upon accurate and timely information. Regarding space weather issues, scintillation is addressed in a number of ways. The U.S. Air Force has developed an interesting approach for addressing equatorial scintillation (i.e., SCINDA), and another program (i.e., C/NOFS) is the scintillation forecasting systems of the future. These programs are briefly described in Chapter 5. Both of these systems emphasize *downstream* data to arrive at predictions.

4.5.4 Benefits of Space Weather Information

The storm period during October-November 2003 was a wake-up call for many telecommunication system managers. The events, described in Chapter 2 (Sections 2.28 and 2.38) and Chapter 3 (Section 3.10.4), generated an array of system effects that were unexpected for a period so late in the solar cycle. Onsager, Poppe, and Murtagh [2004] have described the storm effects in a brief report appearing in the new journal *Space Weather*. In retrospect, it is known that magnetic storms do increase in abundance during the declining phase of the sunspot cycle, but the intensity of solar flares and resultant storm effects was certainly unprecedented. Table 4-15 is a generic listing of system effects that were reported back to the various warning agencies for the Halloween Storm period [Kunches, SEC, 2004; Simpson, 2004; NOAA-NWS, 2004] A number of effects were encountered, but little permanent damage was done. However, when we speak of physical damage we generally refer to power grid failures, satellite failures and the like. These may impact a large and vocal audience of TV and radio subscribers, as well as

users of paging services and cellular phones, for example. The good news is that for radiocommunication systems the effects may be huge but are largely repairable. The bad news is that the "damage" to radio systems, while more subtle, but can be equally dangerous if the radio systems are mandated for emergency comunications, precision landing and navigation, and for critical military operations. In many instances, the effects may have been ameliorated by organic solutions and methods exploiting diversity or redundancy. But to say that the Halloween storms did not cause any significant effects would be a gross overstatement.

From Table 4-15, we note that almost all of the reported radiocommunication disturbances involved bands at HF and below. Exceptions include propagation disturbances on the GPS (i.e., L-band) system transmissions and on WAAS, a system that exploits GPS. Clearly, there were many satellite systems that were also afflicted by scintillation effects, especially VHF and UHF systems, but many were military systems and not faithfully reported in such a way as to be ingested into the NOAA or ISES catalogues of disturbances.

Table 4-15: Sampling of system Impacts during the 2003 Halloween Storm Period (i.e., October 19th – November 7th, 2003)

Aircraft communication systems at HF/VHF suffered severe degradation and periods of complete blackout (above ~57 degrees N) during Polar Cap Absorption (PCA) events.
Trans-polar flights of a major U.S. carrier were re-routed from Polar-3 to Polar-4 routes to avoid the radiation hazards associated with radiation storms over the polar cap.
There were difficulties with long-distance HF communication over trans-Atlantic flights, requiring extra operational staff and use of backup systems
United States Air Force experienced degraded HF communications from stations at San Francisco, Keflavik, Iceland, and Kodiak, Alaska.
The Voice of America experienced outages and anomalies on HF broadcast circuits during Short-Wave-Fades (SWFs) and magnetic storms
HF communication systems encountered radio blackout for dayside paths because of x-ray flares and resultant SWF events. (included aircraft communications)
Terrestrial HF communication systems experienced outages during radiation storms that introduced PCA events.
HF relay operations in Antarctica experienced over 130 hours of blackout during the October-November activity.
Loran-C experienced RFI problems
The Navy Re-locatable OTH radar (ROTHR) had difficulties
The GPS-based WAAS system was interrupted in the continental United States (CONUS). However the system alerted appropriately and no failure of the system was reported.
GPS receiver outages occurred at high latitudes

The provision of definitive forecasts and relevant space weather data can benefit the telecommunications system manager in the following ways:

1. Space weather data can be incorporated in general advisories supplied to high-level policy makers and military tacticians.
2. Space weather data can be utilized by top-level system managers to develop resource management decisions (e.g., mixed-media communications).
3. Space weather data can be used to develop tailored advisories and alerts for use by engineers of specific telecommunication systems. This information allows the system manager to orchestrate system-wide decisions concerning traffic flow control based upon message priority.
4. Space weather data can be utilized to assist the military planner in the area of propagation tactics, for purposes of exploitation, electronic warfare, and surveillance.
5. 3rd party vendors that offer real-time applications supporting telecommunications can use space weather data.
6. Specified space weather data streams can be fed directly to telecommunication system controllers (i.e., system computers) to alter system operational procedures and parameters in near real time.
7. Space weather data can be used to evaluate prior events for: (i) assignment of cause related to impairment and (ii) for the development of mitigation measures.

In summary, we have found that the performance of many important telecommunication systems are influenced by space weather. These are not simply legacy systems, such as shortwave communication and surveillance systems. Satellite systems have encountered a variety of impacts including: spacecraft charging, single-event upsets, station-keeping anomalies, and a range of radio propagation impairments. Of the radio propagation anomalies increased by space weather effects are: amplitude and phase scintillation, ranging and radar tracking errors, and group path delay errors. GPS receiver terminals can lose the capability to track phase, and TEC fluctuations can play havoc with single-frequency users. There have been noble attempts to mitigate space weather impact, and methods include preemptive placement of certain satellites in a "safe" mode, or the reduction of the data rates of terrestrial systems through use of adaptive time diversity and redundancy schemes. Such methods require advance notice of storms. We have described several systems that cope with space weather reasonably well, in the sense that performance degradation can be minimized by some appropriate action. These include the GLOBALink/HF system and the WAAS system. However, it must be said that these systems do not remove the deleterious effects

entirely. Hopefully the reader can now appreciate the importance of space weather information in the operation of telecommunication systems. In the next chapter we will go through some prediction and forecasting services and systems.

4.6 REFERENCES

Aarons, J., 1982, "Global Morphology of Ionospheric Scintillations," *Proc. IEEE,* vol. 70, no. 4, pp. 360-378.

Aarons, J., E. MacKenzie and K. Bhavnani, 1980, "High Latitude Analytic Formulas for Scintillation Levels," *Radio Sci.* ,vol.15, pp. 115-127.

Aarons, J., C. Gurgiolo, and A. S. Rodger, 1988, "The Effects of Magnetic Storm Phases on F-layer Irregularities below the Auroral Oval," *Radio Science,* vol. 23, no. 3, pp. 309-319.

AGARD, 1982, *Medium, Long, and Very Long Wave Propagation,* NATO-AGARD-CP-305, ADA113969.

Akasofu, 1977, *Physics of Magnetospheric Substorms*, D. Reidel Publishing Co., Boston, MA.

ALSA, 2003, "HFALE: Multi-Service Tactics, Techniques, and Procedures for the High Frequency Automatic Link Establishment (HF-ALE) Radio", U.S. Army FM 6-02.74, U.S, Marine Corps MCRP 3-40.3E, U.S. Navy NTTP 6-02.6, U.S, Army AFTTP(I) 3-2-48, published by the Air-Land-Sea Applications (ALSA) Center.

Anderson, D.N. and J. A. Klobuchar, 1983, "Pre-Midnight Enhancements in Total Electron Content at Ascension Island," in *Proc. Beacon Satellite Studies* of the *Earth's Environment*, New Delhi, India, p. 51,

Anderson, D.N., M. Mendillo and B. Hermiter, 1985, "A Semi-Empirical Low Latitude Ionospheric Model," AFGL-TR-85-0254.

Anderson, S.J., 1986, "Remote Sensing of the Jindalee Skywave Radar", *IEEE J. Oceanic Eng.*, OE-11 (2), 158-163.

Bannister, R. 1986, "Simplified Formulas for ELF Propagation at Shorter Distance," *Radio Science,* vol. 21, p. 529.

Bannister, P.R., 1980, "Extremely Low Frequency (ELF) Propagation," NUSC Scientific and Engineering Studies, NUSC, New London, Conn.

Basu, S. and Su. Basu, 1981, "Equatorial Scintillations-A Review," *J. Atmospheric Terrest. Phys.*, vol. 43, p. 473.

Basu, Su, S. Basu, E. MacKenzie, and H. E. Whitney, 1985, "Morphology of Phase and Intensity Scintillations in the Auroral Oval and Polar Cap," *Radio Science,* vol. 20, p. 347.

Basu, S. E. MacKenzie, and Su. Basu, 1988a "Ionospheric Constraints on VHF/UHF Communication Links During Solar Maximum and Minimum Periods", *Radio Science,* vol. 23 (3), pp. 363-378.

Basu, Su. , S. Basu, E. J. Weber, and W. R. Coley, 1988b, "Case Study of Polar Cap Scintillation Modeling Using DE2 Irregularity Measurements at 800 km", *Radio Science,* vol. 23, no. 4, pp. 545-553.

Bean, B.R., G. D. Thayer, and B. A. Hart, 1971, "Worldwide Characteristics of Refractive Index and Climatological Effects" in *Tropospheric Radio Propagation* (part 1), H. J. Albrecht (editor), NATO-AGARD-CP-70, Technical Editing and Reproduction Ltd., London, UK.

Bent, R.B., S. K. Llewellyn, G. Nesterczuk, and P. E. Schmid, 1975, "The Development of a Highly Successful World-wide Empirical Ionospheric Model and its use in Certain Aspects of Space Communications and Worldwide Total Electron Content Investigation," in Proceedings of IES85, J.M. Goodman (editor), pp. 23-38.

Berkey, 1998, "Introduction to the Special Section: Science and Technology of OTH-R", special issue of *Radio Science* (Berkey, guest editor), 33(4), 1043-1044, 10.1029/98RS02158.

Bilitza, D., 2001, "International Reference Ionosphere-2000", Radio Science, 36, No.2, pp.261-275.

Bradley, P.A., Propagation of Radiowaves in the Ionosphere, in *Radiowave Propagation,* IEE Electromagnetic Wave Series 30, Peter Perigrinus Ltd. for IEE, London, UK.

Buchau, J., E. J. Weber, D. N. Anderson, H. C. Carlson, Jr., J. G. Moore, B. E. Reinisch, and R. C. Livingston, 1985, "Ionospheric Sturctures in the Polar Cap: Their Origin and Relation to 250 MHz Scintillation", *Radio Sci.*, vol. 20, pp. 325-338.

CCIR Rpt. 252-2, 1970, "CCIR Interim Method for Estimating Sky-wave Field Strength and Transmission Loss at Frequencies between Approximate Limits of 2 and 30 MHz", in *Recommendations and Reports of the CCIR: Propagation in Ionized Media,* ITU, Geneva.

CCIR Rpt. 252 Supp, 1982, Supplement to Report 252-2, *Second CCIR Computer-based Interim Method for Estimating Sky-wave Field Strength and Transmission Loss at Frequencies between 2 and 30 MHz*", ITU, Geneva.

CCIR Rpt. 894, 1986, "Simple HF Prediction Method for MUF and Field Strength", Rpt 894-1, pp.239-245, in *Recommendations and Reports of the CCIR, Vol. VI, Propagation in Ionized Media,* ITU, Geneva.

Daglis, I.A. (editor), 2001, *Space Storms and Space Weather Hazards*, NATO Science Series, Kluwer Academic Publishers, Dordrecht, The Netherlands.

Davies, K., 1990, *Ionospheric Radio,* Peter Perigrinus Ltd, for IEE, London, UK.

Doherty P., T. Walter, R. Lejeune, B. El-Arini, T. Dehel, T. McHugh, D. Bunce, and D. Burkholder, 2004, "Space Weather Effects on WAAS: A Performance and Status Report", *Space Weather Week*, Boulder, Colorado.

Evans, J.V., and R. Wand, 1975, "Ionospheric Limitations on the Angular Accuracy of satellite Tracking at UHF or VHF" in *Radio Systems and the Ionosphere*, W.T. Blackband (editor), NATO-AGARD-CP-173, Tech. Editing and Reprod. Ltd., London, UK.

Evstratov, F.F., A.A., Kolossov, A.A., Kuzmin, E.I., Shustov, V.A. Yakunin, Yu.I. Abramovich, and V.A. Alebastrov, 1994, "Over-the-Horizon Radio Location in Russia and Ukraine", *Onde Electr.*, 74 (3), 29-33.

Field, E.C., 1982, "ELF Propagation in Disturbed Environments," in *Medium, Long, and Very Long Wave Propagation, NATO*-AGARD-CP-305, 11-1 to 11-10, ADA113969.

Flock, W.L., 1987, *Propagation Effects on Satellite Systems at Frequencies Below 10 GHz. A Handbook for Satellite Systems Design* (Second Edition), NASA Reference Publication 1108(02), December.

Fremouw, E.J., 1985, "Recent HiLat Results," in P*ropagation Effects on Military Systems in the High Latitude Region,* AGARD-CPP-382, paper 2.1, North Atlantic Treaty Organization, Paris.

Fremouw, E.J. and J. M. Lansinger, 1982, "Recent High Latitude Improvement in a Computer-Based Scintillation Model", *Proc. IES81*, NTIS, Springfield VA.

Fremouw, E.J., R. L. Leadabrand, R. C. Livingston, M. D. Cousins, C. L. Rino, B.C. Fair, and R. A. Long, 1978, "Early Results from the DNA Wideband Satellite Experiment - Complex Signal Scintillation", *Radio Science,* vol. 13, pp. 167-187.

Fremouw, E.J., R. C. Livingston and D. A. Miller, 1980, On the Statistics of Scintillating Signals," *J. Atmospheric Phys.*, vol.43, pp. 717-731.

Fremouw, E.J., J. A. Secan, and J. M. Lansinger, 1985a, "Spectral Behavior of Phase Scintillation in the Nighttime Auroral Region," *Radio Science*, vol. 20, p.923.

Fremouw, E.J., H. C. Carlson, T. A. Potemra, P. F. Bythrow, C. L. Rino, J. F. Vickrey, R. L. Livingston, R. E. Huffman, C.Meng, D.A. Hardy, R. J. Rich, R. A. Heelis, W. B. Hanson, and L. A. Wittwer, 1985b, "The HiLat Satellite Mission", *Radio Sci.,* vol. 20, (3), pp.416-424.

Galejs, J., 1972, *Terrestrial Propagation of Long Electromagnetic Waves,* Oxford, UK: Pergamon Press, Oxford, UK.

Goodman, J.M., 1965, "Prediction of Faraday Rotation Angles at VHF and UHF", NRL Report 6234, NRL, Washington, DC

Goodman, J. M. 1967, "Electron Content Inhomogeneities in the Lower Ionosphere", *J. Geophys. Res.*, Vol.72, No.21, pp.5542-5546.

Goodman, John M. 1980, "Environmental Constraints on Earth-Space Propagation", in NATO-AGARD-CP-284, *Propagation Effects in Space-Earth Paths*, 35-1 to 35-27.

Goodman, J.M. and J. Aarons, 1990, "Ionospheric Effects on Modern Electronic Systems", *Proc. IEEE*, Vol. 78, No.3, March.

Goodman, J.M., 1991, *HF Communications: Science & Technology*, Van Nostrand Reinhold, New York (out-of-print); softbound edition from JMG Assoc. Ltd., 8310 Lilac Lane, Alexandria VA 22308.

Goodman, J.M., J.W. Ballard, and R. Sasselli, 1996, "Growing the ALE Standard to Enable Optimum HF Communications", HF Conference on Frequency Management, held at the IEE Headquarters, Savoy Place, London, UK.

Hauser, J.P., F.J. Rhoads, and F. J. Kelly, "VLFACM Program Description and Operational Manual," NRL Report 8530, Naval research Laboratory, Washington, D.C.

Haydon, G.W., M. Leftin, and R. Rosich, 1976, "Predicting the Performance of High Frequency Skywave Telecommunication Systems" (HFMUFES-4), OT Report 76-102, Dept. of Commerce, Boulder CO.

Headrick, J.M., and M. Skolnik, 1974, "Over the Horizon Radar in the HF Band", *Proc. IEEE*, 62(6): 664-673.

Headrick, J.M., 1990, "Looking over the Horizon", *IEEE Spectrum*, 36-39.

Hunsucker, R.D., 1991, *Radio Techniques for Probing the Terrestrial Ionosphere*, Springer-Verlag, Berlin, Heidelberg, New York.

ITS, 1998, "High Frequency Radio Automatic Link Establishment (ALE) Application Handbook", prepared for NCS of the Office of Technology and Standards, NTIA-ITS, Boulder CO (September).

ITU-R, 1996, *Radiowave Propagation Information for Predictions for Earth to Space Path Communications* (Handbook), Radiocommunication Bureau, ITU, Geneva.

ITU-R, 1997, Recommendations on *Radio Propagation*, Volume 1997, P series, Part 2, Radiocommunication Bureau, ITU, Geneva.

ITU-R Rec. P.684, 1997, "Prediction of Field Strength at Frequencies below about 500 kHz", in ITU-R Recommendations on *Radiowave Propagation,* Volume 1997, P series, Part 2, Geneva.

ITU-R Rec. P.1147, 1997, "Prediction of Sky-wave Field Strength at Frequencies between about 150 and 1700 kHz", in ITU-R

Recommendations on *Radiowave Propagation,* Volume 1997, P series, Part 2, Geneva.

ITU-R Rec. P.533, 1997, "HF Propagation Prediction Method", in ITU-R Recommendations on *Radiowave Propagation,* Volume 1997, P series, Part 2, Geneva.

ITU-R Rec. F.1337, 1997, "Frequency Management of Adaptive HF Radio Systems and Networks using FMCW Oblique-Incidence Sounding", WP9C, Geneva.

ITU-R, 1998, *The Ionosphere and its Effects on Radiowave Propagation (Handbook), a Guide with Background to ITU-R Procedures for Radio Planners and Users*, Radiocommunication Bureau, ITU, Geneva.

ITU-R, 2002, *Frequency Adaptive Communication Systems and Networks in the MF/HF Bands* (Handbook), Radiocommunication Bureau, ITU, Geneva.

ITU-WARC, 1984, "World Administrative Radio Conference for the Planning of the HF bands Allocated to the Broadcasting Service", (HFBC-84 contained therein), Report at 2nd Session, ITU, Geneva.

Jursa, A.S. (editor), *Handbook of Geophysics and the Space Environment* (Fourth Edition), published by AFGL with copies available through NTIS, 5245 Port Royal Road, Springfield VA 22161,1985.

Kelly, F.J., F. J. Rhoads, J. P. Hauser, E. S. Byrd, A. J. Martin, and L. J. Richard, 1984, "Longwave Predictions using the Wave Hop and Waveguide Mode Techniques," in *Effect of the Ionosphere on C3/ Systems (IES84), J.* M. Goodman, F. D. Clarke, J. A. Klobuchar, and H. Soicher (editors), pp. 367-374, NTIS, Springfield VA.

Kelly, F.J., 1986, "ELF/VLF/LF Propagation and System Design" in NATO-AGARD-LS on *Interaction of Propagation and Digital Transmission Techniques,* October (also available as NRL Report 9028, Naval Research Laboratory, Washington, D.C. 20375-5000)

Klobuchar, J.A., 1975, "A First-Order, Worldwide, Ionospheric Time Delay Algorithm," AFCRL-TR-75-0502, ADA 018862.

Klobuchar, J.A., and R. S. Allen, 1970, "A First-Order Prediction Model of Total-Electron-Content Group Path Delay for a Midlatitude Ionosphere," AFCRL-70-04033, AD711365.

Klobuchar, J.A., K. N. Tyer, H. O. Vats, and R. G. Rastogi, 1977, "A Numerical Model of Equatorial and Low Latitude Total Electron Content for use by Satellite Tracking Systems for Ionospheric Corrections," Indian *J. Radio Space Phys.*, vol. 6, pp. 159-164.

Klobuchar, J.A., D. N. Anderson, G. J. Bishop, and P. H. Doherty, 1987, "Measurements of Trans-Ionospheric Propagation Parameters in the Polar Cap Ionosphere," AFGL-TR-87-1021.

Knight, P., 1982, "Medium Frequency Propagation: A survey," in *Medium, Long, and Very Long Wave Propagation,* NATO-AGARD-CP-305, 28-1 to 28-17, ADA 113969.

Kunches, J., 2004, private communication.

Lane, G.H., 2001, Signal-to-Noise Predictions Using VOACAP", Rockwell Collins, Cedar Rapids, Iowa.

Lawrence, R.S., C. G. Little, and H. J. A . Chivers, 1964, "A Survey of Ionospheric Effects Upon Earth-Space Radio Propagation," *Proc. IEEE,* vol. 52, pp. 4-27.

Liu, C. and S.J. Franke, "Experimental and Theoretical Studies of Ionospheric Irregularities Using Scintillation Techniques," *Radio Science,* vol. 21, p. 363.

Lucas, D., J. Lloyd, J.M. Headrick, and J. Thomason, 1972, "Computer Techniques for Planning and Management of OTH Radar", NRL Memo Report 2500, NRL, Washington, DC, AD 748588.

McNamara, L., 1991, *The Ionosphere: Communications, Surveillance, and Direction Finding*, Krieger Publishing Company, Malabar, Florida.

Millman, G.H., 1967, "A Survey of Tropospheric, Ionospheric, and Extra-Terrestrial Effects on Radio Propagation Between Earth and Space Vehicles," in *Propagation Factors in Space Communications,* W. T. Blackband (editor), Maidenhead, England, NATO-AGARD publication, Technivision; See also G.E. Report TISR66EMHI.

Millman G.H., and K.A. Olsen, 1980, "Ionospheric Dispersion Effects on Wideband Transmissions", NATO-AGARD-CP-284, *Propagation Effects in Space-Earth Paths*, 26-1 to 26-12.

Morfitt, D.G, J. A. Ferguson, and F. P. Snyder, 1982,"Numerical Modelling of the Propagation Medium at ELF/VLF/LF," in *Medium, Long and Very Long Wave Propagation, NATO*AGARD-CP-305, 32-1 to 32-14, ADA113969.

Mullen, J.P., E. MacKenzie, S. Basu, and H. Whitney, 1985, "UHF/GHz Scintillation Observed at Ascension Island from 1980 through 1982", *Radio Science,* vol. 20, p. 357.

NOAA-NWS, 2004, "Intense Space Weather Storms October 19-November 07, 2003", Service Assessment, U.S. Dept. Commerce, NOAA, National Weather Service, Silver Spring, MD.

Ochs, A., 1970, "The Forecasting System of the FTZ", in *Ionospheric Forecasting*, NATO-AGARD-CP-49, V. Agy (editor), paper No. 43.

Onsager, T., B. Poppe, and W. Murtagh, 2004, "Halloween Storms Star in Space Weather Week 2004 Meeting", *Space Weather*, 2, S08003, doi:10.1029/2004SW00099.

Pappert, R.A., and W. F. Moler, 1978, "A Theoretical Study of ELF Normal Mode Reflection and Absorption Produced by Nighttime

Ionospheres," J. *Atmospheric Terrest. Phys.*, vol. 40, no. xx, pp. 1030-1045.

Pappert, R.A., 1980,"Effects of a Large Patch of Sporadic E on the Nighttime Propagation at Lower ELF," J. *Atmospheric Terrest.* Phys., vol. 42, pp. 417-425.

Patterson, J., 2004, ARINC, private communication.

Rawer, K., J. V. Lincoln and R. O. Conkwright, 1981, "International Reference Ionosphere, IRI-79", Report UAG-82, WDC-A for Solar-Terrestrial Physics (STP), NOAA, Boulder, CO.

Rino, C.L., and S.J.Matthews, 1980, "On the Morphology of Auroral Zone Radio Wave Scintillation", *J. Geophys. Res.*, vol. 85, p. 4139.

Rufenach, C. L., 1972, Power-law Wave Number Spectrum Deducted from Ionospheric Scintillation Observations," *J. Geophys.Res,.* vol.77, pp. 46-71.

Rush, C.M., M. Pokempner, D. N. Anderson, J. Perry, F. G. Stewart, and R. Reasoner, 1984, "Maps of foF2, Derived from Observations and Theoretical Data," *Radio* Science, vol. 19, p. 1083.

Secan, J. A., E. J. Fremouw, and R. E. Robins, 1987, "A Review of Recent Improvements to the WBMOD Ionospheric Scintillation Model," in *Proc IES87*, J.M. Goodman (editor), pp. 607-616.

Secan, J.A., 1998, "Space Weather Effects on the Transionospheric Propagation Channel", *Hazards of Space Weather Conference*, Boulder CO, April 20-23, 1998.

Simpson, S., 2004, 2004, "Massive Solar Storms in October 2003 Inflict Little Damage on Earth", *Space Weather Quarterly*, Spring 2004, AGU.

Stone, R. 1999, *Review of Radio Science 1996-1999*, 1999, Published for URSI by Oxford University Press, New York.

Sutherland, D.A., 1993, "Simulated Effects of Sounding on Automatic Link Establishment HF Radio Network Performance", NTIA-93-291, NTIS, Technical Information Bulletin 92-21.

Tascione, T.F., H. W. Kroeht and B. A. Hausman, 1988, "ICED - A New Synoptic Scale Ionospheric Model," in *Proceedings of IES88*, J.M. Goodman (editor), NTIS, Washington, DC

Tascione, T.F., 1994, *Introduction to the Space Environment*, 2nd Edition, Krieger Publishing Company, Malabar, Florida.

Teters, L.R., J.L. Lloyd, G.W. Haydon, and D.L. Lucas, 1983, "Estimating the Performance of Telecommunication Systems Using the Ionospheric transmission Channel: Ionospheric Communications Analysis and Prediction Program (IONCAP User's Manual)", NTIA Report 83-127, ITS Order No. N70-24144, NTIS, Springfield VA.

Tsunoda, R.T., 1988, "High-Latitude F Region Irregularities: A Review and Synthesis", *Reviews of Geophysics*, vol. 26, pp. 719-760.

Tsurutani, B.T., W.D. Gonzalez, Y. Kamide, and J.K. Arballo (editors), 1997, *Magnetic Storms*, Geophysical Monograph 98, AGU, Washington, DC.

Wang, J.C.H., 1985, "A Sky-wave Propagation Study in Preparation for the 1605-1705 kHz Broadcasting Conference", *IEEE Trans. on Broadcasting*, Vol.BC-31, 10-17.

Wang, J.C.H., P. Knight, and V.K. Lehtoranta, 1993, "A Study of LF/MF Sky-wave Data Collected in ITU Region 1", *Proceedings of IES93*, J.M. Goodman (editor), NTIS, Springfield VA.

Wait, J.R., 1970, *Electromagnetic Waves in Stratified Media,* Pergamon Press, New York.

Weber, E.J., R. T. Tsunoda, J. Buchau, R. E. Sheehan, D. J. Strickland, W. Whiting, and J. G. Moore, 1985, "Coordinated Measurements of Auroral Zone Enchancements," *J. Geophys.* Res., vol. 90, p. 6497.

Whitney, H.E., C. Malik and J. Aarons, 1969, "A Proposed Index for Measuring Ionospheric Scintillation," *Planetary Space Sci.*, vol.17, pp. 1069-1073.

Chapter 5
PREDICTION SERVICES AND SYSTEMS

5.1 INTRODUCTION

For those deeply involved in technological aspects of telecommunications, any variability in the propagation channel can represent more than a distraction. It is a burden to be overcome. In general, measures that can be taken are either adaptive or robust. This author prefers to use the term *robust* to describe a system with a capability to operate satisfactorily, if not efficiently, in the benign environment but designed to provide sufficient margin or processing power to cope with the disturbed environment without further reduction in performance. These robust systems are designed to provide an even level of performance but not necessarily the best possible performance. The robust design approach is usually applied for strategic systems; typically low data rate communication systems. A robust system is designed not to fail, and for the communication systems, this may be at the expense of throughput. Some techniques utilized in robust system design include increases in transmitter power or antenna aperture, reduction in the symbol (information) rate, and various forms of diversity. Of course, these techniques can also be made adaptive. Another form of system architecture uses adaptivity (i.e., parameter flexibility) explicitly. An *adaptive* system exploits information about the propagation channel in order to adjust operational parameters actively. Such a process enables the best match to existing conditions and the delivery of optimal performance under a given set of conditions. Long-term propagation predictions can be used in the design of both types of systems, but short-term predictions (i.e., forecasts or nowcasts) are required in the case of adaptive systems.

In this chapter, we address the need for predictions of telecommunications performance, and we examine the relationships between short-term and long-term predictions. We examine the requirements for space weather data in Section 5.2, and we look at the elements of the prediction process in Section 5.3. A major segment of the chapter deals with organizational elements and the services available to the public. Section 5.4 deals with services that are operated under the aegis of government agencies, and Section 5.5 includes a sampling of commercial services. Complete systems used for forecasting are given in Section 5.6.

An estimation of telecommunication system performance is needed for military and commercial enterprises. Engineering approaches include examination of system attributes, as well as the environment within which the system must operate. The environment includes a number of things, not the least of which is the time-varying propagation medium. Propagation predictions are needed to limit the impact of this variability on system

operation. Predictions may rely upon natural laws of physics, which are capable of being described in theoretical terms, or they may be founded upon the trends and patterns seen in stored data, in which case the prediction method may be based upon climatological models. Predictions have improved over recent years as a result of four factors: (a) high speed computers, (b) advanced computational methods, (c) data dissemination and access technology and (d) the development of advanced sensors.

The advent of communication satellites has prompted a significant advance in our global perspective, especially valuable in weather forecasting and its affect on telecommunications. Satellites have provided a unique collection of scientific data that has supplemented our basic understanding of cause and effect. Radio methods for earth-space and terrestrial skywave telecommunications are clearly influenced by ionospheric phenomena in a manner that is dependent upon the frequency used. HF systems are vulnerable to the widest range of ionospheric effects, and the magnitude of HF propagation effects provides a good index of intrinsic ionospheric variability. Moreover, since the HF medium is so sensitive to ionospheric effects, a major component of ionospheric remote sensing technology has been dominated by HF probes and sounding systems. This is now changing with the advent of satellite sensors and hybrid methods employing data assimilation techniques. Predictions, whether based upon HF sensors or other methods, allow one to cope with propagation variability.

One of the elements that can promote relatively accurate short-term predictions of system performance involves the process of model updating by incorporating live data from sensors that probe the temporal and spatial regions of the path of concern. In the context of HF skywave propagation, any sensor or probe, which permits ionospheric characterization of the critical portions of the path, can be a very useful. Under disturbed conditions, forecasts can lose significance in less than an hour if information from the diagnostic probe is less than complete or if the probe is not in close proximity to the so-called "control point" (*i.e.*, within a few hundred kilometers).

- - -

Control Point Concept

Control point is a term that flows naturally from the mirror model of HF skywave propagation. In view of the fact that most of the refraction experienced by a reflected mode is in the neighborhood of the ray trajectory apogee, exclusive of any high-ray modes, convenience suggests that the control point should refer to the midpoint of the (presumed) great circle trajectory. Accordingly, midpath ionospheric properties that are reckoned at some appropriate height are assumed to control the propagation. Factors that will render the control point notion invalid include: strong tilts and gradients, dominance of the high ray, above-the-MOF modes, non-great-circle modes, and sundry scatter modes. Another difficulty is the azimuthal insensitivity of the control point approach, a fact that certainly affects the capability to associate data derived from nonorganic sounders with operational HF paths. This is especially troublesome when

the sounder path and the wanted path are virtually orthogonal, even when the control points are common (i.e., paths form a cross in plan view).

For transionospheric propagation, and especially measurements of the TEC using Faraday rotation or group-path-delay methods, we use the "mean ionospheric height" along the path to define a form of control point. The mean *height* $<h> = \int hNdh / \int Ndh$ is generally much higher than the F2 maximum height since the ionosphere is top-heavy. This "control point" concept, as applied to transionospheric propagation, while convenient, is not without its own idiosyncrasies.

Other factors may similarly affect forecasts. For instance, the update data from the probe is subject to its own built-in errors in scaling and its own imprecision in converting raw data into useful information. Nevertheless, it is possible, in principle, to prepare forecasts that are accurate and useful. We have previously noted that Kalman filters can be used to account for measurement errors, and lead to an optimal solution.

5.2 REQUIREMENTS

Practitioners of space weather disciplines are driven by a desire to improve upon the basic science and technology thereby enabling space weather effects to be better understood and predicted. The issue of user requirements is at the forefront of the current wave in space weather interest. Still, within the civilian sector, it is not well accepted that space weather is of vital importance to technological systems. This may be an educational matter, but it is also true that commercial activities are not prone to honestly state the extent to which space weather may impact the performance of systems they are trying to market or protect.

For systems in the VLF, LF, MF, and HF bands, such as long wave communication and navigation and short wave broadcasting, the need for space weather data is obvious. Moreover, for these disciplines the requirement for space weather assessment is not suppressed by the entities responsible for systems involved. But, for satellite systems, the space weather effects can sometimes be subtle. One thing is clear. Everyone agrees that there is a firm requirement for reliable and timely communication and navigation capability. Society depends upon these capabilities. However, some parties must be informed or reminded that these top-level system requirements depend upon a space environment that is not always cooperative. It would appear that the word is beginning to be heard judging from the worldwide interest in space weather.

The extent of space weather data usage is probably best documented by "hits" on relevant web sites, although such traffic does not distinguish between the curiosity seekers, scientists, and operational users. Therefore such information is only indicative of actual use, and is not conclusive.

The most profound impact on satellite systems is the total elimination of system functionality. The investment in satellite systems, military and civilian, is enormous and growing. The demise of a satellite system represents not only a loss in capability, but a capital loss as well. While the direct cause of any given satellite malfunction may be unclear, there is no question that solar disturbances have led to the loss of a number of satellites. While the matter is important, it is not the focus of this book. For the interested reader there is a general treatment of this subject by Carlowicz and Lopez [2002].

To gain a grasp of the requirements for space weather information in the context of transient impact upon radio systems, it is best to examine the various programs and efforts that are ongoing or proposed for the future. But first let is examine the relationships between prediction (a generic term) and forecasting, nowcasting and hindcasting.

5.3 ELEMENTS OF THE PREDICTION PROCESS

The term *prediction* has a rather elusive meaning, depending upon the nature of the requirement for knowledge about the future. In the case of the ionosphere, a distinction is made between long-term predictions and short-term predictions. Long-term predictions of ionospheric behavior may be based upon climatological models developed from historical records for specified solar and/or magnetic activity levels, season, time-of-day, geographical area involved, etc. In many models the only space weather driver is the running mean sunspot number. Quasi-theoretical models based upon first-principles physics have also been developed, but these may also depend upon the specification of constraints, boundary conditions, and driving parameters, some being similar to those used in climatological models. The drivers used by both classes of models may themselves be stochastic. Thus, at least two sources of error occur in long-term predictions, one arising because of an imprecise estimate of the driving parameter, such as sunspot number, and the second arising from ionospheric variability, which cannot be properly accounted for in the model. Given these difficulties, it may appear surprising that the process can yield useful results, and yet it often does. Long-term predictions are necessary in HF broadcast planning and in other spectrum management activities where significant lead times are involved. They are also needed for both satellite and terrestrial systems when planning for operations in the future. For example, advanced knowledge of scintillation in a particular operational area will allow satellite communication managers to develop mitigation strategies or provide alternate methods for data retrieval.

Short-term predictions involve time scales from minutes to days. The term *forecast* is sometimes used to describe those prediction schemes that are based on established cause-and-effect relationships, rather than upon simple tendencies based upon crude indices. In the limit, a short-term *forecast* becomes a real-time ionospheric assessment or a *nowcast.* In the context of

HF communications, real-time-channel-evaluation (or RTCE) systems, such as oblique sounders, may be exercised to provide a *nowcast*. Such procedures are useful in adaptive HF communication systems. The term *hindcast* is sometimes used to describe an *after-the-fact* analysis of ionospheric effects and system disturbances. Solar control data are usually available for this purpose, and this may be augmented by ionospheric observation data. Figure 5-1 shows the relationship between the various prediction epochs.

The error associated with any prediction method is critically dependent upon the parameter being assessed, the lead-time for the prediction, and other factors. One of the most important parameters in the prediction of the propagation component of HF communication performance is the maximum electron density of the ionosphere, since this determines the communication coverage at a specified broadcast (or transmission) frequency. Thus, the ability to predict the maximum electron density of the ionosphere, N_{max}, is a necessary step in the prediction of HF system performance if skywave propagation is involved. For satellite systems, the ability to derive the distribution of ionospheric inhomogeneities is critical in any evaluation of scintillation at a specified frequency. In general, any space weather sensor that can be used as a driver for improved modeling or forecasting of the ionospheric state is important. For both skywave systems at HF and earth-space systems at VHF and above, predictions can be based upon climatology, quasi-theoretical models, or a combination of methods. Forecasts can start with a baseline prediction followed by timely updates using information extracted from non-organic space weather diagnostics or by information derived from the system under test. Nowcasts of system performance may also be obtained by direct assessment of the system parameters.

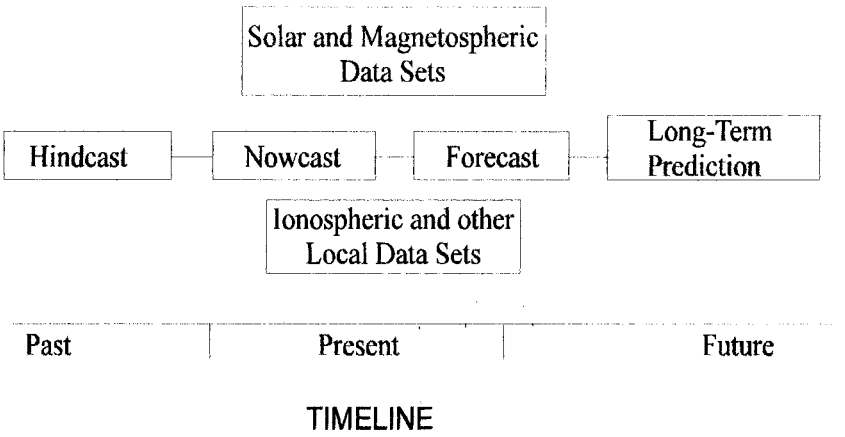


Figure 5-1: Relationships among prediction, forecasting, assessment, nowcasting, and hindcasting

5.4 ORGANIZATIONAL APPROACHES

5.4.1 Forecasting Services

Table 5-1 is a short list of organizations, typically agencies of government (with some exceptions), which are involved in space weather forecasting. In many instances the "products" that are derived from organizations in the table are free of charge and in the public domain (i.e., Internet web and anonymous FTP). By contrast, in Table 5-2 we list several commercial firms that sell advanced services to specified customers. These commercial services (i.e., tailored products) may be based upon (or leveraged by) information derived from organizations listed in Table 5-1. Accordingly the commercial firms have to make a strong case that what they offer is significantly "better" or more pertinent than the information that can be obtained (from the government) free of charge and without restrictions. See Section 5-5 for more information on this matter.

It is important that we recognize that there are an enormous number of organizations involved in space weather research as well as forecasting, most having a presence on multiple Web sites through hypertext linkages. The form and degree of involvement varies. For purposes of this book, and specifically this chapter, we filter the candidate organizations on the basis of the extent to which they are involved with the development of forecasting tools for telecommunication systems. This is an important step since a listing of every organization with involvement in space weather would require many pages, and would have dubious value in the context of telecommunications. Section 6.9 contains a listing of academic institutions, government agencies, private activities, and commercial firms involved in space weather.

Table 5-1 is a restricted list, since we only include organizations that provide operational services. The reader should not be too concerned if his favorite organization is not listed in Table 5-1. Not included are organizations primarily engaged in research and development (i.e., academia, NRL, AFRL, QinetiQ and DSTL, etc.), or its facilitation and funding (e.g., NSF, NASA, ESA, etc.). Major organizations are mentioned, if not discussed, in Section 5.6, which deals with stand-alone forecasting systems, and others are listed in Chapter 6, which deals with programs and resources. Since NRL, AFRL, QinetiQ, and DSTL have developed quasi-operational systems, we have included important examples, such as PROPHET, HF-EEMS, OpSEND, SCINDA, and C/NOFS.

Even with the specified constraints and limitations to Table 5-1, the explanation of which must be rather tedious to the reader, the resulting list may be incomplete. The field of space weather is vast and growing. Moreover, some basic research activities transition to operations in time. We apologize for any omissions. The logic we use is given in Figure 5-2.

In Table 5-2 we have listed a few non-government activities and commercial firms. Table 5-2 does not include many of the companies belonging to the Commercial Space Weather Interest Group (CSWIG) described in Section 5.5 since only a few of these offer services directly related to the effects of space weather on telecommunications. Following Tables 5-1 and 5-2 we shall discuss a number of the more important space weather service organizations and those involved in the development and use of forecasting and prediction systems.

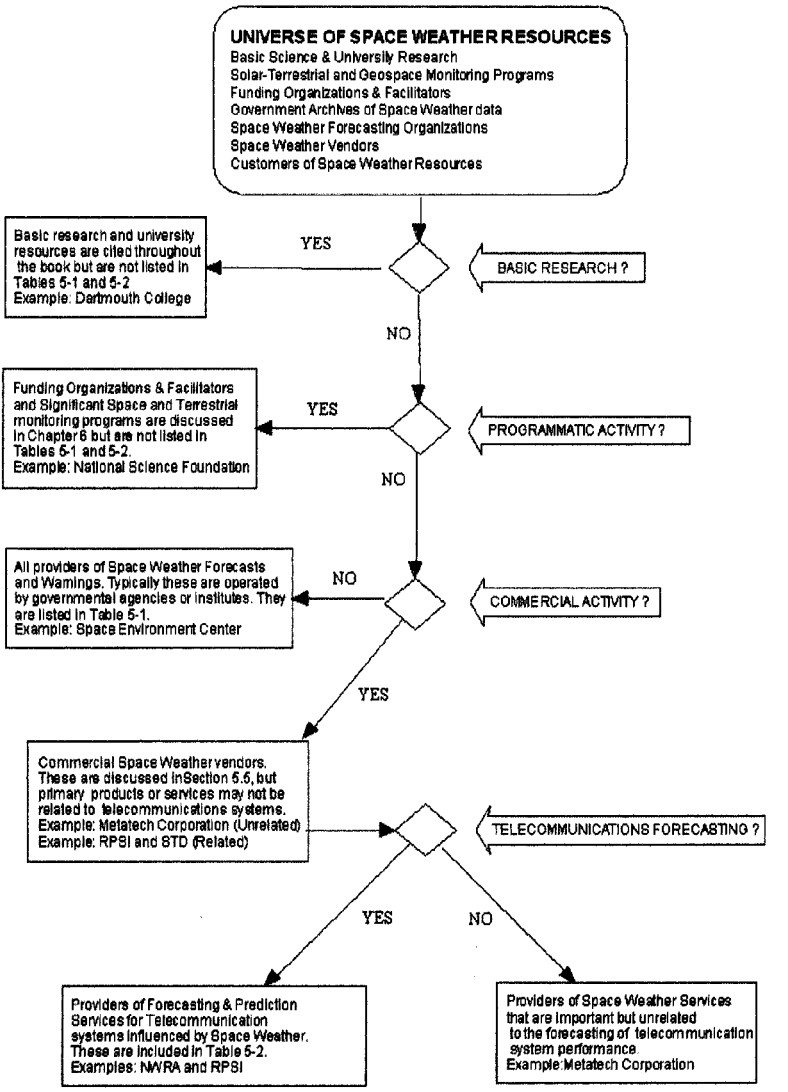


Figure 5-2: Flow Chart depicting the process, which categorizes various elements of the space weather constituency in the book.

We have deliberately avoided specification of the URL for organizational websites within this manuscript since these tend to be volatile, and specific links may become broken over time, or disappear altogether. Hopefully the reader can make use of his favorite browser to easily derive any URLs for sites that should be explored more fully. We apologize for any inconvenience, but it is unavoidable. (See Section 6.10 for a commentary on Internet resources.)

Table 5-1: Organizations involved in space weather observation and forecasting (Note: space weather observation specifically includes the ionosphere)

- International Space Environment Service (ISES)
- NOAA
  - Space Environment Center (SEC) of NOAA (also WWA)
  - National Geophysical Data Center of NOAA (NGDC)
- National Resources Canada (NRCan)
- Ionospheric Prediction Service (IPS-Australia)
- Jet Propulsion Laboratory (JPL)
- Rutherford-Appleton Laboratory (RAL)
- Institute of Communications & Navigation (DLR)
- RWC-Warsaw & IDCE
- Military services
  - Air Force Weather Agency (AFWA)

Table 5-2: Commercial firms offering space weather services for telecom systems. (Note: These firms typically provide selected tailored products and services using original methods and proprietary software, but may also reflect some of the data derived from organizations listed in Table 5-1.)

- Solar-Terrestrial Dispatch: (STD)
- Space Environment Technologies (SET)
- Northwest Research Associates: (NWRA)
- Radio Propagation Services, Inc.: (RPSI)

- - -

There are also international organizations such as the International Telecommunications Union Radio Sector (ITU-R), through its Working Groups, that may encourage certain "space weather" developments in member states during the course of developing radio regulations and recommendations. One such group is the Working Party 3L (dealing with ionospheric propagation). Other organizations include COSPAR, CEDAR, AGU, and URSI Commission G (Ionosphere) to name a few. Professional societies also play a role (viz., IEEE, IEE, and AFCEA). Again these activities will be covered adequately in Chapter 6.

5.4.2 International Space Environment Service

The International Space Environment Service (ISES) has the mission to encourage and facilitate near-real-time international monitoring and prediction of the space environment by the following:

1) Rapid exchange of space environment data
2) Development of standards for data observation and reduction
3) Uniform publication of observational data
4) Application of standardized products/services to assist users in reducing the impact of space-weather

The lineage of ISES is rather interesting. In 1928, The URSI Central Committee of URSIgrams was formed to promulgate the rapid exchange of scientific data. The International Geophysical Year (IGY) led to the formation of the International World Days Service in 1959. These two entities merged in 1962 to form the International URSIgram and World Days Service ((IUWDS). In 1996, the latter service was renamed the International Space Environment Service (ISES). It is organized under URSI in association with the International Astronomical Union (IAU) and the International Union of Geophysics and Geodesy (IUGG).

The following functions enable the mission of ISES to be accomplished:

1) International URSIgram & World Days Service
2) Preparation of the International Geophysical Calendar (IGC)
3) Monthly Spacewarn Bulletins

The URSIgram & World Days Service satisfies the requirement for rapid and free exchange of data. These data sets (including forecasts) are distributed through the Regional Warning Centers (RWCs). The IGC also provides a listing of so-called World Days, or recommended days for concentrated efforts by investigators, to encourage and facilitate collaboration. Information about various satellites and space platforms is provided in the Spacewarn Bulletins, and this data is useful in planning for measurements and conducting analyses. Figure 5-3 is the International Geophysical Calendar for the year 2004.

There are twelve Regional Warning Centers are distributed around the world, including a special one for the European Space Agency (ESA). They are given in Table 5-3. The RWC in Boulder, Colorado is a hub for data and forecast exchange, and it is called the World Warning Agency (WWA).

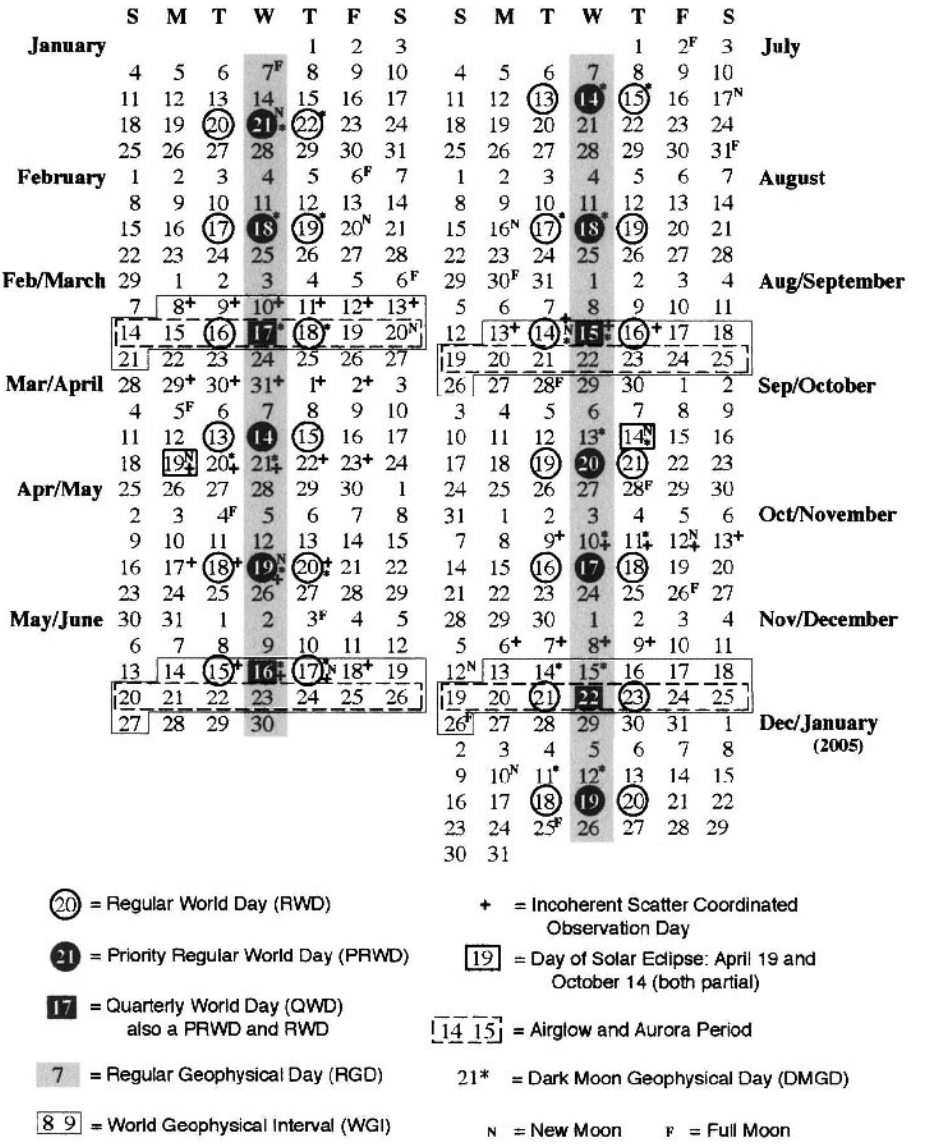


Figure 5-3: Geophysical Calendar for CY 2004, and into January of 2005. This form of calendar can be quite useful for scientific campaign coordination. Global predictions and services require global organization and collaboration. It is noted than many of the "World Days" fall on Tuesday-Thursday. From ISES sources.

Table 5-3: Regional Warning Centers

- Beijing (China)
- Boulder (United States)
- Brussels (Belgium)
- Lund (Sweden)
- Moscow (Russia)
- New Delhi (India)
- Ottawa (Canada)
- Prague (Czech Republic)
- Tokyo (Japan)
- Sydney (Australia)
- Warsaw (Poland)

Note: NOAA-SEC (i.e., RWC-Boulder) is the World Warning Agency (WWA)

- - -

5.4.3 NOAA

5.4.3.1 Space Environment Center

Within the United States, the Space Environment Center of NOAA is the primary source of space weather data. A discussion of the services that are provided by SEC is found in a paper by Joselyn [2001], and we make liberal use of the information in the text that follows. The Space Environment Center is a U.S. Government agency and is currently part of NOAA, which operates under the umbrella of the U.S. Department of Commerce. The Space Environment Center, a relatively small organization, is headquartered in Boulder, Colorado. Despite its size, SEC is at the epicenter of space weather forecasting and data dissemination to the civilian sector of society, and SEC is the official source of space weather alerts, warnings and forecasts within the United States. Table 5-4 is a list of milestones in the history of the forecasting leading up to the efforts at SEC. We have emphasized the telecommunication milestones. In 2004, SEC became part of the U.S. National Weather Service.

Propagation predictions, mostly based upon predictions of sunspot number several months in advance, were produced beginning in the 1950s. The National Bureau of Standards, the predecessor to SEC, published *CRPL Ionospheric Predictions* on a monthly basis, three months in advance. Meanwhile, in the Soviet Union, the Institute of Terrestrial Magnetism, Ionosphere, and Radio Propagation published the *Monthly Predictions of Radio Propagation*. The US Navy published HF communication predictions beginning in the 1960s. This document, *NTP6 Supp-1*, consisted of monthly predictions of optimum frequencies to be used for communication within coverage areas of the global complex of U.S. Navy Communication Area Master Stations (CAMS). It was prepared six months in advance based upon sunspot number predictions [Goodman, 1991]. As a result of imbedded

frequency management technology and the growth of automatic link establishment (ALE) systems, these kinds of long-term predictions are no longer very useful for operations.

5.4.3.1.1 NOAA Space Weather Scales

In the late 1990s, NOAA developed a set of so-called Space Weather Scales that provide some guidance in connection with various forms of solar-terrestrial disturbances. These are listed in Tables 5-5 through 5-7. These scales have educational benefit to be sure, but they also provide an efficient shorthand description for some rather complex phenomena. These standard scales are used in many of SEC's published products. While the reader is advised to peruse the NOAA web site for the full listing, we will restrict the discussion to these elements of concern to telecommunications (i.e., radio propagation) issues.

Table 5-4: Historical Milestones in Development of Forecast Services (With an emphasis on Telecommunications)

- 1913: International Commission on Scientific Radiotelegraphy
- 1919 and years following: International Union of Radio Science established (URSI)
- 1927: The CCIR was established
- 1930 and years following: URSIgrams were established
- 1932-33: International Polar Year (IPY)
- 1940s and following: Central Radio Propagation Laboratory (CRPL) of the National Bureau of Standards (NBS) supported propagation predictions
- 1940s: US Army Radio Propagation Unit (RPU) issued predictions for HF circuits
- 1954: Central Radio Propagation Laboratory of NBS moved to Boulder, Colorado
- 1957-58: International Geophysical Year (IGY)
- 1959: International World Days Service established
- 1962: International URSIgram and World Days Service established (IUWDS)
- 1962: Publication of NBS Handbook 90: *Handbook for CRPL Ionospheric Predictions based on Numerical Methods of Mapping* by S.M. Ostrow.
- 1964-65: International Year of the Quiet Sun
- 1965: Publication of NBS Monograph 80: *Ionospheric Radio Propagation* by K. Davies.
- 1960s (mid): CRPL reorganized itself with part of the organization remaining under NOAA, and another part becoming the Institute for Telecommunication Sciences (ITS), now under NTIA.
- 1965: Space Environment Center (SESC) begins daily service, in concert with the U.S. Air Force Weather Service
- 1967: SESC service becomes operational with full-time operation (24/7)
- 1970: NOAA is created within the U.S. DOC and SEC is incorporated
- 1990s: SEC User Conferences are convened (1990, 1994, 1998)
- 1990s: CCIR abolished and replaced by the Radio Sector under the International Telecommunication Union (ITU-R)
- 1996: IUWDS becomes International Space Environment Service. (ISES)
- 1999-2004: Space Weather Week conferences held (and continuing)

NOAA has developed three basic categories for which space weather scales are defined. They are:

- Geomagnetic Storms
- Solar Radiation Storms
- Radio Blackouts

The geomagnetic storm have been described earlier in the book and NOAA defines it as "disturbances in the geomagnetic field caused by gusts in the solar wind that blows by earth". While an elementary definition, it serves the purpose for public education. The *Geomagnetic Storms* category is probably the most important for modern telecommunication purposes. It enables the user to account for a host of phenomena that impact the operation of terrestrial communication and surveillance systems, satellite communication and navigation, and radar operations. The *Kp* index, a scale of choice for geomagnetic storms, is an important parameter in many models of the ionosphere, and especially those models that track storm time effects [Araujo-Pradere et al., 2002].

The *Solar Radiation Storms* category is also important in the realm of telecommunications, principally because of the association with polar cap absorption events, termed PCA. The PCA events can be a critical factor for commercial airlines that fly over the pole since HF connectivity is impaired during the event. This is a significant problem given the fact that most carriers do not have the capability for satellite communication (using geostationary assets) when a geographic latitude of 80 degrees is exceeded. Moreover, since PCA is a result of a solar radiation storm, there is an appreciable biological hazard.

Radio blackouts are mainly a factor for HF communication systems, HFDF systems, and HF radars. X-ray flares that originate on the surface the sun cause blackouts of short wave systems. NOAA uses the catastrophic term *blackout*, but there is a range of signal absorption amplitudes that can be disruptive, and this is a function of system margin. These events, whether characterized as blackouts or something less catastrophic, are associated with increases in the electron densities in the D-region (and lower E-region) of the ionosphere, where the electron collision frequency becomes elevated. This process leads to an attenuation of radiowave signals that pass through the region. If the events, which are typically short-lived, are significant enough, total blackout of communication can result. This kind of event only occurs on the sunlit side of the earth and is most pronounced near the sub-solar point. Details of this phenomenon are covered elsewhere in the book. NOAA also has a useful product linked to its "Today's Space Weather" site that provides an estimate of the amount of absorption introduced by a solar flare.

As indicated earlier, the NOAA scales provide a useful basis for characterizing the magnitude of effects introduced on specified systems.

They were never intended to be precise. One may use these scales to stipulate broad operational regimes based upon the level of impairment one might anticipate. This author finds the convenient relationships given in Table 5-5a, Table 5-6a, and Table 5-7a to be the most useful. It is interesting that a number of space weather vendors broadcast the NOAA scales as part of their tailored products.

Table 5-5a: Space Weather Scales for Geomagnetic Storms

Scale	Descriptor	*Kp* Value	Frequency
G5	Extreme	*Kp*=9	4 /cycle 4 days/cycle
G4	Severe	*Kp*=8 (including a 9-)	100/cycle 60 days/cycle
G3	Strong	*Kp*=7	200/cycle 130days/cycle
G2	Moderate	*Kp*=6	600/cycle 360days/cycle
G1	Minor	*Kp*=5	1700/cycle 900 days/cycle

Table 5-5b: Effects of Geomagnetic Storms from NOAA Scales

Scale	Effect on Telecommunications
G5	HF propagation conditions may be impossible in many areas for 1-2 days. Satellite navigation may be degraded for days and low frequency navigation can be out for hours. Aurora can descend to ~ 40 degrees geomagnetic.
G4	HF propagation and satellite navigation degraded for hours. Low frequency radio navigation disrupted. Aurora observed as low as 45 degrees geomagnetic.
G3	Some problems for satellite navigation and low frequency radio navigation. HF radio may be intermittent. Aurora may be observed as low as 50 degrees geomagnetic.
G2	HF radio difficulties at higher latitudes. Aurora may be seen as low as 55 degrees geomagnetic.
G1	No significant impact. Aurora visible at high latitudes only

Table 5-6a: Space Weather Scales for Solar Radiation Storms

Scale	Descriptor	Particle Flux Units (PFUs)	Frequency
S5	Extreme	10^5	<1 /cycle
S4	Severe	10^4	3/cycle
S3	Strong	10^3	10/cycle
S2	Moderate	10^2	25/cycle
S1	Minor	10^1	50/cycle

Table 5-6b: Effects from Radiation Storms from NOAA Scales

Scale	Effect on Telecommunications
S5	Complete blackout of HF communications in the polar cap is possible. Position errors will make navigation operations difficult.
S4	Blackout of HF communications in the polar region possible. Increased navigation errors over several days possible.
S3	Degraded HF communications in polar region and navigation position errors are likely.
S2	Some residual effects on HF and navigation systems in the polar region.
S1	Minor impact on HF radio in polar region.

Table 5-7a: Space Weather Scales for Radio Blackouts

Scale	Descriptor	X-Ray Flux	Frequency
R5	Extreme	X20 ($2 \cdot 10^{-3}$)	<1/cycle
R4	Severe	X10 (10^{-3})	8/cycle 8 days/cycle
R3	Strong	X1 (10^{-4})	175/cycle 140 days/cycle
R2	Moderate	M5 ($5 \cdot 10^{-5}$)	350/cycle 300 days/cycle
R1	Minor	M1 (10^{-5})	2000/cycle 950 days/cycle

Table 5-7b: Radio Blackouts Effects from the NOAA Scales

Scale	Effect on Telecommunications
R5	Complete HF blackout on the entire sunlit part of the earth for a number of hours. Low frequency navigation aids experience outages for many hours. Satellite navigation errors on the sunlit side of the earth for a number of hours.
R4	HF radio blackout on most of the sunlit part of the earth for most of the HF band for one to two hours. Outages of terrestrial navigation signals cause position errors for 1-2 hours. Minor disruptions in satellite navigation systems may occur on the sunlit side of the earth.
R3	Wide area blackout of HF communications for up to an hour on the sunlit side of the earth. Low frequency radio navigation systems are degraded for about an hour on the sunlit side.
R2	Limited blackout of HF communication on the sunlit side of the earth for tens of minutes. Some degradation of low-frequency navigation signals for tens of minutes.
R1	Weak or minor impact on the HF band on the sunlit side of the earth. Low-frequency navigation signals degraded for brief intervals.

Author Note-1: Geomagnetic storms may last more than one day. However the incidence of specified *Kp* values (determined 8 times/day) may be several times a day.

Author Note-2: Since a solar cycle is ~ 11 years, the number of days per cycle = ~ 4,015 days. Hence a G1 condition will arise 22% of the days. On the other hand, a G5 condition will occur only 0.1% of the days.

Author Note-3: These effect descriptors are only meant to be representative and are certainly incomplete for many systems. A detailed comparison of the specific system effects and the physical measurements (i.e. *Kp*) upon which the scales are based is certainly recommended.

Author Note-4: There are some system effects that are not mentioned. For example, the occurrence of satellite scintillation can depend upon the value of *Kp*. At high latitudes, magnetic storms tend to increase the amount and intensity of scintillation events.

Author Note-5: The satellite navigation referred to in the scales is not the GNSS (Global Navigation Satellite Systems) family of systems that operate at L-band (i.e., GPS, GLONASS, Galileo). Rather it corresponds to Transit-type systems that employed radio bands at 150 and 400 MHz. The U.S. Navy Transit constellation was the world's 1st operational satellite navigation system. Navigation services using Transit were suspended on Dec. 31, 1996.

Author Note-6: The low frequency radio navigation referenced (as distinguished from satellite navigation in G3, G4, and G5 above) is evidently the family of systems such the LORAN-C, DECCA and OMEGA. DECCA is a hyperbolic navigation system operating at 70-130 kHz and LORAN-C operates at 100 kHz. Recently LORAN-C operations were extended well into the 21st century. OMEGA navigation services at VLF were terminated on September 30, 1997. It is noteworthy that other navigational services such as TACAN, NDB, and VOR are operational, but none is thought to be affected by space weather influences (including ionospheric fluctuations). An exception might be solar radio noise bursts, but this would be a rare occurrence.

Author Note-7: The particle (i.e., proton) flux is measured in particles cm^{-2} sec^{-1}/steradian. For simplicity we sometimes use the term PFU to define the energetic particle flux level.

Author Note-8: Blackout conditions depend upon the level of energetic particle flux. NOAA reports an energetic particle event when the PFU level reaches 10, and it has been suggested that a PCA event is in progress when the PFU level reaches ~40. This would be in the S2 regime. It should be noted that the extent of blackout depends upon the path geometry and the exact frequency of propagation. Since PCA decreases as f^2, radio blackout at 3 MHz (the lowest part of the band) does not necessarily imply blackout at 30 MHz (the highest part of the band).

Author Note-9: The x-ray flux is expressed in Watts/m^2 and is measured in the band in the 1-8 Angstrom unit range (i.e., 0.1 – 0.8 nm).

- - -

5.4.3.1.2 Space Weather Operations of SEC (SWO)

One of the most important functions of NOAA-SEC is embodied in a Divisional structure called *Space Weather Operations*. It is an organization comprised of elements of AFWA (previously the 55th Space Weather Squadron of the U.S. Air Force) and NOAA. This Division came into existence in 1998. The composite SEC/SWO activity list is taken from Joselyn [2001] and paraphrased in Table 5-8.

Table 5-8: NOAA-SEC/SWO Activities

- Procuring solar & space environment sensors
- Operating solar and space environment sensors
- Data ingestion (from other agencies)
- Providing summaries of space environment conditions
- Providing alerts, warnings, and forecasts of environmental conditions
- Conducting focused research related to causes of space environment fluctuations
- Transitioning research into practical solutions (i.e., operational algorithms, etc.)
- Education of space environment users
- Promoting the development of a space weather vendor community

Within NOAA at large, the National Satellite and Data Information Service (NESDIS) maintains the GOES and POES satellites. GOES is comprised of two GEO satellites, one positioned over the Pacific Ocean and the other stationed over the Atlantic. Among other things, GOES monitors the x-ray flux from the sun. The POES system is a complement of two LEO satellites, both operating in high inclination orbits to monitor energetic particles at high latitudes. The orbital planes are separated by approximately ½ a day, so that they pass over the USA in the morning and evening.

NOAA also operates a solar x-ray imager, SXI, designed to provide high resolution, high cadence x-ray images of the sun. Such data is also derived from an instrument on the Japanese YOHKOH satellite. NOAA ingests data from the NASA Advanced Composition Explorer (ACE), which is located at the so-called L1 (i.e., Lagrangian) point, but NOAA is planning to deploy and operate its own monitor of solar wind properties (viz., GEOSTORMS).

Data ingestion is critical for the operation of a world-class forecast center. Part of this is embodied in cost sharing, or more properly – resource sharing. There are a number of national assets and international resources that cannot be ignored. For example, the U.S. Air Force, driven by its own military requirements, operates the Solar Optical Observing Network (SOON) and the U.S. Geological Survey operates the INTERMAGNET network of geomagnetic observation stations. The European Space Agency and NASA have teamed on the SOHO mission, and this platform consists of instruments such as the NRL's LASCO, which delivers information about solar disturbances and eruptions based upon NASA analysis.

There are a number of products and algorithms that are tested by NOAA-SEC. Those of clear relevance to telecommunications include the following:

- The Costello *Kp* Index
- The Fuller-Rowell STORM Model
- High Frequency Absorption Map

The Costello *Kp* Index Model is based upon a neural network solution to the problem of forecasting the magnetic *Kp* index [Costello, 1997; Detman and Joselyn, 1998]. The neural network "trains" on the *Kp* response to a number of solar wind parameters. The driver is solar wind data obtained at the L1 point, and as a result the Costello algorithm can provide forecasts of *Kp* with a lead-time corresponding to the propagation time required to cover the distance from L1 to the earth. Figure 5-4 shows a typical 7-day plot of the Costello *Kp* index compared with the U.S. Air Force estimate of *Kp* (typically used). A more useful plot is the 1-day version given in Figure 5-5, since it clearly exhibits the lead-time (i.e., forecasting) aspect.

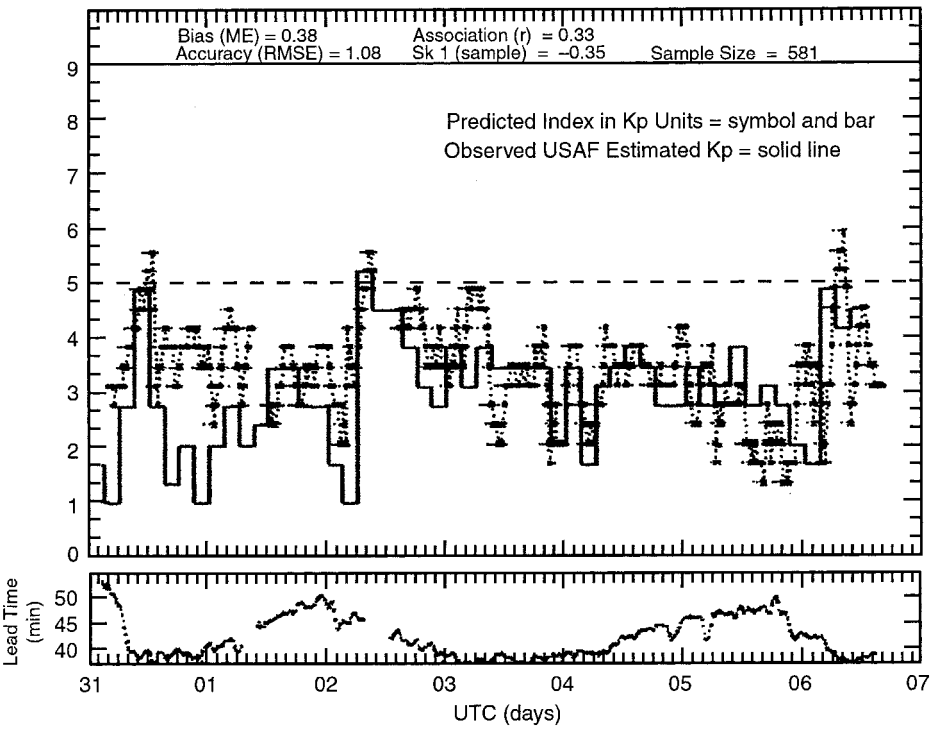


Figure 5-4: The Costello *Kp* Index forecast results for a seven-day period, obtained from the NOAA-SEC Web site. The raw estimates from the Costello algorithm are the dots, and the solid line gives the Air Force estimates of *Kp*. The bottom chart is the lead-time of the forecast. (Information from the Space Environment Center, Boulder, CO, NOAA, Department of Commerce.)

The STORM model developed by SEC is a new development that has the potential to be of great value for telecommunications forecasting. The development is well documented [Fuller-Rowell et al., 2000, 2001; Araujo-Pradere et al., 2002]. While there are a number of shortcomings, largely the result of an inadequate database of vertical incidence soundings upon which

the model is based, the model is certainly a step in the right direction. Given an estimate of *Ap* (or *Kp*) and its time history, one can estimate the global response of the F-region electron density to magnetic storms. The concept is based upon the notion that energy deposited during storms, and represented by magnetic activity indices, takes some time to accomplish redistribution. In general, the consequences of this redistribution, in terms of a departure of *foF2* from the mean, will depend upon geomagnetic latitude, time of day, season, and sunspot number. The results of the STORM model are employed, in modified form, in the development of the quasi-dynamic global frequency plan (i.e., active frequency table, or AFT) for the ARINC GLOBALink/HF system that supports data link communication for commercial aviation. This will be discussed later in the chapter. A sample tabular output of STORM model is given in Figure 5-6 for a significant storm period on October 29, 2003. An interesting feature on the STORM model site is a link to output for significant storms. Retention of these data is helpful for hindcasting purposes (i.e., post-analysis).

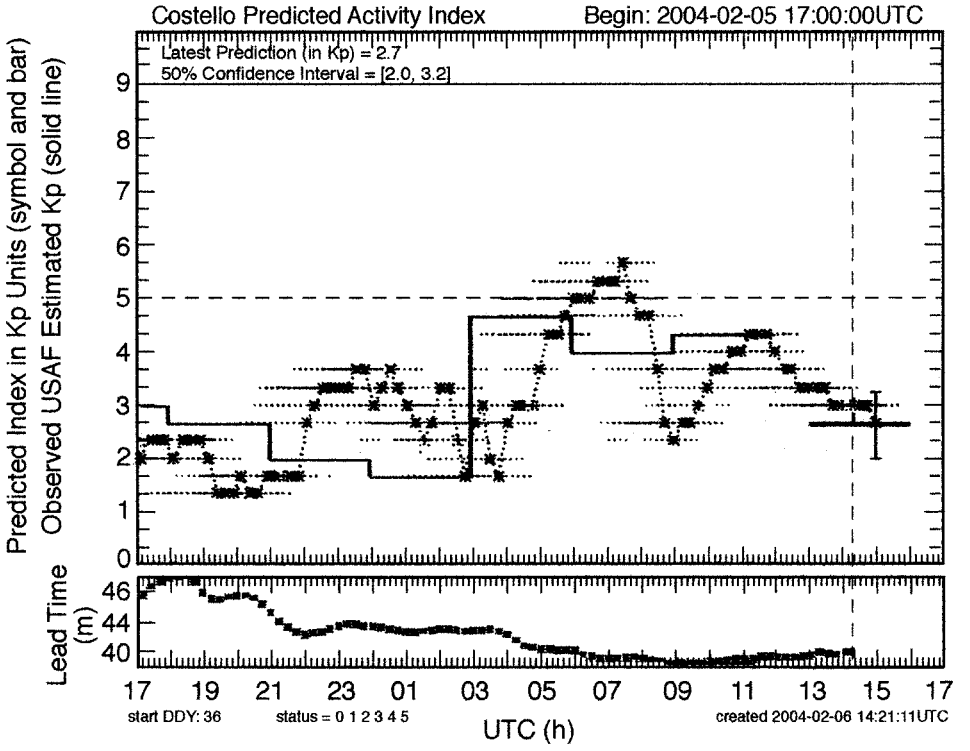


Figure 5-5: The Costello *Kp* Index forecast results for a one-day period, obtained from the NOAA-SEC Web site, by permission. The format is similar to Figure 5-3, except for the time frame. The latest prediction of *Kp* is 2.7 with a confidence interval of [2.0,3.2]. The lead-time is approximately 40 minutes. (Information from the Space Environment Center, Boulder, CO, NOAA, Department of Commerce.)

Prepared by the U.S. Dept. of Commerce, NOAA, Space Environment Center.
Please send comments and suggestions to sec.webmaster@noaa.gov
#
Label: Hap = 3 hour Planetary A Geomagnetic index updated hourly.
Label: int.ap = Integral of Planetary Ap Geomagnetic index over the
previous 33 values
Label: +70 = Correction factor at 70 N Geomagnetic latitude
Label: +50 = Correction factor at 50 N Geomagnetic latitude
Label: +30 = Correction factor at 30 N Geomagnetic latitude
Label: –30 = Correction factor at 30 S Geomagnetic latitude
Label: –50 = Correction factor at 50 S Geomagnetic latitude
Label: –70 = Correction factor at 70 S Geomagnetic latitude
Source: Hap is from USAF Hourly Magnetometer Analysis Report
Missing Data: linearly interpolated: 0 = not interpolated
#
STORM Time Empirical Ionospheric Correction Model
#

# UTC	Hap	int.ap	+70	+50	+30	–30	–50	–70	interpolated
0	24	320.6	1.05	1.04	1.03	1.00	1.00	0.98	0
1	24	330.0	1.05	1.04	1.03	1.00	1.00	0.98	0
2	20	341.6	1.05	1.04	1.04	1.00	0.99	0.97	0
3	26	347.3	1.04	1.04	1.04	1.00	0.99	0.97	0
4	25	351.8	1.04	1.04	1.04	1.00	0.99	0.97	0
5	23	356.1	1.04	1.04	1.00	1.00	0.99	0.97	0
6	15	359.4	1.04	1.04	1.04	1.00	0.99	0.97	0
7	224	358.0	1.04	1.04	1.04	1.00	0.99	0.97	0
8	317	499.6	1.00	1.01	1.05	0.98	0.95	0.94	0
9	400	772.9	0.93	0.97	1.07	0.95	0.88	0.88	0
10	364	1065.6	0.86	0.92	1.10	0.92	0.82	0.83	0
11	231	1260.5	0.81	0.90	1.11	0.90	0.78	0.80	0
12	195	1218.7	0.82	0.90	1.11	0.91	0.79	0.80	0
13	182	1130.9	0.84	0.92	1.10	0.92	0.81	0.82	0
14	143	1149.4	0.84	0.91	1.10	0.91	0.80	0.81	0
15	155	1333.2	0.80	0.89	1.11	0.90	0.77	0.78	0
16	173	1613.3	0.75	0.86	1.13	0.87	0.72	0.74	0
17	155	1899.2	0.70	0.83	1.15	0.85	0.68	0.70	0
18	131	2109.0	0.67	0.82	1.16	0.83	0.65	0.67	0
19	188	2226.0	0.66	0.81	1.16	0.83	0.64	0.66	0
20	293	2334.8	0.64	0.80	1.16	0.82	0.62	0.65	0
21	382	2522.6	0.62	0.80	1.17	0.81	0.61	0.63	0
22	324	2790.6	0.60	0.79	1.18	0.79	0.59	0.61	0
23	353	2998.6	0.59	0.78	1.18	0.78	0.57	0.59	0

Figure 5-6: Tabulation of the output from the Storm model for October 29, 2003. This is found on the SEC listing of significant geomagnetic storms in 2003. The integrated *ap* (the linear version of *Kp*) is seen to grow from a value of 320 to 2998 over the course of the day. This leads to erosion in the *foF2* "multiplier" values for all listed geomagnetic latitudes except 30° N, where the values of *foF2* tend to increase with respect to the long-term median values. These data can be useful in methods for adapting climatological models of the F2 region to reflect the likely distortions introduced by ionospheric storms. (Information from the Space Environment Center, Boulder, CO, NOAA, Department of Commerce.)

With respect to the ramifications of x-ray flares on HF systems, the NOAA-SEC web site permits access to a special *D-Region Absorption Page* (Figure 5-7). There is also a tabular representation that is perhaps more helpful if not as picturesque. D-region absorption is of primary importance to HF communication and surveillance systems. The SEC absorption map published by NOAA indicates the importance of the solar zenith angle (i.e., the subsolar point) in determination of the frequency dependent attenuation. The absorption maps can be quite dramatic, especially for X-category flares. However, from a systems perspective, flare-induced absorption events may not be very important in terms of the attenuation they introduce. This is true if the system response time is equal to or greater than the event duration.

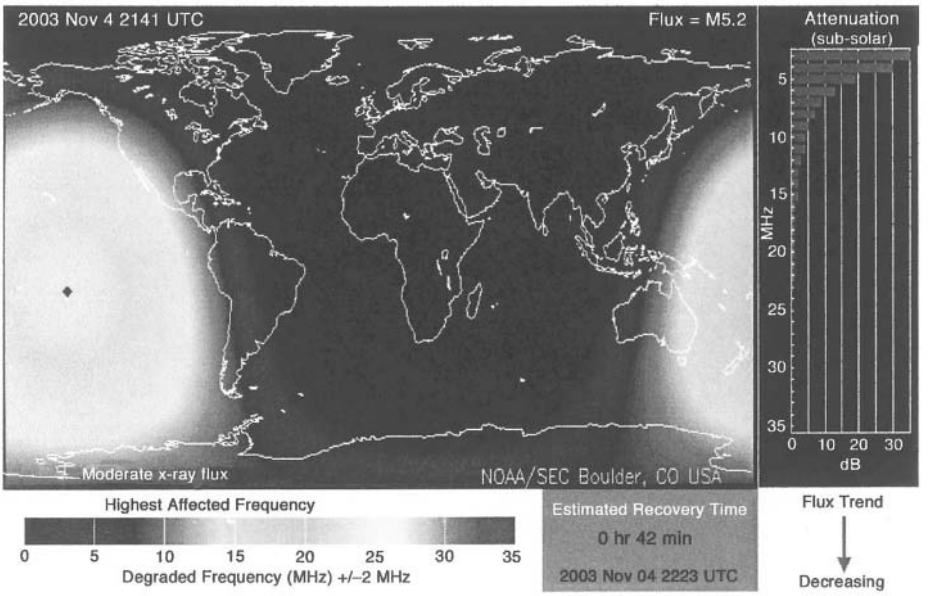


Figure 5-7: Map of D-region absorption based upon GOES X-Ray flux, displayed on the SEC web site. Refer to Chapter 3 for more details on absorption. The original graphic was in color Information in this figure is from the Space Environment Center, Boulder, CO, NOAA, Department of Commerce.

5.4.3.1.3 The NOAA-SEC Web Products

For the public, and certainly for the space weather vendor community, the face if SEC is seen through its web site on the Internet. (Again, one may locate the home page for SEC through use of any good browser.) Most of SEC products, as well as data from other space weather partners, are posted on the SEC web site or are linked to the web site. It will be impossible and unnecessary to go through all of the links to SEC products.

We shall restrict ourselves to those links that appear most pertinent to radio telecommunications. We find that the main SEC web site provides links to *Space Weather Now* and *Today's Space Weather*, two sites of some interest regarding telecommunications.

Space Weather Today is an important site for telecommunications specialists. There is an enormous amount of educational as well as scientific information and data housed at the site. There are the usual sets of solar data that may be somewhat obscure in direct application, but there are a number of items that are of relevance. For example there is a 3-day Solar-Geophysical Forecast. A sample is provided in Figure 5-8. There is also a plot of the GOES *Solar X-ray Flux* (Figure 5-9) and the *Satellite Environment Plot* (Figure 5-10). These items provide important information that is needed in the process of forecasting telecommunication behavior, or in understanding events that have already occurred (i.e., hindcasting). There is access to a variety of data from the main site, including *Space Weather data on SEC's FTP server.*

The SEC Anonymous FTP Server has links to a treasure trove of data. Of special interest telecommunications specialists is the near-real-time ionospheric data found by clicking first on *Lists of Solar Geophysical Data* and then on *Ionospheric Data-Daily Files by Station* or *Ionospheric Data-Monthly files by Station.* Table 5-9 indicates the sort of information to be found, although we have eliminated some of the specialized parameters. Table 5-10 is a list of the stations for which data may be extracted. Some forecasters have taken advantage of this FTP access to update global ionospheric models. This will be discussed later on in the chapter.

Table 5-9: Ionospheric Data obtained from the FTP Site

Parameter	Units	Notes
foF2	MHz	F2 region critical frequency (O-ray)
foEs	MHz	Es layer critical frequency (O-ray)
foE	MHz	E region critical frequency (O-ray)
M(3000)F2	Ratio	*MUF(3000)F2/foF2*
YF2	km	F2 region semi-thickness
hmF2	km	F2 maximum layer height
TEC	10^{16} electrons/m^2	Total electron content

Table 5-10: List of Sounder Stations on the NOAA-SEC FTP Server

Ascension	MacQuarue_Is
Ashkhabad	Madimbo
Athens	Magadan
Beijing	Manzhouli
Brisbane	Millstone_Hill
Camden	Mundaring
Canberra	Narssarssuaq
Casey	Norfolk_Is
Chongqing	Okinawa
Christchurch	Osan
College	Port_Moresby
Darwin	Pt_Arguello
Dixon	Qaanaaq
Dyess	Ramey
Eglin	Rome
Fairford	Salekhard
GooseBay	San_Vito
Grahamstown	Scott_Base
Guangzhou	Sondrestrom
Hobart	Townsville
Juliusruh	Vanimo
Kokubunji	Wakkanai
Ksalmon	Wallops
Learmonth	Warsaw
Louisvale	

The reader is advised to fully explore the SEC site. Another area of interest to users consists of companion links to *All Online Data at SEC*. Real-time data and results from algorithms such as the Fuller-Rowell STORM model and the Costello *Kp* index model discussed in Section 5.4.2.1.2 are easily accessible. Another model that is important for predicting magnetic storm activity from solar wind information is the Wang-Sheeley model. (There is an easy access to reports and summaries, and there are also some *read-me* files of interest.) For telecommunication specialists, click on the *Navigation* and *Radio* hyperlinks to obtain a limited discussion of these topics. The NOAA-SEC site also provides a number of tutorials as well as a glossary of terms.

Joint USAF/NOAA Report of Solar and Geophysical Activity SDF Number 036 Issued at 2200Z on 05 Feb 2004	
Analysis of Solar Active Regions and Activity from 04/2100Z to 05/2100Z	
IA. Solar activity has been low. There have been several B and low-level C-class x-ray flares observed during the last 24 hours. The events were associated with Regions 547 (S08W70), 549 (N14E04), and 552 (S08W20). The largest region on the visible disk is Region 551 (S06E26). This beta group has a 21 sunspot count and is currently over 200 millionths of white light area coverage. A new region was numbered today as Region 553 (S05E01).	
Solar Activity Forecast	
IB. Solar activity is expected to be low. There is a slight chance for an isolated M-class event from Region 549 and 551.	
Geophysical Activity Summary 04/2100Z to 05/2100A	
IIA. The geomagnetic field has been at quiet to active levels. The greater than 2 MeV electron flux at geosynchronous orbit was at high levels today.	
Geophysical Activity Forecast	
IIB. The geomagnetic field is expected to be predominately quiet to unsettled. Isolated periods of active conditions are possible for 06 February.	
III. Event Probabilities 06 Feb to 08 Feb	
Class M Class X Proton PCAF	25/25/25 01/01/01 01/01/01 green
IV. Penticton 10.7 cm Flux	
Observed Predicted 90 Day Mean	05 Feb 106 06 Feb to 08 Feb 105/105/110 05 Feb 120
V. Geomagnetic A Indices	
Observed Afr/Ap 04 Feb 012/015 Estimated Afr/Ap 05 Feb 015/015 Predicted Afr/Ap 06 Feb to 08 Feb 010/015-010/010-010/010	
VI. Geomagnetic Activity Probabilities 06 Feb to 08 Feb	
A. Middle Latitudes	
Active Minor storm Major-severe storm	25/25/25 10/10/10 01/01/01
B. High Latitudes	
Active Minor storm Major-severe storm	35/30/30 25/20/20 10/05/05

Figure 5-8: Sample of a Joint USAF/NOAA Report of Solar and Geophysical Activity. Original printout reformatted for added clarity. Information from the Space Environment Center, Boulder, CO, NOAA, Department of Commerce.

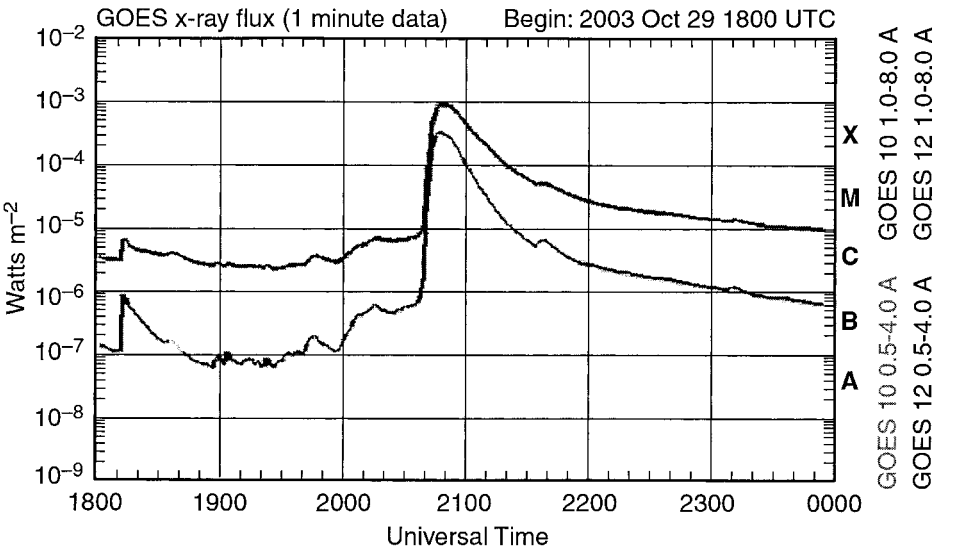


Figure 5-9: X-Ray Flux derived from GOES displayed on the SEC website. The flare depicted was one of the more significant X-category flares during the "Halloween" storm period. Data exhibited in this plot are extracted from GOES 10 and 12. The bands monitored are 1-8 Angstrom units and 0.5-4 Angstrom units. 10 Angstroms = 1 nm or 10^{-9} meters. NOAA-SEC issues alerts at the M5 level and X1 levels. Information from the Space Environment Center, Boulder, CO, NOAA, Department of Commerce.

There are several NOAA satellite systems of importance to telecommunications and the forecasting of effects on systems. One is sun-looking and two are earth-looking. They are GOES (already discussed), POES and TIROS. As indicated above, the GOES system is an important instrument for telecommunications since it provides solar X-ray flux information upon which Short Wave Fade (SWF) assessments may be derived. In addition, large flares are often associated with energetic particle events and/or coronal mass ejections (CMEs). Thus, large flares can be the precursors to magnetic storms, although many storms are not associated with flares. Other NOAA instruments of importance include POES and TIROS. The POES consists of a pair of polar-orbiting satellites that monitor energetic particles at high latitudes, and TIROS (NOAA-16) provides information on auroral electron precipitation in both the Northern and Southern Hemispheres. A NASA satellite, ACE, provides data, ingested by NOAA, to investigate the Interplanetary Magnetic Field (IMF). Indeed the ACE data is used by NOAA in its Costello *Kp* algorithm and test product (See Figures 5-4 and 5-5).

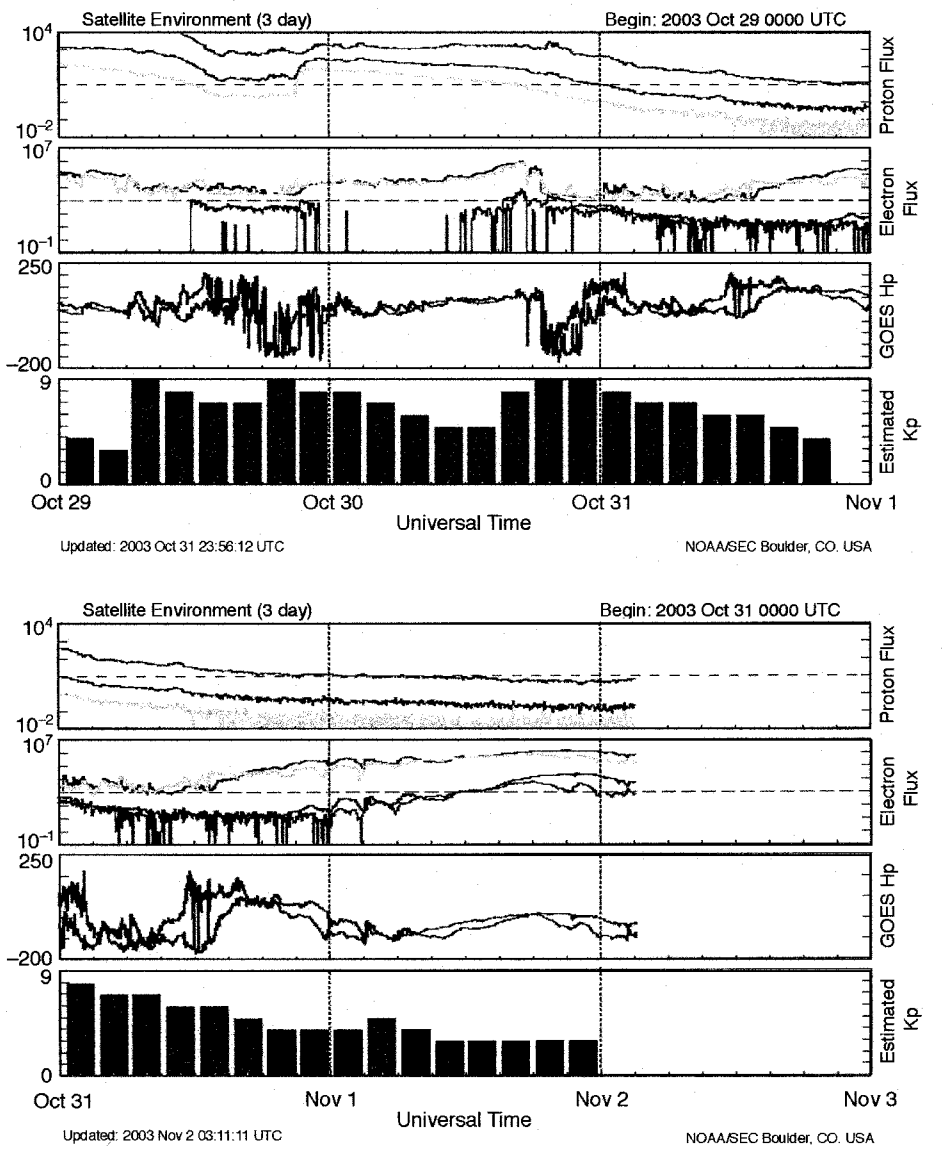


Figure 5-10: Satellite Environment data obtained from the SEC website for the "Halloween" storm 2003 period. The original was color-coded. The topmost plot indicates the energetic particle flux (protons/cm^2-sec-steradian=pfu). An Energetic Particle Event is "called" when the flux equals 10 pfus. Typically one finds that Polar Cap Absorption Events (PCAs) occur in the lower half of the HF band when the flux exceeds ~40 pfus. The bottommost plot gives the *Kp* value estimated by the U.S. Air Force. Information from the Space Environment Center, Boulder, CO, NOAA, Department of Commerce.

Figure 5-11 contains two statistical displays of the auroral oval during an undisturbed period on July 06, 2004. These displays of the ovals in both hemispheres, are derived from POES data (i.e., NOAA-16).

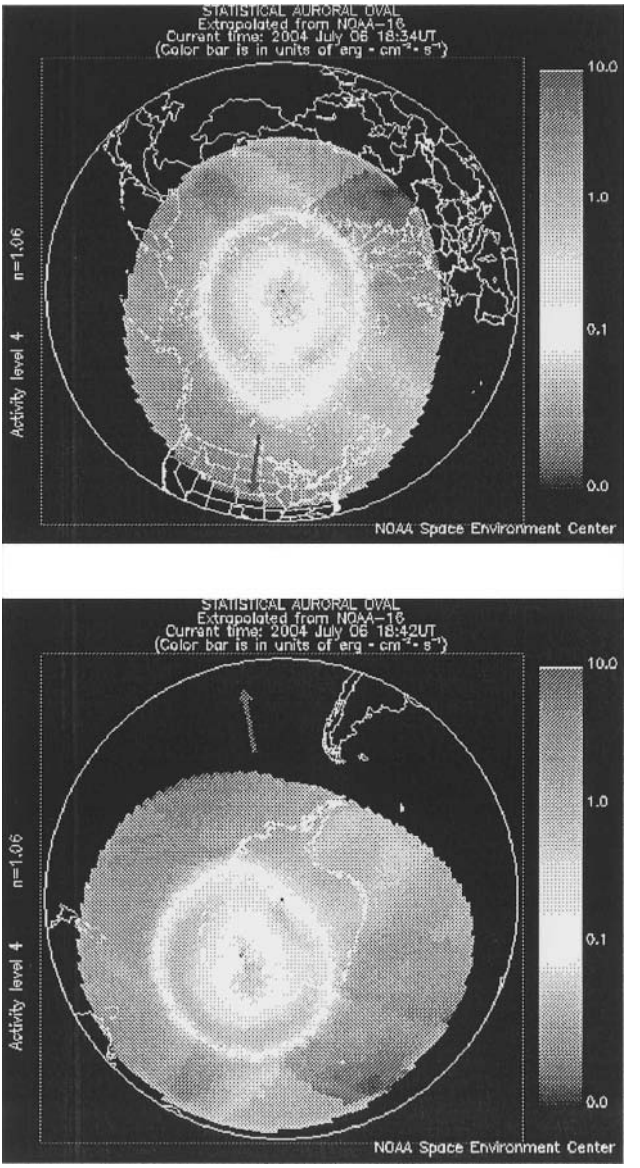


Figure 5-11: Statistical displays of the auroral oval during an undisturbed period on July 06, 2004. Northern Hemispheric (top) and Southern Hemispheric (bottom) data are derived from most recent passes of NOAA/POES. Original plots were in color. Information from the Space Environment Center, Boulder, CO, NOAA, Department of Commerce.

Figure 5-12 is a product from the website of NWRA. It shows the NOAA-TIROS auroral boundary, and is based upon data from SEC. It corresponds to the "Halloween" storm 2003 period, and clearly shows the rapidly changing position of the equatorward boundary of the auroral oval. Both Northern and Southern Hemispheric data are superimposed to derive a composite picture.

Figure 5-13 is an output from POES for the solar proton event of July 15, 2000. All three of the data sets, as represented by Figures 5-11 to Figure 5-13, are useful in the estimation of telecommunication effects. Knowledge of the auroral oval position, from Figures 5-11 and 5-12, is important in determination of the regime of propagation. For example, if the control point for HF communication is sufficiently equatorward of the auroral boundary, but not within the trough region, we can generally regard the propagation path as mid-latitude in nature irrespective of the locations of the receiver or transmitter. If the control point is poleward of the oval, then the path tends to approximate a polar environment. If the control point is within the oval then we must consider auroral effects when evaluating the communication properties. This is a classical registration problem. We must always be mindful where the control points are located in a dynamic environment. It is critical that we get the physics right, given that the mid-latitude region, high-latitude trough, auroral zone, and polar cap are distinctly different in the way they interact with radio waves.

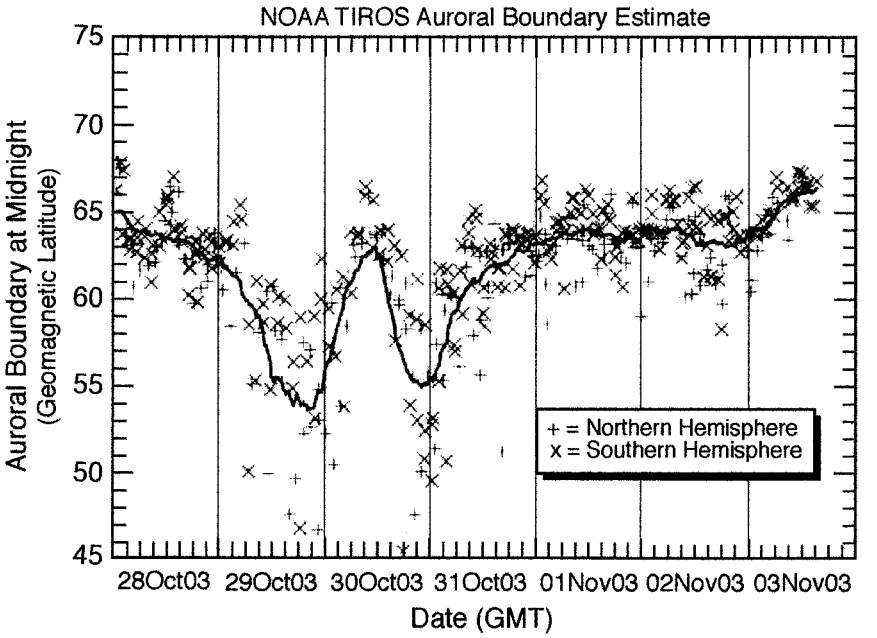


Figure 5-12: The auroral boundary estimate derived by Northwest Research Associates], based upon data from the NOAA TIROS satellite, provided by SEC. The 'Halloween" storm period of 2003 is depicted. From NWRA, by permission.

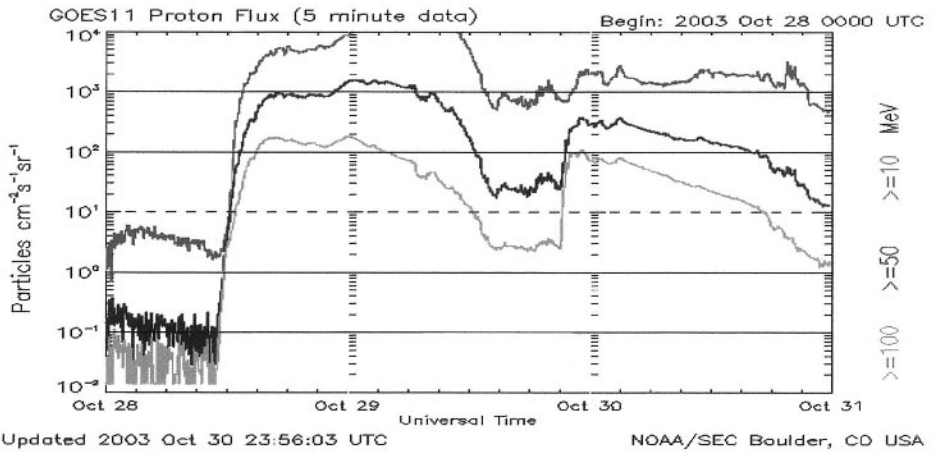


Figure 5-13: Output from GOES-11 for the solar proton events of October 28-30, 2003. Information from the Space Environment Center, Boulder, CO, NOAA, Department of Commerce.

5.4.3.2 National Geophysical Data Center

The National Geophysical Data Center (NGDC), is a one of several data centers operating under NOAA's National Environmental Satellite, Data, and Information Service (NESDIS). The NGDC is in charge of geophysical and environmental data from the sun's surface to the earth's core. There are more than 60 types of data found in the NGDC archives. The types of data of interest to space weather practitioners are mostly found under the heading "Solar-Terrestrial Physics" (STP). The following STP data types are conveniently catalogued by NGDC in Table 5-11. We shall examine a few of these data types. It is also worth noting that NGDC has a Space Physics Interactive Data Resource, called SPIDR (on the Web).

Table 5-11: Types of STP Data Cataloged by NGDC

- Solar & Upper Atmosphere: Data associated with solar activity and the upper atmosphere
- Ionosphere:
- Geomagnetism: Ground-based data about the geomagnetic field
- GOES SEM: X-ray, energetic particle, and magnetic field measurements from geosynchronous satellite platform
- GOES SXI: X-ray Images of the sun
- NOAA POES: Energetic particles from polar orbiter
- DMSP: Energetic particles from Defense Meteorological Satellite

Let us take a look at the ionospheric data that may be obtained from the NGDC archives. The most important data set is derived from ionospheric vertical incidence sounders. Digisonde and earlier analog equipments provide the main source of data. The Digisonde was developed by University of Massachusetts at Lowell, and has been procured by the U.S. Air Force and other agencies and institutions. Data from the Dynasonde system, an advanced sounder developed by NOAA, is also available on the site. There is an ionospheric digital database, available on CD-ROM that covers 40,000 station months from 130 sites around the world for the period 1957-1990. This is primarily useful for studies, such as the development of neural network algorithms for forecasting. However it is also possible to access data online. The SPIDR system has been mentioned as a convenient method for data access.

A *Real-Time Ionograms* page enables access to a number of current ionograms. Table 5-12 gives the list that is available as of February 15, 2004. This list does change from time to time. Some ionograms include scaled values and some do not. Figure 5-14 is a sample ionogram obtained from Dourbes on 15 February 2004. The original is color-coded, but one can clearly see from the B/W version the one-hop and two-hop characteristics, as well as the O-mode and X-mode features.

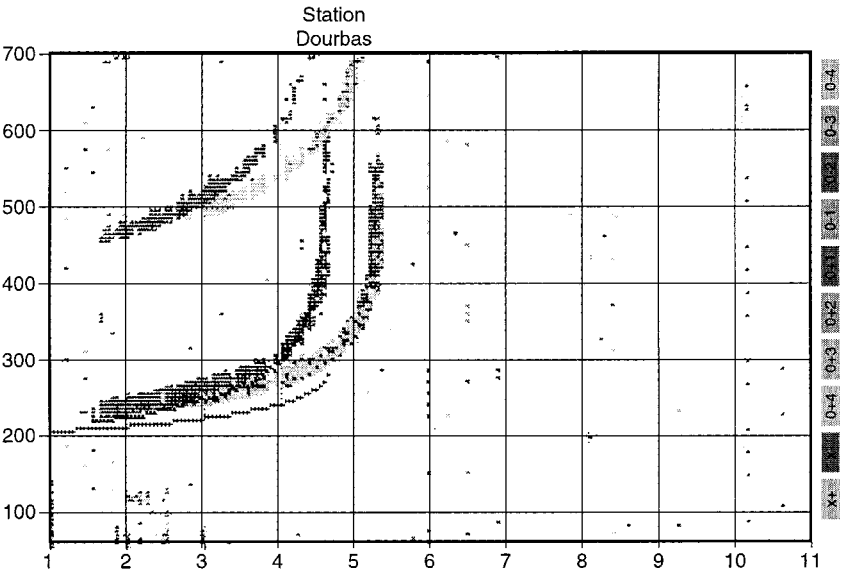


Figure 5-14: Ionogram from Dourbes. This was obtained from the NGDC Anonymous FTP server. The O- and X-modes for both the first and second hops are clearly seen. The electron density profile obtained by "inverting" the ionogram is also exhibited. The ionogram is obtained at 1900 UTC at which time the sun has already set at Dourbes. Therefore neither the E nor the F1 layers can be observed. The Maximun Usable Frequency (for a skip distance of 3000 km) is 14.68 MHz. Hence, with $foF2$ = 4.6 MHz, then M ~ 3.19. (Information from the National Geophysical Data Center of NESDIS, Boulder, CO, NOAA, Department of Commerce.)

Table 5-12: Near-Real-Time Sounding Data on NGDC Site

Station	Latitude	Longitude	Scaled	Restricted
Dourbes	50.1 N	4.6 E	Yes	No
Wallops Island	37.9 N	284.5 E	Yes	Yes
Millstone Hill	42.6 N	288.5 E	Yes	No
Gakona	62.4 N	215.0 E	Yes	No
Chilton	51.6 N	358.7 W	Yes	No
Port Stanley	51.6 S	302.1 W	Yes	No
Tromso	69.6 N	19.2 E	No	No
Uppsala	59.9 N	17.7 E	No	No
Kiruna	67.8 N	20.2 E	No	No
Lycksele	64.5 N	18.6 E	No	No
Okinawa	26 N	128 E	No	No
Kokubunji	36 N	139 E	No	No
Wakkanai	45 N	141 E	No	No
Yamagawa	33.2 N	130.4 E	No	No
Christchurch	43 S	172 E	No	No
Bear lake	55.2 N	96 W	No	No

Note-1: Wallops Island is part of the U.S. Air Force DISS network, and there is a restriction on access to the latest ionogram. The ionograms with scaled data are the easiest to interpret.
Note-2: The sounders providing autoscaled data are University of Massachusetts-Lowell instruments called Digisondes. (Information from the National Geophysical Data Center of NESDIS, Boulder, CO, NOAA, Department of Commerce.)

5.4.4 RWC Canada (NRCan)

Natural Resources Canada (NRCan) is the ISES Regional Warning Center for Canada. The Canadian Space Weather Forecast Center in Ottawa is operated by NRCan with support from the Canadian Space Agency. The RWC Canada provides forecasts for three Canadian zones: subauroral, auroral, and polar cap. There are three versions: (1) a simple graphical map giving predicted geomagnetic activity 6 hours in advance; (2) a chart showing magnetic field strength variation in nanotesla (nT) for the recent past and projected into the near future; and (3) a chart providing a review of magnetic activity and forecast up to 24 hours ahead. Figures 5-15 and 5-16 exhibit products (1) and (3) respectively. These products are especially useful for telecommunication nets in the North American sector.

By virtue of the high latitude location of Canada, there are unique opportunities for investigation of ionospheric effects and coupling of the ionosphere with the magnetosphere and solar wind. Observatories in Canada include many ground-based systems, including radars, magnetometer arrays (i.e., CANOPUS), vertical sounders, and optical instrumentation.

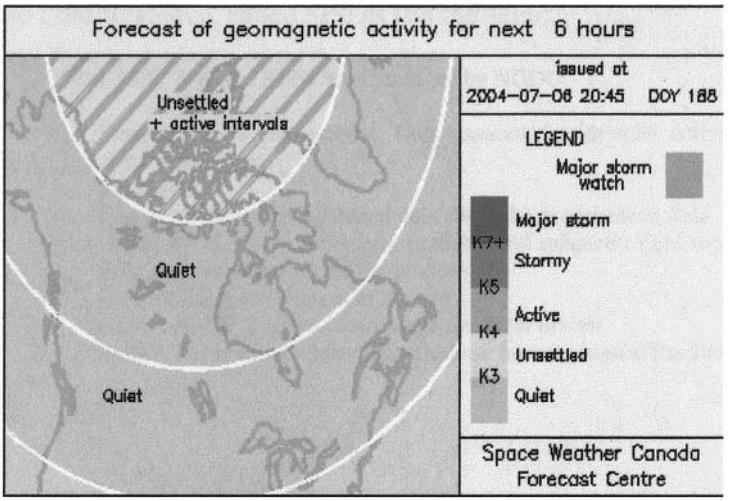


Figure 5-15: Forecast of geomagnetic activity for the next 6 hours. Chart is provided courtesy of David Boteler, Geomagnetic Laboratory, Natural Resources Canada, NRCan

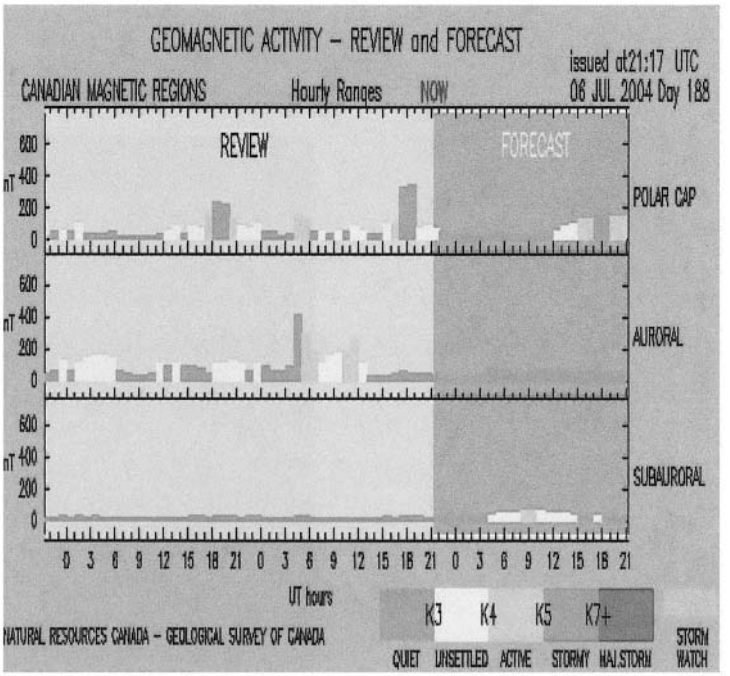


Figure 5-16: Magnetic Activity Review and Forecast. This chart is provided courtesy of David Boteler, Geomagnetic Laboratory, Natural Resources Canada, NRCan.

5.4.5 RWC Australia

The IPS Radio and Space Services (IPS) is under the Australian Space Weather Agency, and is a Regional Warning Center under ISES. The Ionospheric Prediction Service (IPS) has links to most relevant activities involving space weather. It also stresses many aspects of telecommunication impairment. Not unlike SIDC, discussed below, we find that IPS has provided convenient links to data in the following categories:

- Solar conditions
- Geophysical conditions
- HF propagation conditions
- Ionospheric conditions
- Total Electron Content (TEC) conditions

Data sources under the aegis of IPS include:

- Network of ground-based sounders in Australia and surroundings (Australasia) and Antarctica.
- IPS + Australian Geological Survey magnetometers
- Learmonth Solar Observatory (joint with USAF)
- Culgoora Solar Observatory

IPS hosts INAG, the Ionosonde Network Advisory Group. This is Working Group-1 of the URSI Commission G (on the ionosphere) and has the following responsibilities:

- Collecting information on ionogram analysis methods
- Maintenance of conventions for ionogram analysis
- Providing a forum for discussion of issues
- Preservation of the global ionospheric climatology

The World Data Center for Solar Terrestrial Science (WDC-STS) is operated by IPS, and the WDC-STS is located in Sydney, Australia. As would be expected, the WDC is the archive for solar and ionospheric (i.e., ionosonde) data. It also operates a node for the NOAA-SEC SPIDR system.

For purposes of this book, IPS has provided one of the more useful aggregate sites for practitioners of HF communications. In fact, when IPS was formed in 1949, the service was mainly interested in HF systems. To this day, Australia has a major dependence and investment in HF systems, and IPS has developed a number of products to support HF communication, surveillance, and radar systems. Since HF skywave propagation depends heavily upon the ionospheric electron density distribution, IPS has developed a network of sounders to measure ionospheric parameters in near-real-time. But IPS does not stop with Australasia. For example, real-time ionospheric maps are available for the North Atlantic, United States, Europe, as well as Australasia.

It is noted that the preferred solar index at IPS is the so-called T-index, based on the ionospheric response to solar activity. It is used as a proxy for the International Sunspot Number, and many argue that it is a better parameter to drive median models than the sunspot number. Real-time maps of the T-index are available on the IPS Web site, and these maps indicate how the solar activity would have to vary over the region of interest to make the median (climatological) maps of *foF2* match the (observed) *foF2* contours computed from real-time sounder observations. Real time *foF2* maps are also available for the Australian region, Asia, Europe, North America, and the North Atlantic. These maps are produced using the worldwide database of vertical incidence sounder data referred to earlier.

Hourly Area Prediction (HAP) charts are also produced for specified stations. These charts indicate the optimum frequency for communication in the HF band over the specified region at a given hour. They are produced by taking into account the local ionospheric data derived from vertical incidence sounders. Figure 5-17 is a HAP chart for London, England at 0100 UTC. The lowest (skywave) frequencies should always occur in the neighborhood of the base station, and this is observed. This is because the ionosphere will not support near-vertical-incidence skywave signals (NVIS) if the frequency is too high. Within about 500 km of the base station, the highest band is approximately $foF2 \sec \varphi$ where φ is the ray zenith angle. To derive these convenient maps, an intermediate *foF2* map (or its equivalent) is exploited. These resultant ionospheric data are then applied to an HF communication performance model to derive the relevant HF system parameters. One such parameter is the optimum working frequency. This is essentially what the HAP charts depict, although it should be used with considerable caution. This is because actual performance at any given frequency can be very low even at the optimum working frequency. This may happen because of low SNR characteristics arising from poor antenna selection and installation, low transmitter power and elevated noise levels. IPS generally uses a model called ASAPS, although it is understood that the ITU-R model based upon REC533 can be used. HAP charts are available for sites in all world regions specified by IPS.

Local Area Mobile Prediction (LAMP) charts are also available from the IPS web site. The product is available for a number of stations in the Australasian region, using an hourly or daily format. This form of chart provides the optimum HF frequencies for all users within ~ 1000 km of the selected base station. There is no azimuthal dependence, so the predictions are essentially based upon Near-Vertical-Incidence-Skywave (i.e., NVIS) considerations and the secant law. The forecasting procedure uses *foF2* nowcasts and an extrapolation in the time domain. Figure 5-18 is a sample display for Auckland, New Zealand for 02 May, 2004.

The IPS site is an excellent one, especially for HF practitioners. For earth-space users, convenient TEC products are available for Australasia, North America, Europe and Japan. There are also a number of online

prediction tools available. The "Space Weather" page on the IPS site is organized conveniently by an array of icons indicating specific products under the categories given in Table 5-13

Table 5-13: Space Weather Categories and Subcategories at IPS

- Solar conditions
  - Solar wind speed
  - X-ray flux
  - X-ray flares
  - Spectrograph: Culgoora
  - H-alpha: Culgoora
- Geophysical conditions
  - Geomagnetic warning
  - K-index
  - pc3 index
  - Geostat alert
  - Geomagnetic alert
  - Aurora alert
- HF propagation conditions
  - HF communication warning
  - HF fadeout status and warning
  - Polar cap absorption
- Ionospheric conditions
  - Australasia
  - North America
  - Europe
- TEC conditions
  - Australasia
  - North America
  - Europe
  - Japan

5.4.6 Jet Propulsion Laboratory

JPL is a laboratory managed by NASA for the California Institute of Technology. JPL operates NASA's Deep Space Network, incorporating antennas that support communications to many spacecraft and earth terminals. Two of the more significant research products of JPL from the perspective of space weather and telecommunications are as follows:

- Global Ionospheric Maps (GIM) using GPS
- Ionospheric Scintillation Studies using GPS

JPL produces movies of the global TEC as well as differential TEC maps, on the basis of an analysis of two-frequency data from the IGS Global GPS network. The process involves the use of ionospheric modeling and a Kalman filtering technique. The GIM maps have been validated against independent

TEC observations such as those that been derived from the two-frequency TOPEX satellite. The coverage of GPS is illustrated in Figure 5-19. A sample map is given in Figure 5-20. These maps have the potential for use in forecasting.

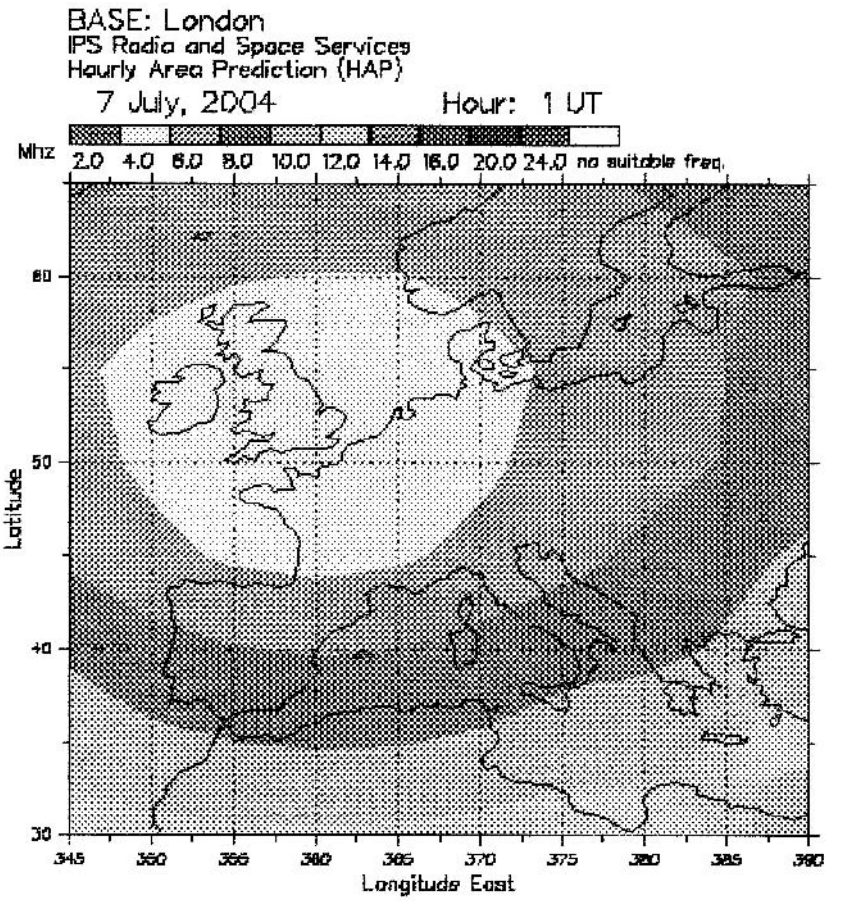


Figure 5-17: Hourly Area Prediction (HAP) chart for London at 0100 UTC on 07 July 2004. Real-time ionospheric data (i.e., *foF2*) is used to produce the chart. Illustration provided courtesy IPS, RWC-Australia.

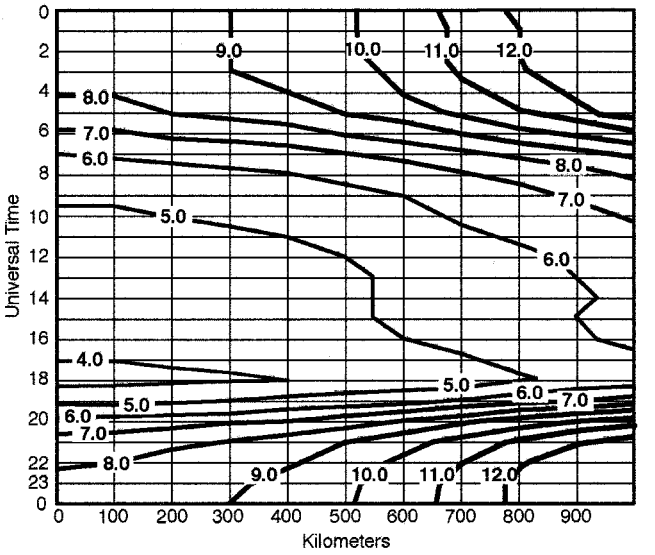


Figure 5-18: Local Area Mobile Predictions (LAMP) for Auckland, New Zealand for 02 May, 2004. Illustration provided courtesy IPS, RWC-Australia.

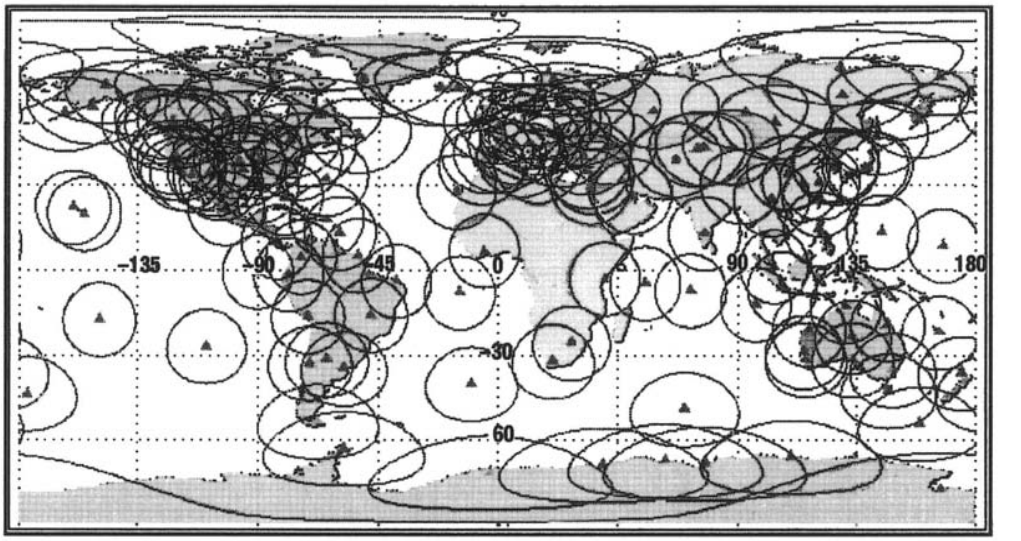


Figure 5-19: The Global Positioning System Network. The coverages are based upon an ionospheric height of 400 km. (Figure from NASA, JPL, by permission).

Scintillation is also of interest to JPL investigators. This is not surprising given the mission of JPL. As of the publication date of this book, the GPS network is comprised of approximately 360 GPS stations. The ground stations are configured to receive the two L-band signals from up to eight (8) satellites, depending upon the latitude of the site. All data is retrieved and downloaded to JPL using Internet resources or dedicated phone lines. The data are accumulated and analyzed to derive information about ionospheric structure and to monitor any radiowave scintillation effects. The "product" is a so-called map showing the Rate-of-TEC Index (ROTI). The ROTI requires a measurement of the signal phase fluctuations (i.e., a measure of the short-term TEC fluctuation). The ROTI is based upon the standard deviation of TEC changes over a specified time interval, and this index can be related to the level of scintillation on L-band signals, and other bands by careful analysis. Given the coverage of the GPS network, the JPL scheme has the potential to provide a significant amount of information in support of space weather and telecommunication system support.

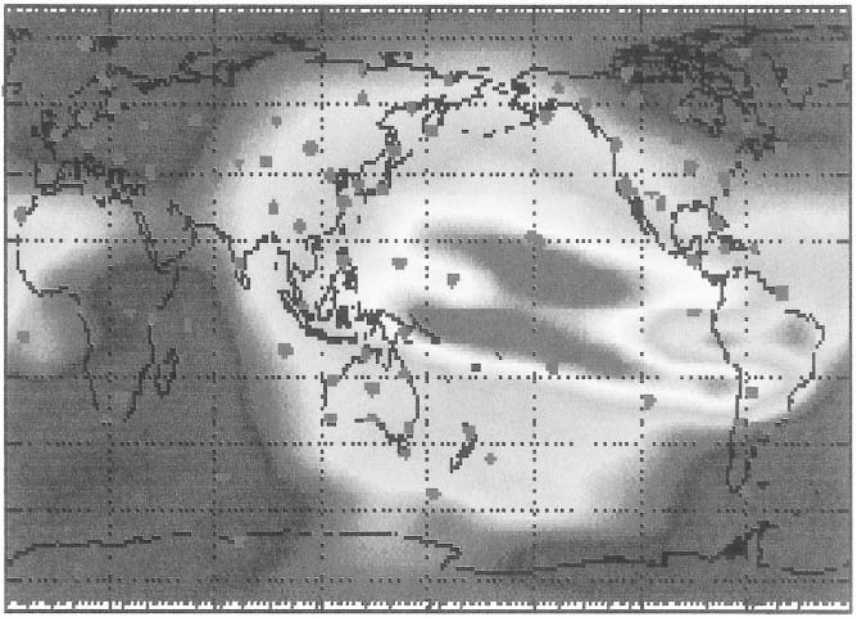


Figure 5-20: Total Electron Content (TEC) map obtained from the Global GPS Network. Global Ionospheric Maps (GIMs) exploit ~100 continuously operating GPS receivers. The TEC "snapshots" of the global TEC distribution are obtained by interpolating, in both space and time, the 6-8 simultaneous TEC measurements obtained from each GPS receiver every 30 seconds. The maps can be produced unattended in a real-time mode, with an update rate of 5-15 minutes. Sample Figure from the NASA-JPL web site.

5.4.7 Rutherford Appleton Laboratory

The Council for Central Laboratory of the Research Councils (CCLRC) is a multidisciplinary research organization, and within its umbrella is the world-renowned Rutherford-Appleton Laboratory (RAL). Located in Oxfordshire, England, RAL has a relatively modest in-house staff but supports ~10,000 scientists and engineers as part of a substantial university research program. The venerable Appleton Laboratory, founded in 1921, is also a part of the present RAL organization since 1979.

Much of this is taken from a report issued by the Radio Communication Agency of the UK [RA, 1998]. The following are selected activities undertaken at RAL.

- World Data Center C1 for Solar Terrestrial Physics
- Model developments for the ITU
- Short-term ionospheric forecasting
- COST 238, COST 251 and COST 271
- Real-time modeling of high latitude effects
- Statistical studies of ionospheric behavior and morphology
- Oblique ionospheric sounding
- Ionosonde services (Chilton, Lerwick and Port Stanley)
- Space Weather Web

The Space Weather Web is a facility for space weather and radio communication users. On the site may be found information of relevance to radio communication, navigation, and surveillance systems. Maps of TEC and *foF2* in the European theater may be accessed. Forecasts for the next hour and for several days are also available. The TEC data is based upon daily RINEX data from GPS measurements gathered and distributed by the International GPS Service for Geodynamics (IGS). The *foF2* and *M(3000)F2* data are obtained from vertical incidence sounders.

Figure 5-21 provides plots of TEC for the Eurasian region for two periods of time on 29 October 2003. These charts are typical of the maps that have been produced as a result of various COST programs.

5.4.8 Institute of Communication and Navigation

The Institute of Communications and Navigation (DLR) organization produces maps of the vertical TEC for the European region, and this is accomplished through the combination of TEC measurements as organized with the help of a regional model of TEC, called the Neustrelitz model (NTCM) [Jakowski et al., 1996-1999]. The model is matched to observed data where measurements are made, and the model is used for extrapolation to areas that are undersampled. DLR also produces TEC maps of the Polar

Regions. GPS ground stations of the International GPS Service (IGS) provide the GPS data used in the DLR mapping programs. Figure 5-22 is a typical polar plot of TEC.

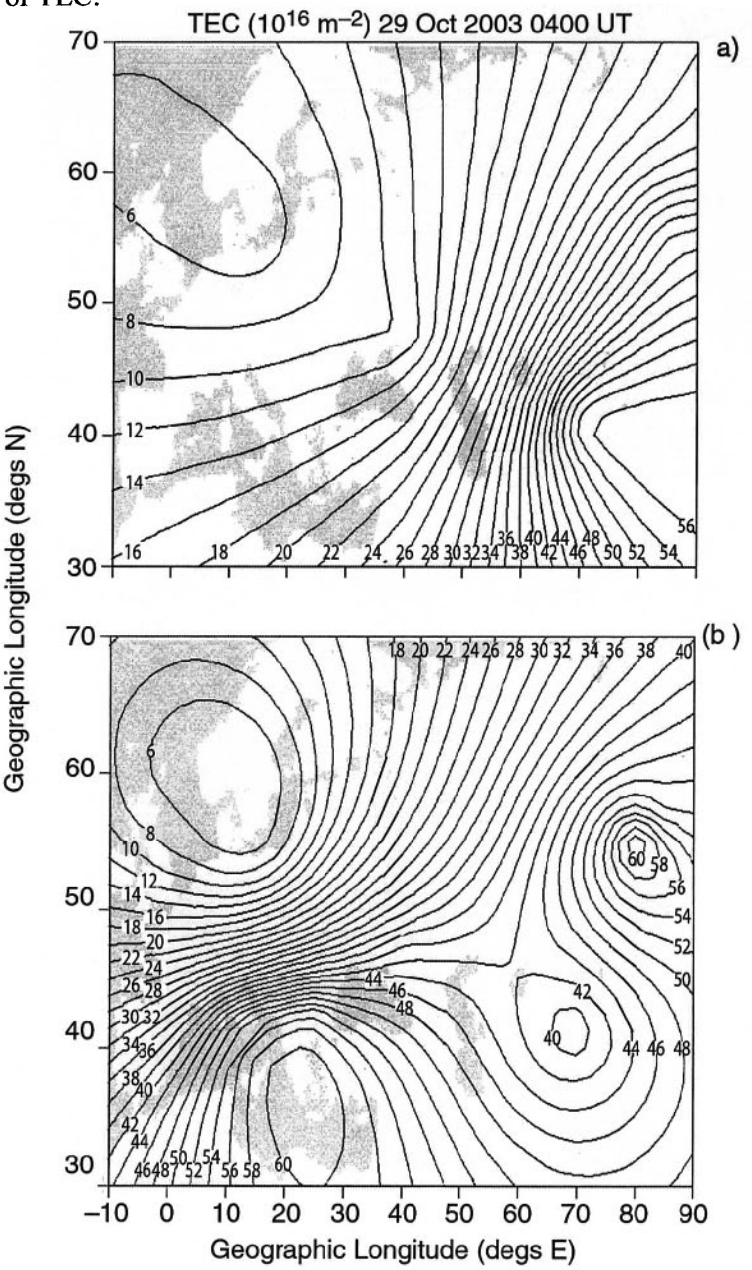


Figure 5-21: Sample TEC maps for the Eurasian region for 29 October 2003. The top curve (a) corresponds to 0400 UTC; the bottom curve (b) corresponds to 1000 UTC. In curve (a) notice the "islands" of increased TEC within the Mediterranean and Asian regions, while the low TEC zones are close to Scandinavia and eastward of Turkey.

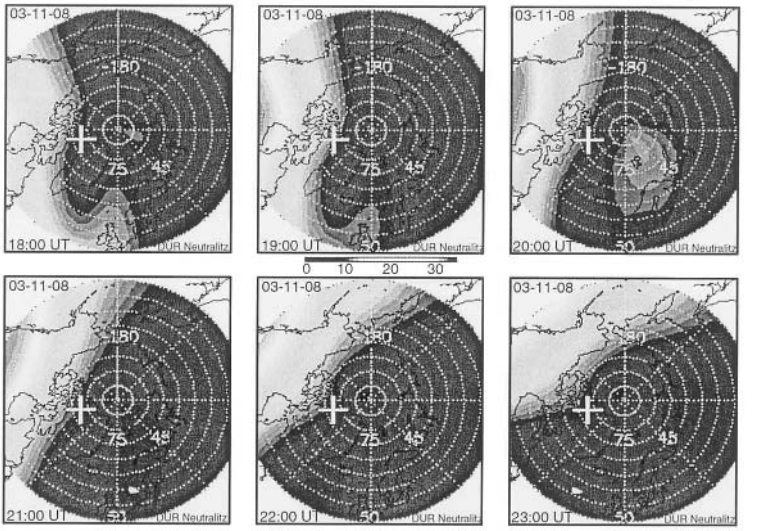


Figure 5-22: TEC maps for the polar region for November 08, 2003. The time separation between maps is 1 hour. Maps are derived from the Institute of Communications and Navigation (DLR) web site. While the originals were in color, we can see the progression in TEC in universal time over the six-hour period.

5.4.9 RWC-Warsaw and IDCE

The Heliogeophysical Prediction Service in Warsaw operates as a Regional Warning Center under the aegis of ISES (see list in Table 5-1). Also, since 1997, the center has been designated the Ionospheric Dispatch Center for Europe (IDCE). The IDCE was established as an initiative of the COST 251 Action. (A discussion of the various COST initiatives is given in Chapter 6. A link to the COST 251 program may be found on the IDCE web site.) The IDCE is a source for current worldwide ionospheric data, basically mimicking the SEC and NGDC data, but in a different format. A new feature is a forecast of *foF2* that can be found on the site. Figure 5-23 exhibits daytime and nighttime maps of *foF2* for the European region. In the *Solar-Terrestrial Reports* area of the site one can find a link to HF Communication Prediction and Forecast Service. Of interest to radio communicators are two products:

- Worldwide maps of Signal-to-Noise Ratio (SNR)
- HF Radio Prediction Calculations from Warsaw to: Johannesburg, Mexico, Moscow, New York, Paris, Sidney, and Tel Aviv.

It is believed that these are climatological predictions, since they appear to have been generated for the 15th of the month. It is likely that the propagation model is REC533 or some equivalent model.

The IDCE also maintains an anonymous FTP site from which a host of solar-terrestrial data can be downloaded.

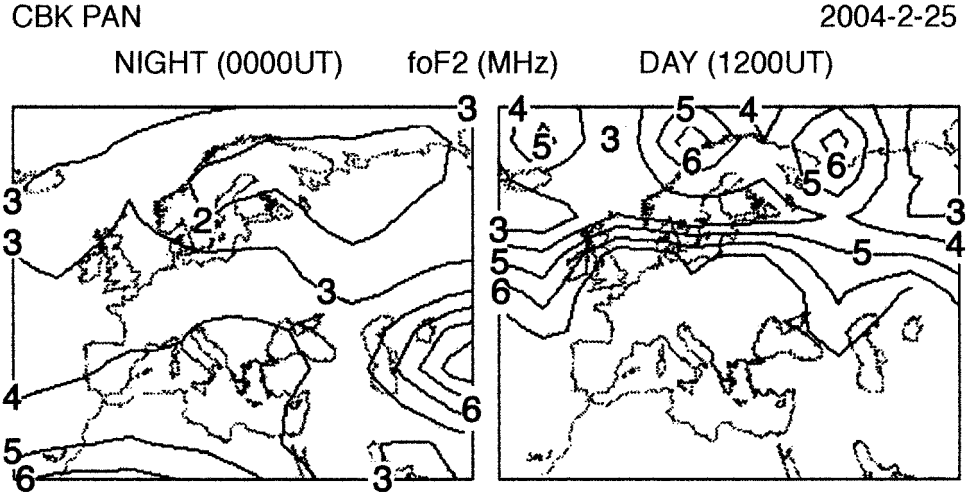


Figure 5-23: Maps of the parameter *foF2* at 0000 and 1200 UTC in the European region. Data obtained from the web site for RWC-Warsaw and IDCE.

5.4.10 RWC Brussels and SIDC

The Solar Influences Data Analysis (SIDC) is run at the Regional Warning Center at Brussels, Belgium. As part of the complex of World Data Centers, RWC-Belgium is the WDC for the Sunspot Index. SIDC has a number of products that may be discovered by perusal of the published website. They include but are not limited to: (i) PRESTO Alerts, fast warnings of important solar events of importance to the space environment, (ii) 3-day forecasts of solar and magnetic activity via the SIDC URSIgram, (iii) ionospheric data for several European sites, (iv) CME detection alerts derived from CACTUS software and data from SOHO/LASCO, and (v) warnings of increase in GPS position errors due to ionospheric disturbances. The SIDC website is very well organized and the icons used to link with specified data sets are both logical and complete.

5.4.11 Military Systems

5.4.11.1 Air Force Weather Agency

Since the 1960s, the U.S. Air Force has taken space weather seriously. The Air Weather Service, headquartered at Scott AFB, managed

radio propagation assessments and prediction services for its Department of Defense clients for many years. The operational arm of the operation was Global Weather Central (AFGWC) located Offutt AFB, near Omaha, Nebraska. A number of changes have taken place over the years, but the mission is still the same ... "that of providing space environment forecasts, warnings, and anomaly assessments to enhance the capability of DoD Forces". In the 1990s, activity was organized under the 55th Space Weather Squadron (i.e., termed 55-SWxS), located at Schriever AFB, Colorado. However, the Air Force has recently moved the operation back to Omaha under the aegis of the Air Force Weather Agency (AFWA). Over the years, operational forecasting in the USAF has been supported by AFCRL in the beginning, then Phillips Lab, and now by Air Force Research Laboratory, all being located at Hanscom AFB, near Boston, Massachusetts.

AFWA is not just an arm of the US Air Force. It is the official agency responsible for the provision of ionospheric and space weather products within the entire Department of Defense (i.e., US-DoD). There was a time when the Navy had planned to develop an operational forecast center of its own. For reasons of efficiency, that plan was dropped.

The predecessors to AFWA were the first to recognize the need for some form of data assimilative model of the ionosphere. In the 1970s, AFGWC developed the concept for a 4-D ionosphere driven by a large number of input drivers, typically sounders and TEC monitors. Regrettably the time was not right for this initiative, and the model was data starved. The computer processing power was decidedly primitive by today's standards, data assimilation methods were crude, and there were an insufficient number of instruments for space weather observation. In recent years, various regional and global models have been developed and the GAIM approach, a joint Air Force/Navy initiative, is making the original concept of massive data assimilation more practical. These issues are addressed more fully in Chapter 3.

Throughout the years the United States Air Force has supported a solar observing network. The Solar Optical Observing Network (i.e., SOON) was replaced by the Solar Electro-Optical Network (SEON), and this is now operated by AFWA. A number of US-DoD agencies require these data, including the United States Space Command, NORAD, and the Air Force Space Command.

Empirical models used by AFWA in the development of its nowcasts and forecasts are driven by three independent sources of ionospheric data:

- Digisonde: $N(h)$ profiles from ~ 17 sites worldwide
- GPS: TEC data from ~24 dual frequency systems worldwide
- DMSP: in-situ plasma density using SSIES sensor

While these assets are insufficient for a full-blown assimilation models as envisioned by the Air Force/Navy MURI program, there is a clear

potential given the possibility to incorporate other sensors into the mix. McCoy [2001] has suggested that additional techniques may soon play a substantial role. These new sensors are GPS occultation, ultraviolet remote sensing, and computerized ionospheric tomography. McCoy's view is that data assimilative models are best served by incorporation of independent and rationalized data sets, and that data sets derived from integrated looks through the ionosphere may be problematic. However, through incorporation of large amounts of data from multiple locations, these issues can be resolved.

5.4.12 Special Product: Email Alerts

A number of agencies and firms provide email alerts and summaries. These are typically provided by subscription and many are free of charge. Such products can be useful since they can serve to alert the customer that operational conditions should be changed to match the potential environmental conditions. Table 5-13 contains three representative alerting services. The examples are taken from government, private industry, and an individual (i.e., amateur radio operator). One can subscribe to these by logging into the respective Web sites. The NOAA-SEC service is free, the amateur radio site suggests a voluntary contribution, and the STD product is fee-for-service, but it is a modest amount. Certainly there are other services, but these are indicative of what is out there.

Table 5-13: Email Alerting Systems

Agency, Firm or Individual	Alert Items
NOAA-SEC	Space Weather Advisories by email
NW7US: HFRadio.org	Solar Flux, *Ap*, *Kp*, Solar Wind, Sunspot Number
Solar Terrestrial Dispatch	Solar Activity, Auroral Conditions, Flare and Storm Warnings & Alerts, Proton Event Warnings and Alerts

5.5 COMMERCIAL FORECASTING SERVICES

A number of companies have evolved out of a need to provide tailored space weather products and services to clients responsible for telecommunication systems, or more properly, radiocommunications. For example a particular client may need to know precisely how his system will perform under specified space weather conditions. Typically the information supplied by government sources found in Table 5-1 is useful but it may not be as useful as it needs to be. Exceptions may include the 55-SWxS (now AFWA) in the United States and the IPS-Australia. In this section we will identify some commercial firms that deal directly with the ultimate (end) users of the information, specifically the managers and operators of telecommunication systems. (Note that the ITU definition of radiocommunications includes navigation and surveillance as well as

communication. Telecommunications is an even broader concept, with radio communication systems as a subset.)

5.5.1 Vendor Industry

The Space Environment Center in Boulder has actively fostered a vendor industry since the late 1990s. They have hosted vendor industry meetings since 1997, typically in conjunction with the annual *Space Weather Week* workshops and symposia. SEC has been obliged to support a healthy vendor industry since it is unable to provide all of the services that its users require. The SEC goal is to encourage value-added vendors to use SEC data for tailored services and the development of commercially available products. While growth of the new industry has been slow, it has shown some signs of maturity. Table 5-14 is a listing of space weather vendors that have advertised the availability of products and services supporting telecommunication systems.

The reader should visit the web sites of the firms listed in Table 5-14 for details. There is a web page hosted on the NOAA-SEC server from which information may be obtained, including links to the various vendors that are listed. One can also visit the *Space Weather Week* link. In the sections that follow, we discuss the products and services of several of the firms. As of the publication date, the widest range of services of interest to telecommunication system operators can be found on the web site of Northwest Research Associates. The eye appeal award probably goes to Solar Terrestrial Dispatch. These are naturally just personal views of the author. The reader can form his own opinion.

Table 5-14: Listing of Space Weather Vendors (Those providing products & services pertaining to communication, surveillance and navigation)

Name of Vendor
ARINC
Northwest Research Associates
Radio Propagation Services
Rockwell-Collins
Solar Terrestrial Dispatch
Space Environment Technologies

Note: A complete listing of the Commercial Space Weather Interest Group (CSWIG) membership is provided in Chapter 6 (i.e., Table 6-14).

5.5.1.1 Northwest Research Associates

Northwest Research Associates offers a wide range of space weather services, but transionospheric signal propagation channel is a specialty of the firm. NWRA is recognized for the development of the only global model of

ionospheric scintillation, WBMOD. However NWRA has the capability to assess the impact of Faraday rotation and time delay effects on space system transmissions. They maintain an extremely useful web site, with tutorials on scintillation, and forecasts for the Far East, the Middle East, South America, European high latitudes, and the American Sector high latitudes. NWRA prepares GPS scintillation impact charts, and using WBMOD and data provided by NOAA-SEC, they also assess the impact of scintillation on other satellite links (i.e., Inmarsat and Norsat-C). They also provide links to all the usual sites; including NOAA-SEC. Figure 5-24 is a sample plot of a Middle East forecast for Solar Maximum conditions.

There are other valuable attributes of the NWRA Web site for those interested in use of indices for various purposes. NWRA has examined the difference between several ionospheric indices that can be used as proxies for the sunspot number. One is the *T-index* and the other is the NWRA "effective" sunspot number (i.e. *SSNe*). Both of these are based upon ionospheric data, but the NWRA-*SSNe* is derived from worldwide vertical-incidence sounder data. In effect, the *SSNe* is a pseudoflux number as described in Chapter 3. It is the sunspot number that would have to be used in a model to best agree with the observed aggregate values of *foF2* worldwide. It can be argued that the pseudoflux concept would best be applied regionally, especially during storm times, given the different geophysical regimes involved. Still the plots of the *SSNe* clearly exhibit the worldwide nature of positive and negative storms. Figure 2-28 (in Chapter 2) a sample plot of the effective sunspot number, *SSNe*.

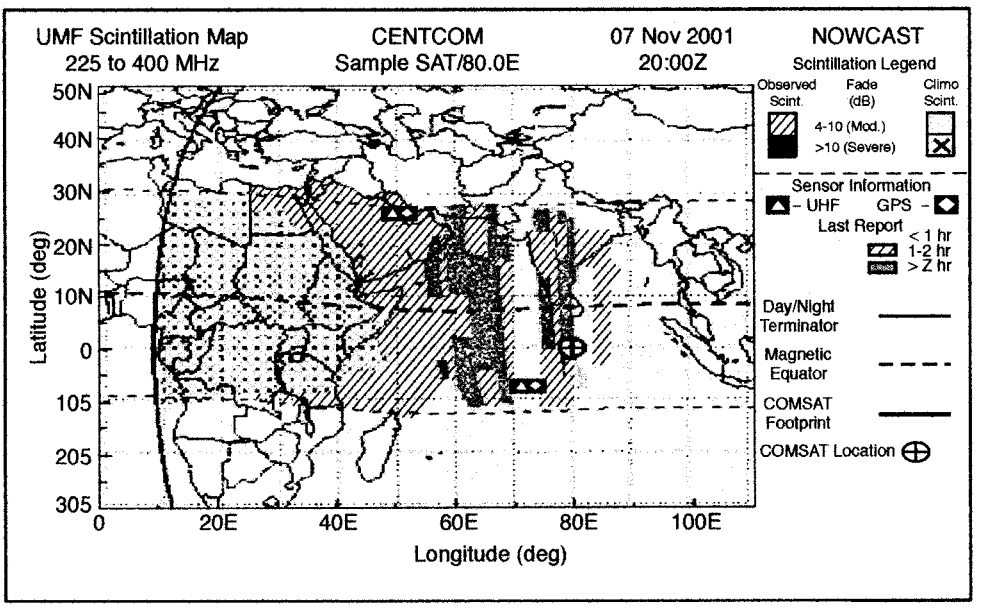


Figure 5-24: Scintillation forecast prepared by NWRA for the Middle East sector, based upon the model WBMOD. (© NWRA, used by permission.)

5.5.1.2 Radio Propagation Services

Radio Propagation Services (RPSI) is a small company specializing in ionospheric support and frequency management services for HF communication systems. Clients include ARINC (i.e., the GLOBALink/HF system), Iceland Telecom, and various unspecified civilian and DoD agencies. The company maintains a warehouse of oblique-incidence Chirpsounder® systems that can be deployed for special campaigns and system evaluations. The company leverages ionospheric data derived from NOAA-SEC and other sources to produce a global map of the ionosphere This map is utilized in conjunction with some proprietary algorithms (i.e., Dynacast®) to evaluate the performance of operational HF systems. A primary use of Dynacast is to prepare global frequency management tables for commercial aviation. The propagation assessment modules include the baseline ionospheric maps as modified by current data. The most challenging aspect of the effort is forecasting, and a major activity is the production of more efficient active frequency information during periods of disturbances. Figure 5-25 is a global map of the ionosphere derived from assimilation of *foF2* data.

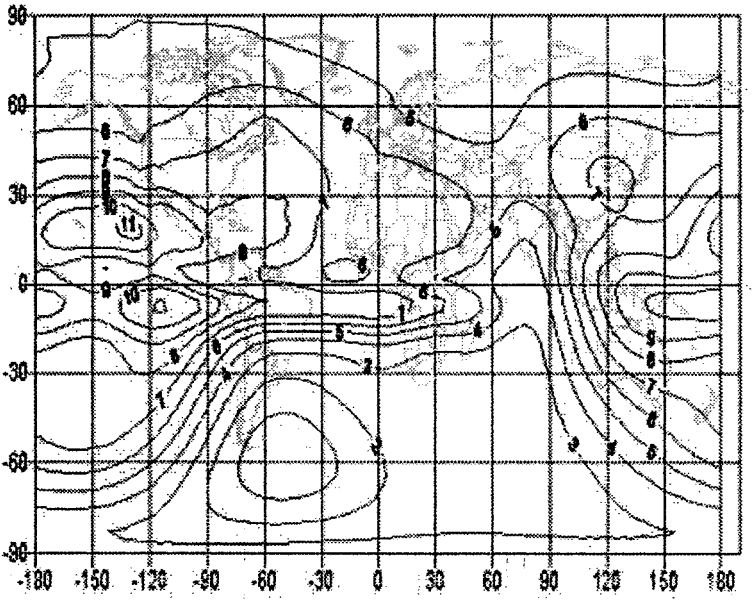


Figure 5-25: RPSI develops maps of *foF2* by means of an update procedure using vertical and oblique sounder data. The map above corresponds to 0000 UT 24 July 2003. The maps are developed within the RPSI Integrated Dynacast® Environment (IDE™). The output from the IDE is an input to one of several Dynacast engines to produce applications products for customers. Nowcasting problems can make good use of the IDE output. The IDE output is augmented by other space weather data sources to address forecasting problems. For HF applications, the kernel within the software engine is the ITS model VOACAP. Options to use other models such as ICEPAC are available .The raw *foF2* data is provided by NOAA-SEC.

5.5.1.3 Solar Terrestrial Dispatch

Solar Terrestrial Dispatch (STD), located in Canada, is primarily a vendor supporting the power industry. However, the company maintains a sophisticated web site where solar-terrestrial data from international resources may be accessed for other purposes. For example, STD provides a prediction of the estimated time of arrival of CMEs as well as the predicted orientation of the IMF at the arrival time. In addition, the company offers certain products that can be useful for analysis of HF communications circuits (i.e., PROPLAB-PRO) and for visualization of solar and auroral activity (i.e., SWIM, Aurora Monitor, and SWARM). For HF practitioners, the PROPLAB-PRO offering includes a three-dimensional ray trace package. This package can be an important analytical tool for evaluation of circuits that transition from one geophysical regime to another (i.e., equatorial anomaly, auroral zone, day-night terminator). STD provides real-time global maps of the parameters MUF, *foF2* and *foE*. The method by which these maps are derived is not described, but macroscopic indices appear to be used as drivers (viz., sunspot number and magnetic activity index), and map updates appear every 5 minutes.

Author Note 1: It is suspected that climatological models of the ionosphere are used as the basis for the STD displays. Moreover, the update burden appears to be borne by real-time estimates of the sunspot number and magnetic activity, and it is likely that the magnetic index is used to modify the position of the auroral oval.

Author Note 2: Ray tracing codes, including the well-known Jones-Stephenson method, are not typically employed in standard HF performance methods such as VOACAP, ICEPAC, ASAPS, or in ITU methods such as REC533. This may have more to do with history and computational efficiency than accuracy. Conceivably, the time has come to merge more sophisticated ray tracing with real-time models of the ionosphere, given the necessity for access to more realistic propagation information by adaptive (HF) systems in the future. But this will not be a trivial exercise.

5.6 SYSTEMS FOR FORECASTING

In Chapter 1 we noted that the U.S. Navy was the first to develop a general approach to propagation assessment and forecasting in the 1970s. In many ways, the US Navy PROPHET system was well ahead of its time, not unlike the original Air Force 4-D model of the ionosphere that was proposed in the same decade. Just as the 4-D model has given way to GAIM, the

PROPHET system has now been superseded by another Air Force system called OPSEND. We will discuss OPSEND in Section 5.6.1.

There are some special purpose programs that address a particular discipline. From an historical perspective, we find that the U.S. Navy CLASSIC PROPHET system, designed to assist the Signal Intelligence (SIGINT) and Electronic Warfare (EW) communities, was probably the first such system hosted on a mini-computer platform. But this was in an era before MS-Windows™ or equivalent operating systems. CLASSIC PROPHET allowed for sounder update, was driven by real-time solar flux data, and allowed for changes in stored values of sunspot number. The kernel of the PROPHET system was a simple propagation model called MINIMUF, but later versions enabled VOACAP to be used instead.

More recently in the late 1990s, an agency of the British MOD (i.e., originally DERA) developed a system similar to CLASSIC PROPHET called HF-EEMS, which operates under a Windows environment [A. Shukla, 1999]. The ownership of HF-EEMS software is thought to be vested in QinetiQ, following the split of DERA into a private company (i.e., QinetiQ) and the Defense Science & Technology Laboratory (DSTL). The kernel of HF-EEMS propagation model is the ITU recommended model REC533, and options include updating of the sunspot number, the *Ap* index, and even the basic MOF data if oblique sounder data is available.

5.6.1 OPSEND

The Air Force Geophysics Laboratory and its predecessors have had a rich history in studies of the space environment and its impact on military systems. In the year 2000, the Space Vehicles Directorate of the Air Force Geophysics Laboratory established a Center of Excellence (CoE) in the area of space weather. The mission of the CoE is to develop technologies for forecasting and mitigating the effects of the space environment. The activities within the Space Weather CoE are largely continuations of prior efforts of several branches within the Battlespace Environment Division.

There are two products developed at AFRL that follow in the PROPHET tradition, but with significant improvements. They are OPSEND and AF-GEOSpace. Both can be considered software structures designed to consolidate a number of activities for the convenience of the scientist and warfighter. AF-GEOSpace is a visualization tool, and while it stresses the environmental aspects of space, it also hosts a number of useful models for evaluation of satellite scintillation, HF ray tracing, and other matters. The second product, OPSEND, also provides for graphical displays and maps, but the emphasis is on system effects at the operational level.

Bishop et al. [2002, 2004] describes the OPSEND system and the product validation approaches. The system itself is a set of graphical products for visualization of space weather effects on theater-based radio systems. Four

of the graphical products are in use at the Air Force Weather Agency (AFWA) at Offutt AFB, Nebraska. The products are:

- Radar auroral clutter maps
- UHF satellite scintillation maps [Groves et al., 1997]
- HF illumination maps
- GPS single-frequency error maps [Smitham et al., 1999]

Each of these graphical products offers nowcasting and forecasting options, and the graphs are updated every hour. In the implementation of OPSEND, it was necessary to utilize a number of near-real-time data sources for purposes of updating the imbedded models. The data is transmitted to AFWA for incorporation in the models, including: (i) the Parameterized Real-Time Ionospheric Specification Model (PRISM) [Anderson, 1993; Daniell et al., 1993], (ii) an auroral oval model, and (iii) the Scintillation Network Decision Aid (SCINDA) [Caton et al., 1999, 2002]. The author notes that the PRISM model has also been suggested as a replacement for the imbedded ionospheric models in ICEPAC and VOACAP to render a real-time HF performance prediction system. The PRISM model is discussed in Chapter 3 and SCINDA is discussed briefly in Chapter 4. More details on SCINDA are given in Section 5.6.2 below.

More information on AFRL space weather activities is provided in a paper by Ginet [2001].

5.6.2 SCINDA

SCINDA [Groves et al., 1997; Caton et al., 1999, 2002] is a scintillation network decision aid. The system was developed by AFRL for the U.S. Air Force Space Command. It is a real-time data-driven system designed to predict scintillation impairments within the equatorial region. A demonstration of the SCINDA system was performed using equatorial stations. At these sites, scintillation parameters were derived from various satellite signals of opportunity. FLTSAT was used as a UHF source; GOES and GPS were used as L-band sources. The basic concept involves measurement of ionospheric drift velocities at the SCINDA sites, transmission of the data to a control center (i.e., AFRL, Hanscom AFB) via the Internet, and development of scintillation impact areas using an empirical model (i.e., a scintillation extrapolation method). The extrapolation process involves an understanding of the phenomenology of scintillation-producing plumes and their evolution.

It should be noted that there are situations in which scintillation data is unavailable, and other situations when situation reports (i.e., forecasts) are required somewhat outside the SCINDA coverage areas. In such instances, SCINDA defaults to WBMOD climatology. The scintillation model WBMOD

was mentioned in Section 5.5.1.1, and a paper by Secan et al. [1995] may be consulted for more details. The SCINDA developers have noted that the some scintillation events may be missed if the source of the disturbance arises between sample points.

The U.S. Air Force Research Laboratory has described the Communication/Navigation Outage Forecasting System (C/NOFS) as the scintillation forecasting system of the future. Unlike SCINDA that relies almost exclusively upon analysis of satellite transmissions to arrive at predictions, C/NOFS involves a dedicated space platform to extract data on ionospheric instabilities. The platform accommodates in-situ and remote sensing approaches. The goal of C/NOFS is to forecast scintillation 3-6 hours before onset.

5.7 CONCLUDING REMARK

The main purpose of this chapter is to identify the hierarchy of forecasting and prediction systems. There are an enormous number of organizations with ongoing activities in space weather forecasting. For the most part these organizations emphasize upstream data (i.e., sun, solar wind, magnetosphere, etc.) and very few concentrate on downstream information (i.e., ionosphere). It is generally true that many of the data sets used to prepare telecommunications forecasts come from the same sources, usually government ones. This is not surprising since primary sources of data (i.e., satellite platforms and large networks of ground-based systems) require an enormous capital investment. While there are numerous forecasting systems identified, the number of independent data sources is relatively small. This can represent vulnerability. Defense-related activities maintain the most sophisticated forecasting systems, but access to data and forecast products from military activities can be problematic for civilian users. Also, while there is growing 3rd party vendor community (viz., CSWIG), the number of vendors that offer forecasting products supporting telecommunications systems can be counted on one hand. The reason for this predicament is an understandable consequence of the fact that the market of telecommunication forecasting services is currently limited. To increase the market, education is required. Many telecommunication system managers are either unaware of the advantages of forecasting or the availability of relevant forecasting systems. This situation needs to be addressed.

5.8 REFERENCES

Anderson, D.N., "The Development of Global, Semi-Empirical Ionospheric Specification Models", in *1993 Ionospheric Effects Symposium*, J.M. Goodman (Editor-in-Chief), NTIS, Springfield VA, pp.353-363.

Araujo-Pradere, E.A., T.J. Fuller-Rowell, and D. Bilitza, 2002, "An Example of Validation of the STORM Response in IRI2000", in *2002 Ionospheric Effects Symposium*, J.M. Goodman (Editor-in-Chief), NTIS, Springfield VA, pp.202-209.

Bakry-El-Arini M., W. Poor, R. Lejeune, R. Conker, J. Fernow, and K. Markin, 1999, "An Introduction to WAAS and its Predicted Performance", MITRE Report MP 99W0000061; also appearing in *Proceedings of IES1999*, edited by J.M. Goodman, NTIS, Springfield, VA.

Bishop, G., T. Bullett, K. Groves, S. Quigley, P.Doherty, E. Sexton, K. Scro, R. Wilkes, and P. Citrone, 2004, "Operational Space Environment Network Display (OPSEND)", *Radio Sci.* 39, RS1S26, doi:10.1029/2002RS002821; also appearing in *2002 Ionospheric Effects Symposium*, J.M. Goodman (Editor-in-Chief), NTIS, Springfield VA, pp.25-32.

Bishop, G., D. Decker, E. Sexton, P. Doherty, O. de la Beaujardiere, T. Bullet, S. Quigley, and K. Groves, 2002, "Space Weather Model and Product Validation", in *2002 Ionospheric Effects Symposium*, J.M. Goodman (Editor-in-Chief), NTIS, Springfield VA, pp.33-39.

Caton, R.G., W.J. McNeil, K.M. Groves, S. Basu, and P. Sultan, 1999, "Real-Time UHF and L-Band Scintillation Measurements with the Scintillation Network Decision Aid (SCINDA)", *1999 Ionospheric Effects Symposium*, J.M. Goodman (Editor-in-Chief), NTIS, Springfield VA, pp.50-57.

Caton, R.G., W.J. McNeil, K.M. Groves, and Sa. Basu, 2002, "GPS Proxy Model for Real-Time UHF Satcom Scintillation Maps from the Scintillation Network Decision Aid (SCINDA)", *2002 Ionospheric Effects Symposium*, J.M. Goodman (Editor-in-Chief), NTIS, Springfield VA, pp.92-99.

Costello, K.A., 1997, "Moving the Rice MSFM into a Real-Time Forecast Mode using Solar Wind Driven Forecast Models", PhD dissertation, Rice University, Houston, TX, June 1997.

Daniell, R.E., W.G. Whartenby, and D.N. Anderson, 1993, "PRISM Validation", in *1993 Ionospheric Effects Symposium*, J.M. Goodman (Editor-in-Chief), NTIS, Springfield VA, pp.364-368.

Detman, T., and J. Joselyn, 1998, "Real-Time Kp Predictions from ACE Real-Time Solar Wind", in Proceedings Solar Wind 9 Conference, October 5-9, 1998 (in Press).

Fuller-Rowell, T.J., E.A. Araujo-Pradere, and M.V. Codrescu, 2000, "An Empirical Ionospheric Storm-Time Correction Model", *Adv. Space Res.*, 25(1), pp.139-148.

Fuller-Rowell, T., M.V. Codrescu, and E.A. Araujo-Pradere, 2001, "Capturing the Storm-Time F-Region Ionospheric Response in an Empirical Model", in *Space Weather*, Geophysical Monograph 125, edited by P. Song, J. Singer, and G.L Siscoe, pp.393-401.

Ginet, G.P., 2001, "Space Weather: An Air Force Research Laboratory Perspective", in *Space Storms and Space Weather Hazards,* edited by I.A. Daglis, Kluwer Academic Publishers, Netherlands, pp.437-457.

Goodman, J.M., *HF Communications: Science & Technology*, Van Nostrand Reinhold, New York, 1991. (JMG Associates, Ltd., 8310 Lilac Lane, Alexandria VA 22308).

Goodman, J.M., J. Ballard, and E. Sharp, 1997, "A Long-Term Investigation of the HF Communication Channel over Middle and High Latitude Paths", *Radio Science*, 32 (4), pp.1705-1715.

Groves, K.M., S. Basu, E.J. Weber, M. Smitham, H. Kuenzler, C.E. Valladares, R. Sheehan, E. MacKenzie, J.A. Secan, P. Ning, W.J. McNeil, D.W. Moonan, and M.J. Kendra, 1997, "Equatorial Scintillation and System Support", *Radio Science*, 32, 2047.

ITS, 1998, "High Frequency Radio Automatic Link Establishment (ALE) Application Handbook", prepared by ITS-Boulder (i.e., the Institute for Telecommunication Sciences of NTIA), Boulder CO, September 1998.

Joselyn, J.A., 2001, "State of the Art in Space Weather Services and Forecasting", in *Space Storms and Space Weather Hazards,* edited by I.A. Daglis, Kluwer Academic Publishers, Netherlands, pp.419-436.

RA, 1998, "Current UK Research into HF Systems, HF Propagation, and the Ionosphere", Technical Working Party on HF Propagation and Ionospheric Effects, National Radio Propagation Committee, RadioCcommunication Agency, United Kingdom

Secan, J.A., R.M. Bussey, and E.J. Fremmouw, 1995, "An Improved Model of Equatorial Scintillation", *Radio Science*, 30, 607.

Shukla, A., 1999, DERA and QinetiQ, private communication

Smitham, M.C., P.H. Doherty, S.H. Delay, and G. Bishop, 1999, "Determination of Position Errors for Single Frequency GPS Receivers", *1999 Ionospheric Effects Symposium*, J.M. Goodman (Editor-in-Chief), NTIS, Springfield VA, pp.647-654.

Chapter 6
RESEARCH ACTIVITIES AND PROGRAMS

6.1 INTRODUCTION

There are a number of initiatives dealing with the role that space weather plays in telecommunications as well as an array of societal needs. Two programs in the USA are the *National Space Weather Program* (NSWP) and NASA's *Living with a Star* (LWS). There are also related efforts that incorporate space weather components. We will discuss a number these programs, indicating their status. Recognizing that these programs will evolve, and that new programs may emerge in the future, it is to be expected that certain aspects of the material in this chapter may become dated. Nonetheless, the material will document the wealth of interest in the subject at the time of publication and will demonstrate the growth in science and technologies related to space weather. It should be stated that the NSWP and LWS are devoted to the management and coordination of a myriad of space weather activities, principally civilian. A parallel effort for the United States DoD through the National Security Space Architect (NSSA) is an architecture of space weather activities through the year 2025, taking into account the known and anticipated needs of the country through that period. There are also emergent space weather activities in Europe and other regions.

There are numerous conferences organized with space weather sessions, including COSPAR and IES. The US Department of Commerce (i.e., NOAA) also sponsors a yearly *Space Weather Week* at which users and researchers gather to communicate ideas and present papers and progress reports. The European Union (EU), through the COST initiatives, s planning a similar forum. These conferences provide a wealth of information on space weather phenomena and applications.

As noted in the NSWP Implementation Plan, there has been a considerable amount of international activity and cooperation in recent years and it is growing. The Plan identifies the following countries as having started major programs in space weather: Australia, Canada, China, France, Sweden, Taiwan, and the USA. The list is growing, and international collaborations are underway, since it is recognized that most aspects of space weather are global, requiring cooperation of scientists from many countries.

Organizations such as the Scientific Committee On Solar-Terrestrial Physics (SCOSTEP) are playing a role in the structuring of space weather campaigns. SCOSTEP organizes and conducts international Solar-Terrestrial Physics (STP) programs of finite duration in cooperation with other bodies belonging to the International Council for Scientific Unions (ICSU). It provides guidance to the STP discipline centers of the ICSU's World Data Center system. SCOSTEP follows earlier entities in the ICSU that were

involved in planning and implementing the International Geophysical Year (IGY: 1957-58) as well as the International Quiet Sun Year (IQSY: 1964-65). SCOSTEP programs that have been completed include: the International Magnetospheric Study (IMS: 1976-79); the Solar Maximum Year (SMY: 1979-81); the Middle Atmosphere Program (MAP: 1982-85); and the Solar-Terrestrial Energy Program (STEP: 1990-97). A number of post-STEP programs are now in progress, and two of these programs are: STEP-Results, Applications, and Modeling Phase (SRAMP) and the International Solar Cycle Study (ISCS). SCOSTEP has embarked upon a new international scientific program for the 2004-2008 time frame termed CAWSES, Climate and Weather of the Sun-Earth System.

As indicated above, a number of space weather initiatives have been established worldwide. The European Space Agency (ESA) coordinates European space weather activities. For example, ESA has initiated a space weather applications pilot project, one purpose of which is to demonstrate the benefits of current and future space weather services. A Space Weather Working Team (SWWT) guides the activity with a membership of experts from the ESA member states. The SWWT acts as a forum for planning and discussion, as well as coordination with other European space weather initiatives such as COST Actions 271 and 724. There are prior COST Actions of interest (viz., 238, 251) that were discussed in Chapter 3. The COST (i.e., Coordination in Science & Technology) activities are quite important in the context of this book, and programmatic will be discussed later on in this chapter.

Before concluding this introduction, it is worth noting the recommendations put forth by the National Research Council (NRC) of the National Academies. A study to assess the current status and future direction of U.S. ground- and space-based programs in solar and space physics research, and a number of pertinent recommendations were made. The report, entitled "The Sun to the Earth – and Beyond" (NRC, 2003) recommends that DoD and NOAA be the lead agencies for acquiring all data sets needed for accurate specification and forecast modeling. Moreover, lead agencies should invest in new ways to acquire real-time data, from both ground- and space-based sources, in view of its importance in forecasting and prediction endeavors. The study indicates, in addition to government activities, that a number of private companies have become involved in the production and dissemination of space weather products and services. Certainly, the growth of such a space weather vendor community, closely synchronized with the real needs of the end user, will add to the vitality of the space weather community.

One should not read this chapter with the view that significant scientific and technical insight may be extracted. Rather, a primary goal is to summarize the organization of the space weather community and identify the various activities. It is heavy on programmatics, and light on the scientific details. Such information is found in earlier chapters and associated citations.

Finally, in the course of the discussion, we shall be mentioning a number of space weather observation techniques and sensors, both ground-based and satellite-borne. Unfortunately space does not permit a full description of these systems. There are a number of documents that deal with such information, including some that may be downloaded from the Internet (see Section 6.10). We recommend a book by Hunsucker [1991] that describes most radio techniques used for investigating the ionosphere, such as ground-based and earth-space methods, and satellite in-situ probes.

6.2 NATIONAL SPACE WEATHER PROGRAM

In the middle 1990s, the National Space Weather Program (NSWP) was established. Useful documents include the *Strategic Plan* (NSWP, 1995) and the *Implementation Plan* (NSWP, 1997, 2000). Goals of the NSWP are found in the latter plan and are duplicated in Table 6-1. Basically there are two groupings of goals: the first deals with the development or improvement of capabilities, while the second group identifies various mitigation schemes or circumvention schemes.

Table 6-1: Goals of the National Space Weather Program

A. Promotion of:
1) Observational Capability
2) Understanding of Processes
3) Numerical Modeling
4) Data Processing & Analysis
5) Research to Operations (including algorithms)
6) Forecasting Accuracy and Reliability
7) Space Weather Products & Services
8) Space Weather Education

B. Prevention/Mitigation of:
1) Over- or Under-design of Technical Systems
2) Blackouts of Power Utilities
3) Premature Loss of Expensive Satellite Systems
4) Disruption of HF, VHF, Satellite Communications
5) Navigation System Errors
6) Radiation Hazards for Humans

While all of the promotional goals are important, the vested interests for telecommunications, and radiocommunications in particular, are directed principally toward goals A-5, A-6, and A-7. The deleterious space weather consequences defined as goals B-1, B-3, B-4, and B-5 all have relevance to telecommunication disciplines. Even B-2 is important if terrestrial radio stations suffer from power outage or brownout. In any case, the listed goals of the NSWP are certainly necessary if not sufficient.

The Implementation Plan [NSWP, 2000] clearly recognizes that the class of forecast/specification services is the main driver of the National

Space Weather Program. It states that "the accuracy, reliability, and timeliness of space weather specification and forecasting must become comparable to that of conventional weather forecasting." This is a tall order. Much of the progress in weather forecasting in the last 25 years has derived from the observation and analysis of satellite images of weather patterns, the use of advanced weather radars, and the networking of weather stations. Thus conventional weather forecasting is blessed with an enormous amount of data upon which to develop forecasts and predictions. The region of prime interest to us here, the ionosphere, is vastly under sampled by comparison.

Without going into great detail, it is worth noting that the NSWP *Implementation Plan* is an excellent source of summary information regarding the current space weather activity and plans for the future. Being a USA document it naturally stresses national programs, and therefore stresses the observational systems and models supporting forecasting operations at NOAA-SEC and the US Air Force equivalent (viz., currently the Air Force Weather Agency, AFWA.) Prior organizations have been Air Force Global Weather Central (AFGWC) and the Air Force 55th Space Weather Squadron. Table 6-2 is a listing of combined resources derived from the *Implementation Plan*. The reader should refer to the compilation of acronyms at the end of this book if the specified system names are unfamiliar.

Table 6-2: Space Weather Resources (circa 2003)

1) GOES
2) POES
3) DMSP
4) ACE
5) Ionosonde Network
6) SCINDA
7) Magnetometer Chain
8) GPS
9) Ground-based Solar Observations

Table 6-3 is a list of operational space weather models in use at NOAA and at the Air Force Weather Agency. Other models are under development. Space weather domains and goals have also been specified. From the ionospheric subgroup, the *Implementation Plan* calls for treatment of the following domains: properties, electric fields, disturbances, and scintillation. The goal is to specify and forecast elements of these domains. For example, with respect to ionospheric properties, the goal is to specify and forecast electron density, plasma temperature, composition, and drift velocity. With respect to disturbances, the goal is to specify and forecast SIDs, TIDs, and critical propagation parameters.

The capabilities of existing space weather assets, in terms of derivative nowcasting and forecasting products is rather mixed. It largely depends upon the requirement of the customer. If the customer requires a short-term forecast that must be valid to within some stated error bars, for

system planning or operation, it should be a relatively easy matter to evaluate the efficiency of the forecasting process and the algorithm employed.

Table 6-3: Operational Models (circa 2003)

1. Magnetospheric Specification Model
2. The Proton Model
3. Wang-Sheeley Model
4. Costello Model
5. Ionospheric Activity Index, IACTIN
6. Ionospheric Correction Model
7. Bent Model
8. Auroral Prediction Model, IAPM
9. HF Prediction Models, ICEPAC, IONCAP, and ITS-78
10. Magnetospheric Specification Model, MSM
11. Magnetospheric Specification & Forecasting Model, MSFM
12. PRISM
13. Parameterized Ionospheric Specification Model, PIM
14. Wideband Model, WBMOD
15. Proton Prediction System, PPS
16. Total Electron Content Model, RBTEC
17. Shock Time-of-Arrival, STOA
18. Global Ionospheric Forecast, IFM
19. Magnetic Field Models, MFM

Unfortunately, one finds that the current capability for nowcasting and forecasting ionospheric properties is not sufficient for many customer requirements. The NSWP *Plan* admits to this deficiency and looks at four kinds of requirements: warnings, nowcasts, forecasts, and post-analyses. The author has a preference for the term "hindcasting" instead of post-analysis. This hierarchy is described in the published *Plan*. In fact, the *Plan* asserts that there is either no capability (i.e., for warnings and forecasts) or limited capability (i.e., for nowcasts and hindcasts). This is a chilling self-assessment; even accounting for the fact that one subliminal purpose of the document is to justify additional space weather research to Congress and the funding agencies. The author believes it is a little overstated in some cases, but he generally agrees with the assessment. We can all agree that there is considerable room for improvement in the type and texture of space weather sensors employed, forecasting algorithms and models utilized, and in data assimilation and dissemination procedures. Refer to Chapters 3-5 for a more complete discussion of this situation.

The NSWP is organized under the convenient umbrella, the Office of the Federal Coordinator for Meteorological Services and Supporting Research (OFCM), and is effectively managed by the National Space Weather Program Council (NSWPC). The Committee for Space Weather (CSW) acts as a steering group for tracking NSWP progress and recommends action to the NSWPC. The CSW itself is comprised of a number of representatives from

agencies such as NASA, NSF, DoD, DoT, DoE, and DoI. Clearly the NSWP is broadly based, and it represents considerable depth as well as breadth.

As mentioned in the introduction for this chapter, the NSWP has goals that are in general harmony with those of the National Security Space Architect (NSSA). The latter office is under the aegis of the DoD, and has completed a study of long-term agency requirements (i.e., for the next 15 to 25 years). While the architecture has been organized under the DoD, there was considerable input provided by civilian agencies, including NOAA, NASA, NSF, and FAA. The NSSA goals, being directed to requirements of the Defense Department, are slightly different than those of the civilian NSWP as expressed earlier. We shall discuss this DoD activity in a following section.

The NSWP coordinates with other agency initiatives such as the NASA *Living with a Star* initiative. We will discuss this program in the section that follows. Coordination with the research community and the user community is also stipulated in the *Implementation Plan*. As mentioned above, the NOAA-SEC sponsored *Space Weather Week* provides an excellent opportunity for the government and civilian users of space weather products to meet with scientists and developers of these products. There are other forums as well, too numerous to mention here.

Research is the engine in the space weather program evolutionary process. . Figure 6-1 exhibits the research areas of interest.

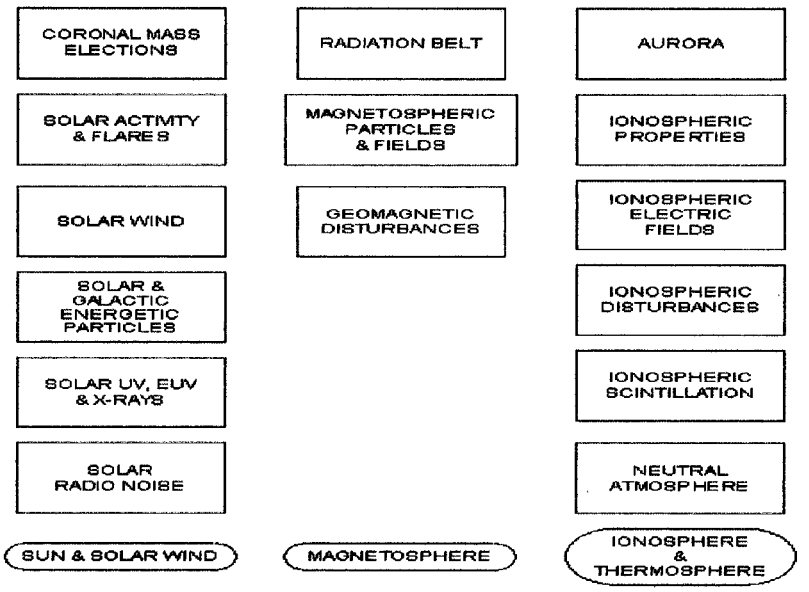


Figure 6-1: Research topics specified in the National Space Weather Program

It is noteworthy that each of these research areas can be associated with a possible operational model or model suite. NSF regards three broad research area as critical in the development of a viable space and ionospheric forecasting system: (i) sun and solar wind, (ii) magnetosphere, and (iii) ionosphere. The thermosphere is regarded by the NSWP as coupled to the ionosphere, and this recognizes (among other things) the relationship between thermospheric properties and the composition and dynamics of the ionosphere. Supporting the research activity is a substantial number of experimental observation systems. These are listed in Tables 6-4 (space-based) and 6-5 (ground-based).

Table 6-4: Space Observing Systems

ACE	Interplanetary Monitoring Platform 8 (IMP-8)
ARGOS	Living with a Star
Arizona Airglow Instrument (GLO)	MSX
ASTRID-2	ORSTED
C/NOFS	SAMPEX
COSMIC	Solar Probe
FAST	TIMED
GPS Particle Detectors	Solar-B
HESSI	STEREO
IMAGE	Magnetospheric Multiscale
WIND	Global Electrodynamics Connectons (GEC)
POLAR	Magnetospheric Constellation
Geotail	Ulysses
SOHO	Yohkoh/SXT
Interplanetary CME Imager	

Table 6-5: Ground-based Observing Systems

Automatic Geophysical Observatories (AGOs)
Balloon-borne Vector Magnetograph
Coronal Magnetic Field Measurements
Incoherent Scatter Radars
Interplanetary Scintillation Modeling
Relocatable Atmospheric Observatory (RAO)
Riometers
Scintillation Network
SuperDARN
Vector Magnetographs

6.3 LIVING WITH A STAR

NASA's Office of Space Sciences (OSS) was reorganized in 1996 and stipulated four major science themes for the future. One of these, "The Sun-Earth Connection" addresses much of what we now consider to fall under

the space weather umbrella. A roadmap for the space weather theme was organized as a strategic plan for the period 2000-2020. Following this reorganization, a new initiative called *Living with a Star* was established in the year 2000.

Living with a Star (LWS) was established by the National Aeronautics and Space Administration (NASA), through US Congressional mandate, in 2000. The science goals and implementation of the LWS *Geospace Mission* have been provided in a published report, and a short summary has been published in the AGU Transactions, EOS [Kintner et al., 2003]

It is of interest to note that the LWS Geospace Mission is focused on the following: the near-earth interplanetary medium, the magnetosphere, the ionosphere, and the upper atmosphere. Therefore, it is felt by the author that this project can provide the basis for improved understanding of many of the factors of importance to telecommunication systems that must operate within the geoplasma, and especially the ionosphere. The stated goal of this project is to "understand and characterize the geospace phenomena that most affect life and society". This should include communication, navigation and surveillance systems, both military and civilian. But the project is directed toward an understanding and characterization, and does not address specific applications that may be important to telecommunication system designers and operators. This is as it should be. LWS Geospace is, after all, a science project. Still these science objectives are quite important, ultimately, in the development of models that can be tailored for use in specific applications. Hopefully this will come to pass.

As one would expect, the LWS program is multi-faceted and long-term. Spacecraft missions out to year 2011 have been identified. Science investigations will focus on understanding and characterization leading toward physics-based and empirical models that can be used to diagnose and predict a number of space weather effects. In the EOS article, Kintner et al. [2003] indicate that such prediction capabilities cover communication, navigation, and radar disruptions among others. This will be helpful. As stated in their article, the LWS Geospace program will focus on two regions, the ionosphere and the radiation belts. They correctly identify magnetic storms as disturbances that can adversely affect military and civilian communication and navigation systems. They allude to storm-time impact on HF communications systems, military radar systems, and navigation systems based upon GPS, such as WAAS being developed by the FAA.

Programs such as LWS Geospace are important ingredients in the mix required to improve space weather services. One hopes that attempts will be made to develop a synergy between actual users of the services, the service providers, and the LWS Geospace scientists. This will be essential for success.

There are a number of challenges ahead. LWS workers will rely on data sets that are not generated within their own mission. One of these data

sets involves the measurement of low-latitude ionospheric irregularities. It seems to the author that there are additional ionospheric data sets that may also be of interest, including the worldwide distribution of electron density and its variation, a data set that can only derived from the global constellation of vertical incidence sounders. Kintner et al. [2003] indicate that the greatest challenge will be coordination of the science data analyses with applications and with related government efforts. This is always a challenge, given turf wars than can ensue, but it is a noble objective.

6.4 DATA ASSIMILATION AND TRANSFER

Up until recent years the International URSIgram and World Days Service (IUWDS) was the vehicle for fusion of those kinds of data that pertain to the environment of space, the heliosphere, and the geosphere. A focus of the IUWDS was clearly solar-terrestrial in nature, and a major component related to the implications for the ionosphere and its electron density distribution. Recently the name of the IUWDS has been changed to the International Space Environment Service ((ISES). The various responsibilities have been described [NSWP, 2000]. Regional warning centers, operated within ISES, provide information to the World Warning Agency (WWA) in the USA on a daily basis. As it stands, the WWA provides a consolidated forecast set and data summaries to the regional centers for dissemination within the areas they serve.

6.5 MILITARY SPACE WEATHER INVOLVEMENT

6.5.1 Early DoD Activity

The US DoD has been involved in the investigation of space weather effects for decades, long before the term "space weather" became a part of our vocabulary. The same is true of other nations. Efforts within the various services was directed toward the solution of problems associated with command, control, communication, and intelligence systems, called C^3I. Even before the dawn of the space age with the successful launch of satellites, the US Navy was involved in the examination of the so-called Kennelly-Heaviside layer (i.e., the ionosphere) to the extent that it effected radio communications.

The history of military interest in the ionosphere and space weather was examined in Chapter 1. Given the importance of communications, radar, and electronic surveillance to the success of military objectives, it is not surprising that various military organizations have played a key role in the exploration of near-space and the upper atmosphere. It is imperative that any vulnerability of electronic and radio systems, induced by space weather effects, be fully understood so that countermeasures can be developed. Navies

showed the earliest interest in space and the ionosphere for historical reasons. For one thing, ships preceded airplanes, and in the USA context, the Navy was the only service to provide truly global reach until the middle of the 20th century. Over time, and certainly after the advent of satellite technologies, many activities originated by Navy scientists were transitioned to other services, notably the Air Force. While Army, Navy, and Air Force all have space weather requirements, the U.S. Air Force serves as the focal point for operational forecasting and data dissemination to military customers. It is also recognized that the DoD has a synergistic relationship to NOAA, since many sensors satisfy dual military and civilian requirements. Indeed, space weather is an equal opportunity discipline, impacting military and civilian systems in similar ways.

6.5.2 Space Weather Architecture

Much of material in this section is based upon the Space Weather Architecture Transition Plan. It is the definitive guidance from the DoD on the implementation of the Space Weather Architecture as developed by DoD, DoC, and a number of other federal agencies. It is noteworthy that the space weather architecture developed under the aegis of the NSSA is wholly consistent with recommendations found in the NSWP documents, but the DoD view provides somewhat more depth, a greater focus on the long term (i.e., 2010 and beyond), and gives consideration to fiscal constraints. The vision of National Space Weather is "as a nation, move forward to dramatically improve space weather understanding, forecasts, and services to meet customer needs". This is a dramatic statement, carrying with it the view that dramatic improvements are required and possible to achieve. Such a vision is optimistic and worth pursuing.

The National Space Weather goals are provided in Table 6-6. It is worth comparing them to the NSWP goals given in Table 6-1. The tone is quite different. The NSWP goals are very specific, and largely based upon what could (and should) be done, independent of the resources made available in a realistic operational and fiscal climate. The Architecture, while consistent with the detailed technical goals of the NSWP and taking no issue with them, provides a practical, albeit vague, template within which one can achieve most elements provided in Table 6-1. Realism is a good thing.

The linkages between the Space Weather Architecture Transition Plan and the NSWP are spelled out in the Transition Plan [NSWP, 2000] and will not be detailed herein. It also indicates the coordinating structures, the methodology for assessment of progress, and for resolution of conflicts between the stakeholder agencies. An important part of this process is that a vehicle for adjustment in the program is part of the coordination process, taking into account any breakthroughs that emerge as technology evolves.

Table 6-6: National Space Weather Goals in the NSSA-Sanctioned Architecture Document

- Achieve improved space weather response and support capability to:
  - Provide timely, accurate, and reliable observations and forecasts
  - Establish national priorities
  - Focus agency efforts
  - Leverage resources
- Pursue the space weather architecture "vector" to:
  - Increase the emphasis on operational model development
  - Ensure space weather operational capabilities are based on user needs
  - Improve the forecast capabilities based upon improved:
    - physics
    - models
    - user requirements

6.5.3 Existing Capabilities

The catalogue of space weather sensors and capabilities is sizable and growing. The space segment of this catalogue is depicted in Figure 6-2. Satellite systems are generally controlled by either the DoD or the DoC. The civilian sector and commercial users derive forecasting products from NOAA-SEC, and military users derive specialized forecasting products from the Air Force Weather Agency, AFWA. Data from all space assets are used in both NOAA-SEC and AFWA products, since SEC and AFWA share data, with the exception of data from classified systems. As would be expected, tailored products may be different for each class of users.

Table 6-7 is a listing of ground stations that make up the non-space component of the Space Weather Support System according to the Space Weather Baseline Operations Report. These systems, combined with those shown in Figure 6-2, provide the backbone of space weather observational capabilities. It should be noted that there exist other assets, not part of this "official" backbone. These assets may be controlled by so-called 3rd party vendors and commercial activities, and can be exploited to leverage data and forecasts provided by the backbone. There is the potential for feedback from the "independent" sources, and this should be explored.

Basically there are three sources for space weather data, and the choice and availability depends upon the customer category. Military customers obviously receive tailored products from AFWA, but may also derive additional information from NOAA or from 3rd party vendors (mentioned above) who subscribe to the NOAA-SEC data sets or generate their own proprietary products from other sources. The civilian sector derives data from the Space Environment Center, but may also get tailored outputs from 3rd party vendors. An organization that represents the 3rd party vendors is the Commercial Space Weather Interest Group, CSWIG.

Table 6-7: Ground Stations within the Space Weather Support Network

SOON (Solar Optical Observing Network)
RSTN (Radio Solar Telescope Network)
DISS (Digital Ionospheric Sounding System)
Ionospheric Measuring System
Neutron Monitor
Riometer
Canadian Radio Observatory
Australian Observatory
Australian Ionospheric Network
National Solar Observatories
NASA-JPL Total Electron Content Monitors
Archive Center
USGS Magnetometer Network

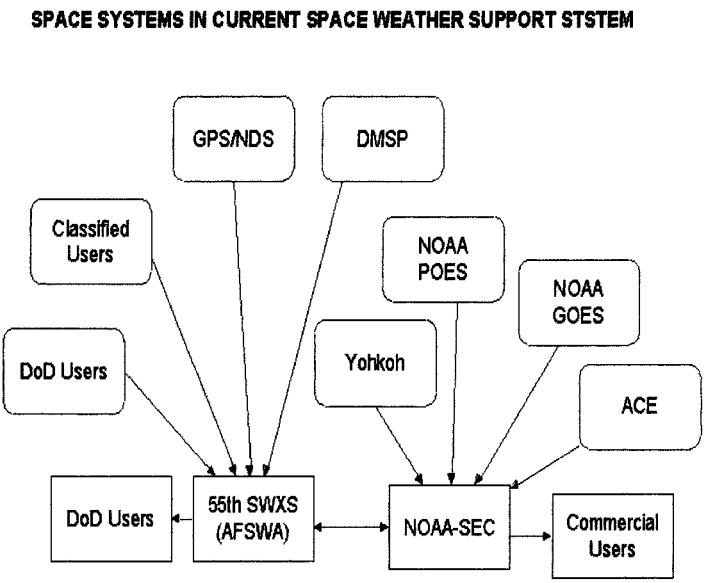


Figure 6-2: Data Flow for Various Space Systems Controlled by Government Agencies

6.5.4 Areas of Improvement

Space weather technology is undergoing constant evolution. New models are being developed and the sensor backbone is being improved. Additional areas of improvement are indicated in Figure 6-3.

Among the modeling efforts are those principally undertaken by the civilian community (i.e., NOAA). As would be expected there are plans to improve models of coronal mass ejections, interplanetary shocks, magnetic storm effects and related phenomena. A pleasant entry from an operational perspective is the development of assimilative models that combine data from diverse sensors to provide the best possible representation of the ionosphere

and magnetosphere. The opinion of the author is that this is certainly the way ahead.

It is noteworthy that there is no generalized space weather model. A specific NOAA program envisions an ensemble of models from which the most appropriate one can be selected under specialized circumstances. It is not clear why this effort is identified as a specific NOAA modeling program, but it is certainly a good idea. This could lead to an operational solution for a vexing short-term forecasting problem, one of rapidly selecting from a catalog of competing models. It would also be useful in post-analysis (i.e., hindcasting) or in the performance of "what if" or "thought" experiments.

The improvement in the solar optical and radio telescopes is a part of the planned improvement in ground-based assets. The existing systems are called the Solar Observing Optical Network (SOON) and Radio Solar Telescope Network (RSTN) respectively. The RSTN will be replaced by a Solar Radio Spectrograph (SRS) and a Solar Radio Burst Locator (SRBL). The optical system is to be replaced by ISOON, or improved SOON. The replacement systems will be smaller, efficient, and more reliable. All to the good.

The DoD and NOAA have a long tradition in flying "traditional" weather satellites. Over the years, these satellites have also carried some sensors that are more applicable to space weather that terrestrial weather. The DMSP platform is a workhorse for DoD, and several improvements are being made to the polar orbiting satellites. To be added is a Special Sensor Ultraviolet Limb Imager (SSULI) that can deduce vertical profiles of airglow from constituents in the altitude regime: 50-750 km.

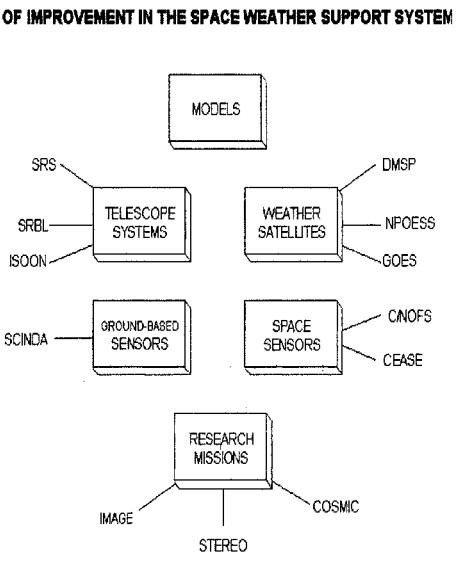


Figure 6-3: Specified systems with planned improvements

Another new system is the Special Sensor Ultraviolet Spectrographic Imager (SSUSI) that monitors UV emission bands from the upper atmosphere. DoD and NOAA are planning to jointly develop and operate a National Polar-orbiting Operational Environmental Satellite System (NPOESS). This system will consist of two satellites in its space segment. Eventually these two birds will be added to Eumetsat to form a joint USA-European system for monitoring the terrestrial and space environment. GOES will continue to be a part of the space weather support environment. New sensors will be added, including x-ray and ultraviolet monitors. There is a new sensor carried by GOES (i.e., Solar x-ray Imager, SXI), having the capability to provide x-ray imagery of the disk and corona. It can also detect x-rays from behind the limb.

Improvements are also being planned in areas very specifically directed to the solution of important telecommunication problems. The ones cited in this paragraph take the form of Advanced Concepts Technical Demonstrations, ACTDs. Two new programs are the ground-based Scintillation Network Decision Aid (SCINDA) and the space-based Communications/Navigation Outage Forecasting System (C/NOFS). These two systems will provide a greatly improved capability to monitor and forecast radiowave scintillation. C/NOFS has the purpose of detecting ionospheric conditions deemed favorable to the generation of scintillation events, and therefore might be useful in the prediction of scintillation for certain earth-space paths. The SCINDA exploits radio receivers to generate scintillation maps over equatorial regions where scintillation is most pronounced. What is currently missing is a similar system for polar regions, a matter that is to be considered in the longer term. There is another instrument called CEASE that evaluates system outages from anomalies such as spacecraft charging. This system, in tandem with SCINDA and C/NOFS, can also determine if spacecraft outages are due to radiowave scintillation or system failure arising from high-energy protons and cosmic rays.

Several research missions can also play a role in the likelihood of significant improvement in capability. These programs include (i) the Constellation Observing System for Meteorology, Ionosphere and Climate (COSMIC), (ii) the Solar Terrestrial Relations Observatory (STEREO), and (iii) the International Monitor for Auroral Geomagnetic Effects (IMAGE). The magnetosphere is the focus of IMAGE while solar activity is the focus of STEREO. A consortium including the Taiwan National Space Program Office, NASA, JPL, and several universities are responsible for the ambitious COSMIC mission. The purpose of COSMIC is to measure electron densities in the upper atmosphere using eight micro-satellites and a global network of data collection centers.

6.5.5 Space Weather Architecture "Vector"

The design of the DoD architecture resulted in what is referred to as an architecture vector. This construction presents one with the notion of active change from the present baseline configuration, through minimal architecture, target architecture, and desired architectures phases. The invention of this notional vector is useful since it provides direction and focus. It also recognizes the nuances of technological breakthroughs or bottlenecks as well as programmatic and fiscal constraints. Details about the desired architecture models and programs are found in the architecture document. We have listed the sensors in Table 6-8 and have depicted the models in Figure 6-4.

Models required include those in the solar, magnetosphere, ionosphere and neutral categories. For telecommunications the priority order should be the ionosphere, magnetosphere, solar, and then neutral. Some models do exist but improvements are needed for the activities of assessment, warning and forecasting. The DoD asserts that forecast models for the ionosphere and magnetosphere are in the best shape of all. This is because of the wealth of ionospheric data available and comprehensive studies over the last fifty years.

Table 6-8: Space and Ground-based Sensors in the Ultimate Architecture

- Space
  - LEO equatorial satellite to measure ionospheric properties
  - Sensors on NPOESS to measure electron density profiles, etc.
  - Sensors on two GOES satellites (i.e., a candidate) with EUV and X-ray imaging capability
  - Satellite on Sun-Earth line for solar and interplanetary measurements
  - Piggyback particle detectors on many satellites, such as NPOESS
  - Piggyback energetic neutral atom imager on many satellites
  - Telescope on high earth orbit satellite (HEO) to observe Northern Polar Cap continuously
  - STEREO system deployed
  - Piggyback GPS/Occultation Sensor (OS) receivers hosted by 18-24 low altitude Space –Based Infrared System (SBIRS) satellites
- Ground
  - Ten sensors for polar scintillation measurements
  - Twenty sensors for equatorial scintillation measurements
  - Fifty sensor packages located globally at JPL and USGS sites and other selected sites: GPS receivers, VHF receivers, ionosondes, magnetometers
  - Ten specialized all-sky video recording systems deployed at selected polar sites
  - Four solar radio and solar optical sites (currently SEON)
  - Riometer deployed to polar cap (currently Thule)
  - Measurements of satellite drag from satellite tracking network

The DoD Architecture recommendations are a useful roadmap for the future and may guide major acquisition, development, and research activities

in the future. They are too general to outline here, but we do take note of the following statement made regarding space weather importance awareness:

"Space weather effects have the most impact on communications, Position, Navigation, and Timing (PNT), and Intelligence, Surveillance, and Reconnaissance (ISR)" ... activities.

We certainly agree.

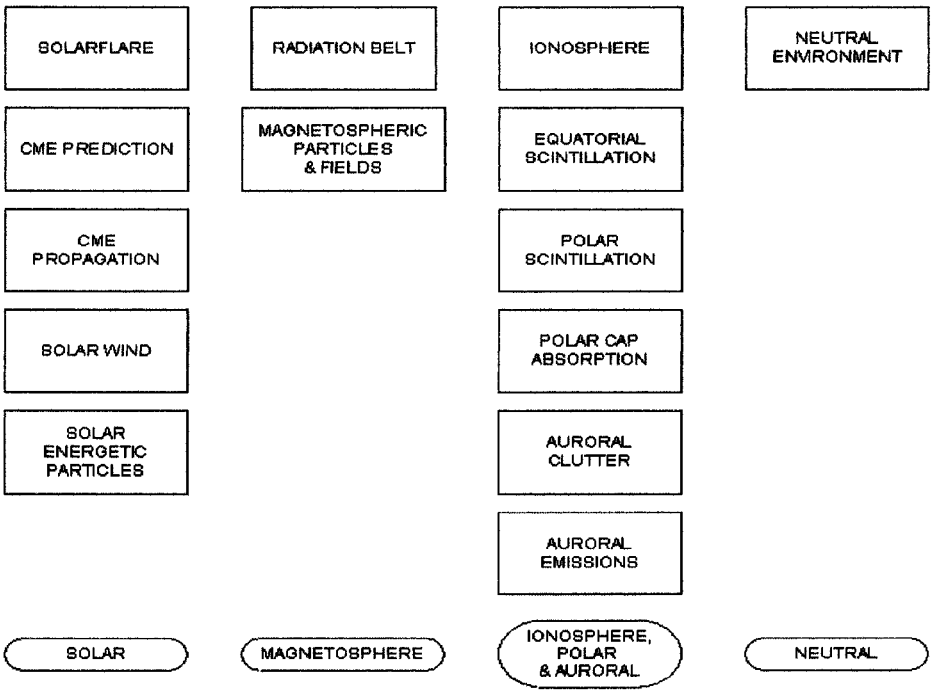


Figure 6-4: Models needed in the ultimate or desired architecture.

6.6 INTERNATIONAL INITIATIVES

In addition to the United States, an increasing number of nations are embarking on space weather programs, or have reorganized existing space science activities to be in harmony with space weather objectives. This calls for coordination across bureaucratic boundaries and national borders. Moreover, traditional science must be merged with some engineering groups to facilitate operational prediction and forecasting services. The European Space Agency (ESA) has embarked upon an ambitious space weather

campaign, and it collaborates with the European Union (EU). For its part, the EU is involved in a number of collaborative enterprises among the member countries, and several European COST (i.e., Cooperation in the Field of Scientific and Technical Research) *Actions* bear directly upon the ability to understand the ionosphere and space weather. Aside from the EU and its member states, national space weather efforts are underway in Sweden, Japan, France, Australia, and Canada. The list is growing.

6.6.1 European Union COST Actions

There are four specific EU activities, called *Actions* within the (COST) vernacular, which are important to recognize in the context of the ionosphere, space weather, and telecommunications. Reports for the first three of these Actions were available as this book went to press. These reports contain a wealth of information on state-of-the-art techniques and should be on the bookshelf of every ionosphericist and telecommunications specialist. While the thrusts of the efforts are directed to the European region, the general concepts are applicable to other geographical areas in the majority of cases. The technical issues addressed by these Actions will not be covered in this largely programmatic chapter. Selected aspects are described elsewhere in this manuscript.

6.6.1.1 COST Action 238

The first COST action organized by the EU to examine a direct relationship between space weather effects and telecommunications was Action 238, although space weather was not the primary focus or driver for the activity. The main focus was the ionosphere as an influence on HF communication systems and earth-space systems. The Action was dubbed PRIME, standing for "Prediction and Retrospective Ionospheric Modelling over Europe". Action 238 was a four-year activity that was begun in March 1991. Thirty-one organizations from seventeen member states were involved in the activity. Objectives of the Action were to develop techniques for using ionospheric sounding information taken from existing measurement systems to develop improved ionospheric models for Europe. The final report was accepted on June 1, 1995. See Bradley [1999].

6.6.1.2 COST Action 251

The second COST Action of significance was Action 251. It was entitled "Improved Quality of Service in Ionospheric Telecommunication Systems Planning and Operation". The activity was supported by a group of 122 participants from 46 organizations in twenty nations. The main objectives

of Action 251 were to (i) collect various types of ionospheric data, (ii) to develop forecasting procedures for use in the European environment, (iii) to develop models that would be directed toward system performance evaluation, and (iv) develop methods for communication channel simulation. Outputs of COST 251 included not only models, but also the formation of the Ionospheric Dispatch Center in Europe (IDCE), located in Warsaw, Poland. The Action began on April 7, 1995 and was concluded in 1999. See Hanbaba [1999].

6.6.1.3 COST Action 271

This COST Action is on *Effects of the Upper Atmosphere on Terrestrial and Earth-Space Communication*. The objectives of COST 271 are to stimulate international cooperation in predicting and forecasting the ionosphere and the plasmasphere. In this process, the Action would lead to the development and implementation of new communication services, and to the minimization of ionospheric effects on communication systems. At the same time, Action 271 would provide for the collection of new data for nowcasting and forecasting.

Action 271 was commissioned on August 16, 2000 and the termination was scheduled for August 15, 2004. Four Working Groups (WGs) were established, and a number of Work Programs (WPs) organized under each. A number of significant papers were presented at the Action 271 Workshop, "Significant Results in COST 271 Action", held in Spetses Island, Greece in September 2003. A list of the presentations may be found on the COST 271 website.

6.6.1.4 COST Action 724

This most recent COST Action is on *Developing the Scientific Basis for Monitoring, Modeling, and Predicting Space Weather*. This Action is described in a news article in the Journal of Space Weather as well as the ESA website. It is anticipated that Action 724 will form the basis of a central coordinator for European Space Weather. As such, this new activity would eventually serve as a European equivalent to NOAA-SEC in Boulder. One of the plans is to organize a European equivalent to the U.S. Space Weather Week orchestrated by NOAA-SEC. The inaugural event is to be held in late 2004 at ESTEC in Noordwijk, the Netherlands.

As indicated by Lilensten et al. [2004], the origins of Action 724 can be traced to 1999 when the European Space Agency organized two consortia, one headed by Rutherford-Appleton Laboratory (RAL) in the UK and the other by ALCATEL in France, to examine the range of European space weather issues. A Space Weather Working team (SWWT) examined the findings of the consortia and reported back to ESA with recommendations. Recommendations consisted of a number of pilot projects plus the institution

of COST Action 724. By 2003, there were 21 countries signed on to the Action: Finland, France, Germany, Greece, Scotland, Austria, Armenia, Belgium, Bulgaria, Czech Republic, Denmark, Great Britain, Hungary, Israel, Italy, Poland, Russia, Slova Republic, Spain, Switzerland, and Ukraine. ESA joined the group as an associated institution. The inaugural meeting was held on November 14, 2003.

6.6.2 European Space Agency

The European Space Agency (ESA) coordinates European space weather activities. For example, ESA has initiated a space weather applications pilot project, one purpose of which is to demonstrate the benefits of current and future space weather services. A Space Weather Working Team (SWWT) guides the activity with a membership of experts from the ESA member states. The SWWT acts as a forum for planning and discussion, as well as coordination with other European space weather initiatives such as the EU COST Actions 238, 251, 271 and 724.

ESA is comprised of fifteen countries within Europe that collaborate on space science and technology. As represented on the ESA website, the technology objectives include the development of telecommunication systems, earth observation satellites, and launch vehicles through the prototype phase. The final operational systems are the responsibility of Eutelsat, Eumetsat, Arianespace, Inmarsat, and others.

A space weather website is maintainted by the Space Environments and Effects Analysis Section of ESTEC within ESA. The organization also publishes the Space Weather Euro News (SWEN), and these newsletters may be downloaded from the ESTEC space weather web server. The server hosts features typical of such web sites including: tutorials, international activities, models and data, workshop information, and links to other sites such as the NOAA-SEC *Space Weather Now.*

ESA sponsored a space weather workshop, "Developing a European Space Weather Service Network", in the Fall of 2003. The purpose was to orchestrate the development of a Space Weather European Network (SWENET). The SWENET system is a pilot project of space weather service development and collaboration. The objective of this is to achieve a long-term perspective of the space weather applications and services, along with the societal benefits and relevance of such services. A noble objective indeed.

6.6.3 Sweden

The space weather activity in Sweden is centralized within the Institutet för Rymdfysik (IRF) or the Swedish Institute of Physics. This government agency has its principal office in Kiruna with other locations in Uppsala, Umeå, and Lund. At Kiruna, the research activities include

atmospheric physics, solar system physics, and space technology. At Uppsala, the research program includes space plasma physics, and at Umeå, the activity includes space science data analysis tools. Lund has a number of research projects including solar activity, solar activity and climate, GIC effects, and effects on radiocommunication systems.

The Swedish Institute of Space Physics and the Swedish Regional Warning Center (RWC) are located at Lund. Both organizations may be accessed at the Lund Space Weather Center website. Solar-terrestrial data and activity forecasts are available from the RWC, including SOHO/MDI data. A link to the COST Action 724 activity is also available.

6.6.4 France

France is the host country for the regional forecast center serving Western Europe under the aegis of the International Space Environment Service (ISES). France is heavily involved in the EU COST Actions related to space weather. The forecast center is located at Paris-Meudon University. According to the National Space Weather Program documentation [NSWP, 2000], 23% of the customers of the French service are from France, 47% are from the remainder of Europe (including Eastern Europe) and 12% are from the rest of the world. The Meudon Center cooperates mainly with CNES and ESA, but it also provides forecasts to Canada and Japan.

6.6.5 Japan

The Hiraiso Solar Terrestrial Research Center operates the Space Environment Information service. Using the Japanese meteorological satellite, SMS-4, the services include daily representations of high-energy particle flux measured using the Space Environment Monitor (SEM) package. The center provides geomagnetic and solar activity data, and real-time data from the ACE satellite. The Center also operates SERDIN, the Space Environment Real-Time Intercommunication Network.

It should be noted that Japan operates a vertical-incidence sounder network for deriving ionospheric parameters. These data may be accessed from the Internet. Sites are at Okinawa, Kokubunji, Wakkanai, and Yamagawa. These data may also be accessed from websites managed by NGDC. Japan maintains the World Data Center for the Ionosphere, WCA-C2, as part of the original WDC system.

Japan has an active interest in space weather, and a working group on the subject was formed in 1999. Steps are underway to integrate space weather activities in the Asia Pacific region, and a space weather forecast center is being planned at the Communication Research Laboratory.

As a side note, a survey of space weather customers of CRL products indicates that ~ 40% are involved in communications or amateur radio.

Supplementary Note: Other centers that archive ionospheric data are World Data Centers for Solar Terrestrial Research in Boulder, USA (WDC-A), Rutherford-Appleton Lab in Didcot, UK (WDC-C1), and in Moscow (WDC-B). Ionospheric data is also archived by the Ionopheric Prediction Service in Haymarket, Australia, which is the WDC for Solar-Terrestrial Science.

6.6.6 Canada

The agency responsible for space weather data acquisition and dissemination in Canada is Natural Resources Canada, NRCan. We have discussed NRCan products of interest in Chapter 5.

6.6.7 Australia

It is well known that the Ionospheric Prediction Service (IPS) is an equivalent to NOAA-SEC for the Southern Hemisphere, in matters related to space weather and telecommunications. We have discussed IPS in Chapter 5. The IPS web site is one of the best for our purposes, although much of the original data is derived from non-Australian sources. The umbrella organization in Australia is the Australian Space Forecast Center (ASFC). The role of ASFC is to monitor the solar-terrestrial environment, including the sun, the solar wind, and the ionosphere. IPS serves as the WDC for Solar-Terrestrial Science in the World Data Center system.

6.7 SCIENTIFIC & PROFESSIONAL ORGANIZATIONS

6.7.1 URSI

URSI consists of a number of Commissions. Of most relevance to space weather is Commission G entitled: On the Ionosphere. This commission is broken into a number of Study Groups as indicated in Table 6-9. Working Groups within Study Group G are provided in Table 6-10. Joint Working Groups involving Commission G and other Commissions are provided in Table 6-11. A listing of some Inter-Union Working Groups is given in Table 6-12.

Commission G: Ionospheric Radio and Propagation (including ionospheric communications and remote sensing of ionized media) is the group of primary interest for purposes of this manuscript. The Commission deals with the study of the ionosphere in order to provide the broad understanding necessary for radio communications. Quite naturally space weather aspects are always involved in the studies undertaken.

Specifically, the Commission G study includes the following areas: (i) global morphology and modeling of the ionosphere, (ii) ionospheric space-time variations, (iii) development of tools and networks needed to measure ionospheric properties and trends, (iv) theory and practice of radio

propagation via the ionosphere, and (v) application of ionospheric information to radio communications.

Table 6-9: URSI Commissions

Commission	Title
A	Electromagnetic Metrology
B	Fields and Waves
C	Radio-communication Systems and Signal Processing
D	Electronics and Photonics
E	Electromagnetic Noise and Interference
F	Wave Propagation and remote Sensing
G	Ionospheric Radio and Propagation
H	Waves in Plasmas
J	Radio Astronomy
K	Electromagnetics in Biology and medicine

Table 6-10: Working Groups of Commission G of URSI

Group	*Title*
G.1	Ionosonde Network Advisory Group (INAG)
G.2	Studies of the Ionosphere using Beacon Satellites
G.3	Incoherent Scatter
G.4	Ionospheric Research to Support Radio Systems

Table 6-11: Joint Working Groups Involving Commission G of URSI

Group	Title
EGH	Lithosphere-Atmosphere-Ionosphere
FG	Ionosphere and Atmosphere remote sensing
GF	Middle Atmosphere
GH.1	Active Experiments in Plasmas
GH.2	Computer Experiments, Simulation and Analysis of Wave Plasma Processes
GH.3	Wave Turbulence Analysis

Table 6-12: Inter-Union Groups of Interest to Commission G of URSI

Group	Title
URSI-IAGA	VLF/ELF Remote Sensing of the Ionosphere and the Magnetosphere (VERSIM)
URSI-COSPAR	International Reference Ionosphere

6.7.2 COSPAR

COSPAR stands for Committee on Space Research, a body established by the International Council for Science (ICSU) in 1958. COSPAR acts as a forum for the presentation of latest scientific information and as a vehicle for data exchange. By mandate, COSPAR also advises the

United Nations and other international bodies, and serves as an advocate for international cooperation of space science activity. COSPAR organizes scientific assemblies, colloquia, workshops and symposia.

6.7.3 SCOSTEP

Organizations such as the Scientific Committee On Solar-TErrestrial Physics (SCOSTEP) are playing a role in the structuring of space weather campaigns. SCOSTEP organizes and conducts international Solar-Terrestrial Physics (STP) programs of finite duration in cooperation with other bodies belonging to the International Council for Scientific Unions (ICSU). It provides guidance to the STP discipline centers of the ICSU's World Data Center system. SCOSTEP follows earlier entities in the ICSU that were involved in planning and implementing the International Geophysical Year (IGY: 1957-58) as well as the International Quiet Sun Year (IQSY: 1964-65). SCOSTEP programs that have been completed include: the International Magnetospheric Study (IMS: 1976-79); the Solar Maximum Year (SMY: 1979-81); the Middle Atmosphere Program (MAP: 1982-85); and the Solar-Terrestrial Energy Program (STEP: 1990-97). A number of post-STEP programs are now in progress, and two of these programs are: STEP-Results, Applications, and Modeling Phase (SRAMP) and the International Solar Cycle Study (ISCS). SCOSTEP has embarked upon a new international scientific program for the 2004-2008 time frame termed CAWSES, Climate and Weather of the Sun-Earth System.

6.7.4 ITU-R

Within the International Telecommunications Union (ITU), the Radiocommunication Sector (i.e., ITU-R) is responsible for "ensuring the rational, equitable, efficient and economical use of the radio-frequency spectrum by all radiocommunication services". The Sector performs studies from which official ITU Recommendations are formulated. Study Groups (SGs) of the ITU-R are responsible for specialized deliberations on technical matters of concern, and the regulatory and policy functions are performed by World and Regional Radiocommunication Conferences and Assemblies supported by the SGs. From the point of view of space weather, the ionosphere, and propagation information supporting earth-to-space and terrestrial communications, we find that the primary Study Group is SG-3: dealing with radio propagation and prediction systems. Table 6-13 is a listing of all of the designated Study Groups. While SG-3 has the most application to space weather, other groups deal with space assets (i.e., satellite systems) and systems that exploit space science and technologies.

Table 6-13: ITU-R Study Groups

Group	Title
SG 1	Spectrum management
SG 3	Radiowave propagation
SG 4	Fixed satellite service
SG 6	Broadcasting services
SG 7	Science services
SG 8	Mobile, radio-determination, amateur and related satellite services
SG 9	Fixed service

6.7.5 NCEP

The National Centers for Environmental Prediction (NCEP) is organized under the National Weather Service. The Space Environment Center (SEC) belongs to the NCEP family. The group includes: the Aviation Weather Center, the Climate Prediction Center, the Environmental Modeling Center, the Hydrometeorological Modeling Center, the Ocean Prediction Center, the Space Environment Center, the Storm Prediction Center, and the Tropical Prediction Center.

6.7.6 CSWIG

A number of companies have emerged offering services based upon Space weather data. Such companies, termed space weather vendors, are not merely parroting the source data from NOAA, NASA, or other government agencies. In some instances they possess independent sources of data, and more generally utilize proprietary models or methods for analysis of the data. Above all, the companies tend to be quite close to the ultimate user, having an intimate knowledge of systems owned by these customers. The government activities, owners of the primary data sources, cannot efficiently invest in these ultimate applications products. Accordingly the space weather vendors perform a vital service. Not only does this arrangement provide the ultimate user with end products that are tailored for very specific applications, it also provides the source organizations with more time to develop improved primary data sources and products.

Dr. Ernest Hildner, director of the Space Environment Center at NOAA, has stated that it is the policy of NOAA to foster a viable space weather vendor industry. As indicated on the NOAA-SEC web site: "because SEC is unable to provide all the services users want, we are anxious to work with value-added vendors who will use our data and products to develop commercially available products. Chapter 7 (Epilogue), which contains a brief interview with Dr. Hildner, is recommended to the reader.

A Commercial Space weather Services Interest Group SWIG) has been established, and NOAA has hosted meetings for this group at Boulder as

part of the annual Space Weather Week activities. Table 6-12 is a listing of organizations that have identified themselves as vendors of Space Weather services and products. We have italicized those firms related to telecommunications, our primary focus in this book.

Table 6-14: Listing of Space Weather Vendors

Note: The italicized listings are those providing products and services pertaining to radiocommunication, navigation and surveillance services. A number of these vendors are members of the Commercial Space Weather Interest Group (CSWIG).

Name of Vendor
Aerospace Corporation
ARINC
Metatech Corporation
Northwest Research Associates
Radio Propagation Services
Rockwell-Collins
Solar Terrestrial Dispatch
Space Environment Technologies/SpaceWx
Exploration Physics International
Community Alert Network
In-Flight Radiation Protection Services, Inc.
High Altitude Radiation Monitoring Service
Federal Data Corporation
Exploration Physics International, Inc.
Federal Data Corporation
Electric Research & Management, Inc.

6.7.7 Space Weather Week

The Space Environment Center (SEC) of NOAA has managed and hosted annual Space weather Week (SWW) workshops and symposia for a number of years. These activities bring together a relatively large group of scientists and engineers that are involved in various aspects of space weather. The event began in the 1990s as a series of user conferences. A synopsis of the events for 1999, 2000, 2001, 2002, 2003, and 2004 can be found on the NOAA-SEC website. The SWW event has become so successful that ESTEC of the European Space Agency (in collaboration with the EU) is planning the invocation of a similar series dedicated to European requirements and activities, as stimulated by the COST Action 724 sponsored by the EU.

The Space Weather Week is not the typical URSI or COSPAR conference. While science is an important aspect of SWW, the idea is to encourage the participation of the developers, managers and users of systems thought vulnerable to space weather, collectively called "customers of space weather products". This is never as successful as one would like, for it is often hard to get managers of some systems (e.g., telecommunications industry) to

admit vulnerabilities in a highly competitive marketplace. It is an easier "sell" with government customers, since mission requirements relating to performance will generally trump other factors.

6.8 RESEARCH PROGRAMS & ACTIVITIES

We have already mentioned the NSWP and NASA's Living with a Star (LWS) research program. Several NSF initiatives involving space weather are CEDAR, GEM, and SHINE, and these are listed in Table 6-15. Some additional missions sponsored by NASA and other organizations are also listed. A new CAWSES effort organized under the aegis of SCOSTEP is worth noting.

Table 6-15: Sampling of Programs & Activities Related to Space Weather

NSF	NASA	SCOSTEP	OTHER
CEDAR	ACE	STEP	ISTP
GEM	FAST	SRAMP	CLUSTER
SHINE	IMAGE	ISCS	SOHO
CISM	GEOTAIL	CAWSES	INTERBALL
	POLAR		
	WIND		
	RHESSI		
	TIMED		
	TRACE		

Note-1: The NSF programs are discussed in Sections 6.8.1 – Sections 6.8.4
Note-2: The SCOSTEP programs are discussed in Section 6.7.3 and CAWSES is separately discussed in Section 6.8.5.
Note-3: The ISTP is an international effort including: the NASA GGS Program, the ESA CLUSTER program, the Russian INTERBALL, and SOHO.
Note-4: WIND, GEOTAIL, and POLAR are part of the NASA GGS Program. The Canadian CANOPUS program is a partner.
Note-5: NASA programs ACE, FAST, IMAGE, RHESSI, TIMED, and TRACE are identified in Section 6.8.6.
Note-6: Terrestrial sensors and data gathering systems are listed in Table 6-16. This includes SuperDARN, incoherent scatter radar, sounders, etc.

6.8.1 CEDAR

CEDAR stands for "Coupling, Energetics and Dynamics of Atmospheric Regions", and is sponsored by the National Science foundation. The scientific objectives of CEDAR are may be found on the "CEDARweb". The purpose of the effort is to "enhance the capability of ground-based instruments to measure the upper atmosphere, and to coordinate instrument and model data to the benefit of the scientific community".

CEDAR provides a number of services to the community, centered about education and the promotion of science. Aside from the periodic

meetings with tutorial lectures, which are typically made available to the public in a variety of media, CEDAR also orchestrates a community mailing with announcements of meetings, job opportunities, etc. The CEDAR POST is a newsworthy bulletin that is available.

The CEDAR Data System is a cooperative venture between NSF, the High Altitude Observatory (HAO), the National Center for Atmospheric research (NCAR) and other organizations that provide data to the system. The primary mission of the CEDAR database is the provision for: (i) an archive for models and data, (ii) a browsing capability, (iii) an interactive capability, and (iv) a repository for detailed documentation on data acquisition and processing. The CEDAR Database, hosted by NCAR and HAO, has an association with the TIMED satellite program in connection with ground-based data sets. Some of the ground-based systems include incoherent scatter radar (ISR) and HF radar (HFR) systems, to name a few.

Table 6-16 is a listing of ground-based programs that are important in the promotion of a successful space weather program. Of those listed in Table 6-16, only the ISR and HFR are contained in the CEDAR Database. Table 6-17 and Table 6-18 contain listings of the incoherent scatter and HF radars respectively. There are a number of other system types that contribute to the overall space weather effort, and those listed are more directly relevant to the furtherance of telecommunication performance prediction capabilities.

Table 6-16: Some Ground-Based Systems of Interest

- Incoherent Scatter Radar (ISR) (e.g., Millstone Hill)
- HF Radar (HFR) (e.g., SuperDARN)
- GPS-TEC monitors
- Scintillation monitors (e.g., CNOFS)
- Vertical Incidence Sounders (e.g. Digisonde, Dynasonde)
- Oblique Incidence Sounders (e.g. Chirpsounder)
- Magnetometer networks (e.g., Intermagnet, Canopus)
- Solar Optical and Radio Telescopes (e.g. SOON, SEON, etc.)

Listings of various sounding stations are found in the NGDC archives and at WDC sites for Solar-Terrestrial Physics. See also Chapter 5 and specifically Table 5-10.

6.8.2 GEM

The National Science Foundation established the Geospace Environment Modeling (GEM) program. Its goal is to provide a focus on the near-earth region of geospace. This region is defined to lie between the earth's ionosphere and the earth-solar wind interaction region. The ultimate purpose is to support basic research directed toward the development of a "Global

Geospace General Circulation Model (GGCM)" with a capability for predictions. In truth, GEM supports a number of campaigns, with the GGCM initiative being a primary example. The 1st GEM campaign (on the magnetospheric cusp and boundary layer) ran from 1991-1996; the 2nd campaign (on the magnetotail and substorms) ran from 1994-2003; the 3rd campaign (on the inner magnetosphere) is ongoing; and a 4th campaign (on magnetosphere-ionosphere coupling) is also ongoing.

GEM organizes workshops at AGU meetings and has held joint workshops with the CEDAR crowd. GEM publishes a newsletter, the GEM Messenger, which is available from the GEM Website. UCLA manages the GEM Homepage on the Web.

6.8.3 SHINE

The National Science Foundation established the SHINE program in the year 2001, following the GEM and CEDAR examples. It is recalled that GEM supports space weather research in the magnetosphere and the near-earth portion of geospace, while CEDAR supports space weather research and data derived from ground-based sensors. The SHINE initiative emphasizes solar disturbances that propagate in the direction of earth. Like CEDAR and GEM, workshops are organized under the SHINE initiative.

SHINE is advertised as an affiliation of scientists actively involved with solar and heliospheric research, and specifically science directed toward an improved understanding of solar disturbances that propagate toward earth.

6.8.4 CISM

The Center for Integrated Space Weather Modeling (CISM) is a Science and technology Center (STC) sponsored by NSF. The center consists of research activities at eight universities, augmented by activities within government, commerce, and private research institutions. The effort is led by Boston University, and includes: University of California, Stanford University, SAIC, University of Colorado (NCAR/HAO), University of Texas at El Paso, Rice University, Alabama A&M, NCSA, Dartmouth College, Brown University, NRL-CCMC.

The goal of CISM is to build a physics-based model of space weather that will enable forecasting of the near-earth environment based upon the solar influences. CISM offers a two-week summer school on space weather phenomena, modeling, and consequences, typically at Boston University.

6.8.5 CAWSES

CAWSES, Climate and Weather of the Sun-Earth System, is a new SCOSTEP program for the period 2004-2008. The basis and purposes for CAWSES follow naturally from prior SCOSTEP programs: IMS (1976-1979), SMY (1976-1979), MAP (1982-1985), STEP (1990-1997), and S-RAMP (1998-2002). Specifically, CAWSES leverages the STEP and S-RAMP programs. The major areas of concentration include: (i) solar influence on climate and (ii) the science and applications of space weather. The second area is of greatest interest for purposes of this book.

6.8.6 Additional Missions & Activities

Under the International Solar Terrestrial Physics Program (ISTP), NASA has sponsored the Global Geosciences Mission (GGS). The GGS includes GEOTAIL, WIND, and POLAR as part of the space complement, and involves the Canadian CANOPUS ground-based systems. Other parts of ISTP incorporate the ESA CLUSTER, the ESA/NASA SOHO satellite, and the Russian INTERBALL. Below are a few comments about some of the programs that were identified in Table 6-15 and Table 6-16.

Incoherent Scatter Radar (ISR): Otherwise known as Thomson scatter radar, ISR provides considerable information about the electron and ion density profiles of the ionosphere, and can provide additional data on plasma temperatures and ionospheric drifts. Unlike vertical-incidence sounders that are restricted to bottomside investigation, ISR facilities, listed in Table 6-17, can extract electron density profiles of the entire ionosphere. ISR can also detect ionization valleys, a situation that is problematic for ionospheric sounders. On the other hand, ISR requires a high-gain antenna and significant transmitter power, leading to a significantly greater expense for operations than sounding systems.

Table 6-17: Incoherent Scatter Radars (ISR) in the CEDAR Database

Station	Latitude (degrees E)	Longitude (degrees N)
Jicamarca (Peru)	-11.95	-76.0
Arecibo (Puerto Rico)	+18.3	-66.8
Millstone Hill (MA, USA)	+42.6	-71.5
Kharkov (Ukraine)	+50.0	+36.2
Irkutsk (Russia)	+52.85	+103.1
Sondrestrom (Greenland)	+67.0	-51.0
EISCAT Sodankyla (Finland)	+67.4	+26.6
EISCAT Kiruna (Sweden)	+67.9	+20.4
EISCAT Tromso (Norway)	+69.6	+19.2
EISCAT Svalbard (Norway)	+78.0	+15.0

SuperDARN: The HF radars indicated in Table 6-18 are oblique-incidence radars, and are part of the SuperDARN network of radars, operating in the northern and southern polar regions. The raw ionospheric data derived from the SuperDARN radars includes line-of-sight ion velocity for regions that present scattering irregularities. Continuous maps of ionospheric convection can be derived from operations, and Northern Hemispheric data are readily available from the SuperDARN webpage via APL. Refined data are available from the sites managed by CEDAR/TIMED. The Southern Hemispheric data sets are typically delayed due lack of an adequate method for data relay.

Table 6-18: SuperDARN Radars in the CEDAR Database

Station	Latitude (degrees N)	Longitude (degrees E)
Pykkvibaer (Iceland)	+63.86	-19.20
Stokkseyri (Iceland)	+63.86	-22.02
Hankasalmi (Finland)	+62.32	+26.61
King Salmon (AK, USA)	+58.68	-156.65
Kodiac Island (AK, USA)	+57.60	-152.20
Prince George (Canada)	+53.98	-122.59
Goose Bay (Canada)	+53.32	-60.46
Saskatoon (Canada)	+52.16	-103.53
Kapuskasing (Canada)	+49.39	-82.32
TIGER (Australia)	-43.38	+147.23
Kergeulen Island	-49.39	+70.26
Syowa East (Antarctica)	-69.01	+39.61
Syowa South (Antarctica)	-69.00	+39.58
SANAE (Antarctica)	-71.68	-2.85
Halley (Antarctica)	-75.52	-26.63

CANOPUS: This system is especially valuable for terrestrial communications applications in North America, Canada, and other portions of the northern hemisphere polar region. It is associated with the NASA GGS under the ISTP international effort.

ACE: The Advanced Composition Explorer is a satellite system designed to monitor solar wind information in real time. The location of ACE is at the L1 libration point between the sun and earth. This is ~ 1.5 million km from the earth, or about one percent of the earth-sun distance. This vantage point gives roughly a 1-hour warning of possible disturbances of the near geospace and the ionosphere arising from solar wind interactions with the geoplasma. Data are provided to NASA ground stations and to the NOAA SWO Center in Boulder. Real-time data include the EPAM data (electrons, and protons), MAG data (Bx, By, Bz, Bt, theta, phi), SIS data (energetic protons) and SWEPAM data (density, temperature, speed, and spacecraft position).

Data are accessed at the NOAA-SEC Website. A geomagnetic activity test product based upon ACE data has been developed.

FAST: The Fast Auroral Snapshot Explorer is one of a number of small explorer satellite (SMEX) missions managed under the long-standing NASA Explorer program.

IMAGE: This system was launched into a highly elliptical orbit with an apogee of about 7 earth radii above the northern polar region, and the period of the orbit is approximately 13.5 hours. Real-time data is transmitted to a number of ground stations and then to NOAA-SEC for public availability. The data includes auroral images, and global maps of disturbances. Such data can be used for model development and validation; and since it is available in real-time, it can have operational value.

RHESSI: A NASA Small Explorer satellite. RHESSI is designed to examine the physics of solar flares using imaging and spectroscopic observations of hard x-rays and gamma rays. While Skylab, SMM, and the US/Japanese Yohkoh and many other satellite missions have examined solar x-ray flares, RHESSI is believed to be the first platform to combine gamma rays, hard x-rays and high-resolution spectroscopy. This should enable scientists to construct an improved understanding of the flare process.

TIMED: The Thermosphere, Ionosphere, Mesosphere, Energetics and Dynamics mission is designed to (i) understand the influence of the sun on the atmosphere, (ii) understand the influence of human activity on the atmosphere, and (iii) to improve the capability of space weather prediction. The concept involves study of the energy budget of the ionosphere, lower thermosphere, and the mesosphere. Future programs (as noted on the TIMED website) include the Solar Terrestrial Relations Observatory (STEREO), the SOLAR-B mission, Magnetosphere Multiscale (MMS), the Geospace Electrodynamic Connections (GEC), and the Magnetospheric Constellation (MC).

TRACE: The Transition Region and Coronal Explorer is designed to evaluate the 3-D magnetic structures that emerge through the solar photosphere. This information is then used to define the dynamics and the geometry of the uppermost parts of the solar atmosphere, which includes the so-called transition region and the corona.

WIND: The WIND satellite is part of the NASA GGS mission under ISTP project. Two of the science objectives are: (i) the provision for

complete plasma, energetic particle and magnetic field data for use in ionospheric and magnetospheric studies, (ii) investigate plasma processes within the near-earth solar wind.

POLAR: The NASA Polar satellite is in a highly elliptical (near polar) orbit with an 86 degree inclination and a period of ~ 17 hours. Polar carries out multi-wavelength imaging of the aurora. It is a major component of the Sun-Earth Connections fleet. The other systems are Wind and Geotail.

CLUSTER: The CLUSTER program is an ESA mission under ISTP. Four identical satellites are part of the "cluster". These satellites are relatively close together, having separations between 200 and 1800 km. The program design goal is to examine the small-scale spatial and temporal properties of the magnetospheric plasma and the solar wind plasma in the vicinity of the earth. The key plasma regions being examined are (i) solar wind and bow shock, (ii) the magnetopause, (iii) the polar cusp, (iv) the magnetotail, and (v) the auroral zone. Each satellite in the cluster will have 11 instruments on board. Five instruments were developed by the Cluster Wave Experiment Consortium (WEC). One of the more interesting experiments in the WEC complement is WHISPER. This experiment is an intermittent transceiver than can also be operated in the passive mode. The transmitter emits short pulses to stimulate plasma resonance phenomena, while the receiver can sense plasma densities in the range from 0.2 to 80 cm^{-3} from received signals.

GEOTAIL: GEOTAIL is part of the NASA GGS mission under ISTP. It is a collaborative project between NASA and the Institute of Space and Astronautical Science (ISAS). The principal goal of the program is to study the dynamics of the magnetotail region from the near-earth region (i.e., 8 earth radii, Re) to the remote tail region (~ 200 Re).

SOHO: NASA and ESA have teamed on the Solar and Heliospheric Observatory (SOHO) mission, which is a part of the ISTP program. Following two other ESA missions, Cluster and Ulysses, SOHO is examining sun-earth interactions. SOHO is located at approximately the L1 position, so that it is effectivcly locked along the earth-sun line. One of the key technologies used in the SOHO program is helioseismology, and this study of sound waves have provided scientists with a glimpse of sunspot activity on the far side of the sun. This can have important forecasting potential. There are 12 complementary instruments in the SOHO, with the majority being developed by European scientists. A sampling of some of the more interesting instruments include: (i) CELIAS, which monitors the solar

wind and warns of solar storms, (ii) GOLF, which monitors velocity oscillations over the solar disk, (iii) LASCO, which monitors the corona using a coronograph, (iv) SWAN, which uses a unique method to map the solar wind, (v) VIRGO, which measures solar irradiance variation. LASCO provides forecasters with information on coronal mass ejections (CMEs).

6.9 AGENCIES, INSTITUTIONS & COMPANIES

There are many organizations that have directly or indirectly participated in space weather research and model development, data analysis and distribution, prediction and forecasting, provision of services, and education. In Table 6-19, we have listed a number of the organizations. Since the space weather discipline is evolving, at any given time the list may be incomplete. At the same time some of the listed organizations may leave the space weather field. In general, however, we find that the constituency is growing. Hopefully the list will provide the reader with a feel for the array of assets that are addressing the space weather discipline.

Table 6-19: Listing of Academic Institutions, Government Agencies, Private Activities, and Commercial Firms involved in Space Weather

Note: The listing was compiled by examination of (i) attendance lists at *Space Weather Week* and various topical conferences such as IES and COSPAR that organize space weather sessions, and (ii) a perusal of space weather activity participants and sponsors. Unless otherwise noted, the country associated with the listing is the United States. The listing is really a sampling, and therefore only indicative of the breadth of space weather activity. To consolidate the list (i.e., limit the depth of activity), we have often, but not always, suppressed the names of subordinate divisions, branches, and affiliated laboratories, etc. We have also excluded the names of professional societies that may sponsor or host space weather sessions or activities.

- Abdas Salam International Center for Theoretical Physics, Italy
- Adelaide University, Australia
- Aerospace Corporation, The
- AFTAC
- Arecibo Observatory, Puerto Rico
- Aeronautical Radio Inc.
- ANSER
- ASRC Aerospace
- Ball Aerospace & Technologies
- Belgian Institute for Space Aeronomy, Belgium
- Bell Laboratories
- Boeing Company
- Boston College
- Boston University
- Brown University
- Byron Institute of Auroral Study
- California Institute of Technology
- Carmel Research Center
- Catholic University of America
- Center for Remote Sensing
- CIRES/University of Colorado
- Clemson University
- CNRS, France
- Communications Research Center, Canada
- Communications Research Laboratory, Japan
- Computational Physics, Inc.
- Cornell University
- Dartmouth University

- Defense Science and Technology Organization, Australia
- DeVry University
- Dynamics Research Corporation
- European Space Agency
- European Space Research & Technology Centre (ESTEC)
- European Union
- Exploration Physics International, Inc.
- Finnish Meteorological Institute, Finland
- Federal Aviation Administration of DOT
- FMA Research, Inc.
- Fugro Chance, Inc
- General Dynamics
- Geoloc Corporation
- Geological Survey of Canada
- Geophysical Institute, Academy of Sciences of Czech Republic
- George Mason University
- George Washington University
- Geospace Corporation
- High Latitude Observatory
- Holloman Solar Observatory
- Ionospheric Prediction Service (IPS), Australia
- Ionospheric Systems Research, Australia
- Institute for Applied Geophysics, RWC-Moscow, Russia
- Institute for Space Sciences, Taiwan
- Intelsat (Europe)
- Israel Cosmic Ray and Space Weather Center, Israel
- IZMIRAN, Russia
- Japan Aerospace Exploration Agency, Japan
- Jet Propulsion Laboratory, California Institute of Technology, NASA
- Johns Hopkins University
- Kyoto University, Japan
- Kyungpook National University, Korea
- Laboratory for Atmospheric and Space Physics
- La Trobe University, Australia
- Learmonth Solar Observatory
- Lockheed Martin Advanced Technology Center
- LASP
- Loral Skynet
- Los Alamos National Laboratory
- ManTech Aegis Research Corporation
- Max-Planck-Institut fur Aeronomy, Germany
- Metatech Corporation
- MCR, Inc.
- Micro-g Solutions, Inc.
- Mission Research Corporation
- MIT Lincoln Laboratory
- MIT Haystack Observatory
- Moscow State University, Russia
- Mullard Space Science Laboratory, Switzerland
- Nagoya University, Japan
- NASA Goddard Space Flight Center
- NASA Johnson Space Center
- NASA Marshall Space Flight Center
- National Air and Space Intelligence Center
- National Astronomical Observatories, China
- National Astronomical Observatory, Japan
- National Center for Atmospheric Research (NCAR)
- National Centers for Environmental Prediction
- National Geodetic Survey
- National Geophysics Research Institute, India
- National Observatory of Athens, Greece
- National Physical Laboratory, India
- Natural Resources Canada, Geomagnetic Laboratory
- National Reconnaissance Office
- National Research Council
- National Science Foundation
- National Weather Service of NOAA
- New Jersey Institute of Technology
- New Mexico Institute of Mining and Technology
- NOAA National Geophysical Data Center
- NOAA/OAR

- NOAA Space Environment Center (SEC)
- NOAA/NESDIS
- Northrop Grumman
- Office of Naval Research
- Orbital Sciences Corporation
- ONERA/DESP, France
- Palehua Solar Observatory
- Peterson AFB Weather Station
- Polar Geophysical Institute of the Russian Academy of Sciences, Russia
- QinetiQ, UK
- Raben Systems, Inc.
- Radio Propagation Services, Inc.
- Raytheon Corporation
- RWC-Moscow
- Rice University
- Rockwell-Collins
- Rostov State University, Russia
- Rutherford-Appleton Laboratory, UK
- Sachs-Freeman Associates
- Sandia National Labs
- SED Systems, Canada
- SIDC- Royal Observatory of Belgium, Belgium
- SolarMetrics Limited, UK
- Solar Physics Research Corporation, Japan
- Solar Terrestrial Dispatch
- Southern Polytechnic State University
- Southwest Research Institute
- Space and Missile Systems Center
- Space Environment Corporation
- Space Environment Technologies
- Space Policy Institute
- Stanford University
- Swales Aerospace
- Swedish Defence Research Agency, Sweden
- Swedish Institute of Space Physics, Lund, Sweden
- TASC, Inc.
- Telesat Canada
- Universität Bonn, Germany
- University of Alabama
- University of Alaska, Fairbanks
- University of Alberta, Canada
- University of Bath, UK
- University of Bern, Switzerland
- University of Calcutta, India
- University of Calgary, Canada
- University of California at Berkeley
- University of California at San Diego
- University of California at Los Angeles
- University of Chicago
- University of Colorado
- University of Graz, Austria
- University of Hull, UK
- University of Illinois
- University of Lancaster, UK
- University of Leicester, UK
- University of Maryland
- University of Massachusetts-Lowell
- University of Michigan
- University of Minnesota
- University of New Brunswick, Canada
- University of Newfoundland
- University of New Hampshire
- University of Rennes, France
- University of Saskatchewan, Canada
- University of Sheffield, UK
- University of Southern California
- University of Texas at Austin
- University of Texas at Dallas
- University of Texas at El Paso
- University of Toronto, Canada
- University of Wales, UK
- University of Washington
- U.S. Air Force Academy
- U.S. Air Force Office of Scientific Research
- U.S. Air Force Research Laboratory
- U.S. Air Force Space Command
- U.S. Air Force Weather Agency
- U.S. Air Force SPC
- U.S. Army Electronic Proving Ground
- U.S. Coast Guard of DHS
- U.S. Department of Energy
- U.S. National Geodetic Survey of NOAA
- U.S. Geological Survey of DOI
- U.S. Naval Research Laboratory
- U.S. Navy Stennis Space Center
- Utah State University

6.10 A COMMENT ON INTERNET RESOURCES

There are a large number of Internet resources from which space weather information may be obtained. A favorite is the NOAA-SEC web site. Space weather data may be retrieved from web sites associated with a variety of organizations, including those listed in Table 6-17. The categories of space weather information include: (i) organizational, (ii) programmatic, (iii) observational data, (iv) forecast products and services, and (v) educational information. As has been stated elsewhere in the text, and in consultation with the publisher, we have decided to resist the temptation to list URLs of relevant web sites. The reasons are numerous. We have discovered that many links are transient in nature, are not updated consistently, and may be broken by the time of publication or within a few years from publication. This can be an annoyance to the reader. There are a number of websites that provide listings of space weather links, but many of these are limited in scope and some do not update the listings very often.

As suggested above, it is felt that the best starting point for Internet discovery is the NOAA-SEC home page, while equivalent data may be extracted from websites affiliated with the World Data Centers and the Regional Warning Centers of ISES. A useful non-government site is managed by Rice University. With some reluctance, we shall break our self-imposed rule and list the URLs for the SEC home page and the Rice University resources page. They are as follows: http://www.noaa.sec.gov and http://dragonrider.rice.edu/ISTP/. For the SEC site, simply "click" on the hyperlink *Online Data* and a wealth of opportunities for data mining will emerge.

One should be mindful that broken URLs are unlikely to be associated with sites developed by the larger government organizations, although there are a number of private companies that have also done an excellent job in site maintenance. Still it would be unwise to presume the long-term integrity of URLs and web site content, even for those organizations with an established track record. Fortunately, it is remarkably easy to locate information on the Internet, assuming one is familiar with the use of web search engines. There are a number of packages in use including: Google, Yahoo!, AOL, MSN, Excite, and AltaVista, to name a few. Typically a few attempts, and a little patience, will lead to a successful outcome. A general search using the keyword "space weather" or "ionosphere" generates a large number of useful sites containing relevant information and hyperlinks. Some of the entities in Table 6-19 may have space weather links. Typically you can find the home pages by simply typing in the name of the organization using your favorite search engine. The subject index for this book can also be exploited. Good luck.

6.11 REFERENCES

ASD-C3I, 2000, "Space Weather Architecture Transition Plan", Office of the Assistant Secretary of Defense for Command, Control, Communication, and Intelligence, 22 May 2000.

Bradley, P. (Editor), 1999 (February), "PRIME, Prediction and Retrospective Ionospheric Modelling over Europe", COST Action 238, Final Report, ISBN 0902376853, Commission of European Countries, printed by Council for the Central Laboratory of the Research Councils, Rutherford-Appleton Laboratory, Chilton, Didcot, Oxfordshire OX110QX, UK.

Hanbaba, R. (Editor), 1999 (April), "Improved Quality of Service in Ionospheric Telecommunication Systems Planning and Operation", COST Action 251, Commission of European Countries Final Report, ISBN 83-902319-3-X, Published by the Space Research Centre, Warsaw, Poland.

Hunsucker, R. D., 1999, "Radio techniques for Probing the Terrestrial Ionosphere", Physics and Chemistry in Space 22, Springer-Verlag, New York.

Kintner, P.M., M. Guhathakurta, , J. Spann, and B. Giles, 2003, "Definition Team of NASA's 'Living with a Star' Geospace Mission sets Science Priorities", *EOS*, Vol.84, No.7, pp. 61, 64.

Lilensten, J., T. Clark, and A. Belehaki, 2004, "Europe's First Space Weather Think Tank", in the *Space Weather Journal*, 2003SW000021, 13 April 2004.

NSWP, 2000, "National Space Weather Program Implementation Plan, 2nd Edition, prepared by the Committee for Space Weather for the National Space Weather Program Council, Office of the Federal Coordinator for Meteorology, FCM-P31-2000, Washington DC.

Chapter 7
EPILOGUE

Space weather has been a factor in the evolution of telecommunication systems since the time of Marconi with his verification of long-distance radio signaling in 1901. The term *space weather*, as used currently, may be troubling to some purists since it could be looked upon as simply a convenient way to organize and humanize the array of solar-terrestrial phenomena that influence various technological systems. Since society understands fully the implication of ordinary weather on the lives of people, the grafting of weather and space is certainly an astute political maneuver. Indeed, R&D conducted under the space weather moniker should be more attractive to the funding agencies than if less provocative banners were to be used. But this is a cynical view and an inaccurate portrayal of the motives of the various institutions and funding agencies that comprise the space weather constituency. Space science and aeronomy have not been redefined for convenience. Rather, the term weather has been generalized to include the earth's total environment, as it should, and not limited to the troposphere. The author argues that the term space weather, and all that it represents, is an intellectually honest representation, and that 21st Century technology is making the merger of space science and generalized weather forecasting both logical and inevitable.

This having been said, it is true that the space environment does exhibit some characteristics that are analogous to tropospheric weather and climate, as well as others that are unique to space. For example, there are space weather patterns that can be monitored and forecast. There are also climatological tendencies that are catalogued and parameterized. There are even space weather stations, although the parameters being measured within the upper atmosphere and space are not humidity, temperature, and pressure. From the vantage point of telecommunications, and radio communication in particular, the ionospheric personality is of primary significance. When we speak of solar storms or geomagnetic storms, we are talking about behavioral influences on what really matters, the ionosphere. The ionospheric storm is quite important in the scheme of things since it can be directly related to the geomagnetic storm. The ionospheric storm is but one component in the hierarchy of ionospheric weather conditions.

It should be obvious to the readership, including practicing scientists, engineers, academicians and space weather vendors, that one of the leading resources for information regarding current space weather conditions is the Space Environment Center of NOAA located at Boulder, Colorado. It also functions as the World Warning Agency under the ISES umbrella, and convenes annual Space Weather Week symposia that are important channels for collaboration and retrieval of the latest programmatic, scientific, and operational activity. SEC maintains a limited but high quality R&D activity,

and leverages its scientific mission through a robust collaborative research program, both internationally and domestically. SEC and its managers have recognized the need for a viable space weather vendor community and have fostered its growth.

Given the position of SEC in the grand scheme of things, it is fitting that we obtain some insight from Dr. Ernest Hildner, the Director of that fine organization. Dr. Hildner is also manager of the Space Weather program at NOAA. Dr. Hildner provided testimony before a Hearing of the U.S. House of Representatives Science Committee (Subcommittee on Environment, Technology, and Standards) on October 30, 2003. In his testimony, which is a matter of public record, he made a strong case for space weather support. We have made reference to some his remarks within several chapters of this book, because we feel they are worth emphasizing. We certainly recommend that the readership take the opportunity to peruse the Congressional Record vis-à-vis the testimony provided by Dr. Hildner and other scientists who appeared before the House Subcommittee.

Goodman: The NOAA Space Environment Center (in its various forms) has long been the leading source for solar-terrestrial data and related information, and it has been loosely affiliated with the U.S. military for many decades. How do you see, or can you describe the current and future relationship between SEC and the U.S. Air Force? How is this apt to change, if, as anticipated, your agency becomes a part of the National Weather Service?

Hildner: SEC enjoys very close and beneficial relationships with our DoD partners in the Air Force Weather Agency, with the USAF Office of Scientific Research AFOSR), with the Air Force Research Laboratory, and with the Naval Research Laboratory and the Office of Naval Research. SEC's new home in the NWS, the National Centers for Environmental Prediction (NCEP), already has close ties with the U.S. Air Force for meteorological activities, so I expect no change in our relations with the DoD and maybe even a better relationship between SEC and the U.S. Air Force.

Goodman: Becoming a part of the National Weather Service certainly offers a logical umbrella for SEC space weather support activities. The average U.S. citizen generally recognizes the need for tropospheric weather predictions and forecasts in everyday planning for recreation and day-to-day activities. I haven't seen a recent survey of public opinion, but my perception is that there is less complaining about bad weather forecasts than there used to be. Clearly methods have improved, and technological enhancements, including advanced radar and satellite systems

are a part of this overall improvement. The same may now be occurring in the space weather prediction business. My question is twofold: (1) Do you think the National Weather Service and SEC are embracing each other, or is it a one-sided embrace; and (2) where are we now in terms public acceptance of space weather forecasting as a important (if not essential) aspect of their everyday lives? As a follow-up, under the presumption that the public will never regard space weather as important to them as "regular" weather, will the acceptance of space weather importance by specialized commercial and military activities be sufficient?

Hildner: I'm pleased to say that the NWS is embracing space weather – and SEC – with great enthusiasm and energy. The new head of the NWS, BGEN D. L. Johnson, learned about the importance of space weather when he was Director of Weather in the Air Force and is a great supporter, as is Dr Louis Uccellini, Director of the National Centers for Environmental Prediction, where SEC will be one of the Centers.

I think your perception of where we are in public acceptance of the importance and value of space weather services is quite accurate, and the analogy with improving weather forecasts holds true. The operators of affected systems – such as airlines, radio communicators, electric power grids - are well aware of NOAA's space weather services and use them to make operational decisions.

However, so many of the affected systems are advertised as being very reliable, and the owners and operators do not wish to advertise their vulnerability to space weather. That is, the effects of space weather are not so obvious as meteorological weather and there is little incentive to inform the public that their electricity prices, or the length of their airline flight, are being affected by space weather. So the public awareness of the impacts of space weather – and that space weather services exist and are improving - is growing more slowly.

Goodman: The reality (or a perception) of a paucity in funding has been a source of aggravation for basic and, to some extent, applied research in aeronomy and space sciences for many years. Are you comfortable with the level of support you are currently receiving to support your current and future SEC goals? And, if not, do you see a time when SEC may privatize a segment of its activities to find a solution to this problem?

Hildner: For the last few years the President's Budget has requested sufficient funds for SEC to continue at its current level of effort, but Congress has not seen fit to appropriate as much as the President has requested. This has caused undesirable constraints on some activities SEC feels it should be doing. Especially, SEC would like to be able to transition into operations some of the data driven, physics based models that have been developed in academia, often with DoD, NASA, and NSF support.
As part of NWS, SEC will follow NWS policy regarding privatization of its activities; so far, I am not aware of any consideration of privatization. However, there is a policy that allows for a federal laboratory to receive royalties from the private sector if an idea developed in the lab is commercialized; this is often the result of a Cooperative Research And Development Agreement (CRADA) between a lab and a for-profit company.

Goodman: Your center has fostered the creation and development of so-called 3rd Party Vendor organization. I believe the current name is CSWIG for Commercial Space Weather Interest Group, and it is ably headed by John Kappenman of MetaTech Corporation. Barbara Poppe of your staff has done a fine job orchestrating yearly gatherings of CSWIG during *Space Weather Week* held in Boulder every Spring. The CSWIG is in its formative stages, and the member companies are developing, and in some cases actually providing, new products that are specifically tailored for end-users. Do you see any problems in managing your research staff who might perceive that CSWIG is simply "skimming the cream", or merely providing copies of SEC products for a fee.

Hildner: Thank you, John, for commending Barbara and her efforts on behalf of commercial sector space weather folks such as yourself and the members of CSWIG. Following the historical development of a meteorological services industry, primarily based on government data and model outputs, we feel that a space weather services industry is a logical and appropriate path into the future. Part of SEC's mission is to foster a space weather services industry, and we feel very strongly that this is the right thing for SEC to do. If we at SEC try to understand the environment and provide environmental products, SEC's researchers agree there is more than enough for us to do. This leaves to the private sector the development and provision of products about the effects of space weather, products tailored to specific industries or even specific companies.

Goodman: There has been a strong programmatic growth in the space weather community in recent years with the institution of the *National Space Weather Program* (NSWP), and NASA's *Living with a Star*, to name a few. There is also a growing international effort underway, and SEC, in its role as the World Warning Agency under the ISES framework, plays a key role in space weather activities and forecasting. How much of the space weather activity now ongoing is simply repackaging, and how much of it involves new initiatives and a real focus on the problem?

Hildner: John, I'm pleased to say that there is a considerable upsurge in the real level of activity and interest in space weather. NSF has put new money into annual grants solicited under the NSWP, and just a year ago began to fund – with $4 million per year - a new Science and Technology Center, the Center for Integrated Space weather Modeling (CISM). As you point out, NASA's new *Living with a Star* program, with its multiple missions, is about space weather. USAF has "mainstreamed" space weather into meteorological weather, so that the standard form for the pilot getting a preflight weather briefing shows meteorological and space weather on the same page. NOAA (with USAF partnership for the polar orbiting satellites) is planning to significantly increase its investment in sensors to monitor space weather conditions. In sum, the Nation has significantly raised the level of effort in space weather over the last few years.

Goodman: As I'm sure you know, I have a strong professional interest in the ionosphere. It has been stated by some workers that the ionosphere actually constitutes about 70% of all space weather. I don't really know where that estimate comes from, but in terms of the impact on telecommunication systems, I'm willing to accept a number even higher than that. It has been said that SEC has only limited involvement in ionospheric activity, perhaps a result of the perception that most of the challenging aeronomic and ionospheric problems have already been solved. Is this an inaccurate assessment, and do you see this as a problem, if the ionosphere is so important to an important class of users.

Hildner: The ionosphere is a very important part of space weather, whether it is 70 percent or not. Some years ago, recognizing that HF communication was not fading from the scene and that GPS was going to be widely used, SEC made an investment in ionospheric expertise. This decision reversed an earlier decision that SEC should zero out its ionospheric activities. I am pleased

to say that our customers are seeing payoffs from that decision now and soon will see much more. Right now, SEC has a graphical product, which shows the expected absorption of radio signals in the ionosphere's D-region after a flare. This fall we intend to go operational with a US-TEC map (and provide the associated gridded numerical values described by the map), which will show, the total electron content (TEC) in a column vertically above each point in the contiguous United States, every 15 minutes. The model, which produces the map, will be driven by data from more than 100 dual-frequency GPS receivers in the Continuously Operating Reference Station (CORS) network, as well as by other data from ionosondes. We think that this map will find many applications for GPS navigation and surveying, as well as for HF radio communications. In the future, our ultimate goal is to use a data assimilative model to predict the three dimensional state of the ionosphere every 15 minutes, worldwide, taking into account both whatever current observations are available and the best understanding of ionospheric physics. With this model output, communicators, navigators, transpolar airline routers, satellite operators, and others will be able to optimize their operations, as never before, to minimize the deleterious effects of ionospheric disturbances.

Goodman: Ernie, you have had an outstanding career with Government and NOAA, specifically in connection with your direction of SEC, leading the Center through some challenging events and circumstances, and navigating the treacherous waters of budgetary constraints while satisfying agency missions. At this point in time, what gives you the most satisfaction, and what are some things you would like to accomplish in the near term? The long term?

Hildner: John, my time at SEC has been an amazing ride! When I think back one 11-year solar cycle ago, and I remember the limited data, the limited display capability, the infant capability of the Internet and digital imaging we had then, and compare it to what we have now, I chuckle with delight. We have so much more data to work with, we can exchange opinions and data with our distant colleagues almost instantaneously and nearly for free, and we now have models that were then only dreams. We are doing a far better job of predicting space weather storms now than we did then, and our verification statistics back that up. Real-time solar wind data from NASA's satellite ACE out in front of Earth give us an excellent indication of the intensity of the

geomagnetic activity which will occur when the solar wind hits Earth about 30 minutes later, something we didn't have until a little over five years ago.

I guess I am most proud of how far SEC's capabilities have come and how much we accomplish with how few dollars. We have good people who are passionate about SEC's mission, about customer service, and about space research. Ideally, as I look into the future, I see the concept of space weather, and its importance, percolating into the consciousness of more decision makers, so that space weather gets its due recognition and adequate support.

In the near term, we have some exciting ionospheric services coming along, most of which will enable the private sector to develop and sell applications. And, of course, the ripples caused by our transition to the National Weather Service will take a year or two to smooth out. Guided by the history of meteorological services, in the mid-term, we see SEC's implementation of physics-based numerical models to forecast space weather conditions. In the longer term, we see ensembles of coupled models simulating current and predicting future space weather conditions from the Sun to Earth's neutral atmosphere, we see the possible extension of SEC's space weather activities to predict and monitor space weather at Mars to support the national initiative to send humans there, and we see forecasts so accurate that systems operators take action to mitigate the effects of space weather storms based upon the forecast rather than waiting to take action until a parameter exceeds a threshold.

There are a number of challenges facing ionospheric specialists and aeronomists. Space weather is now in vogue, and it is important that opportunities for technical and scientific advance not be missed. While theories explaining most facets of ionospheric behavior exist and are generally accepted, the theories do not always provide a good basis for prediction of future behavior. This is because the driving forces and boundary conditions needed in a physical model are not always known, and estimates must be used. This has led to the development of semi-empirical models for the purpose of system design and these are used for operations as well. By and large these models exploit large ionospheric databases and yield only median representations of ionospheric parameters. To fix this problem, various "update" schemes have been developed to make the specification of the ionospheric state as current as possible. The physics is then used to let the system evolve. All of this can be very unsatisfactory unless an understanding of the nature of ionospheric variability (viz., in both space and time) is

established. There are many sources within the earth-sun system that contribute to the growth of ionospheric structure. While these have been characterized to some extent, the characterizations are not sufficient to provide predictions acceptable for many users of the ionospheric channel. Currently this is a major challenge facing the ionospheric research community. This makes it a challenge for space weather advocates as well.

The following topics require more attention from ionospheric specialists: (a) the driving forces of upper atmospheric winds and the impact on ionospheric structure and dynamics; (b) the hierarchy of energy sources within the earth-sun system that influence ionospheric behavior; (c) the development of geomagnetic storms and the impact that storms have on ionospheric behavior; (d) the development and evolution of ionospheric inhomogeneities; and (e) various methods for ionospheric predictions. Many of these topics are being addressed independently and in the context of various space weather programs and initiatives. University programs are being established and there are a number of public domain educational opportunities addressing space weather and sun-earth connections.

In the new millennium, the researcher is confronted with an enormous amount of data, both near real-time and archived, that may be accessed via the Internet. Harnessing this information stream, and using the state-of-the-art computational assets, it should be possible to leverage ongoing science efforts, organize more efficient experimental campaigns, and enhance collaborative efforts, all resulting in a more fulsome understanding of ionospheric physics. Finally, the establishment of the National Space Weather Program in the United States and similar international programs should provide abundant opportunities for synergistic relationships to develop between space weather advocates, the ionospheric research community, and telecommunication engineers.

LIST OF ACRONYMS AND SELECTED TERMS

Note: This list of acronyms and terms is not intended to provide a complete definition or description. The reader should refer to the book Index and cited references within the book for more details. There are also other glossaries that can be useful. For example, there are the "NPOESS consolidated acronym list", and the "On-Line Glossary of Solar-Terrestrial Terms" (from NOAA-SEC and NGDC/STP) that may be accessed over the Internet. One may use the quoted segments above as search items.

ACE:	Advanced Composition Explorer (solar wind monitor at L1 point)
ACTD:	Advanced Concepts Technical Demonstration
AEEC:	Airline Electronic Engineering Committee
AF 55-SWxS:	Air Force 55th Space Weather Squadron (now defunct)
AFT:	Active Frequency Table (ARINC HFDL system)
AFCEA:	Armed Forces Communications and Electronics Association
AFCRL:	Air Force Cambridge Research Laboratory
AF-GEOSpace:	Visualization tool for environmental analysis and evaluation of system effects
AFGL:	Air Force Geophysics Laboratory
AFGWC:	Air Force Global Weather Central
AFOSR:	Air Force Office of Scientific Research
AFRL:	Air Force Research Laboratory
AFWA:	Air Force Weather Agency
AGARD:	Advisory Group for Aerospace Research and Development (NATO)
AGO:	Automatic Geophysical Observatories
AGU:	American Geophysical Union
AIP:	Atmospheric and Ionospheric Profiling
ALE:	Automatic Link Establishment
Alouette:	Canadian topside sounder system
Apollo:	NASA moon exploration mission
ARGOS:	Advanced Research and Global Observation Satellite
ARINC:	Aeronautical Radio Incorporated
ASAPS:	Advanced Stand Alone Prediction System
ASFC:	Australian Space Forecast Center
ASTRID:	Microsatellite that carries two UV instruments for imaging the aurora. (Sweden)
ATS:	Advanced Technology Satellite
CACTUS:	Software system used at RWC-Brussels
CAMS:	Communication Area Master Station
CANOPUS:	Canadian Auroral Network for the OPEN Program Unified Study. CANOPUS was originally an acronym based on the

	role of the project as a component experiment of the NASA OPEN program. OPEN has now been renamed GGS and integrated into the International Solar Terrestrial Physics program which involves NASA, ESA and ISAS (the Japanese Space Agency).
CAT 1:	Category 1 Flight Operations
CAWSES:	Climate and Weather of the Space Earth System
CCIR:	International Radio Consultative Committee
CCLRC:	Council for Central Laboratory of the Research Councils (UK)
CEASE:	Compact Environment Anomaly Sensor. Instrument to monitor spacecraft charging
CEDAR:	Coupling, Energetics, and Dynamics of Atmospheric Regions
CELIUS:	Instrument on SOHO that monitors the solar wind
CGCS:	Corrected Geomagnetic Coordinate System
CHAMP:	Satellite mission for global geo-monitoring (Germany)
CISM:	Center for Integrated Space Weather Modeling
CITFM:	Coupled Ionosphere-Thermosphere Forecast Model
CLUSTER:	Four polar-orbiting satellites for study of solar wind and magnetosphere (ESA)
CME:	Coronal Mass Ejection
C/NOFS:	Communications/Navigation Outage Forecasting System
CONOPS:	Concept of Operations
CONUS:	Continental United States
CORLPRED:	COST Action model to predict *foF2* and *M3000F2*
CORS:	Continuously Operating Reference Stations
COSMIC:	Constellation Observation System for Meteorology, Ionosphere and Climate
COSPAR:	Committee of Space Research
COST:	Coordination in Science & Technology (European Commission)
COSTPROF:	COST Action model to predict TEC based on sounders
COSTTEC:	COST Action model to predict the TEC (long-term map)
CRC:	Communication Research Centre (Canada)
CSW:	Committee for Space Weather
CSWIG:	Commercial Space Weather Interest Group (3rd party vendors)
CTIM:	Coupled Thermosphere-Ionosphere Model
CTIP:	Coupled Thermosphere-Ionosphere-Plasmasphere (model)
DAMSON:	Doppler and Multipath Sounding Network
DARN:	Dual Auroral Radar Network (also superDARN)
DECCA:	A low frequency radio navigation system (defunct; also DNS)
DERA:	Defence Evaluation & Research Agency (UK). DERA was disestablished in 2001.
DGPS:	Differential GPS

DISS:	Digital Ionospheric Sounding System
DLR:	Institute for Communications and Navigation (was German Space Agency)
DMSP:	Defense Meteorological Satellite program
DNA:	Defense Nuclear Agency
DNA-002:	DNA Wideband Satellite
DoC:	Department of Commerce
DoD:	Department of Defense
DoE:	Department of Energy
DoI:	Department of Interior
DoJ:	Department of Justice
DoT:	Department of Transportation
DSP:	Defense Support Program
DSTL:	Defence Science and Technology Laboratory (UK)
DSTO:	Defence Science and technology Organization (Australia)
Dynacast©:	Ionospheric modeling and HF performance prediction program (RPSI)
EC:	Electron Content (also TEC)
EHF:	Extremely High Frequency
EISCAT:	European Ionospheric Scatter program
ELF:	Extremely Low Frequency
EMOF	Elevated Maximum Observable Frequency
EM:	Electromagnetic
EMP:	Electromagnetic Pulse
EOS:	*Transactions*, American Geophysical Union
EPPIM:	Eulerian Parallel Polar Ionosphere Model
ESA:	European Space Agency
ESTEC:	European Space Research and Technology Center
EUMETSAT:	European Organization for Exploitation of Meteorological Satellites
EUV:	Extreme Ultraviolet (10-100 nanometers)
FAA:	Federal Aviation Administration
FAST:	NASA Fast Auroral Snapshot Explorer
FAIM:	Fully Analytical Ionospheric Model
FLTSAT:	Fleet Communication Satellite
foF2:	Ordinary ray critical frequency for F2 layer in the ionosphere
foF1:	Ordinary ray critical frequency for F1 ledge in the ionosphere
foE:	Ordinary ray critical frequency for E layer in the ionosphere
foEs:	Ordinary ray critical frequency for sporadic E in the ionosphere
FTP:	File Transfer Protocol
GAIM:	Global Assimilation of Ionospheric Measurements
GALILEO	European Space Agency SATNAV (similar to GPS)
GEC:	Global Electrodynamics Connections
GEM:	Geospace Environment Modeling program

Gemini:	NASA two-astronaut space mission
GENESIS:	JPL's environmental and earth science information system
GEO:	Geostationary Earth Orbiting (satellite)
GEOSTORMS:	Joint Air Force and NOAA program to monitor solar wind properties
GGCM:	Geospace General Circulation Model
GIM:	Global Ionospheric Maps
GINS:	Geomagnetic Information Nodes
GIVEs:	Grid Ionospheric Vertical Errors (error bounds for ionospheric errors in WAAS system)
GLOBALink:	Commercial aviation HFDL service (ARINC)
GLONASS:	Russian SATNAV (similar to GPS)
GNSS:	Global Navigation Satellite System
GOES:	Geostationary Operations Environmental Satellite (consists of 2 GEOs)
GPS:	Global Positioning System
GRACE:	Satellite mission for global gravity field measurements and modeling (Germany)
GTIM:	Global Theoretical Ionospheric Model
GWEN:	Ground Wave Emergency Network
HAARP:	High Frequency Active Auroral Research Program
HANE:	High Altitude Nuclear Effect
HAO:	High Altitude Observatory
HAP:	Hourly Area Prediction
HEO:	High Earth Orbit (satellite)
HESSI:	High Energy Solar Spectroscopic Imager
HF:	High Frequency (3-30 MHz)
HF-EEMS:	High Frequency assessment and prediction system (DERA/QinetiQ)
HFDF:	High Frequency Direction Finding
HFDL:	High Frequency Data Link
HFIA:	High Frequency Industry Association
HIRAAS:	High Resolution Airglow/Aurora Spectroscopy Experiment
hmF2:	Maximum height of the F2 layer of the ionosphere
IACTIN	Ionospheric Activity Index
IAGA:	International Association of Geomagnetism and Aeronomy
IAPM:	Auroral prediction model
IAU:	International Astronomical Union
ICAO:	International Civil Aviation Organization
ICED:	Ionospheric Conductivity and Electron Density (model)
ICEPAC:	Ionospheric Communications Enhanced Profile Analysis & Circuit Prediction Program
ICSU:	International Council for Scientific Unions
ICTP:	Abdus Salam International Center for Theoretical Physics
IDCE:	Ionospheric Dispatch Centre for Europe (RWC-Warsaw)

IEE: Institute of Electrical Engineers (UK)
IEEE: Institute of Electrical and Electronics Engineers
IES: Ionospheric Effects Symposium
IFM: Ionospheric Forecast Model
IGC: International Geophysical Calendar
IGP: Ionospheric Grid Point (WAAS system)
IGRF: International Geomagnetic Reference Field
IGS: International GPS Service (for Geodynamics)
IGY: International Geophysical Year (1957-1958)
IMAGE: International Monitor for Auroral Geomagnetic Effects
IMF: Interplanetary Magnetic Field
IMS: International Magnetospheric Study
IMP-8: Interplanetary Monitoring Platform. It measures the magnetic fields, plasmas, and energetic charged particles (*e.g.*, cosmic rays) of the Earth's magnetotail and magnetosheath and of the near-Earth solar wind. IMP-8 is the last of ten IMP or AIMP (Anchored-IMP) satellites.
INAG: Ionosonde Network Advisory Group
INSPIRE: Interactive NASA Space Physics Ionosphere Radio Experiment
INTERBALL: A program to study plasma processes in the magnetosphere using a system of spacecraft consisting of one satellite-subsatellite pair above the polar aurora and another in the magnetospheric tail region.
INTER-MAGNET: Global network of geomagnetic observatories
IONCAP: Ionospheric Communications Analysis and Prediction (model for HF)
IOX: Ionospheric Occultation Experiment (on PICOSat) that used a space-based dual frequency GPS receiver to measure ionospheric properties.
IPS: Ionospheric Prediction Service (Australia)
IPY-2: International Polar Year (2nd) (1932-1933)
IQSY: International Quiet Sun Year (1964-1965)
IRI: International Reference Ionosphere
ISAS: Institute of Atmospheric and Space Studies (Canada)
ISAS: Japanese Space Agency
ISCS: International Solar Cycle Study
ISEE: International Sun-Earth Explorer program. An international cooperative program between NASA and ESA to study the interaction of the solar wind with the Earth's magnetosphere.
ISES: International Space Environment Service
ISGI: International Service of Geomagnetic Indices
ISO: International Standardization Organization

ISOON:	Improved Solar Optical Observing Network
ISR:	Incoherent Scatter Radar (Thomson scatter)
ISTP:	International Solar Terrestrial Physics
ITRAY:	Ionosphere and Troposphere Raytrace (model)
ITS-78:	Early HF performance prediction program (ITS-Boulder)
ITU:	International Telecommunication Union
ITU-R:	International Telecommunication Union, Radio Sector
IUGG:	International Union of Geophysics and Geodesy
IUWDS:	International URSIgram and World Days Service
JINDALEE:	OTH radar system (Australia)
JORN:	Jindalee Operational Radar Network
JPL:	Johns Hopkins University
L1:	Lagrangian point
LAMP:	Local Area Mobile Prediction charts
LASCO:	Large Angle Spectrometric Coronograph
L-Band:	950 MHz to 2200 MHz
LEO:	Low Earth Orbiting (satellite)
LF:	Low Frequency
LOF:	Lowest Observable Frequency
LORAAS:	Low Resolution Airglow and Aurora Spectrograph (NRL)
LORAN:	A maritime navigation system for U.S. coastal areas. The system provides navigation, location, and timing services for both civil and military air, land and marine users, and it is approved as an en route supplemental air navigation system.
LQA:	Link Quality Analysis (matrix); used in HF-ALE systems.
LWS:	Living With a Star (NASA program)
LUF:	Lowest Usable Frequency
M(3000)F2:	Ratio of MUF(3000)F2 and foF2
MAP:	Middle Atmosphere Program
Mercury:	NASA single-astronaut space mission
MFM:	Magnetic Field Model
MINIMUF:	Model to predict the Maximum Usable Frequency for HF (NOSC)
MIT:	Massachusetts Institute of Technology
MLT:	Magnetic Local Time
MOF:	Maximum Observed Frequency
MSFM:	Magnetospheric Specification and Forecasting Model
MSM:	Magnetospheric Specification Mode
MSX:	Midcourse Space Experiment (mapping)
MUF:	Maximum Usable Frequency
MUF(3000)F2:	MUF corresponding to a skip distance of 3000 km using the F2 layer
MURI:	Multi-University Research Initiative
NASA:	National Aeronautics and Space Administration

NATO:	North Atlantic Treaty Organization
NAVSPASUR:	Navy Space Surveillance System (VHF radar)
NAVSTAR:	Program name for GPS system (i.e., NAVSTAR-GPS)
NCAR:	National Center for Atmospheric Research
NCEP:	National Centers for Environmental Prediction
NESDIS:	National Satellite and Data Information Service
NF:	Number of solar flares
NGDC:	National Geophysical Data Center (NOAA)
NOAA:	National Oceanographic and Atmospheric Administration
NORAD:	North American Aerospace Defense Command
NOSC:	Naval Ocean Systems Center
NPA:	Nonprecision Approach
NPV:	Nonprecision Approach with Vertical Guidance
NPOESS:	National Polar-orbiting Operational Satellite System
NRC:	National Research Council (USA)
NRCan:	Natural Resources Canada
NRL:	U.S. Naval Research Laboratory
NSSA:	National Security Space Architect
NSSDC:	National Space Science Data Center
NSWP:	National Space Weather Program
NSWPC:	National Space Weather Program Council
NTCM:	Neustrelitz Total (electron) Content Model
NTP6 Supp-1	Naval Telecommunications Publication (dealing with HF coverage)
NTS-2:	Navy Timation Satellite No.2; NAVSTAR/GPS prototype
NVIS:	Near Vertical Incidence Skywave
NWP:	Numerical Weather Prediction
NWRA:	Northwest Research Associates (USA)
OFCM:	Office of the Federal Coordinator for Meteorological Services and Supporting Research
O-mode:	Ordinary wave mode of radio propagation
OMEGA:	Longwave terrestrial navigation system. It was the first worldwide navigation system. (System terminated in 1997)
OpSEND:	Operational Space Environment Network Display
ORSTED:	Danish satellite that carries five science instruments with the objective of mapping the Earth's magnetic field and measuring its associated high-energy charged particle environment. Data from the mission will be used to improve geomagnetic models and study the auroral phenomena.
OSD	Office of Secretary of Defense
OSS:	Office of Space Sciences (NASA)
OTH:	Over-the-Horizon
OTH-R:	Over-the-Horizon Radar
PA:	Precision Approach
PCA:	Polar Cap Absorption

PIM:	Parameterized Ionospheric Model
PFU:	Particle Flux Units (particles cm^{-2} sec^{-1}/steradian)
POES:	Polar Operations Environmental Satellite (consists of 2 LEOs)
POLAR:	Spacecraft measures solar wind properties, ionospheric output, and energy deposition at high latitudes (ISTP program)
PPS:	Proton Prediction System
PRARE:	Two-way microwave tracking system on satellite ERS-2 (for TEC determination)
PRESTO:	Alert system for RWC-Brussels
PRIME:	Prediction and Retrospective Ionospheric Modelling over Europe
PRISM:	Parameterized Real-Time Ionospheric Specification Model
PROPHET:	Propagation Forecasting Terminal (NOSC)
PROPLAB-PRO:	Commercial HF communication software package (STD)
Q-index:	Magnetic activity index defining the shape and position of the auroral oval
QinetiQ:	Privatized component of the DERA organization (UK)
RA:	Radiocommunication Agency (UK)
RAL:	Rutherford-Appleton Laboratory (UK)
RBTEC:	Ramsey-Bussey Total Electron Content (model)
REC533:	HF system performance model based on ITU-R Rec.P.533
RFC:	Regional Forecast Center
RHESSI:	NASA small Explorer satellite to examine solar flares
RIBG:	Raytrace/ICED, Bent, Gallagher (model) of the ionosphere
RBTEC:	Ramsey-Bussey Total Electron Content model.
RINEX:	Receiver Independent Exchange Format
RIOMETER:	Relative Ionospheric Opacity Meter (absorption monitor)
ROTHR:	Relocatable Over-the-Horizon Radar
ROTI:	Rate of TEC Index
RPSI:	Radio Propagation Services, Inc. (USA)
RPU:	Radio Propagation Unit (U.S. Army: circa 1940s)
RSTN:	Radio Solar Telescope Network
RTCA:	Radio Technical Commission for Aeronautics
RTCE:	Real Time Channel Evaluation
RWC:	Regional Warning Center
SAC-C:	System to provide multispectral imaging of terrestrial and coastal environments. The spacecraft will study the structure and dynamics of the Earth's atmosphere, ionosphere and geomagnetic field.
SAMPEX:	Solar Anomalous and Magnetospheric Particle Explorer
SATCOM:	Satellite Communication
SATNAV:	Satellite Navigation

SC:	Storm commencement
SCINDA:	Scintillation Network Decision Aid
SCOSTEP:	Scientific Committee On Solar-Terrestrial Physics
SEC:	Space Environment Center (NOAA)
SED:	Storm-Enhanced Density (plume)
SEDAC:	Space Environment Data Analysis Center
SEM:	Space Environment Monitor
SERDIN:	Space Environment Real Time Interconnection Network
SEON:	Solar Electro-optical Network
SESC:	Space Environment Services Center
SET:	Space Environment Technologies
SFD:	Sudden Frequency Deviation
SHF:	Super High Frequency
SHINE:	NSF program having as its goal to build a physics-based model of space weather enabling forecasting of the near earth environment based on solar influences.
SID:	Sudden Ionospheric Disturbance
SIDC:	Solar Index Data Center (RWC-Belgium)
SLIM:	Low-Latitude Ionospheric Model
SMART:	Segmented Method for Analytic Raytracing
SMY:	Solar Maximum Year
SNR:	Signal-to-Noise Ratio
SOHO:	The Solar and Heliospheric Observatory, a project of international cooperation between ESA and NASA
SOLAR2000	EUV model (Space Environment Technologies)
SOLRAD:	Solar Radiation Satellite
SOLAR-B:	Satellite to focus on the Sun's photosphere, the chromosphere and the corona. Active regions on the Sun, and interactions among these three solar layers, will be examined.
SOON:	Solar Optical Observing Network
SPA:	Sudden Phase Anomaly
SPAWAR:	Space and Naval Warfare Systems Command
SPIDR:	Space Physics Interactive Data Resource
SPUTNIK:	First artificial earth satellite (Soviet Union)
SRAMP:	STEP-Results, Applications, and Modeling Phase
SRBL:	Solar Radio Burst Locator
SRS:	Solar Radio Spectrograph
SSN:	Sunspot Number
SSNe:	Effective sunspot number (NWRA)
SSULI:	Special Sensor Ultraviolet Limb Imager
SSUSI:	Special Sensor Ultraviolet Spectrographic Imager
STC:	Science and Technology Center
STD:	Solar Terrestrial Dispatch
STEP:	Solar-Terrestrial Energy Program

STEREO:	Solar Terrestrial Relations Observatory
STOA:	Shock Time-of-Arrival
STORM:	Magnetic storm model (for estimating *foF2* from *Ap* time history)
STP:	Solar-Terrestrial Physics
STEP:	Solar Terrestrial Energy Program
STEREO:	Solar Terrestrial Relations Observatory
SWARM:	Visualization software for solar and auroral data (STD)
SWEN:	Space Weather News
SWENET:	Space Weather European Network
SWF:	Short Wave Fade
SWIM:	Visualization software for solar and auroral data (STD)
SWW:	Space Weather Week
SWWT:	Space Weather Working Team (ESA)
SWXS:	Space Weather Squadron
STD:	Solar Terrestrial Dispatch (Canada)
STOA:	Science Technology Options Assessment
SuperDARN:	Super Dual Auroral Radar Network
SURFER:	Mapping software (Golden Software, USA)
SWAN:	Solar Wind Anisotropies. SWAN is an instrument onboard SOHO (SOlar Heliospheric Observatory) that observes interplanetary Lyman alpha radiation from all directions of the sky.
SWO:	Space Weather Operations (NOAA-SEC)
SXI:	Solar X-ray Imager
TACSAT:	Tactical Satellite
TDIM:	Time Dependent Ionospheric Model
TE:	Transverse Electric (mode)
TEC:	Total Electron Content
TID:	Traveling Ionospheric Disturbance
TIGCM:	Thermosphere-Ionosphere Global Circulation Model
TIMED:	Thermosphere, Ionosphere, Mesosphere, Energetics and Dynamics (mission)
TIME-GCM:	Thermosphere-Ionosphere-Mesosphere-Electrodynamic General Circulation Model
T-Index:	Proxy for sunspot number (IPS-Australia)
TIROS:	NOAA-16 satellite; with sensors to monitor electron precipitation
TM:	Transverse Magnetic (mode)
TOPEX:	Satellite equipped with dual frequency radar altimeter
TRACE:	Transition Region and Coronal Explorer
UAF:	University of Alaska-Fairbanks
UDRE:	User Differential Range Error. An error metric for the WAAS system that exploits the GPS waveform.
UHF:	Ultra High Frequency

ULYSSES:	A NASA/ESA satellite designed to survey the solar environment from the poles to the equator, and to study the solar spectrum, solar flares and the solar wind.
URL:	Universal Resource Locator (e.g., web site)
URSI:	International Union of Radio Science
USAF:	United States Air Force
USGS:	United States Geological Survey
UV:	Ultraviolet (~ 100 – 400 nanometers)
VERSIM:	VLF/ELF Remote Sensing of the Ionosphere and the Magnetosphere
VHF:	Very High Frequency
VIRGO:	An instrument aboard SOHO that monitors solar irradiance variations.
VIS:	Vertical Incidence Sounder
VLF:	Very Low Frequency
VOACAP:	Voice of America Communications Analysis Program
WAAS:	Wide Area Augmentation System (FAA)
WBMOD:	Wideband Model (of radio wave scintillation)
WDC:	World Data Center
WDC-STS:	World Data Center for Solar-Terrestrial Science (Sidney)
WIND:	The first of two NASA spacecraft in the Global Geospace Science initiative and part of the ISTP Project, to be followed by a halo orbit at the Earth-Sun L1 point. Objectives of the WIND mission include an investigation of basic plasma processes occurring in the near-Earth solar wind.
WMS:	WAAS Master Station
WRS:	WAAS Reference Station
WWA:	World Weather Agency (NOAA-SEC)
X-mode:	Extra-ordinary wave mode of radio propagation
XUV:	soft x-rays in the range ~1 – 30 nanometers
YF2:	F2 region semi-thickness
YOHKOH:	Satellite hosting solar x-ray imager instrument (Japan)

INDEX

Note: This subject index is a convenient vehicle for finding topics covered in the manuscript without referring to the Table of Contents. While the index is generally complete, discretionary editing of the page listings for some topics has carried out to limit minor references and redundancies, thereby making searches more efficient. For example, the term "SEC" appears so many times throughout the book that a complete catalog of the associated pages would not be very helpful. We have chosen not to incorporate an author index, but the reader is encouraged to make use of sizable reference lists that appear at the end of each chapter. On the other hand, we include the page numbers associated with references to prominent scientists if no specific citation is given (i.e., Marconi, Gauss, etc.). The reader should also refer to the separate "List of Acronyms and Selected Terms"(pp.355-365) for additional information.

Aarons, J., 19
A-index, 63, 127 (see geomagnetic activity indices)
Advanced Composition Explorer (ACE), satellite, 42, 146, 271, 279, 312, 315, 320, 334, 338-339
Advanced Concepts Technical Demonstrations (ACTD), 322
AEEC, 226
AFCRL, 19 (See AFRL)
AFGL, 19, 175 (See AFRL)
AFGWC, 17 (See AFWA)
AFRL, 156-157, 160, 260
Air Force Weather Agency (AFWA), 149, 262, 270, 296-298, 312, 320
Airglow Experiment-Arizona (GLO), 315
Alcatel, 326
Alerts (E-mail), 298
Alouette, 14-15
American Geophysical Union (AGU), 262, 336
Appleton, E.V., 8-10
Appleton layer, 10; (See F layer)
Applied Physics Lab (APL), 338
Apollo program, 14
ARGOS satellite, 149, 155, 314
ARINC, 299, 301
Armed Forces Communications and Electronics Association (AFCEA), 262
ASTRID, 315
Aurora, 6, 7, 116
Auroral oval, 6, 68-71, 117, 281
Auroral Prediction Model (IAPM), 313
Australian Space Forecast Center (ASFC), 329

Automatic Geophysical Observatories (AGO), 315
Bartels, J., 7
Boston University, 336
Breit, G., 8
Carpenter, D., 183
CAWSES, 334, 337
CCIR (See ITU, ionospheric models)
CEASE, 322
CEDAR, 262, 334-336
    CEDARweb, 334
    CEDAR POST, 335
    CEDAR Data System, 335
CELIAS, 340-341
Celsius, A., 7
CHAMP, 156
Chapman, S., 9
Center for Integrated Space Weather Modeling (CISM), 334, 336
CLUSTER, 183, 334, 340
Collision frequency, 211
Commercial Space Weather Interest Group (CSWIG), 23, 261, 299, 305, 332-333
    List of 3rd-party vendors, 333
Committee for Space Weather (CSW), 313-314
Control point, 256-257
Cornell University, 160
Coronal holes, 39-42, 50, 67
Coronal Mass Ejection (CME), 53, 65, 67, 73, 177, 193, 341
COSPAR, 21, 144-145, 155, 262, 309, 330, 333
COSMIC, 156, 315, 322
Coordination in Science and Technology (COST), 142, 146-147, 149-153, 163, 310, 328
    Action-238 (PRIME), 150, 293, 325
    Action-251, 151, 293, 325-326
    Action-271, 293, 326
    Action-724, 326-327
Costello *Kp* index, 271-273, 279-280, 313
Defence Science and technology Organization (DSTO), 195
Department of Defense (DOD), 314, 321
Department of the Interior (DOI), 314
Department of Transportation (DOT), 314
DERA, 151, 303
Digital Ionospheric Sounding System (DISS), 320
DMSP program, 67, 156, 283, 312, 320-321
DNA-Wideband satellite, 19
D region, 97-97

DSTL, 260, 303
Dynacast®, 234, 301
Dynamics Explorer satellite, 67, 69
Eccles, W.H., 9
Echo satellite, 13
EISCAT, 337
EMP, 183
E region, 98-100
ESTEC, 326-327, 333
Eumetsat, 322
European Space Agency (ESA), 152, 260, 324, 326-327
    Space Weather Working Team (SWWT), 152, 310, 326-327
    Space Weather European Network (SWENET), 327
    Space Weather News (SWEN), 327
European Union (EU), 325, 333
Explorer program, 13
Evans, J.V., 13
FAST, 315, 334, 339
Federal Aviation Administration (FAA), 316
F1 region, 101-102
F2 region, 103
    Anomalies, 104-106
        Diurnal anomaly, 105
        Appleton anomaly, 105, 140 (see equatorial anomaly)
        December anomaly, 106
        Winter anomaly, 106
        Trough, 106
Faraday, M., 7-8
GAIM, (See ionospheric models)
Galileo, 4
Galileo navigation system, 18, 270
Gauss, J.C.F., 7
GEOSTORMS, 271
GEM initiative, 334-336
    GEM Messenger, 336
Gemini program, 14
Geomagnetic activity indices, 62-64, 118-119
    Costello *Kp* index, 271-273
Geomagnetic field, 55-60
    B-L coordinate system, 58
    Geomagnetic coordinate system, 58
    Geomagnetic data, 64
    Geomagnetic latitudes, 59-60
    GIN stations, 64
    INTERMAGNET program, 64, 335

Magnetic latitude vs. dip angle, 59
Geomagnetic storm, 65-76, 188, 267
TEC variations, 108, 111
Ionospheric storm, 129-140
Modeling, 130-134
Propagation studies, 134-137
Geospace General Circulation Model (GGCM), 336
Geotail, 315, 334, 340
Global Electrodynamics Connections (GEC), 315
Global Navigation Satellite System (GNSS), 270
Global Positioning System (GPS), 17-18, 134, 156, 159, 224, 270, 304, 312, 315-316, 320
CORS, 156, 158
IGS, 156
WAAS, 158-159, 224, 316
GPS network of ground stations, 291
GLONASS, 18, 270
GOES satellites, 53, 271, 275, 279, 283, 304, 312, 320, 322
Golden, T., 19
GOLF, 341
GRACE, 156
Halloween 2003 storm, 53-54, 73-76, 137-140, 233-234, 237, 240, 243-244, 279-280, 282
System impact, 244
HAARP, 183
Hartree, D.R., 9
Helliwell, R., 183
Hertz, H., 8
HESSI, 315
High Altitude Observatory (HAO), 335
High Altitude Nuclear Explosions (HANE), 185
High Frequency Industry Association (HFIA), 195
High Frequency (HF)
Prediction programs, 48
HIRASS instrument, 155
ICAO, 226
IDCE (See regional warning centers)
IEE, 175
IEEE, 175
IMAGE satellite, 6, 67-68, 183, 315, 322, 334 339
IMP satellite, 42
Incoherent scatter radar (ISR) (i.e., Thomson scatter), 315, 335, 337
Inmarsat, 300
Innovative Solutions International, 158
INSPIRE, 183

Institute of Communication and Navigation (DLR), 262, 293-295
European and polar TEC maps, 294-295
INTERBALL, 334
INTERMAGNET, 271
International Association of Geomagnetism and Aeronomy (IAGA), 63, 330
International Council for Science (ICSU), 330-331
International Service of Geomagnetic Indices (ISGI), 63
International Geophysical Year (IGY), 11-12, 310, 331
International GPS Service for Geodynamics (IGS), 293
International Magnetospheric Study (IMS), 310
International Polar Year, 10
International Solar Cycle Study (ISCS), 310, 331, 334
International space weather initiatives, 324-329
Australia, 329
Canada, 329
European Union, 325
European Space Agency, 327
France, 328
Regional Forecast Center (RFC-Meudon), 328
Japan, 328
Sweden, 327-328
International Standardization Organization (ISO), 155
International Telecommunications Union (ITU), 155, 162, 176, 178, 262, 331-332
International Union of Geophysics and Geodesy (IUGG), 64
International URSIgram and World Days Service (IUWDS), 317
International Years of the Quiet Sun (IQSY), 12, 310, 331
Interplanetary CME Imager, 315
Interplanetary Magnetic Field (IMF), 29, 41-42, 61, 65-66, 118, 146, 177, 179
Interplanetary Monitoring Platform, 315
Ionosphere, 81-164
Chapman layer, 90-95
Production rate, 91
Continuity equation, 92
Current systems, 141
Diurnal variations, 108-111
Electron density distributions, 86
Equatorial anomaly, 140
Equilibrium processes, 92-95
High latitudes, 116-127
Plasma patches, 120-121, 126
Ion concentrations, 85
Irregularities, 106-108
Layer descriptions, 95-111
Layer properties, 87-89

Solar activity dependence, 112-113
Sporadic E, 114-116, 214-216
Spread F, 214-215
Storms, 52
Structure, 82-83
Ionospheric Activity Index (IACTIN), 313
Ionospheric Effects Symposia, 81, 148, 160, 309
IES2002 Modeling Panel, 153-161
Ionospheric models, 141-146
ASAPS, 196-197, 302
Bent model, 146, 313
Bradley-Dudeney profile, 142
CCIR model, 12, 103-104, 142, 145
Ching-Chiu model, 146
COST Action models
CORLPRED, 150-151
COSTPROF, 150-152
COSTTEC, 150-151
Data assimilation models, 157
Kalman filter, 146-147, 163
GAIM, 25, 147-149, 156, 160, 164, 297
EPPIM model, 146
FAIM, 144
International Reference Ionosphere (IRI), 133, 142-143, 150, 154-155
ICED, 144
ICEPAC, 141, 196-197, 302, 304, 313
IONCAP, 141-143, 196-197, 313
ITS-78, 313
MINIMUF, 196-197, 303
NTCM-Neustrelitz, 293
PIM, 144, 313
PRISM, 144, 304, 313
PROPLAB-PRO, 302
REC533, 141, 196-197, 302
RIBG, 144
VOACAP, 141, 196-197, 302, 304
Ionospheric predictions, 161-163
Ionospheric Forecast Model (IFM), 313
Ionospheric Prediction Service (IPS), 262, 287-289, 298, 329
Hourly Area Prediction (HAP) charts, 288, 290
Ionosonde Network Advisory Group (INAG), 287, 330
Local Area Mobile Prediction (LAMP) charts, 288, 291
Space weather categories at IPS, 289
WDC for Solar-Terrestrial Science, 287
Ionospheric propagation

Arctic radio propagation, 122
Diagnostic studies, 122-127
Channel availability, 127
Geomagnetic storm effects, 134-137
MOF studies, 124-125
Near Vertical Incidence Skywave (NVIS), 223
O and X modes, 96-97
Propagation properties, 179-181
Storm Enhanced Density (SED) plume, 140, 242
Short Wave Fade (SWF), 185, 192, 223, 279
Sudden Frequency Deviation, 192
Sudden Phase Anomaly (SPA), 185
WBMOD scintillation, 157, 300, 300
Whistler mode, 182
Ionospheric sounding, 95-97, 159, 191, 284-285, 312
Digisonde, 96, 284, 335
Dynasonde, 284, 335
Chirpsounder®, 335
Chirpsounder® studies, 124-127, 230-232
Northern Experiment geometry, 231
Ionospheric storm, 129-140 (See geomagnetic storm)
ISEE satellite, 42
ISES, 46-47, 64, 262-264, 317
Regional Warning Centers (RWCs), 265
Mission and functions, 263
Geophysical calendar, 264
World Warning Agency (WWA), 317
ISTP program, 334
Kelvin, Lord W.T., 7
Kennelly-Heaviside layer, 9
K-index, 63, 70, 130-133, 267 (see geomagnetic activity indices)
Kriging, 151
Larmor, J., 9
LASCO, 271, 296, 341
Living with a Star (LWS), 309, 315-318
Loomis, E., 5
LORAAS instrument, 149, 155
Lorentz, H., 9
Magnetic Field Model (MFM), 313
Magnetometer chain, 312
Magnetosphere, 60-62
Magnetospheric Constellation, 315
Magnetospheric Multiscale, 315
Magnetospheric Specification Model (MSM), 313
Magnetospheric Specification and Forecasting Model (MSFM), 313

Magnetospheric substorm, 66-67
Marconi, G., 8
Maunder minimum, 4
Maxwell, 8
Mercury program, 14
Metatech Corporation, 53
Middle Atmospheric Program (MAP), 310, 337
Minitrack system, 19
MIT Haystack Observatory, 140
MSX, 315
MURI program, 148
NASA, 145, 260, 314, 332, 334
    Jet Propulsion Laboratory, 156, 262
        GENESIS web site, 156
        GIM TEC maps, 289, 292
        Deep Space Network, 289
        ROTI index, 292
    Office of Space Sciences (OSS), 315
National Center for Atmospheric Research (NCAR), 335
National Centers for Environmental Prediction (NCEP), 332
National Geophysical Data Center (NGDC), 64, 96, 262, 283-285, 335
    NESDIS, 283
    SPIDR on the web, 283
National Oceanographic and Atmospheric Administration (NOAA), 321, 332
National Polar-Orbiting Operational Environmental Satellite System (NPOESS), 322
National Research Council (NRC), 310
National Satellite and Data Information Service (NESDIS), 271
National Science Foundation (NSF), 260, 314, 334-336
National Security Space Architect (NSSA), 309, 314
    National space weather goals, 319
    Space weather architecture vector, 323
        Ultimate architecture components, 323
    Space weather support network, 320
    Space weather support network improvements, 321
National Space Science Data Center (NSSDC), 145
National Space Weather Program (NSWP), 2, 20-21, 25, 309, 311-315
    Goals, 311
    Ground-based observing systems, 315
    Operational models, 313
    Research topics of NSWP, 314
    Space observing systems, 315
    Space weather resources, 312
    Strategic and Implementation Plans, 311-314
National Space Weather Program Council (NSWPC), 313

National Weather Service (NWS), 73, 75
NATO-AGARD, 175
Natural Resources Canada (NRCan), 262, 285-286, 329
    CANOPUS system, 285, 335, 338
Naval Ocean Systems Center (NOSC), 17
Naval Research Laboratory, 9, 134, 260
Northwest Research Associates (NWRA), 19, 68-69, 71-72, 157, 160, 262, 299-300
    Auroral boundary plot, 282
Office of the Federal Coordinator for Meteorological Services (OFCM), 313
ORSTED, 315
Poincaré, H., 8
Poisson, S., 7
POES, 271, 279, 281, 283, 312, 320
POLAR, 183, 315, 334, 340
Polar Cap Absorption (PCA), 61, 123, 185-186, 188, 192, 210, 223
Prediction services and systems, 255-305
    AF-GEOSpace, 303
    C/NOFS, 157, 243, 260, 305, 315, 322, 335
    Elements of the prediction process, 258-259
    HF-EEMS, 260, 303
    Organizations offering forecasting services, 260-262
    OpSEND, 24, 241, 260, 302-304
    PROPHET, 14-17, 22, 241, 260, 302-303
    Requirements for predictions, 257-258
    SCINDA, 24, 243, 260, 304-305, 312, 322
Proton Prediction System (PPS), 313
QinetiQ, 260
Radio blackout, 267
Radio Propagation Services (RPSI), 68, 104, 124-127, 146, 262, 299, 301, 301
Radio Solar Telescope Network (RSTN), 320-321
Radio systems, 21
    System influences, 22
Rayleigh, Lord,
Real-Time Channel Evaluation (RTCE), 190, 231-232
Regional Warning Centers, 64 (See ISES)
    RWC-Warsaw and IDCE, 262, 295-296, 326
    RWC-Brussels and SIDC, 296
        CACTUS, 296
        PRESTO alerts, 296
RHESSI, 334, 339
Ring current, 5
Riometer, 315, 320
Rockwell-Collins, 299

Rutherford-Appleton Laboratory (RAL), 262, 293, 326
Space Weather Web, 293
SAMPEX, 315
Schuster, A., 5
Science and Technology Center (STC), 336
SCINDA, (See prediction services and systems)
Scintillation, 19-20, 157
SCOSTEP, 309-310, 331, 334, 337
Space Environment Real-Time Intercommunication Network (SERDIN), 328
SHINE initiative, 334, 336
Shock Time of Arrival model (STOA), 313
Skylab satellite, 40-41
SOHO satellite, 53, 271, 296, 315, 328, 334, 340
Solar Influences Data Center (SIDC), 43 (See RWC-Brussels)
Solar Maximum Year (SMY), 310, 331, 337
SOLRAD, 14, 24
Solar-B, 315
Solar and geophysical activity report, 278
Solar flares, 50-51, 186
Number of, 51
Flare classification, 51
Short wave fade (SWF), 128-129, 185, 193
Sudden Ionospheric Disturbance (SID), 50-52, 127-128, 188, 312
Sudden Phase Anomaly, 185-186
X-ray flares, 73-77
Solar flux, 43
Ottawa solar flux, 43, 49
Penticton Radio Observatory, 43
Solar proton event, 186, 283
Solar radiation storms, 73, 75, 267
Solar Radio Burst Locator (SRBL), 321
Solar Radio Spectrograph (SRS), 321
Solar Terrestrial Dispatch (STD), 68, 262, 298-299, 302
PROPLAB-PRO, 302
SWARM, 302
SWIM, 302
Solar Terrestrial Energy Program (STEP), 310, 331, 334, 337
Solar Terrestrial Relations Observatory (STEREO), 315, 322
Solar variability, 45-50
27-day recurrence, 48-50
Solar wind, 39-42, 50
Solar X-ray Imager (SXI), 271, 283, 322
Sommerfeld, A., 8
Solar Optical Observing Network (SOON), 271, 297, 320-321, 335
Improved SOON (ISOON), 321

Solar Electro-Optical Network (SEON), 297, 335
Space Environment Center (SEC), 64, 71-72, 132-134, 138-139, 149, 262, 265-283, 332-333
E-mail alerts, 298
FTP data server, 276
Historical milestones, 266
Space Weather Operations (SWO), 270-275
Space weather scales, 266-270
For geomagnetic storms, 268
For Solar radiation storms, 268-269
For radio blackouts, 269
Vertical incidence sounder station list, 277
Web site: "Today's Space Weather", 267, 276
Web site: "Space Weather Now", 276
Space Environment Monitor (SEM), 328
Space Environment Services Center (SESC), 17
(See Space Environment Center)
Space Environment Technologies (SET), 45, 68, 157, 262, 299
Space Research Center-Warsaw, 152
Space weather
Data utilization, 23
Definition, 2-3
Historical perspectives, 3-20
Observational motivation, 76
Programs, 20
Space weather forecast benefits, 245
Space Weather Week (SWW), 160, 299, 309, 314, 333-334
Space weather email alerts 298
Space weather forecasting services (commercial), 298-302
SPAWAR, 241
Sputnik, 13
SSIES, 297
SSULI, 156, 321
SSUSI, 156, 322
STEP-Results, Applications and Modeling Phase (SRAMP), 310, 330, 334, 337
Stewart, B., 5, 7-8
Stormer, B., 7
STORM model, 132-134, 158, 197, 271-274
SuperDARN, 156, 196, 315, 335, 338
SURFER mapping program, 151
Sun, 31-51
Butterfly diagram, 39
Composition, 31
Structure and irradiance, 31-36

Solar2000 model, 45, 157
Sun-Earth Connections, 315-316
Sunspots 5, 36-39, 42-45, 178
T-index, 144, 196, 300
Wolf number, 42
Zurich number, 43
Predictions, 43-45
SWAN, 341
Swedish Institute of Space Physics
RWC-Lund, 328
Website: Lund Space Research Center
Telecommunication systems
Automatic Link Establishment (ALE), 194-195, 224-225
DECCA, 270
DGPS, 224
Fleetsatcom (FLTSAT), 304
GLOBALink/HF system, 194, 225-236, 245, 273, 301
Air traffic patterns, 228
Diversity experiments, 230-232
Ground stations, 226-227
Frequency management, 227, 229, 234
Storm impact on HFDL (See Halloween storm)
Technical characteristics, 229
Global Positioning System, 222, 237
Groundwave Emergency Network (GWEN), 183
HF communication systems, 187-198, 316
Polar communication services, 234-236
LDOC and ATC, 235-236
Polar flight patterns, 236
HF data link communications (HFDL; see GLOBALink/HF)
HFDF, 223
HF OTHR, 9, 193, 195-196, 223
Jindalee radar, 195
Jindalee Operational Radar Network (JORN), 195
LORAN, 270
LQA matrix, 194
Military C3I requirements, 221
NAVSPASUR, 158
NORAD, 297
OMEGA, 15, 270
Relocatable OTHR (i.e., ROTHR), 195, 223
TACSAT, 19, 214
Utilization, 181
WAAS system, 18, 73, 158, 224, 237-240, 245, 316
CONOPS, 237-238

Error metrics (GIVEs, UDREs), 237-240
Space weather response (See Halloween storm)
System architecture, 237, 239
Telecommunication system effects
Absorption map for HF, 271, 275
Channel availability, 127
Earth-space effects, 198-220
Absorption, 198, 209-211
Differential effects, 214-221
Electron content effects, 199
Integrated effects, 198-199
Ionospheric Doppler, 206
Faraday rotation, 198, 206-209
Frequency dependence, 208
Magnetic field parameter, 208
Phase and group path effects, 202-205
Ionospheric time delay, 203
Range error limits, 204
Refraction, 198-201
Wedge refraction, 200
Ionospheric refraction error, 205
Scintillation, 214-221
Diurnal variation, 214-216
Global morphology, 216-219
Mechanisms, 218
Mitigation, 220
Modeling, 219-221
Intensity spectrum, 219-221
Nakagami distribution, 219
Phase spectrum, 220-221
Rayleigh distribution, 219
Ringing irregularities, 214
VHF scintillation, 216
UHF/L-Band scintillation, 217
Time dispersion, 198, 209-210
ELF effects, 184
HF effects, 188-189
HF Propagation mechanisms, 190-191
HF System Performance Models, 196-198 (See ionospheric models)
MF effects, 187
Real-Time Channel Evaluation (RTCE), 162
Storm effects on satellite navigation signals, 134-137
Waveguide mode, 184-185
Wavehop mode, 184-185
WBMOD scintillation model, 157-158

TIMED, 315, 334, 339
TIROS satellite, 69, 71, 279, 282
TOPEX satellite, 156, 290
Total electron content (TEC), 151, 156, 163, 198-199, 202-203, 206-213, 237, 335
    GIM mapping, 156
    RBTEC model, 313
TRACE, 334, 339
Traveling Ionospheric Disturbance (TID), 22-23, 108, 160, 162-163, 188, 193, 223, 312
Tuve, M.A., 8
Ulysses, 315
University of Alaska-Fairbanks, 146
University of Leicester, 145
University of Massachusetts-Lowell, 96
University of Southern California, 148, 156
URSI, 144, 155, 262, 329-330, 333
    Coefficients, 103-104
    Commission G, 329
Utah State University, 148, 157
Van Allen, J., 13
    Van Allen radiation belts, 13, 57
Vanguard, 12-13
VERSIM, 330
VIRGO, 341
Von Braun, W., 13
WAAS, (See Telecommunication systems)
Wang-Sheeley Model, 313
WBMOD, 19, 157, 304, 313 (See Telecommunication system effects)
WIDEBAND satellite, 218
Wien's displacement law, 34
WIND satellite, 42, 146, 315, 334, 339-340
World Data Centers, 64, 328
    WDC-A, 64
    WDC-B, 328
    WDC-C1 (UK), 328
    WFDC-C2 (Japan), 328
YOHKOH satellite, 271, 320

ABOUT THE AUTHOR

John Goodman received his BS in Nuclear Engineering from N.C. State University in 1960 and his PhD in Physics from Catholic University of America in 1970. He has 44 years of government and industry experience in the RDT&E associated with radio and radar systems with emphasis on those categories that are influenced by the ionosphere. Specialties have included SATCOM and HF system impairment studies and the development of real-time-channel evaluation subsystems. He was with the Naval Research Laboratory from 1960-1991, and served a brief stint as Principal Scientific Consultant for Radio Communications at the SHAPE Technical Center at The Hague in the mid-80s. He was Program Manager for Radio Communications Technology at SRI International from 1991-1994, and he was Vice President for Applied Technology at TCI/BR Communications, headquartered in Sunnyvale California between 1994 and 1998. He is currently Vice President and Chief Technical Officer for Radio Propagation Services, Inc. (RPSI). Dr. Goodman has numerous publications, and he has been the Guest Editor for Special Issues of Radio Science issues on several occasions. He has organized a number of topical conferences, most notably the series of IES conferences held every three years since 1975. He is also author of the text: *HF Communications: Science & Technology* published by Van Nostrand Reinhold [1992], and a Chapter on "Meteor Burst Communications" in the *Encyclopedia of Telecommunications* published by Marcel Dekker. [1995]. He has been a guest author of an article entitled "Characteristics of the Ionosphere" appearing in the *Wiley Encyclopedia of Electrical and Electronics Engineering* [2002]. Dr. Goodman has lectured on a variety of space science issues, and has conducted specialized training courses under the aegis of the George Washington University.

Dr. Goodman has been actively involved in national and international bodies responsible for consideration of industry and government standards for radio communications. Specifically he has been engaged in ITU-R activities, and has represented the United States at various meetings of Study Groups and Working Parties both in the United States and abroad. He has been a member of Working Groups within URSI, and he is a member of the AGU. Dr Goodman has taken an active role in various bodies responsible for coordinating, developing, and evaluation of aeronautical communications standards and systems. In this context, he has participated in the AEEC, RTCA, C/SOIT, ICAO and other bodies involved in HF communications for aviation purposes.

Early in his career at NRL, Dr. Goodman was involved in radar investigations of the atmosphere and space objects of interest. He developed an interest in space science, and began measurement of the ionospheric electron content using Faraday rotation of lunar echoes. He conducted studies of the ionosphere using incoherent scatter radar technology, eventually using

this topic as inspiration for his PhD dissertation. He was one of the first investigators to observe positive phase excursions in TEC associated with geomagnetic storms. He was the Principal Investigator for GEMINI Experiment D14 designed to investigate ionospheric inhomogeneities, at a time when such measurements were either sparse or nonexistent. He also investigated UHF and L-Band scintillation phenomena associated with the Timation Satellite, an early prototype of the NAVSTAR/GPS system. He managed a team responsible for recovery and dissemination of SOLRAD 11A/B data, and. and he was the originator of a well-known method for updating climatological models based upon pseudo-sunspot numbers derived from sounders. With RPSI, Dr Goodman is the co-inventor of a real-time forecasting procedure, Dynacast®, that enables specification of the ionosphere by taking space weather data into account. He has also been involved in the investigation of various patented methods that could be implemented in a real-time system for specification of optimal sets of propagating frequencies for a global HF communication system, GLOBALink/HF, managed by ARINC Corporation, and used by commercial carriers worldwide.